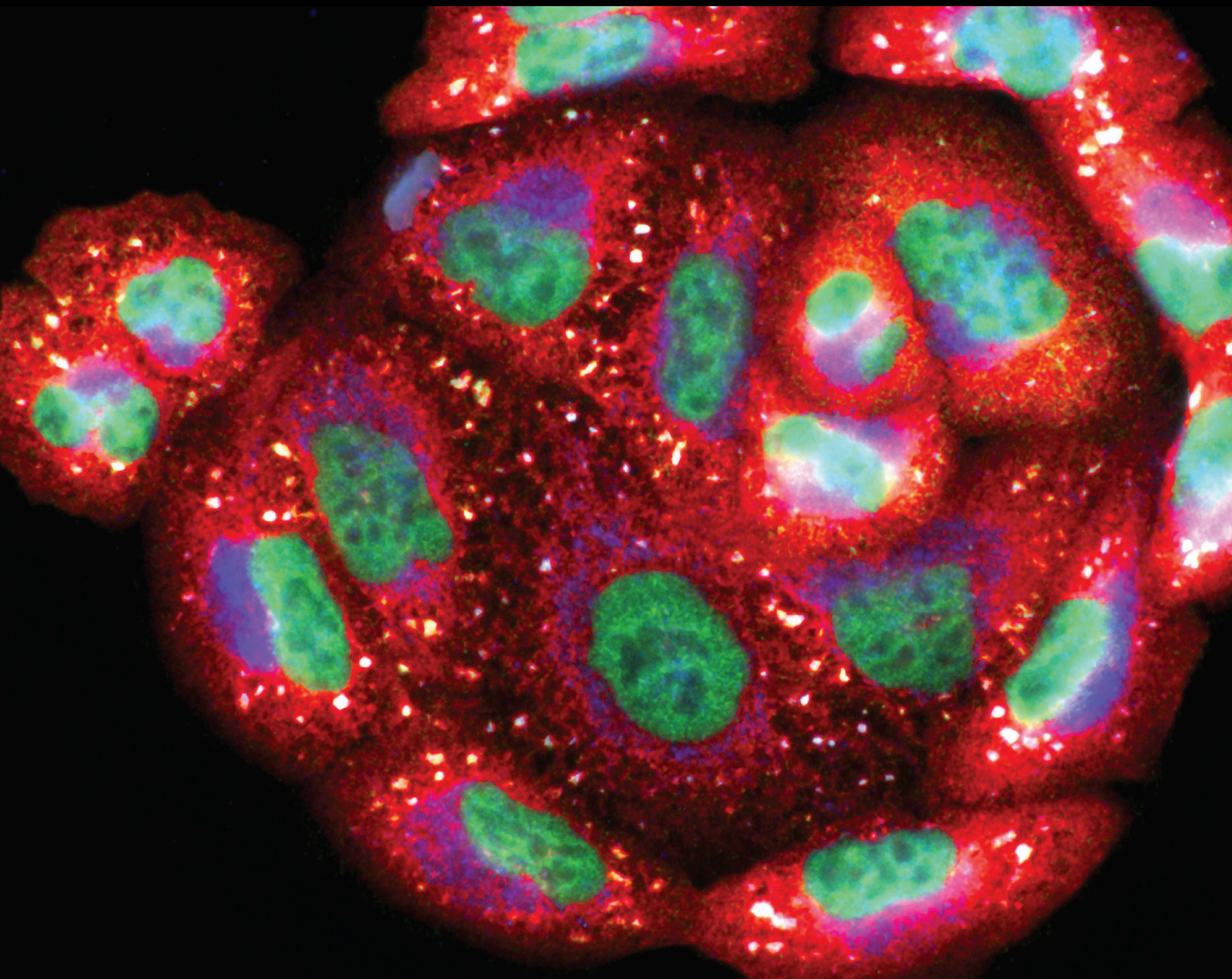# Mitochondrial Oxidative Stress and Energy Metabolism: Impact on Aging and Longevity

Lead Guest Editor: Ravirajsinh Jadeja
Guest Editors: Pamela M. Martin and Wei Chen

Mitochondrial Oxidative Stress and Energy Metabolism: Impact on Aging and Longevity

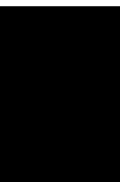# Mitochondrial Oxidative Stress and Energy Metabolism: Impact on Aging and Longevity

Lead Guest Editor: Ravirajsinh Jadeja
Guest Editors: Pamela M. Martin and Wei Chen

Chief Editor

Jeannette Vasquez-Vivar, USA

Editorial Board

Contents

Contents

Editorial

Mitochondrial Oxidative Stress and Energy Metabolism: Impact on Aging and Longevity

Ravirajsinh N. Jadeja [ID],[1] Pamela M. Martin [ID],[1,2,3] and Wei Chen [ID][4]

[1]*Department of Biochemistry and Molecular Biology, Augusta University, Georgia, USA*
[2]*Department of Ophthalmology, Medical College of Georgia, Augusta University, Augusta, GA 30912, USA*
[3]*James and Jean Culver Vision Discovery Institute and Medical College of Georgia at Augusta University, Augusta, GA, USA*
[4]*Department of Food Science and Nutrition, National Engineering Laboratory of Intelligent Food Technology and Equipment,
   Zhejiang Key Laboratory for Agro-Food Processing, Zhejiang University, Hangzhou 310058, China*

Correspondence should be addressed to Ravirajsinh N. Jadeja; rjadeja@augusta.edu
and Pamela M. Martin; pmmartin@augusta.edu

Understanding better processes governing normal aging and the pathogenesis of age-related conditions is essential to potential lifespan extension and/or improvement of quality of life in the geriatric population. Mitochondria are key players in the process of aging because of their critical role in the regulation of bioenergetics, oxidative stress, and cell death [1, 2]. Thus, therapeutic strategies targeted at minimizing oxidative stress and maintaining healthy mitochondrial energy metabolism for productive aging are of noticeable interest to aging researchers. The maintenance of an adequate supply of energy during aging is essential for cellular repair, homeostatic mechanisms, and mitochondrial biogenesis [3, 4]. Numerous studies have shown mitochondrial bioenergetic deterioration to be an important factor in normal physiological aging and in the pathogenesis of age-related ailments in various cell and tissue types [5, 6], with reactive oxygen species- (ROS-) induced mitochondrial DNA damage being a prominent factor [7]. Furthermore, epigenetic modifications have been shown to greatly influence oxidative stress and mitochondrial dysfunction during aging [8]. Related to the above, evidence from recent studies highlights the importance of alterations in the metabolism of nicotinamide adenine dinucleotide (NAD), a coenzyme central to cellular metabolism and epigenetic regulation, in aging [9, 10]. This Special Issue aims to provide recent updates on the role of mitochondrial oxidative stress and energy metabolism in aging and longevity. Following the stringent peer review of many submitted manuscripts, 17 articles were incorporated for publication in this special issue. The article collection for this Special Issue can be subdivided into the following major categories: cardiovascular, retinal and neurological aging, mitochondrial ROS and energy metabolism, and hyperglycemia, as detailed more closely below.

This issue contains two research manuscripts and two review articles focused on cardiovascular aging. The study by E. Qaed et al. evaluated the role of phosphocreatine (PCr) on mitochondrial respiratory function in diabetic cardiomyopathy (DCM). The pretreatment with PCr was found to be effective against cardiac damage in experimental diabetic mice. Another article by Y. Qiao et al. focused on the protective role of capsaicin (CAP) in regulating mitochondrial function in anoxic or anoxic/reoxygenated cardiomyocyte injury. CAP-mediated upregulation of 14-3-3η, a protective phosphoserine-binding protein in cardiomyocytes, ameliorated mitochondrial function caused by a disruptive redox status and an impaired ETC (electron transport chain). The other two review articles

focused on the role of mitochondrial ROS and mitophagy in maintaining mitochondrial dynamics during cardiovascular aging and collectively provide an excellent review of the existing literature on the field of cardiac aging. Further and importantly, a thorough discussion of potential future therapeutic avenues is also provided.

This special issue also contains three research articles focusing on the role of the mitochondrial function in cerebral injury and aging. The study by Y. Li et al. evaluated the proteomic profile of the aging mouse brain to identify proteins involved in mitochondrial dysfunction and oxidative damage. The proteomic changes of young (4-month) and aged (16-month) B6129SF2/J male mouse hippocampus and cerebral cortex were investigated. Compared with the young animals, 390 hippocampal proteins (121 increased and 269 decreased) and 258 cortical proteins (149 increased and 109 decreased) changed significantly in the aged mice. Bioinformatic analysis indicated that these proteins are mainly involved in mitochondrial function, oxidative stress, synapses, ribosomes, cytoskeletal integrity, transcriptional regulation, and GTPase function. Reutzel et al. performed a longitudinal evaluation of the cerebral mitochondrial function and cognitive performance in aging female NMRI mice. These authors measured brain mitochondrial function, cognitive performance, and molecular markers every 6 months until mice reached the age of 24 months. During the physiological aging process, several changes in cognitive performance, mitochondrial brain energy metabolism, and mRNA expression of genes involved in mitochondrial biogenesis were detected in a longitudinal study over a period of 24 months. Most of the impairments on cognition and mitochondria bioenergetics were detected starting at the age of 18 months, which shows that aged NMRI mice are an appropriate model to study the neurological aging process. Another study by W. Chen et al. evaluated the efficacy of mitoquinone (MitoQ), a newly developed selective mitochondrial reactive oxygen species (ROS) scavenger against intracerebral hemorrhage (ICH) in mice. They demonstrated that the selective mitochondrial ROS scavenger MitoQ can attenuate white matter injury and improve neurological impairment after ICH and supported the potential future use of MitoQ as a therapeutic agent for neuroprotection after ICH.

Review articles from our research group and P. G. Sreekumar et al. provide recent updates on retinal aging. We highlighted specifically the importance of NAD$^+$, a coenzyme that participates in various energy metabolism pathways, including glycolysis, β-oxidation, and oxidative phosphorylation, in addition to being a required cofactor for important enzymes such as (ADP-ribose) polymerases (PARPs) and sirtuins, with emphasis on the relevance of the above to metabolism in the aging retina and in retinal degeneration. We also discussed possible therapeutic avenues to improve energy metabolism in the aging retina. Alternately, P. G. Sreekumar et al. focused on the topic of ocular senescence. This review provided an overview of the types of senescence, pathways of senescence, and senescence-associated secretory phenotype (SASP). Furthermore, the authors also discussed the role of mitochondria in ocular senescence and possible therapeutic avenues.

This issue also contains several articles focused on understanding the associations between oxidative stress, energy metabolism, and mitochondrial function under various physiological conditions. Y. Du et al. showed that knockdown of mitochondrial antiviral signaling proteins (MAVS) alleviated radiation-induced mitochondrial dysfunction, downregulated the expression of proapoptotic proteins, and reduced the generation of ROS in cells after irradiation. L. Zhao and colleagues showed that autophagy deficiency impairs the antioxidant defense system and could play an important role in the process of aging. In another article by A. Keller et al., it was reported that (–)-epicatechin modulates mitochondrial redox in vascular cell models of oxidative stress. The other two research articles and one review article provided important information related to energy metabolism in various organ systems. C. X. Li et al. reported that inhibition of aldose reductase accelerates liver regeneration by regulating energy metabolism and could serve as a therapeutic target. Using *Caenorhabditis elegans* as an experimental system, B. Dilberger et al. reported that mitochondrial oxidative stress impairs energy metabolism and reduces stress resistance and longevity. The authors further proposed that paraquat-treated *C. elegans* could be a readily accessible in vivo model for mitochondrial dysfunction as it displays the characteristics of oxidative stress, restricted energy metabolism, and reduced stress resistance and longevity. Lastly, the review article by S. Zhang et al. summarized the importance of adropin in the crosstalk between energy regulation and immune regulation.

Finally, this special issue also contains one basic and one clinical research study related to diabetes. L. Lyu et al. evaluated the relationship between leukocyte telomere length (LTL) and mitochondrial DNA copy number (mtDNAcn) in a noninterventional rural community of China with different glucose tolerance statuses. Based on their observation, the authors concluded that tumor necrosis factor-α (TNFα) may be considered a potential therapeutic target against aging-related disease in hyperglycemia, whereas H. Su et al. demonstrated that andrographolide exerted a glucose-lowering effect through strengthening the intestinal barrier function and increasing the microbial species of *A. muciniphila*. The authors of the latter study also suggested that it might be plausible to prevent type-2 diabetes by regulating gut barrier integrity and shaping intestinal microbiota composition.

In summary, we hope that readers find this special issue to be as interesting as it is important. The overarching goal of the review articles and original research manuscripts assembled herein is to advance the current knowledge of the mechanisms governing normal aging and the development and progression of age-related diseases by providing new insights into the role of mitochondrial oxidative stress and energy metabolism in aging and longevity.

Conflicts of Interest

The editors declare that they have no conflicts of interest regarding the publication of this special issue.

Acknowledgments

References

[1] M. Panel, B. Ghaleh, and D. Morin, "Mitochondria and aging: a role for the mitochondrial transition pore?," *Aging Cell*, vol. 17, no. 4, article e12793, 2018.

[2] N. Sun, R. J. Youle, and T. Finkel, "The mitochondrial basis of aging," *Molecular Cell*, vol. 61, no. 5, pp. 654–666, 2016.

[3] N. N. Wu, Y. Zhang, and J. Ren, "Mitophagy, mitochondrial dynamics, and homeostasis in cardiovascular aging," *Oxidative Medicine and Cellular Longevity*, vol. 2019, Article ID 9825061, 15 pages, 2019.

[4] P. V. S. Vasileiou, K. Evangelou, K. Vlasis et al., "Mitochondrial Homeostasis and Cellular Senescence," *Cells*, vol. 8, no. 7, p. 686, 2019.

[5] S. Srivastava, "The Mitochondrial Basis of Aging and Age-Related Disorders," *Genes (Basel)*, vol. 8, no. 12, p. 398, 2017.

[6] H. Cui, Y. Kong, and H. Zhang, "Oxidative stress, mitochondrial dysfunction, and aging," *Journal of Signal Transduction*, vol. 2012, Article ID 646354, 13 pages, 2012.

[7] M. Nita and A. Grzybowski, "The role of the reactive oxygen species and oxidative stress in the pathomechanism of the age-related ocular diseases and other pathologies of the anterior and posterior eye segments in adults," *Oxidative Medicine and Cellular Longevity*, vol. 2016, Article ID 3164734, 23 pages, 2016.

[8] A. Guillaumet-Adkins, Y. Yañez, M. D. Peris-Diaz, I. Calabria, C. Palanca-Ballester, and J. Sandoval, "Epigenetics and oxidative stress in aging," *Oxidative Medicine and Cellular Longevity*, vol. 2017, Article ID 9175806, 8 pages, 2017.

[9] S. Johnson and S. I. Imai, "NAD+ biosynthesis, aging, and disease," *F1000Research*, vol. 7, p. 132, 2018.

[10] L. Rajman, K. Chwalek, and D. A. Sinclair, "Therapeutic ootential of NAD-boosting molecules: the *in vivo* evidence," *Cell Metabolism*, vol. 27, no. 3, pp. 529–547, 2018.

Research Article

Andrographolide Exerts Antihyperglycemic Effect through Strengthening Intestinal Barrier Function and Increasing Microbial Composition of *Akkermansia muciniphila*

Hongming Su,[1] Jianling Mo,[2] Jingdan Ni,[2] Huihui Ke,[1] Tao Bao,[1] Jiahong Xie,[1] Yang Xu,[1] Lianghua Xie,[1] and Wei Chen [1,2,3]

[1]*Department of Food Science and Nutrition, National Engineering Laboratory of Intelligent Food Technology and Equipment, Zhejiang Key Laboratory for Agro-Food Processing, Zhejiang University, Hangzhou 310058, China*
[2]*Department of Traditional Chinese Medicine, Sir Run Run Shaw Hospital, School of Medcine, Zhejiang University, Hangzhou 310016, China*
[3]*Ningbo Research Institute, Zhejiang University, Ningbo 315100, China*

Correspondence should be addressed to Wei Chen; zjuchenwei@zju.edu.cn

Accumulating evidence indicates that type 2 diabetes (T2D) is associated with intestinal barrier dysfunction and dysbiosis, implying the potential targets for T2D therapeutics. Andrographolide was reported to have several beneficial effects on diabetes and its associated complications. However, the protective role of andrographolide, as well as its underlying mechanism against T2D, remains elusive. Herein, we reported that andrographolide enhanced intestinal barrier integrity in LPS-induced Caco-2 cells as indicated by the improvement of cell monolayer barrier permeability and upregulation of tight junction protein expression. In addition, andrographolide alleviated LPS-induced oxidative stress by preventing ROS and superoxide anion radical overproduction and reversing glutathione depletion. In line with the *in vitro* results, andrographolide reduced metabolic endotoxemia and strengthened gut barrier integrity in db/db diabetic mice. We also found that andrographolide appeared to ameliorate glucose intolerance and insulin resistance and attenuated diabetes-associated redox disturbance and inflammation. Furthermore, our results indicated that andrographolide modified gut microbiota composition as indicated by elevated Bacteroidetes/Firmicutes ratio, enriched microbial species of *Akkermansia muciniphila*, and increased SCFAs level. Taken together, this study demonstrated that andrographolide exerted a glucose-lowering effect through strengthening intestinal barrier function and increasing the microbial species of *A. muciniphila*, which illuminates a plausible approach to prevent T2D by regulating gut barrier integrity and shaping intestinal microbiota composition.

1. Introduction

Type 2 diabetes (T2D) is characterized by insulin resistance, glucose intolerance, and hyperglycemia [1]. The development and progression features of T2D among individuals can vary considerably as results of diverse genetic backgrounds and lifestyles. Although several antidiabetic treatment strategies have been recommended including pharmacological medications and lifestyle modifications (weight loss and exercise), the health benefits from these strategies are limited. Antidiabetic agents such as pioglitazone and acarbose are effective in pre-

venting diabetes [2]. However, the potential side-effect of those antidiabetic agents cannot be overlooked [3]. In the face with a large number of T2D populations, it is urgently needed to develop novel, safe, and effective antidiabetic medications.

Gut microbiota has been recognized to be implicated with whole-body glucose and lipid homeostasis [4]. The connection between the microbial community and the human body is linked and separated by the intestinal barrier. The intestinal barrier function could be disrupted under obesity and diabetes conditions, which contribute to the increased gut permeability, leading to a more readily translocation of

lipopolysaccharide (LPS) into the circulation [5]. LPS is confirmed to play a critical role in triggering systematic inflammation, which is also linked to the onset and development of insulin resistance [6]. Therefore, the intestinal epithelial barrier could be an alternative therapeutic target to prevent metabolic endotoxemia and thus provide metabolic benefits [7]. In addition, accumulating evidence implicates gut microbiota as a promising target for T2D therapeutics [8]. Recently, the species of *Akkermansia muciniphila*, a mucin-degradation and strictly anaerobic bacteria, has received considerable attention for its beneficial effect on metabolic disorders [9–11]. Multiple bioactive components such as metformin, cranberry extract, and dietary polyphenols are reported to confer metabolic benefits through changing the bacterial abundance of *A. muciniphila* [12–14]. Therefore, the investigation of potential candidate prebiotics, which could promote the growth of *A. muciniphila*, might provide possible strategies for the prevention and treatment of metabolic diseases including T2D.

Andrographolide is a diterpenoid lactone derived from *Andrographis paniculata* (Burm. F.) Nees [15]. This plant is widely distributed in Southeast Asia, such as China, India, and Thailand [16]. Andrographolide has been demonstrated to have a broad range of pharmacological activities such as anticancer, anti-inflammation, antiobesity, and anti-NAFLD [16–18]. Our previous studies have shown that andrographolide suppressed preadipocyte proliferation and inhibited hepatic carcinogenesis [15, 16]. Regarding the effect of andrographolide on diabetes, a previous study indicated the antihyperglycemic effect of andrographolide in streptozotocin- (STZ-) induced diabetic mice [19]. Andrographolide was also reported to attenuate postprandial hyperglycemia by inhibiting α-glucosidase and α-amylase enzyme activities [20]. However, whether andrographolide could enhance the gut epithelial barrier integrity or modulate the intestinal microbiota composition in diabetes remains unclear. Here, we established a colorectal cell monolayer barrier model to investigate the protective effect of andrographolide against LPS-induced disruption of monolayer barrier integrity and oxidative stress. Furthermore, the effect of andrographolide on gut barrier integrity and gut microbiota composition in a murine model of T2D was examined. Our results indicated that andrographolide prevented hyperglycemia through strengthening intestinal barrier function and increasing *A. muciniphila*.

2. Materials and Methods

2.1. Reagents. Dichlorodihydrofluorescein diacetate (DCFH-DA), dihydroethidium (DHE), lipopolysaccharide (LPS), and fluorescein-isothiocyanate- (FITC-) dextran (average MW 3,000-5,000) were purchased from Sigma-Aldrich (California, USA). Naphthalene-2,3-dicarboxal-dehyde (NDA) was obtained from Life Technologies (Carlsbad, CA, USA). SYBR Green PCR Master Mix was purchased from Roche (Basel, Switzerland). All other reagents used were of analytical grade.

2.2. Extraction and Purification of Andrographolide. The dry leaves of *A. paniculata* were mixed with 95% aqueous ethanol solution and then ultrasound extracted twice at 45°C for 1 h.

Then, the ethanol extracts were combined, filtered, and concentrated. The crude mixture was reextracted with petroleum ether twice and followed by ethyl acetate extraction. The residue was obtained after the evaporation of ethyl acetate portion and used for high-speed countercurrent chromatography (HSCCC, TBE-300A, Tauto Biotechnique Company, Shanghai, China) separation and HPLC (Dionex Ultimate 3000, Thermo Fisher Scientific, USA) analysis [21]. The purity of andrographolide was 98.8%.

The structure of andrographolide was identified by NMR. Andrographolide was dissolved in 0.5 mL of CD_3OD. The experiment was performed on a Bruker AVANCE™ III spectrometer (14.1 Tesla), with a Larmor frequency of 150 MHz for ^{13}C and 600 MHz for ^1H. ^1H NMR of andrographolide (CD_3OD, 600 MHz) is as follows: δ 6.86-6.88 (m, 1H), 5.03 (d, $J = 6.0$ Hz, 1H), 4.91 (d, $J = 6.0$ Hz, 1H), 4.69 (s, $J = 6.0$ Hz, 1H), 4.49 (dd, $J = 10.2$ Hz, 6.6 Hz, 1H), 4.18 (dd, $J = 10.2$ Hz, 1.8 Hz, 1H), 4.14 (d, $J = 10.8$ Hz, 1H), 3.38-3.44 (m, 2H), 2.57-2.68 (m, 2H), 2.43-2.47 (m, 1H), 2.03-2.08 (m, 1H), 1.94-1.96 (m, 1H), 1.84-1.89 (m, 2H), 1.80-1.83 (m, 2H), 1.36-1.43 (m, 1H), 1.30-1.35 (m, 2H), 1.24 (s, 3H), and 0.77 (s, 3H). ^{13}C NMR of andrographolide (CD_3OD, 150 MHz) is as follows: 172.6, 149.4, 148.8, 129.8, 109.2, 80.9, 76.1, 66.7, 65.0, 57.4, 56.3, 43.7, 40.0, 39.0, 38.1, 29.0, 25.7, 25.2, 23.4, and 15.5.

2.3. Cell Culture. Human Caco-2 cells were obtained from the Cell Bank of Type Culture Collection of Chinese Academy of Sciences (CBTCCCAS, Shanghai, China). Caco-2 cells were cultured in DMEM medium containing 10% fetal bovine serum, 100 IU/mL penicillin, and 100 μg/mL streptomycin in a humidified cell incubator with an atmosphere of 5% CO_2 at 37°C.

2.4. In Vitro Caco-2 Cell Monolayer Permeability Assay. Transepithelial electrical resistance (TEER) was determined using a Millicell-ERS-2 Volt-Ohm meter (Millipore) according to a previous report [22]. Briefly, Caco-2 cells (2×10^5) were seeded onto Transwell plates (0.4 μm pores; Corning, USA) for 21 days to reach confluence. After that, a Caco-2 monolayer grown on the apical side of Transwell plates was treated with andrographolide (2.5 and 5 μM), followed by treatment of LPS (10 μg/mL). The effect of andrographolide on the permeability of large molecular substances across the Caco-2 cell monolayer barrier was determined using FITC-dextran. After treatment, the medium in the basolateral and apical compartment was replaced with 1.5 mL DMEM or 0.5 mL DMEM containing FITC-dextran (1 mg/mL). After 2 h incubation, the concentration of FITC-dextran in the basolateral compartment was determined by a fluorescence microplate at a wavelength of 495 nm.

2.5. Fluorescence Microscopy. Reactive oxygen species (ROS), superoxide anion radicals (O_2^-), and glutathione (GSH) are determined according to previously described methods [23, 24]. Briefly, cells were seeded into 12-well plates a density of 6×10^4 cells/well for 24 h. Cells were treated with andrographolide (2.5 and 5 μM) for 24 h, followed by treating with LPS (10 μg/mL) for further 24 h. After incubating with 10 μM

DCFH-DA (for ROS labeling) or 10 μM DHE (for superoxide anion radical labeling) or 50 μM NDA (for GSH labeling) for 30 min, cells were washed with PBS twice and then immediately evaluated by fluorescence microscopy. The results from the fluorescence microscope were expressed as mean fluorescence intensity. The fluorescence intensity was analyzed by Image-Pro Plus 6.0 (Media Cybernetics, Inc.).

2.6. Real-Time Reverse Transcription-PCR. We followed the methods of Su et al. [25]. Total RNA was isolated from the caecal tissue using TRIzol (Invitrogen, CA, USA) and then pooled for the RT-PCR analysis. cDNA was synthesized using the PrimeScript RT Reagent Kit (TaKaRa, Japan) according to the manufacturer's instruction. Quantitative real-time PCR was carried out in the QuantStudio 3 Real-Time PCR System (Applied Biosystems, CA, USA). The primers used in this study are shown in Table S1.

2.7. Western Blot. Western blot analysis was performed as previously described [15]. Total protein fraction was extracted using RIPA Lysis Buffer (BOSTER Biological Technology Co. Ltd.) with the addition of Roche cOmplete™ Protease Inhibitor Cocktail. Protein was separated by electrophoresis on SDS-polyacrylamide gels and transferred to polyvinylidene fluoride (PVDF) membranes (Millipore, ISEQ00010). After blocking with 10% nonfat dry milk in PBS buffer containing 0.1% Tween-20 (PBST), the membrane was incubated with the primary antibody overnight at 4°C. After three washes, the membrane was incubated with horseradish peroxidase-conjugated secondary antibodies (Bio-Rad, 170-6515 and 170-6516, 1:1000) for 1 h. After three washes with PBST, the immunoreactive protein bands were visualized by Chemiluminescent HRP Substrate (Millipore, WBKLS0100). The following primary antibodies were used: Occludin (Abcam, ab216327, 1:1000), ZO-1 (Abcam, ab61357, 1:1000), and GAPDH (Abcam, ab181602, 1:10,000).

2.8. In Vivo Experimental Design. All animal experiments were conducted according to the guidelines and laws on the use and care of laboratory animals in China (GB/T 35892-2018 and GB/T 35823-2018). The animal experimental procedures were performed in the Animal Experiment Center of Zhejiang Chinese Medical University (Hangzhou, China). The animal protocol was approved by the laboratory animal management and ethics committee of Zhejiang Chinese Medical University (201610087). Male Lepr^db mutation (db/db) mice with C57BL/6J background, aged six weeks, were purchased from the Model Animal Research Center of Nanjing University (Nanjing, China). All mice have *ad libitum* access to autoclaved water and diet. The temperature in the cage was maintained with constant temperature (23°C) and humidity. After one week of acclimatization, the mice were divided into two groups: (1) db/db mice were orally administered with vehicle (normal saline (NS)/Tween-80 (25:1, *v/v*) ($n = 12$); (2) db/db mice were orally administered with 150 mg/kg per mice andrographolide (AG) ($n = 12$), according to a previous report [26]. Andrographolide was dissolved in normal NS/Tween-80 (25:1, *v/v*) by grinding with a mortar and pestle. After eight weeks' administration, the mice

were sacrificed under anesthesia using carbon dioxide, following 12 h fasting. Blood was collected by cardiac puncture and centrifuged at 5000 rpm for 10 min for serum collection. Caecal contents were collected immediately after euthanasia and preserved in sterilized tubes. Caecal contents, serum, and all of the tissues were snap-frozen and stored at -80°C.

2.9. Glucose Tolerance Test (GTT) and Insulin Tolerance Tests (ITT). GTT and ITT were determined as previously described [25]. At week 7, mice fasted for 12 h, and GTT was performed after 0.5 g/kg glucose was administered intraperitoneally. Blood glucose levels were measured from the tail before glucose administration and 15, 30, 60, 90, and 120 min after administration. ITT was performed after mice fasted for 6 h. Insulin (2 IU/kg) was administered intraperitoneally. Blood glucose levels were measured from the tail before insulin administration and 15, 30, 60, 90, and 120 min after the administration.

2.10. Biochemical Analysis. The blood samples were collected and centrifuged at 5000 rpm for 10 min, and then serum was collected for biochemical analysis. Triglyceride (TG), cholesterol, free fatty acids (FFAs), aspartate transaminase (AST), alanine aminotransferase (ALT), lactate dehydrogenase (LDH), and glucose were measured by the Hitachi automatic biochemistry analyzer. Serum insulin, LPS, and LPS-binding protein (LBP) were determined using ELISA kits according to the manufacturer's instructions (Elabscience, Wuhan, China).

2.11. Homeostasis Model Assessment-Insulin Resistance (HOMA-IR). The HOMA-IR index was calculated using the fasting values of glucose and insulin with the following formula: HOMA index = insulin (μU/mL) × glucose (mM)/22.5.

2.12. Fecal Microbiota Identification. We followed the methods as previously described [25]. The genomic DNA from fecal samples was extracted using the QIAamp DNA Stool Mini Kit (Qiagen, Germany) according to the manufacturer's instruction. 16S rRNA comprising V3-V4 regions was amplified using 16S universal primers. Amplicons were purified using the AxyPrep DNA Gel Extraction Kit (Axygen Biosciences, CA, USA). The purified amplicons were sequenced on the Illumina MiSeq platform. Raw sequences were analyzed and processed using the Quantitative Insights into the Microbial Ecology (QIIME) software package. All sequences were clustered into Operational Taxonomic Units (OTUs) with a 97% threshold by using UPARSE. The taxonomy of each 16S rRNA gene sequence was analyzed by UPARSE mapping to Greengene (default): V201305 for species annotation. The relative abundance of each bacterial taxa was analyzed. Heatmaps were drawn using the ggplot2 package of the R software (v.3.1.1).

2.13. Short-Chain Fatty Acids (SCFAs) Identification and Quantification. SCFA levels in fecal content were analyzed using gas chromatography on Agilent 6890 (Agilent Technologies, CA, USA) in comparison with known standards as previously described [14].

2.14. Statistical Analysis. Data are expressed as the mean ± SEM. Two-tailed Student's *t*-test was performed to evaluate

the significant differences between two groups. One-way analysis of variance (ANOVA) followed by Bonferroni's post hoc test was performed to evaluate the significant differences between multiple groups. Metastats analysis was used to determine the bacterial species with a statistically significant difference. $p < 0.05$ was considered to be a significant difference. The statistical analyses were performed using Graph-Pad Prism (V.7.0a, GraphPad Software, USA) and SPSS (Version 20.0).

3. Results

3.1. Andrographolide Attenuated LPS-Induced Disruption of Caco-2 Cell Monolayer Barrier Integrity. Andrographolide was extracted and purified from the dry leaves of *A. paniculata* using high-speed countercurrent chromatography (HSCCC) and HPLC techniques, with a purity of 98.8% (Figures 1(a)–1(e)). The structure of andrographolide identified by NMR (Figures 1(f)–1(h)). The final yield of andrographolide in dry leaves of *A. paniculata* was 400 mg/kg. Accumulating evidence indicates that lipopolysaccharide (LPS), a principal component originated from bacteria, poses damage to gut barrier integrity [27]. Therefore, we employed the LPS-induced Caco-2 cell monolayer barrier model to investigate the gut barrier function involved in metabolic endotoxemia according to previous reports [22, 28]. To evaluate the protective role of andrographolide on cell monolayer permeability *in vitro*, the TEER and FITC-dextran concentration in the Transwell plates were determined. As shown in Figure 2(a), LPS (10 μg/mL) treatment caused a significant reduction of TEER compared to the control, indicating the monolayer barrier permeability increased in Caco-2 cells upon LPS treatment. Andrographolide (2.5 μM and 5 μM) treatment significantly reversed LPS-induced TEER reduction compared with that in the LPS-treated group, indicating andrographolide improved monolayer barrier integrity. In line with the TEER results, we observed a significantly increased FITC-dextran concentration in LPS-induced cells, which indicated that large molecular substances were easier to pass through the LPS-induced Caco-2 cell monolayer barrier compared to the control (Figure 2(b)). However, andrographolide treatment significantly mitigated LPS-induced FITC-dextran fluorescence increase, indicating that andrographolide protected against LPS-induced intestinal monolayer barrier dysfunction. Since the monolayer barrier permeability was improved upon andrographolide treatment, we thus hypothesized that andrographolide reinforced intestinal barrier function through inducing tight junction protein expression. To test this possibility, we determined the effect of andrographolide on the expressions of tight junction protein including occluding (Ocln) and Zona occludin-1 (ZO-1). As anticipated, andrographolide treatment abolished LPS-induced reduction of occludin and ZO-1 protein expressions (Figures 2(c)–2(e)). Moreover, andrographolide treatment facilitated the upregulation of *Ocln* and *ZO-1* mRNA expressions compared with those in the LPS-induced cells (Figures 2(f) and 2(g)). Together, these results confirmed that andrographolide ameliorated LPS-

induced disruption of cell monolayer permeability by inducing tight junction proteins.

3.2. Andrographolide Prevented LPS-Induced Oxidative Stress in Caco-2 Cells. Increasing evidence indicates that metabolic endotoxemia is associated with oxidative stress [29, 30]. To uncover the protective effect of andrographolide against LPS-induced oxidative stress, we detected reactive oxygen species (ROS) using a fluorescence probe DCFH-DA. As shown in Figures 3(a) and 3(b), LPS (10 μg/mL) treatment contributed to a significant increase of DCF fluorescence intensity compared with that in control, indicating an excessive production of ROS. Andrographolide treatment dramatically inhibited LPS-induced ROS overproduction in Caco-2 cells compared with the LPS-induced group, suggesting andrographolide is capable of preventing LPS-induced ROS production. As superoxide anion radical (O_2^-) is a particular type of ROS, which may lead to the generation of highly oxidizing derivative hydroxyl radical (·OH), we next determined whether andrographolide suppressed LPS-induced superoxide anion radical production. As shown in Figures 3(c) and 3(d), superoxide anion radical was measured by a DHE fluorescence probe. The results exhibited that LPS treatment contributed to a significant increase of DHE fluorescence intensity in comparison with that in control. However, andrographolide treatment markedly reduced the DHE fluorescence intensity compared with that in LPS-induced cells, indicating andrographolide inhibited LPS-induced superoxide anion radical production in Caco-2 cells. Intracellular GSH level as an essential indicator reflects cellular redox status. Therefore, we determined the effect of LPS on intracellular GSH level in the presence or absence of andrographolide. Cellular GSH level was monitored by a fluorescence probe NDA. As shown in Figures 3(e) and 3(f), LPS treatment resulted in a pronounced decrease of NDA fluorescence intensity compared with that in control. However, andrographolide treatment attenuated the reduction of NDA fluorescence intensity triggered by LPS, indicating andrographolide recovered LPS-induced GSH depletion. Collectively, our results suggest that andrographolide alleviated LPS-induced oxidative stress by inhibiting ROS, superoxide anion radical overproduction, and preventing GSH depletion.

3.3. Andrographolide Ameliorated Glucose Intolerance and Insulin Resistance by Enhancing Gut Barrier Integrity in db/db Mice. Numerous studies have established the role of metabolic endotoxemia in the development of type 2 diabetes (T2D) [6], and the gut barrier integrity appeared to be disturbed in diabetic condition [31, 32]. To elucidate the protective role of andrographolide against T2D, we performed the glucose tolerance test (GTT) and insulin tolerance test (ITT) in db/db mice orally treated with andrographolide (150 mg/kg per mice) or vehicle for 8 weeks. Metformin, a widely used antidiabetic agent, was used as a positive control. The area under the curve (AUC) of GTT and ITT was calculated. Our results showed that andrographolide significantly improved glucose tolerance and insulin tolerance in db/db diabetic mice compared with those in control (Figures 4(a)–4(d)), which was similar to the results of
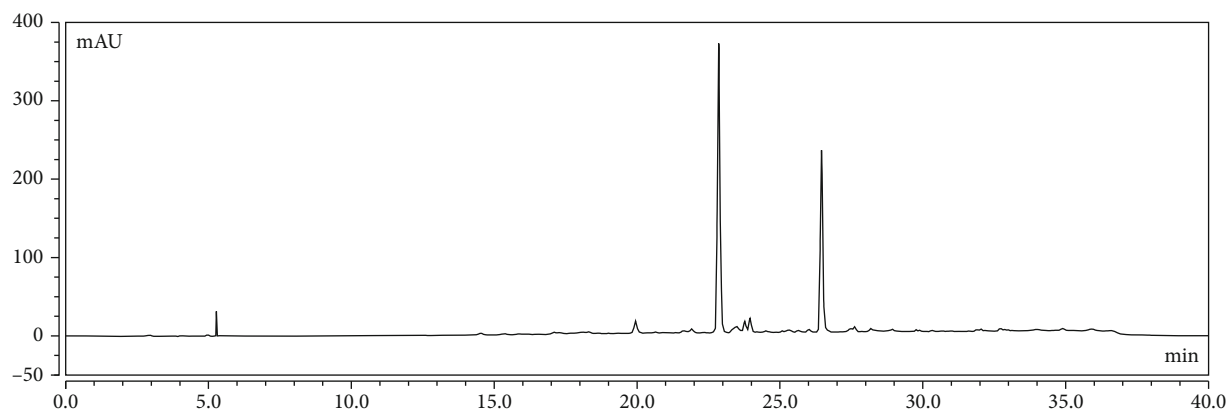
(a)
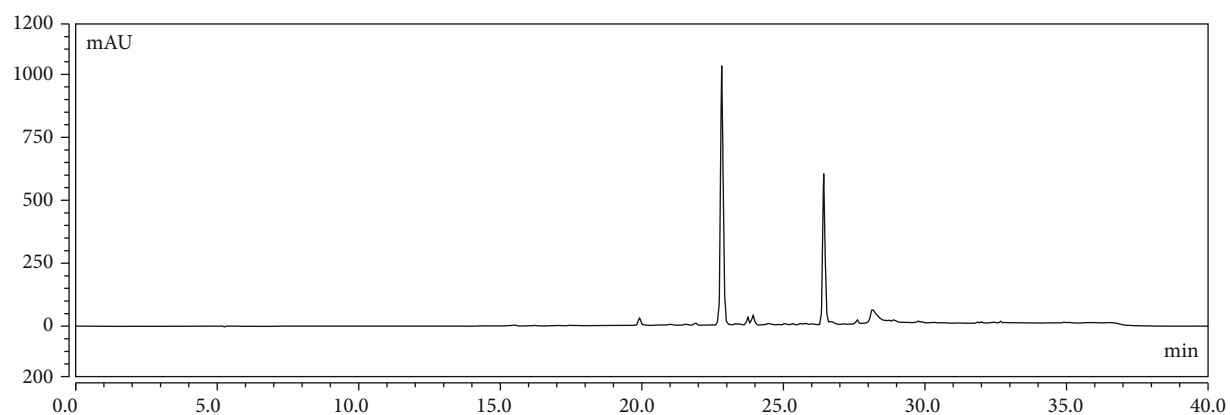
(b)
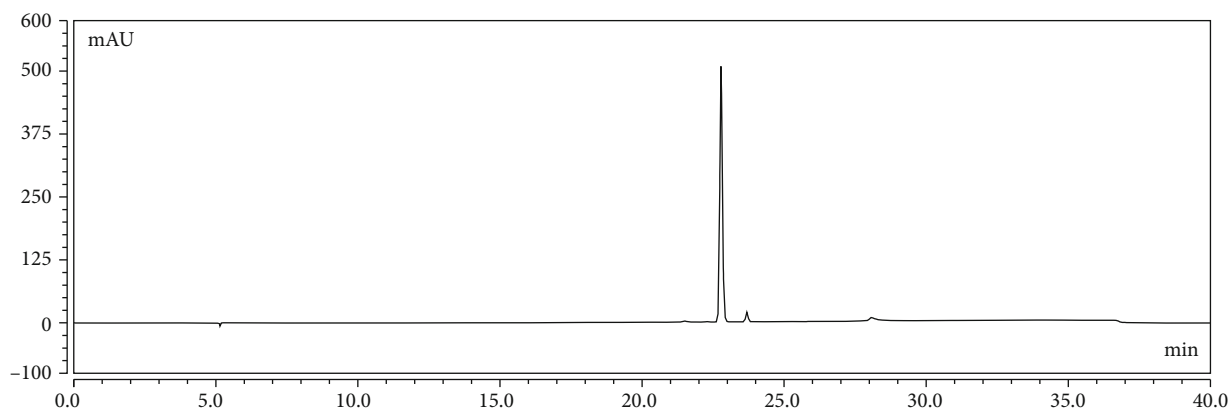
(c)

Figure 1: Continued.

(d)

(e)

(f)

(g)
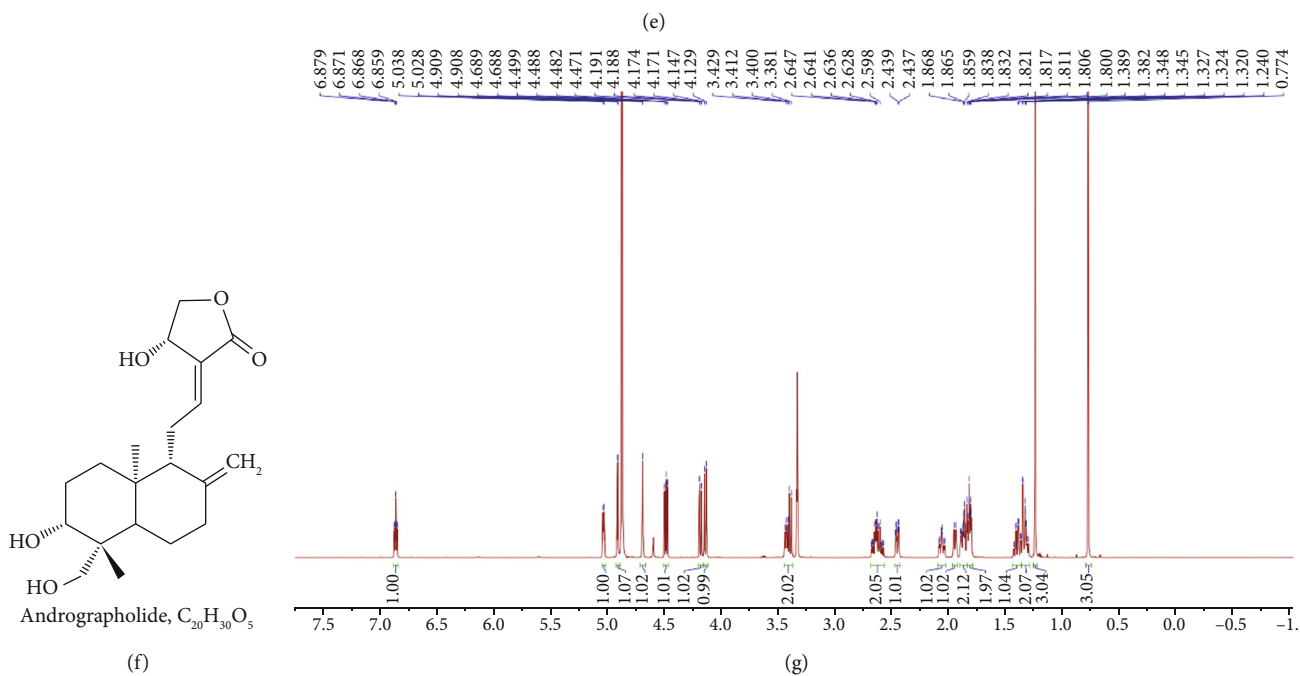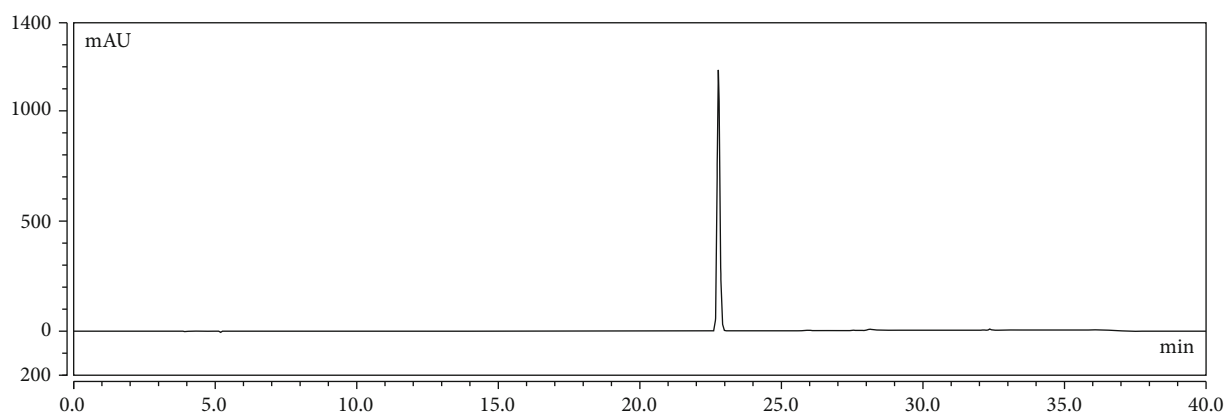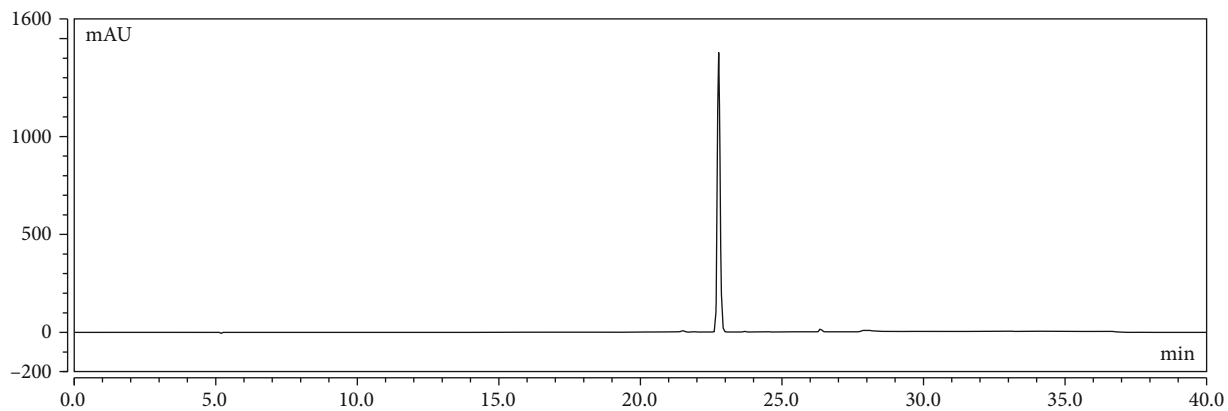
Figure 1: Continued.
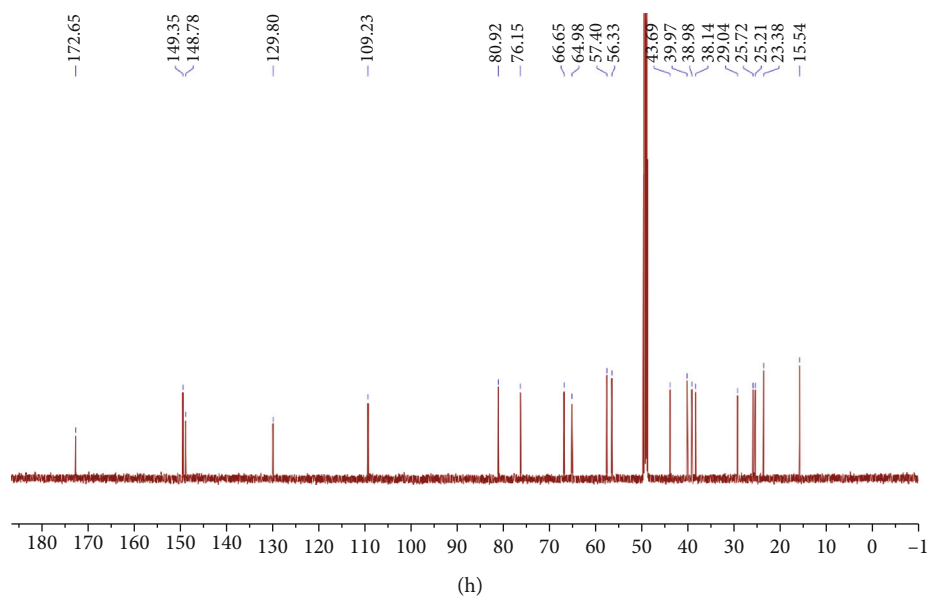
Figure 1: Purification and identification of andrographolide from *A. paniculata*. (a) The crude mixture was reextracted with petroleum ether twice and followed by ethyl acetate extraction. The ethyl acetate portion was analyzed by HPLC at 254 nm. (b) The fraction of 75-88 min in HSCCC separation was analyzed by HPLC at 254 nm. (c) The fraction of 75-88 min in HSCCC separation was evaporated and then washed with the solvent of ethyl acetate/methanol/water (1 : 2 : 4, *v/v/v*). (d) The andrographolide was isolated and was analyzed by HPLC at 254 nm. (e) HPLC analysis of the andrographolide of chromatographic grade at 254 nm. (f) Chemical structure of andrographolide. NMR spectrums of andrographolide, (g) ^{1}H NMR of andrographolide, and (h) ^{13}C NMR of andrographolide.

metformin treatment (200 mg/kg per mice). In addition, fasting insulin level and HOMA-IR index significantly reduced after 8 weeks of andrographolide treatment (Figures 4(e) and 4(f)), which was in accordance with metformin treatment, suggesting andrographolide prevents insulin resistance in diabetic mice. However, andrographolide treatment did not influence daily food intake between groups (Figure 4(g)), indicating andrographolide did not change the appetite of mice. These results suggest that andrographolide ameliorates glucose intolerance and insulin resistance in db/db diabetic mice.

Since the *in vitro* results showed that andrographolide attenuated LPS-induced monolayer barrier dysfunction in Caco-2 cells, we speculated that andrographolide could improve intestinal barrier function in db/db mice. To examine the effect of andrographolide on metabolic endotoxemia, we determined the serum LPS and LPS-binding protein (LBP) levels. As shown in Figures 4(h) and 4(i), andrographolide administration contributed to a significant increase of LPS and LBP levels compared to the control, indicating the reduction of endotoxemia. To ascertain the effect of andrographolide on gut barrier integrity, we determined the relative gene expression of *Ocln* and *ZO-1*. Andrographolide administration led to the upregulation of *Ocln* and *ZO-1* mRNA expression compared with those in control (Figures 4(j) and 4(k)), indicating andrographolide improved the gut barrier integrity. Given that mucin 2 (*Muc2*) have a beneficial role in the gut barrier [33], we determined *Muc2* gene expression. Our study displayed that andrographolide significantly increased *Muc2* gene expression compared with that in control (Figure 4(l)). Toll-like receptor 2 (*Tlr2*) was reported to regulate tight junction proteins [34]. Hence, we

investigated whether andrographolide could activate *Tlr2*. As shown in Figure 4(m), *Tlr2* expression was significantly increased upon andrographolide administration compared to the control. In addition, cannabinoid receptor 1 (*Cnr1*) activation was confirmed to increase intestinal permeability, whereas blocking *Cnr1* reduced gut permeability [35]. However, in the present study, the expression of *Cnr1* was not influenced by andrographolide administration (Figure 4(n)). To further investigate the protective role of andrographolide on intestinal barrier function, we determined the intestinal expression of glucose transporter 2 (*Glut2*), as a recent study reported that hyperglycemia drives the intestinal barrier dysfunction through Glut2-dependent mechanism [31]. We observed that *Glut2* gene expression was slightly decreased with no significant difference in andrographolide-treated mice compared to the control (Figure 4(o)). Altogether, these data suggest that andrographolide enhanced gut barrier function might through activating Tlr2.

3.4. Andrographolide Improved Serum Biochemical Profiles. To investigate the effect of andrographolide on serum biochemical profile, we determined serum triglyceride (TG) (Figure S1 (A)), cholesterol (Figure S1(B)), and free fatty acids (FFAs) (Figure S1 (C)). After 8 weeks' andrographolide treatment, serum TG, cholesterol, and FFAs significantly reduced on db/db diabetic mice compared with those in control. In addition, andrographolide administration contributed to a significant decrease of AST (Figure S1 (D)), ALT (Figure S1 (E)), and LDH (Figure S1 (F)) compared with those in control, suggesting andrographolide could improve hepatic function. These results indicate andrographolide improves serum biochemical profiles in db/db mice.

(a)

(b)

(c)

(d)

(e)

(f)

(g)
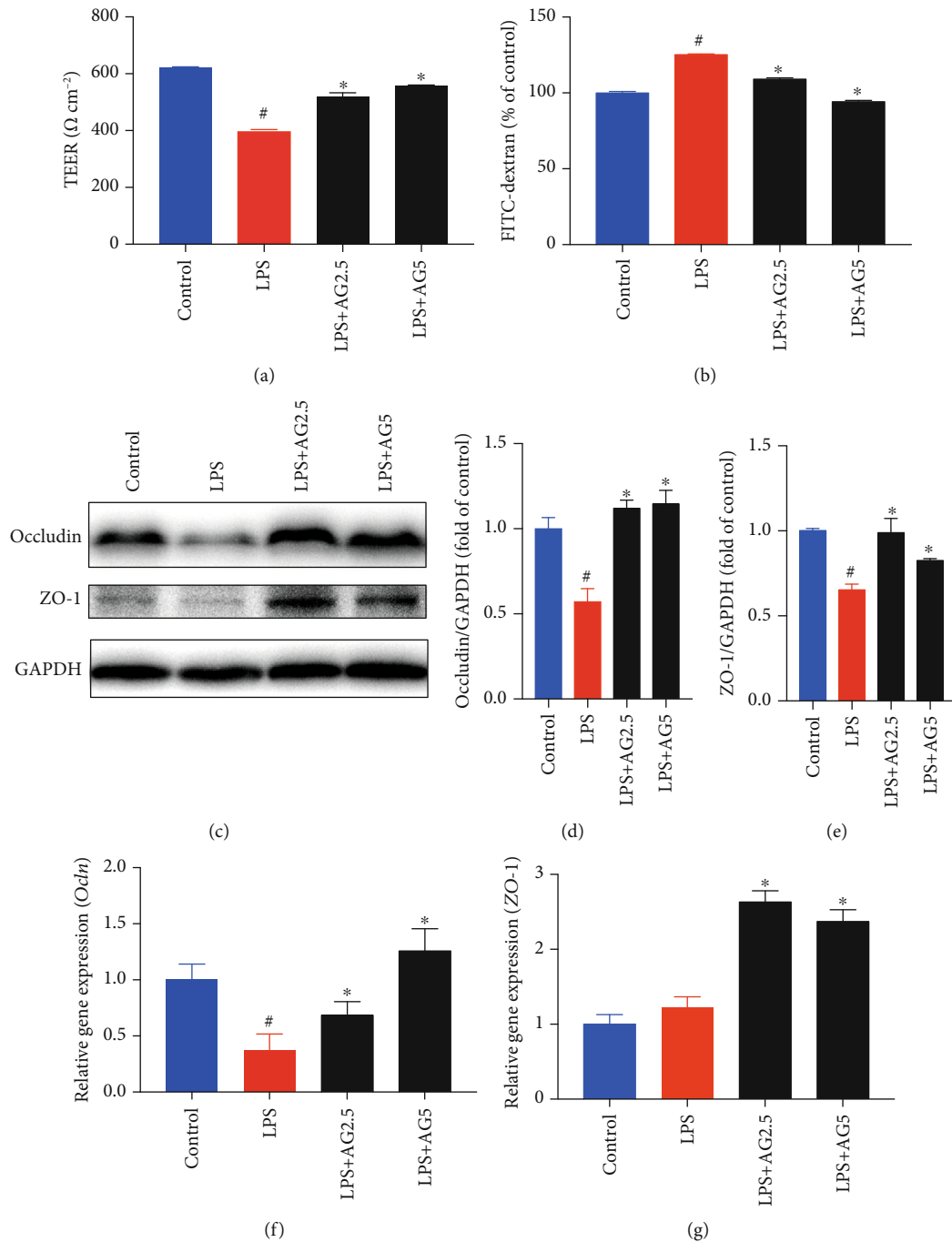
Figure 2: Andrographolide improved LPS-induced disruption of the intestinal barrier in Caco-2 cells. (a) Effect of andrographolide on TEER in LPS-induced Caco-2 cells. The Caco-2 cells were seeded in Transwell cell plates and cultured for 21 days to form a cell monolayer. Then, the cells were treated with andrographolide (2.5 and 5 μM) for 24 h, followed by the treatment of LPS (10 μg/mL) for a further 24 h. The TEER value was measured using a Millicell-ERS-2 Volt-Ohm meter (Millipore). (b) Effect of andrographolide on FITC-dextran concentration. The Caco-2 cells in Transwell cell plates were treated with andrographolide (2.5 and 5 μM) for 24 h, followed by the treatment of LPS (10 μg/mL) for a further 24 h. After treatment, the medium in the apical compartment was replaced with fresh DMEM containing FITC-dextran (1 mg/mL). After 2 h incubation, the medium from the basolateral compartment was subjected to spectrofluorometric measurement. (c–e) Immunoblot analysis of Occludin and ZO-1 protein expression from LPS-induced Caco-2 cells in the presence and absence of andrographolide (2.5 and 5 μM) for 24 h. The protein bands were subjected to densitometric analysis using ImageJ. Relative mRNA expression of (f) *Ocln* and (g) *ZO-1* were determined by RT-PCR. Data represent means $\pm$ SEM ($n = 3$), [#]$p < 0.05$ versus the control group, $*p < 0.05$ versus the LPS group.

(a)

(b)

(c)

(d)

(e)

(f)
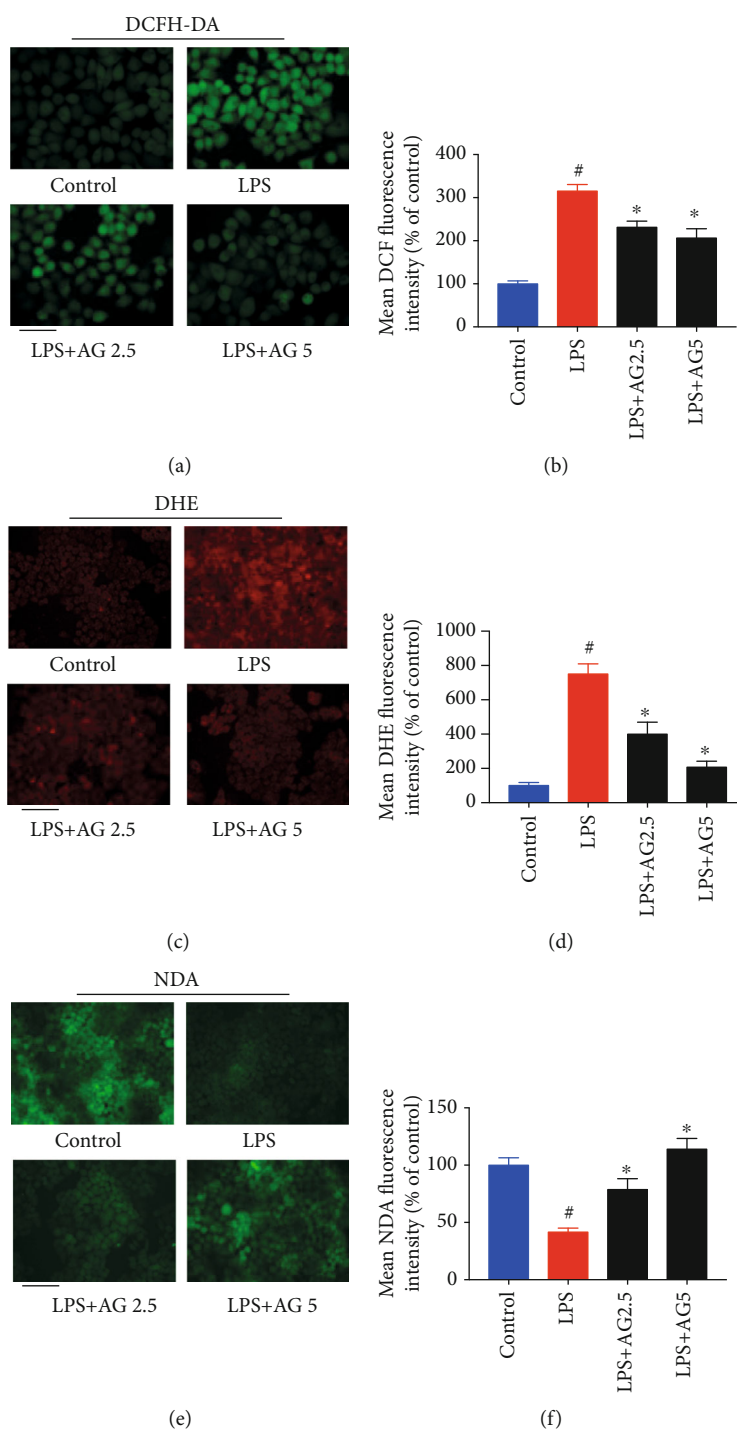
FIGURE 3: Andrographolide prevented LPS-induced oxidative stress. (a) Effect of andrographolide on LPS-induced ROS production. The Caco-2 cells were pretreated with andrographolide (2.5 and $5\,\mu$M) for 24 h, followed by the treatment of LPS ($10\,\mu$g/mL) for a further 24 h. After that, the medium was removed and incubated with $10\,\mu$M of DCFH-DA for 30 min, and then cells were evaluated by fluorescence microscopy. The scale bar represents $25\,\mu$m. (b) The quantitative data of panel (a), and results were expressed as mean DCF fluorescence intensity ($n = 6$). (c) Effect of andrographolide on LPS-induced superoxide anion radical production. After treatment, cells were collected and incubated with $10\,\mu$M of DHE for 30 min, and then cells were evaluated by fluorescence microscopy. The scale bar represents $50\,\mu$m. (d) The quantitative data of panel (c), and results were expressed as mean DHE fluorescence intensity ($n = 6$). (e) Effect of andrographolide on GSH content in LPS-induced Caco-2 cells. After treatment, cells were collected and incubated with $50\,\mu$M of NDA for 30 min, and then cells were evaluated by fluorescence microscopy. The scale bar represents $50\,\mu$m. (f) The quantitative data of panel (e), and results were expressed as mean NDA fluorescence intensity ($n = 6$). Data represent means $\pm$ SEM ($n = 6$), $^{\#}p < 0.05$ versus control group, $*p < 0.05$ versus the LPS group.

(a)

(b)

(c)

(d)

(e)

(f)

(g)

(h)

(i)

(j)

(k)

(l)

(m)

(n)

(o)
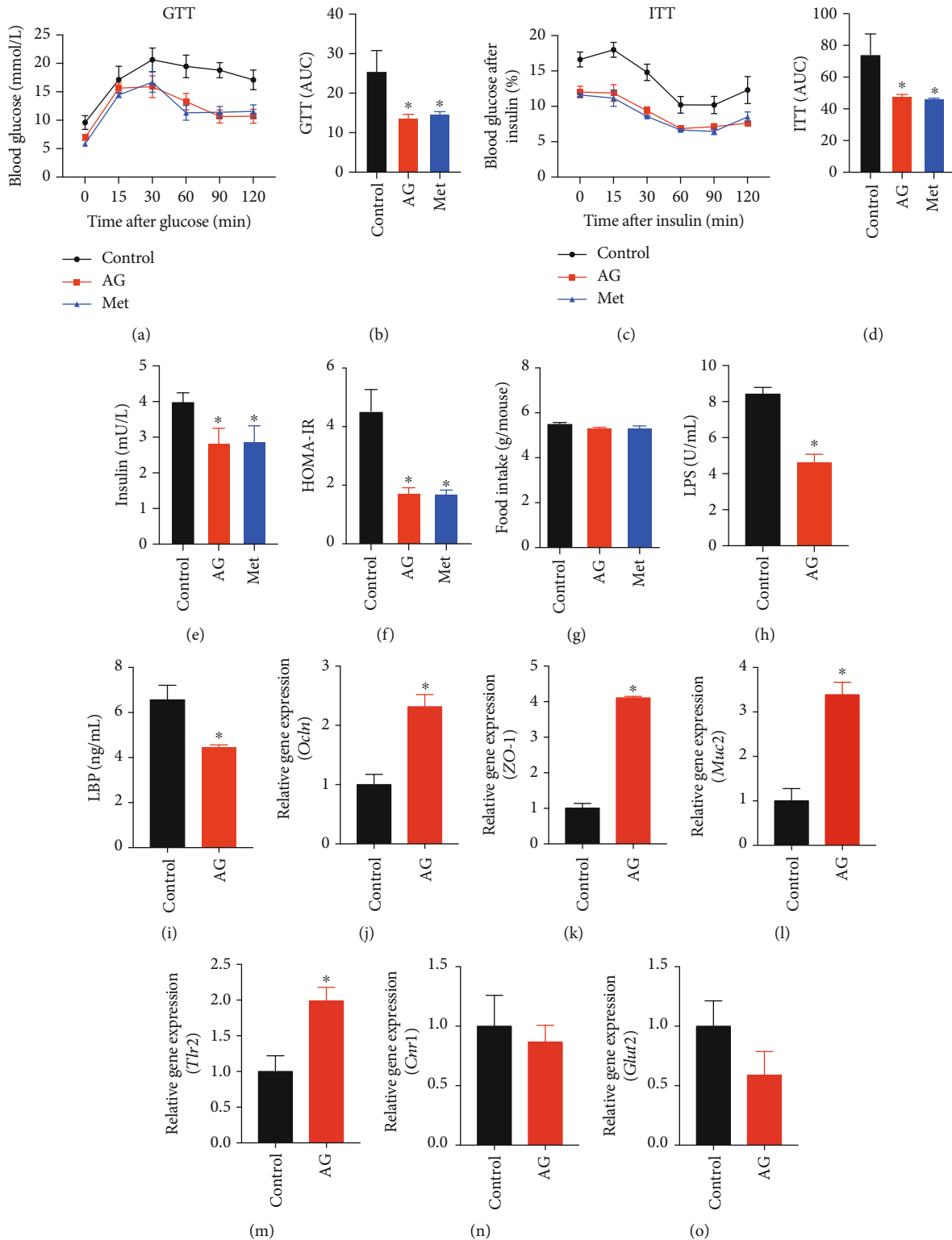
FIGURE 4: Andrographolide ameliorated glucose intolerance and insulin resistance by enhancing gut barrier integrity. 12 db/db mice were treated daily with vehicle, and 12 db/db mice were treated daily with andrographolide (150 mg/kg per day) or metformin (200 mg/kg per day) for 8 weeks by oral gavage. (a) At the eighth week, glucose tolerance test (GTT) was performed. (b) The area under the curve (AUC) of GTT was calculated. (c) Insulin tolerance test was performed at the end of the eighth week. (d) The AUC of ITT was calculated. (e) The serum insulin level and (f) HOMA-IR index were determined. (h) Serum LPS and (i) LBP were determined by the ELISA assay. The relative gene expression of (j) *Ocln*, (k) *ZO-1*, (l) *Muc2*, (m) *Tlr2*, (n) *Cnr1*, and (o) *Glut2* were determined. Control: db/db mice administered with vehicle; AG: db/db mice administered with 150 mg/kg andrographolide; Met: db/db mice administered with 200 mg/kg metformin. Data represent means ± SEM ($n = 12$), ∗$p < 0.05$ versus the control group.

(a)

(b)

(c)
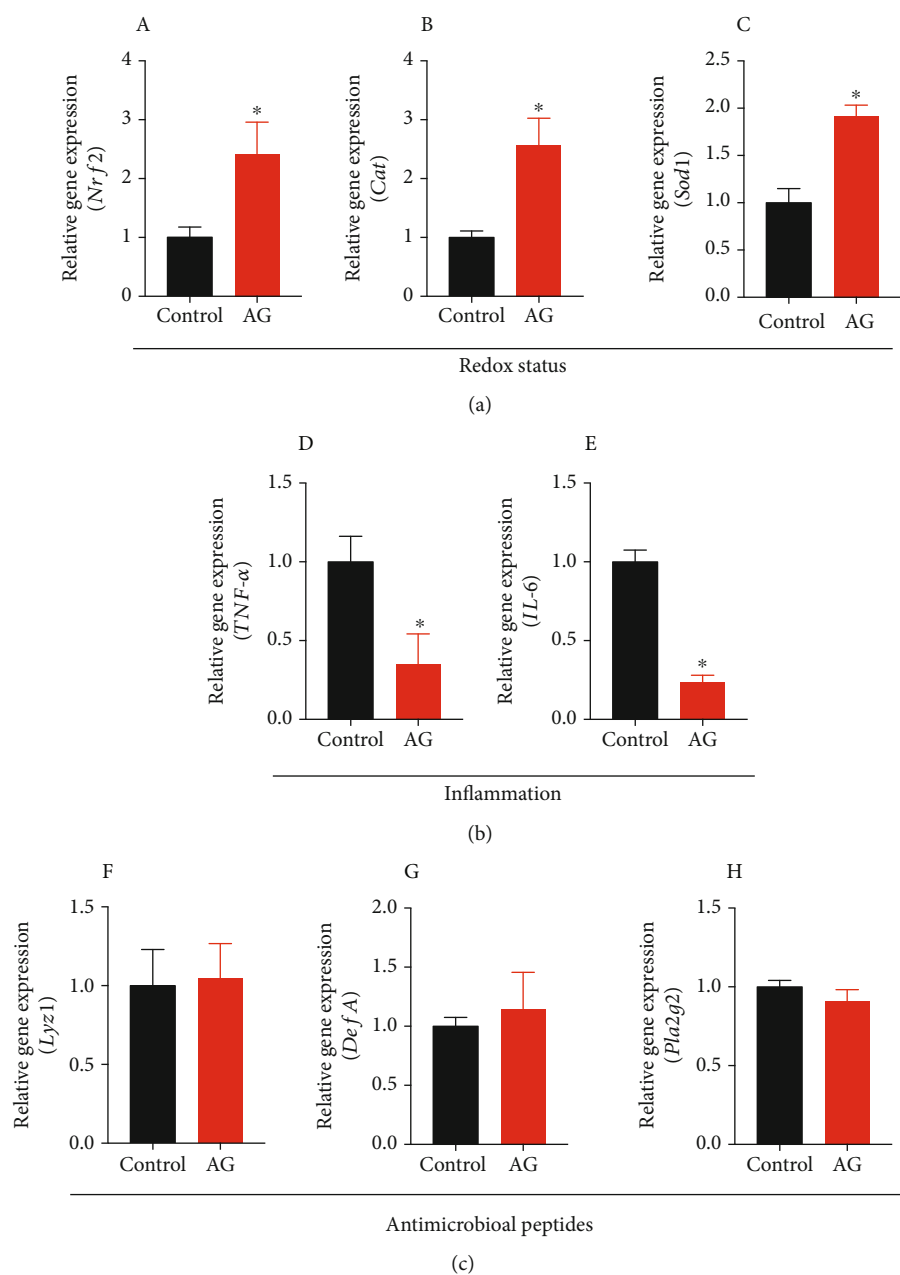
FIGURE 5: Andrographolide attenuated diabetes-associated redox disturbance and inflammation. (a) The relative gene expression from caecal tissue corresponding to redox status (A) *Nrf2*, (B) *Cat*, and (C) *Sod1* was determined. (b) The relative gene expression of inflammatory factors from caecal tissue including (D) *TNF-α* and (E) *IL-6* were determined. (c) The relative gene expression of the antimicrobial peptides from caecal tissue including (F) *Lyz1*, (G) *DefA*, and (H) *Pla2g2* was determined. Control: db/db mice administered with vehicle; AG: db/db mice administered with 150 mg/kg andrographolide. Data represent means $\pm$ SEM ($n = 6$), $*p < 0.05$ versus the control group.

3.5. Andrographolide Improved Intestinal Redox Status and Inflammatory Response.

To further investigate the effect of andrographolide on intestinal redox status, we determined the relative gene expressions of nuclear factor- (erythroid-derived 2) like 2 (*Nrf2*), catalase (*Cat*), and superoxide dismutase 1 (*Sod1*), which play critical roles in maintaining redox balance. We found that andrographolide significantly increased the relative gene expressions of *Nrf2*, *Cat*, and *Sod1* compared with those in control (Figures 5(a)–5(c)), indicating andrographolide attenuates diabetes-associated oxidative stress. To examine the role of andrographolide on

intestinal epithelial inflammation, we determined the relative gene expressions of tumor necrosis factor-*α* (TNF-*α*) and interleukin 6 (IL-6). Our study showed that the gene expressions of TNF-*α* and IL-6 were significantly decreased by andrographolide treatment (Figures 5(d) and 5(e)). Given that antimicrobial peptides play a crucial role in maintaining intestinal barrier function, redox status, and inflammation [36], we determined *Lyz1* (encoding for Lysosome-1), *DefA* (encoding defensin), and *Pla2g2* (encoding phospholipase A2 group-II) expressions (Figures 5(f)–5(h)). However, andrographolide had no significant impact on *Lyz1*, *DefA*,

(a)   (b)   (c)   (d)

(e)   (f)

(g)   (h)
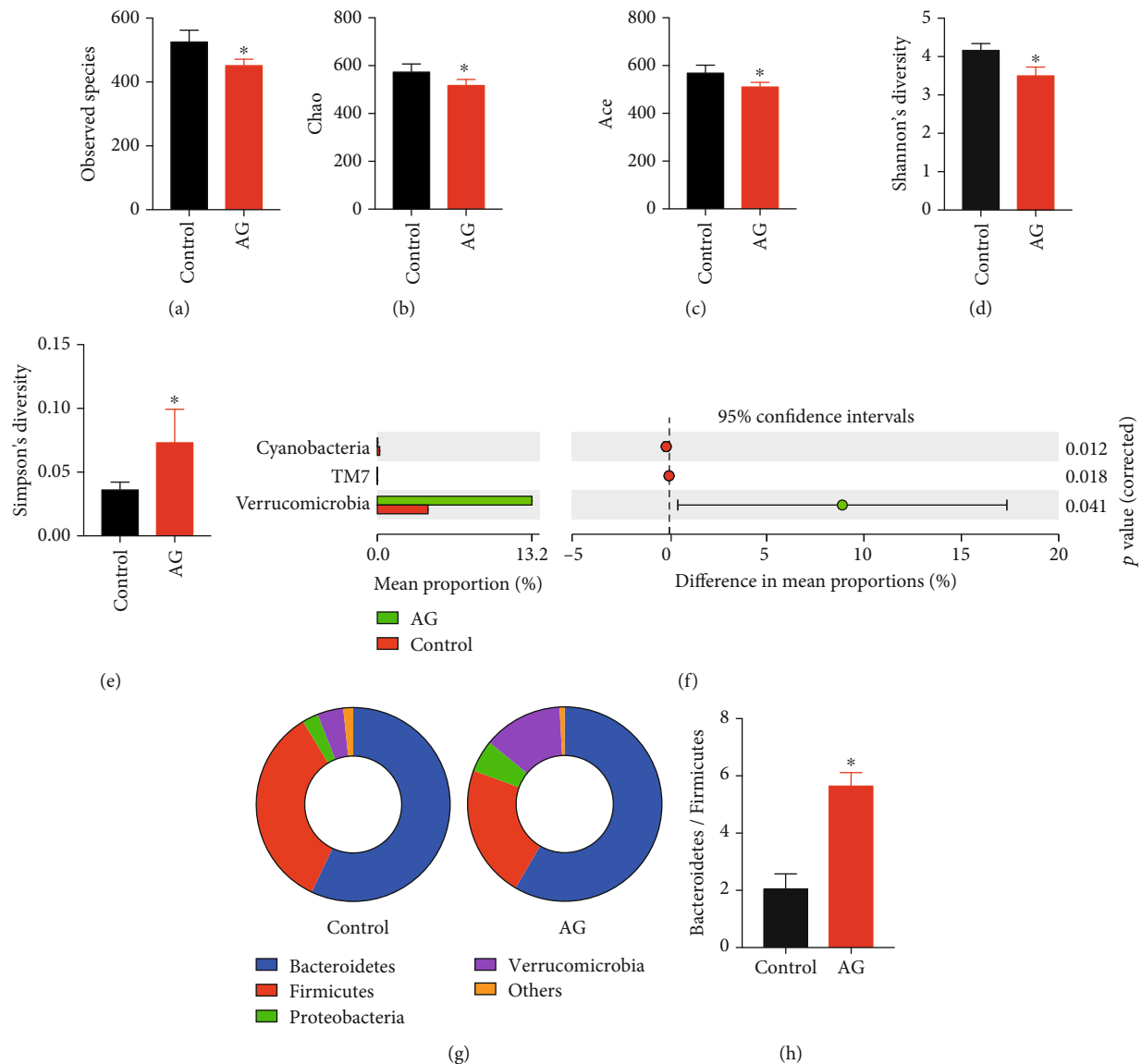
FIGURE 6: Andrographolide modulated gut microbiota composition. (a) Observed species, (b) Chao, (c) Ace, (d) Shannon's diversity, and (e) Simpson's diversity were obtained by analyzing 16S rDNA sequencing. (f) Statistical comparisons of gut bacterial profiles at the phylum level. (g, h) The Bacteroidetes/Firmicutes ratio was calculated. Control: db/db mice administered with vehicle; AG: db/db mice administered with 150 mg/kg andrographolide. Data represent means ± SEM ($n = 6$), $*p < 0.05$ versus the control group.

and *Pla2g2* gene expressions. Together, our study suggests that andrographolide improves diabetes-associated intestinal redox imbalance and inflammation without affecting antimicrobial peptides expression.

3.6. Andrographolide Modified the Gut Microbiota Composition and Increased the Bacterial Species of a. Muciniphila. Gut microbiota can directly contact with the intestinal barrier and thereby exert its beneficial or detrimental impact on host health [7]. Although our study has shown that andrographolide improved gut barrier function both *in vivo* and *in vitro*, we cannot exclude the potential action of gut microbiota on host metabolic health. To further elucidate the potential involvement of gut microbiota on diabetes, we identified the caecal microbial composition using 16S rRNA sequencing. Beta-diversity analysis indicated that the observed

species in the andrographolide-treated group was lower than that in the control group, suggesting a reduced enrichment of gut microbiota (Figure 6(a)). In addition, andrographolide caused reduced parameters of Chao, Ace, and Shannon's diversity compared with those in control (Figures 6(b)–6(d)). Simpson's diversity in andrographolide-treated group was higher than that in the control group (Figure 6(e)). To ascertain the enrichment alteration of specific gut microbiota in each taxa level, the OTUs were annotated, and their relative abundance was computed. As shown in Figure 6(f), andrographolide treatment resulted in a significant enrichment of *Verrucomicrobia* at the phylum level, whereas *TM7* and *Cyanobacteria* were significantly reduced compared with those in control. The increased abundance of Bacteroidetes/Firmicutes was associated with a beneficial effect on glucose metabolism [37]. In the present study, we observed an

(a)

(b)

Figure 7: Continued.

(c)
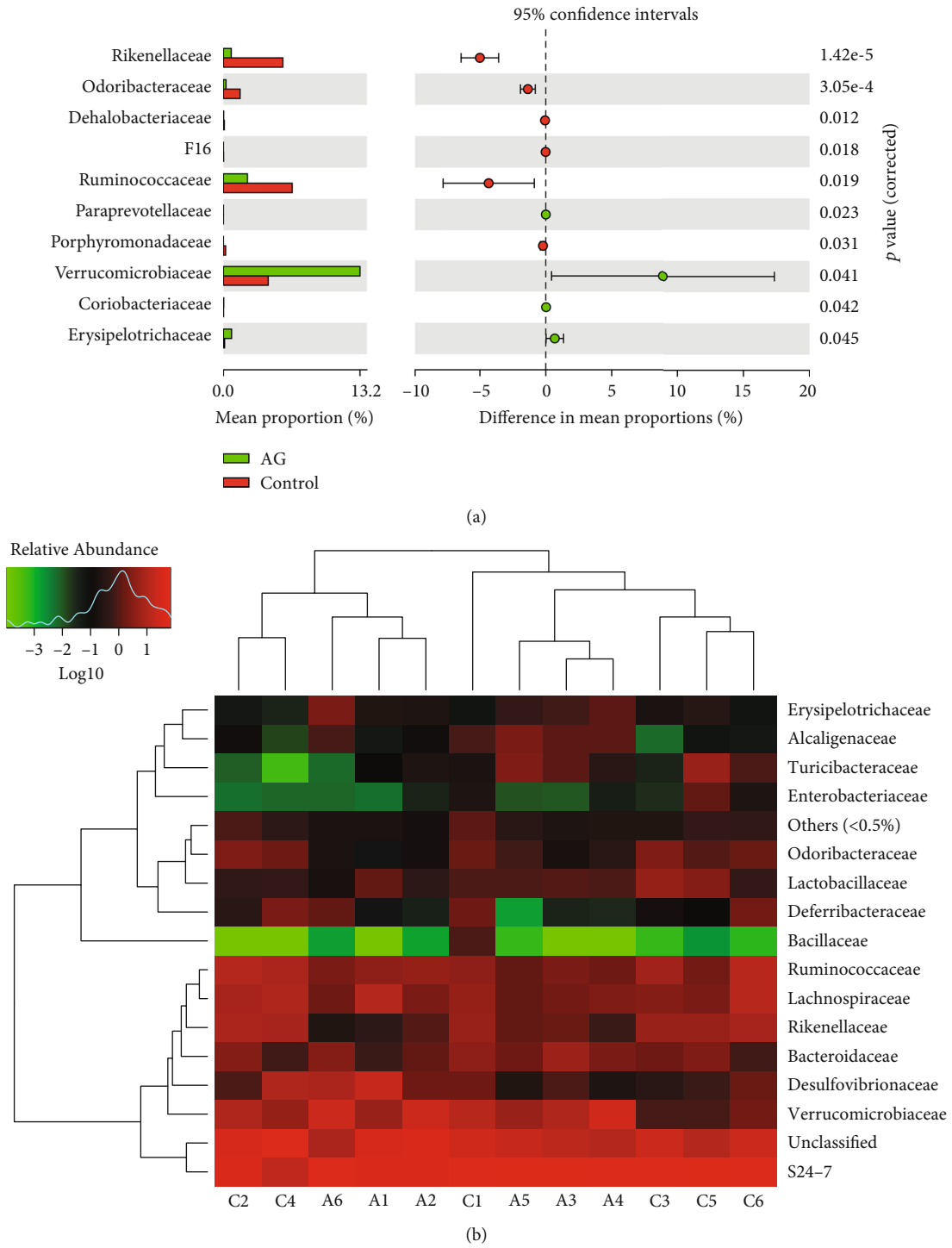
(d)

Figure 7: Continued.

(e)

(f)
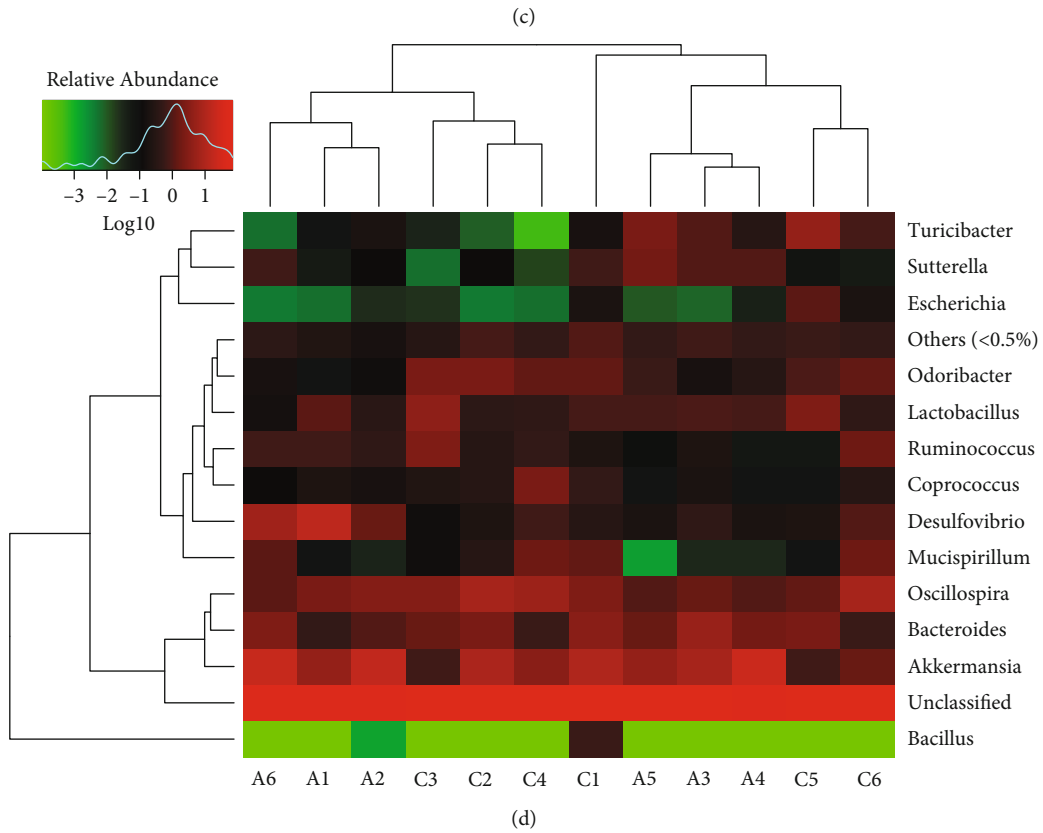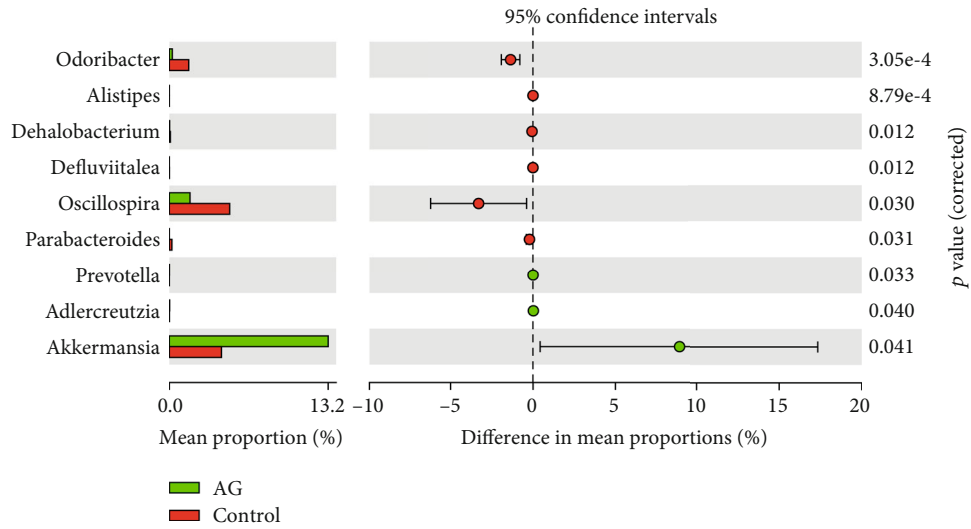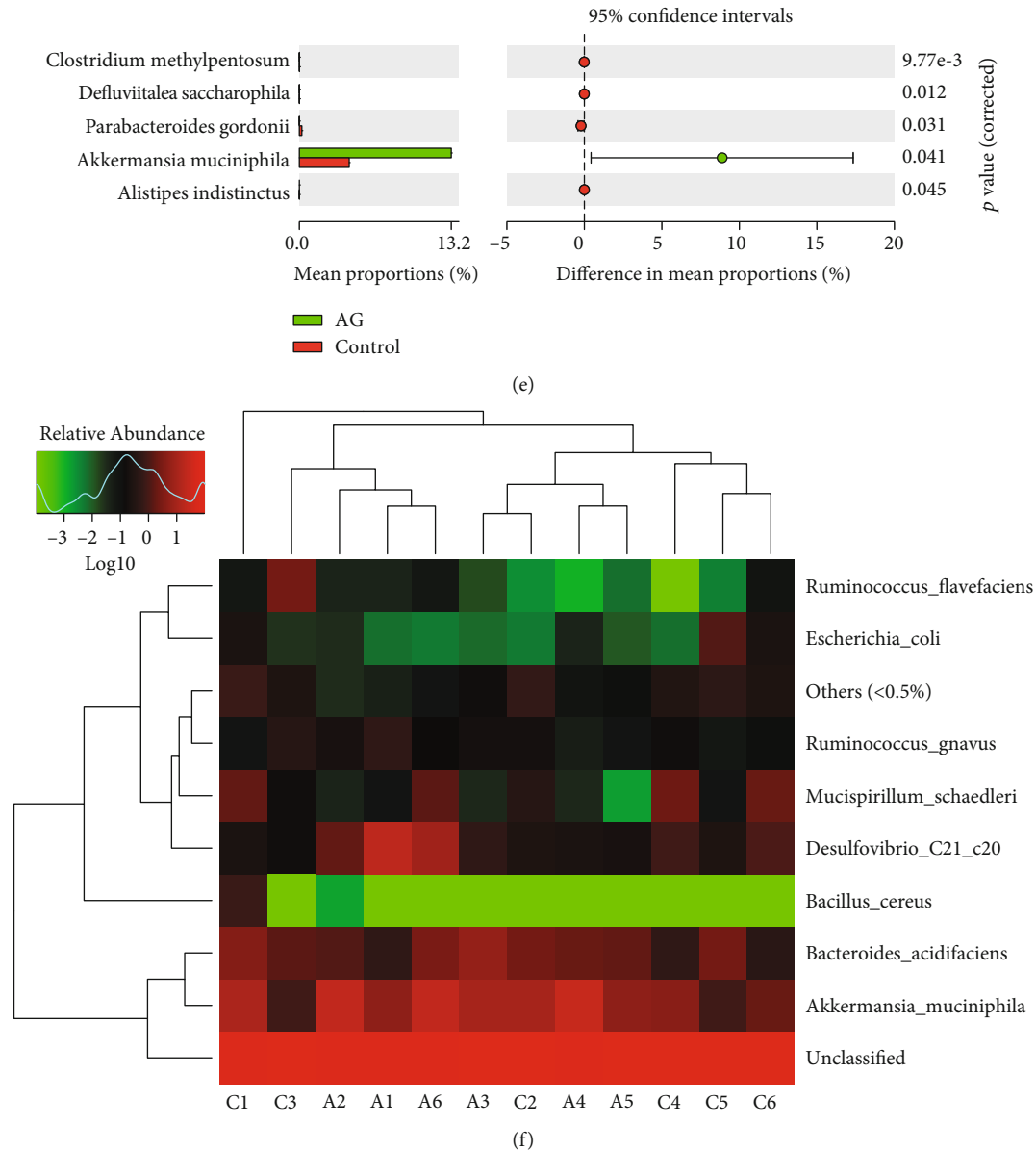
FIGURE 7: Andrographolide promoted the growth of *Akkermansia muciniphila*. (a) Statistical comparisons of gut bacterial profiles at the family level. (b) Heatmap of gut bacterial profiles at the family level. (c) Statistical comparisons of gut bacterial profiles at the genus level. (d) Heatmap of gut bacterial profiles at the genus level. (e) Statistical comparisons of gut bacterial profiles at the species level. (f) Heatmap of gut bacterial profiles at the species level. Control: db/db mice administered with vehicle; AG: db/db mice administered with 150 mg/kg andrographolide. Data represent means ± SEM ($n = 6$), $*p < 0.05$ versus the control group.

increased ratio of Bacteroidetes/Firmicutes (Figures 6(g) and 6(h)), suggesting the beneficial effect andrographolide on modulating gut microbiota composition. The heatmap shown in Figure S2 indicates the overall enrichment of gut microbiota in each group.

To further distinguish the differences of microbial community between the control and andrographolide-treated mice, the gut microbiota composition at family, genus, and species levels was specified. As shown in Figures 7(a) and 7(b), andrographolide treatment contributed to a significant enrichment of Verrucomicrobiaceae, Porphyromonadaceae, Coriobacteriaceae, and Erysipelotrichaceae at the family level, whereas Rikenellaceae, Odiribacteraceae, and Ruminococca-

ceae reduced. At the genus level, andrographolide increased the levels of *Akkermansia*, *Prevotella*, and *Adlercreutzia* and decreased the levels of *Odoribacter*, *Alistipes*, *Dehalobacterium*, *Defluviitalae*, *Oscillospira*, and *Parabacteroides* (Figures 7(c) and 7(d)). Interestingly, we observed that a beneficial bacterial species of *A. muciniphila* was significantly enriched in andrographolide-treated mice (Figures 7(e) and 7(f)). Together, these results suggest that andrographolide might provide metabolic benefits by shaping the microbiota composition and promoting the growth of *A. muciniphila*.

3.7. Andrographolide Increased Fecal Short-Chain Fatty Acids (SCFAs). SCFAs have been proposed to play a critical role on
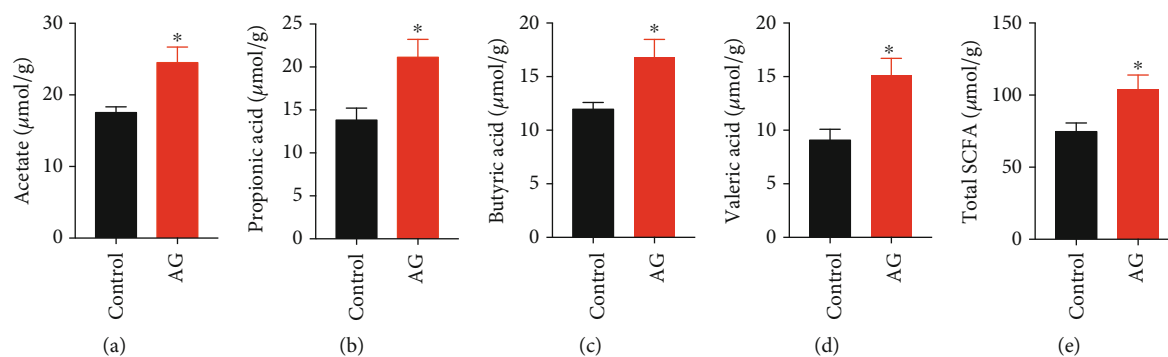
FIGURE 8: Andrographolide improved the short-chain fatty acids (SCFAs) composition. (a) acetate, (b) propionic acid, (c) butyric acid, and (d) valeric acid were measured in fecal samples by gas chromatography (GC) in comparison with known standards. (e) Total SCFAs were the sum of each amount of individual fatty acids. Control: db/db mice administered with vehicle; AG: db/db mice administered with 150 mg/kg andrographolide. Data represent means ± SEM ($n = 6$), $*p < 0.05$ versus the control group.

the maintenance of the intestinal barrier [38]. Therefore, we determined the fecal concentration of SCFAs, including acetic acid, propionic acid, butyric acid, and n-valeric acid by gas chromatography. As expected, we found that andrographolide significantly increased the fecal concentration of total SCFAs, particularly acetic acid, propionic acid, and butyric acid in diabetic mice (Figures 8(a)–8(e)). Those results suggest an involvement of SCFAs on the protective action of andrographolide against leaky gut.

4. Discussion

Previous studies have confirmed the usefulness of andrographolide in preventing diabetes and its associated metabolic disorders through regulating multiple pathways. For example, andrographolide was reported to prevent diabetes-associated cognitive deficits [39]. In addition, andrographolide not only ameliorated diabetic nephropathy by inhibiting hyperglycemia-induced renal oxidative stress and inflammation via the Akt/NF-κB pathway [40] but also attenuated diabetic retinopathy by inhibiting retinal angiogenesis and inflammation [41]. Andrographolide derived from *Andrographis paniculata* (Burm. F.) Nees exhibited profound antidiabetic promise [42], suggesting its potential preclinical and clinical application on preventing diabetes. Although the hypoglycemic effect of andrographolide has been reported long before [19, 43], its underlying mechanism is still largely unknown. Yu et al. indicated that andrographolide reduced the plasma glucose level in streptozotocin- (STZ-) induced diabetic mice through an increase of glucose utilization. The increase of GLUT4 gene expression was considered as one of the mechanisms of andrographolide [19]. Zhang et al. indicated that the andrographolide-lipoic acid conjugate (AL-1) prevented diabetes in alloxan-treated diabetic mouse model by protecting beta cell mass, preserving insulin-secreting function, and stimulating GLUT4 translocation [43]. Moreover, andrographolide was reported to prevent postprandial hyperglycemia by inhibiting α-glucosidase activity [20]. In the present study, we unveiled a novel mechanism that andrographolide ameliorated insulin resistance and glucose intolerance through reinforcement of the intestinal barrier function and modulation of the gut microbiota composition.

The intestinal barrier plays a critical role in making digested food components selectively absorbed. The increased intestinal barrier permeability may lead to a more readily permeation of xenobiotics or microbe-derived small molecules such as LPS [25, 27]. The increase of circulating LPS results in systemic inflammation and insulin resistance [6]. Accordingly, the gut barrier plays pivotal roles in maintaining host metabolic health. Tight junction proteins including occludin and ZO-1 constitute the wall between gut epithelial cells. Previous studies demonstrated that deficiency of tight junction protein might increase intestinal permeability [44], which led to the translocation of LPS into blood, suggesting an important connection between tight junction protein and inflammation. Andrographolide derivative was found to ameliorate dextran sulfate sodium-induced colitis by suppressing inflammation in mice [45], suggesting the potential protective role of andrographolide on gut barrier. However, little information is available concerning the direct role of andrographolide on intestinal barrier permeability.

In the present study, our results revealed that andrographolide restored LPS-induced disruption of monolayer barrier permeability *in vitro* as indicated by increased TEER and reduced FITC-dextran concentration. In addition, this study demonstrated that andrographolide strengthened the intestinal barrier integrity by inducing occludin and ZO-1. In consistence with the *in vitro* results, andrographolide displayed a profound protective role in enhancing gut barrier function by increasing the intestinal gene expression of occludin and ZO-1 in diabetic mice. Antimicrobial peptides produced by the host play crucial roles in maintaining gut microbiota homeostasis and gut barrier function [36]. However, andrographolide had no impact on *Lyz1*, *DefA*, and *Pla2g2* expressions, suggesting antimicrobial peptides were not involved in the protective action of andrographolide on gut barrier integrity. SCFAs including acetate, butyrate, and propionate, which are produced by bacterial fermentation, are the dominant SCFAs in the large intestine [27, 36]. SCFAs mediated several beneficial effects on host metabolic health. The reduction of SCFAs is associated with weakened tight junctions and permeability [46]. Andrographolide treatment increased total SCFAs, particularly acetic acid, propionic acid, butyric acid, and valeric acid levels, suggesting SCFAs are
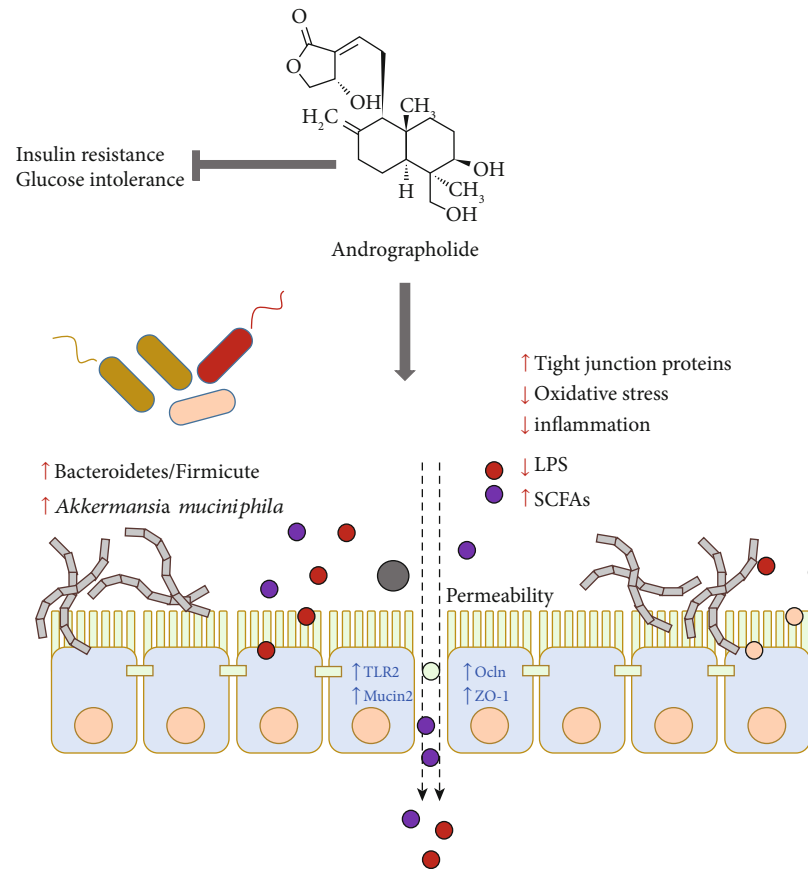
FIGURE 9: Brief summary of the mechanism of andrographolide on diabetes. This study demonstrated that andrographolide ameliorated glucose intolerance and insulin resistance in db/db diabetic mice. Andrographolide exerted glucose-lowering effect through strengthening intestinal barrier function and increasing microbial composition of *A. muciniphila*, which illuminates a plausible approach to ameliorate T2D.

involved in andrographolide's beneficial effects on gut barrier function. Collectively, our results suggest that andrographolide provides metabolic benefits partially through the enhancement of intestinal barrier function by inducing tight junction proteins and promoting SCFAs.

Previous studies reveal that endotoxemia triggers cellular oxidative stress. The disrupted redox balance is responsible for the initiation and progression of inflammation [29, 30]. Andrographolide was found to inhibit TNF-α-induced ROS generation and GSH content depletion [24]. We demonstrated that andrographolide prevented LPS-induced oxidative stress by scavenging excessive ROS and superoxide anion radicals, as well as restoring GSH depletion in Caco-2 cells. A large number of evidences confirmed the critical role of Nrf2, a transcriptional factor regulating cellular redox homeostasis [47]. Activation of Nrf2 contributes to the upregulation of its target genes involved in the antioxidant signaling pathway. *In vivo* study confirmed that andrographolide promoted the expressions of *Nrf2*, *Cat*, and *Sod1*, suggesting andrographolide confers antioxidant defense against diabetes-associated oxidative stress. In addition, andrographolide alleviated inflammatory responses as indicated by the downregulation of IL-6 and TNF-α. It is possible that the decreased oxidative stress and inflammation might be extrapolated from the reinforced intestinal barrier by andrographolide.

Numerous studies indicate the association of intestinal microbiota with T2D [25, 48]. Structural modulation of gut microbiota is a putative strategy for the alleviation of T2D. In the present study, we performed Illumina sequencing of the V3 and V4 regions of the 16S rRNA gene and identified the taxonomic composition of caecal microbiota from andrographolide and vehicle-treated mice. We found the gut microbiota of andrographolide-treated mice were strikingly distinct from the control mice, implying the possible involvement of gut microbiota in preventing diabetes. Increasing evidence confirmed that increased abundance of Bacteroidetes/Firmicutes was associated with decreased glucose level and reduced insulin resistance [37]. As anticipated, andrographolide treatment exhibited an increased ratio of Bacteroidetes/Firmicutes. Of note, we found a microbial species of *A. muciniphila* was significantly enriched in andrographolide-treated mice. *A. muciniphila*, a Gram-positive strictly anaerobic bacterium, resides in intestinal mucosa showed great capability on the maintenance of host lipid and glucose homeostasis [9]. Recently, several natural products that promote the growth of *A. muciniphila* have been found, such as metformin, cranberry extract, and grape polyphenols [12–14]. The purified membrane proteins derived from *A. muciniphila* exerted its beneficial effects on diabetes and obesity [33], suggesting that *A. muciniphila* could be a potential bacterial target for antidiabetic drug development. Interestingly, in the present study, we also observed the

phenomena that andrographolide increased the abundance of *A. muciniphila* in diabetic mice. Therefore, these results reveal that andrographolide prevents T2D in db/db mice presumably through increasing the Bacteroidetes/Firmicutes ratio and promoting the abundance *A. muciniphila*.

5. Conclusion

In the present study, we aimed at investigating the protective effect of andrographolide derived from *A. paniculata* against T2D through regulating gut barrier integrity and gut microbiota composition. This study uncovers that andrographolide appears to attenuate insulin resistance and glucose intolerance in db/db mice through enhancing gut barrier integrity, elevating Bacteroidetes/Firmicutes ratio, and promoting the species abundance of *A. muciniphila*. In addition, andrographolide improved diabetes-associated redox disturbance and inflammation. The antidiabetic action of the mechanism of andrographolide is summarized in Figure 9. Those results illuminate a plausible approach to prevent T2D through regulating gut barrier integrity and modulating gut microbiota composition, which shed a novel insight that andrographolide may represent a promising agent in the prevention and treatment of T2D. Our results also suggest beneficial roles of andrographolide against oxidative stress and intestinal dysbiosis.

Abbreviations

T2D:	Type 2 diabetes
AG:	Andrographolide
HSCCC:	High-speed counter-current chromatography
TEER:	Transepithelial electrical resistance
FITC-dextran:	Fluorescein-isothiocyanate-dextran
Ocln:	Occludin
ZO-1:	Zonula occludens-1
ROS:	Reactive oxygen species
DCFH-DA:	Dichlorodihydrofluorescein diacetate
DHE:	Dihydroethidium
NDA:	Naphthalene-2,3-dicarboxal-dehyde
GSH:	Glutathione
GTT:	Glucose tolerance test
ITT:	Insulin tolerance test
AUC:	Area under the curve
HOMA-IR:	Homeostasis model assessment of insulin resistance
LPS:	Lipopolysaccharide
LBP:	LPS-binding protein
Muc2:	Mucin 2
Tlr2:	Toll-like receptor 2
Cnr1:	Cannabinoid receptor 1
Glut2:	Glucose transporter 2
FFAs:	Free fatty acids
AST:	Aspartate transaminase
ALT:	Alanine aminotransferase
LDH:	Lactate dehydrogenase
Nrf2:	Nuclear factor- (erythroid-derived 2) like 2
Cat:	Catalase
Sod1:	Superoxide dismutase 1
SCFAs:	Short-chain fatty acids
TNF-α:	Tumor necrosis factor-α
IL-6:	Interleukin-6
Lyz1:	Lysosome-1
DefA:	Defensin A
Pla2g2:	Phospholipase A2 group-II.

Data Availability

The data used to support the findings of this study are available from the corresponding author upon request.

Conflicts of Interest

The authors declare that they have no conflicts of interest.

Acknowledgments

Supplementary Materials

Table S1: primers used for quantitative RT-PCR. Figure S1: andrographolide improved serum biochemical profiles. (A) Serum triglyceride, (B) cholesterol, (C) FFAs, (D) AST, (E) ALT, and (F) LDH levels were determined. Control: db/db mice administered with vehicle; AG: db/db mice administered with 150 mg/kg andrographolide. Data represent means ± SEM ($n = 12$), *$p < 0.05$ versus the control group. Figure S2: heatmap of gut bacterial profiles. OUT annotation of gut microbiota with significant difference between control (C) and andrographolide (A) groups. Control: db/db mice administered with vehicle; AG: db/db mice administered with 150 mg/kg andrographolide, $n = 6$, *$p < 0.05$ versus the control group. *(Supplementary materials)*

References

[1] R. A. DeFronzo, E. Ferrannini, L. Groop et al., "Type 2 diabetes mellitus," *Nature Reviews. Disease Primers*, vol. 1, no. 1, 2015.

[2] American Diabetes Association, "5. Prevention or delay of type 2 Diabetes:Standards of medical care in diabetes-2018," *Diabetes Care*, vol. 41, Supplement 1, pp. S51–S54, 2017.

[3] N. A. Calcutt, M. E. Cooper, T. S. Kern, and A. M. Schmidt, "Therapies for hyperglycaemia-induced diabetic complications: from animal models to clinical trials," *Nature Reviews. Drug Discovery*, vol. 8, no. 5, pp. 417–430, 2009.

[4] C. L. Gentile and T. L. Weir, "The gut microbiota at the intersection of diet and human health," *Science*, vol. 362, no. 6416, pp. 776–780, 2018.

[5] J. R. Turner, "Intestinal mucosal barrier function in health and disease," *Nature Reviews. Immunology*, vol. 9, no. 11, pp. 799–809, 2009.

[6] P. D. Cani, R. Bibiloni, C. Knauf et al., "Changes in gut microbiota control metabolic endotoxemia-induced inflammation in high-fat diet-induced obesity and diabetes in mice," *Gastroenterology*, vol. 57, no. 6, pp. 1470–1481, 2008.

[7] M. A. Odenwald and J. R. Turner, "The intestinal epithelial barrier: a therapeutic target?," *Nature Reviews. Gastroenterology & Hepatology*, vol. 14, no. 1, pp. 9–21, 2017.

[8] L. Zhao, F. Zhang, X. Ding et al., "Gut bacteria selectively promoted by dietary fibers alleviate type 2 diabetes," *Science*, vol. 359, no. 6380, pp. 1151–1156, 2018.

[9] A. Everard, C. Belzer, L. Geurts et al., "Cross-talk between Akkermansia muciniphila and intestinal epithelium controls diet-induced obesity," *Proceedings of the National Academy of Sciences of the United States of America*, vol. 110, no. 22, pp. 9066–9071, 2013.

[10] R. L. Greer, X. Dong, A. C. F. Moraes et al., "_Akkermansia muciniphila_ mediates negative effects of IFN γ on glucose metabolism," *Nature Communications*, vol. 7, no. 1, 2016.

[11] A. Hanninen, R. Toivonen, S. Poysti et al., "Akkermansia muciniphila induces gut microbiota remodelling and controls islet autoimmunity in NOD mice," *Gut*, vol. 67, no. 8, pp. 1445–1453, 2018.

[12] D. E. Roopchand, R. N. Carmody, P. Kuhn et al., "Dietary polyphenols promote growth of the gut BacteriumAkkermansia muciniphilaand attenuate high-fat diet-induced metabolic syndrome," *Gastroenterology*, vol. 64, no. 8, pp. 2847–2858, 2015.

[13] F. F. Anhe, D. Roy, G. Pilon et al., "A polyphenol-rich cranberry extract protects from diet-induced obesity, insulin resistance and intestinal inflammation in association with increased Akkermansia spp. population in the gut microbiota of mice," *Gut*, vol. 64, no. 6, pp. 872–883, 2015.

[14] H. Wu, E. Esteve, V. Tremaroli et al., "Metformin alters the gut microbiome of individuals with treatment-naive type 2 diabetes, contributing to the therapeutic effects of the drug," *Nature Medicine*, vol. 23, no. 7, pp. 850–858, 2017.

[15] W. Chen, H. Su, L. Feng, and X. Zheng, "Andrographolide suppresses preadipocytes proliferation through glutathione antioxidant systems abrogation," *Life Sciences*, vol. 156, pp. 21–29, 2016.

[16] W. Chen, L. Feng, H. Nie, and X. Zheng, "Andrographolide induces autophagic cell death in human liver cancer cells through cyclophilin D-mediated mitochondrial permeability transition pore," *Carcinogenesis*, vol. 33, no. 11, pp. 2190–2198, 2012.

[17] E. Toppo, S. S. Darvin, S. Esakkimuthu et al., "Effect of two andrographolide derivatives on cellular and rodent models of non-alcoholic fatty liver disease," *Biomedicine & Pharmacotherapy*, vol. 95, pp. 402–411, 2017.

[18] M. T. Islam, E. S. Ali, S. J. Uddin et al., "Andrographolide, a diterpene lactone from _Andrographis paniculata_ and its therapeutic promises in cancer," *Cancer Letters*, vol. 420, pp. 129–145, 2018.

[19] B. C. Yu, C. R. Hung, W. C. Chen, and J. T. Cheng, "Antihyperglycemic effect of andrographolide in streptozotocin-induced diabetic rats," *Planta Medica*, vol. 69, no. 12, pp. 1075–1079, 2003.

[20] R. Subramanian, M. Z. Asmawi, and A. Sadikun, "In vitro alpha-glucosidase and alpha-amylase enzyme inhibitory effects of Andrographis paniculata extract and andrographolide," *Acta Biochimica Polonica*, vol. 55, no. 2, pp. 391–398, 2008.

[21] D. Wu, X. Cao, and S. Wu, "Overlapping elution-extrusion counter-current chromatography: a novel method for efficient purification of natural cytotoxic andrographolides from Andrographis paniculata," *Journal of Chromatography. A*, vol. 1223, pp. 53–63, 2012.

[22] H. Guo, Y. Xu, W. Huang et al., "Kuwanon G preserves LPS-induced disruption of gut epithelial barrier in vitro," *Molecules*, vol. 21, no. 11, p. 1597, 2016.

[23] H. Su, Y. Li, D. Hu et al., "Procyanidin B2 ameliorates free fatty acids-induced hepatic steatosis through regulating TFEB-mediated lysosomal pathway and redox state," *Free Radical Biology & Medicine*, vol. 126, pp. 269–286, 2018.

[24] C. Y. Lu, Y. C. Yang, C. C. Li, K. L. Liu, C. K. Lii, and H. W. Chen, "Andrographolide inhibits TNFalpha-induced ICAM-1 expression via suppression of NADPH oxidase activation and induction of HO-1 and GCLM expression through the PI3K/Akt/Nrf2 and PI3K/Akt/AP-1 pathways in human endothelial cells," *Biochemical Pharmacology*, vol. 91, no. 1, pp. 40–50, 2014.

[25] H. Su, L. Xie, Y. Xu et al., "Pelargonidin-3-O-glucoside derived from wild raspberry exerts antihyperglycemic effect by inducing autophagy and modulating gut microbiota," *Journal of Agricultural and Food Chemistry*, 2019.

[26] C. Zhang, L. Gui, Y. Xu, T. Wu, and D. Liu, "Preventive effects of andrographolide on the development of diabetes in autoimmune diabetic NOD mice by inducing immune tolerance," *International Immunopharmacology*, vol. 16, no. 4, pp. 451–456, 2013.

[27] G. Chen, X. Ran, B. Li et al., "Sodium butyrate inhibits inflammation and maintains epithelium barrier integrity in a TNBS-induced inflammatory bowel disease mice model," *eBioMedicine*, vol. 30, pp. 317–325, 2018.

[28] T. R. Wu, C. S. Lin, C. J. Chang et al., "Gut commensal Parabacteroides goldsteinii plays a predominant role in the anti-obesity effects of polysaccharides isolated from Hirsutella sinensis," *Gut*, vol. 68, no. 2, pp. 248–262, 2019.

[29] M. B. Kadiiska, S. Peddada, R. A. Herbert et al., "Biomarkers of oxidative stress study VI. Endogenous plasma antioxidants fail as useful biomarkers of endotoxin-induced oxidative stress," *Free Radical Biology & Medicine*, vol. 81, pp. 100–106, 2015.

[30] W. Wu, S. Wang, Q. Liu, X. Wang, T. Shan, and Y. Wang, "Cathelicidin-WA attenuates LPS-induced inflammation and redox imbalance through activation of AMPK signaling," *Free Radical Biology & Medicine*, vol. 129, pp. 338–353, 2018.

[31] C. A. Thaiss, M. Levy, I. Grosheva et al., "Hyperglycemia drives intestinal barrier dysfunction and risk for enteric infection," *Science*, vol. 359, no. 6382, pp. 1376–1383, 2018.

[32] A. Martin and S. Devkota, "Hold the door: role of the gut barrier in diabetes," *Cell Metabolism*, vol. 27, no. 5, pp. 949–951, 2018.

[33] H. Plovier, A. Everard, C. Druart et al., "A purified membrane protein from _Akkermansia muciniphila_ or the pasteurized bacterium improves metabolism in obese and diabetic mice," *Nature Medicine*, vol. 23, no. 1, pp. 107–113, 2017.

[34] E. Cario, G. Gerken, and D. K. Podolsky, "Toll-like receptor 2 controls mucosal inflammation by regulating epithelial barrier function," *Gastroenterology*, vol. 132, no. 4, pp. 1359–1374, 2007.

[35] G. G. Muccioli, D. Naslain, F. Backhed et al., "The endocannabinoid system links gut microbiota to adipogenesis," *Molecular Systems Biology*, vol. 6, no. 1, p. 392, 2010.

[36] A. Everard, V. Lazarevic, N. Gaia et al., "Microbiome of prebiotic-treated mice reveals novel targets involved in host

response during obesity," *The ISME Journal*, vol. 8, no. 10, pp. 2116–2130, 2014.

[37] J. C. Clemente, L. K. Ursell, L. W. Parfrey, and R. Knight, "The impact of the gut microbiota on human health: an integrative view," *Cell*, vol. 148, no. 6, pp. 1258–1270, 2012.

[38] J. Hu, S. Lin, B. Zheng, and P. C. K. Cheung, "Short-chain fatty acids in control of energy metabolism," *Critical Reviews in Food Science and Nutrition*, vol. 58, no. 8, pp. 1243–1249, 2017.

[39] A. K. Thakur, G. Rai, S. S. Chatterjee, and V. Kumar, "Beneficial effects of an Andrographis paniculata extract and andrographolide on cognitive functions in streptozotocin-induced diabetic rats," *Pharmaceutical Biology*, vol. 54, no. 9, pp. 1528–1538, 2016.

[40] X. Ji, C. Li, Y. Ou et al., "Andrographolide ameliorates diabetic nephropathy by attenuating hyperglycemia-mediated renal oxidative stress and inflammation via Akt/NF-kappaB pathway," *Molecular and Cellular Endocrinology*, vol. 437, no. C, pp. 268–279, 2016.

[41] Z. Yu, B. Lu, Y. Sheng, L. Zhou, L. Ji, and Z. Wang, "Andrographolide ameliorates diabetic retinopathy by inhibiting retinal angiogenesis and inflammation," *Biochimica et Biophysica Acta*, vol. 1850, no. 4, pp. 824–831, 2015.

[42] G. Brahmachari, "Andrographolide," in *Discovery and Development of Antidiabetic Agents from Natural Products*, pp. 1–27, Elsevier, 2017.

[43] Z. Zhang, J. Jiang, P. Yu, X. Zeng, J. W. Larrick, and Y. Wang, "Hypoglycemic and beta cell protective effects of andrographolide analogue for diabetes treatment," *Journal of Translational Medicine*, vol. 7, no. 1, p. 62, 2009.

[44] M. C. Arrieta, L. Bistritz, and J. B. Meddings, "Alterations in intestinal permeability," *Gut*, vol. 55, no. 10, pp. 1512–1520, 2006.

[45] B. J. Guo, Z. Liu, M. Y. Ding et al., "Andrographolide derivative ameliorates dextran sulfate sodium-induced experimental colitis in mice," *Biochemical Pharmacology*, vol. 163, pp. 416–424, 2019.

[46] X. Shi, X. Wei, X. Yin et al., "Hepatic and fecal metabolomic analysis of the effects of lactobacillus rhamnosus GG on alcoholic fatty liver disease in mice," *Journal of Proteome Research*, vol. 14, no. 2, pp. 1174–1182, 2014.

[47] N. Nagata, L. Xu, S. Kohno et al., "Glucoraphanin ameliorates obesity and insulin resistance through adipose tissue browning and reduction of metabolic endotoxemia in mice," *Gastroenterology*, vol. 66, no. 5, pp. 1222–1236, 2017.

[48] J. Qin, Y. Li, Z. Cai et al., "A metagenome-wide association study of gut microbiota in type 2 diabetes," *Nature*, vol. 490, no. 7418, pp. 55–60, 2012.

Hindawi

Research Article

Proteomic Profile of Mouse Brain Aging Contributions to Mitochondrial Dysfunction, DNA Oxidative Damage, Loss of Neurotrophic Factor, and Synaptic and Ribosomal Proteins

Yingchao Li [1,2] **Haitao Yu** [1,2] **Chongyang Chen** [1,2] **Shupeng Li,**[3] **Zaijun Zhang** [4] **Hua Xu** [2] **Feiqi Zhu,**[5] **Jianjun Liu,**[1] **Peter S. Spencer,**[6] **Zhongliang Dai** [7] **and Xifei Yang** [1]

[1]*Key Laboratory of Modern Toxicology of Shenzhen, Shenzhen Center for Disease Control and Prevention, Shenzhen 518055, China*
[2]*College of Pharmacy, Jinan University, Guangzhou 510632, China*
[3]*State Key Laboratory of Oncogenomics, School of Chemical Biology and Biotechnology, Peking University Shenzhen Graduate School, Shenzhen 518055, China*
[4]*Institute of New Drug Research and Guangzhou, Key Laboratory of Innovative Chemical Drug Research in Cardio-Cerebrovascular Diseases, Jinan University College of Pharmacy, Guangzhou 510632, China*
[5]*Cognitive Impairment Ward of Neurology Department, The 3rd Affiliated Hospital of Shenzhen University, China*
[6]*Department of Neurology, School of Medicine, Oregon Institute of Occupational Health Sciences, Oregon Health & Science University, Portland, Oregon 97239, USA*
[7]*The Department of Anesthesiology, Shenzhen People's Hospital, The Second Clinical Medical College, Jinan University, Shenzhen 518020, China*

Correspondence should be addressed to Hua Xu; huax_mail@126.com, Zhongliang Dai; daizhongliang@jnu.edu.cn, and Xifei Yang; xifeiyang@gmail.com

The deleterious effects of aging on the brain remain to be fully elucidated. In the present study, proteomic changes of young (4-month) and aged (16-month) B6129SF2/J male mouse hippocampus and cerebral cortex were investigated by using nano liquid chromatography tandem mass spectrometry (NanoLC-ESI-MS/MS) combined with tandem mass tag (TMT) labeling technology. Compared with the young animals, 390 hippocampal proteins (121 increased and 269 decreased) and 258 cortical proteins (149 increased and 109 decreased) changed significantly in the aged mouse. Bioinformatic analysis indicated that these proteins are mainly involved in mitochondrial functions (FIS1, DRP1), oxidative stress (PRDX6, GSTP1, and GSTM1), synapses (SYT12, GLUR2), ribosome (RPL4, RPS3), cytoskeletal integrity, transcriptional regulation, and GTPase function. The mitochondrial fission-related proteins FIS1 and DRP1 were significantly increased in the hippocampus and cerebral cortex of the aged mice. Further results in the hippocampus showed that ATP content was significantly reduced in aged mice. A neurotrophin brain-derived neurotrophic factor (BNDF), a protein closely related with synaptic plasticity and memory, was also significantly decreased in the hippocampus of the aged mice, with the tendency of synaptic protein markers including complexin-2, synaptophysin, GLUR2, PSD95, NMDAR2A, and NMDAR1. More interestingly, 8-hydroxydeoxyguanosine (8-OHdG), a marker of DNA oxidative damage, increased as shown by immunofluorescence staining. In summary, we demonstrated that aging is associated with systemic changes involving mitochondrial dysfunction, energy reduction, oxidative stress, loss of neurotrophic factor, synaptic proteins, and ribosomal proteins, as well as molecular deficits involved in various physiological/pathological processes.

1. Introduction

Molecular and cellular changes occurring with the passage of time provide an indispensable foundation with which to detect and define deviations from the normal aging process that surfaces in the form of various neurodegenerative diseases [1, 2]. While a minority of these diseases results from defined genetic mutations that can be modeled in transgenic rodents, especially mice, many occur sporadically and develop with aging. Therefore, understanding the evolution of brain aging would be of paramount importance to provide novel molecular and cellular clues leading to neurodegenerative diseases. To determine the specific molecular mechanisms and related biomarkers of brain aging, we have used 4- and 16-month-old B6129SF2/J mice to study the systemic changes of proteins in the hippocampus and cortex by using nano liquid chromatography tandem mass spectrometry (NanoLC-ESI-MS/MS) coupled with tandem mass tag (TMT) labeling technology, a robust, sensitive, and accurate high-resolution analytical method [3].

Several studies of physiological brain aging in mice have been published, some of which have examined gene expression changes and, more recently, proteomic differences. These studies have employed mice of various strains (BALB/c, C57BL/6NHsd, and C57BL/10J), ages (range of 1-30 months), and sexes (males, females, or both), with comparisons variably among various brain areas of the cerebral cortex, hypothalamus, and cerebellum [4–10]. A recent quantitative proteomic analysis of the hippocampus, cortex, and cerebellum of postnatal (1 month) and middle-aged (12 months) C57BL/10J mice found total protein expression levels to be similar in the two age groups, and the hippocampus showed the most variable in protein expression across age [10]. The ability of aging neurons to oxidize glucose through glycolysis and mitochondria, as well as the ability to utilize fatty acids, increases and decreases from early to middle life (12 months) [9]. However, till now, the general picture of systemic molecular changes with aging, which was proposed to involve metabolic, immunological, inflammatory, and cellular functional, has now been explored. In the present study, hippocampal and cerebral cortical quantitative proteomics were explored through the age of 16 months (relative to 4 months) in a related mouse strain (B6129SF2/J). Our results showed that aging accompanying protein changes are related to mitochondrial dynamics, energy metabolism, GTPase function, oxidative stress, ribosome, synapses, loss of neurotrophic factor, and transcriptional regulation, among others.

2. Materials and Methods

2.1. Animals and Treatment Protocol. Animal treatment and housing were carried out in accordance with the Principles of Laboratory Animal Care (NIH publication no. 8–23, revised 1985) and the Regulations of the Animal Care and Use Committee of the Experimental Animal Center at Shenzhen Center for Disease Control and Prevention (SZCDCP). This study was approved by the SZCDCP Ethics Committee.

Mice of strain B6129SF2/J (JAX stock #101045) were purchased from Jackson Laboratory (Maine, USA). These F2 hybrid mice are the offspring of an F1 × F1 mating, itself the product of a cross between C57BL/6J females (B6) and 129S1/SvImJ males (129S) [11]. Ten mice were housed in per cage ($470 \times 350 \times 200$ mm) with sufficient water and food. The nutritional profile of the diet was as follows: moisture 8.02%, crude protein 22.30%, crude fat 5.35%, crude fiber 4.45%, crude ash 6.36%, calcium 1.332%, total phosphorus 0.673%, copper 20.8 mg/kg, iron 209 mg/kg, magnesium 2182 mg/kg, manganese 91.5 mg/kg, potassium 5317 mg/kg, zinc 111 mg/kg, sodium 2704 mg/kg, selenium 0.424 mg/kg, total arsenic 0.315 mg/kg, chromium 3.08 mg/kg, iodine 2.318 mg/kg, vitamin E 146.1 mg/kg, vitamin A 17670 IU/kg, and vitamin C 9.397 mg/kg, mercury-free and lead-free. Male animals were of two age groups: 4 months old ($n = 10$) and 16 months old ($n = 10$). The animal room has a stable indoor environment: temperature ($20 \pm 2°C$), humidity ($55 \pm 5\%$), and 12 hours of light and dark cycle.

2.2. Sample Protein Extraction for Proteomic Analysis. After euthanizing mice with 1% sodium pentobarbital, we performed a series of operations to ensure the freshness of the samples, including removing the mouse brain from the skull, excising the hippocampus and cerebral cortex on an ice-cold plate, rapidly freezing tissues in liquid nitrogen, and finally storing the tissue at −80°C. Samples (five or six for each group) were suspended in lysis buffer, containing 8 M urea in PBS, pH 8.0, 1 cocktail, and 1 mM phenylmethanesulfonyl fluoride (PMSF), and ultrasonicated for 90 s (4 s on and 6 s off) at 45% power with a Fisher 550 Sonic Dismembrator (Pittsburgh, PA, USA). After 30-minute incubation time, we proceed as follows: removing debris from the sample centrifugation at $12,000 \times g$ at 4°C for 15 min and transferring the supernatant to a fresh 1.5 mL tube, using Nanodrop 2000c (Thermo Fisher Scientific, Waltham, MA, USA) to determine the protein concentration.

2.3. Tandem Mass Tag Labeling. The unilateral hippocampus and cortex of 5 or 6 mice were randomly selected from each group, and 100 μg totaled protein was pooled in equal proportions (1 : 1 : 1 : 1 : 1 or 1 : 1 : 1 : 1 : 1 : 1) for subsequent proteomic analysis (Figure 1). The mixed proteins (per group) were incubated with 10 mM dithiothreitol (DTT, Sigma-Aldrich) at 55°C for 1 h and then incubated with 25 mM iodoacetamide (IAA, Sigma-Aldrich) in the dark at room temperature (RT) for 1 h and digested for 12 h at 37°C with trypsin/Lys-C Mix (Promega, V5072) (protease : protein ratio of 1 : 50). After terminating the reaction, the samples (per group) were acidified with 1% formic acid (FA, Thermo Fisher 167136), desalted with a reverse phase column (Oasis HLB; Waters, MC), and dried with a vacuum concentrator (RVC 2-18 CD plus), then dissolved in TEAB (triethylammonium bicarbonate buffer, 200 mM, pH 1/4 8.5, Thermo Fisher 90114).

According to the TMT 4-plex reagent (Thermo Fisher 90066) instructions, the samples (per group) were labeled with different TMT labels. The 4- and 16-month-old mouse hippocampal/cortical samples were individually labeled with TMT-126, TMT-128, TMT-129, and TMT-130, respectively. Samples (per group) added into the TMT tag were incubated
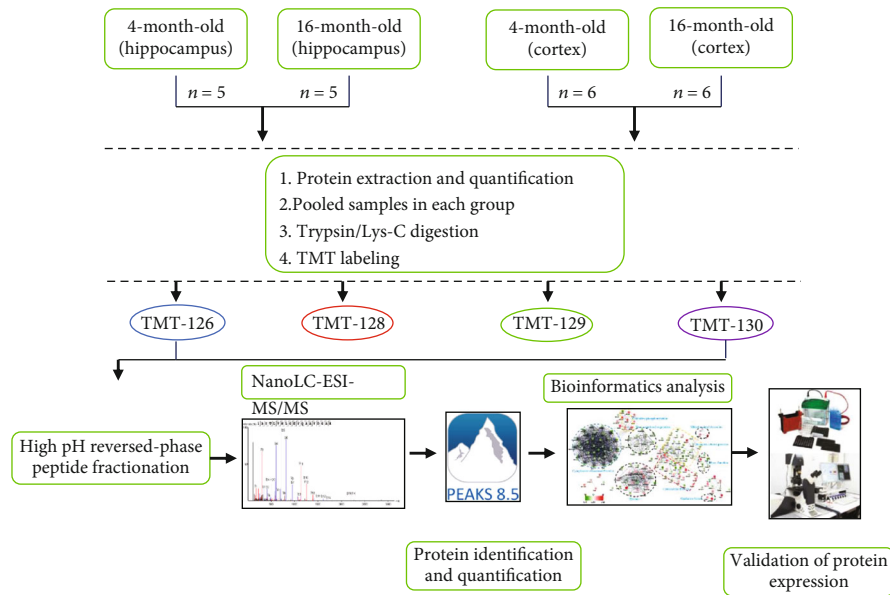
FIGURE 1: Experimental flowchart. We employed 4-month-old and 16-month-old mice, respectively, each group of 10 mice. From each group, hippocampal and cerebral cortical tissues of 5 or 6 animals were randomly selected for proteomic analysis. For each group, proteins were extracted from 5 or 6 individual samples and pooled (1 : 1 : 1 : 1 : 1 or 1 : 1 : 1 : 1 : 1 : 1) for subsequent proteomic experiments. The pooled proteins were digested into peptides using trypsin/Lys-C Mix and subjected to 4-plex TMT labeling, High pH reversed-phase peptide fractionation and subsequent NanoLC-ESI-MS/MS analysis. The raw data were identified and quantified using PEAKS 8.5 software and subjected to bioinformatics analysis (GO, KEGG, STRING, and Wiki pathways). Selected key proteins were verified by Western blot.

for 1 hour at RT, followed by the addition of 5% hydroxyl-amine (Thermo Fisher 90115) to terminate the reaction, and finally, the TMT-labeled peptides were mixed together for subsequent experiments.

2.4. High-pH Reversed-Phase Chromatography Separation. Labeled peptides were fractionated by Pierce High-pH Reversed-Phase Peptide Fractionation Kit (Thermo Fisher 84868) for further NanoLC-ESI-MS/MS analysis. First, the adjustment of the spin columns consisted of removing the solution, packing the resin material, and washing the spin column twice with 300 μL acetonitrile (ACN) and 0.1% FA solution, respectively, all of which were centrifuged at 5,000 $\times$ g for 2 min. Second, peptide separation involved dissolving each sample with 300 μL of 0.1% FA, loading onto a column, and eluting twice with a gradient elution solution of 300 μL (ACN: triethylamine) (Thermo Fisher 84868 (5%, 10%, 12.5%, 15%, 17.5%, 20.0%, 22.5%, 25.0%, and 50.0%)), all of which were maintained at 3,000 $\times$ g for 2 min. After drying in a vacuum concentrator, 20 μL of 0.1% FA was added to each tube for NanoLC-ESI-MS/MS analysis.

2.5. Data Collection of TMT-Labeled Peptides Using NanoLC-ESI-MS/MS. We loaded the peptide fraction from 2.4 into a ChromXP C18 (3 μm, 120 Å) trap column and analyzed using TripleTOF 5600+ mass spectrometer (SCIEX, Concord, ON, Canada). To acquire ESI/MS/MS data, running in positive ion mode, the first MS scan range is 400-1800 m/z, based on survey scans (250 ms) and acquisition of up to 40 ions in 80 ms (threshold value 160 cps, charge number 2-5) for IDA (information-dependent acquisition), and dynamically excludes selected ions due to the random-

ness of parent ion selection during MS/MS IDA. In this process, the rolling collision energy setting is adapted to the dissociation of all precursor ions.

Overall, protein extracts from selected brain regions of 5 or 6 mice were mixed before digestion, and then the mixtures were subjected to TMT labeling, peptide fractionation, and NanoLC-ESI-MS/MS analysis (Figure 1). For each group, the proteins were extracted from 5 or 6 individual samples and pooled (1 : 1 : 1 : 1 : 1 or 1 : 1 : 1 : 1 : 1 : 1) for subsequent proteomic analysis. The pooled proteins were digested into peptides using trypsin/Lys-C mix and subjected to 4-plex TMT labeling, high-pH reversed-phase peptide fractionation, and subsequent NanoLC-ESI-MS/MS analysis (Figure 1).

2.6. Database Searching and Protein Quantification. We use PEAKS 8.5 software (Bioinformatics Solutions, Waterloo, Canada) to identify and quantify proteins (Figure 1). The UniProt-*Mus musculus* database, containing 51,697 protein entries (released in July 2017), can be used to search the raw mass spectra. The parameters were as follows: parent mass error tolerance of 30 ppm and fragment mass error tolerance of 0.1 Da; FDR (false discovery rate) $\leq 1.0\%$ at peptide-spectrum match level, which can be determined by PEAKS 8.5 searching the related database; peptide scores ($-10 \log p$) > 19.5, equivalent to a p value of ~1%, were regarded as confidently identified. The TMT 6-plex method was used to relatively quantify peptides and proteins. The summed area, including all reported ion spectra with TMT tags of identified peptides, was taken as the normalized factor across different samples. According to the Peaks Q algorithm, proteins were considered to be significantly different

when the ratio ≥ 1.2 or<0.80-fold and the protein significance score ≥ 5.

2.7. Bioinformatics Analysis.

Visualization of differential proteins by different software and related databases is as follows: DAVID version 6.7 (https://david-d.ncifcrf.gov/) [12, 13] was used to elucidate the biological function of the identified proteins. STRING database version 10.0 (https://string-db.org/) [14, 15] was used to analyze the protein-protein interaction (PPI) network. For logistic analysis of tissue proteomes, Venn Diagram Generator (http://www.pangloss.com/seidel/Protocols/venn.cgi) was used. To analyze Wiki paths, Cytoscape 3.6.1 software and plug-ins were used to STRING-generated network and Wiki path visualization analysis [16, 17].

2.8. Western Blot Analysis.

After protein quantification, we added the loading buffer for protein denaturation. Then, the samples are separated on SDS-PAGE, transferred to PVDF membranes, and blocked with 5% skim milk. After treatment with the primary antibody (Table 1) of the target proteins and the corresponding secondary antibody, we performed an exposure development operation using an ECL kit (Thermo Scientific Pierce ECL, USA) and analyzed using Image Quant 1D software (GE Healthcare, Pittsburgh, PA, United States).

2.9. Assay of ATP Content.

ATP levels were determined with an ATP Assay Kit (S0026, Beyotime Institute of Biotechnology, Haimen, China). Approximately 200 μL of lysate was added per 20 mg of tissue, and the mixture was homogenized with a glass or other homogenizer to affect complete tissue lysis. Lysed cells were centrifuged at 12, 000 × g for 5 min at 4°C, and the supernatant was taken for subsequent measurement. We can calculate the relative ATP level with the ratio of the ATP value to the protein value. These values were measured with a multifunctional microplate reader (Tecan Infinite M1000 PRO, Männedorf, Switzerland).

2.10. Immunofluorescence Staining.

We performed immunofluorescence staining as described previously [18]. Briefly, coronal mouse brain slices were cut into 30 μm thick sections and rinsed 4 times with PBS for 5 min. For immunochemistry of FIS1 and 8-hydroxydeoxyguanosine (8-OHdG), sections were incubated at 4°C for 12 h with the primary antibody (FIS1 at 1:100, 8-OHdG at 1:100) (Table 1), then washed with PBST and stained with the secondary antibody (1:200) for 1 h, Alexa Fluor ®-488 goat anti-rabbit, and Alexa Fluor ®-488 donkey anti-goat (Invitrogen, USA), counterstained for 5 min with DAPI (Beyotime, Haimen, China) to reveal the nuclei, and analyzed using a laser scanning confocal microscope (Leica, Wetzlar, Germany).

2.11. Statistical Analysis.

The data were expressed as the mean ± SEM with GraphPad Prism 7.0 (GraphPad Software, Inc.), assessed with Student's t-test about the level of significance between two groups, and p value < 0.05 was considered to be significant.

3. Results

3.1. Differentially Expressed Hippocampal and Cortical Proteins.

All the proteins of the hippocampus and cerebral cortex were identified by the mass spectra (Supplementary Excel 1). By using the LC-MS/MS analysis combined with TMT labeling technology, based on two unique peptides, we identified a total of 3530 proteins in the hippocampus and cerebral cortex with a false discovery rate (FDR) of less than 1% (Figure 2(c)). Among these proteins, a total of 1857 were common to the hippocampus and cortex (Figure 2(c)). Proteins with at least 1.2 or <0.80-fold and significant score ≥ 5 were considered differentially expressed. We can get the names, accession numbers, and relative abundance ratios of the differential proteins Figures 2(a) and 2(b) from the Swiss-Prot database.

3.2. Aging Contributes to Proteomic Alterations in a Mouse Hippocampus.

Three hundred-ninety hippocampal proteins were differentially expressed between 4- and 16-month-old mice (Figure 2(a)). Among these proteins, 121 proteins were increased and 269 decreased in aged vs. young mice; these involved mitochondria (29 increased and 22 decreased), synapses (12 increased and 33 decreased), oxidative stress (7 increased and 9 decreased), cytoskeletal integrity (3 increased and 15 decreased), ribosome (37 decreased), transcriptional regulation (2 increased and 18 decreased), GTPase function (3 increased and 13 decreased), and histone (11 increased and 5 decreased). Gene ontology analysis was performed to reveal the strongly enriched biological processes: translation process, nucleosome assembly process, macromolecular complex subunit organization process, vesicle-mediated transport process, cytoskeleton organization process, and regulation of synaptic transmission process (Figure 3(a)). In addition, we also revealed the strongly enriched molecular function of differential proteins: structural constituent of ribosome activity, structural molecule activity, RNA binding activity, GTP binding activity, cytoskeletal protein binding activity, and guanyl nucleotide binding activity (Figure 3(c)). Further KEGG analysis indicates that these differential proteins are also highly enriched in some pathways associated with aging: ribosome, long-term potentiation, neurotrophin signaling pathway, regulation of actin cytoskeleton, oxidative phosphorylation, and axon guidance (Figure 3(e)).

3.3. Aging Contributes to Proteomic Alterations in a Mouse Cerebral Cortex.

Two hundred-fifty-eight cortical proteins were differentially expressed between 4- and 16-month-old mice (Figure 2(b)). Among these proteins, 149 proteins were increased and 109 decreased in aging vs. young mice, involving mitochondria (25 increased and 12 decreased), synapses (29 increased and 19 decreased), oxidative stress (8 increased and 5 decreased), cytoskeletal integrity (7 increased and 14 decreased), ribosome (5 increased and 5 decreased), transcriptional regulation (10 increased and 16 decreased), and GTPase function (8 increased and 5 decreased).

Gene ontology analysis was performed to reveal the strongly enriched biological processes: vesicle-mediated transport process, secretion process, protein localization

TABLE 1: Brands and usages of the primary antibodies.

Antibody	Specificity	Type	Dilution	Source	CAT no.
β-Actin	Beta-actin	Mouse	1/3000	Santa Cruz	sc-47778
α-Tubulin	Alpha-tubulin	Mouse	1/3000	Santa Cruz	sc-73242
FIS1	Fission 1	Rabbit	1/1000	Proteintech	10956-1-AP
DRP1	Dynamin-related protein 1	Mouse	1/1000	Santa Cruz	sc-271583
OPA1	OPA1 (D-9)	Mouse	1/1000	Santa Cruz	sc-393296
MFN1	Mitofusin 1	Mouse	1/1000	Abcam	ab57602
NFN2	Mitofusin 2	Rabbit	1/1000	Proteintech	12186-1-AP
NDUAA	NDUFA10	Rabbit	1/1000	Abcam	ab103026
SDHB	Succinate dehydrogenase subunit B	Mouse	1/1000	Abcam	ab14714
UCRI	UQCRFS1	Rabbit	1/1000	Abcam	ab131152
COX5A	COX5a (A-5)	Mouse	1/3000	Santa Cruz	sc-376907
COX5B	Cytochrome c oxidase subunit 5B	Rabbit	1/1000	Abcam	ab180136
ATP5A	ATP synthase F1 subunit alpha	Mouse	1/1000	Abcam	ab14748
PGAM1	Phosphoglycerate mutase 1	Rabbit	1/1000	Abcam	ab184232
MPC2	Mitochondrial pyruvate carrier 2	Rabbit	1/1000	Cell Signaling	#46141
PRDX6	Peroxiredoxin 6	Mouse	1/1000	Abcam	ab16947
CHOP	CHOP (L63F7)	Mouse	1/1000	Cell Signaling	#2895
SYT1	Synaptotagmin-1	Rabbit	1/1000	Abcam	ab131551
SYT12	Synaptotagmin-12	Rabbit	1/1000	Proteintech	55015-1-AP
CPLX2	Complexin-2	Goat	1/1000	Abcam	ab215046
SYN II	Total synapsin-2	Rabbit	1/1000	Abcam	ab76494
Synaptophysin	Total synaptophysin	Rabbit	1/1000	Abcam	ab32127
GluR 2	Total GLUR2	Rabbit	1/1000	Abcam	13607s
PSD-95	Total postsynaptic density 95	Rabbit	1/1000	Abcam	ab76115
NMDAR 2A	Total NMDA receptor 2A	Rabbit	1/1000	Abcam	ab124913
NMDAR 1	Total NMDA receptor 1	Rabbit	1/1000	Abcam	ab109182
BDNF	Brain-derived neurotrophic factor	Rabbit	1/1000	Abcam	ab108319
8-OHdG	8-Oxo-2′-deoxyguanosine	Goat	1/100	Abcam	ab10802

process, cell recognition process, small GTPase-mediated signal transduction process, and protein transport process (Figure 3(b)). In addition, we also revealed the strongly enriched molecular function of differential proteins: GTP binding activity, GTPase activity, nucleotide binding activity, calmodulin binding activity, ribonucleotide binding activity, and purine ribonucleotide binding activity (Figure 3(d)). Further KEGG analysis indicates that these differential proteins are also highly enriched in some pathways associated with aging: pentose phosphate pathway, MAPK signaling pathway, gap junction, ribosome, axon guidance, and glycolysis (Figure 3(f)).

3.4. Bioinformatics Analysis for Hippocampal/Cortical Proteins. To identify the potential relationships among the proteins, as shown in Figures 4(a) and 4(b), we used Cytoscape 3.6.1 to visualize the STRING network. We found that many proteins in the PPI map are associated with brain aging processes: cytoplasmic ribosomal pathway, transcriptional regulation, synapses, oxidative phosphorylation, mitochondrial dynamics, oxidative stress, GTPase function, and IL-3 signaling pathway were associated with the aged brain. This indicated that brain aging may involve the deterioration of multiple cellular pathways including the cytoplasmic ribosomal pathway, transcriptional regulation, synapses, mitochondrial dysregulation, and oxidative stress.

Based on the PPI map, aging had a greater impact on the hippocampus, which leads to collective imbalances in multiple hippocampal features including transcription, ribosomes, and synapses (Figure 4(a)). Interactions among the hippocampal proteins related to ribosomal metabolism were evident, including the following: 60S ribosomal protein L4 (RPL4), 60S ribosomal protein L7 (RPL7), 60S ribosomal protein L6 (RPL6), 60S ribosomal protein L7a (RPL7a), 60S ribosomal protein L10 (RPL10), 60S ribosomal protein L34 (RPL34), 60S ribosomal protein L8 (RPL8), 60S ribosomal protein L9 (RPL9), 60S ribosomal protein L28 (RPL28), 60S ribosomal protein L13a (RPL23a), 40S ribosomal protein S3 (RPS3), 40S ribosomal protein S15a (RPS15a), 40S ribosomal protein S30 (RPS30), and 40S ribosomal protein S14 (RPS14) (Figure 5(d)). Furthermore, Wiki pathway analysis revealed that cytoplasmic ribosomal proteins were generally decreased in the aged hippocampus, with only a few disorders in the corresponding cerebral cortex (Figure 5(e)). Collectively,

(a)

FIGURE 2: Continued.

(b)

(c)
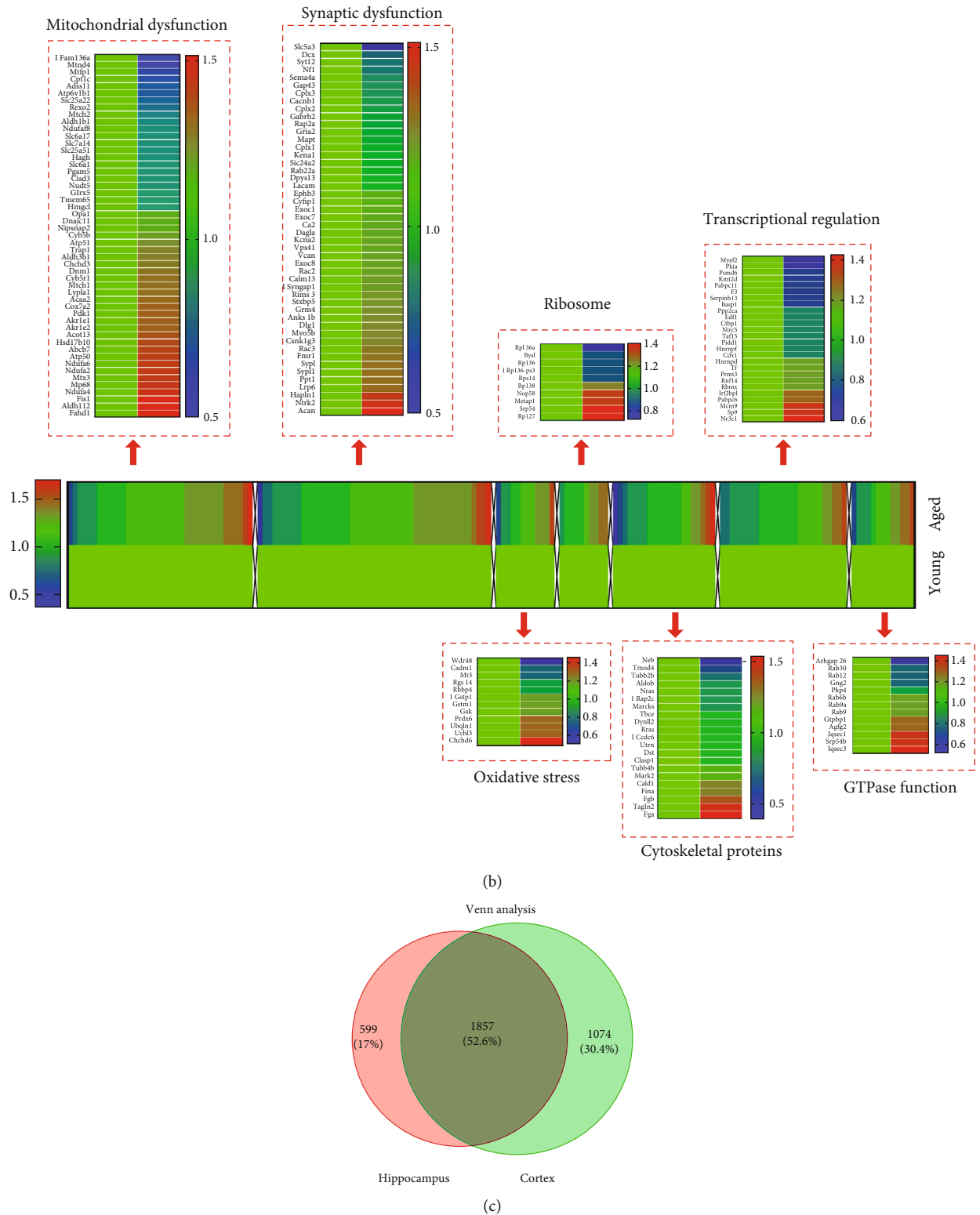
FIGURE 2: Differentially expressed hippocampal and cortical proteins in aged vs. young mice identified by NanoLC-ESI-MS/MS. (a and b) Proteins differentially expressed in 390 hippocampi and 258 cerebral cortices were hierarchically clustered for 4-month and 16-month-old mice. Differential expression was defined as at least 1.2 times (increased) or ≤0.8-fold (decreased) expression in aged vs. young animal brain. The color of each cell represents the expression level of the protein: red signifies an increase and blue a decreased level relative to that of the control group (4-month-old mice). $n = 5/6$ for per group. Identified proteins are primarily involved in mitochondrial dysfunction, synaptic dysfunction, oxidative stress, ribosome, cytoskeletal integrity, transcriptional regulation, and GTPase function. (c) The Venn logic diagram between the dysregulated proteins of the hippocampus and cerebral cortex in 4-month and 16-month-old mice.

(a)

(b)

(c)

(d)

FIGURE 3: Continued.

(e)

(f)
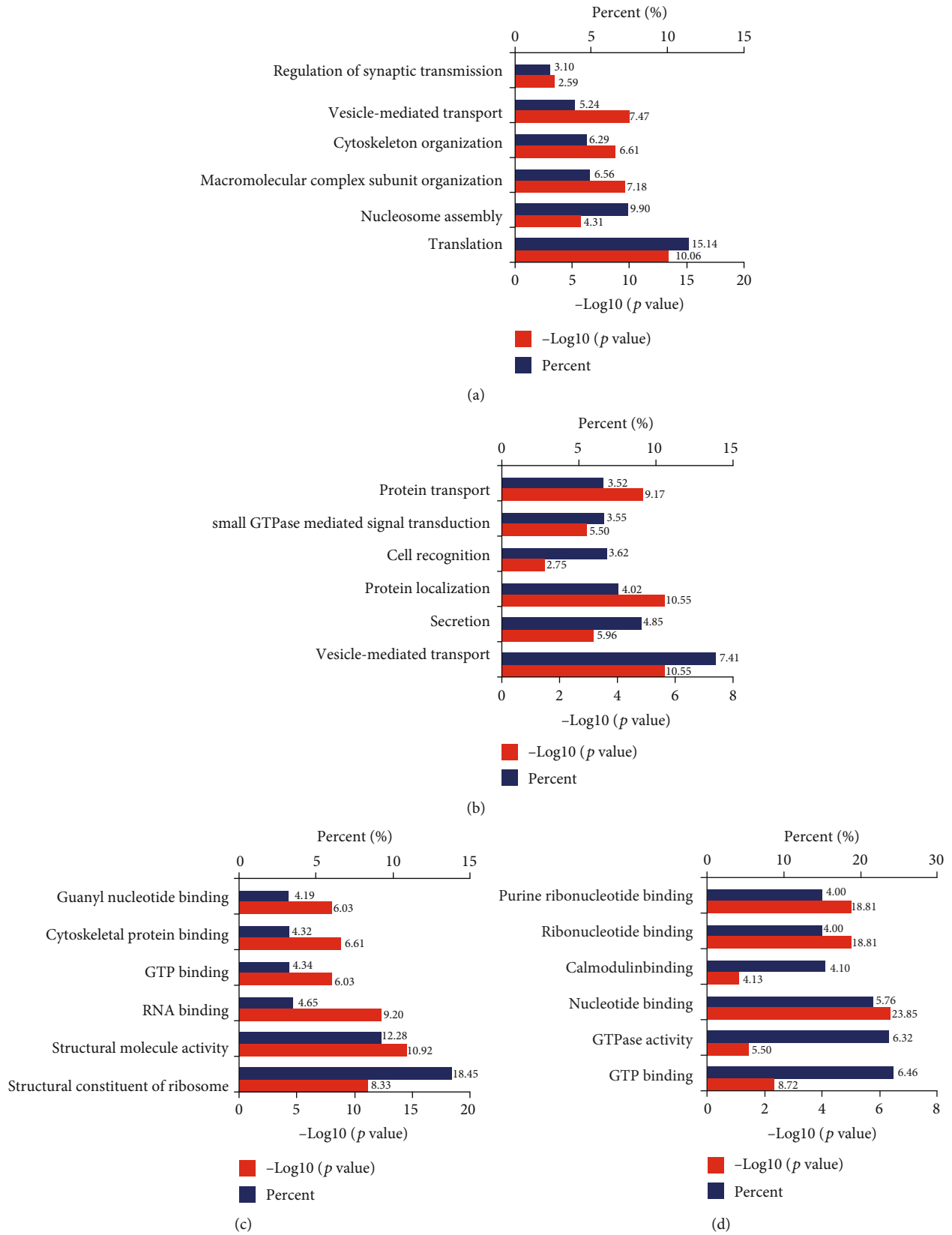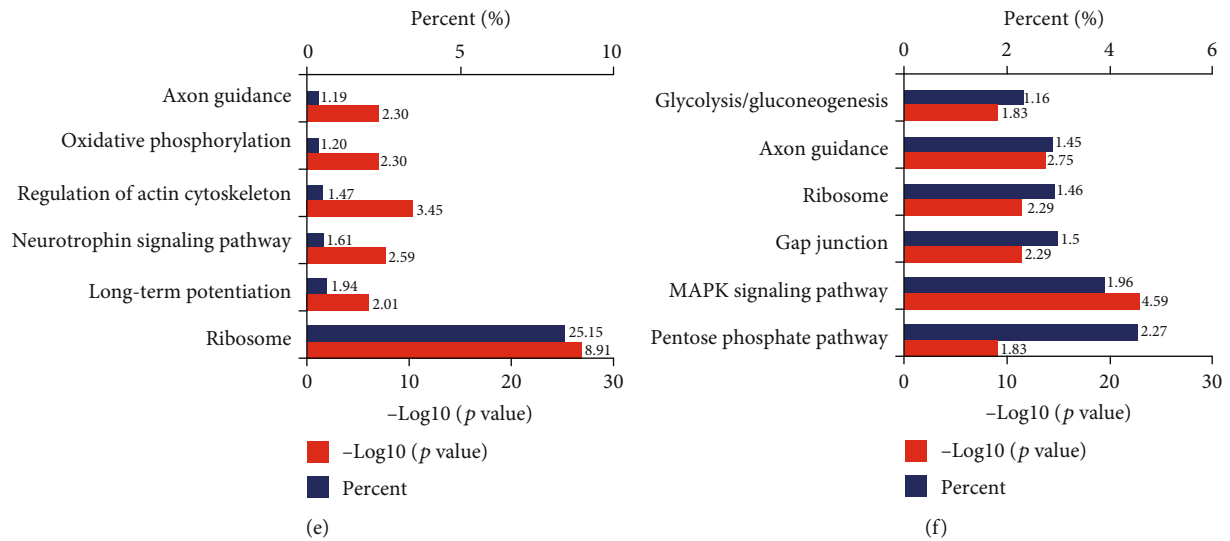
FIGURE 3: DAVID Gene Ontology and KEGG enrichment analysis for the hippocampal and cerebral cortical proteins of young vs. aged mice. Enrichment analysis for the following: (a) hippocampal proteomics by biological processes, (b) cerebral cortical proteomics by biological process, (c) hippocampal proteomics by molecular function, (d) cerebral cortical proteomics by molecular function, and (e and f) hippocampal and cerebral cortical proteomics by KEGG analysis, respectively.

the translation function of hippocampal protein in aged mice was degraded.

Proteomics analysis revealed an increase in a large number of electron transfer- (ECT-) related proteins; such changes in the hippocampus were more pronounced in the cerebral cortex (Figure 5(a)). Wiki pathway analysis also revealed that these dysregulated proteins are located in the electron transport chain Complexes I-V (Figures 5(b) and 5(c)) such as Complex I subunits (NDUAA, NDUA2, NDUA4, and NDUA6), Complex II subunits (SDHB), Complex III subunits (QCRI, QCR8), Complex IV subunits (COX5A, COX5B), and Complex V subunits (ATP5A, ATP5H). Collectively, these suggest a disordered electron transport chain in the aged brain.

In sum, proteomic alterations detected in the aged vs. younger brain revealed a large number of protein disorders, particularly impacting hippocampal transcription, translation, and synaptic and mitochondrial proteins.

3.5. Further Validation of the Dysregulated Expressed Proteins. Brain proteomic analysis revealed abnormal expression of mitochondrial dynamics, oxidative stress, synapse, energy metabolism, and ribosomal metabolism-related proteins in the hippocampus and cerebral cortex of aged vs. young mice. For mitochondrial dynamics, we determined the expression of key molecules involved in mitochondrial fission by Western blot and immunofluorescence staining analysis (Figures 6(a)–6(f)). For energy metabolism, we examined the expression of subunits involved in the electron transport chain and the glycolysis-related protein phosphoglycerate mutase 1 (PGAM1) and by Western blot analysis (Figures 7(a)–7(d)). We also validated oxidative stress-related protein Peroxiredoxin 6 (PRDX6) (Figures 8(c) and 8(d)). Brain proteomic analysis also revealed a relative decrease of many synapse-related proteins: of these, some representative proteins, such as Syntaxin12 (STX12),

complexin-2 (CPLX2), synapsin-2, glutamate receptor 2 (GLUR2), synaptophysin, PSD95, NMDAR2A, and NMDAR1 were confirmed by Western blot analysis (Figures 9(a)–9(e)). Consistent with the proteomics data, glycolysis-related protein PGAM1 and synaptic proteins were decreased significantly, while ECT-related proteins, mitochondrial fission protein FIS1, and oxidative stress protein PRDX6 were increased significantly in aged vs. young mice. All verification raw data of Western blot analysis are shown in Supplementary Excel 2.

3.6. Decreased ATP Levels in the Hippocampus of Aged in Comparison with Young Mice. To further investigate the effects of aging on energy metabolism, we evaluated ATP levels in the hippocampus of aged vs. young mice. The former showed significantly reduced ATP levels (Figure 7(e)), suggesting that aging is linked with mitochondrial dysfunction in the murine hippocampal respiratory chain.

3.7. DNA Oxidative Damage in Aged Mice. To determine the potential effects of aging on regional brain DNA, we measured two markers of DNA damage, namely, CHOP and 8-OHdG. Quantification of green fluorescence intensity showed that 8-OHdG immunoreactivity was markedly increased in the cerebral cortex and hippocampal regions CA1, CA3, and DG of aged vs. young mice (Figures 8(a) and 8(b)). Western blot analysis showed that CHOP was also significantly increased in the cerebral cortex and hippocampus of aged mice vs. young mice (Figures 8(c) and 8(d)). These data suggest that brain DNA oxidative damage accrues with aging.

3.8. Decreased BDNF Levels in the Hippocampus of Aged Mice. Considering the broad role of BDNF in neuroprotection, including synaptic plasticity, oxidative, metabolic, and excitotoxic stress [19, 20], we explored the expression

(a)

(b)
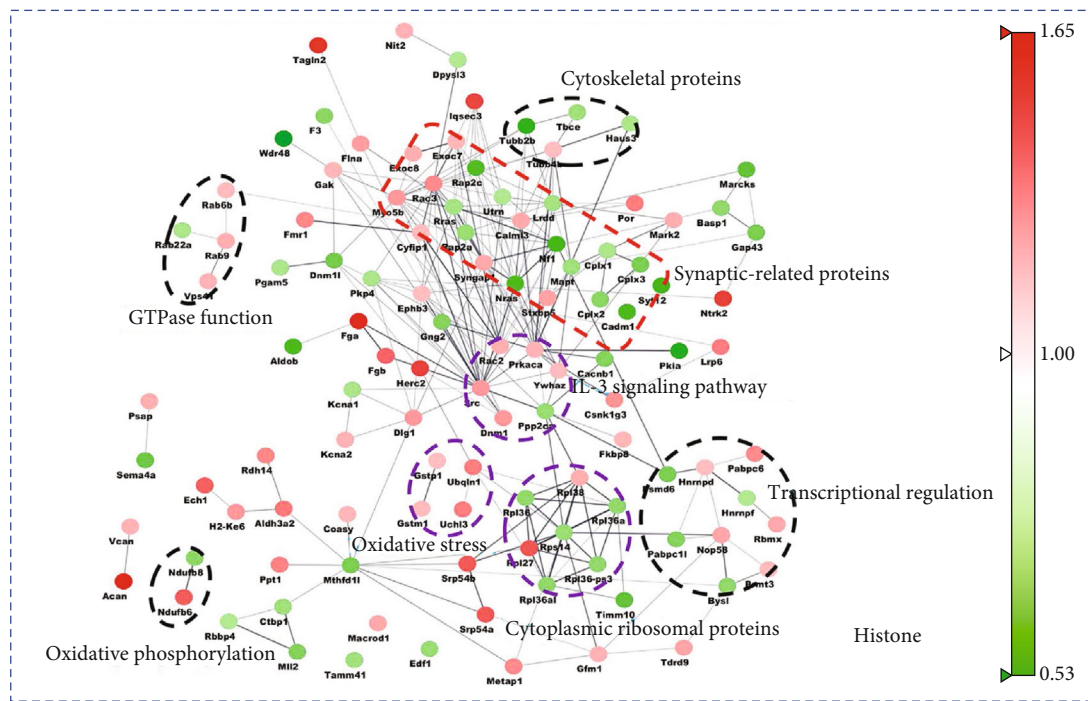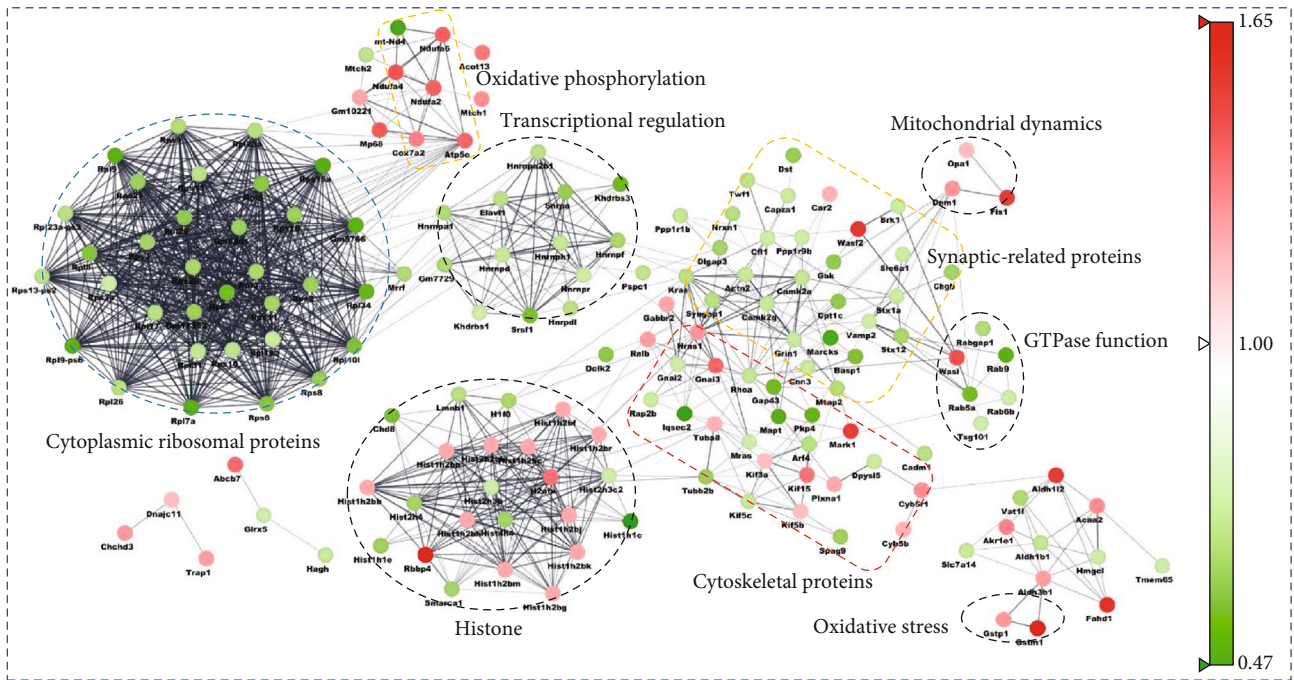
FIGURE 4: Protein-protein interaction analysis of 390 hippocampal proteins and 258 cortical proteins using the STRING database. All the differentially expressed proteins were visualized and mapped using Cytoscape 3.6.1. STRING analyses of hippocampal differentially expressed proteins (a) and cerebral cortical differential proteins (b). Unconnected proteins were removed from the networks. Interactions between two proteins are indicated with gray edges. Red and green nodes indicate increased or decreased protein levels, respectively.

changes of BDNF in the hippocampus and cerebral cortex of aged vs. young mice. Western blot analysis showed significantly reduced levels of BDNF in both the cerebral cortex and hippocampus of aged mice vs. young mice (Figures 10(a) and 10(b)).

4. Discussion

Proteomic analysis detected a total of 3530 proteins, of which 1857 proteins were common to the hippocampus and cerebral cortex. 390 hippocampal proteins and 258 cerebral

(a)

(b)

(c)

FIGURE 5: Continued.

(d)   (e)
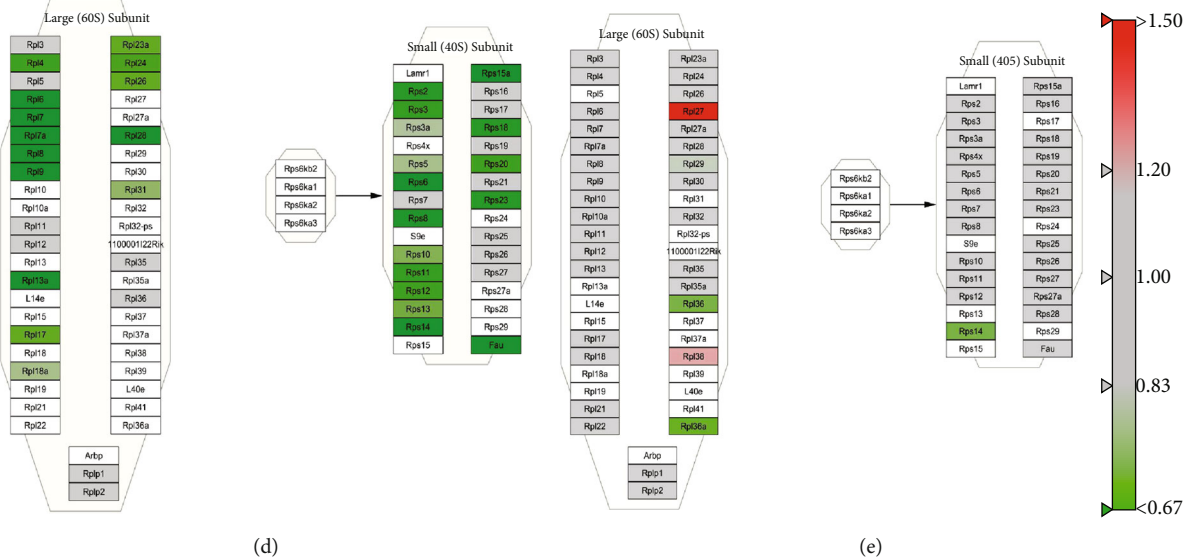
FIGURE 5: Wiki pathway analysis of all proteins. (a) Heat map analysis of hippocampal and cerebral cortical electron transport chain proteins. Red and green indicate increased or decreased protein levels in aged vs. young mouse brain, respectively. X indicates unscreened protein. Electron transport chain in the hippocampus (b) and cerebral cortex (c) and cytoplasmic ribosomal proteins in the hippocampus (d) and cerebral cortex (e). All proteins were mapped to the related Wiki pathway based on the published database. Proteins are represented by boxes labeled with the protein's name. Relative protein levels in 16-month-old mouse brain compared to those in 4-month-old animals are indicated by colors. Red and green indicated increased or decreased levels, respectively. Proteins in white were not identified in this study.

cortical proteins showed altered levels in the 16-month-old vs. the 4-month-old mouse brain, and these proteins were involved in mitochondrial function, energy metabolism, synaptic function, the cytoplasmic ribosomal pathway, transcriptional regulation, and oxidative stress. Aging seemed to have a more pronounced effect on protein levels in the hippocampus than those in the cerebral cortex, as noted in previous proteomic studies of mouse brain [10, 21], whereas the main pathways affected are shared between the two regions encompassing altered mitochondrial dynamics, synapse proteins, and oxidative stress in the hippocampus and cerebral cortex, with transcriptional regulation, energy metabolism, and changes in the cytoplasmic ribosome pathway more obvious in the hippocampus of aged mice. In this study, samples in each age group were pooled together to evaluate the differences of protein profiles among groups. However, it was difficult to reveal the individual variation in the same group, which is also one of the limitations for this study.

4.1. Mitochondrial Dynamics. Our results found aging was associated with simultaneous increase of fission 1 protein (mitochondrial outer membrane) in both the hippocampus and cerebral cortex of aged mice. In addition, dynamin-like protein DRP1 (dynamin 1-like) was significantly increased in the cerebral cortex of aged mice in comparison to young mice. In the pathological study of Alzheimer's disease and Huntington's disease, fis1 was found to aggravate the aggregation of DRP1 in mitochondria by interacting with DRP1 oligomers, which can induce mitochondrial division [22–25]. In addition, FIS1 knockdown promotes mitochondrial fusion and inhibits apoptosis [26, 27]. Compared with non-neuronal cells, DRP1 plays a significant role not only in the regulation of mitochondrial morphology but also in the dis-

tribution of mitochondria in axons, dendrites, and synapses [28–33]. Mitochondrial fission is vital for mitotic segregation of mitochondria to daughter cells, distribution of mitochondria to subcellular locations, and mitophagy [34, 35]. Unopposed fission leads to mitochondrial fragmentation, loss of OXPHOS function, mtDNA depletion, and ROS production, which are associated with metabolic dysfunction or disease [36]. Mitochondrial fission may enhance apoptosis by increasing the availability of outer membrane surface area for pore formation. Increased mitochondrial fission proteins disrupt mitochondrial membrane potential and respiration, resulting in slow cell growth and accelerated cell aging [37]. Taken in concert, these findings suggest that aging may dysregulate brain mitochondrial dynamics via increased levels of FIS1 and DRP1.

4.2. Energy Metabolism. Brain aging has been previously associated with abnormal energy metabolism, including increases in enzymes associated with glycogen metabolism and altered levels of proteins in the ETC, the function of which is required for ATP production [14, 21, 38]. We found major changes in the levels of energy metabolism-related proteins in the hippocampus and cerebral cortex of aged vs. young mice, and ETC-related proteins were most obviously increased in the hippocampus (Figure 5(a)). As an essential glycolytic enzyme [39], phosphoglycerate mutase 1 (PGAM1) was increased in the hippocampus of aged compared to young mice. However, mitochondrial pyruvate carrier 2 (MPC2), a heterooligomer complex, can be formed in the mitochondrial inner membrane (IMM), involved in pyruvate transport, for mitochondrial pyruvate oxidation and carboxylation [40], decreased in the cerebral cortex of aged mice. Wiki pathway analysis showed a general disorder

(a)

(b)

(c)

(d)

(e)

(f)
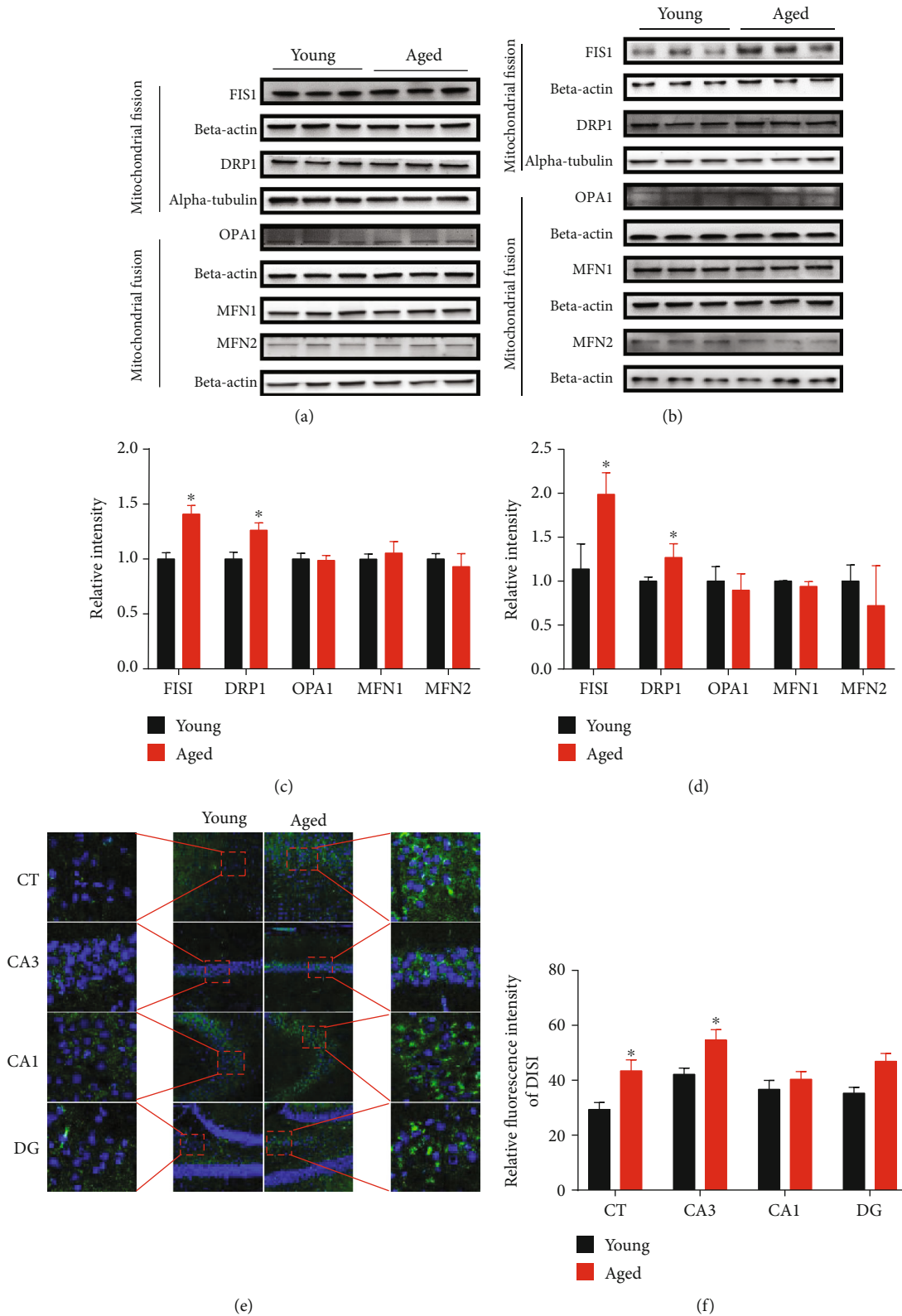
FIGURE 6: Validation of differentially expressed hippocampal and cortical mitochondrial dynamics proteins. (a and c) Relative levels of hippocampal mitochondrial dynamic proteins in 16-month-old mice compared to 4-month-old mice; (b and d) Relative levels of cerebral cortical mitochondrial dynamics proteins in aged vs. young animals. Data are presented as the mean ± SEM. $^{*}p < 0.05$ vs. the control mice. $n = 3$ for each group. (e and f) The brain sections containing hippocampal CA1, CA3, dentate gyrus (DG), and cerebral cortex (CT) were stained with anti-FIS1 antibody to detect the level of mitochondrial fission protein. The representative images were selected from 4-month-old mice and 16-month-old mice. Scale bar = 100 μm. Data are presented as the mean ± SEM. $^{*}p < 0.05$ vs. the control mice.

(a)

(b)

(c)

(d)

(e)

FIGURE 7: Validation of differentially expressed energy metabolism proteins by Western blot analysis. Relative levels of hippocampal energy metabolism proteins (a and c) and cerebral cortical energy metabolism proteins (b and d) in 16-month-old mice compared to 4-month-old mice. Data are presented as the mean ± SEM. $^*p < 0.05$ vs. the control mice. $n = 3$ for each group. (e) ATP levels in the hippocampus of 4-month-old mice and 16-month-old mice. ATP levels in young and aged animals were determined with an ATP Assay Kit. Data are presented as the mean ± SEM. $^*p < 0.05$ vs. the control mice. $n = 3$ for each group.

(a)

(b)

(c)

(d)
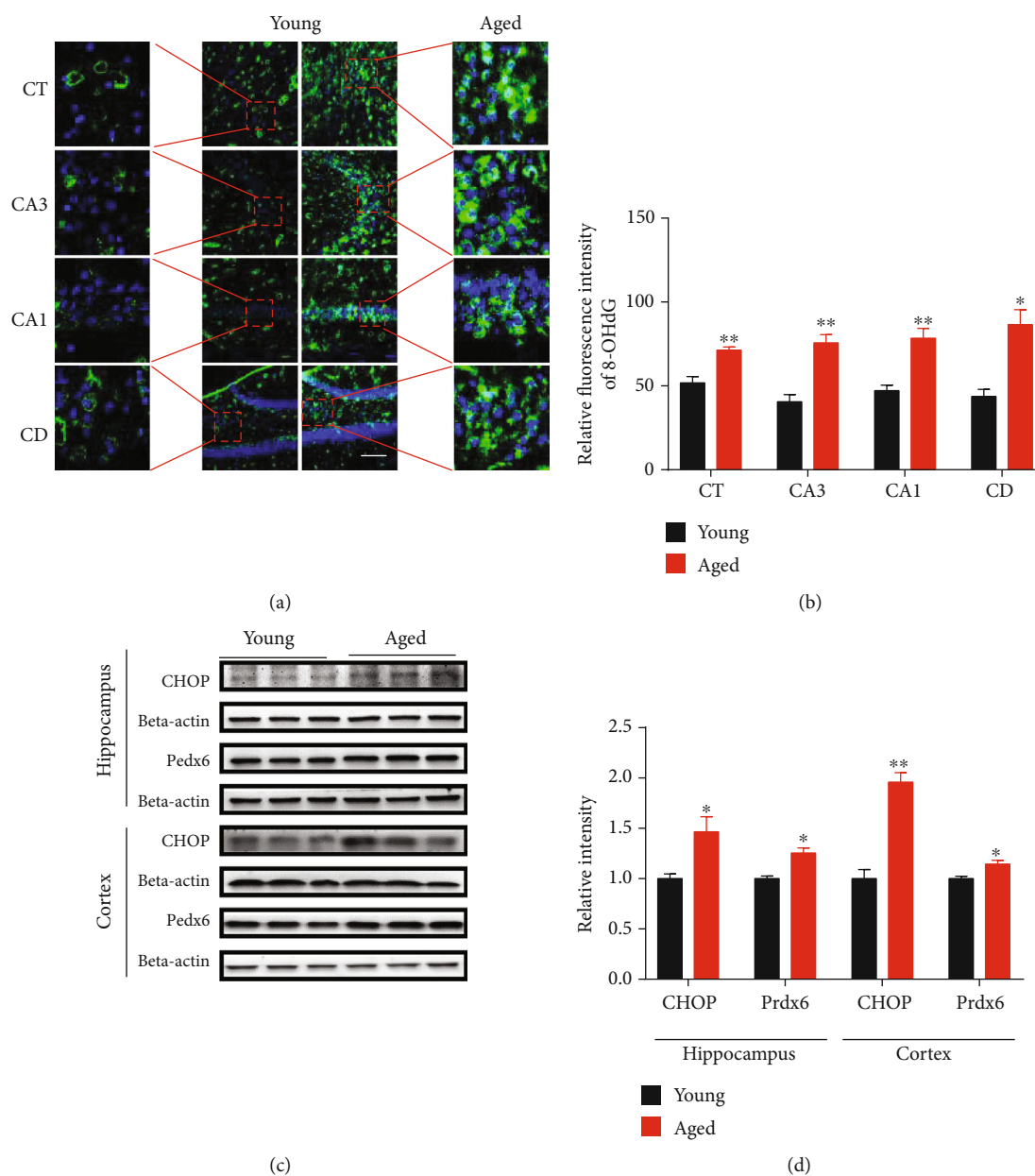
FIGURE 8: Elevation of PRDX6, CHOP, and 8-OHdG in the hippocampus and cerebral cortex of aged vs. young mice. (a and b) Brain sections containing hippocampal CA1, CA3, dentate gyrus (DG), and cerebral cortex (CT) were stained with anti-8-OHdG antibody to detect the level of these DNA lesions. Representative images were selected from 4-month-old mice and 16-month-old mice. Scale bar = $100\,\mu$m. Data are presented as the mean ± SEM. $^{*}p < 0.05$ and $^{**}p < 0.01$ vs. the control mice. (c and d) The levels of PRDX6 and CHOP were measured by Western blot analysis. Data are shown as the mean ± SEM. $^{*}p < 0.05$ vs. the control mice. $n = 3$ for each group.

of ETC-related proteins, Complex I-V subunits [41] (Figures 5(b) and 5(c)). In summary, the abnormal changes in many energy metabolism pathways, including the glycolysis (PGAM1), pyruvate oxidation and carboxylation (MPC2), and oxidative phosphorylation (OXPHOS) [42, 43], suggest that widespread disruption of brain energy metabolism occurs during mouse aging. As a process of the mitochondrial electron transport chain, oxidative phosphorylation is particularly important in the process of producing ATP, but as age increases, electrons leak and increase in reactive oxygen species, causing mitochondrial dysfunction and increased oxidative stress [44].

4.3. Oxidative Stress. Concomitantly, glutathione metabolism represents a key defense system that provides resistance to oxidative stress which involves increased protein glutathione S-transferase (GST), peroxidase (PRDX), and superoxide dismutase (SOD). During oxidative stress, GST protects against reactive molecules via catalyzing the nucleophilic attack of glutathione on electrophilic substrates [45]. Furthermore, the H2O2-scavenging peroxiredoxins (Prxs), a thiol-specific antioxidant enzyme with six isozymes (PRDX1, 2, 3, 4, 5, and 6) [46], play a significant effect on the regulation of reactive oxygen species (ROS) [47]. We found increased levels of GSTP1, GSTM1, and PRDX6 in the hippocampus and

(a)

(b)

(c)

(d)
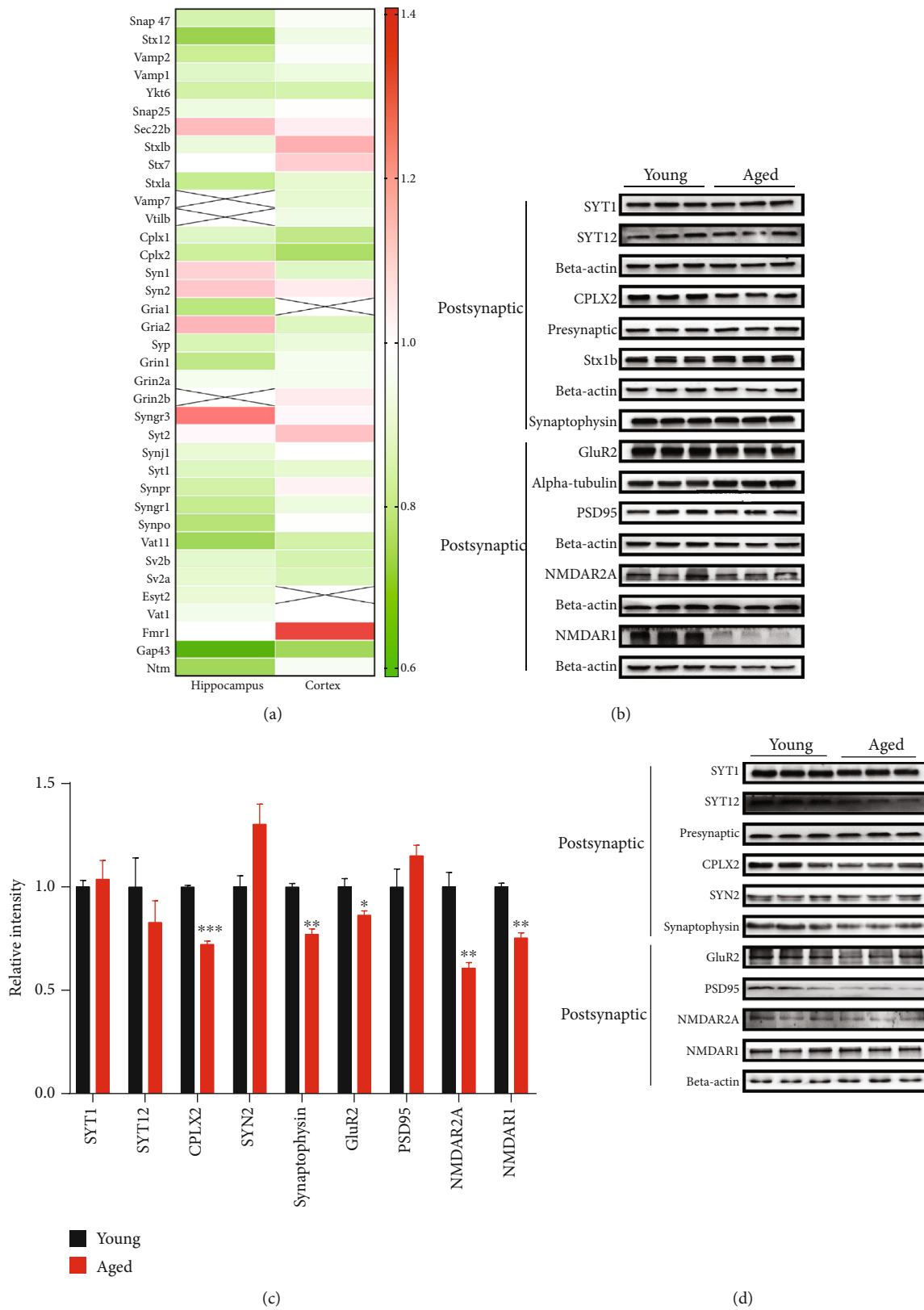
Figure 9: Continued.
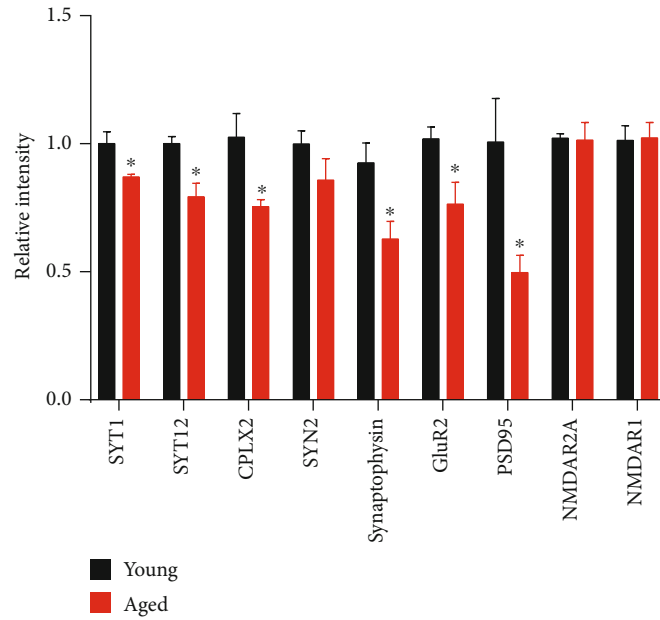
(e)

FIGURE 9: Validation of differentially expressed synaptic proteins by Western blot analysis. (a) Heat map analysis of synaptic proteins in the hippocampus and cerebral cortex. Red and green, respectively, indicate increased or decreased levels in 16-month-old vs. 4-month-old mice. X indicates unscreened protein. (b and c) Relative levels of hippocampal synaptic proteins in aged vs. young mice. (d and e) Relative levels of cerebral cortical synaptic proteins in aged vs. young mice. Data are presented as the mean ± SEM. $^*p < 0.05$, $^{**}p < 0.01$, and $^{***}p < 0.001$ vs. the control mice. $n = 3$ for each group.
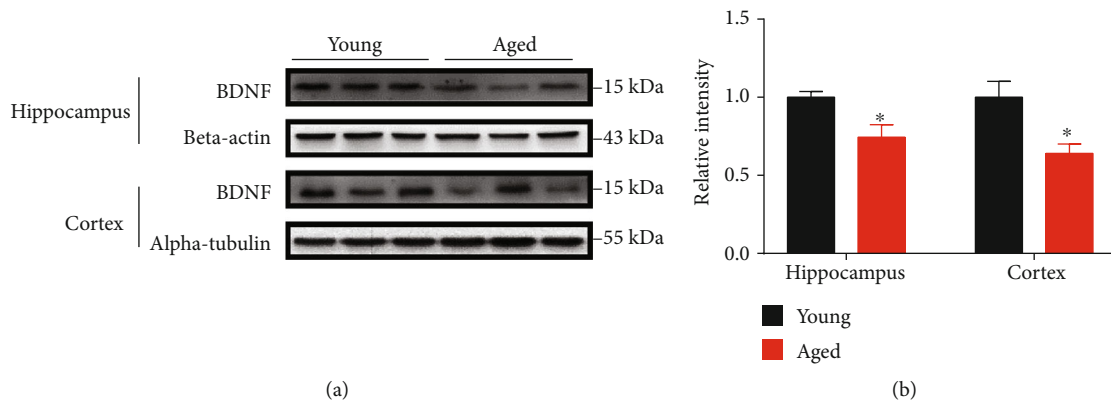
(a)

(b)

FIGURE 10: Expression level of BDNF analyzed by Western blot. (a and b) Relative levels of hippocampal and cortical BDNF in 16-month-old mice compared to 4-month-old mice. Data are shown as the mean ± SEM. $^*p < 0.05$ vs. the control mice. $n = 3$ for each group.

cerebral cortex of aged mice compared with young animals. A previous study also reported that the protein GSTP1 participating in the regulation of oxidative stress was significantly increased in the brain of aged rats [48]. Recent transcriptomics studies are in accordance with our results, since GST, subunits mu1, mu3, mu7, pi2, theta 1, and theta2 are all significantly increased in aged mouse brain tissue [49]. The increased levels of glutathione metabolism-related proteins GSTP1, GSTM1, and PRDX6 in aged vs. young brain suggest that a protective antioxidant compensatory mechanism becomes more active as aging advances [50].

4.4. Synaptic Dysfunction. Synaptic decline and plasticity deficiency contribute to age-related retardation in learning and memory [51], and there is also evidence of deficits in synaptic transmission [52] consistent with the decreased number of synaptic connections with the advance of age [53]. Our proteomics results show that aging promotes an overall imbalance of synapse-associated proteins. Consistent with the proteomics results, levels of complexin-2, synaptophysin, GLUR2, PSD95, NMDAR2A, and NMDAR1 were reduced significantly in aged mice contrasted with young mice. Synaptotagmin-12 is a synaptic vesicle phosphoprotein

that regulates the release of spontaneous neurotransmitters, controlled by cAMP-dependent phosphorylation. It is differentially expressed in the aging hippocampus and cerebral cortex of aging mice [54]. Complexin-2 plays an important regulatory role in synaptic structure and can be replaced by synaptic-binding proteins, facilitating transport of vesicles to synaptic membrane [55, 56]. Our observations suggest that aging causes a deficiency of synaptic connections and plasticity, supporting the theory of regulation or diminishment synaptic transmission with aging. A recent proteomics study of mouse brain found that in the learning and memory formation, the expression of some receptors and signaling cascade proteins of young and middle-aged mice is different significantly [10].

4.5. Cytoplasmic Ribosomes. Translation is the most important process in the regulation of protein expression that affects the ability of cellular proteins to stabilize, a function associated with the lifespan of multiple model organisms [57]. Numerous studies have shown that many ribosome-associated proteins and translational regulators are closely related to lifespan [58–60]. We found in aged vs. young mice that a large number of cytoplasmic ribosomes-related proteins were decreased in the hippocampus but not significantly altered in the cerebral cortex. In addition, it is well known that translation of ribosomal protein L4 (RPL4) is necessary for rapid axonal regeneration [61] and ribosomal protein S3 (RPS3) is involved in DNA repair mechanisms [62]. In sum, the overall decrease of ribosomal proteins may be closely related to the physiology of brain aging.

4.6. Loss of Neurotrophic Factor. BDNF (neurotrophin brain-derived neurotrophic factor) plays an important part in modulating the synaptic function of neurons. Following biosynthesis, the combination of BDNF to TrkB is required to transport BDNF from dense core vesicles to axon terminals, where it is secreted into the synaptic cleft following membrane depolarization [63, 64]. The efficacy of excitatory synapses is enhanced by recombinant BDNF delivery to hippocampal slices [65, 66]. These effects are primarily mediated through changes in NMDA receptor function [67]. A more recent study showed that BDNF can enhance mitochondrial ATP production by increasing respiratory coupling, thus contributing to neuroprotective mechanisms associated with neural plasticity [68].

In addition to neural plasticity, studies have clearly shown that BDNF plays an important role in a variety of nerve damages, and its reduction is closely related to a variety of neurodegenerative diseases. [19, 20]. Moderate amounts of BDNF exposed to hippocampus or cortical neurons prevent acute and/or chronic neurodegenerative diseases associated with: mitochondria toxins [68], oxidative stressors [69], glucose and oxygen deprivation [70], glutamate and excitotoxins [71, 72], and amyloid-β peptide [73]. In this study, we found that compared with young mice, the level of BDNF in hippocampus of aged mice was significantly reduced, indicating that decreased BDNF may contribute to brain aging by disrupting multiple complex physiological processes, including

mitochondrial dysregulation, energy metabolism, synaptic dysfunction, and oxidative stress.

5. Conclusions

In summary, a lot of proteins in the hippocampus and cerebral cortex of aged mice were differentially expressed. Such changes predictably promote the decline of physiological brain function by decreasing ATP content, increasing DNA oxidative damage, and synaptic dysfunction. Hippocampal and cortical proteomics and bioinformatic analysis revealed that aging is related to abnormal expression of proteins related to mitochondrial dynamics (FIS1, DRP1), energy metabolism (PGAM1, MPC2), oxidative stress (PRDX6, GSTM1, and GSTP1), synapses (SYT12, GLUR2), ribosome (RPL4, RPS3), loss of neurotrophic factor, transcriptional regulation, and GTPase function. Through comprehensive proteomic analysis, we can reasonably interpret the functional significance of altered protein profiles in the brains of early aging mice, as well as the relationships and pathways involved in various physiological/pathological processes.

The critical importance of diet composition and housing conditions in regulating the longevity of mice may limit the generalizability of our observations across laboratories. While every effort was made to standardize these variables, longevity outcomes may vary across laboratories even when the same strain, diet, and husbandry practices are employed. In this study, 10 male mice were housed in a large cage ($470 \times 350 \times 200$ mm). I believe this is a limitation of this study, housing one-group mice in a big cage, although previous data showed no significant change in the aging characteristics explored between the mice (8-10 mice) housed in a big cage and the mice housed in a small age (3-5 mice) [16, 74]. Median lifespan variations of up to 31% (704-925 days) have been observed for a single mouse strain housed and fed under identical conditions in collaborating laboratories, and strain and sex differences can modify responses to dietary restriction, which is known to extend the lifespan. Furthermore, the food intake of mice, which in turn can affect lifespan, is greater when animals are held in rooms at temperatures lower than their thermoneutral zones (30-34°C) [75].

Data Availability

All data used to support the findings of this study are included within the article. Raw data used to generate the figures are available from the corresponding author upon request.

Conflicts of Interest

The authors declare that they have no conflict of interest to disclose.

Authors' Contributions

Yingchao Li and Haitao Yu contributed equally to this work.

Acknowledgments

Supplementary Materials

Supplementary 1. Supplementary Excel 1: all the proteins of the hippocampus and cerebral cortex identified by the mass spectra.

Supplementary 2. Supplementary Excel 2: all verification raw data of Western blot analysis.

References

[1] J. V. Hindle, "Ageing, neurodegeneration and Parkinson's disease," *Age and Ageing*, vol. 39, no. 2, pp. 156–161, 2010.

[2] N. A. Bishop, T. Lu, and B. A. Yankner, "Neural mechanisms of ageing and cognitive decline," *Nature*, vol. 464, no. 7288, pp. 529–535, 2010.

[3] R. A. Scheltema, J. P. Hauschild, O. Lange et al., "The Q Exactive HF, a Benchtop mass spectrometer with a pre-filter, high-performance quadrupole and an ultra-high-field Orbitrap analyzer," *Molecular & Cellular Proteomics*, vol. 13, no. 12, pp. 3698–3708, 2014.

[4] C. H. Jiang, J. Z. Tsien, P. G. Schultz, and Y. Hu, "The effects of aging on gene expression in the hypothalamus and cortex of mice," *Proceedings of the National Academy of Sciences of the United States of America*, vol. 98, no. 4, pp. 1930–1934, 2001.

[5] C. K. Lee, R. Weindruch, and T. A. Prolla, "Gene-expression profile of the ageing brain in mice," *Nature Genetics*, vol. 25, no. 3, pp. 294–297, 2000.

[6] P. M. Loerch, T. Lu, K. A. Dakin et al., "Evolution of the aging brain transcriptome and synaptic regulation," *PLoS One*, vol. 3, no. 10, article e3329, 2008.

[7] D. M. Walther and M. Mann, "Accurate quantification of more than 4000 mouse tissue proteins reveals minimal proteome changes during aging," *Molecular & Cellular Proteomics*, vol. 10, no. 2, p. M110.004523, 2011.

[8] S. Yang, T. Liu, S. Li et al., "Comparative proteomic analysis of brains of naturally aging mice," *Neuroscience*, vol. 154, no. 3, pp. 1107–1120, 2008.

[9] D. Drulis-Fajdasz, A. Gizak, T. Wojtowicz, J. R. Wisniewski, and D. Rakus, "Aging-associated changes in hippocampal glycogen metabolism in mice. Evidence for and against astrocyte-to-neuron lactate shuttle," *Glia*, vol. 66, no. 7, pp. 1481–1495, 2018.

[10] P. Duda, O. Wojcicka, J. R. Wisniewski, and D. Rakus, "Global quantitative TPA-based proteomics of mouse brain structures reveals significant alterations in expression of proteins involved in neuronal plasticity during aging," *Aging*, vol. 10, no. 7, pp. 1682–1697, 2018.

[11] E. M. Simpson, C. C. Linder, E. E. Sargent, M. T. Davisson, L. E. Mobraaten, and J. J. Sharp, "Genetic variation among 129 substrains and its importance for targeted mutagenesis in mice," *Nature Genetics*, vol. 16, no. 1, pp. 19–27, 1997.

[12] D. W. Huang, B. T. Sherman, and R. A. Lempicki, "Bioinformatics enrichment tools: paths toward the comprehensive functional analysis of large gene lists," *Nucleic Acids Research*, vol. 37, no. 1, pp. 1–13, 2009.

[13] D. W. Huang, B. T. Sherman, and R. A. Lempicki, "Systematic and integrative analysis of large gene lists using DAVID bioinformatics resources," *Nature Protocols*, vol. 4, no. 1, pp. 44–57, 2009.

[14] B. Xu, Y. Gao, S. Zhan et al., "Quantitative protein profiling of hippocampus during human aging," *Neurobiology of Aging*, vol. 39, pp. 46–56, 2016.

[15] H. Yu, X. Jiang, X. Lin et al., "Hippocampal subcellular organelle proteomic alteration of copper-treated mice," *Toxicological Sciences*, vol. 164, no. 1, pp. 250–263, 2018.

[16] H. Yu, X. Lin, D. Wang et al., "Mitochondrial molecular abnormalities revealed by proteomic analysis of hippocampal organelles of mice triple transgenic for Alzheimer disease," *Frontiers in Molecular Neuroscience*, vol. 11, p. 74, 2018.

[17] H. Yu, D. Wang, L. Zou et al., "Proteomic alterations of brain subcellular organelles caused by low-dose copper exposure: implication for Alzheimer's disease," *Archives of Toxicology*, vol. 92, no. 4, pp. 1363–1382, 2018.

[18] M. Dobrivojevic, N. Habek, K. Kapuralin, M. Curlin, and S. Gajovic, "Krüppel-like transcription factor 8 (Klf8) is expressed and active in the neurons of the mouse brain," *Gene*, vol. 570, no. 1, pp. 132–140, 2015.

[19] A. M. Marini, X. Jiang, X. Wu et al., "Preconditioning and neurotrophins: a model for brain adaptation to seizures, ischemia and other stressful stimuli," *Amino Acids*, vol. 32, no. 3, pp. 299–304, 2007.

[20] M. Jiang, J. Wang, J. Fu et al., "Neuroprotective role of Sirt1 in mammalian models of Huntington's disease through activation of multiple Sirt1 targets," *Nature Medicine*, vol. 18, no. 1, pp. 153–158, 2011.

[21] H. S. Hamezah, L. W. Durani, D. Yanagisawa et al., "Proteome profiling in the hippocampus, medial prefrontal cortex, and striatum of aging rat," *Experimental Gerontology*, vol. 111, pp. 53–64, 2018.

[22] M. Manczak, M. J. Calkins, and P. H. Reddy, "Impaired mitochondrial dynamics and abnormal interaction of amyloid beta with mitochondrial protein Drp1 in neurons from patients with Alzheimer's disease: implications for neuronal damage," *Human Molecular Genetics*, vol. 20, no. 13, pp. 2495–2509, 2011.

[23] U. P. Shirendeb, M. J. Calkins, M. Manczak et al., "Mutant huntingtin's interaction with mitochondrial protein Drp1 impairs mitochondrial biogenesis and causes defective axonal transport and synaptic degeneration in Huntington's disease," *Human Molecular Genetics*, vol. 21, no. 2, pp. 406–420, 2011.

[24] M. Manczak and P. H. Reddy, "Abnormal interaction between the mitochondrial fission protein Drp1 and hyperphosphorylated tau in Alzheimer's disease neurons: implications for mitochondrial dysfunction and neuronal damage," *Human Molecular Genetics*, vol. 21, no. 11, pp. 2538–2547, 2012.

[25] Q. Zhang, J. Wu, R. Wu et al., "DJ-1 promotes the proteasomal degradation of Fis1: implications of DJ-1 in neuronal protection," *The Biochemical Journal*, vol. 447, no. 2, pp. 261–269, 2012.

[26] Y. J. Lee, S. Y. Jeong, M. Karbowski, C. L. Smith, and R. J. Youle, "Roles of the mammalian mitochondrial fission and fusion mediators Fis1, Drp1, and Opa1 in apoptosis," *Molecular Biology of the Cell*, vol. 15, no. 11, pp. 5001–5011, 2004.

[27] Y. S. Yoon, D. S. Yoon, I. K. Lim et al., "Formation of elongated giant mitochondria in DFO-induced cellular senescence: involvement of enhanced fusion process through modulation of Fis1," *Journal of Cellular Physiology*, vol. 209, no. 2, pp. 468–480, 2006.

[28] M. Roy, P. H. Reddy, M. Iijima, and H. Sesaki, "Mitochondrial division and fusion in metabolism," *Current Opinion in Cell Biology*, vol. 33, pp. 111–118, 2015.

[29] P. H. Reddy, T. P. Reddy, M. Manczak, M. J. Calkins, U. Shirendeb, and P. Mao, "Dynamin-related protein 1 and mitochondrial fragmentation in neurodegenerative diseases," *Brain Research Reviews*, vol. 67, no. 1-2, pp. 103–118, 2011.

[30] H. Chen and D. C. Chan, "Mitochondrial dynamics–fusion, fission, movement, and mitophagy–in neurodegenerative diseases," *Human Molecular Genetics*, vol. 18, no. R2, pp. R169–R176, 2009.

[31] X. Wang, B. Su, H. Fujioka, and X. Zhu, "Dynamin-like protein 1 reduction underlies mitochondrial morphology and distribution abnormalities in fibroblasts from sporadic Alzheimer's disease patients," *The American Journal of Pathology*, vol. 173, no. 2, pp. 470–482, 2008.

[32] X. Wang, G. Perry, M. A. Smith, and X. Zhu, "Amyloid-beta-derived diffusible ligands cause impaired axonal transport of mitochondria in neurons," *Neurodegenerative Diseases*, vol. 7, no. 1-3, pp. 56–59, 2010.

[33] T. Uo, J. Dworzak, C. Kinoshita et al., "Drp1 levels constitutively regulate mitochondrial dynamics and cell survival in cortical neurons," *Experimental Neurology*, vol. 218, no. 2, pp. 274–285, 2009.

[34] H. Otera, N. Ishihara, and K. Mihara, "New insights into the function and regulation of mitochondrial fission," *Biochimica et Biophysica Acta*, vol. 1833, no. 5, pp. 1256–1268, 2013.

[35] L. C. Gomes and L. Scorrano, "Mitochondrial morphology in mitophagy and macroautophagy," *Biochimica et Biophysica Acta*, vol. 1833, no. 1, pp. 205–212, 2013.

[36] M. Liesa and O. S. Shirihai, "Mitochondrial dynamics in the regulation of nutrient utilization and energy expenditure," *Cell Metabolism*, vol. 17, no. 4, pp. 491–506, 2013.

[37] P. H. Reddy, "Mitochondrial medicine for aging and neurodegenerative diseases," *Neuromolecular Medicine*, vol. 10, no. 4, pp. 291–315, 2008.

[38] M. Manczak, Y. Jung, B. S. Park, D. Partovi, and P. H. Reddy, "Time-course of mitochondrial gene expressions in mice brains: implications for mitochondrial dysfunction, oxidative damage, and cytochrome c in aging," *Journal of Neurochemistry*, vol. 92, no. 3, pp. 494–504, 2005.

[39] L. A. Fothergill-Gilmore and H. C. Watson, "The phosphoglycerate mutases," *Advances in Enzymology and Related Areas of Molecular Biology*, vol. 62, pp. 227–313, 1989.

[40] K. S. McCommis and B. N. Finck, "Mitochondrial pyruvate transport: a historical perspective and future research directions," *The Biochemical Journal*, vol. 466, no. 3, pp. 443–454, 2015.

[41] N. Yadav and D. Chandra, "Mitochondrial DNA mutations and breast tumorigenesis," *Biochimica et Biophysica Acta*, vol. 1836, no. 2, pp. 336–344, 2013.

[42] M. Saraste, "Oxidative phosphorylation at the fin de siècle," *Science*, vol. 283, no. 5407, pp. 1488–1493, 1999.

[43] D. D. Newmeyer and S. Ferguson-Miller, "Mitochondria: releasing power for life and unleashing the machineries of death," *Cell*, vol. 112, no. 4, pp. 481–490, 2003.

[44] D. C. Liemburg-Apers, P. H. Willems, W. J. Koopman, and S. Grefte, "Interactions between mitochondrial reactive oxygen species and cellular glucose metabolism," *Archives of Toxicology*, vol. 89, no. 8, pp. 1209–1226, 2015.

[45] J. Pajaud, S. Kumar, C. Rauch, F. Morel, and C. Aninat, "Regulation of signal transduction by glutathione transferases," *International Journal of Hepatology*, vol. 2012, Article ID 137676, 11 pages, 2012.

[46] M. H. Park, M. Jo, Y. R. Kim, C. K. Lee, and J. T. Hong, "Roles of peroxiredoxins in cancer, neurodegenerative diseases and inflammatory diseases," *Pharmacology & Therapeutics*, vol. 163, pp. 1–23, 2016.

[47] B. Kim, J. Park, K. T. Chang, and D. S. Lee, "Peroxiredoxin 5 prevents amyloid-beta oligomer-induced neuronal cell death by inhibiting ERK–Drp1-mediated mitochondrial fragmentation," *Free Radical Biology & Medicine*, vol. 90, pp. 184–194, 2016.

[48] E. Martinez-Lara, E. Siles, R. Hernandez et al., "Glutathione S-transferase isoenzymatic response to aging in rat cerebral cortex and cerebellum," *Neurobiology of Aging*, vol. 24, no. 3, pp. 501–509, 2003.

[49] C. Frahm, A. Srivastava, S. Schmidt et al., "Transcriptional profiling reveals protective mechanisms in brains of long- lived mice," *Neurobiology of Aging*, vol. 52, pp. 23–31, 2017.

[50] L. W. Durani, H. S. Hamezah, N. F. Ibrahim et al., "Age-related changes in the metabolic profiles of rat hippocampus, medial prefrontal cortex and striatum," *Biochemical and Biophysical Research Communications*, vol. 493, no. 3, pp. 1356–1363, 2017.

[51] T. C. Foster, "Involvement of hippocampal synaptic plasticity in age-related memory decline," *Brain Research. Brain Research Reviews*, vol. 30, no. 3, pp. 236–249, 1999.

[52] C. A. Barnes, "Normal aging: regionally specific changes in hippocampal synaptic transmission," *Trends in Neurosciences*, vol. 17, no. 1, pp. 13–18, 1994.

[53] D. L. Dickstein, D. Kabaso, A. B. Rocher, J. I. Luebke, S. L. Wearne, and P. R. Hof, "Changes in the structural complexity of the aged brain," *Aging Cell*, vol. 6, no. 3, pp. 275–284, 2007.

[54] A. Maximov, O. H. Shin, X. Liu, and T. C. Sudhof, "Synaptotagmin-12, a synaptic vesicle phosphoprotein that modulates spontaneous neurotransmitter release," *The Journal of Cell Biology*, vol. 176, no. 1, pp. 113–124, 2007.

[55] J. J. Hill, D. A. Callaghan, W. Ding, J. F. Kelly, and B. R. Chakravarthy, "Identification of okadaic acid-induced phosphorylation events by a mass spectrometry approach," *Biochemical and Biophysical Research Communications*, vol. 342, no. 3, pp. 791–799, 2006.

[56] K. Reim, M. Mansour, F. Varoqueaux et al., "Complexins regulate a late step in Ca2+-dependent neurotransmitter release," *Cell*, vol. 104, no. 1, pp. 71–81, 2001.

[57] B. K. Kennedy and M. Kaeberlein, "Hot topics in aging research: protein translation, 2009," *Aging Cell*, vol. 8, no. 6, pp. 617–623, 2009.

[58] A. N. Rogers, D. Chen, G. McColl et al., "Life span extension via eIF4G inhibition is mediated by posttranscriptional remodeling of stress response gene expression in C. elegans," *Cell Metabolism*, vol. 1, pp. 55–66, 2011.

[59] K. Z. Pan, J. E. Palter, A. N. Rogers et al., "Inhibition of mRNA translation extends lifespan in Caenorhabditis elegans," *Aging Cell*, vol. 6, no. 1, pp. 111–119, 2007.

[60] B. M. Zid, A. N. Rogers, S. D. Katewa et al., "4E-BP extends lifespan upon dietary restriction by enhancing mitochondrial activity in Drosophila," *Cell*, vol. 139, no. 1, pp. 149–160, 2009.

[61] J. L. Twiss, D. S. Smith, B. Chang, and E. M. Shooter, "Translational control of ribosomal protein L4 mRNA is required for rapid neurite regeneration," *Neurobiology of Disease*, vol. 7, no. 4, pp. 416–428, 2000.

[62] C. H. Lee, K. Y. Yoo, J. H. Choi, I. K. Hwang, S. Y. Choi, and M. H. Won, "Ribosomal protein s3 immunoreactivity in the young, adult and aged gerbil hippocampus," *The Journal of Veterinary Medical Science*, vol. 73, no. 3, pp. 361–365, 2011.

[63] J. M. Conner, J. C. Lauterborn, Q. Yan, C. M. Gall, and S. Varon, "Distribution of brain-derived neurotrophic factor (BDNF) protein and mRNA in the normal adult rat CNS: evidence for anterograde axonal transport," *The Journal of Neuroscience*, vol. 17, no. 7, pp. 2295–2313, 1997.

[64] S. Dieni, T. Matsumoto, M. Dekkers et al., "BDNF and its propeptide are stored in presynaptic dense core vesicles in brain neurons," *The Journal of Cell Biology*, vol. 196, no. 6, pp. 775–788, 2012.

[65] M. Korte, P. Carroll, E. Wolf, G. Brem, H. Thoenen, and T. Bonhoeffer, "Hippocampal long-term potentiation is impaired in mice lacking brain-derived neurotrophic factor," *Proceedings of the National Academy of Sciences of the United States of America*, vol. 92, no. 19, pp. 8856–8860, 1995.

[66] S. L. Patterson, T. Abel, T. A. S. Deuel, K. C. Martin, J. C. Rose, and E. R. Kandel, "Recombinant BDNF rescues deficits in basal synaptic transmission and hippocampal LTP in BDNF knockout mice," *Neuron*, vol. 16, no. 6, pp. 1137–1145, 1996.

[67] H. Park and M. M. Poo, "Neurotrophin regulation of neural circuit development and function," *Nature Reviews Neuroscience*, vol. 14, no. 1, pp. 7–23, 2013.

[68] A. Markham, I. Cameron, R. Bains et al., "Brain-derived neurotrophic factor-mediated effects on mitochondrial respiratory coupling and neuroprotection share the same molecular signalling pathways," *The European Journal of Neuroscience*, vol. 35, no. 3, pp. 366–374, 2012.

[69] M. M. Harper, L. Adamson, B. Blits, M. B. Bunge, S. D. Grozdanic, and D. S. Sakaguchi, "Brain-derived neurotrophic factor released from engineered mesenchymal stem cells attenuates glutamate- and hydrogen peroxide-mediated death of staurosporine-differentiated RGC-5 cells," *Experimental Eye Research*, vol. 89, no. 4, pp. 538–548, 2009.

[70] B. Cheng and M. P. Mattson, "NT-3 and BDNF protect CNS neurons against metabolic/excitotoxic insults," *Brain Research*, vol. 640, no. 1-2, pp. 56–67, 1994.

[71] A. Wu, Z. Ying, and F. Gomez-Pinilla, "The interplay between oxidative stress and brain-derived neurotrophic factor modulates the outcome of a saturated fat diet on synaptic plasticity and cognition," *The European Journal of Neuroscience*, vol. 19, no. 7, pp. 1699–1707, 2004.

[72] X. Wu, D. Zhu, X. Jiang et al., "AMPA protects cultured neurons against glutamate excitotoxicity through a phosphatidylinositol 3-kinase-dependent activation in extracellular signal-regulated kinase to upregulate BDNF gene expression," *Journal of Neurochemistry*, vol. 90, no. 4, pp. 807–818, 2004.

[73] S. E. Counts and E. J. Mufson, "Noradrenaline activation of neurotrophic pathways protects against neuronal amyloid toxicity," *Journal of Neurochemistry*, vol. 113, no. 3, pp. 649–660, 2010.

[74] C. Chen, X. Jiang, Y. Li et al., "Low-dose oral copper treatment changes the hippocampal phosphoproteomic profile and perturbs mitochondrial function in a mouse model of Alzheimer's disease," *Free Radical Biology & Medicine*, vol. 135, pp. 144–156, 2019.

[75] V. K. Gibbs and D. L. Smith Jr., "Nutrition and energetics in rodent longevity research," *Experimental Gerontology*, vol. 86, pp. 90–96, 2016.

Research Article

(–)-Epicatechin Modulates Mitochondrial Redox in Vascular Cell Models of Oxidative Stress

Amy Keller [ID],[1,2] **Sara E. Hull,**[1,2] **Hanan Elajaili** [ID],[3] **Aspen Johnston,**[1] **Leslie A. Knaub,**[1,2] **Ji Hye Chun,**[1,2] **Lori Walker,**[4] **Eva Nozik-Grayck,**[3] **and Jane E. B. Reusch**[1,2]

[1]*Division of Endocrinology, Metabolism & Diabetes, University of Colorado Anschutz Medical Campus, Aurora, CO 80045, USA*
[2]*Rocky Mountain Regional VA Medical Center, Aurora, CO 80045, USA*
[3]*Cardiovascular Pulmonary Research Laboratories and Pediatric Critical Care, University of Colorado Anschutz Medical Campus, Aurora, CO 80045, USA*
[4]*Division of Cardiology, University of Colorado Anschutz Medical Campus, Aurora, CO 80045, USA*

Correspondence should be addressed to Amy Keller; amy.keller@ucdenver.edu

Diabetes mellitus affects 451 million people worldwide, and people with diabetes are 3-5 times more likely to develop cardiovascular disease. In vascular tissue, mitochondrial function is important for vasoreactivity. Diabetes-mediated generation of excess reactive oxygen species (ROS) may contribute to vascular dysfunction via damage to mitochondria and regulation of endothelial nitric oxide synthase (eNOS). We have identified (–)-epicatechin (EPICAT), a plant compound and known vasodilator, as a potential therapy. We hypothesized that mitochondrial ROS in cells treated with antimycin A (AA, a compound targeting mitochondrial complex III) or high glucose (HG, global perturbation) could be normalized by EPICAT, and correlate with improved mitochondrial dynamics and cellular signaling. Human umbilical vein endothelial cells (HUVEC) were treated with HG, AA, and/or 0.1 or 1.0 μM of EPICAT. Mitochondrial and cellular superoxide, mitochondrial respiration, and cellular signaling upstream of mitochondrial function were assessed. EPICAT at 1.0 μM significantly attenuated mitochondrial superoxide in HG-treated cells. At 0.1 μM, EPICAT nonsignificantly increased mitochondrial respiration, agreeing with previous reports. EPICAT significantly increased complex I expression in AA-treated cells, and 1.0 μM EPICAT significantly decreased mitochondrial complex V expression in HG-treated cells. No significant effects were seen on either AMPK or eNOS expression. Our study suggests that EPICAT is useful in mitigating moderate ROS concentrations from a global perturbation and may modulate mitochondrial complex activity. Our data illustrate that EPICAT acts in the cell in a dose-dependent manner, demonstrating hormesis.

1. Introduction

Diabetes mellitus (DM) confers an excess risk of cardiovascular disease (CVD), preceded by dysfunction in vascular reactivity [1]. In the context of DM, excess reactive oxygen species (ROS) correlate with vascular inflammation and vascular stiffness [2–4]. Disruptions in redox regulation and elevated ROS are linked to hyperglycemia, dampened antioxidant defenses, insulin resistance, and dysfunctional cellular signaling [2, 3, 5–8]. It is established that elevated ROS promotes vascular pathology; however, multiple clinical attempts at establishing the efficacy of antioxidants have failed [9, 10]. Stochiometric approaches to excess ROS allevi-

ation do not consider the important signaling role of ROS in cellular homeostasis [11, 12]. Therefore, studies targeting elevated ROS must approach redox from a broad perspective. For example, mitochondria are a central source of cellular superoxide under normal physiological conditions; however, excess mitochondrial-derived oxidative damage has been shown to cause age-related vascular inflammation and arterial stiffness [13–16]. As the mitochondrial function is critical to effective vasoreactivity, targeting redox homeostasis in this organelle is a promising therapeutic direction.

Flavonoids are a class of botanical compounds found ubiquitously in common plant-based foods that impact vasomotion. Flavonoids are characterized by a two-benzene ring

basal structure and include well-known subclasses of compounds such as anthocyanins and catechins; as a class, these chemicals promote vasodilation and have specific antioxidant activity [17, 18]. The botanical flavonoid (–)-epicatechin (EPICAT) is found in commonly consumed foods, primarily chocolate (*Theobroma cacao*, Sterculiaceae) and tea (*Camellia sinensis*, Theaceae). This compound has been shown to induce vasorelaxation in rat femoral artery ex vivo, increase mitochondrial respiration in cardiomyocytes, prevent derangements in mitochondrial membrane potential and decrease in mitochondrial complex expression in mouse kidney cells, and activate nitric oxide synthase (NOS) activity, the enzyme upstream of both vasodilation and mitochondrial activity, in rat aorta and human coronary arterial endothelial cells [19–23].

Importantly, EPICAT has been reported to have antioxidant activity in multiple tissues and cells. Specifically, EPICAT supports the activation of ROS-regulating transcription factors and decreases ROS in aortic rings and HepG2 cells, measured with immunohistochemistry (IHC) and dihydroethidium (DHE) [24, 25]. EPICAT inhibits cardiac, hepatic, adipose, and HepG2 ROS-generating enzymatic or protein expression activity, such as NADPH oxidases (NOXs) and related proteins [26–28]. EPICAT has also been shown to alleviate hydrogen peroxide production in damaged cardiac and brain mitochondria by modifying mitochondrial respiration [29]. In plasma and urine, EPICAT promotes the activity of superoxide dismutase (SOD) and glutathione peroxidase [30]. In human lung fibroblasts, EPICAT restored SOD activity and complex I expression dampened by damaged mitochondria [31]. Despite this consistent antioxidant paradigm in numerous models and tissues, EPICAT's mechanism(s) at the cellular level remain largely unverified.

We hypothesized that in a vascular cell model, human umbilical vein endothelial cells (HUVECs), treated with antimycin (mitochondrial perturbation, AA) or high glucose (cellular perturbation, HG) will generate mitochondrial ROS and that treatment with EPICAT will reduce mitochondrial ROS concentrations while not impacting untreated cells, restoring mitochondrial function and cellular homeostasis. We chose these two cellular perturbations to test EPICAT against oxidative stress targeted to the mitochondria as well as global cellular stress. It is imperative to have these two models, as EPICAT has mixed results as an antioxidant. Employing a mitochondrial specific versus global model allows for specific determination about its activity. Here, we report our results from testing concentrations of 0.1 or $1.0\,\mu M$ of EPICAT, based on previous literature, in cells exposed to either AA or HG. We measured cytosolic or mitochondrial-derived superoxide, mitochondrial respiration, and cellular nutrient signaling, as well as endogenous redox defenses. Our study demonstrates the dose-dependent redox and mitochondrial regulatory activity of EPICAT. This effect is of interest for diseases characterized by chronic redox dysfunction impacting the vasculature, such as diabetes. To our knowledge, this is a singular, comprehensive effort to investigate EPICAT's bioactivity in a human vascular cell model with the goal of expanding the understanding of the actions of this compound beyond its well-established activity as a vasodilator.

2. Methods and Materials

2.1. Reagents. For cell culture, Hyclone Ham's Nutrient Mixture F12 Media (Fisher #SH30526.01) was purchased from Fisher. Penicillin/streptomycin, trypsin, and fetal bovine serum (FBS) were purchased from Gemini Bioproducts (CA, USA). For Western blotting and general experiments, gels were from BioRad, PVDF membranes from Millipore, fluorescent secondary antibodies were from Licor. Mammalian Protein Extraction Reagent (M-PER,) was obtained from Thermo Scientific Hyclone (MA, USA), and dimethyl sulfoxide (DMSO), sodium chloride, sucrose, and bovine serum albumin were purchased from Fisher Scientific (PA, USA). For Western blot and respiration experiments, collagenase, ethylenediaminetetraacetic acid (EDTA), ethylene glycol tetraacetic acid (EGTA), sodium pyrophosphate, sodium orthovanadate, sodium fluoride, okadaic acid, 1% protease inhibitor cocktail, dithiothreitol, magnesium chloride, K-lactobionate, taurine, potassium phosphate, HEPES, digitonin, pyruvate, malic acid, glutamic acid, adenosine diphosphate, succinic acid, oligomycin, carbonyl cyanide 4 (trifluoromethoxy)phenylhydrazone (FCCP), antibody to β-actin (mouse), phenylephrine and acetylcholine, trypsin inhibitor, and cytochrome c were procured from Sigma-Aldrich (MO, USA). EPICAT was sourced from Cayman Chemical (MI, USA).

2.2. Antibodies. Antibodies to total adenosine monophosphate kinase (AMPK, Cell Signaling #2532S, 1 : 500, mouse), phosphorylated AMPK (pAMPK, Cell Signaling #2532S, 1 : 500, rabbit), Sirtuin 3 (SIRT3, Cell Signaling #2627S, 1 : 500, rabbit), total endothelial nitric oxide synthase (eNOS, Cell Signaling #9572S, 1 : 500-1 : 250, mouse), Ser1177 phosphorylated eNOS (Cell Signaling #9571S, 1 : 500-1 : 250 rabbit), were obtained from Cell Signaling (MA, USA). Antibody cocktail to representative subunits of mitochondrial oxidative phosphorylation (Total OXPHOS Blue Native WB Antibody Cocktail Abcam #ab110412, 1 : 1000-1 : 500, mouse) complexes I (subunit NDUFA9), II (subunit SDHA), III (subunit UQCRC2), IV (subunit IV), and V (subunit ATP5A); PPARγ coactivator 1 alpha (PGC-1α, Abcam #ab54481, 1 : 500, rabbit); and MnSOD antibody (Anti-SOD2/MnSOD antibody [2a1], Abcam, #ab16956, 1 : 1000-1 : 500) were obtained from Abcam (Cambridge, MA). Secondary Fluorescent antibodies (IRDye 680RD goat antimouse, Li-COR, #926-68070 1 : 5,000, IRDye 680RD goat antirabbit, Li-COR, #926-68071 1 : 5,000, IRDye 800CW goat antimouse, Li-COR, #926-32210, 1 : 10,000, IRDy 800CW goat antirabbit, Li-COR, #926-32211, 1 : 10,000) for Western blot detection were purchased from Li-COR (NE, USA).

2.3. Cell Experiments. Human umbilical vein endothelial cells (HUVECs) were purchased from ATCC and grown in media supplemented with 10% FBS and 1% penicillin/streptomycin at 7 mM glucose. Cells were incubated in 0.1% FBS starvation media for 12-15 hours. HUVECs were then preincubated for 1 hour with either 0.1 or $1.0\,\mu M$ EPICAT diluted into

phosphate-buffered saline (PBS) or PBS alone. Following this incubation, antimycin (10 μM, AA), ethanol, glucose (30 mM, high glucose [HG]), or PBS were directly added into media for a 2-hour incubation. The antimycin concentration was chosen based on previous studies of mitochondrial ROS generation [32, 33]. Cells were then harvested for electron paramagnetic resonance spectroscopy, respiration, or Western blotting. No evidence of cell death was observed. All experiments were conducted in triplicate or quadruplicate.

2.4. Electron Paramagnetic Resonance Spectroscopy (EPR).

Total ROS production was measured by EPR using the superoxide sensitive spin probe 1-hydroxy-3-methoxycarbonyl-2,2,5,5-tetramethylpyrrolidine (CMH), while mitochondrial ROS production was measured using the mitochondrial spin probe 1-hydroxy-4-[2-triphenylphosphonio)-acetamido]-2,2,6,6-tetramethyl-piperidine,1-hydroxy-2,2,6,6-tetramethyl-4-[2-(triphenylphosphonio)acetamido] piperidinium dichloride (mito-TEMPO-H). HUVEC Cells were seeded in 6-well plates, and experiments were completed prior to the EPR measurements. Spin probes CMH and mito-TEMPO-H were prepared in deoxygenated 50 mM phosphate buffer. Cells were washed and treated with CMH and mito-TEMPO-H 0.25 mM in Krebs-HEPES buffer (KHB) containing 100 μM of a metal chelator DTPA. Cells were incubated for 50 min at 37°C then gently scraped and transferred to ice. 50 μl of cell suspension was loaded in an EPR capillary tube, and EPR measurements were performed at room temperature using Bruker EMXnano X-band spectrometer. EPR acquisition parameters are microwave frequency = 9.6 GHz; center field = 3432 G; modulation amplitude = 2.0 G; sweep width = 80 G; microwave power = 19.9 mW; total number of scans = 10; sweep time = 12.11 s; and time constant = 20.48 ms. CMH or mito-TEMPO-H both are detected as nitroxide radicals; the concentration was obtained by simulating the spectra using the SpinFit module incorporated in the Xenon software of the bench-top EMXnano EPR spectrometer followed by the SpinCount module (Bruker). Nitroxide concentrations were normalized to total protein.

2.5. Western Blotting.

HUVECs were harvested in 4°C mammalian lysis buffer (MPER with 150 mM sodium chloride, 1 mM of EDTA, 1 mM EGTA, 5 mM sodium pyrophosphate, 1 mM sodium orthovanadate, 20 mM sodium fluoride, 500 nM okadaic acid, 1% protease inhibitor cocktail), and protein was measured using Western blotting as previously described [34]. Cell lysates were sonicated at 4°C centrifuged at 18,000 x g at 4°C for 10 min, and the Bradford protein assay was used to measure the protein concentration of the lysate. Protein samples (15 μg to 40 μg) in Laemmli sample buffer (boiled with 100 mM dithiothreitol) were run on precast SDS-4-15% polyacrylamide gels. Proteins were transferred to PVDF membranes. Ponceau S staining was used to evaluate protein loading. Blots were probed with antibodies described above and left overnight at 4°C. Fluorescent secondary antibodies were applied following the primary antibody incubation (1 : 10,000 IRDye800CW and 1 : 5,000 IRDye680RD, 1 hour at room

temperature). Proteins were detected by fluorescence with the Li-COR Odyssey CLX, and Image Studio v 4.1 was used for densitometric analysis. All protein data has been normalized to β-actin protein expression. Specific activity was determined as the ratio of phosphorylated signal to total signal following β-actin normalization. To rule out bleed-through, antibodies were probed on the same blot using different animal primary antibodies between the phosphorylated (rabbit) and total protein (mouse) allowing for two-color detection and analysis when used with secondary fluorescent antibodies with differing wavelengths (IRDye 680RD and IRDye 800CW).

2.6. Respiration.

Oroboros Oxygraph-2k (O2k, OROBOROS INSTRUMENTS Corp., Innsbruck, Austria) was used for mitochondrial respiration analysis. Permeabilized HUVEC protocols were optimized according to previously described protocols [34–36]. HUVECs were trypsinized using 0.25% trypsin/EDTA, washed with PBS, and spun (3 minutes at 800 g). Cells were then resuspended in MiR05 respiration buffer (0.5 mM EGTA, 3 mM magnesium chloride, 60 mM K-lactobionate, 20 mM taurine, 10 mM potassium phosphate, 20 mM HEPES, 110 mM sucrose, 1 g/l fatty acid-free bovine serum albumin) and counted under a microscope using a hemocytometer. HUVECs were added to the O2k chamber at a cell count of 0.5×10^6 and 1×10^6 per chamber and permeabilized with 3 μg of digitonin. Substrates and inhibitors designed to mimic carbohydrate metabolism were added to assess respiration rates. State 2 (leak state) was defined following the addition of 5 mM pyruvate, 2 mM malate, and 10 mM glutamate (PMG); state 3 (ATP-generating respiration) was defined as PMG with 2 mM adenosine diphosphate (ADP); state 3S was defined as PMG, ADP, and 6 mM succinate; 2 μg/ml oligomycin revealed state 4 (leak state); and 0.5 μM of carbonyl cyanide 4-(trifluoro-methoxy)phenylhydrazone (FCCP) was added incrementally until a peak uncoupling state was reached (uncoupled). Cells were recounted following the experiments, and respiration rates normalized to cell count. An area of consistent respiration rate of 3-5 minutes or longer was representative of the various states.

2.7. Statistical Analysis.

A two-way ANOVA was used for data analysis with Tukey multiple comparisons post hoc analysis for comparing each group. Data are presented on separate graphs to represent each ANOVA comparison. For analysis of the mitochondrial superoxide data, controls (negative and positive for both HG and AA) from all experiments were pooled. A p value of less than 0.05 for interaction, treatment, or EPICAT effects was used as the cutoff for statistical significance in all tests. A p value of equal or less than 0.08 was considered indicative of data trends approaching significance. Data are expressed as mean ± SEM.

3. Results

3.1. Differential Measurement of Total Cellular Versus Mitochondrial Superoxide.

We employed electron paramagnetic resonance spectroscopy using two different spin probes

to differentiate total cell (CMH) and mitochondrial (Mito-TEMPO-H) superoxide to measure both total cellular and mitochondrial-derived superoxide. When the mitochondrial probe was used in these same experiments, we measured elevated superoxide concentrations in both AA ($p = 0.05$, Figure 1(a)) and HG-treated cells ($p < 0.05$, Figure 1(b)). Representative nitroxide spectra for mitochondrial-specific superoxide are shown in Figure 1(c). To determine whether we could isolate the measurement of mitochondrial-derived superoxide from total cellular superoxide, we tested cells with HG and measured superoxide in total cells (Figures 1(a) and 1(d)). HG failed to generate significantly higher concentrations of superoxide in the total cell as compared with the control (Figure 1(d)), demonstrating the mitochondrial specificity of our superoxide measurements.

3.2. (−)-Epicatechin Attenuated Mitochondrial Superoxide Production. In all experiments, the mitochondrial toxin and superoxide generator AA significantly increased superoxide production ($p < 0.05$, Figure 1(a)). AA plus EPICAT at $1.0 \,\mu$M (Figure 1(a)) tended to decrease superoxide in cells compared to AA alone ($p = 0.06$, EPICAT effect, Figure 1(a)). Post hoc analysis revealed that AA-treated cells showed significantly elevated superoxide as compared with controls, and cells with control plus EPICAT at both concentrations had significantly lower superoxide as compared with treated cells ($p < 0.05$, Figure 1(a)). Cells with AA plus EPICAT were significantly different than both controls with and without EPICAT (both concentrations, $p < 0.05$, Figure 1(a)). At $1.0 \,\mu$M, EPICAT significantly attenuated superoxide production stimulated by HG, with post hoc analysis revealing significantly less superoxide in cells with EPICAT as compared with HG-treated cells ($p = 0.05$ and $p < 0.05$, interaction and EPICAT effects, respectively, Figure 1(b)). EPICAT at $0.1 \,\mu$M concentrations did not show any significant impact on mitochondrial-derived superoxide (Figure 1(b)). MnSOD expression was not altered by either AA or HG, alone or in the presence of EPICAT treatment (Figure 1(e)).

3.3. (−)-Epicatechin Had No Significant Impact on Mitochondrial Respiration. Permeabilized HUVECs were exposed to a suite of substrates and inhibitors designed to mimic carbohydrate metabolism; respiration was measured as mitochondrial oxygen disappearance. No significant differences were observed in any respiration state in response to HG and EPICAT treatment (Figure 2). However, a nonsignificant increase in all respiration states was observed with $0.1 \,\mu$M EPICAT (Figure 2). Cells treated with AA showed decreased respiration at all states, as expected with a mitochondrial toxin; however, the toxic effect of AA did not permit full respiration measurements (data not shown).

3.4. (−)-Epicatechin Modulated AMPK Expression. AA treatment resulted in a significant increase in pAMPK expression, regardless of EPICAT concentrations ($p < 0.05$, Figure 3(a)). AA treatment also elevated AMPK specific activity at $0.1 \,\mu$M EPICAT ($p < 0.01$, Figure 3(a)). Post hoc analysis revealed significant differences in pAMPK expression between control

and treated cells in the $0.1 \,\mu$M EPICAT experiments, and also in AMPK specific activity between control cells plus EPICAT and AA-treated cells, and between control and AA-treated cells with EPICAT ($p < 0.05$, Figure 3(a)). Post hoc analyses showed no differences between groups in the $1.0 \,\mu$M EPICAT experiments (Figure 3(a)). In cells treated with AA, EPICAT did not impact pAMPK expression (Figure 3(a)). In cells treated with HG, no effects were noted on pAMPK expression (Figure 3(a)).

3.5. (−)-Epicatechin Nonsignificantly Impacted eNOS Activity. In cells treated with AA, $0.1 \,\mu$M EPICAT resulted in no change in peNOS expression (Figure 3(a)). In cells treated with HG, $1.0 \,\mu$M EPICAT resulted in a nonsignificant elevation of eNOS specific activity ($p = 0.08$, Figure 3(b)).

3.6. (−)-Epicatechin Modulated the Expression of SIRT3 but Did Not Impact PCG1-α. Cells exposed to AA showed a significant decrease of PGC1-α expression ($p < 0.01$, treatment effect and significant post hoc differences between control and AA-treated cells, $p < 0.05$, Figure 3(a)). Post hoc analysis revealed significant differences between both AA-treated groups and the control cells ($p < 0.05$, Figure 3(a)). No effect of EPICAT was observed. A significant interaction effect between treatment and EPICAT was observed in SIRT3 expression in HUVECs treated with AA and $1.0 \,\mu$M EPICAT ($p < 0.01$, interaction effect, $p < 0.05$ difference between vehicle control ± EPICAT, Figure 3(a)); however, no differences were noted in post hoc analyses. No effects were noted with HG-treated cells (Figure 3(b)).

3.7. (−)-Epicatechin Attenuated the Expression of Mitochondrial Complexes I and V. In cells exposed to AA, there was a significant decrease in complex I expression with $0.1 \,\mu$M EPICAT (interaction ($p < 0.05$), treatment ($p < 0.01$), and EPICAT effect ($p < 0.05$), with significant post hoc differences between control cells with EPICAT and both control and AA-treated cells, and between control and AA-treated cells with EPICAT $p < 0.05$ for all, Figure 4(a)). Complex III expression was significantly decreased by AA treatment ($p < 0.05$, treatment effect, Figure 4(a)). In HUVECs exposed to HG, EPICAT at $1.0 \,\mu$M concentration significantly attenuated the expression of mitochondrial complex V ($p < 0.05$, EPICAT effect, $p < 0.05$, significant differences between vehicle control ± EPICAT, Figure 4(b)). No impact on complex expression was observed with $0.1 \,\mu$M concentration (Figure 4(b)).

4. Discussion

Here, we report our results from an acute in vitro study investigating the bioactivity of two concentrations of EPICAT in vascular cells. Endothelial cells were exposed to insults designed to mimic either direct mitochondrial insult (AA) or broad metabolic stress (HG). These perturbations were specifically designed to gauge the biological activity of EPICAT at the cellular level, harnessing HUVEC's, a human endothelial cell, versatility for in vitro vascular studies. The dosage range of EPICAT 0.1-1.0 μM has been used extensively in the literature, particularly in in vitro experiments

(a)

(b)

(c)

(d)
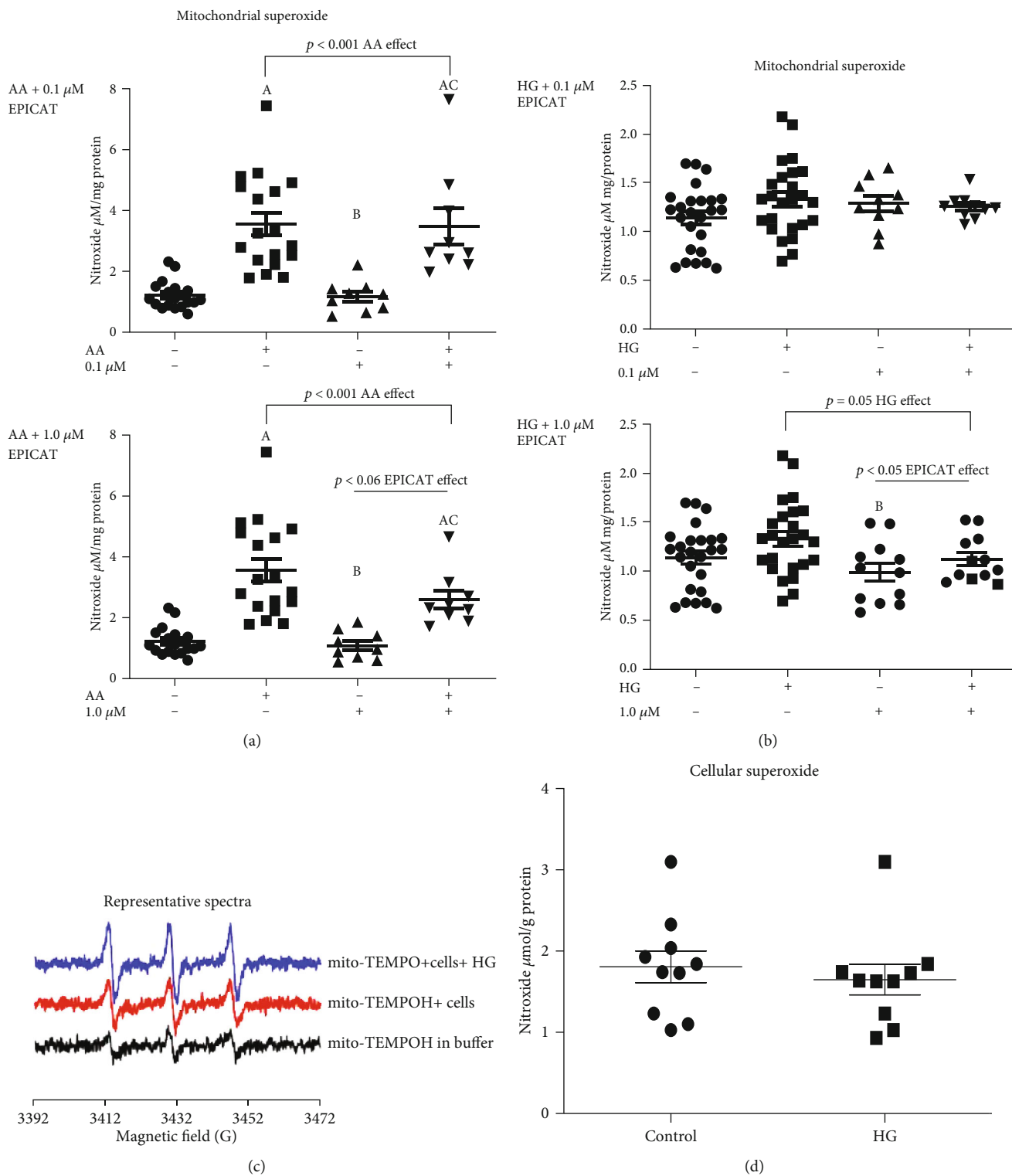
Figure 1: Continued.
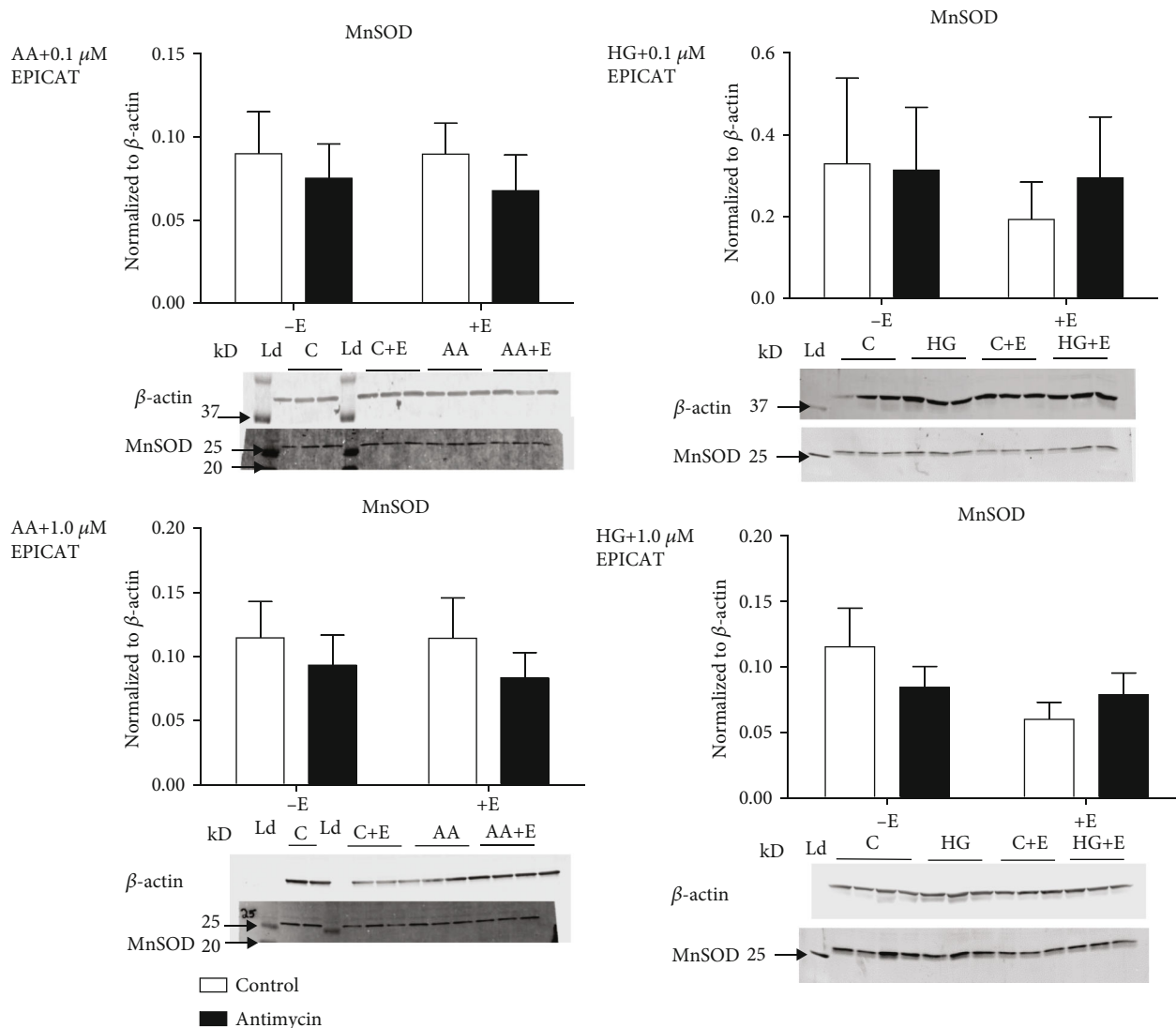
(e)

FIGURE 1: (a–d) Mitochondrial and cellular superoxide measurement in both HG and AA perturbations: Superoxide concentrations were measured in HUVECs by electron paramagnetic resonance spectroscopy using two different spin probes to differentiate mitochondrial (Mito-TEMPO-H) and total cell (CMH) superoxide. CM or mito-TEMPO nitroxide radicals concentration was obtained by simulating the spectra using the SpinFit module incorporated in the Xenon software of the bench-top EMXnano EPR spectrometer followed by the SpinCount module (Bruker). Nitroxide concentrations were normalized to total protein. Mitochondrial superoxide (a–c) and MnSOD protein expression (e) was assessed in cells exposed to $0.1\,\mu M$ and $1.0\,\mu M$ EPICAT $n = 3 - 4$, in control, and HG- and AA-treated cells. Representative spectra is shown (c), and total cellular superoxide during a HG perturbation is shown (d), $n = 3$. For analysis of superoxide, control data from all experiments was pooled $n = 8$, and separate tests were run on each experiment of different EPICAT concentrations. AA experiments, $p < 0.001$ AA effect, both experiments, $\dagger p = 0.06$ EPICAT effect for $1.0\,\mu M$ concentration only (a). HG experiments, $p = 0.05$ glucose effect, $*p < 0.05$ EPICAT effect, $1.0\,\mu M$ concentration only (b), two-way ANOVA, Tukey multiple comparisons analysis. A long horizontal bar over the entire graph indicates an interaction effect, smaller bars over the EPICAT groups indicates an EPICAT effect, while bars with tabs indicate a single main effect of either AA or HG. Post hoc analyses are described as $a = p < 0.05$ as compared to control, $b = p < 0.05$ as compared to treatment, $c = p < 0.05$ as compared to EPICAT control. Data are expressed as mean ± SEM.

[21, 37]. At these concentrations in cells, EPICAT attenuated mitochondrial superoxide in HG-treated cells but not in AA-treated cells, stimulated a nonsignificant mitochondrial respiration signal, and modulated mitochondrial complex expression. Although others have reported an impact of EPICAT on cellular signaling, we do not observe this in our acute study at 2 hours of treatment.

To date, very little research has been conducted in an informative vascular cell model to provide a detailed understanding of the vasoreactivity results observed with EPICAT in vivo. Using a comprehensive suite of endpoints to pinpoint EPICAT bioactivity on mitochondrial ROS and content and function, we found a difference between the response of a mitochondrial poison (AA) versus nutrient
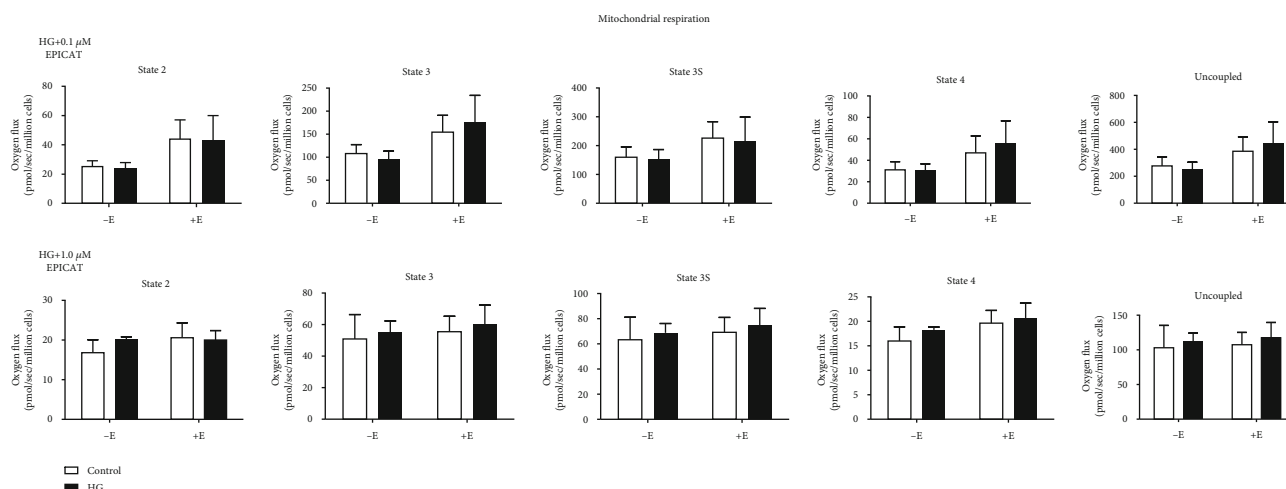
FIGURE 2: Mitochondrial respiration of permeabilized cells. Permeabilized HUVECs were exposed to substrates and inhibitors mimicking carbohydrate metabolism and states 2 (leak state), 3, 3S (both ATP-generating respiration), 4 (leak state), and uncoupled were determined. Respiration rates normalized to cell count ($n = 4$). $*p < 0.05$, $†p < 0.08$, interaction, treatment, or EPICAT effect, two-way ANOVA, Bonferroni's multiple comparisons analysis. Data are expressed as mean ± SEM.

stress (HG) on ROS profiles and mitochondrial respiration using state of the art approaches. EPR enables precise and specific superoxide measurement to delineate superoxide concentrations of mitochondrial origin. We chose our cell model, HUVECs, as they are a human-derived in vitro model widely used in vascular cellular studies. A 2-hour incubation period was chosen based on preliminary experiments addressing specific intercellular ROS pools, mimicking the acute postmeal state. The novelty of our current study lies, in part, in its assessment of cellular signaling and bioactivity upstream of vasodilation during an acute AA (targeted) or HG (global) exposure.

4.1. (–)-Epicatechin Suppresses Mitochondrial Superoxide.
Here, we observed a suppression of AA-induced mitochondrial superoxide at the higher concentration of EPICAT, albeit not significant, and significant lowering effect of EPICAT on HG-induced superoxide, confirming previous studies suggesting that EPICAT is an antioxidant [22, 24–31, 38]. We also demonstrate that both AA and HG specifically increase mitochondrial ROS acutely. Surprisingly, we did not observe a concurrent response in mitochondrial superoxide dismutase (MnSOD); however, we did capture significant elevation of SIRT3 expression with $1.0\,\mu M$ EPICAT concentration in our AA perturbation experiments. EPICAT has previously been shown to have antioxidant activity [22, 38], but the mechanisms of this activity are not entirely elucidated. Taken together, our data strongly suggest that EPICAT does not work stoichiometrically, as has been seen with other compounds such as vitamin C [10, 11], but modulates endogenous cellular redox defenses. These data show EPICAT as an intriguing solution to excess mitochondrial superoxide, a known phenomenon in chronic disease, such as diabetes and metabolic syndrome [2, 3, 5–8].

4.2. (–)-Epicatechin Modulated Mitochondrial Activity. EPI-
CAT has been shown to increase mitochondrial respiration

[23, 39]. However, we did not observe any significant impact on mitochondrial respiration at 2 hours. Interestingly, EPI-CAT treatment at the higher concentration resulted in a significantly less expression of complex V in cells treated with HG; this may indicate a dose-dependent impact of EPICAT depressing mitochondrial function and therefore lessening the generation of superoxide. At the AA experiment with $0.1\,\mu M$ EPICAT treatment, EPICAT significantly increased complex I expression in control cells but failed to rescue the AA-dampened response in AA-treated cells. EPICAT also failed to restore complex III expression dampened in AA-treated cells. This suggests a stimulatory effect of EPICAT on mitochondrial activity that is not sufficient to overcome the toxicity caused by AA. This dampening of complex expression is expected in AA-treated cells, as AA targets complex III of the electron transport chain. Employing the use of the Oxygraph 2k Oroboros in conjunction with protein expression measurements is a highly rigorous way to assess mitochondrial function; here, we show that EPICAT may stimulate mitochondrial respiration while protecting against resultant oxidant damage, but cannot restore cell function in the context of a specific mitochondrial insult.

4.3. (–)-Epicatechin Has Only a Moderate Effect on Cellular Signaling Upstream of Mitochondria Regulation. EPICAT has been shown to increase or modulate AMPK and eNOS signaling in previous studies [20, 21, 40, 41]. Our results show that AA had a significant stimulatory effect on AMPK expression, but EPICAT was unable to modulate this effect. Our results may not agree with those previously reported due to the acute nature of our study (2 hours of incubation with AA or HG), or other experimental differences. Other studies report that EPICAT induces and increases eNOS expression, but we failed to see a significant increase in the eNOS expression or specific activity in either AA- or HG-treated cells. We acknowledge that we measured protein expression, not a true enzymatic activity for either pAMPK
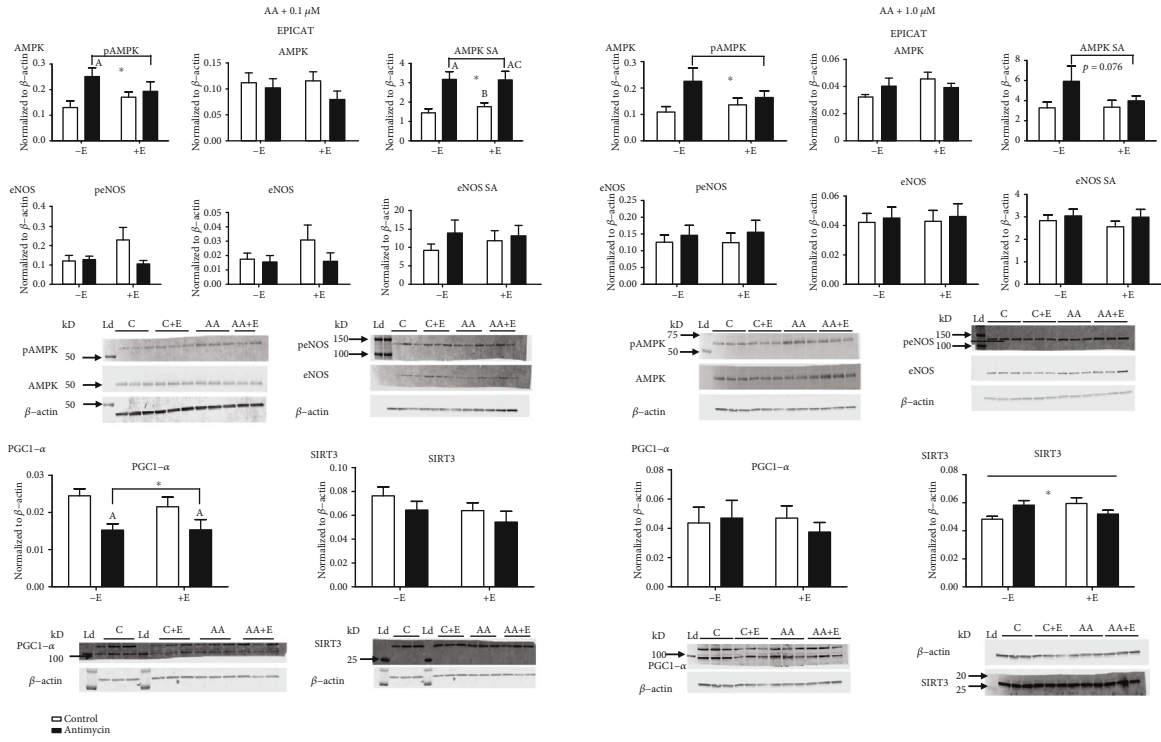
(a)
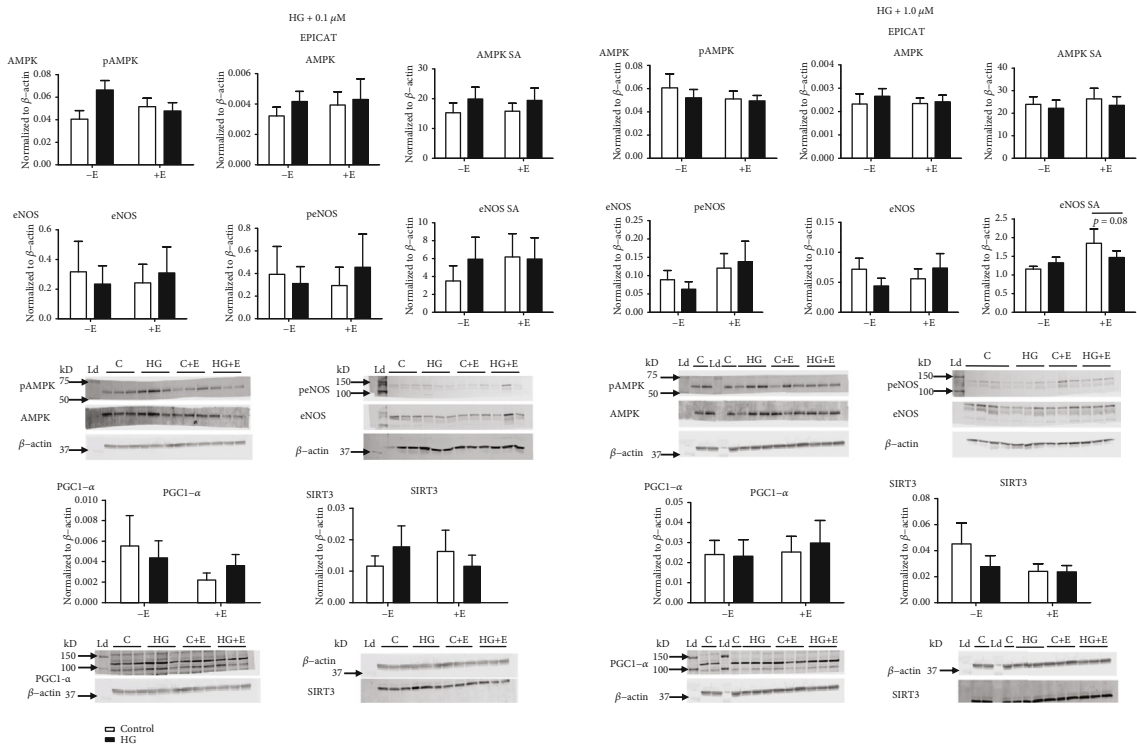
(b)

Figure 3: (a, b) Cellular signaling: Cells were harvested and lysates processed for protein expression via Western blot analysis ($n = 3 - 4$). Blots were probed for pAMPK, AMPK, peNOS, eNOS, SIRT3, and PGC1-α. Specific activity (SA) was calculated as phosphorylated signal normalized to total signal for AMPK and eNOS. ∗$p < 0.05$, interaction, treatment, or EPICAT effect, two-way ANOVA, Tukey multiple comparisons analysis. A long horizontal bar over the entire graph indicates an interaction effect, smaller bars over the EPICAT groups indicates an EPICAT effect, while bars with tabs indicate a single main effect of either AA or HG. Post hoc analyses are described as $a = p < 0.05$ as compared to control, $b = p < 0.05$ as compared to treatment, $c = p < 0.05$ as compared to EPICAT control. Data are expressed as mean ± SEM.
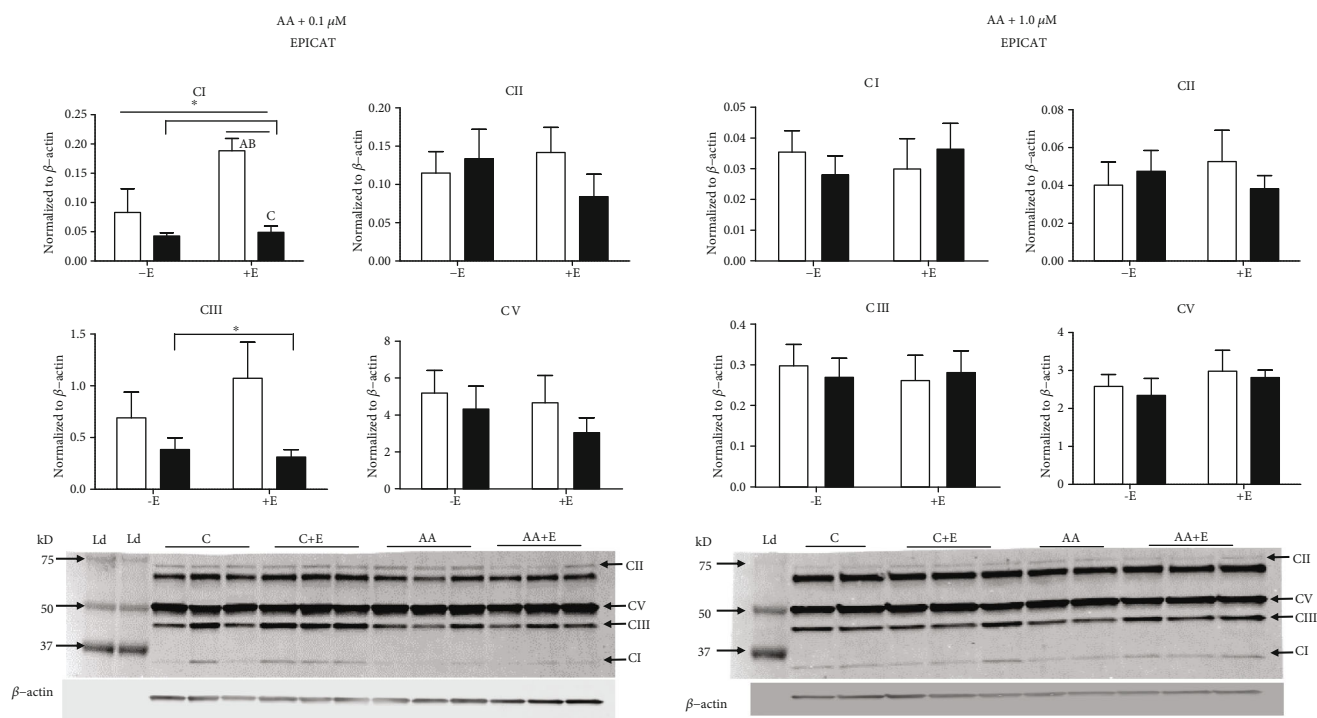
(a)
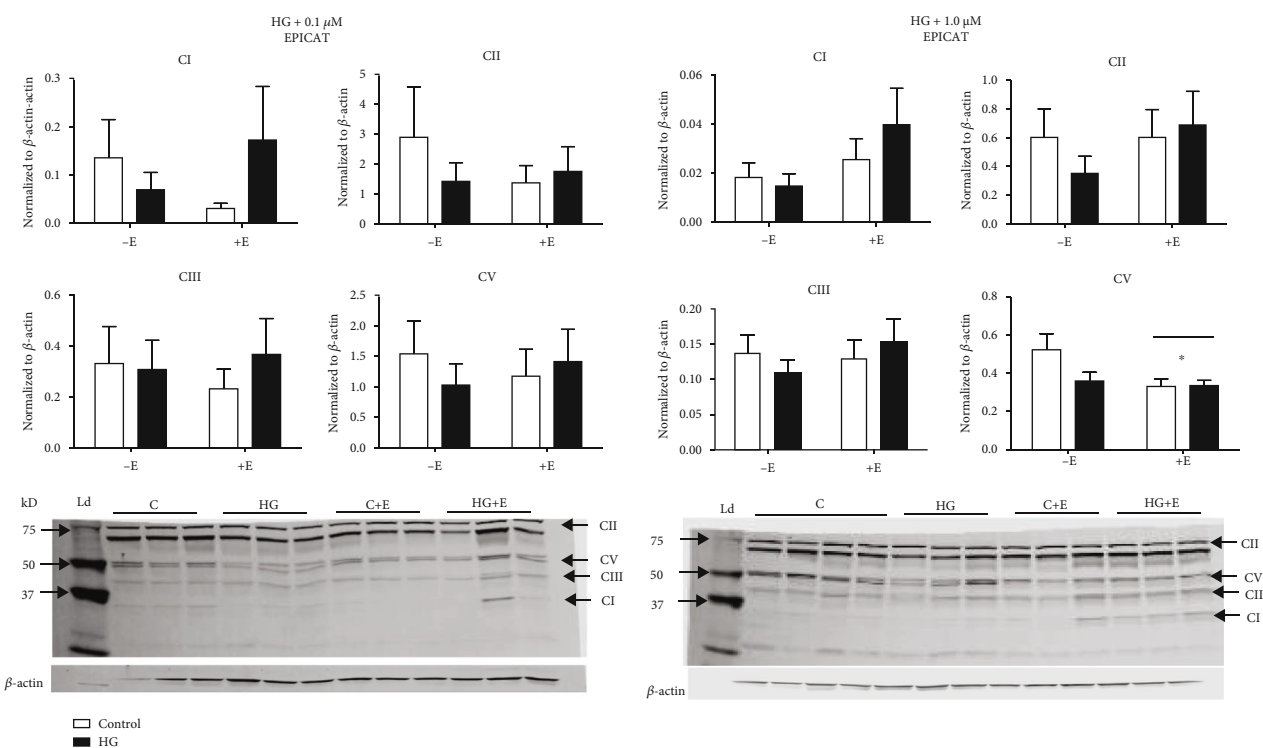
(b)

FIGURE 4: (a, b) Mitochondrial complex expression: Cells were harvested and lysates processed for protein analysis via Western blot analysis ($n = 3 - 4$). Blots were probed for mitochondrial complexes I, II, III, and IV using a single antibody-containing subunits of all complexes. ∗$p < 0.05$, †$p < 0.08$, interaction, treatment, or EPICAT effect, two-way ANOVA, Tukey multiple comparisons analysis. A long horizontal bar over the entire graph indicates an interaction effect, smaller bars over the EPICAT groups indicates an EPICAT effect, while bars with tabs indicate a single main effect of either AA or HG. Post hoc analyses are described as $a = p < 0.05$ as compared to control, $b = p < 0.05$ as compared to treatment, $c = p < 0.05$ as compared to EPICAT control. Data are expressed as mean ± SEM.

or eNOS. We anticipated that the impact on cellular signaling would be detectable after 2 hours of perturbation. Further studies will be needed to determine whether EPICAT signals more acutely, whereas longer incubations may result in indirect effects. Further in vitro experiments in other vascular cell lines and experimental designs may clarify the activity of these and additional mechanisms of action of EPICAT in cellular signaling.

4.4. Hormesis. Our data largely demonstrate that EPICAT is more bioactive at the lower concentration tested as compared with the higher concentration. This phenomenon, known as hormesis, refers to a biphasic response of beneficial stimulation of cellular response at low doses, but toxic or null activity promoted by compounds at higher concentrations [42]. Hormesis is observed with many phytochemicals, including catechins [43], and the overall result is homeostatic adaptation [42]. This concept agrees with other reports of a peak bioactive EPICAT concentration for the stimulation of mitochondrial complex expression in vitro, with higher concentrations showing diminished bioactivity [44, 45]. This observation of EPICAT's hormetic effect is also reported in certain hormones sharing a common structural backbone [45], perhaps explaining this commonality in demonstrating hormesis. Taken together, these results show that EPICAT is an agent of hormesis, ultimately promoting cellular and physiological adaptation. These results also agree with a recent paradigm shift on the role of ROS and antioxidants in health [46, 47]. Current understanding on mitochondrial-derived ROS considers the possibility that this excess mitochondrial ROS may have a hormetic effect on cellular pathways in the context of chronic glucose exposure, providing cellular adaptation to nutrient excess [47]. Our results showing bioactivity at a lower dose of EPICAT, and those of others reporting lack of clinical impact of antioxidant supplements [46], align with this new paradigm. It is possible that EPICAT has an adaptive effect on cellular homeostasis at a low concentration but allows for cells' necessary responsiveness to higher ROS concentrations of mitochondrial-derived ROS.

4.5. Limitations. Previous preliminary and scout experiments in our laboratory pointed to the acute bioactivity of EPICAT, impacting downstream cellular activity in incubation periods shorter than 4 hours. Two-hour incubations were chosen to determine whether EPICAT works acutely and signals at the cellular level. As most of our cellular signaling and respiration data failed to yield significant activity, longer incubation periods may be necessary in future experiments. We did not measure enzymatic activity directly; we assessed protein expression, a proxy measurement. Also, we chose the HUVECs as a widely used model of vascular cells; however, these cells are venous in origin, and using cells from arteries may be more representative of vascular physiology. Lastly, we report many endpoints showing only nonsignificant results ($0.05 \leq p \leq 0.08$). We are confident that we have repeated our experiments sufficiently; thus, this may be due to reasons stated above.

5. Conclusions

Our study shows that EPICAT acutely supports cellular homeostasis in the context of oxidative stress, but not cellular signaling. EPICAT is found in several commonly consumed foods, such as chocolate and tea, and although we made no attempt to compare our dosage in vitro with that of edible EPICAT-containing sources, future studies will ideally investigate this further. Our future experiments will elucidate the mechanism behind EPICAT's redox normalization and modulation of mitochondrial regulation and as a potential therapeutic target. We also made use of an exciting tool (EPR) for the measurement of cellular superoxide. In conclusion, EPICAT shows promise as a potential modulator of oxidant stress that needs to be further studied in the setting of chronic ROS.

Data Availability

Data will be provided upon request to the corresponding author.

Conflicts of Interest

The authors declare that they have no conflicts of interest.

Acknowledgments

References

[1] Z. Bloomgarden, "Cardiovascular disease and diabetes," *Diabetes Care*, vol. 26, no. 1, pp. 230–237, 2003.

[2] N. Bashan, J. Kovsan, I. Kachko, H. Ovadia, and A. Rudich, "Positive and negative regulation of insulin signaling by reactive oxygen and nitrogen species," *Physiological Reviews*, vol. 89, no. 1, pp. 27–71, 2009.

[3] Z. A. Ma, Z. Zhao, and J. Turk, "Mitochondrial dysfunction and β-cell failure in type 2 diabetes mellitus," *Experimental Diabetes Research*, vol. 2012, Article ID 703538, 11 pages, 2012.

[4] J. Y. Youn, K. L. Siu, H. E. Lob, H. Itani, D. G. Harrison, and H. Cai, "Role of vascular oxidative stress in obesity and metabolic syndrome," *Diabetes*, vol. 63, no. 7, pp. 2344–2355, 2014.

[5] E. J. Anderson, M. E. Lustig, K. E. Boyle et al., "Mitochondrial H_2O_2 emission and cellular redox state link excess fat intake to insulin resistance in both rodents and humans," *Journal of Clinical Investigation*, vol. 119, no. 3, pp. 573–581, 2009.

[6] S. K. Chacko and R. Cheluvappa, "Increased ceruloplasmin and fibrinogen in type 2 diabetes corresponds to decreased anti-oxidant activity in a preliminary tertiary south Indian hospital study," *Experimental and Clinical Endocrinology & Diabetes*, vol. 118, no. 1, pp. 64–67, 2010.

[7] S. Kawashima, "The two faces of endothelial nitric oxide synthase in the pathophysiology of atherosclerosis," *Endothelium*, vol. 11, no. 2, pp. 99–107, 2004.

[8] T. Nishikawa, D. Edelstein, X. L. du et al., "Normalizing mitochondrial superoxide production blocks three pathways of hyperglycaemic damage," *Nature*, vol. 404, no. 6779, pp. 787–790, 2000.

[9] E. Lonn, J. Bosch, S. Yusuf et al., "Effects of long-term vitamin E supplementation on cardiovascular events and cancer: a randomized controlled trial," *Journal of the American Medical Association*, vol. 293, no. 11, pp. 1338–1347, 2005.

[10] D. P. Vivekananthan, M. S. Penn, S. K. Sapp, A. Hsu, and E. J. Topol, "Use of antioxidant vitamins for the prevention of cardiovascular disease: meta-analysis of randomised trials," *The Lancet*, vol. 361, no. 9374, pp. 2017–2023, 2003.

[11] M. Ristow, K. Zarse, A. Oberbach et al., "Antioxidants prevent health-promoting effects of physical exercise in humans," *Proceedings of the National Academy of Sciences of the United States of America*, vol. 106, no. 21, pp. 8665–8670, 2009.

[12] D. X. Zhang and D. D. Gutterman, "Mitochondrial reactive oxygen species-mediated signaling in endothelial cells," *American Journal of Physiology: Heart and Circulatory Physiology*, vol. 292, no. 5, pp. H2023–H2031, 2007.

[13] Z. Ungvari, W. E. Sonntag, and A. Csiszar, "Mitochondria and aging in the vascular system," *Journal of Molecular Medicine*, vol. 88, no. 10, pp. 1021–1027, 2010.

[14] R. H. Zhou, A. E. Vendrov, I. Tchivilev et al., "Mitochondrial oxidative stress in aortic stiffening with age: the role of smooth muscle cell function," *Arteriosclerosis, Thrombosis, and Vascular Biology*, vol. 32, no. 3, pp. 745–755, 2012.

[15] M. S. Shah and M. Brownlee, "Molecular and cellular mechanisms of cardiovascular disorders in diabetes," *Circulation Research*, vol. 118, no. 11, pp. 1808–1829, 2016.

[16] D. J. Ceradini, D. Yao, R. H. Grogan et al., "Decreasing intracellular superoxide corrects defective ischemia-induced new vessel formation in diabetic mice," *The Journal of Biological Chemistry*, vol. 283, no. 16, pp. 10930–10938, 2008.

[17] F. Luna-Vázquez, C. Ibarra-Alvarado, A. Rojas-Molina, I. Rojas-Molina, and M. Zavala-Sánchez, "Vasodilator compounds derived from plants and their mechanisms of action," *Molecules*, vol. 18, no. 5, pp. 5814–5857, 2013.

[18] B. Almeida Rezende, A. C. Pereira, S. F. Cortes, and V. S. Lemos, "Vascular effects of flavonoids," *Current Medicinal Chemistry*, vol. 23, no. 1, pp. 87–102, 2016.

[19] M. Galleano, I. Bernatova, A. Puzserova et al., "(-)-Epicatechin reduces blood pressure and improves vasorelaxation in spontaneously hypertensive rats by NO-mediated mechanism," *IUBMB Life*, vol. 65, no. 8, pp. 710–715, 2013.

[20] I. Ramirez-Sanchez, H. Aguilar, G. Ceballos, and F. Villarreal, "(-)-epicatechin-induced calcium independent eNOS activation: roles of HSP90 and AKT," *Molecular and Cellular Biochemistry*, vol. 370, no. 1-2, pp. 141–150, 2012.

[21] I. Ramirez-Sanchez, L. Maya, G. Ceballos, and F. Villarreal, "(-)-epicatechin activation of endothelial cell endothelial nitric oxide synthase, nitric oxide, and related signaling pathways," *Hypertension*, vol. 55, no. 6, pp. 1398–1405, 2010.

[22] K. Tanabe, Y. Tamura, M. A. Lanaspa et al., "Epicatechin limits renal injury by mitochondrial protection in cisplatin nephropathy," *American Journal of Physiology: Renal Physiology*, vol. 303, no. 9, pp. F1264–F1274, 2012.

[23] K. G. Yamazaki, A. Y. Andreyev, P. Ortiz-Vilchis et al., "Intravenous (-)-epicatechin reduces myocardial ischemic injury by protecting mitochondrial function," *International Journal of Cardiology*, vol. 175, no. 2, pp. 297–306, 2014.

[24] M. Gómez-Guzmán, R. Jiménez, M. Sánchez et al., "Epicatechin lowers blood pressure, restores endothelial function, and decreases oxidative stress and endothelin-1 and NADPH oxidase activity in DOCA-salt hypertension," *Free Radical Biology & Medicine*, vol. 52, no. 1, pp. 70–79, 2012.

[25] A. B. Granado-Serrano, M. A. Martín, G. Haegeman, L. Goya, L. Bravo, and S. Ramos, "Epicatechin induces NF-κB, activator protein-1 (AP-1) and nuclear transcription factor erythroid 2p45-related factor-2 (Nrf2) via phosphatidylinositol-3-kinase/protein kinase B (PI3K/AKT) and extracellular regulated kinase (ERK) signalling in HepG2 cells," *The British Journal of Nutrition*, vol. 103, no. 2, pp. 168–179, 2010.

[26] A. Bettaieb, M. A. Vazquez Prieto, C. Rodriguez Lanzi et al., "(−)-Epicatechin mitigates high-fructose-associated insulin resistance by modulating redox signaling and endoplasmic reticulum stress," *Free Radical Biology & Medicine*, vol. 72, pp. 247–256, 2014.

[27] V. Calabró, B. Piotrkowski, L. Fischerman, M. A. Vazquez Prieto, M. Galleano, and C. G. Fraga, "Modifications in nitric oxide and superoxide anion metabolism induced by fructose overload in rat heart are prevented by (-)-epicatechin," *Food & Function*, vol. 7, no. 4, pp. 1876–1883, 2016.

[28] M. C. Litterio, M. A. Vazquez Prieto, A. M. Adamo et al., "(-)-Epicatechin reduces blood pressure increase in high-fructose-fed rats: effects on the determinants of nitric oxide bioavailability," *The Journal of Nutritional Biochemistry*, vol. 26, no. 7, pp. 745–751, 2015.

[29] R. Lagoa, I. Graziani, C. Lopez-Sanchez, V. Garcia-Martinez, and C. Gutierrez-Merino, "Complex I and cytochrome c are molecular targets of flavonoids that inhibit hydrogen peroxide production by mitochondria," *Biochimica et Biophysica Acta*, vol. 1807, no. 12, pp. 1562–1572, 2011.

[30] Y. V. Simos, I. I. Verginadis, I. K. Toliopoulos et al., "Effects of catechin and epicatechin on superoxide dismutase and glutathione peroxidase activity, in vivo," *Redox Report*, vol. 17, no. 5, pp. 181–186, 2012.

[31] L. F. Silva Santos, A. Stolfo, C. Calloni, and M. Salvador, "Catechin and epicatechin reduce mitochondrial dysfunction and oxidative stress induced by amiodarone in human lung fibroblasts," *Journal of Arrhythmia*, vol. 33, no. 3, pp. 220–225, 2017.

[32] Q. Chen, E. J. Vazquez, S. Moghaddas, C. L. Hoppel, and E. J. Lesnefsky, "Production of reactive oxygen species by mitochondria: central role of complex III," *The Journal of Biological Chemistry*, vol. 278, no. 38, pp. 36027–36031, 2003.

[33] N. B. Madungwe, N. F. Zilberstein, Y. Feng, and J. C. Bopassa, "Critical role of mitochondrial ROS is dependent on their site of production on the electron transport chain in ischemic heart," *American Journal of Cardiovascular Disease*, vol. 6, no. 3, pp. 93–108, 2016.

[34] A. C. Keller, L. A. Knaub, M. W. Miller, N. Birdsey, D. J. Klemm, and J. E. B. Reusch, "Saxagliptin restores vascular mitochondrial exercise response in the Goto-Kakizaki rat," *Journal of Cardiovascular Pharmacology*, vol. 65, no. 2, pp. 1–147, 2014.

[35] K. E. Boyle, D. Zheng, E. J. Anderson, P. D. Neufer, and J. A. Houmard, "Mitochondrial lipid oxidation is impaired in

cultured myotubes from obese humans," *International Journal of Obesity*, vol. 36, no. 8, pp. 1025–1031, 2012.

[36] A. V. Kuznetsov, V. Veksler, F. N. Gellerich, V. Saks, R. Margreiter, and W. S. Kunz, "Analysis of mitochondrial function in situ in permeabilized muscle fibers, tissues and cells," *Nature Protocols*, vol. 3, no. 6, pp. 965–976, 2008.

[37] I. Ramirez-Sanchez, C. Mansour, V. Navarrete-Yañez et al., "(-)-Epicatechin induced reversal of endothelial cell aging and improved vascular function: underlying mechanisms," *Food & Function*, vol. 9, no. 9, pp. 4802–4813, 2018.

[38] M. Grzesik, K. Naparło, G. Bartosz, and I. Sadowska-Bartosz, "Antioxidant properties of catechins: comparison with other antioxidants," *Food Chemistry*, vol. 241, pp. 480–492, 2018.

[39] D. M. Kopustinskiene, A. Savickas, D. Vetchý, R. Masteikova, A. Kasauskas, and J. Bernatoniene, "Direct effects of (−)-epicatechin and procyanidin B2 on the respiration of rat heart mitochondria," *BioMed Research International*, vol. 2015, Article ID 232836, 7 pages, 2015.

[40] A. Moreno-Ulloa, A. Cid, I. Rubio-Gayosso, G. Ceballos, F. Villarreal, and I. Ramirez-Sanchez, "Effects of (-)-epicatechin and derivatives on nitric oxide mediated induction of mitochondrial proteins," *Bioorganic & Medicinal Chemistry Letters*, vol. 23, no. 15, pp. 4441–4446, 2013.

[41] H. Si, Z. Fu, P. V. A. Babu et al., "Dietary epicatechin promotes survival of obese diabetic mice and Drosophila melanogaster," *The Journal of Nutrition*, vol. 141, no. 6, pp. 1095–1100, 2011.

[42] E. J. Calabrese, "Converging concepts: adaptive response, preconditioning, and the Yerkes–Dodson Law are manifestations of hormesis," *Ageing Research Reviews*, vol. 7, no. 1, pp. 8–20, 2008.

[43] M. P. Mattson and A. Cheng, "Neurohormetic phytochemicals: low-dose toxins that induce adaptive neuronal stress responses," *Trends in Neurosciences*, vol. 29, no. 11, pp. 632–639, 2006.

[44] T. P. Ciaraldi, *Personal Communication*, 2019.

[45] I. Ramirez-Sanchez, C. Mansour, A. Moreno-Ulloa et al., *A Class of Steroids That Are Structural Analogues of (+)-Epicatechin As Possible Molecular Mediators of Exercise Effects*, American College of Sports Medicine, San Diego, CA, USA, 2018.

[46] G. Riccioni, T. Bucciarelli, B. Mancini, C. di Ilio, V. Capra, and N. D'Orazio, "The role of the antioxidant vitamin supplementation in the prevention of cardiovascular diseases," *Expert Opinion on Investigational Drugs*, vol. 16, no. 1, pp. 25–32, 2007.

[47] K. Sharma, "Mitochondrial hormesis and diabetic complications," *Diabetes*, vol. 64, no. 3, pp. 663–672, 2015.

Review Article

Implications of NAD+ Metabolism in the Aging Retina and Retinal Degeneration

Ravirajsinh N. Jadeja [ID],[1] **Menaka C. Thounaojam** [ID],[2,3] **Manuela Bartoli** [ID],[2,3] **and Pamela M. Martin** [ID][1,2,3]

[1]*Department of Biochemistry and Molecular Biology, Medical College of Georgia, Augusta University, Augusta, GA 30912, USA*
[2]*Department of Ophthalmology, Medical College of Georgia, Augusta University, Augusta, GA 30912, USA*
[3]*James and Jean Culver Vision Discovery Institute and Medical College of Georgia at Augusta University, Augusta, GA, USA*

Correspondence should be addressed to Ravirajsinh N. Jadeja; rjadeja@augusta.edu
and Pamela M. Martin; pmmartin@augusta.edu

Nicotinamide adenine dinucleotide (NAD+) plays an important role in various key biological processes including energy metabolism, DNA repair, and gene expression. Accumulating clinical and experimental evidence highlights an age-dependent decline in NAD+ levels and its association with the development and progression of several age-related diseases. This supports the establishment of NAD+ as a critical regulator of aging and longevity and, relatedly, a promising therapeutic target to counter adverse events associated with the normal process of aging and/or the development and progression of age-related disease. Relative to the above, the metabolism of NAD+ has been the subject of numerous investigations in various cells, tissues, and organ systems; however, interestingly, studies of NAD+ metabolism in the retina and its relevance to the regulation of visual health and function are comparatively few. This is surprising given the critical causative impact of mitochondrial oxidative damage and bioenergetic crises on the development and progression of degenerative disease of the retina. Hence, the role of NAD+ in this tissue, normally and aging and/or disease, should not be ignored. Herein, we discuss important findings in the field of NAD+ metabolism, with particular emphasis on the importance of the NAD+ biosynthesizing enzyme NAMPT, the related metabolism of NAD+ in the retina, and the consequences of NAMPT and NAD+ deficiency or depletion in this tissue in aging and disease. We discuss also the implications of potential therapeutic strategies that augment NAD+ levels on the preservation of retinal health and function in the above conditions. The overarching goal of this review is to emphasize the importance of NAD+ metabolism in normal, aging, and/or diseased retina and, by so doing, highlight the necessity of additional clinical studies dedicated to evaluating the therapeutic utility of strategies that enhance NAD+ levels in improving vision.

1. Introduction

Nicotinamide adenine dinucleotide (NAD+) was discovered in 1906 as a coenzyme involved in yeast fermentation [1]. We now know it to be an important cofactor, required for at least 500 different enzymatic reactions in the body including those central to key metabolic pathways such as glycolysis, fatty acid (β) oxidation, the tricarboxylic acid (TCA) cycle, and oxidative phosphorylation as the redox interplay between the oxidized (i.e., NAD+) and reduced forms of NAD (i.e., NADH) governs the activity of critical enzymes

in these pathways [2, 3]. NAD+ is also consumed in the processes of protein deacetylation and ADP-ribosylation by sirtuin and poly (ADP-ribose) polymerase (PARP), respectively [2, 4]. Further, the NAD glycohydrolases, CD38 and CD157 (BST1), consume NAD+ through the conversion of NAD into ADP-ribose (ADPR) or cyclic-ADPR [5]. Thus, the facilitation of biologic processes central to the maintenance of the living mammalian (e.g., metabolism, DNA repair, and gene expression) hinges upon the availability of NAD+. Congruent with its obligatory requirement in numerous extremely important biologic reactions, NAD+ levels in
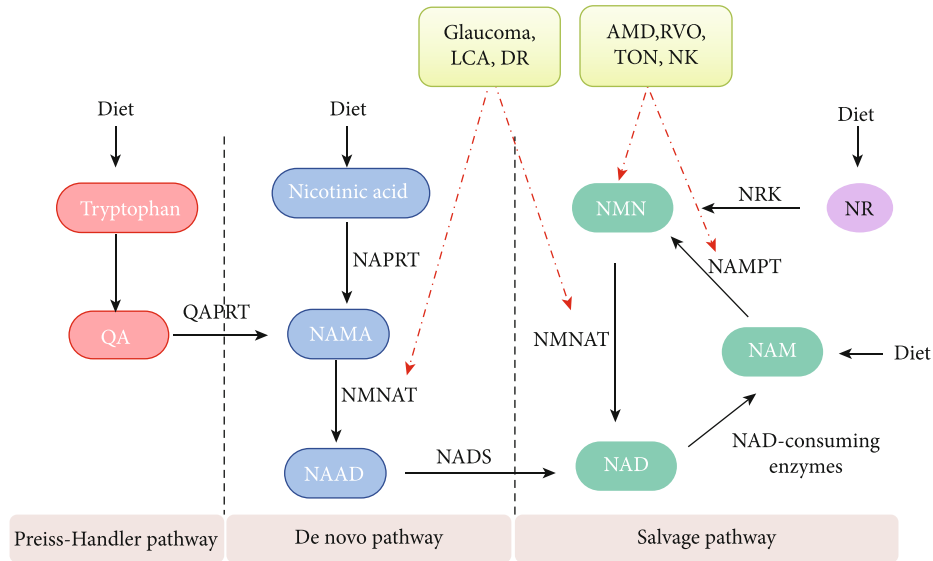
FIGURE 1: Overview of NAD$^+$ biosynthesis pathways. NAD$^+$ is mainly synthesized via the Preiss-Handler, *de novo*, and salvage pathways using tryptophan, nicotinic acid, and nicotinamide, respectively. The red dotted arrow highlights key enzyme alterations that underlie decreased NAD$^+$ availability during disease conditions. QA: quinolinic acid; QAPRT: quinolinate phosphoribosyltransferase; NAPRT: nicotinate phosphoribosyltransferase; NAAD: nicotinic acid adenine dinucleotide; NADS: NAD synthase; NAMPT: nicotinamide phosphoribosyltransferase; NMNAT: nicotinamide mononucleotide adenylyltransferase; NAMN: nicotinic acid mononucleotide; NMN: nicotinamide mononucleotide; NAM: nicotinamide; NR: nicotinamide ribose; NRK: nicotinamide riboside kinase; LCA: Leber congenital amaurosis; DR: diabetic retinopathy; AMD: age-related macular degeneration; RVO: retinal vein occlusion; TON: traumatic optic neuropathy; NK: neurotrophic keratopathy.

the average, healthy human adult are maintained relatively high, ~3 grams [6]! However, as age increases, NAD$^+$ levels decline gradually. This age-related decrease in the availability of NAD$^+$ has been linked strongly to processes relevant to normal aging and importantly also to the development and progression of a number of age-related diseases [6–8]. In 2000, Imai et al. made the groundbreaking discovery that yeast SIR2 (silent information regulator 2) and the mouse ortholog, SIRT1, transcriptional silencers and thereby regulators of longevity, are NAD$^+$-dependent [9]. This discovery helped to explain mechanistically the link between impaired mitochondrial bioenergetics, reactive oxygen species generation, and aging and fueled new interest in understanding NAD$^+$ biology and the importance of NAD$^+$ metabolism in aging. It also renewed interest in the decades-old search for strategies to effectively augment NAD$^+$ levels for therapeutic purposes.

The relationship between NAD$^+$, health, and longevity though not completely understood undeniably exists. The current understanding of this subject has perhaps been most uniformly presented by Imai who in 2009 introduced the concept of the NAD World to explain the novel systemic regulatory network for metabolism and aging. Imai established that there are two critical components: (1) NAMPT- (nicotinamide phosphoribosyltransferase-) mediated systemic NAD biosynthesis as the pacemaker and driver of metabolism in tissues and organs and (2) the NAD-dependent deacetylase SIRT1 as the universal mediator of metabolic functions in various tissues [10]. He later revised the concept (NAD World 2.0), to better emphasize the importance of the intertissue communication between three key organs and tis-

sues, namely, the hypothalamus, skeletal muscle, and adipose tissue which he referred to functionally as the controller, the effector, and the modulator, respectively [11]. With such rapid progress in this field, there have already been many excellent review articles about general NAD$^+$ biology and its relevance to health and disease [4, 8, 12–16]. However, none has focused, as we do in the current review, on the specific importance of NAD$^+$ metabolism in ocular diseases, an area that has received comparatively less attention.

2. NAD$^+$ Synthesis in the Retina

NAD$^+$ can be derived from dietary sources via three principal routes: the Preiss-Handler, *de novo*, and salvage pathways (Figure 1) [17, 18]. In mammals, however, the majority of NAD is thought to be generated via the salvage pathway which is controlled by two key enzymes, nicotinamide phosphoribosyltransferase (NAMPT) and nicotinamide mononucleotide adenylyltransferase (NMNAT) [3]. NAMPT converts nicotinamide (NAM) and phosphoribosyl pyrophosphate (PRPP) to nicotinamide mononucleotide (NMN), and NMNAT generates NAD by transferring the adenylyl moiety from ATP to NMN [19, 20]. NMN can also be generated from nicotinamide ribose (NR) when phosphorylated by nicotinamide riboside kinase (NRK). In the final step of NAD biosynthesis, NMN is adenylylated by nicotinamide mononucleotide adenylyltransferase (NMNAT) to form NAD$^+$. The salvage pathway is referred to as the salvage pathway because not only does it take advantage of multiple dietary substrates for NAD synthesis but the nicotinamide that is generated as a consequence of NAD$^+$ utilization (e.g., by

PARP and sirtuin as a substrate for ADP-ribosylation and deacetylation activities, respectively [9, 21] or by the NAD glycohydrolases, CD38 and CD157, which also consume a relatively small percentage of NAD for their activities [5, 22]) is also recouped and recycled to generate more NAD by NAMPT. The significance of the salvage pathway, specifically NAMPT, to retinal health is highlighted by a 2015 report by Kaja et al. [23] that showed that alterations in circulating levels of NAMPT correlate strongly with risk for retinal vein occlusions, conditions in which both ischemia and metabolic disruption are common. Subsequently, Lin et al. [24] confirmed the functional relevance of NAMPT to retinal function by demonstrating that the photoreceptor-specific deletion of this enzyme leads to culminate in retinal degeneration. Recent work in our labs [25] (Thounaojam et al., unpublished work) have similarly demonstrated the importance of this enzyme and the related availability of NAD^+ also to human retinal pigment epithelial (RPE) and endothelial cells, retinal cell types in which an early senescent phenotype is promoted in the face of inhibition of NAMPT expression and activity and related deficits in NAD^+ bioavailability. Thus, while there are multiple avenues to NAD^+ generation, in the ocular environment, involving NAMPT appears to be of paramount importance.

3. Approaches to Increase NAD^+ Levels in Humans

The potential therapeutic utility of NAD^+ supplementation was demonstrated as early as 1937 when it was demonstrated that it could cure the black tongue in the canine and successfully treat pellagra in the human [26–28]. Accordingly, more recent studies have shown that supplementation with NAD^+ precursors improves NAD^+ levels in aged tissues and thereby protects against aging and the development and progression of aging-related diseases [14, 29–33]. Indeed, boosting NAD^+ metabolism has been shown to extend the lifespan of various organisms, such as yeast, worms, flies, and rodents [11]. A study by Belenky et al. (2007) showed that nicotinamide ribose (NR) supplementation could extend the replicative lifespan of wild-type yeast by more than ten generations [34]. Similarly, in *C. elegans*, NR supplementation extended the average lifespan of wild-type worms [35]. Remarkably, NR has been shown to improve the C57BL/6J mouse lifespan by 5% [36]. Collectively, these data suggest that NAD^+ replenishment delays normal aging in laboratory animal models.

Different approaches such as modifying diet and exercise and supplementation with various NAD^+ precursors have found to be clinically relevant in comparison to approaches to reduce NAD^+ utilization. Herein, we discuss various clinical studies that are conducted using these approaches.

3.1. Diet and Exercise.
It is well known that daily exercise and caloric restriction boost metabolic health in humans [37]. Exercise in humans influences NAMPT expression; endurance-trained athletes have a twofold higher expression of NAMPT in the skeletal muscle compared with baseline levels in sedentary obese, nonobese, and type 2 diabetic individuals [38]. In another study involving six weeks of endurance exercise, NAMPT protein levels increased in the trained leg only compared to the untrained leg [39]. Also, NAMPT and the subsequent expression of SIRT1 in the adipose tissue of healthy obese participants were found to be increased during a caloric weight loss intervention [40]. A study by Seyssel et al. (2014) provided additional evidence that a state of obesity or overnutrition lowers NAD^+ levels [41]. Hence, fed versus fasting states influence heavily the NAD^+/-SIRT1 axis. Further studies are required to evaluate the influence of calorie restriction and exercise on retinal NAD^+ levels and NAMPT expression.

3.2. Elevating NAD^+ Levels via Supplementation with NAD^+ Precursors.
Numerous experimental studies including our own have explored the relevance of enhancing NAD^+ levels in various cell and tissue types using nicotinamide. Importantly, several clinical trials have demonstrated tolerance and safety of nicotinamide in daily pharmacological doses up to 3.5 g [42–46] and single doses of up to 6 g [47–49]. Very recently, the result of the first clinical trial on NMN was published [50]. The single oral administration of NMN was reported to be safe in healthy men without causing any significant deleterious effects. However, this trial was conducted in only 10 patients receiving a single dose of NMN. Hence, more clinical trials with the larger patient population and longer NMN treatments are required to have a meaningful interpretation of its clinical benefits. In this regard, several ongoing clinical trials (NCT03151239, UMIN000030609, and UMIN000025739) are expected to provide better clinically relevant results.

Nicotinic acid is another NAD^+ precursor that is well tolerated in humans; however, at high doses, flushing is a major adverse event [51]. The flushing effect is limited when using newly developed synthetic extended- and sustained-release formulations of nicotinic acid; however, exploratory use of nicotinic acid for the purpose of elevating levels of NAD^+ remains limited [29]. In contrast to nicotinic acid, nicotinamide riboside, another very effective NAD^+ precursor, does not cause flushing [52]. Indeed, clinical studies demonstrate that daily doses of nicotinamide riboside up to 2000 mg are well tolerated with few side effects and effectively increase NAD^+ levels by ~60% in peripheral blood mononuclear cells [53–56].

NAD^+ levels can also be enhanced via dietary means using tryptophan (Trp), an essential amino acid that is metabolized into NAD^+ through *de novo* biosynthesis in the liver and kidneys. This route is critical for maintaining the NAD^+ pool, even though the conversion ratio of Trp to NAD^+ is low in humans, averaging 60 : 1 [57]. Nonetheless, Trp is deemed capable of meeting the metabolic demands of NAD^+ metabolism in nicotinic acid- and nicotinamide-deficient diets and is well tolerated at high doses, between 30 and 50 mg/kg bodyweight, apart from inducing minor side effects such as drowsiness or sleepiness [58]. To date, however, no dietary supplementation studies are available that assess directly whether boosting NAD^+ through Trp might be metabolically beneficial in humans.

3.3. Reducing NAD$^+$ Utilization. With respect to improving NAD$^+$ availability to therapeutically enhance mitochondrial function and prevent the bioenergetic crisis that often precipitates cell damage and death in degenerative retinal disease, many have considered raising NAD$^+$ levels through exogenous supplementation with NAD$^+$ directly or its precursors. However, few have considered the alternate, reducing overall NAD$^+$ utilization. As such, no clinical trials with PARP-1 or CD38 inhibitors that focus on improving metabolic variables relevant to the preservation of NAD$^+$ have been conducted in humans [29]. This, however, does not imply that this strategy must be abandoned altogether, as a viable work-around to exploit the theoretical metabolic benefit of inhibition of NAD$^+$ consumers may present itself in due time, allowing us to assess the efficacy of this strategy in clinical trials.

4. Significance of NAD$^+$ Metabolism in Ocular Diseases

4.1. Leber Congenital Amaurosis 9. Many discussions of the importance of NAD$^+$ are related directly to its direct impact on aging and/or the pathogens of age-related disease. This is understandable given that the consequences of altered NAD$^+$ metabolism are most often exposed in these conditions. However, while we are aware of the numerous biologic processes that are dependent upon the availability of an adequate supply of NAD$^+$, it is important to understand better the significance of NAD$^+$ under normal or basal conditions and, therefore, in the absence of aging or related disease. As such, it is quite fitting to start our more detailed discussion of the significance of NAD$^+$ metabolism to retinal health and function with Leber congenital amaurosis (LCA), a family of congenital retinal dystrophies that results in severe vision loss at an early age [59]. Leber congenital amaurosis 9 (LCA9) is an autosomal recessive retinal degeneration condition caused specifically by mutations in NMNAT1, a key NAD$^+$ biosynthetic enzyme [60] (Figure 1). This was validated by Falk et al. who, using whole-exome sequencing, identified a homozygous missense mutation (c.25G>A, p.Val9Met) in the NAD synthase gene NMNAT1 encoding nicotinamide mononucleotide adenylyltransferase 1 [61]. Around the same time, Koenekoop et al. identified 10 mutant alleles of NMNAT1 in eight families with LCA [62]. Like Falk et al., Koenekoop et al. suggested that the variants would result in altered NMNAT1 structure and function, a hypothesis that these two investigative groups validated via *in vivo* and *in vitro* functional assays. These studies demonstrate convincingly the essential relevance of NAD$^+$ not only to the maintenance of retinal structure and function in the adult but importantly also to retinal development and visual function in general. These studies also highlight the sensitivity of retinal neurons in particular to insufficient supplies of NAD$^+$, a finding supported also by the more recent work of Lin et al. [24] and Kuribayashi et al. [63] which confirmed the importance of NMNAT1 in retinal development and related photoreceptor health and function.

4.2. Glaucoma. Like photoreceptors, the health of retinal ganglion cells (RGCs), cells that serve as a direct liaison between the retina and brain, is too heavily dependent upon NAD$^+$. This is evidenced in glaucoma, a complex and multifactorial disease characterized by the progressive dysfunction and loss of RGCs [64]. Major risk factors for glaucoma are increased intraocular pressure (IOP) and age [65]. During aging, the optic nerve, which is formed by the bundled axons of the RGCs, becomes more prone to damage caused by elevated IOP [66]. Indeed, axonal degeneration of RGCs is a hallmark of glaucoma, and studies focused on identifying the mechanisms responsible for the progressive degeneration of RGC axons and how to prevent it are of pivotal importance in the field of glaucoma [67]. Related to axonal health, NMNAT, specifically isoform 1, has been shown to play crucial roles in axonal protection [68, 69]. NMNAT1 is one of three mammalian NAD synthase isoforms whose whole coding sequence has been described as part of the chimeric protein Wallerian degeneration slow allele (Wlds) that is fused to the amino (N)-terminal 70-amino acid fragment of a ubiquitin-protein [70]. Wlds has been reported to be functionally protective with respect to axonal health, and this axon-protective phenotype in the peripheral nervous system has been linked to enhanced expression of the Wlds protein component of NMNAT1 [70]. More specifically, Zhu et al. [67] evaluated the involvement of NMNAT1 and its subcellular localization to the cytoplasm in both acute and chronic RGC disease models. Their study using cytNMNAT1-Tg mice showed that cytoplasmic overexpression of NMNAT1 significantly protects RGC (both axons and soma) from ischemic and glaucomatous injury. Collectively, these findings signify that cytoplasmic overexpression of NMNAT1 can provide RGC's pancellular defense against both acute and chronic retinal injuries. Additionally, this study highlighted the therapeutic importance of nonnuclear NMNAT1 expression in protecting RGCs.

Other mammalian NMNAT isoforms such as NMNAT2 (located in the Golgi apparatus and cytosol) and NMNAT3 (located in the mitochondria) are also reported to exert axonal protection in different neuronal models [71]. Kitaoka and colleagues evaluated the protective effect of NMNAT3 overexpression on optic nerve axonal protection in two different mouse models of glaucoma (the TNF injection model and the hypertensive glaucoma model). Overexpression of NMNAT3 exerted axonal protection against both TNF-induced and IOP elevation-induced optic nerve degeneration. Further, it was reported that the overexpression of NMNAT3 can alter the autophagy machinery, and NMNAT3 may be involved in decreased p62 and increased LC3-II levels in optic nerve degeneration [72]. The above studies have reported on the link between alterations in isoforms of NMNAT, a major player with respect to the biosynthesis of NAD$^+$, and axonal health. However, the direct relevance of NAD$^+$ itself to aging and/or glaucomatous retina was illustrated directly by Williams et al. who confirmed significant reductions in retinal NAD$^+$ content both in normal aging and in glaucoma-prone mice (DBA/2J) [73]. Although the death of RGCs in these models was not indisputably proven to be attributed solely to the reduced availability of NAD$^+$, the investigators were able to conclude with confidence that the differences in gene expression and total

NAD$^+$ levels did impact RGC function. Further, they hypothesized that the age-dependent decline in NAD$^+$ levels and subsequent dysregulated energy metabolism, when combined with the stress of elevated intraocular pressure, could have a deleterious impact on mitochondrial function and thereby contribute to the loss of RGCs. The validity of this hypothesis was confirmed by the dose-dependent protection against structural and functional retinal ganglion cell damage conferred in association with dietary supplementation of nicotinamide. Additionally, in the same mouse model, intravitreal injection of an adenoviral vector (AAV2.2) to facilitate overexpression of NMNAT1 also provided significant protection against the development and progression of a glaucomatous phenotype. When used in combination, gene therapy plus nicotinamide treatment, the benefit exceeded that derived from the use of either strategy alone. In another study, Williams et al. demonstrated that Wlds, a protein already shown to be axonal protective, increases retinal NAD$^+$ levels [74]. When combined with nicotinamide treatment, Wlds was found to significantly protect mice from glaucomatous neurodegeneration, more than Wlds or nicotinamide alone. Importantly, nicotinamide and Wlds protected somal, synaptic, and axonal compartments, prevented the loss of anterograde axoplasmic transport, and protected animals from visual impairment, a finding demonstrated to be true in 94% of the mouse eyes that were studied [74]. In a follow-up study, Williams et al. provided additional evidence for nicotinamide-mediated protection by including the results from axon counting and optic nerve head analyses [75]. They also show analyses of age- and intraocular pressure-dependent changes in transcripts of NAD-producing enzymes within retinal ganglion cells and that nicotinamide treatment prevents these transcriptomic changes. These data demonstrate that nicotinamide-treated nerves that show no nerve damage are as healthy as nonglaucomatous age-matched controls in terms of their cross-sectional area, axon number, and general morphology, without obvious glial changes. Nicotinamide-treated eyes were also protected from the remodeling and atrophy of the optic nerve head that produces optic nerve cupping, a characteristic feature of human glaucoma. These findings extend previous studies implicating mitochondria in glaucoma by showing that mitochondrial dysfunction is among the first glaucoma-initiating changes within RGCs and that NAD-boosting therapy is potently protective [75]. Collectively, these experiments emphasize the importance of NAD$^+$ to the health and function of retinal neurons and additionally suggest that improving mitochondrial health by enhancing the energy metabolism of RGCs through genetic and/or therapeutic augmentation of NAD$^+$ could be of benefit in glaucoma [73].

5. NAD$^+$ and Aging Retina

Although not completely understood with respect to underlying mechanisms, the relevance of NAD$^+$ metabolism to aging and longevity has been known for decades. Recent studies have brought to the forefront once again the importance of NAD$^+$ metabolism in these processes. The age-dependent decline in NAD$^+$ levels has been demonstrated to occur in animal models and humans, in multiple organs including the brain, liver, muscle, pancreas, adipose tissue, and skin [6, 14, 76, 77]. Our recent work coupled with that of others has added the retina, specifically photoreceptor, ganglion, endothelial, and retinal pigment epithelial (RPE) cells, to this growing list of tissues/cell types [24, 25, 67, 68, 72]. Not only do NAD$^+$ levels decline with increased age but also an extensive metabolic study conducted by Wang et al., using the cornea, RPE/choroid, and lens, confirmed significant difference in metabolites present within aged (73 weeks old) mouse tissues compared to those present in mice of a relatively young age (6 weeks old) [78]. Together, these data suggest that there is a universal age-dependent decrease of cellular NAD$^+$ across species and that most if not all tissues and cell types, excluding possibly only those cells in which mitochondria are absent (e.g., red blood cells), are impacted, to some degree, by the consequent metabolic alterations that emanate. The decrease in NAD$^+$ levels is attributed to an imbalance between NAD$^+$ synthesis and consumption given that the expression and activity of enzymes critical to NAD$^+$ synthesis decline with increasing age despite the fact that the obligatory requirement for NAD$^+$ remains high.

5.1. Age-Related Macular Degeneration. Age-related macular degeneration (AMD) is a complex multifactorial disease, and as its name implies, age is a primary risk factor for its development [79–81]. Retinal pigment epithelial (RPE) cells and photoreceptor cells, cell types that as discussed above are critically dependent upon the adequate availability of and proper metabolism of NAD$^+$, are the principal retinal cell types affected in AMD [82–84]. Congruent with this, studies from our laboratory and others have provided a wealth of evidence in support of the critical importance of NAD$^+$ to RPE and photoreceptor health in aging and AMD.

Bai and Sheline [85] showed that in the rodent model of light-induced retinal damage, a model used commonly to model processes relevant to disease development in AMD, retinal NAD$^+$ content is significantly reduced. Similarly, NAD$^+$ levels in *ex vivo* primary retinal cultures were significantly reduced in association with increased exposure to oxidative stress. Supportive of the prominent causative role that reductions in NAD$^+$ have on the propagation of retinal damage in these experimental model systems, nicotinamide injection restored NAD$^+$ levels and attenuated light-induced damage to RPE and photoreceptors. The same benefit was attainable via cytoplasmic overexpression of the key biosynthetic enzyme NMNAT1. This study provided pioneering evidence of critical relevance of NAD$^+$ to outer retinal health and the potential that therapeutic strategies to restore or augment NAD$^+$ might have in treating degenerative retinal diseases such as AMD in which NAD$^+$ depletion and consequent damage to photoreceptor cells and RPE are paramount. This finding is supported strongly by several additional studies such as that by Zhu et al. which not only demonstrated the benefit of enhancing NAD$^+$ levels in retina/RPE but also further provided insight into the underlying mechanisms to explain this effect: decreased intracellular ROS, inhibition of PARP-1, and upregulated autophagy in

(a)

(b)
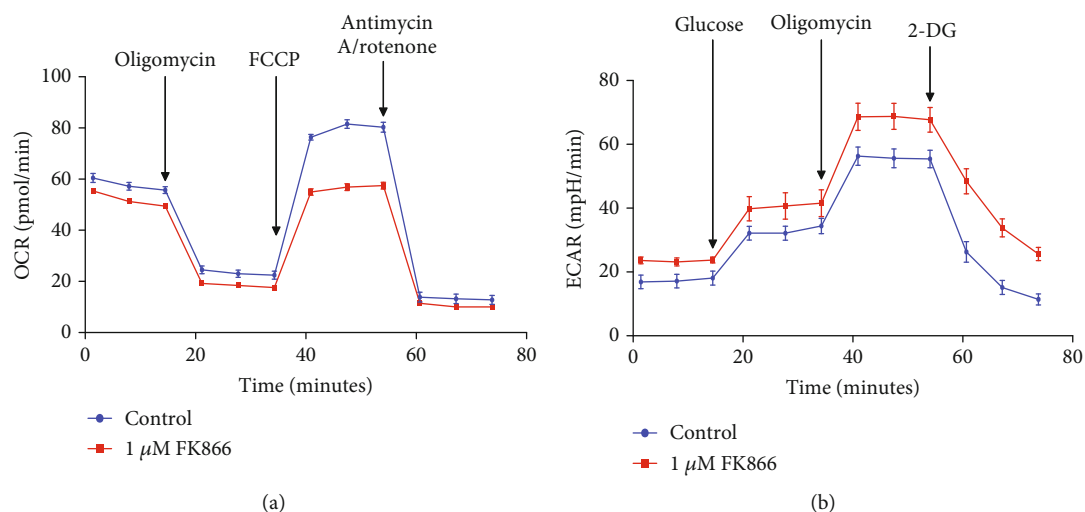
FIGURE 2: Inhibition of NAMPT activity decreases oxidative phosphorylation and increases glycolysis in human retinal pigment epithelial cells. Human retinal pigment epithelial cells were treated with $1\,\mu M$ FK866 for 72 hours, and change in oxidative phosphorylation and glycolysis was evaluated using the Seahorse extracellular flux (XF) analyzer. Results are expressed as mean $\pm$ SEM for $n = 6$ independent replicates. FCCP: carbonyl cyanide-4-phenylhydrazone; 2-DG: 2-deoxy-d-glucose.

RPE cells exposed to prooxidant stimuli [86]. The relevance of NAD$^+$ metabolism to AMD is perhaps even more directly demonstrated by a recent report [87], which, using human-induced pluripotent stem cell-derived RPE (hiPSC-RPE) cells, prepared from donors with and without AMD, showed the benefit of the NAD$^+$ precursor, nicotinamide, in limiting the expression of key complement and inflammatory proteins linked directly to drusen development and AMD.

In a recent study conducted in our laboratory [25], we too observed a decline in NAD$^+$ levels in aged mouse retinas. When searching for the mechanism to explain this phenomenon, we found interestingly that the expression of major contributors in the *de novo* pathway of NAD$^+$ biosynthesis was unchanged; however, NAMPT expression declined significantly with age and in RPE specifically. The importance of NAMPT expression and activity was further demonstrated in subsequent *in vitro* and *in vivo* studies using the NAMPT inhibitor FK866. NAMPT inhibition promoted RPE senescence, an effect that was prevented by the exogenous provision of nicotinamide. Thus, while a number of prior studies have demonstrated the impact of modulating NMNAT1 expression on retinal health and function, work by Lin et al. [24] coupled with that of our own implicates NAMPT as a key rate-limiting enzyme in the determination of NAD$^+$ availability and the consequent health and function of cells in the outer retina, namely, RPE and photoreceptors. Further evidence for the importance of the NAMPT-mediated NAD$^+$ synthesis pathway in the retina comes from the cancer field. NAMPT is overexpressed in many different types of tumors, and its expression appears to be associated with cancer progression [22, 88]. Thus, many cancer biologists have explored the strategy of inhibiting NAMPT expression as a means of reducing tumor growth [88–90]. Although preclinical studies have shown this approach to be very beneficial for reducing various tumor types, this anticancer benefit is associated, unfortunately, with severe retinal toxicity. Additional studies conducted in zebrafish and rodents subjected to NAMPT

inhibition have similarly reported severe retinal damage, defined as disruption of architecture and cellular degeneration and loss of cellular layers, vacuolation and thinning of noncellular layers, and, with time and severity, a reactive mononuclear cell infiltrate (interpreted as glial cells) and fibroplasia [91, 92]. Indeed, suppressing NAMPT precipitates a pathologic state that involves photoreceptor and outer nuclear layers and, with progressed severity, the RPE, outer plexiform, and inner nuclear layers. Hence, approaches such as the coadministration of nicotinic acid along with NAMPT inhibitors have been proposed to reduce the incidence of retinal toxicity associated with anticancer NAMPT-inhibiting therapies [93]. Collectively, these studies from an unrelated field to vision science provide further evidence that maintenance of adequate NAD$^+$ levels is pivotal for overall retinal health and provide additional strong support of the rationale for targeting NAMPT expression and activity in the retina and, thereby, NAD$^+$ metabolism therapeutically to prevent and treat AMD. There is a burgeoning literature in support of the theory that mitochondrial dysfunction contributes significantly to the onset of senescence [94–96]. Hence, building on the information above and our prior report on the significance of the age-associated decline in NAD$^+$ levels in RPE senescence, we investigated the role of NAD$^+$ in maintaining mitochondrial energy metabolism in RPE cells. As shown in Figure 2, inhibition of NAMPT activity in primary human retinal pigment epithelial (HRPE) cells resulted in a significant decline in oxidative phosphorylation. Alternately, glycolytic respiration was upregulated in NAD$^+$-depleted HRPE cells. These observations were a bit surprising as they are in contrast to the findings reported by others using photoreceptor cells wherein FK866 treatment-induced NAD$^+$ depletion results in significant impairment in both oxidative phosphorylation and glycolysis [24]. However, these observations highlight the contrasting capabilities of photoreceptors and RPE to handle impairments in energy metabolism. Neuronal cell types (e.g., photoreceptors) appear to be more sensitive to
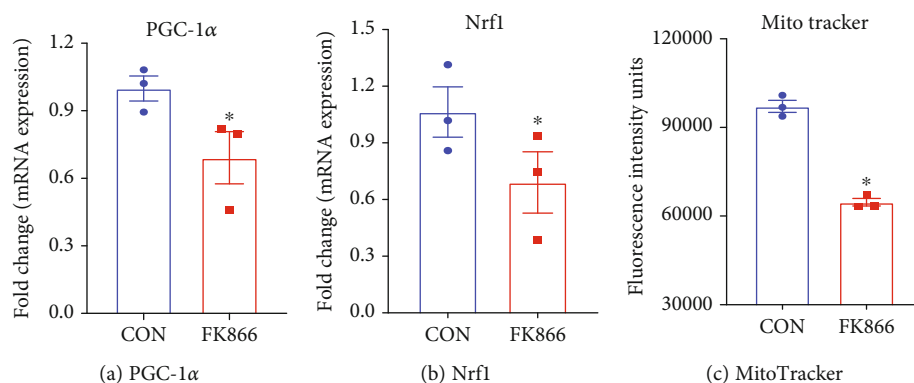
FIGURE 3: Inhibition of NAMPT activity affects mitochondrial biogenesis in human retinal pigment epithelial cells. Human retinal pigment epithelial cells were treated with $1\,\mu M$ FK866 for 72 hours, and change in mRNA expression of PGC1a and Nrf1 and density of healthy respiring mitochondria (MitoTracker Green positive) were determined using qPCR and FACS analysis, respectively. Results are expressed as mean $\pm$ SEM for $n = 3$ independent experiments. $^{*}p < 0.05$ vs. control. PGC-1α: peroxisome proliferator-activated receptor gamma coactivator 1-alpha; Nrf1: nuclear respiratory factor 1.

NAD$^+$ depletion as it may result in the death of these cells; in contrast, in RPE, cell viability is preserved in lieu of the development of a senescent phenotype. Interestingly, the switch in energy metabolism in RPE from oxidative phosphorylation to glycolysis under stress conditions, though different from energy metabolism in photoreceptor cells subjected to the same conditions, is in accordance with previous studies by others in RPE [97]. We found additionally that NAD$^+$ depletion also induced significant downregulation in the expression of the mitochondrial biogenesis markers Nrf1, PGC-1α, and TFAM (Figure 3). Of interest, in a hypothesis article, Wei et al. (2019) proposed that NAD$^+$ supplementation may restore RPE metabolic dysfunction by inducing mitophagy in AMD [98]. Collectively, these data and recent reports by others and us suggest that NAD$^+$ levels are important for maintaining a healthy state of RPE cells, a characteristic that may directly or indirectly impact photoreceptor cell health and function given the major supportive role of RPE relative to this cell type, factors that are highly relevant to the prevention of age-related RPE dysfunction.

Up to this point, our discussion regarding the relevance of NAD$^+$ metabolism to AMD has focused largely on RPE. Again, however, photoreceptor cells are too majorly impacted in this disease. The importance of NAD$^+$ metabolism to photoreceptor health and function was readily apparent as it relates to the function of the development and function of these cells in Leber congenital amaurosis, a congenital and therefore nonage-associated disease. There is considerable evidence also of the dysfunction of these cells in the aging retina and/or AMD congruent with the decline of NAD$^+$ under these conditions. Studies performed by a research group at Washington University School of Medicine, USA, demonstrated that nicotinamide supplementation (100 and 300 mg/kg/day NMN doses) prevented deficits in rod cell function as ascertained by electroretinography studies in aged mice [99]. The critical relevance of NAD$^+$ metabolism in photoreceptor cells was additionally demonstrated in mice in which NAMPT was deleted specifically in rod and/or cone photoreceptors. Rod-specific

deletion of NAMPT in mice significantly impaired impairs photoreceptor survival and vision, whereas NAMPT deletion in cone photoreceptors of mice significantly decreased photopic visual acuity, phenotypes that the authors demonstrated to be linked strongly to altered function of the mitochondrial deacetylase SIRT3 consequent to NAD$^+$ deficiency [24]. Thus, it appears that augmenting NAD$^+$ availability whether through exogenous supplementation or genetic modifications that promote endogenous biosynthesis may be of benefit in protecting photoreceptors and RPE thereby preserving visual health and function in aging and/or diseased (AMD) retina [24, 100].

5.2. The Relevance of NAD$^+$ Metabolism in Other Eye Diseases. In addition, to the major sight-threatening retinal diseases mentioned previously, alterations in NAD$^+$ metabolism have been reported to occur also in association with other retinal and nonretinal ocular diseases including diabetic retinopathy [101], retinal vein occlusion [23], neurotrophic keratopathy [102], and traumatic optic neuropathy [103]. A brief mention of current information available relevant to these ocular disorders is provided below. Retinal vascular occlusions (RVOs) are prevalent in about 0.5% of the population. However, the incidence of RVOs increases with increasing age though variable with ethnicity and/or race. Indeed, retinal vein occlusions are a common cause of retinal vascular disease, second only to diabetic retinopathy, a leading cause of blindness worldwide. About half of the cases of RVOs occur in patients older than 65 years of age, and more than half of these cases are found in patients with cardiovascular diseases. Interestingly, reduced serum levels of NAMPT have been reported to be associated inversely with the incidence and severity of RVOs [23]. However, little detailed confirmatory information is available. As such, this clinical observation should be further evaluated in detail to better undertint the role of NAMPT in RVOs.

RGC injury is an important pathological feature in the pathological process of diabetic retinopathy. Hence, protecting RGCs from high glucose-induced injury is a promising strategy that improves neuronal damage in diabetic

retinopathy. Zhou et al. evaluated the role of NMNAT1, in high glucose-induced RGC injury [101]. The data in this study show that NMNAT1 knockdown could aggravate RGC injury and accelerate the development of RGC apoptosis in response to high glucose stress. Additionally, our recent unpublished work highlights the importance of NAD$^+$ metabolism to retinal endothelial cells, photoreceptors, and RPE, cell types too affected robustly in the diabetic retina. NAD$^+$ metabolism in aging and therefore age-related diseases such as AMD has received much attention; however, additional effort to understand the importance of NAD$^+$ metabolism in the diabetic retina is also warranted.

Recent work suggests that NAD$^+$ metabolism may also impact the susceptibility of retinal cells to traumatic injury. Therefore, augmentation of NAD$^+$ availability may be of therapeutic relevance also in this ocular condition. Supportive of this, it has been shown that P7C3, a member of the aminopropyl carbazole class, activates NAMPT contributing to increased NAD$^+$ generation [104]. This is supported by a study from the research group of Dr. Hidehiro Oku that evaluated the protective effects of P7C3 on optic nerve injury and found that 5 mg/kg/day of P7C3-A20 for 3 days had a neuroprotective effect on RGCs after the optic nerve crush in rats [103].

The impact of NAD$^+$, particularly reductions in its availability, certainly extends beyond the retina. Neurotrophic keratopathy is a degenerative disease characterized by impaired corneal epithelium healing and the absence of corneal sensitivity that renders the cornea vulnerable to injury [105]. The incidence of neurotrophic keratitis increases with age. To determine how corneal epithelial denervation induces apoptosis, Li et al. [102] studied the significance of NAD$^+$ levels and NAMPT expression in a mouse model of corneal denervation. The results showed that the denervation decreased epithelial NAD$^+$ content by reducing NAMPT expression resulting in corneal epithelial apoptosis. Further, the inhibition of NAD biosynthesis by the NAMPT inhibitor recapitulated corneal denervation-induced epithelial detachment and cell apoptosis, which was partially improved by the replenishment of NAD$^+$ or NMN. In conclusion, this study demonstrated that corneal denervation which impaired the epithelial NAD$^+$ level caused apoptosis and epithelial detachment, suggesting that corneal innervations may control epithelial homeostasis by regulating NAD$^+$ biosynthesis. This phenomenon is worthy also of additional exploration.

6. Concluding Remarks

NAD$^+$ is a key cofactor required for the propagations of a plethora of reactions of metabolic importance. Therefore, is not surprising that when levels of NAD$^+$ levels are compromised, the consequences can be and often are quite severe as we have discussed in aging and/or diseased retina. NAD$^+$ is certainly a critical regulator of aging and longevity and, therefore, a promising target for the development of therapies aimed a treating aging and aging-associated diseases. Thus, any discussion of the impact of mitochondrial oxidative stress and altered energy metabolism to aging and longevity would be incomplete without considering factors

relevant to the biosynthesis and utilization of NAD$^+$, hence, the basis of this review. Numerous studies using mouse models have demonstrated the beneficial effects of NAD precursors against metabolic disorders, cancer, and neurological disorders. Additionally, several studies have clearly shown that genetic or nutritional activation of NAD metabolism promotes lifespan extension in various organisms including mammals. However, comparatively few studies have investigated the role of NAD$^+$ metabolism in the regulation of visual health and function. Based on the available literature, it can be surmised that while the salvage pathway for NAD$^+$ synthesis is significantly altered in retinal aging and various conditions of retinal degeneration, the *de novo* pathway seems to be unaffected. Moreover, there seem to be cell type-dependent differences in the affected enzymes. For example, while NAMPT expression is more important to outer retinal cells (RPE and photoreceptors), NMNAT plays a significant role in maintaining the health and function of RGC cells, neurons of the inner retina. Overall, various strategies aimed at improving retinal NAD$^+$ metabolism have shown some promising results in improving visual function in laboratory animals. Thus, similar detailed studies in humans are warranted. Collectively, we hope that the present review will confirm the importance of NAD$^+$ metabolism in the aging retina and other retinal diseases and lead to further clinical studies on evaluating the role of NAD supplementation in improving vision.

Conflicts of Interest

The authors declare that there is no conflict of interest regarding the publication of this article.

Authors' Contributions

RNJ and PMM conceptualized the topic. RNJ and MCT drafted the manuscript. MB and PMM edited and proofed the manuscript. All authors have agreed upon the submission and publication of this work.

Acknowledgments

References

[1] A. Harden and W. J. Young, "The alcoholic ferment of yeast-juice," *Proceedings of the Royal Society of London. Series B, Containing Papers of a Biological Character*, vol. 77, no. 519, pp. 405–420, 1906.

[2] G. Magni, A. Amici, M. Emanuelli, G. Orsomando, N. Raffaelli, and S. Ruggieri, "Enzymology of NAD+ homeostasis in man," *Cellular and Molecular Life Sciences CMLS*, vol. 61, no. 1, pp. 19–34, 2004.

[3] K. Yaku, K. Okabe, and T. Nakagawa, "NAD metabolism: implications in aging and longevity," *Ageing Research Reviews*, vol. 47, pp. 1–17, 2018.

[4] C. Canto, K. J. Menzies, and J. Auwerx, "NAD$^+$ Metabolism and the Control of Energy Homeostasis: A Balancing Act between Mitochondria and the Nucleus," *Cell Metabolism*, vol. 22, no. 1, pp. 31–53, 2015.

[5] V. Quarona, G. Zaccarello, A. Chillemi et al., "CD38 and CD157: a long journey from activation markers to multifunctional molecules," *Cytometry Part B: Clinical Cytometry*, vol. 84, no. 4, pp. 207–217, 2013.

[6] L. Rajman, K. Chwalek, and D. A. Sinclair, "Therapeutic potential of NAD-boosting molecules: the *in vivo* evidence," *Cell Metabolism*, vol. 27, no. 3, pp. 529–547, 2018.

[7] S. Johnson and S. I. Imai, "NAD$^+$ biosynthesis, aging, and disease," *F1000Research*, vol. 7, p. 132, 2018.

[8] S. Imai and L. Guarente, "NAD$^+$ and sirtuins in aging and disease," *Trends in Cell Biology*, vol. 24, no. 8, pp. 464–471, 2014.

[9] S. Imai, C. M. Armstrong, M. Kaeberlein, and L. Guarente, "Transcriptional silencing and longevity protein Sir2 is an NAD-dependent histone deacetylase," *Nature*, vol. 403, no. 6771, pp. 795–800, 2002.

[10] S. Imai, "The NAD World: a new systemic regulatory network for metabolism and aging–Sirt1, systemic NAD biosynthesis, and their importance," *Cell Biochemistry and Biophysics*, vol. 53, no. 2, p. 65, 2009.

[11] S. I. Imai and L. Guarente, "It takes two to tango: NAD$^+$ and sirtuins in aging/longevity control," *npj Aging and Mechanisms of Disease*, vol. 2, no. 1, article 16017, 2016.

[12] P. Belenky, K. L. Bogan, and C. Brenner, "NAD$^+$ metabolism in health and disease," *Trends in Biochemical Sciences*, vol. 32, no. 1, pp. 12–19, 2007.

[13] C. C. S. Chini, M. G. Tarrago, and E. N. Chini, "NAD and the aging process: role in life, death and everything in between," *Molecular and Cellular Endocrinology*, vol. 455, pp. 62–74, 2007.

[14] E. F. Fang, S. Lautrup, Y. Hou et al., "NAD$^+$ in Aging: Molecular Mechanisms and Translational Implications," *Trends in Molecular Medicine*, vol. 23, no. 10, pp. 899–916, 2017.

[15] E. Verdin, "NAD$^+$ in aging, metabolism, and neurodegeneration," *Science*, vol. 350, no. 6265, pp. 1208–1213, 2015.

[16] Y. Yang and A. A. Sauve, "NAD$^+$ metabolism: Bioenergetics, signaling and manipulation for therapy," *Biochimica et Biophysica Acta (BBA) - Proteins and Proteomics*, vol. 1864, no. 12, pp. 1787–1800, 2016.

[17] A. A. B. Badawy, "Kynurenine pathway of tryptophan metabolism: regulatory and functional aspects," *International Journal of Tryptophan Research*, vol. 10, 2017.

[18] N. Hara, K. Yamada, T. Shibata, H. Osago, T. Hashimoto, and M. Tsuchiya, "Elevation of cellular NAD levels by nicotinic acid and involvement of nicotinic acid phosphoribosyltransferase in human cells," *Journal of Biological Chemistry*, vol. 282, no. 34, pp. 24574–24582, 2007.

[19] H. N. Jayaram, P. Kusumanchi, and J. A. Yalowitz, "NMNAT expression and its relation to NAD metabolism," *Current Medicinal Chemistry*, vol. 18, no. 13, pp. 1962–1972, 2011.

[20] J. R. Revollo, A. A. Grimm, and S. Imai, "The NAD biosynthesis pathway mediated by nicotinamide phosphoribosyltransferase regulates Sir2 activity in mammalian cells,"

[21] M. Y. Kim, T. Zhang, and W. L. Kraus, "Poly(ADP-ribosyl)ation by PARP-1: 'PAR-laying' NAD$^+$ into a nuclear signal," *Genes & Development*, vol. 19, no. 17, pp. 1951–1967, 2005.

[22] K. Yaku, K. Okabe, K. Hikosaka, and T. Nakagawa, "NAD metabolism in cancer therapeutics," *Frontiers in Oncology*, vol. 8, p. 622, 2018.

[23] S. Kaja, A. Shah, S. Haji et al., "Nampt/PBEF/visfatin serum levels: a new biomarker for retinal blood vessel occlusions," *Clinical Ophthalmology*, vol. 9, pp. 611–618, 2015.

[24] J. B. Lin, S. Kubota, N. Ban et al., "NAMPT-Mediated NAD$^+$ Biosynthesis Is Essential for Vision In Mice," *Cell Reports*, vol. 17, no. 1, pp. 69–85, 2016.

[25] R. N. Jadeja, F. L. Powell, M. A. Jones et al., "Loss of NAMPT in aging retinal pigment epithelium reduces NAD$^+$ availability and promotes cellular senescence," *Aging*, vol. 10, no. 6, pp. 1306–1323, 2018.

[26] C. A. Elvehjem, "Pellagra, a deficiency disease," *Proceedings of the American Philosophical Society*, vol. 93, no. 4, pp. 335–339, 1949.

[27] C. A. Elvehjem, R. J. Madden, F. M. Strong, and D. W. Wolley, "The isolation and identification of the anti-black tongue factor. 1937," *Journal of Biological Chemistry*, vol. 277, no. 34, article e22, 2002.

[28] C. A. Elvehjem, R. J. Madden, F. M. Strong, and D. W. Woolley, "Relation of nicotinic acid and nicotinic acid amide to canine black tongue," *Journal of the American Chemical Society*, vol. 59, no. 9, pp. 1767-1768, 1937.

[29] N. J. Connell, R. H. Houtkooper, and P. Schrauwen, "NAD$^+$ metabolism as a target for metabolic health: have we found the silver bullet?," *Diabetologia*, vol. 62, no. 6, pp. 888–899, 2019.

[30] Y. S. Elhassan, A. A. Philp, and G. G. Lavery, "Targeting NAD + in metabolic disease: new insights into an old molecule," *Journal of the Endocrine Society*, vol. 1, no. 7, pp. 816–835, 2017.

[31] L. Mouchiroud, R. H. Houtkooper, and J. Auwerx, "NAD$^+$ metabolism: a therapeutic target for age-related metabolic disease," *Critical Reviews in Biochemistry and Molecular Biology*, vol. 48, no. 4, pp. 397–408, 2013.

[32] K. Okabe, K. Yaku, K. Tobe, and T. Nakagawa, "Implications of altered NAD metabolism in metabolic disorders," *Journal of Biomedical Science*, vol. 26, no. 1, p. 34, 2019.

[33] G. Sultani, A. F. Samsudeen, B. Osborne, and N. Turner, "NAD$^+$: a key metabolic regulator with great therapeutic potential," *Journal of Neuroendocrinology*, vol. 29, no. 10, article e12508, 2017.

[34] P. Belenky, F. G. Racette, K. L. Bogan, J. M. McClure, J. S. Smith, and C. Brenner, "Nicotinamide riboside promotes Sir2 silencing and extends lifespan via Nrk and Urh1/Pnp1/-Meu1 pathways to NAD$^+$," *Cell*, vol. 129, no. 3, pp. 473–484, 2007.

[35] E. F. Fang, H. Kassahun, D. L. Croteau et al., "NAD$^+$ Replenishment Improves Lifespan and Healthspan in Ataxia Telangiectasia Models via Mitophagy and DNA Repair," *Cell Metabolism*, vol. 24, no. 4, pp. 566–581, 2016.

[36] H. Zhang, D. Ryu, Y. Wu et al., "NAD$^+$ repletion improves mitochondrial and stem cell function and enhances life span in mice," *Science*, vol. 352, no. 6292, pp. 1436–1443, 2016.

Journal of Biological Chemistry, vol. 279, no. 49, pp. 50754–50763, 2004.

[37] R. L. Smith, M. R. Soeters, R. C. I. Wust, and R. H. Houtkoo-per, "Metabolic flexibility as an adaptation to energy resources and requirements in health and disease," *Endocrine Reviews*, vol. 39, no. 4, pp. 489–517, 2018.

[38] S. R. Costford, S. Bajpeyi, M. Pasarica et al., "Skeletal muscle NAMPT is induced by exercise in humans," *American Journal of Physiology-Endocrinology and Metabolism*, vol. 298, no. 1, pp. E117–E126, 2010.

[39] J. Brandauer, S. G. Vienberg, M. A. Andersen et al., "AMP-activated protein kinase regulates nicotinamide phosphoribo-syl transferase expression in skeletal muscle," *The Journal of Physiology*, vol. 591, no. 20, pp. 5207–5220, 2013.

[40] E. Rappou, S. Jukarainen, R. Rinnankoski-Tuikka et al., "Weight loss is associated with increased NAD$^+$/SIRT1 expression but reduced PARP activity in white adipose tis-sue," *The Journal of Clinical Endocrinology & Metabolism*, vol. 101, no. 3, pp. 1263–1273, 2016.

[41] K. Seyssel, M. Alligier, E. Meugnier et al., "Regulation of energy metabolism and mitochondrial function in skeletal muscle during lipid overfeeding in healthy men," *The Journal of Clinical Endocrinology & Metabolism*, vol. 99, no. 7, pp. E1254–E1262, 2014.

[42] G. Mendola, R. Casamitjana, and R. Gomis, "Effect of nico-tinamide therapy upon B-cell function in newly diagnosed type 1 (insulin-dependent) diabetic patients," *Diabetologia*, vol. 32, no. 3, pp. 160–162, 1989.

[43] P. Pozzilli, N. Visalli, G. Ghirlanda, R. Manna, and D. Andreani, "Nicotinamide increases C-peptide secretion in patients with recent onset type 1 diabetes," *Diabetic Medi-cine*, vol. 6, no. 7, pp. 568–572, 1989.

[44] P. Pozzilli, N. Visalli, A. Signore et al., "Double blind trial of nicotinamide in recent-onset IDDM (the IMDIAB III study)," *Diabetologia*, vol. 38, no. 7, pp. 848–852, 1995.

[45] P. Vague, R. Picq, M. Bernal, V. Lassmann-Vague, and B. Vialettes, "Effect of nicotinamide treatment on the residual insulin secretion in type 1 (insulin-dependent) diabetic patients," *Diabetologia*, vol. 32, no. 5, pp. 316–321, 1989.

[46] N. Visalli, M. G. Cavallo, A. Signore et al., "A multi-centre randomized trial of two different doses of nicotinamide in patients with recent-onset type 1 diabetes (the IMDIAB VI)," *Diabetes/Metabolism Research and Reviews*, vol. 15, no. 3, pp. 181–185, 1999.

[47] J. Dragovic, S. H. Kim, S. L. Brown, and J. H. Kim, "Nicotin-amide pharmacokinetics in patients," *Radiotherapy and Oncology*, vol. 36, no. 3, pp. 225–228, 1995.

[48] A. Petley, B. Macklin, A. G. Renwick, and T. J. Wilkin, "The pharmacokinetics of nicotinamide in humans and rodents," *Diabetes*, vol. 44, no. 2, pp. 152–155, 1995.

[49] M. R. L. Stratford, A. Rojas, D. W. Hall et al., "Pharmacoki-netics of nicotinamide and its effect on blood pressure, pulse and body temperature in normal human volunteers," *Radio-therapy and Oncology*, vol. 25, no. 1, pp. 37–42, 1992.

[50] J. Irie, E. Inagaki, M. Fujita et al., "Effect of oral adminis-tration of nicotinamide mononucleotide on clinical param-eters and nicotinamide metabolite levels in healthy Japanese men," *Endocrine Journal*, vol. 67, no. 2, pp. 153–160, 2020.

[51] Z. Benyo, A. Gille, C. L. Bennett, B. E. Clausen, and S. Offermanns, "Nicotinic acid-induced flushing is mediated by activation of epidermal langerhans cells," *Molecular Phar-macology*, vol. 70, no. 6, pp. 1844–1849, 2006.

[52] K. L. Bogan and C. Brenner, "Nicotinic acid, nicotinamide, and nicotinamide riboside: a molecular evaluation of NAD$^+$ precursor vitamins in human nutrition," *Annual Review of Nutrition*, vol. 28, no. 1, pp. 115–130, 2008.

[53] S. E. Airhart, L. M. Shireman, L. J. Risler et al., "An open-label, non-randomized study of the pharmacokinetics of the nutritional supplement nicotinamide riboside (NR) and its effects on blood NAD+ levels in healthy volunteers," *PLoS One*, vol. 12, no. 12, article e0186459, 2017.

[54] R. W. Dellinger, S. R. Santos, M. Morris et al., "Repeat dose NRPT (nicotinamide riboside and pterostilbene) increases NAD$^+$ levels in humans safely and sustainably: a randomized, double-blind, placebo-controlled study," *npj Aging and Mechanisms of Disease*, vol. 3, no. 1, p. 17, 2017.

[55] C. R. Martens, B. A. Denman, M. R. Mazzo et al., "Chronic nicotinamide riboside supplementation is well-tolerated and elevates NAD$^+$ in healthy middle-aged and older adults," *Nature Communications*, vol. 9, no. 1, article 1286, 2018.

[56] S. A. J. Trammell, M. S. Schmidt, B. J. Weidemann et al., "Nicotinamide riboside is uniquely and orally bioavailable in mice and humans," *Nature Communications*, vol. 7, no. 1, article 12948, 2016.

[57] T. Fukuwatari and K. Shibata, "Nutritional aspect of trypto-phan metabolism," *International Journal of Tryptophan Research*, vol. 6, Supplement 1, pp. 3–8, 2013.

[58] J. D. Fernstrom, "Effects and side effects associated with the non-nutritional use of tryptophan by humans," *The Journal of Nutrition*, vol. 142, no. 12, pp. 2236S–2244S, 2012.

[59] N. Kumaran, A. T. Moore, R. G. Weleber, and M. Michaelides, "Leber congenital amaurosis/early-onset severe retinal dystrophy: clinical features, molecular genetics and therapeutic interventions," *British Journal of Ophthal-mology*, vol. 101, no. 9, pp. 1147–1154, 2017.

[60] Y. Sasaki, Z. Margolin, B. Borgo, J. J. Havranek, and J. Milbrandt, "Characterization of Leber congenital amaurosis-associated NMNAT1 mutants," *Journal of Biolog-ical Chemistry*, vol. 290, no. 28, pp. 17228–17238, 2015.

[61] M. J. Falk, Q. Zhang, E. Nakamaru-Ogiso et al., "*NMNAT1* mutations cause Leber congenital amaurosis," *Nature Genet-ics*, vol. 44, no. 9, pp. 1040–1045, 2012.

[62] R. K. Koenekoop, H. Wang, J. Majewski et al., "Mutations in *NMNAT1* cause Leber congenital amaurosis and identify a new disease pathway for retinal degeneration," *Nature Genet-ics*, vol. 44, no. 9, pp. 1035–1039, 2012.

[63] H. Kuribayashi, Y. Baba, T. Iwagawa, E. Arai, A. Murakami, and S. Watanabe, "Roles of Nmnat1 in the survival of retinal progenitors through the regulation of pro-apoptotic gene expression via histone acetylation," *Cell Death & Disease*, vol. 9, no. 9, p. 891, 2018.

[64] H. A. Quigley and A. T. Broman, "The number of people with glaucoma worldwide in 2010 and 2020," *The British Journal of Ophthalmology*, vol. 90, no. 3, pp. 262–267, 2006.

[65] C. W. McMonnies, "Glaucoma history and risk factors," *Jour-nal of Optometry*, vol. 10, no. 2, pp. 71–78, 2017.

[66] S. Baltan, D. M. Inman, C. A. Danilov, R. S. Morrison, D. J. Calkins, and P. J. Horner, "Metabolic vulnerability disposes retinal ganglion cell axons to dysfunction in a model of glau-comatous degeneration," *Journal of Neuroscience*, vol. 30, no. 16, pp. 5644–5652, 2010.

[67] Y. Zhu, L. Zhang, Y. Sasaki, J. Milbrandt, and J. M. Gidday, "Protection of mouse retinal ganglion cell axons and soma

from glaucomatous and ischemic injury by cytoplasmic over-expression of Nmnat1," *Investigative Opthalmology & Visual Science*, vol. 54, no. 1, pp. 25–36, 2013.

[68] Y. Sasaki, B. P. S. Vohra, R. H. Baloh, and J. Milbrandt, "Transgenic mice expressing the Nmnat1 protein manifest robust delay in axonal degeneration *in vivo*," *Journal of Neuroscience*, vol. 29, no. 20, pp. 6526–6534, 2009.

[69] Y. Sasaki, B. P. S. Vohra, F. E. Lund, and J. Milbrandt, "Nicotinamide mononucleotide adenylyl transferase-mediated axonal protection requires enzymatic activity but not increased levels of neuronal nicotinamide adenine dinucleotide," *Journal of Neuroscience*, vol. 29, no. 17, pp. 5525–5535, 2009.

[70] M. P. Coleman and M. R. Freeman, "Wallerian degeneration, wld^s, and nmnat," *Annual Review of Neuroscience*, vol. 33, no. 1, pp. 245–267, 2010.

[71] B. L. Tang, "Why is NMNAT protective against neuronal cell death and axon degeneration, but inhibitory of axon regeneration?," *Cells*, vol. 8, no. 3, p. 267, 2019.

[72] Y. Kitaoka, Y. Munemasa, K. Kojima, A. Hirano, S. Ueno, and H. Takagi, "Axonal protection by Nmnat3 overexpression with involvement of autophagy in optic nerve degeneration," *Cell Death & Disease*, vol. 4, no. 10, article e860, 2013.

[73] P. A. Williams, J. M. Harder, N. E. Foxworth et al., "Vitamin B$_3$ modulates mitochondrial vulnerability and prevents glaucoma in aged mice," *Science*, vol. 355, no. 6326, pp. 756–760, 2017.

[74] P. A. Williams, J. M. Harder, N. E. Foxworth, B. H. Cardozo, K. E. Cochran, and S. W. M. John, "Nicotinamide and WLD^S act together to prevent neurodegeneration in glaucoma," *Frontiers in Neuroscience*, vol. 11, p. 232, 2017.

[75] P. A. Williams, J. M. Harder, B. H. Cardozo, N. E. Foxworth, and S. W. M. John, "Nicotinamide treatment robustly protects from inherited mouse glaucoma," *Communicative & Integrative Biology*, vol. 11, no. 1, article e1356956, 2018.

[76] H. Massudi, R. Grant, N. Braidy, J. Guest, B. Farnsworth, and G. J. Guillemin, "Age-associated changes in oxidative stress and NAD$^+$ metabolism in human tissue," *PLoS One*, vol. 7, no. 7, article e42357, 2012.

[77] X. H. Zhu, M. Lu, B. Y. Lee, K. Ugurbil, and W. Chen, "In vivo NAD assay reveals the intracellular NAD contents and redox state in healthy human brain and their age dependences," *Proceedings of the National Academy of Sciences of the United States of America*, vol. 112, no. 9, pp. 2876–2881, 2015.

[78] Y. Wang, A. Grenell, F. Zhong et al., "Metabolic signature of the aging eye in mice," *Neurobiology of Aging*, vol. 71, pp. 223–233, 2018.

[79] L. G. Fritsche, R. N. Fariss, D. Stambolian, G. R. Abecasis, C. A. Curcio, and A. Swaroop, "Age-related macular degeneration: genetics and biology coming together," *Annual Review of Genomics and Human Genetics*, vol. 15, no. 1, pp. 151–171, 2014.

[80] L. García-Quintanilla, A. Luaces-Rodríguez, M. Gil-Martínez et al., "Pharmacokinetics of intravitreal anti-VEGF drugs in age-related macular degeneration," *Pharmaceutics*, vol. 11, no. 8, p. 365, 2019.

[81] S. Mukhtar and B. K. Ambati, "The value of nutritional supplements in treating age-related macular degeneration: a review of the literature," *International Ophthalmology*, vol. 39, no. 12, pp. 2975–2983, 2019.

[82] C. R. Fisher and D. A. Ferrington, "Perspective on AMD pathobiology: a bioenergetic crisis in the RPE," *Investigative Opthalmology & Visual Science*, vol. 59, no. 4, pp. AMD41–AMD47, 2018.

[83] T. Léveillard, N. Philp, and F. Sennlaub, "Is retinal metabolic dysfunction at the center of the pathogenesis of age-related macular degeneration?," *International Journal of Molecular Sciences*, vol. 20, no. 3, p. 762, 2019.

[84] E. Pawlowska, J. Szczepanska, A. Koskela, K. Kaarniranta, and J. Blasiak, "Dietary polyphenols in age-related macular degeneration: protection against oxidative stress and beyond," *Oxidative Medicine and Cellular Longevity*, vol. 2019, Article ID 9682318, 13 pages, 2019.

[85] S. Bai and C. T. Sheline, "NAD$^+$ maintenance attenuates light induced photoreceptor degeneration," *Experimental Eye Research*, vol. 108, pp. 76–83, 2013.

[86] Y. Zhu, K. K. Zhao, Y. Tong et al., "Exogenous NAD$^+$ decreases oxidative stress and protects H$_2$O$_2$-treated RPE cells against necrotic death through the up-regulation of autophagy," *Scientific Reports*, vol. 6, no. 1, article 26322, 2016.

[87] A. A. Bergen, "Nicotinamide, iRPE-in-a dish, and age-related macular degeneration therapy development," *Stem Cell Investigation*, vol. 4, no. 9, p. 81, 2017.

[88] V. Audrito, A. Manago, F. Gaudino, and S. Deaglio, "Targeting metabolic reprogramming in metastatic melanoma: the key role of nicotinamide phosphoribosyltransferase (NAMPT)," *Seminars in Cell & Developmental Biology*, vol. 98, pp. 192–201, 2020.

[89] S. Lucas, C. Soave, G. Nabil et al., "Pharmacological inhibitors of NAD biosynthesis as potential an ticancer agents," *Recent Patents on Anti-Cancer Drug Discovery*, vol. 12, no. 3, pp. 190–207, 2017.

[90] A. Roulston and G. C. Shore, "New strategies to maximize therapeutic opportunities for NAMPT inhibitors in oncology," *Molecular & Cellular Oncology*, vol. 3, no. 1, article e1052180, 2016.

[91] S. Cassar, C. Dunn, A. Olson et al., "From the cover: inhibitors of nicotinamide phosphoribosyltransferase cause retinal damage in larval zebrafish," *Toxicological Sciences*, vol. 161, no. 2, pp. 300–309, 2018.

[92] T. S. Zabka, J. Singh, P. Dhawan et al., "Retinal toxicity, *in vivo* and *in vitro*, associated with inhibition of nicotinamide phosphoribosyltransferase," *Toxicological Sciences*, vol. 144, no. 1, pp. 163–172, 2015.

[93] G. Zhao, C. F. Green, Y. H. Hui et al., "Discovery of a highly selective NAMPT inhibitor that demonstrates robust efficacy and improved retinal toxicity with nicotinic acid coadministration," *Molecular Cancer Therapeutics*, vol. 16, no. 12, pp. 2677–2688, 2017.

[94] C. Correia-Melo, F. D. Marques, R. Anderson et al., "Mitochondria are required for pro-ageing features of the senescent phenotype," *The EMBO Journal*, vol. 35, no. 7, pp. 724–742, 2016.

[95] M. Schuliga, D. V. Pechkovsky, J. Read et al., "Mitochondrial dysfunction contributes to the senescent phenotype of IPF lung fibroblasts," *Journal of Cellular and Molecular Medicine*, vol. 22, no. 12, pp. 5847–5861, 2018.

[96] P. V. S. Vasileiou, K. Evangelou, K. Vlasis et al., "Mitochondrial homeostasis and cellular senescence," *Cells*, vol. 8, no. 7, p. 686, 2019.

[97] E. E. Brown, A. J. DeWeerd, C. J. Ildefonso, A. S. Lewin, and J. D. Ash, "Mitochondrial oxidative stress in the retinal pigment epithelium (RPE) led to metabolic dysfunction in both the RPE and retinal photoreceptors," *Redox Biology*, vol. 24, article 101201, 2019.

[98] Q. Wei, W. Hu, Q. Lou, and J. Yu, "NAD$^+$ inhibits the metabolic reprogramming of RPE cells in early AMD by upregulating mitophagy," *Discovery Medicine*, vol. 27, no. 149, pp. 189–196, 2019.

[99] K. F. Mills, S. Yoshida, L. R. Stein et al., "Long-Term Administration of Nicotinamide Mononucleotide Mitigates Age-Associated Physiological Decline in Mice," *Cell Metabolism*, vol. 24, no. 6, pp. 795–806, 2016.

[100] M. Yoshida, A. Satoh, J. B. Lin et al., "Extracellular Vesicle-Contained eNAMPT Delays Aging and Extends Lifespan in Mice," *Cell Metabolism*, vol. 30, no. 2, pp. 329–342.e5, 2019.

[101] R. M. Zhou, Y. Shen, J. Yao et al., "Nmnat 1: a security guard of retinal ganglion cells (RGCs) in response to high glucose stress," *Cellular Physiology and Biochemistry*, vol. 38, no. 6, pp. 2207–2218, 2016.

[102] Y. Li, X. Ma, J. Li et al., "Corneal denervation causes epithelial apoptosis through inhibiting NAD$^+$ biosynthesis," *Investigative Opthalmology & Visual Science*, vol. 60, no. 10, pp. 3538–3546, 2019.

[103] H. Oku, S. Morishita, T. Horie et al., "P7C3 suppresses neuroinflammation and protects retinal ganglion cells of rats from optic nerve crush," *Investigative Opthalmology & Visual Science*, vol. 58, no. 11, pp. 4877–4888, 2017.

[104] G. Wang, T. Han, D. Nijhawan et al., "P7C3 neuroprotective chemicals function by activating the rate-limiting enzyme in NAD salvage," *Cell*, vol. 158, no. 6, pp. 1324–1334, 2014.

[105] A. Lambiase and M. Sacchetti, "Diagnosis and management of neurotrophic keratitis," *Clinical Ophthalmology*, vol. 8, pp. 571–579, 2014.

Research Article

TNFα Mediates the Interaction of Telomeres and Mitochondria Induced by Hyperglycemia: A Rural Community-Based Cross-Sectional Study

Lu Lyu [ID],[1] **Shuli He**,[2] **Huabing Zhang**,[1] **Wei Li**,[1] **Jingbo Zeng**,[3] **Fan Ping** [ID],[1] and **Yu-Xiu Li** [ID][1]

[1]*Key Laboratory of Endocrinology, Ministry of Health, Department of Endocrinology, Peking Union Medical College Hospital, Peking Union Medical College, Chinese Academy of Medical Sciences, Beijing 100730, China*
[2]*Department of Clinical Nutrition, Peking Union Medical College Hospital, Peking Union Medical College, Chinese Academy of Medical Sciences, Beijing 100730, China*
[3]*Department of Endocrinology, Fuxing Hospital, The Eighth Clinical Medical College, Capital Medical University, Beijing 100038, China*

Correspondence should be addressed to Fan Ping; pingfan6779@163.com and Yu-Xiu Li; liyuxiu@medmail.com.cn

This study is aimed at evaluating the relationship between leukocyte telomere length (LTL) and mitochondrial DNA copy number (mtDNAcn) in a noninterventional rural community of China with different glucose tolerance statuses. In addition, we investigate whether the indicators of oxidative stress and inflammation were involved and identify mediators among them. A total of 450 subjects in rural China were included and divided into two groups according to a 75 g oral glucose tolerance test (OGTT): the abnormal glucose metabolism (AGM, $n = 257$, 57.1%) group and the normal glucose tolerance (NGT, $n = 193$, 42.9%) group. Indicators of oxidative stress (superoxide dismutase (SOD) and glutathione reductase (GR)) and inflammatory indices (tumor necrosis factor α (TNFα) and interleukin-6 (IL-6)) were all determined by ELISA. LTL and mtDNAcn were measured using a real-time PCR assay. Linear regressions were used to adjust for covariates that might affect the relationship between LTL and mtDNAcn. Mediation analyses were utilized to evaluate the mediators. In the AGM, LTL was correlated with mtDNAcn ($r = 0.214$, $p = 0.001$), but no correlation was found in the NGT. The association between LTL and mtDNAcn was weakened after adjusting for inflammatory factors in the AGM ($p = 0.087$). LTL and mtDNAcn were both inversely related to HbA1c, IL-6, TNFα, and SOD activity. Mediation analysis demonstrated that TNFα was a significant mediator in the telomere-mitochondrial interactome in the AGM. This result suggests that inflammation and oxidative stress may play a vital role in telomere shortening as well as mitochondrial dysfunction. In the subjects with hyperglycemia, a significant positive correlation is observed between LTL and mtDNAcn, which is probably mediated by TNFα. TNFα may be considered a potential therapeutic target against aging-related disease in hyperglycemia.

1. Introduction

Type 2 Diabetes (T2DM) is a worldwide epidemic characterized by insulin resistance and abnormal insulin secretion, which can result in severe complications and increased medical care costs. Unfortunately, China has become the world's most massive diabetes epidemic since the prevalence of T2DM increased at a substantial rate, which was primarily driven by population aging. Despite the fact that diabetes was more common in urban areas, it was the rural areas that were associated with higher diabetes-related mortality [1].

Telomere damage and mitochondrial dysfunction are both hallmarks of aging. In the past ten years, these two hallmarks were studied, respectively. Recently, a few reports have revealed that there are profound links between telomere attrition and mitochondrial reprogramming, which promote their interaction in aging and degenerative diseases [2]. Previous studies suggest that certain cytokines shuttle between

the nucleus and mitochondria upon oxidative stress, which may influence both telomere biology and mitochondrial function [3]. Meanwhile, oxidative stress and inflammatory responses were both involved in the onset and progression of T2DM. However, the specific factors involved in oxidative stress or inflammation contributing to the malfunction of the mitochondrial-telomere axis remain unclear.

The present study sought to assess the relationship between leukocyte telomere length (LTL) and mitochondrial DNA copy number (mtDNAcn) based on a noninterventional rural population with different oral glucose tolerance statuses. The indicators of oxidative stress or inflammatory cytokines involved in the interaction of telomere attrition and mitochondrial dysfunction were also analysed.

2. Materials and Methods

2.1. Study Population. The current study was conducted within the frame of a type 2 diabetes project in the Nankou Community of Changping, Beijing, in China between March 2014 and January 2015. A questionnaire of essential demographic information, including age, gender, previous medical history, and medication history, was assigned among 599 subjects who all signed written informed consent voluntarily.

Exclusion criteria include the following: (1) use of antidiabetic medications in the past three months with known diabetes; (2) use of lipid-lowering drugs or steroids in the past three months; (3) positive detection of antibodies related to type 1 diabetes including insulin autoantibodies (IAA), islet-cell antibodies (ICA), islet antigen-2 antibodies (IA2), and glutamic acid decarboxylase autoantibodies (GAD-Ab); (4) complication with cardiovascular and cerebrovascular diseases or chronic kidney diseases; and (5) refusal to the telomere length or mitochondrial copy number test. Eventually, a total of 450 subjects were included in this study. The clinical trial was approved by the ethics committee of Peking Union Medical College Hospital (ZS-1274).

2.2. Clinical Measurement. All subjects received a physical examination, including measurements of waist circumference (WC), hip circumference (HC), height, and weight (wearing lightweight clothes without shoes), and blood pressure was collected. Body mass index (BMI) was calculated as weight/(height × height) (kg/m^2). Waist circumference (the level of the midpoint line between the iliac crest and the costal margin on both sides) and hip circumference (the level of the hip rotor) were measured twice by the same observer. The mean values were recorded. Blood pressure was measured twice using the same standard mercury sphygmomanometer at rest, and the mean value was calculated.

2.3. Biochemical Measurements. A 75 g oral glucose tolerance test (OGTT) was performed after overnight fasting. Blood samples were collected at 0, 30, 60, and 120 min following the OGTT. Plasma glucose was determined by the glucose oxidase assay. Lipid metabolism-related indices, including cholesterol (TC), triglyceride (TG), high-density lipoprotein (HDL-C), and low-density lipoprotein (LDL-C), were determined using an automated analyser (AU5800 automatic bio-

chemistry analyser, Beckman Coulter). Chemiluminescent enzyme immunoassay (ADVIA Centaur XP, Siemens) was developed to quantify insulin and C peptide. HbA1c concentrations were assayed by high-performance liquid chromatography (D10 hemoglobin testing system, Bio-Rad; intra-assay coefficient of variation (CV) < 3%, interassay CV < 10%).

2.4. Assessment of Insulin Resistance (IR) and β Cell Function. The homeostatic model assessment of insulin resistance (HOMA-IR) was used to evaluate the degree of insulin resistance [4]: HOMA-IR = fasting blood glucose (mmol/L) × fasting insulin (IU/mL)/22.5. Insulin secretion of the steady-state model (homeostasis model assessment of insulin secretion (HOMA-β)) was calculated as the evaluation of islet beta-cell function [4]: HOMA-β = fasting insulin (IU/mL)/(fasting blood glucose (mmol/L) − 3.5).

2.5. Measurement of LTL. The determination of telomere length in peripheral blood has been described in detail previously [5]. QIAamp DNA blood mid kit (Qiagen, Hilden, Germany) was used to extract Genomic DNA in leukocytes. Purified DNA samples were diluted and quantified using a NanoDrop 1000 spectrophotometer (Thermo Fisher Scientific, Wilmington, DE, USA). The ratio of telomere repeat copy number to single-gene copy number (*T/S*) was determined by the novel monochrome multiplex quantitative PCR. The *T/S* ratio was used to indicate the telomere length [6]. The CV within the plate was 18%, and the interassay CV was 7%.

2.6. Measurement of Peripheral Blood mtDNAcn. The specific method of measurement of peripheral blood mtDNAcn has been described in detail. In brief, the nicotinamide adenine dinucleotide (NADH) dehydrogenase subunit 1 (ND1) genes were used as representatives of mitochondrial genes, and single-copy nuclear gene beta-actin served as the control gene. Quantitative RT-PCR was used to determine ND1 and β-actin reference genes quantitatively. The ratio of mtDNAcn to β-actin copy number represented the relative copy number of mtDNAcn. The ratio of each specimen was normalized to the alignment of the calibrated DNA samples. The intra-plate CV was 4.2% (1.6-9.8%), and the interassay CV was 4.6% (0.9-7.8%).

2.7. Measurement of Oxidative Stress and Inflammatory Indicators. Fasting blood samples were collected. Determinations of serum GR, SOD activity, TNFα, and IL-6 were done using the Elisa kit (Cloud-Clone Corp, Houston, USA) by the Beijing Institute of Biotechnology.

2.8. Statistical Analysis. All data were analysed using SPSS 22.0 (IBM Corp., Chicago, IL, USA). The normal distribution data were presented as the mean ± standard deviation, and parameters that were not normally distributed were expressed as the median (p25th, p75th). The data of the normal distribution were compared by Student's *t*-test, and the data not normally distributed were transformed. Nonparametric tests were used to analyse the data that could not be transformed. Correlation between data was assessed using

TABLE 1: Clinical and demographic characteristics in groups with different glucose tolerance statuses.

Parameter	NGT ($n = 193$)	AGM ($n = 257$)	p
Age (years)	49 ± 11.26	55.21 ± 10.21	$\leq 0.001^{**}$
Sex, male : female[†]	$62 : 131$	$97 : 160$	0.120
BMI (kg/m^2)	25.31 ± 3.55	26.64 ± 3.85	$\leq 0.001^{**}$
Waist circumference (cm)	84.94 ± 9.93	88.83 ± 9.88	$\leq 0.001^{**}$
Hip circumference (cm)	90.08 ± 9.93	88.83 ± 9.88	$\leq 0.001^{**}$
SBP (mmHg)	125.03 ± 19.00	130.36 ± 19.26	0.004^{*}
DBP (mmHg)	75.70 ± 9.43	76.4 ± 10.52	0.486
HbA1c%	5.3 (5.1, 5.6)	5.90 (5.5, 6.6)	$\leq 0.001^{**}$
HOMA-IR	2.22 (1.54, 3.07)	3.23 (2.16, 4.99)	$\leq 0.001^{**}$
HOMA-β	91.32 (67.99, 130.56)	65.09 (41.08, 98.29)	$\leq 0.001^{**}$
FPG (mmol/L)	5.46 (5.22, 5.72)	6.57 (6.13, 7.90)	$\leq 0.001^{**}$
2hPG (mmol/L)	6.03 (5.04, 6.89)	9.7 (7.83, 14.83)	$\leq 0.001^{**}$
TC (mmol/L)	5.30 ± 0.1	5.68 ± 0.1	$\leq 0.001^{**}$
TG (mmol/L)	1.20 (0.78, 1.66)	1.71 (1.13, 2.36)	$\leq 0.001^{**}$
HDL-C (mmol/L)	1.29 (1.11, 1.50)	1.25 (1.08, 1.44)	0.050
LDL-C (mmol/L)	2.71 ± 0.07	2.99 ± 0.07	$\leq 0.001^{**}$
GR (U/L)	7.20 ± 3.22	7.00 ± 3.33	0.538
SOD activity (U/mL)	60.69 ± 18.51	59.57 ± 18.57	0.46
IL-6 (pg/mL)	3.96 ± 3.33	3.98 ± 2.93	0.932
TNFα (fmol/mL)	23.96 ± 10.32	23.93 ± 10.67	0.977
LTL	28.72 ± 0.83	28.67 ± 0.851	0.583
mtDNAcn	108.88 ± 44.31	100.47 ± 41.04	0.023^{*}

$^{*}p < 0.05$; $^{**}p < 0.01$; [†]chi-square test. NGT: normal glucose tolerance; AGM: abnormal glucose metabolism; BMI: body mass index; SBP: systolic blood pressure; DBP: diastolic blood pressure; HOMA-IR: homeostatic model assessment of insulin resistance; HOMA-β: homeostasis model assessment of insulin secretion; FPG: fasting plasma glucose; 2hPG: 2 h postprandial plasma glucose; TC: cholesterol; TG: triglyceride; HDL-C: high-density lipoprotein; LDL-C: low-density lipoprotein; GR: glutathione reductase; SOD: superoxide dismutase; IL-6: interleukin-6; TNFα: tumor necrosis factor α; LTL: telomere length; mtDNAcn: mitochondrial DNA copy number.

Spearman's correlation analysis. Linear regression analyses were used to establish five sets of models to adjust for covariates that might affect the relationship between LTL and mtDNAcn. Model 1 was adjusted for age and gender. Model 2 was adjusted for antioxidant indices (GR, SOD activity) based on Model 1. Model 3 was adjusted for inflammatory indices (IL6, TNFα) based on Model 1. Model 4 made an adjustment of lipid metabolism indicators (TC, TG, HDL-C, and LDL-C) based on Model 1. The mediation analysis was performed by a three-step test model. In the first step, the independent variables were significantly correlated with the mediator variable. Next, the relationship between the independent variable and the dependent variable would be tested. The third step was to investigate the association between intermediate variables and the dependent variables controlling the independent variables. For the model with the insignificant three-step test, the Sobel test was used to verify the results again.

3. Results

3.1. Clinical and Demographic Characteristics in Groups with Different Glucose Tolerance Statuses.
Based on the 1999 World Health Organization criteria, normal glucose tolerance (NGT, $n = 193$) was defined as fasting blood glucose (FPG) < 6.1 mmol/L and 2 h postprandial glucose (2hPG) < 7.8 mmol/L. Abnormal glucose metabolism (AGM) was classified as FPG ≥ 6.1 mmol/L or Glu120 ≥ 7.8 mmol/L. The general demographic characteristics of the two groups are shown in Table 1. Based on the Working Group for Obesity in China (WGOC) criteria, overweight and obesity were defined as $24 \leq$ BMI < 28 and BMI ≥ 28 [7].

It was unexpected that the AGM group had a higher proportion than the NGT group (57.1% vs. 42.9%), which implicated the current situation of glucose metabolism in rural China was not optimistic. Compared with the NGT, the AGM was older (NGT vs. AGM: 49 ± 11.26 y vs. 55.21 ± 10.21 y, $p \leq 0.001$) and had higher BMIs, larger WCs, and HCs ($p \leq 0.001$). Over 450 subjects (41.5%, $n = 187$) were overweight, and 27.5% ($n = 124$) were obese. Systolic blood pressure was higher in the AGM ($p = 0.01$). The insulin resistance index HOMA-IR and the insulin secretion index HOMA-β of the AGM were higher than those of the NGT ($p < 0.01$). In terms of lipid metabolism, TC, TG, and LDL-C in the AGM were higher ($p < 0.01$), while HDL-c rendered no significant difference between the two groups ($p = 0.05$).
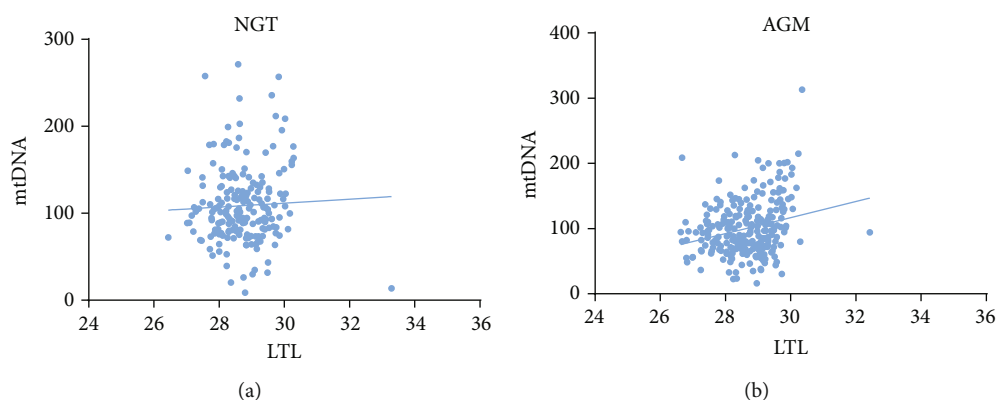
FIGURE 1: Correlation analysis between mtDNAcn and LTL in populations with different glucose tolerance statuses: (a) correlation analysis between mtDNAcn and LTL in the NGT ($r = 0.071$, $p = 0.325$) and (b) correlation analysis between mtDNAcn and LTL in the AGM ($r = 0.214$, $p = 0.001$).

No differences were found in oxidative stress and inflammatory factors (including GR, SOD activity, Il-6, and TNFα) between the NGT and the AGM. Among the aging indices, mtDNAcn was significantly decreased in the AGM (NGT vs. AGM: 108.88 ± 44.31 vs. 100.47 ± 41.04, $p = 0.023$), while LTLs in the AGM did not differ from those in the NGT (NGT vs. AGM: 28.72 ± 0.83 vs. 28.67 ± 0.851, $p = 0.583$).

3.2. MtDNAcn Was Positively Correlated with LTL in People with AGM and the Correlation Disappeared after Correcting Inflammatory Factors. Spearman's correlation analysis was used to explore the relationship between LTL and mtDNAcn in people with different blood glucose levels (Figure 1). In the NGT, no correlation was found between LTL and mtDNAcn ($r = 0.071$, $p = 0.325$). Among the subjects in the AGM, LTL was positively correlated with mtDNAcn ($r = 0.214$, $p = 0.001$). After adjusting for age and gender, the relationship between LTL and mtDNAcn did not significantly change ($p \leq 0.001$) (Model 1 (M1)) (Table 2). Further analyses of the relationships of LTL and mtDNAcn were conducted separately after correcting oxidative stress, inflammatory indicators, and lipid metabolism-related indices based on adjusting for age and gender (Table 2). There was still a positive correlation between LTL and mtDNAcn after correcting antioxidant indices (GR, SOD activity) and lipid metabolism indices ($p < 0.01$). However, the correlation between LTL and mtDNAcn disappeared when we accounted for inflammatory indicators (IL-6, TNFα) (nonstandardized $\beta = 6.237$, $p = 0.087$).

3.3. The SOD Activity Was Negatively Correlated with FPG, and TNFα Was Positively Correlated with HbA1c and 2hPG in the AGM. The relationship between oxidative stress and glucose metabolism was analysed in AGM (Table 3). SOD activity value was negatively correlated with FPG ($r = -0.161$, $p = 0.016$), and SOD activity was not related to 2hPG, HbA1c, HOMA-IR, HOMA-β. No correlation was observed between GR and the indicators of glucose metabolism above.

In investigating the relationship between inflammatory and glucose metabolism indices in AGM (Table 3), TNFα

TABLE 2: Correlation analysis between LTL and mtDNAcn in a correction model of abnormal glucose metabolism.

Correction model	Unstandardized coefficients (β)	Standardized coefficients (β)	R^2	p
M1	11.884	0.245	0.073	$\leq 0.001^{**}$
M2	11.232	0.224	0.074	0.001^{**}
M3	6.237	0.125	0.112	0.087
M4	11.813	0.242	0.106	$\leq 0.001^{**}$

Model 1 (M1): adjusted for age and gender. Model 2 (M2): adjusted for antioxidants (GR and SOD activity) based on Model 1. Model 3 (M3): adjusted for inflammatory (IL-6 and TNFα) based on Model 1. Model 4 (M4): adjusted for lipid metabolism indicators (TC, TG, HDL-C, LDL-C) based on Model 1. $^{*}p < 0.05$; $^{**}p < 0.01$.

was positively correlated with 2hPG ($r = 0.247$, $p \leq 0.001$) and HbA1c ($r = 0.16$, $p = 0.016$), and TNFα was not correlated with FPG, HOMA-IR, and HOMA-β. IL-6 was not observed to be associated with indices of glucose metabolism above.

3.4. Telomere Shortening Was Associated with Increased HbA1c, Inflammatory Markers, and SOD Activity. LTL was negatively correlated with HbA1c ($r = -0.174$, $p \leq 0.001$) (Figure 2(a)). Further analysis found that LTL was significantly negatively correlated with SOD activity ($r = -0.236$, $p \leq 0.001$), IL-6 ($r = -0.133$, $p = 0.008$), TNFα ($r = -0.477$, $p \leq 0.001$) (Table 4). There was no correlation between LTL and GR ($r = -0.064$, $p = 0.205$).

3.5. Decreased mtDNAcn Was Associated with Elevated SOD Activity, IL-6, and TNFα Levels. There was no statistical relationship between mtDNAcn and HbA1c ($r = -0.085$, $p = 0.072$) (Figure 2(b)). Decreased mtDNAcn was significantly associated with an elevated level of SOD activity ($r = -0.236$, $p \leq 0.001$), IL-6 ($r = -0.133$, $p = 0.008$), and TNFα ($r = -0.219$, $p = 0.001$) (Table 4). MtDNAcn was not statistically correlated with GR ($r = 0.040$, $p = 0.548$).

3.6. TNFα Played a Mediating Role in Telomere-Mitochondria Interactome when Glucose Metabolism Is Abnormal. Through mediation analysis, it was found that

TABLE 3: Correlation analysis of antioxidants and inflammatory indicators with glucose metabolism indices in the AGM.

| | HbA1c% | p | FPG (mmol/L) | p | 2hPG (mmol/L) | p | HOMA-IR | p | HOMA-β | p |
	r		r		r		r		r	
GR (U/L)	-0.086	0.199	-0.052	0.436	-0.022	0.745	0.012	0.864	0.027	0.687
SOD activity (U/mL)	-0.037	0.587	-0.161	0.016*	-0.13	0.052	-0.105	0.12	0.055	0.416
IL-6 (pg/mL)	-0.012	0.858	-0.09	0.179	-0.03	0.66	0.014	0.831	0.098	0.150
TNFα (fmol/mL)	0.247	$\leq$0.001**	-0.059	0.379	0.16	0.017*	0.036	0.595	0.045	0.510

*$p < 0.05$; **$p < 0.01$. FPG: fasting plasma glucose; 2hPG: 2 h postprandial plasma glucose; HOMA-IR: homeostatic model assessment of insulin resistance; HOMA-β: homeostasis model assessment of insulin secretion; GR: glutathione reductase; SOD: superoxide dismutase; IL-6: interleukin-6; TNFα: tumor necrosis factor α.

(a)

(b)
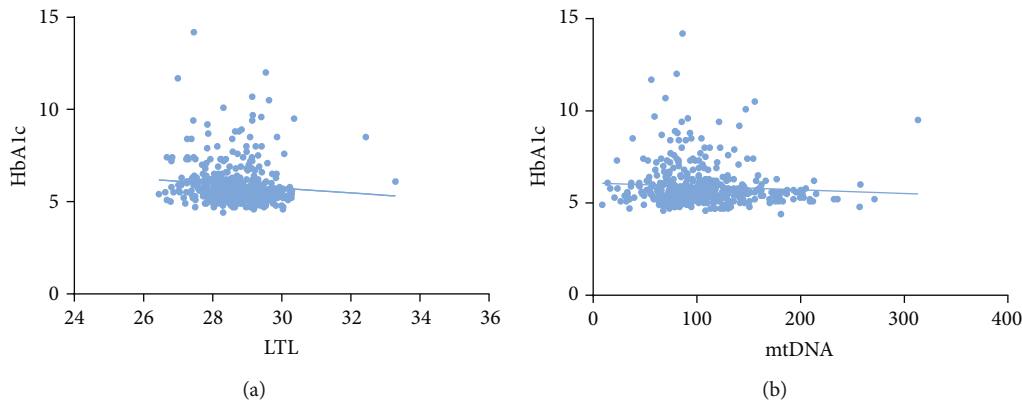
FIGURE 2: Correlation analysis between HbA1c and LTL and mtDNAcn: (a) correlation analysis between HbA1c and LTL ($r = -0.174$, $p \leq 0.001$) and (b) correlation analysis between HbA1c and mtDNAcn ($r = -0.085$, $p = 0.072$).

TABLE 4: Correlation analysis of antioxidants and inflammatory indicators with LTL and mtDNAcn.

| | LTL | p | mtDNAcn | p |
	r		r	
GR (U/L)	-0.064	0.205	0.011	0.833
SOD activity (U/mL)	-0.229	$\leq$0.001**	-0.139	0.006**
IL-6 (pg/mL)	-0.133	0.008**	-0.144	0.004**
TNFα (fmol/mL)	-0.477	$\leq$0.001**	-0.236	$\leq$0.001**

*$p < 0.05$; **$p < 0.01$. GR: glutathione reductase; SOD: superoxide dismutase; IL-6: interleukin-6; TNFα: tumor necrosis factor α; LTL: telomere length; mtDNAcn: mitochondrial DNA copy number.

TNFα played a full mediating effect in the positive correlation between LTL and mtDNAcn (c' was not significant, $p = 0.058$). However, GR, SOD viability, IL-6 had no mediating effect on LTL and mtDNAcn (Figure 3).

4. Discussion

This study investigated the association between oxidative stress and inflammatory markers, LTL, and mtDNAcn in groups with different glucose tolerance status in a rural community of Beijing. Despite a higher prevalence of prediabetes, the diagnosis and treatment of hyperglycemia patients in rural China lag far behind to that in urban areas.

To minimize the effect of the medication, diabetic patients who had recently taken antidiabetic drugs, as well as the individuals who received lipid-lowering agents or steroids recently, were excluded. The present study found a higher prevalence of AGM, which was 57.1% in this rural community, than that (50.9%) in the previous report of Chinese rural areas [8]. Additionally, the study population has a larger number of people with overweight and obesity compared with the population studied in the northeast rural community of China in 2012, where the prevalence of overweight and obesity was 31.6% and 14.6% [9]. These data alerted us the prevention and risk factor management of aging-related metabolic disease in rural northern China is urgent. This real-world study revealed that LTL was positively correlated with mtDNAcn only in the AGM, and the correlation disappeared after the adjustment of the inflammatory indices. There was an inverse correlation between SOD activity and fasting blood glucose in the AGM, while TNFα was positively correlated with HbA1c level and 2hPG. At the same time, this study also found that LTL was negatively correlated with SOD activity, TNFα, and IL-6. The decreased mtDNAcn was found in those with higher SOD activity, TNFα, and IL-6 levels. The mediation analysis revealed that TNFα acted as a mediator between LTL and mtDNAcn.

Previous studies have confirmed a positive correlation between mtDNAcn and LTL in the elderly [10]. LTL and mtDNAcn are both hallmarks of aging, which might accelerate the progression of diabetes. There is abundant evidence that the abrasion of telomere could activate the tumor suppressor gene p53 and inhibit the expression of PGC1a,
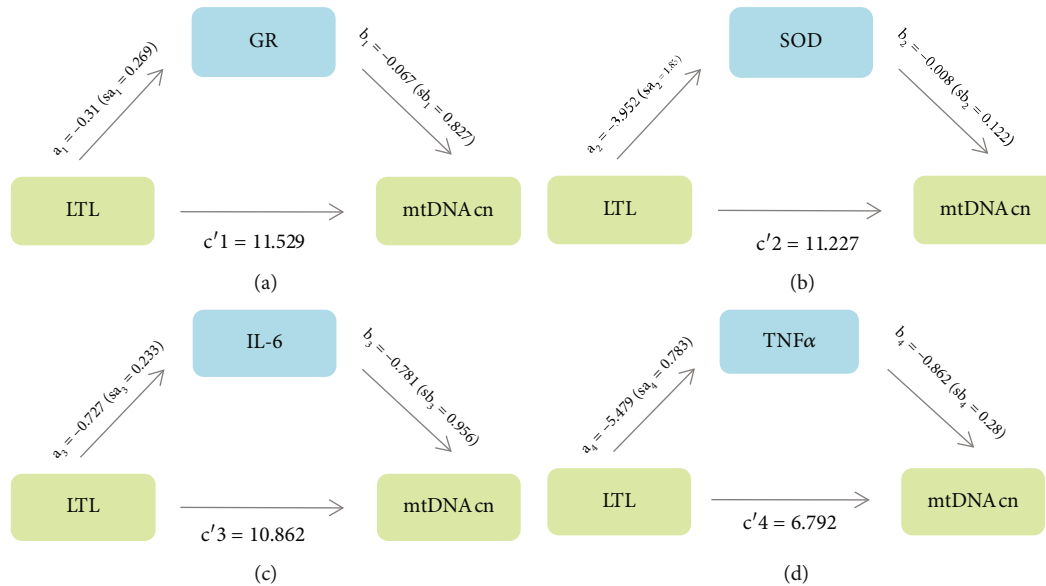
Figure 3: Mediational analysis of antioxidants and inflammatory indicators on the relationship between LTL and mtDNAcn after adjusting for age and gender. (a) a1: the effect of LTL on GR ($p = 0.251$); b1: the effect of GR on mtDNAcn ($p = 0.925$); a1 × b1: mediating effect of GR on mtDNAcn; $c'1$: the direct effect of LTL on mtDNAcn after the correction of GR ($p = 0.001$). (b) a2: the effect of LTL on SOD activity ($p = 0.032$); b2: the effect of SOD activity on mtDNAcn ($p = 0.472$); a2 × b2: mediating effect of SOD activity on mtDNAcn; $c'2$: the direct effect of LTL on mtDNAcn after the correction of SOD activity ($p = 0.001$). (c) a3: the effect of LTL on IL-6 ($p = 0.002$); b3: the effect of IL-6 on mtDNAcn ($p = 0.415$); a3 × b3: mediating effect of IL-6 on mtDNAcn; $c'3$: the direct effect of LTL on mtDNAcn after the correction of IL-6 ($p = 0.001$). (d) a4: the effect of LTL on TNFα ($p \leq 0.001$); b4: the effect of TNFα on mtDNAcn ($p = 0.002$); a4 × b4: mediating effect of TNFα on mtDNAcn; $c'4$: the direct effect of LTL on mtDNAcn after the correction of TNFα ($p = 0.058$).

leading to the dysfunction of mitochondrial synthesis [11]. On the other hand, excessive acetyl-CoA in the mitochondria has been shown to increase the production of NADH resulting in an aggravation of telomere attrition. Our previous study has revealed that mtDNAcn is negatively correlated with plasma glucose levels measured at 30 and 120 min during 75 g OGTT in population with different glucose status [12]. The present study has indicated that LTL is positively correlated with mtDNAcn only in the AGM group, which indicated that the decrease in mtDNAcn might imply a decline of glucose-stimulate insulin secretion (GSIS) of β-cell [12]. The activation of telomere-mitochondrial interaction in the glucose intolerance population might induce deterioration of β-cell and insulin resistance. In other words, the vicious cycle between telomere shortening and mitochondria dysfunction might be formed by hyperglycemia. However, based upon the evidence of the cross-sectional characteristics, this study cannot provide a definitive causal link between the telomere-mitochondrial axis and hyperglycemia.

HbA1c, a critical biomarker that reflects long-term glycemic control, has its value in predicting the complications associated with aging among diabetic patients [13]. This study demonstrates that LTL is shortened with the elevation of HbA1c, indicating that telomere damage might be involved in poorly controlled hyperglycemia. However, no correlation has been found between mtDNAcn and HbA1c, which suggests that the interaction between telomere and mitochondria is not mediated by hyperglycemia itself. Inflammation and oxidative stress have been firmly established as central roles in the development of hyperglycemia,

which is also a promoter of mitochondria disorder [14]. Although previous studies have proved that lipid metabolism and oxidative stress were closely related to inflammatory factors [15], this study suggests that neither lipid metabolism nor antioxidant indices affected the telomere-mitochondrial interaction. The present study shows that the positive correlation between LTL and mtDNAcn disappears after adjusting for inflammatory factors, including IL6 and TNFα, indicating that inflammatory factors are critical factors for the interaction between telomere and mitochondria.

Among several antioxidants and inflammatory markers, this study has revealed that only TNFα exerts a complete mediating effect on the telomere-mitochondrial interactome and confirmed that TNFα is negatively correlated with mtDNAcn on a higher level of HbA1c. However, how TNFα mediated the telomere-mitochondria axis in hyperglycemia remains unclear and has yet to be further explored. TNFα is a proinflammatory cytokine and can be downregulated by the activation of the SIRT1 (sirtuin1) gene. Research in the elderly has proved that the expression of the SIRT1 gene mediates a 40% positive correlation between LTL and mtDNAcn [16]. It can be hypothesized that the LTL shortening in hyperglycemia may increase the TNFα level by reducing SIRT1 activity, which leads to a reduction of mtDNAcn. The treatment aimed at lowering the TNFα level is expected to delay the progression of mitochondrion dysfunction caused by telomere attrition due to hyperglycemia. Meanwhile, the improvement of mitochondrion function can benefit the glucose uptake driven by the oxidative phosphorylation and slow down the cell senescence of

individuals with hyperglycemia [17]. Given the limited evidence, further research is required to look into the specific mechanisms of TNFα-mediated telomere attrition and mitochondria dysfunction.

5. Conclusions

This is a cross-sectional study based on a noninterventional rural community in Beijing, China. Over half of adults in this rural population are found to have AGM by OGTT, including diabetes and prediabetes. It is also shown that mitochondrial dysfunction is closely related to telomere shortening, which is fully mediated by elevation of TNFα in AGM depending on hyperglycemia.

Data Availability

338 The datasets analysed in this manuscript are not publicly available. Requests to access the datasets should be directed to the datasets supporting the conclusions of this manuscript arebavailable from the corresponding author (pingfan6779@163.com or liyuxiu@medmail.com.cn) on reasonable request.

Conflicts of Interest

All authors declare no conflict of interest.

Acknowledgments

References

[1] F. Bragg, M. V. Holmes, A. Iona et al., "Association between diabetes and cause-specific mortality in rural and urban areas of China," *Journal of the American Medical Association*, vol. 317, no. 3, pp. 280–289, 2017.

[2] Q. Zheng, J. Huang, and G. Wang, "Mitochondria, telomeres and telomerase subunits," *Frontiers in Cell and Developmental Biology*, vol. 7, p. 274, 2019.

[3] W. Udomsinprasert, Y. Poovorawan, V. Chongsrisawat, P. Vejchapipat, J. Jittikoon, and S. Honsawek, "Leukocyte mitochondrial DNA copy number as a potential biomarker indicating poor outcome in biliary atresia and its association with oxidative DNA damage and telomere length," *Mitochondrion*, vol. 47, pp. 1–9, 2019, Epub 2019 Apr 20.

[4] D. R. Matthews, J. P. Hosker, A. S. Rudenski, B. A. Naylor, D. F. Treacher, and R. C. Turner, "homeostasis model assessment: insulin resistance and beta-cell function from fasting plasma glucose and insulin concentrations in man," *Diabetologia*, vol. 28, no. 7, pp. 412–419, 1985.

[5] M. Zhou, L. Zhu, X. Cui et al., "Influence of diet on leukocyte telomere length, markers of inflammation and oxidative stress in individuals with varied glucose tolerance: a Chinese population study," *Nutrition Journal*, vol. 15, p. 39, 2016.

[6] R. M. Cawthon, "Telomere length measurement by a novel monochrome multiplex quantitative PCR method," *Nucleic Acids Research*, vol. 37, no. 3, article e21, 2009.

[7] B. F. Zhou and C Cooperative Meta-Analysis Group of the Working Group on Obesity in China, "Predictive values of body mass index and waist circumference for risk factors of certain related diseases in Chinese adults–study on optimal cut-off points of body mass index and waist circumference in Chinese adults," *Biomedical and Environmental Sciences*, vol. 15, pp. 83–96, 2002.

[8] Y. Xu, L. Wang, J. He et al., "Prevalence and control of diabetes in Chinese adults," *Journal of the American Medical Association*, vol. 310, no. 9, pp. 948–959, 2013.

[9] R. Wang, P. Zhang, C. Gao et al., "Prevalence of overweight and obesity and some associated factors among adult residents of Northeast China: a cross-sectional study," *BMJ Open*, vol. 6, no. 7, article e010828, 2016.

[10] J. H. Kim, H. K. Kim, J. H. Ko, H. Bang, and D. C. Lee, "The relationship between leukocyte mitochondrial DNA copy number and telomere length in community-dwelling elderly women," *PLoS One*, vol. 8, no. 6, article e67227, 2013.

[11] L. J. Yan, "Pathogenesis of chronic hyperglycemia: from reductive stress to oxidative stress," *Journal Diabetes Research*, vol. 2014, article 137919, 11 pages, 2014.

[12] M. C. Zhou, L. Zhu, X. Cui et al., "Reduced peripheral blood mtDNA content is associated with impaired glucose-stimulated islet β cell function in a Chinese population with different degrees of glucose tolerance," *Diabetes/Metabolism Research and Reviews*, vol. 32, no. 7, pp. 768–774, 2016.

[13] E. Selvin, M. W. Steffes, H. Zhu et al., "Glycated hemoglobin, diabetes, and cardiovascular risk in nondiabetic adults," *The New England Journal of Medicine*, vol. 362, no. 9, pp. 800–811, 2010.

[14] X. Bao, Y. Borné, L. Johnson et al., "Comparing the inflammatory profiles for incidence of diabetes mellitus and cardiovascular diseases: a prospective study exploring the 'common soil' hypothesis," *Cardiovascular Diabetology*, vol. 17, no. 1, p. 87, 2018.

[15] H. P. Kopp, C. W. Kopp, A. Festa et al., "Impact of weight loss on inflammatory proteins and their association with the insulin resistance syndrome in morbidly obese patients," *Arteriosclerosis, Thrombosis, and Vascular Biology*, vol. 23, no. 6, pp. 1042–1047, 2003.

[16] N. Pieters, B. G. Janssen, L. Valeri et al., "Molecular responses in the telomere-mitochondrial axis of ageing in the elderly: a candidate gene approach," *Mechanisms of Ageing and Development*, vol. 145, pp. 51–57, 2015.

[17] M. T. Lewis, J. D. Kasper, J. N. Bazil, J. C. Frisbee, and R. W. Wiseman, "Quantification of mitochondrial oxidative phosphorylation in metabolic disease: application to type 2 diabetes," *International Journal of Molecular Sciences*, vol. 20, no. 21, p. 5271, 2019.

Research Article

Cerebral Mitochondrial Function and Cognitive Performance during Aging: A Longitudinal Study in NMRI Mice

Martina Reutzel,[1] Rekha Grewal,[1] Benjamin Dilberger,[1] Carmina Silaidos,[1] Aljoscha Joppe,[2] and Gunter P. Eckert [ID][1]

[1]*Institute of Nutritional Sciences, Laboratory for Nutrition in Prevention and Therapy, Justus-Liebig-University of Giessen, Biomedical Research Center Seltersberg (BFS), Schubertstrasse 81, 35392 Giessen, Germany*
[2]*Department of Biological Sciences & Cluster of Excellence Macromolecular Complexes, Institute of Molecular Biosciences, Johann Wolfgang Goethe University Frankfurt, Frankfurt am Main, Germany*

Correspondence should be addressed to Gunter P. Eckert; eckert@uni-giessen.de

Brain aging is one of the major risk factors for the development of several neurodegenerative diseases. Therefore, mitochondrial dysfunction plays an important role in processes of both, brain aging and neurodegeneration. Aged mice including NMRI mice are established model organisms to study physiological and molecular mechanisms of brain aging. However, longitudinal data evaluated in one cohort are rare but are important to understand the aging process of the brain throughout life, especially since pathological changes early in life might pave the way to neurodegeneration in advanced age. To assess the longitudinal course of brain aging, we used a cohort of female NMRI mice and measured brain mitochondrial function, cognitive performance, and molecular markers every 6 months until mice reached the age of 24 months. Furthermore, we measured citrate synthase activity and respiration of isolated brain mitochondria. Mice at the age of three months served as young controls. At six months of age, mitochondria-related genes (complex IV, creb-1, β-AMPK, and Tfam) were significantly elevated. Brain ATP levels were significantly reduced at an age of 18 months while mitochondria respiration was already reduced in middle-aged mice which is in accordance with the monitored impairments in cognitive tests. mRNA expression of genes involved in mitochondrial biogenesis (cAMP response element-binding protein 1 (creb-1), peroxisome proliferator-activated receptor gamma coactivator 1-alpha (PGC1-α), nuclear respiratory factor-1 (Nrf-1), mitochondrial transcription factor A (Tfam), growth-associated protein 43 (GAP43), and synaptophysin 1 (SYP1)) and the antioxidative defense system (catalase (Cat) and superoxide dismutase 2 (SOD2)) was measured and showed significantly decreased expression patterns in the brain starting at an age of 18 months. BDNF expression reached, a maximum after 6 months. On the basis of longitudinal data, our results demonstrate a close connection between the age-related decline of cognitive performance, energy metabolism, and mitochondrial biogenesis during the physiological brain aging process.

1. Introduction

The average life expectancy has increased considerably to over 80 years in developed countries [1], and the multifactorial aging process is characterized by several changes on the cellular level [2, 3]. Mitochondria are cell organelles with central functions such as energy metabolism, including ATP production and generation of reactive oxygen species (ROS); however, mitochondrial dysfunction has been identified as an important hallmark of aging [4–9]. In addition, there are many studies that describe the close relationship between various age-related diseases and impaired mitochondrial function, which makes mitochondria interesting as a potential target for the treatment and prevention of neurodegenerative diseases [10, 11]. Mitochondrial dysfunction is characterized by a reduced efficiency of the respiratory chain system diminishing the synthesis of high-energy molecules such as ATP and the expression of genes involved in mitochondrial biogenesis, cellular longevity, and the antioxidant defense systems [12]. Evidences point out that the

activity of complex I and complex IV of the respiratory chain system is impaired in aged brains which leads to a reduced capability to produce ATP [13, 14]. In 1956, the "free radical, theory of aging" was postulated by Harman which states that cellular aging is a direct consequence of free radicals, especially the superoxide anion radical ($O_2^{\cdot-}$), attacking cells and tissue [3, 15–17]. This framework has been refined over the last years. In 1979, mitochondria were identified as the key producer of ROS that significantly contribute to aging processes [18–21]. However, low "physiological" ROS levels are known to have important functions for signaling mechanisms in the cell [22]. Under physiological conditions, the antioxidative defense system, including superoxide dismutase (SOD) and the glutathione (GSH) system, is able to eliminate highly reactive molecules [23]. However, if there is an imbalance between the generation of ROS and the cellular defense system, oxidative damage occurs which can initiate apoptosis and trigger neurodegenerative diseases. Furthermore, aging is characterized by changes in mitochondrial dynamics [24]: these organelles are able to fuse and to divide. The later process, the so-called fission, is part of the cellular quality control and results in fragments of different sizes that are cleared by mitophagy [25, 26]. The fission processes also help to regulate the cellular ATP levels. Fusion leads to enrichment of mtDNA and finally reduces mutations, [24].

Most of the aging studies in rodents conducted so far compared aged animals to young ones but did not collect longitudinal data over the entire lifetime. Thus, studies on cognitive performance and bioenergetic parameters in the brain covering the lifespan are rare. Therefore, we measured the development of the energy metabolism and mRNA expression of genes involved in mitochondrial biogenesis, antioxidant capacity, and synaptic plasticity in the brain as well as the cognitive performance every six months in the same cohort of female NMRI mice. Female NMRI mice are a well-described outbred mouse model for the physiological, "normal" aging process which reflects a high variability of the genome [27–29]. This model has been described as most suitable for studies on physiological aging compared to inbred or genetically modified mouse models with accelerated aging or reduced lifespans [30, 31].

2. Material and Methods

2.1. Animals and Treatment. Female NMRI mice (Navar Medical Research Institute) were purchased at the age of 3 weeks from Charles River (Sulzbach, Germany) and kept in the animal station until they reached the ages of 3, 6, 12, 18, and 24 months. All mice had ad libitum access to a standard pelleted diet (cat. no.1324; Altromin, Lage, Germany) and drinking water. Behavioral testing was performed before all time points. Mice were sacrificed by decapitation. The brain was quickly dissected on ice after the removal of the cerebellum, the brain stem, and the olfactory bulb. All experiments were carried out by individuals with appropriate training and experience according to the requirements of the Federation of European Laboratory Animal Science Associations and the European Communities Council Direc-

tive (Directive 2010/63/EU). Experiments were approved by the regional authority (Regierungspraesidium Darmstadt; #V54–19 c 20/15–FU/1062).

2.2. Passive Avoidance Test. The test was carried out using a passive avoidance step-through system (cat. no. 40533/mice; Ugo Basile, Germonio, Italy) and a protocol similar to the protocol published by Shiga et al. [32]. On day one of the experiment, the mouse was put into the light chamber (light intensity 75%). The door toward the dark chamber was opened after a 30 s delay, and time was recorded until the mouse enters into the dark chamber. In the dark chamber, the mouse received an electric shock (0.5 mA, 1 s duration). If the mouse did not enter the dark chamber after 180 s, the test was stopped. The same test was repeated 24 h later. This time, the door toward the dark chamber was already opened after 5 s and time was measured until the mouse entered the dark chamber but the electric shock was turned off. The test was aborted after 300 s.

2.3. One-Trial Y-Maze Test. A one-trial Y-maze test was conducted using a custom-made Y-maze (material: polyvinyl chloride; length of arms: 36 cm; height of arms: 7 cm; width of arms: 5 cm; and angle between arms: 120°). At the beginning of the test, the mouse was put into one of the three arms of the Y-maze, and the sequence of the entries was recorded for 5 min. Spontaneous alternation was determined using the formula (number of alternations/number of entries)/2 [33].

2.4. Preparation of Dissociated Brain Cells. One hemisphere of the brain was used to prepare dissociated brain cells (DBCs) for ex vivo studies. The brain was washed once in medium 1 (138 mM NaCl, 5.4 mM KCl, 0.17 mM Na_2HPO_4, 0.22 mM KH_2PO_4, 5.5 mM glucose $*$ H_2O, and 58.4 mM sucrose; pH = 7.35). Afterwards, it was cut into small pieces in 2 ml of medium 1 using a scalpel. The chopped brain was then pressed through a 200 μm nylon mesh into a beaker containing 16 ml of medium 1 using a plastic Pasteur pipette with a wide opening. In the last step, the brain homogenate was filtered through a 102 μm nylon mesh. The resulting brain homogenate was centrifuged (2000 rpm, 5 min, and 4°C) before the pellet was redissolved in 20 ml of medium 2 (110 mM NaCl, 5.3 mM KCl, 1.8 mM $CaCl_2$ $*$ 2 H_2O, 1 mM $MgCl_2$ $*$ 6 H_2O, 25 mM Glucose $*$ H_2O, 70 mM sucrose, and 20 mM HEPES). The centrifugation step was repeated twice; after the last centrifugation, the pellet was redissolved in 4.5 ml of Dulbecco's modified without supplements. DBCs were seeded in 250 μl aliquots in 12 replicates into a 24-well plate for the measurement of the mitochondrial membrane potential. For the measurement of the ATP level, DBCs were seeded in 50 μl aliquots into a 96-well plate. Cells were incubated for 3 h in a humidified incubator (5% CO_2). Respectively, 6 wells were incubated for 3 h with sodium nitroprusside (0.5 mM for ATP measurement; 2 mM for the measurement of the mitochondrial membrane potential) in DMEM. The remaining cell suspension was reserved for protein determination and stored at -80°C.

2.5. Measurement of ATP Concentrations in DBCs. The Via-Light Plus bioluminescence kit (Lonza, Walkersville, USA)

was used for assessing ATP concentrations in DBC. At the end of the incubation, the 96-well plate was removed from the incubator and allowed to cool to room temperature for 10 min. Afterwards, all wells were incubated with 25 μl lysis buffer in the dark for 10 min. In the next step, wells were incubated with 50 μl monitoring reagent. The emitted light (bioluminescence) was recorded using a luminometer (Victor X3 multilabel counter). The ATP concentrations in the wells were determined using a standard curve; ATP concentrations of DBC were normalized to protein content.

2.6. Measurement of Mitochondrial Membrane Potential. MMP was measured in DBC using the fluorescence dye Rhodamine123 (R123). DBCs were incubated in an incubator (37°C, 5% CO_2) for 15 min with 0.4 μM R123. Afterwards, the reaction was stopped by adding Hank's Balanced Salt Solution (HBSS) into the wells. DBCs were centrifuged (914 g, 5 min, room temperature), the medium was aspirated, and DBCs were supplemented with new HBSS. DBCs were triturated to obtain a homogenous sample. Subsequently, MMP was assessed by reading the R123 fluorescence at an excitation wavelength of 490 nm and an emission wavelength of 535 nm (Victor X3 multilabel counter). The fluorescence in each well was read in four consecutive runs. The fluorescence values were then normalized to protein content.

2.7. Isolation of Brain Mitochondria and High-Resolution Respirometry. Half a brain hemisphere (the frontal part) was used to isolate brain mitochondria. The protocol is described in Hagl et al. [34]. The pellet obtained from the last centrifugation step was dissolved in 250 μl MIRO5 (0.5 mM EGTA, 3 mM $MgCl_2 * 6 H_2O$, 60 mM K-lactobionat, 20 mM taurine, 10 mM KH_2PO_4, 20 mM HEPES, 100 mM sucrose, 1 g/l BSA). Subsequently, 80 μl of the resulting cell suspension was injected into an Oxygraph 2k-chamber. A complex protocol was used to investigate the function of the respiratory chain complexes. The capacity of the oxidative phosphorylation (OXPHOS) was determined using complex I-related substrates pyruvate (5 mM), malate (2 mM), and ADP (2 mM) followed by the addition of succinate (10 mM). Mitochondrial integrity was measured by addition of cytochrome c (10 μM). Oligomycin (2 μg/ml) was added to determine leak respiration (leak (omy)), and afterwards, uncoupling was achieved by carbonyl cyanide p-(trifluoro-methoxy)phenylhydrazone (FCCP, injected stepwise up to 1-1.5 μM). Complex II respiration was measured after the addition of rotenone (0.5 μM). Complex III inhibition was achieved by the addition of antimycin A (2.5 μM) and was subtracted from all respiratory parameters. COX activity was measured after ROX determination by applying 0.5 mM tetramethylphenylenediamine (TMPD) as an artificial substrate of complex IV and 2 mM ascorbate to keep TMPD in the reduced state. Autoxidation rate was determined after the addition of sodium azide (>100 mM), and COX respiration was additionally corrected for autoxidation.

2.8. Citrate Synthase Activity. Citrate synthase activity was measured photometrically in isolated brain mitochondria as described in Hagl et al. [34].

2.9. Protein Quantification. Protein content was determined according to the BCA method using a Pierce™ Protein Assay Kit (Fisher Scientific, Waltham, MA, USA) according to the manufacturer's instructions.

2.10. Transcription Analysis by Quantitative Real-Time PCR (qRT-PCR). Total RNA was isolated using the RNeasy Mini Kit (Qiagen, Hilden, Germany) according to the manufacturer's instructions using ~20 mg RNAlater stabilized samples (Qiagen, Hilden, Germany). RNA was quantified measuring the absorbance at 260 and 280 nm using a Nano-Drop™ 2000c spectrometer (Thermo Fisher Scientific, Waltham, MA, USA). RNA purity was assessed using the ratio of absorbance 260/280 and 260/230. To remove residual genomic DNA, samples were treated with a TURBO DNA-free™ kit according to the manufacturer's instructions (Thermo Fisher Scientific, Waltham, MA, USA). Complementary DNA was synthesized from 250 ng total RNA using the iScript cDNA Synthesis Kit (BioRad, Munich, Germany) according to the manufacturer's instructions and was stored at -80°C. qRT-PCR was conducted using a CfX 96 Connect™ system (BioRad, Munich Germany). Oligonucleotide primer sequences, primer concentrations, and product sizes are listed in Table 1. All primers were received from Biomol (Hamburg, Germany) or Biomers (Ulm, Germany). cDNA for qRT-PCR was diluted 1 : 5 with RNase-free water (Qiagen, Hilden, Germany), and all samples were performed in triplicates. PCR cycling conditions were an initial denaturation at 95°C for 3 min, followed by 45 cycles of 95°C for 10 s, 58°C for 45 s, and 72°C for 29 s. Gene expression was analyzed using the $-(2\Delta\Delta C_q)$ method using BioRad CfX manager software and was normalized to the expression levels of beta 2 microglobulin (B2M) and phosphoglycerate kinase 1 (PGK1).

2.11. Statistics. Unless otherwise stated, values are presented as mean ± standard error of the mean (SEM). Statistical analyses were performed by applying one-way ANOVA with Tukey's multiple comparison post-test (Prism 8.0 GraphPad Software, San Diego, CA, USA). Statistical significance was defined for p values of < 0.05.

3. Results

Female NMRI mice of one cohort were investigated at 3, 6, 12, 18, and 24 months of age. Mice aged 24 months had to be excluded from both of the cognitive tests, since they were too impaired in their mobility.

3.1. Effect of Aging on Cognitive Performance. Spatial learning memory and locomotor activity were determined using the Y-maze spontaneous alternation test in 3-, 6-, 12-, and 18-month-old mice [29, 35, 36].

Mice, aged 6 or 12 months, showed slightly but not significantly decreased changes in alternation rates compared to young controls during a five-minute testing phase (Figure 1(a)). Significant changes were observed at an age of 18 months (-21%) (Figure 1(a)). Regarding the number of alternations, 6- and 12-month-old NMRI mice showed numerically but not significantly reduced performance

TABLE 1: Oligonucleotide primer sequences, product sizes, and primer concentrations for quantitative real-time PCR.

Primer	Sequence	Product size (bp)	Conc. (μM)
AMPK (β-subunit)	5′-agtatcacggtggttgctgt-3′ 5′-caaatactgtgcctgcctct-3′	190	0.1
B2M	5′-ggcctgtatgctatccagaa-3′ 5′-gaaagaccagtccttgctga-3′	198	0.4
BDNF	5′-gatgccagttgctttgtctt-3′ 5′-atgtgagaagttcggctttg-3′	137	0.1
CI (NADH-ubiquinone oxidoreductase 51 kDa subunit)	5′-acctgtaaggaccgagaga-3′ 5′-gcaccacaaacacatcaaaa-3′	227	0.1
CIV (cytochrome c oxidase subunit 5A)	5′-ctgttccattcgctgctatt-3′ 5′-gcgaacagcactagcaaaat-3′	217	0.1
Creb-1	5′-tagctgtgacttggcattca-3′ 5′-ttgttctgtttgggacctgt-3′	184	0.5
CS	5′-aacaagccagacattgatgc-3′ 5′-atgaggtcctgctttgtcct-3′	184	0.1
GAP43	5′-agggagatggctctgctact-3′ 5′-gaggacggggagttatcagt-3′	190	0.15
Nrf-1	5′-tcggagcacttactggagtc-3′ 5′-ctagaaaacgctgccatgat-3′	228	0.5
PGC1-α	5′-tgtcaccaccgaaatcct-3′ 5′-cctggggaccttgatctt-3′	124	0.05
PGK1	5′-gcagattgtttggaatggtc-3′ 5′-tgctcacatggctgacttta-3′	185	0.4
SOD2	5′-acagcgcatactctgtgtga-3′ 5′-gggggaacaactcactttt-3′	183	0.1
SYP1	5′-tttgtggttgttgagttcct-3′ 5′-gcatttcctccccaaagtat-3′	204	0.1
Tfam	5′-agccaggtccagctcactaa-3′ 5′-aaacccaagaaagcatgtgg-3′	166	0.5

bp: base pairs; conc.: concentration.

compared to young animals (Figure 1(b)). Significantly reduced changes in the number of alternations were recorded starting at an age of 12 months (-28%) (Figure 1(b)).

The fear-based passive avoidance test was used to assess the cognitive performance in 3-, 6-, 12-, and 18-month-old mice [37, 38]. Young mice remembered the foot shock they received when they entered the dark chamber 24 hours before quite well as indicted by an increased latency time on day two (Figure 2). On day two, old animals reentered the dark chamber faster than young control animals resulting in significantly lower latency times (Figure 2) indicating a lack in memory in mice aged 12 (-60%) and 18 months (-65%). At the age of 24 months, mice showed severe impairments in mobility. Thus, they were no longer usable for the test and had to be excluded.

3.2. Effect of Aging on Gene Expression. The expression of genes involved in longevity, mitochondrial biogenesis and function, synaptic plasticity, and antioxidative properties was determined in brains of 3-, 6-, 12-, 18-, and 24-month-old mice. All genes considered showed significant changes in the expression pattern during the observed aging process in the brain. It was observed that the mRNA expression of creb-1, Tfam, complex IV, BDNF, and β-AMPK, which are mainly involved in mitochondrial biogenesis and physical activity, significantly increased during the young adulthood (6 months) and showed a significantly reduced expression with 24 months compared to that of young control animals (Figures 3(a)–3(e)). Furthermore, PGC1-α and Nrf-1, two other important transcription factors involved in mitochondrial biogenesis, showed an approximately constant

(a)

(b)
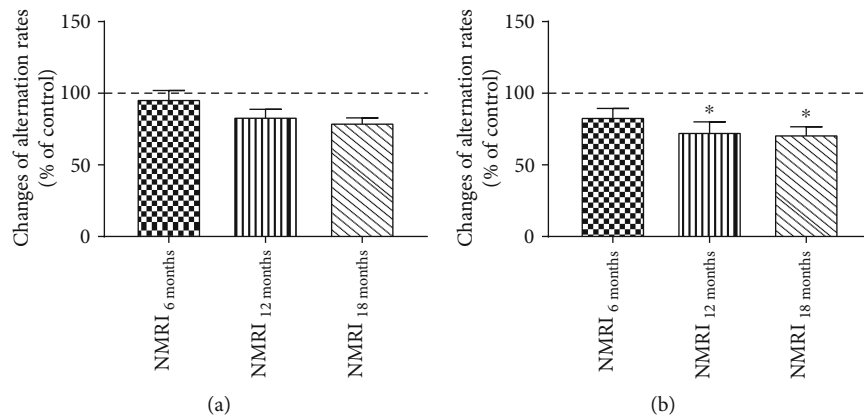
FIGURE 1: Y-Maze spontaneous alternation test of 3-, 6-, 12-, and 18-month-old mice during a five-minute period time of testing. Changes of alternation rates (% of control) (a) and changes of number of alternations (% of control) (b); $n = 12$, mean $\pm$ SEM, and one-way ANOVA with Tukey's post hoc test; $*p < 0.05$. Performance of young control mice (3 months) is defined as 100%.
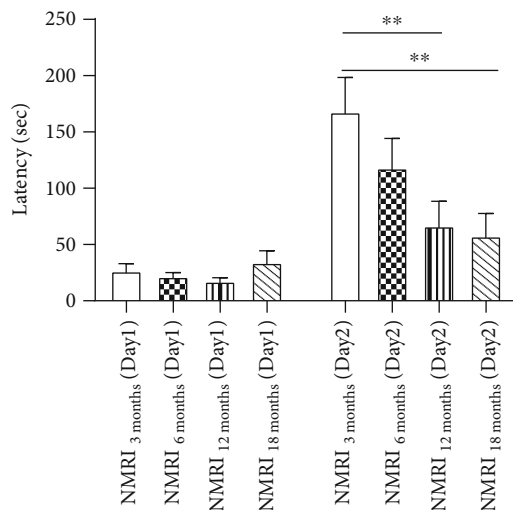
FIGURE 2: Passive avoidance test with 3-, 6-, 12-, and 18-month-old NMRI mice. On day one, mice receive a mild electric shock (0.5 mA) and time that the mouse needs to enter into the dark chamber is recorded; 24 h after the first testing period, the test is repeated and time that the mouse needs to reenter the dark chamber is recorded; $n = 15$, mean $\pm$ SEM, and one-way ANOVA with Tukey's post hoc test; $*p < 0.05$ and $**p < 0.01$.

expression level until the age of 24 months where mRNA expression decreased significantly in comparison to young mice (Table 2). Additionally, gene expression of the mitochondrial mass marker citrate synthase was significantly reduced starting at the age of 18 months. mRNA expression of SOD2 and Cat, enzymes responsible for the antioxidative cellular properties, significantly started to decline with 18 months. However, complex I mRNA expression was approximately constant until the age of 24 months. Expression of the synaptosomal markers SYP1 and GAP43 decreased at an age of 6 months. Unexpectedly, SYP1 mRNA expression was unchanged in 18-month-old mice only (Table 2).

3.3. Effect of Aging on Brain ATP Levels and Mitochondrial Membrane Potential (MMP).
ATP and MMP levels were measured in dissociated brain cells (DBCs) of 3-, 6-, 12-, 18-, and 24-month-old NMRI mice [28, 39]. ATP levels of 6- and 12-month-old mice showed no significant changes compared to those of young control animals. ATP levels were significantly reduced in DBC isolated from 18-month-old NMRI mice (-33%). However, ATP levels showed a numerical increase with 24-month-old compared to 3-month-old mice (+25%). MMP levels were significantly reduced in brains of 24-month-old NMRI mice compared to 18-month-old animals (-28%, Table 3).

3.4. High-Resolution Respirometry in Isolated Mitochondria.
The complexes of the inner mitochondria membrane (complex I, NADH: ubiquinone oxidoreductase (CI); complex II, succinate-coenzyme Q reductase (CII); complex III, cytochrome c oxidoreductase (CIII); and complex IV, cytochrome c oxidase (CIV)) are essential for building up the mitochondrial membrane potential (MMP) which is the driving force for complex V of the mitochondrial respiration chain (F_1/F_0-ATPase (CV)) that produces ATP [40]. Adult mice, aged 6 months, did not show any differences concerning mitochondrial respiration compared to 3-month-old control animals (Table 3). However, mitochondrial respiration of complexes I (-30.3%) and IV (-20.4%) was significantly reduced starting at an age of 12 months compared to that of young animals (Table 3). Respiration of CI+CII (-25.6%) and CII_{ETS} (-32%) in isolated mitochondria gradually declines during aging starting at an age of 12 months (Table 4).

4. Discussion

In order to understand the physiological brain aging process, longitudinal aging studies are superior to single point studies since they provide a good indication of when the first cognitive deficits occurred during lifetime [41, 42]. The special characteristic of our study is that we used a single cohort of NMRI mice to examine the effects of the physiological aging
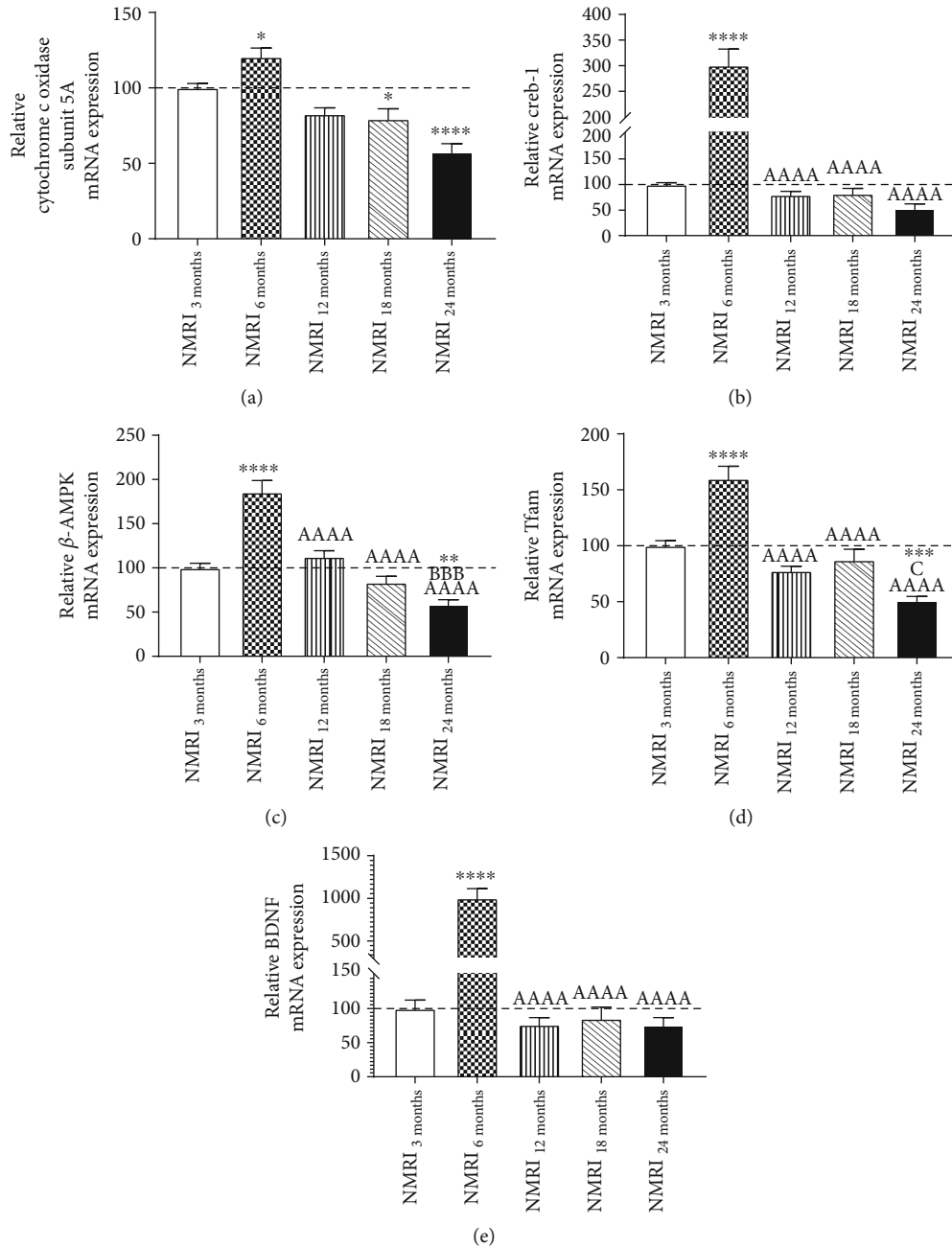
FIGURE 3: Relative normalized mRNA expression levels of cytochrome c oxidase subunit 5A (a), cAMP response element-binding protein (creb-1) (b), AMP-activated protein kinase (β-AMPK) (c), mitochondrial transcription factor A (Tfam) (d), and brain-derived neurotrophic factor (BDNF) (e) in brain homogenate of 3-, 6-, 12-, 18-, and 24-month-old mice. mRNA expression of 3-month-old control mice is 100%. $n = 9$, mean $\pm$ SEM with one-way ANOVA and Tukey's post hoc test with $^*p < 0.05$, $^{**}p < 0.01$, $^{***}p < 0.001$, and $^{****}p < 0.0001$ against 3-month-old control animals. "A" indicates one-way ANOVA and Tukey's post hoc test against 6-month-old mice, "B" against 12-month-old mice, and "C" against 18-month-old animals. Results are normalized to the mRNA expression levels of beta 2 microglobulin (B2M) and phosphoglycerate kinase 1 (PGK1).

process in the brain while most previous studies focused on one time point only to examine the brain aging process (Table 5). To our knowledge, we are the first who used NMRI mice of 3, 6, 12, 18, and 24 months of age to explore changes during the aging process in one cohort. In the end, these data allow a more detailed picture of mitochondrial and cognitive functions during the aging process. Overall, our data show an early decline of cognitive functions in middle-aged NMRI mice, which do not seem to go along simultaneously with the identified impairments on the molecular level and the bioenergetics of the brain. These findings are potentially important for the prevention of neurodegenerative diseases, for which aging processes are an important risk factor and can start early, well before the first symptoms appear.

TABLE 2: Relative normalized mRNA expression levels in brain homogenate from 3-, 6-, 12-, 18-, and 24-month-old mice determined using quantitative real-time PCR in comparison to 3-month-old control animals. mRNA expression of 3-month-old control mice is 100%; $n = 9$; mean ± SEM with one-way ANOVA and Tukey's post hoc test with $*p < 0.05$, $**p < 0.01$, $***p < 0.001$, and $****p < 0.0001$. "A" indicates one-way ANOVA and Tukey's post hoc test against 6-month-old mice, "B" against 12-month-old mice, and "C" against 18-month-old animals. Results are normalized to the mRNA expression levels of beta 2 microglobulin (B2M) and phosphoglycerate kinase 1 (PGK1).

Gene	6 months	12 months	18 months	24 months
Complex I (CI)	95.0 ± 3.3	102.1 ± 6.8	89.3 ± 7.0	$60.3 \pm 5.4^{***/AA/BBB/CC}$
Citrate synthase (CS)	83.1 ± 4.7	86.4 ± 7.7	$69.9 \pm 6.0^{*}$	$50.5 \pm 5.1^{***/A/B}$
Growth-associated protein (GAP43)	$66.5 \pm 2.8^{****}$	$66.6 \pm 4.8^{****}$	$80.2 \pm 4.8^{*}$	$58.7 \pm 4.6^{****/C}$
Synaptophysin 1 (SYP1)	$81.4 \pm 4.4^{*}$	86.6 ± 2.4	103.8 ± 6.0^{AA}	$66.9 \pm 4.8^{****/B/CCCC}$
Superoxide dismutase 2 (SOD2)	109.0 ± 5.3	81.6 ± 8.2^{A}	$72.7 \pm 6.9^{*/AAA}$	$50.1 \pm 4.6^{****/AAAA/B}$
Catalase (Cat1)	104.5 ± 3.7	89.5 ± 5.4	$66.4 \pm 6.3^{****/AAAA/B}$	$64.2 \pm 6.8^{****/AAAA/B}$
Peroxisome proliferator-activated receptor gamma coactivator 1-alpha (PGC1-α)	83.3 ± 3.9	82.7 ± 5.9	88.3 ± 8.5	$62.5 \pm 9.9^{*}$
Nuclear respiratory factor-1 (NRF-1)	93.9 ± 7.8	85.7 ± 6.9	86.8 ± 9.6	$51.2 \pm 4.8^{****/AA/B/CC}$

TABLE 3: Basal ATP and MMP levels of dissociated brain cells (DBCs) as well as protein-normalized respiration of complexes I and IV in isolated mitochondria from 3-, 12-, 18-, and 24-month-old mice; $n = 10$; mean ± SEM; with one-way ANOVA and Tukey's post hoc test with $*p < 0.05$, $**p < 0.01$, and $****p < 0.0001$ compared to young control animals. # indicates significant changes against 18-month-old mice with $p < 0.05$.

	ATP level (nmol/mg protein)	MMP level (AU/mg protein)	CI (pmol/(s∗mg protein))	CIV (pmol/(s∗mg protein))
3 mo	1.2 ± 0.1	79323 ± 3401	1906 ± 133	8060 ± 660
6 mo	1.4 ± 0.1	86166 ± 6272	1799 ± 131	8048 ± 495
12 mo	1 ± 0.1	83357 ± 5612	$1327 \pm 84^{**}$	$6412 \pm 202^{*}$
18 mo	$0.8 \pm 0.1^{*}$	104125 ± 11331	$1199 \pm 131^{**}$	$5591 \pm 313^{**}$
24 mo	1.5 ± 0.2	$74770 \pm 4217^{\#}$	$1232 \pm 145^{**}$	$4814 \pm 489^{****}$

TABLE 4: Protein-normalized respiration of CI+CII and CII$_{ETS}$ in isolated brain mitochondria from 3-, 12-, 18-, and 24-month-old mice; $n = 10$; mean ± SEM; with one-way ANOVA and Tukey's post hoc test with $*p < 0.05$, $**p < 0.01$, $***p < 0.001$, and $****p < 0.0001$ compared to young control animals.

	CI+II (pmol/(s∗mg protein))	CII$_{ETS}$ (pmol/(s∗mg protein))
3 mo	3416 ± 240	1904 ± 140
6 mo	3222 ± 158	1827 ± 79
12 mo	$2539 \pm 119^{**}$	$1292 \pm 90^{**}$
18 mo	$2149 \pm 107^{***}$	$1000 \pm 104^{****}$
24 mo	$1605 \pm 163^{****}$	$995 \pm 109^{****}$

One important finding in our cohort study was that mice at the age of 6 months showed a significantly different phenotype in comparison to young but also to older mice. It seems that extensive changes take place in the brain of animals at the age of 6 months, which need to be investigated in future studies. Interestingly, most aging studies use 3-month-old NMRI mice as young controls [35, 43]. Moreover, these observations demonstrate the importance of longitudinal aging studies, investigating more than one time point to describe the brain aging process and cognitive decline. Spe-

cific aspects of our study, such as study type, behavioral tests, and the role of mitochondria in brain aging, are discussed in the following sections.

4.1. Longitudinal Study. Longitudinal studies (Table 5, A) of the brain aging process, which provide information on mitochondrial bioenergetics in combination with cognitive function, are rare. Most longitudinal studies only consider behavioral tests or mitochondrial parameters during lifetime. More importantly, most studies did not examine mice from a cohort but reported differences at individual points in time (Table 5, B), which makes it difficult to give a clear picture of the development and course of the physiological aging process in the brain.

4.2. Behavioral Testing. Monitoring the following aging process, 18-month-old mice had a significantly reduced alternation rate and number of alternations compared to young control animals, indicating a reduced spatial learning memory and mobility in 18-month-old NMRI mice (Figures 1(a) and 1(b)) which is in agreement with previous studies [29, 36]. In comparison, other studies already showed a significantly decreased performance in the Y-maze test in middle-aged mice [43, 49]. Furthermore, our findings indicate that long-term memory seems to be already impaired in middle-aged mice during the physiological aging process whereas spatial learning memory

TABLE 5: Results from longitudinal studies (A) and single point studies (B) focused on the results of mitochondrial bioenergetics and cognitive functions. Unless otherwise stated, 3-month-old animals served as young controls. Arrows indicate the age at which significant effects were first observed ($\uparrow$ increase, $\downarrow$ decrease, and $\leftrightarrow$ no significant effect).

	MMP	ATP	CI	CIV	Cognitive function	Mouse strain	Lit.
(A) Longitudinal studies							
Current study	$\downarrow$ (24 m)	$\downarrow$ (18 m)	$\downarrow$ (12 m)	$\downarrow$ (12 m)	$\downarrow$ (12 m)	NMRI	
Navarro et al. 2005	n.d.	$\leftrightarrow$ (13 m) $\leftrightarrow$ (19 m)	$\uparrow$ (13 m) $\downarrow$ (19 m)	$\downarrow$ (13 m) $\downarrow$ (19 m)	n.d.	CD-1	[44]
Kwong et al. 2000	n.d.	n.d.	$\leftrightarrow$ (13 m) $\leftrightarrow$ (29 m)	$\leftrightarrow$ (13 m) $\leftrightarrow$ (29 m)	n.d.	C57Bl/6	[45]
Lamberty et al. 1990	n.d.	n.d.	n.d.	n.d.	$\downarrow$ (9 m) $\downarrow$ (12 m)	NMRI	[43]
Gower et al.1993	n.d.	n.d.	n.d.	n.d.	$\downarrow$ (9 m) $\downarrow$ (12 m)	NMRI	[36]
(B) Single point studies							
Reutzel et al. 2018	$\leftrightarrow$	$\downarrow$ (18 m)	$\leftrightarrow$	$\leftrightarrow$	$\downarrow$ (18 m)	NMRI	[28]
Hagl et al. 2016	$\leftrightarrow$	$\downarrow$ (18 m)	$\leftrightarrow$	$\downarrow$ (18 m)	$\downarrow$ (18 m)	NMRI	[27]
Afshordel et al. 2015	n.d.	$\downarrow$ (24 m)	$\leftrightarrow$ (24 m)	$\leftrightarrow$ (24 m)	n.d.	NMRI	[46]
Hagl et al. 2015	$\leftrightarrow$ (18 m)	$\leftrightarrow$	$\downarrow$ (18 m)	$\leftrightarrow$ (18 m)	n.d.	NMRI	[47]
Stoll et al. 1996	n.d.	n.d.	n.d.	n.d.	$\leftrightarrow$ (12 m) $\leftrightarrow$ (22 m)	NMRI	[48]

n.d.: not determined.

seems to be more or less unaffected until the age of 18 months. The signaling molecule BDNF has several functions in brain aging and plasticity. It is an important component in biochemical pathways and is a key player in energy metabolism, neuronal survival, and neurogenesis [50–52] and has been shown to play a crucial role in hippocampus-dependent learning behavior [53]. However, during the physiological aging process, we have measured a strong decrease in gene expression of this important neurotrophic factor starting at 12 months of age. During the young adulthood of mice (6 months), BDNF mRNA expression reaches a maximum and maintains at a constant level throughout aging which is in agreement with previous findings from Webster et al. who reported a significant rise in the prefrontal cortex of BNDF in young adults [54]. Furthermore, mice lacking SYP1 show significantly reduced learning behavior [55], and an enriched environment has been reported to have positive effects on the SYP1 brain level [56]. In accordance with these findings, we detected numerically decreased SYP1 mRNA expression levels during the brain aging process starting in young adulthood which is in agreement with the observed deficits on cognition. Surprisingly, SYP1 mRNA expression increased numerically at an age of 18 months compared to 12-month-old animals. Synaptophysin is reported to be a component of neurotransmitter-containing presynaptic vesicle membranes, and its increase is closely connected to an improved neurotransmission and cognitive performance [56, 57]. However, data availability and the connection between SYP1 mRNA levels in the brain are not consistent. According to this, other studies did not show any age-related changes in SYP1 brain levels [58, 59], while others reported significantly decreased SYP1 with age [60–62]. GAP43, another nervous

tissue-specific protein, is mainly involved in neurite outgrowth and elongation during the neuronal development and is also regarded as a marker for neural plasticity [63–65]. In our study, GAP43 was highly expressed in brains of 3-month-old animals which is in accordance with findings from Rosskothen-Kuhl and Illing who found the highest expression of GAP43 during the early development of the nervous system [66]. Recently, we reported that mRNA levels of all three proteins involved in neuronal plasticity were significantly decreased in brains of aged NMRI mice [39], which is confirmed by our recent data. The reduced expression of those genes indicates less synaptic plasticity and neuronal remodelling in brains of aged NMRI mice which might be one possible reason for the cognitive impairments in memory and motor performance during the aging process [67, 68].

4.3. Mitochondrial Bioenergetics during the Physiological Aging Process. In accordance with most of the previous studies from our group, we measured significantly reduced ATP levels in dissociated brain cells isolated from brains of 18-month-old NMRI mice in comparison to young control animals. In accordance with the finding of reduced ATP levels in brains of aged NMRI mice, we found reduced mRNA expression levels of complex IV in the brain of 18-month-old mice, which is one of the most important protein complexes involved in the oxidative phosphorylation process consistent with previous studies [28, 29, 39]. A reduced complex IV expression was associated with an increase in apoptosis [69, 70]. Bowling et al. showed an age-associated progressive decline of the respiratory chain complexes I and IV in cortices of primates [71], and Petrosillo et al. measured a reduced complex I activity in brain mitochondria of 24-month-old rats [72], whereas other studies could not confirm those

findings in brains of aged mice [45]. The mitochondrial membrane potential (MMP) reflects the mitochondrial functional status and is mainly produced by complex I, complex III, and complex IV that transport protons from the mitochondrial matrix into the intermembrane space [73]. However, at the age of 24 months, we detected a small, but only numerical, increase of ATP brain levels which is in contrast to the results from Afshordel et al. who reported significantly reduced brain ATP levels in 24-month-old mice [46]. Furthermore, the group of Navarro et al. did not show any significant changes of ATP levels in brains of 13- and 19-month-old CD-1 mice [44]. Thus, age-dependent changes in ATP levels seem to depend on the strain of mice that was investigated.

Regarding the mitochondrial membrane potential, we detected reduced MMP in brains of 24-month-old mice compared to young animals which is in accordance with the reduced complex I and IV mRNA expression in brains of aged mice. Based on these data, one would expect a reduced respiration of the respiratory chain complexes [74, 75]. Accordingly, in the current study, activity of respiratory chain complexes I and IV as well as CI+CII and CII$_{ETS}$ was significantly reduced starting at 12 months of age compared to that of young animals (Tables 3 and 4) which is in accordance with previous studies of our group detecting reduced complex activity in brains of 18-month-old animals [28, 29]. Surprisingly, our longitudinal study shows that complex activity seems to be reduced already in middle-aged animals while brain ATP and MMP levels stay constant until mice reach the age of 18 and 24 months.

4.4. Mitochondrial Biogenesis and the Antioxidative Defense System during the Aging Process. Mitochondrial biogenesis is a process in which new mitochondria are formed from existing mitochondria and is regulated by peroxisome proliferator-activated receptor gamma (PPARγ) coactivator 1-alpha (PGC1-α). PGC1-α as a master regulator of mitochondrial biogenesis is activated by AMPK-activated kinase and Sirt-1 which are the two major pathways to induce mitochondrial biogenesis. AMPK is able to phosphorylate PGC1-α, or it activates Sirt-1 through increasing the NAD+ level. Alternatively, the transcription factor creb-1 pathway is induced which finally leads to the generation of new mitochondria [76]. During the brain aging process, we detected a significantly reduced mRNA expression of PGC1-α, Nrf-1, Tfam, creb-1, AMPK, and citrate synthase (CS), which is a key enzyme in mitochondria involved in the citric acid cycle (TCA) and thus provides information on mitochondrial mass. However, we did not find reduced citrate synthase activity, which is a common marker for mitochondrial mass (data not shown). In accordance with other studies, we were able to confirm that during the aging process, mitochondrial biogenesis seems to be impaired. For example, Picca et al. described an impaired protein expression of PGC1-α and Nrf-1 in liver tissue of aged rats [77]. Furthermore, overexpression of Tfam is able to reverse age-dependent memory loss in mice which shows the close connection between the detected cognitive impairments and the reduced mRNA expression of genes involved in mitochondrial biogenesis

found in aged mice [78]. In contrast to our previous work which described a reduced gene expression in brains of 18-month-old mice [28, 29], in this longitudinal study, we were only able to confirm a reduced mRNA expression of most of the considered genes in brains of mice aged 24 months. We therefore hypothesize that rodents can keep physiological mRNA expression until at least the age of 18 months, but the decrease detected at 24 months of age is finally a result of the ongoing senescence [75].

Antioxidant enzymes like SOD2 and Cat1 are involved in the antioxidative defense system of the cell and are able to protect macromolecules like DNA, lipids, and proteins from oxidative damage. Thus, our findings show an age-dependent decrease of SOD2 and Cat1 starting at an age of 18 months which gives evidence that damaging effects could occur more probably in the aged mouse brain. Thus, the data availability shows variable results concerning the antioxidative enzymes. Leutner et al. showed an increased SOD activity in brains of NMRI mice starting at an age of 10 months, while other studies could not find any changes of SOD or Cat in 24-month-old rats [29, 79].

In particular, mRNA gene expression is affected first in brains of very old animals. These observations suggest that SYP1 and GAP43 [80, 81], two genes involved in synaptic plasticity and synaptogenesis, may be one possible reason for the early decline in the passive avoidance test. Furthermore, we hypothesize that the brain, as an energy-demanding organ, is able to maintain stable ATP levels until mice reach the age of 18 months, although the oxidative phosphorylation is already affected in middle-aged animals in our study. These observations suggest that glycolysis and its metabolites should be further investigated to determine the exact mechanisms behind these results since several studies showed deficits in glucose metabolism in brains of aged rats as well as healthy, old people [82, 83]. Any changes in the physiological brain glucose metabolism, mainly supported by mitochondria, affect neuronal function, cognition, learning, and memory [84].

5. Conclusion

Many clinical and neuropathological symptoms of AD occur parallel to the normal aging process which makes it difficult to keep them apart from each other. During the physiological aging process, several changes on cognitive performance, mitochondrial brain energy metabolism, and mRNA expression of genes involved in mitochondrial biogenesis were detected in a longitudinal study over 24 months. Most of the impairments on cognition and mitochondria bioenergetics were detected starting at an age of 18 months which in fact shows that aged NMRI mice are an appropriate model to study the physiological (brain-) aging process.

Data Availability

The data set generated during this study is available from the corresponding author on reasonable request.

Conflicts of Interest

The authors declare that they have no conflicts of interest.

Acknowledgments

References

[1] M. Kritsilis, S. V. Rizou, P. Koutsoudaki, K. Evangelou, V. Gorgoulis, and D. Papadopoulos, "Ageing, cellular senescence and neurodegenerative disease," *International Journal of Molecular Sciences*, vol. 19, no. 10, article 2937, 2018.

[2] J. Y. Jang, A. Blum, J. Liu, and T. Finkel, "The role of mitochondria in aging," *The Journal of Clinical Investigation*, vol. 128, no. 9, pp. 3662–3670, 2018.

[3] A. Grimm and A. Eckert, "Brain aging and neurodegeneration: from a mitochondrial point of view," *Journal of Neurochemistry*, vol. 143, no. 4, pp. 418–431, 2017.

[4] D. A. Chistiakov, I. A. Sobenin, V. V. Revin, A. N. Orekhov, and Y. V. Bobryshev, "Mitochondrial aging and age-related dysfunction of mitochondria," *BioMed Research International*, vol. 2014, Article ID 238463, 7 pages, 2014.

[5] A. Bratic and N.-G. Larsson, "The role of mitochondria in aging," *The Journal of Clinical Investigation*, vol. 123, no. 3, pp. 951–957, 2013.

[6] H.-C. Lee and Y.-H. Wei, "Mitochondria and aging," *Advances in Experimental Medicine and Biology*, vol. 942, pp. 311–327, 2012.

[7] Y.-H. Wei and H.-C. Lee, "Oxidative stress, mitochondrial DNA mutation, and impairment of antioxidant enzymes in aging," *Experimental Biology and Medicine (Maywood, N.J.)*, vol. 227, no. 9, pp. 671–682, 2002.

[8] D. V. Ziegler, C. D. Wiley, and M. C. Velarde, "Mitochondrial effectors of cellular senescence: beyond the free radical theory of aging," *Aging Cell*, vol. 14, no. 1, pp. 1–7, 2015.

[9] M. Gonzalez-Freire, R. de Cabo, M. Bernier et al., "Reconsidering the role of mitochondria in aging," *The Journals of Gerontology Series A, Biological Sciences and Medical Sciences*, vol. 70, no. 11, pp. 1334–1342, 2015.

[10] C. Cadonic, M. G. Sabbir, and B. C. Albensi, "Mechanisms of mitochondrial dysfunction in Alzheimer's disease," *Molecular Neurobiology*, vol. 53, no. 9, pp. 6078–6090, 2016.

[11] G. Cenini and W. Voos, "Mitochondria as potential targets in Alzheimer disease therapy: an update," *Frontiers in Pharmacology*, vol. 10, p. 902, 2019.

[12] C. Desler, T. L. Hansen, J. B. Frederiksen, M. L. Marcker, K. K. Singh, and L. Juel Rasmussen, "Is there a link between mitochondrial reserve respiratory capacity and aging?," *Journal of Aging Research*, vol. 2012, Article ID 192503, 9 pages, 2012.

[13] A. K. Pollard, E. L. Craig, and L. Chakrabarti, "Mitochondrial complex 1 activity measured by spectrophotometry is reduced across all brain regions in ageing and more specifically in neurodegeneration," *PLoS One*, vol. 11, no. 6, article e0157405, 2016.

[14] J. D. Pandya, J. E. Royland, R. C. MacPhail, P. G. Sullivan, and P. R. S. Kodavanti, "Age- and brain region-specific differences in mitochondrial bioenergetics in brown Norway rats," *Neurobiology of Aging*, vol. 42, pp. 25–34, 2016.

[15] E. Veal, T. Jackson, and H. Latimer, "Role/s of "antioxidant" enzymes in ageing," *Sub-Cellular Biochemistry*, vol. 90, pp. 425–450, 2018.

[16] J. Viña, "The free radical theory of frailty: mechanisms and opportunities for interventions to promote successful aging," *Free Radical Biology and Medicine*, vol. 134, pp. 690–694, 2019.

[17] G. Barja, "The mitochondrial free radical theory of aging," *Progress in Molecular Biology and Translational Science*, vol. 127, pp. 1–27, 2014.

[18] D. Harman, "The biologic clock: the mitochondria?," *Journal of the American Geriatrics Society*, vol. 20, no. 4, pp. 145–147, 1972.

[19] M. F. Alexeyev, "Is there more to aging than mitochondrial DNA and reactive oxygen species?," *The FEBS Journal*, vol. 276, no. 20, pp. 5768–5787, 2009.

[20] G. Barja, "Updating the mitochondrial free radical theory of aging: an integrated view, key aspects, and confounding concepts," *Antioxidants & Redox Signaling*, vol. 19, no. 12, pp. 1420–1445, 2013.

[21] M. C. Gomez-Cabrera, F. Sanchis-Gomar, R. Garcia-Valles et al., "Mitochondria as sources and targets of damage in cellular aging," *Clinical Chemistry and Laboratory Medicine*, vol. 50, no. 8, pp. 1287–1295, 2012.

[22] J. M. Son and C. Lee, "Mitochondria: multifaceted regulators of aging," *BMB Reports*, vol. 52, no. 1, pp. 13–23, 2019.

[23] I. Liguori, G. Russo, F. Curcio et al., "Oxidative stress, aging, and diseases," *Clinical Interventions in Aging*, vol. 13, pp. 757–772, 2018.

[24] A. Chauhan, J. Vera, and O. Wolkenhauer, "The systems biology of mitochondrial fission and fusion and implications for disease and aging," *Biogerontology*, vol. 15, no. 1, pp. 1–12, 2014.

[25] J. Bereiter-Hahn, "Do we age because we have mitochondria?," *Protoplasma*, vol. 251, no. 1, pp. 3–23, 2014.

[26] E. M. Fivenson, S. Lautrup, N. Sun et al., "Mitophagy in neurodegeneration and aging," *Neurochemistry International*, vol. 109, pp. 202–209, 2017.

[27] S. Leutner, A. Eckert, and W. E. Müller, "ROS generation, lipid peroxidation and antioxidant enzyme activities in the aging brain," *Journal of Neural Transmission*, vol. 108, no. 8, pp. 955–967, 2001.

[28] M. Reutzel, R. Grewal, C. Silaidos et al., "Effects of long-term treatment with a blend of highly purified olive secoiridoids on cognition and brain ATP levels in aged NMRI mice," *Oxidative Medicine and Cellular Longevity*, vol. 2018, Article ID 4070935, 10 pages, 2018.

[29] S. Hagl, H. Asseburg, M. Heinrich et al., "Effects of long-term rice bran extract supplementation on survival, cognition and brain mitochondrial function in aged NMRI mice," *Neuromolecular Medicine*, vol. 18, no. 3, pp. 347–363, 2016.

[31] L. Harkema, S. A. Youssef, and A. de Bruin, "Pathology of mouse models of accelerated aging," *Veterinary Pathology*, vol. 53, no. 2, pp. 366–389, 2016.

[30] S. Kõks, S. Dogan, B. G. Tuna, H. González-Navarro, P. Potter, and R. E. Vandenbroucke, "Mouse models of ageing and their relevance to disease," *Mechanisms of Ageing and Development*, vol. 160, pp. 41–53, 2016.

[32] T. Shiga, T. J. Nakamura, C. Komine et al., "A single neonatal injection of ethinyl estradiol impairs passive avoidance learning and reduces expression of estrogen receptor α in the

hippocampus and cortex of adult female rats," *PLoS One*, vol. 11, no. 1, article e0146136, 2016.

[33] A. Wolf, B. Bauer, E. L. Abner, T. Ashkenazy-Frolinger, and A. M. S. Hartz, "A comprehensive behavioral test battery to assess learning and memory in 129S6/Tg2576 mice," *PLoS One*, vol. 11, no. 1, article e0147733, 2016.

[34] S. Hagl, A. Kocher, C. Schiborr et al., "Rice bran extract protects from mitochondrial dysfunction in guinea pig brains," *Pharmacological Research*, vol. 76, pp. 17–27, 2013.

[35] A. J. Gower and Y. Lamberty, "The aged mouse as a model of cognitive decline with special emphasis on studies in NMRI mice," *Behavioural Brain Research*, vol. 57, no. 2, pp. 163–173, 1993.

[36] A.-K. Kraeuter, P. C. Guest, and Z. Sarnyai, "The Y-maze for assessment of spatial working and reference memory in mice," in *Pre-Clinical Models*, P. Guest, Ed., vol. 1916 of Methods in Molecular Biology, pp. 105–111, Humana Press, New York, NY, USA, 2019.

[37] I. Izquierdo, C. R. G. Furini, and J. C. Myskiw, "Fear memory," *Physiological Reviews*, vol. 96, no. 2, pp. 695–750, 2016.

[38] P. E. Gold, "The use of avoidance training in studies of modulation of memory storage," *Behavioral and Neural Biology*, vol. 46, no. 1, pp. 87–98, 1986.

[39] S. Hagl, D. Berressem, R. Grewal, N. Sus, J. Frank, and G. P. Eckert, "Rice bran extract improves mitochondrial dysfunction in brains of aged NMRI mice," *Nutritional Neuroscience*, vol. 19, no. 1, pp. 1–10, 2016.

[40] V. Larosa and C. Remacle, "Insights into the respiratory chain and oxidative stress," *Bioscience reports*, vol. 38, no. 5, 2018.

[41] A. Sowa, B. Tobiasz-Adamczyk, R. Topór-Mądry, A. Poscia, and D. I. la Milia, "Predictors of healthy ageing: public health policy targets," *BMC Health Services Research*, vol. 16, Supplement 5, 2016.

[42] M. McGue, A. Skytthe, and K. Christensen, "The nature of behavioural correlates of healthy ageing: a twin study of lifestyle in mid to late life," *International Journal of Epidemiology*, vol. 43, no. 3, pp. 775–782, 2014.

[43] Y. Lamberty and A. J. Gower, "Age-related changes in spontaneous behavior and learning in NMRI mice from maturity to middle age," *Physiology & Behavior*, vol. 47, no. 6, pp. 1137–1144, 1990.

[44] A. Navarro, C. Gómez, M.-J. Sánchez-Pino et al., "Vitamin E at high doses improves survival, neurological performance, and brain mitochondrial function in aging male mice," *American Journal of Physiology. Regulatory, Integrative and Comparative Physiology*, vol. 289, no. 5, pp. R1392–R1399, 2005.

[45] L. K. Kwong and R. S. Sohal, "Age-related changes in activities of mitochondrial electron transport complexes in various tissues of the mouse," *Archives of Biochemistry and Biophysics*, vol. 373, no. 1, pp. 16–22, 2000.

[46] S. Afshordel, S. Hagl, D. Werner et al., "Omega-3 polyunsaturated fatty acids improve mitochondrial dysfunction in brain aging – Impact of Bcl-2 and NPD-1 like metabolites," *Prostaglandins, Leukotrienes, and Essential Fatty Acids*, vol. 92, pp. 23–31, 2015.

[47] S. Hagl, A. Kocher, C. Schiborr, N. Kolesova, J. Frank, and G. P. Eckert, "Curcumin micelles improve mitochondrial function in neuronal PC12 cells and brains of NMRI mice – Impact on bioavailability," *Neurochemistry International*, vol. 89, pp. 234–242, 2015.

[48] S. Stoll, K. Scheuer, O. Pohl, and W. E. Müller, "*Ginkgo biloba* extract (EGb 761) independently improves changes in passive avoidance learning and brain membrane fluidity in the aging mouse," *Pharmacopsychiatry*, vol. 29, no. 4, pp. 144–149, 1996.

[49] Y. Lamberty and A. J. Gower, "Age-related changes in spontaneous behavior and learning in NMRI mice from middle to old age," *Physiology & Behavior*, vol. 51, no. 1, pp. 81–88, 1992.

[50] B. Lu, P. T. Pang, and N. H. Woo, "The yin and yang of neurotrophin action," *Nature Reviews. Neuroscience*, vol. 6, no. 8, pp. 603–614, 2005.

[51] A. Ghosh, J. Carnahan, and M. Greenberg, "Requirement for BDNF in activity-dependent survival of cortical neurons," *Science*, vol. 263, no. 5153, pp. 1618–1623, 1994.

[52] G. Leal, P. M. Afonso, I. L. Salazar, and C. B. Duarte, "Regulation of hippocampal synaptic plasticity by BDNF," *Brain Research*, vol. 1621, pp. 82–101, 2015.

[53] B. Lu, K. H. Wang, and A. Nose, "Molecular mechanisms underlying neural circuit formation," *Current Opinion in Neurobiology*, vol. 19, no. 2, pp. 162–167, 2009.

[54] M. J. Webster, C. S. Weickert, M. M. Herman, and J. E. Kleinman, "BDNF mRNA expression during postnatal development, maturation and aging of the human prefrontal cortex," *Brain Research. Developmental Brain Research*, vol. 139, no. 2, pp. 139–150, 2002.

[55] U. Schmitt, N. Tanimoto, M. Seeliger, F. Schaeffel, and R. E. Leube, "Detection of behavioral alterations and learning deficits in mice lacking synaptophysin," *Neuroscience*, vol. 162, no. 2, pp. 234–243, 2009.

[56] K. M. Frick and S. M. Fernandez, "Enrichment enhances spatial memory and increases synaptophysin levels in aged female mice," *Neurobiology of Aging*, vol. 24, no. 4, pp. 615–626, 2003.

[57] B. Wiedenmann and W. W. Franke, "Identification and localization of synaptophysin, an integral membrane glycoprotein of Mr 38,000 characteristic of presynaptic vesicles," *Cell*, vol. 41, no. 3, pp. 1017–1028, 1985.

[58] M. E. Calhoun, D. Kurth, A. L. Phinney et al., "Hippocampal neuron and synaptophysin-positive bouton number in aging C57BL/6 mice," *Neurobiology of Aging*, vol. 19, no. 6, pp. 599–606, 1998.

[59] M. M. Nicolle, M. Gallagher, and M. McKinney, "No loss of synaptic proteins in the hippocampus of aged, behaviorally impaired rats," *Neurobiology of Aging*, vol. 20, no. 3, pp. 343–348, 1999.

[60] T. D. Smith, M. M. Adams, M. Gallagher, J. H. Morrison, and P. R. Rapp, "Circuit-specific alterations in hippocampal synaptophysin immunoreactivity predict spatial learning impairment in aged rats," *The Journal of Neuroscience*, vol. 20, no. 17, pp. 6587–6593, 2000.

[61] K. S. Chen, E. Masliah, M. Mallory, and F. H. Gage, "Synaptic loss in cognitively impaired aged rats is ameliorated by chronic human nerve growth factor infusion," *Neuroscience*, vol. 68, no. 1, pp. 19–27, 1995.

[62] S. Saito, S. Kobayashi, Y. Ohashi, M. Igarashi, Y. Komiya, and S. Ando, "Decreased synaptic density in aged brains and its prevention by rearing under enriched environment as revealed by synaptophysin contents," *Journal of Neuroscience Research*, vol. 39, no. 1, pp. 57–62, 1994.

[63] G. Grasselli and P. Strata, "Structural plasticity of climbing fibers and the growth-associated protein GAP-43," *Frontiers in Neural Circuits*, vol. 7, p. 25, 2013.

[64] D. Gorup, I. Bohaček, T. Miličević et al., "Increased expression and colocalization of GAP43 and CASP3 after brain ischemic lesion in mouse," *Neuroscience Letters*, vol. 597, pp. 176–182, 2015.

[65] L. Aigner and P. Caroni, "Depletion of 43-kD growth-associated protein in primary sensory neurons leads to diminished formation and spreading of growth cones," *The Journal of Cell Biology*, vol. 123, no. 2, pp. 417–429, 1993.

[66] N. Rosskothen-Kuhl and R.-B. Illing, "*Gap43* transcription modulation in the adult brain depends on sensory activity and synaptic cooperation," *PloS One*, vol. 9, no. 3, article e92624, 2014.

[67] A. S. Buchman, L. Yu, P. A. Boyle, J. A. Schneider, P. L. de Jager, and D. A. Bennett, "Higher brain BDNF gene expression is associated with slower cognitive decline in older adults," *Neurology*, vol. 86, no. 8, pp. 735–741, 2016.

[68] M. P. Mattson, S. Maudsley, and B. Martin, "BDNF and 5-HT: a dynamic duo in age-related neuronal plasticity and neurodegenerative disorders," *Trends in Neurosciences*, vol. 27, no. 10, pp. 589–594, 2004.

[69] Y. Poirier, A. Grimm, K. Schmitt, and A. Eckert, "Link between the unfolded protein response and dysregulation of mitochondrial bioenergetics in Alzheimer's disease," *Cellular and Molecular Life Sciences*, vol. 76, no. 7, pp. 1419–1431, 2019.

[70] Y. Li, J.-S. Park, J.-H. Deng, and Y. Bai, "Cytochrome c oxidase subunit IV is essential for assembly and respiratory function of the enzyme complex," *Journal of Bioenergetics and Biomembranes*, vol. 38, no. 5-6, pp. 283–291, 2006.

[71] A. C. Bowling, E. M. Mutisya, L. C. Walker, D. L. Price, L. C. Cork, and M. F. Beal, "Age-dependent impairment of mitochondrial function in primate brain," *Journal of Neurochemistry*, vol. 60, no. 5, pp. 1964–1967, 1993.

[72] G. Petrosillo, M. Matera, G. Casanova, F. Ruggiero, and G. Paradies, "Mitochondrial dysfunction in rat brain with aging: Involvement of complex I, reactive oxygen species and cardiolipin," *Neurochemistry International*, vol. 53, no. 5, pp. 126–131, 2008.

[73] L. D. Zorova, V. A. Popkov, E. Y. Plotnikov et al., "Mitochondrial membrane potential," *Analytical Biochemistry*, vol. 552, pp. 50–59, 2018.

[74] A. Navarro, "Mitochondrial enzyme activities as biochemical markers of aging," *Molecular Aspects of Medicine*, vol. 25, no. 1-2, pp. 37–48, 2004.

[75] M. Manczak, Y. Jung, B. S. Park, D. Partovi, and P. H. Reddy, "Time-course of mitochondrial gene expressions in mice brains: implications for mitochondrial dysfunction, oxidative damage, and cytochrome *c* in aging," *Journal of Neurochemistry*, vol. 92, no. 3, pp. 494–504, 2005.

[76] P. A. Li, X. Hou, and S. Hao, "Mitochondrial biogenesis in neurodegeneration," *Journal of Neuroscience Research*, vol. 95, no. 10, pp. 2025–2029, 2017.

[77] A. Picca, V. Pesce, F. Fracasso, A. M. Joseph, C. Leeuwenburgh, and A. M. S. Lezza, "Aging and calorie restriction oppositely affect mitochondrial biogenesis through TFAM binding at both origins of mitochondrial DNA replication in rat liver," *PloS One*, vol. 8, no. 9, article e74644, 2013.

[78] Y. Hayashi, M. Yoshida, M. Yamato et al., "Reverse of age-dependent memory impairment and mitochondrial DNA damage in microglia by an overexpression of human mitochondrial transcription factor a in mice," *The Journal of Neuroscience*, vol. 28, no. 34, pp. 8624–8634, 2008.

[79] F. Cand and J. Verdetti, "Superoxide dismutase, glutathione peroxidase, catalase, and lipid peroxidation in the major organs of the aging rats," *Free Radical Biology & Medicine*, vol. 7, no. 1, pp. 59–63, 1989.

[80] J. Bu and H. Zu, "Effects of pregnenolone intervention on the cholinergic system and synaptic protein 1 in aged rats," *The International Journal of Neuroscience*, vol. 124, no. 2, pp. 117–124, 2014.

[81] A. Mohan, A. Thalamuthu, K. A. Mather et al., "Differential expression of synaptic and interneuron genes in the aging human prefrontal cortex," *Neurobiology of Aging*, vol. 70, pp. 194–202, 2018.

[82] A. Miccheli, C. Puccetti, G. Capuani et al., "[1-^{13}C]Glucose entry in neuronal and astrocytic intermediary metabolism of aged rats: A study of the effects of nicergoline treatment by ^{13}C NMR spectroscopy," *Brain Research*, vol. 966, no. 1, pp. 116–125, 2003.

[83] J. L. Eberling, T. E. Nordahl, N. Kusubov, B. R. Reed, T. F. Budinger, and W. J. Jagust, "Reduced temporal lobe glucose metabolism in aging," *Journal of Neuroimaging*, vol. 5, no. 3, pp. 178–182, 1995.

[84] F. Yin, H. Sancheti, I. Patil, and E. Cadenas, "Energy metabolism and inflammation in brain aging and Alzheimer's disease," *Free Radical Biology & Medicine*, vol. 100, pp. 108–122, 2016.

Review Article

Mitochondrial ROS-Modulated mtDNA: A Potential Target for Cardiac Aging

Yue Quan (ID),[1] **Yanguo Xin** (ID),[2] **Geer Tian** (ID),[1] **Junteng Zhou** (ID),[2] and **Xiaojing Liu** (ID)[1,2,3]

[1]*Laboratory of Cardiovascular Diseases, Regenerative Medicine Research Center, West China Hospital, Sichuan University, Chengdu 610041, China*
[2]*Department of Cardiology, West China Hospital, Sichuan University, Chengdu 610041, China*
[3]*Laboratory of Mitochondrial Biology, West China-Washington Mitochondria and Metabolism Center, West China Hospital, Sichuan University, Chengdu 610041, China*

Correspondence should be addressed to Xiaojing Liu; liuxq@scu.edu.cn

Mitochondrial DNA (mtDNA) damage is associated with the development of cardiovascular diseases. Cardiac aging plays a central role in cardiovascular diseases. There is accumulating evidence linking cardiac aging to mtDNA damage, including mtDNA mutation and decreased mtDNA copy number. Current wisdom indicates that mtDNA is susceptible to damage by mitochondrial reactive oxygen species (mtROS). This review presents the cellular and molecular mechanisms of cardiac aging, including autophagy, chronic inflammation, mtROS, and mtDNA damage, and the effects of mitochondrial biogenesis and oxidative stress on mtDNA. The importance of nucleoid-associated proteins (Pol γ), nuclear respiratory factors (NRF1 and NRF2), the cGAS-STING pathway, and the mitochondrial biogenesis pathway concerning the development of mtDNA damage during cardiac aging is discussed. Thus, the repair of damaged mtDNA provides a potential clinical target for preventing cardiac aging.

1. Introduction

Cardiovascular diseases (CVDs) account for 31% of all deaths worldwide [1]. Age is widely recognized as the leading risk factor for CVDs. Cardiac aging is defined as the gradual deterioration of cardiac structure and function with age [2]. Diastolic dysfunction and left ventricular hypertrophy often occur in the elderly. Valvular calcification and fibrosis cause the development of aortic stenosis with age. The ventricular and valvular changes above make the aged heart more vulnerable to stress and contribute to the increased mortality and morbidity of CVDs in the elderly [3, 4]. The aged heart also exhibits a decrease in the number of myocytes, an increase in the size of cardiomyocyte, and an increase in the accumulation of lipids and fibrosis [5]. The interrelationship between the underlying mechanisms of cardiac aging and the interaction between cellular and molecular aging processes and disease-specific pathways are intricate. Elucidating the potential mechanisms of cardiac aging can promote the

development of "antiaging" therapies to prevent or delay the cardiovascular changes.

To explore potential targets of heart aging, it is important to obtain knowledge of adequate preclinical models, which can be used to study the mechanisms of cardiac aging. Canine hearts develop myocardial hypertrophy and accumulate lipofuscin and amyloid, leading to increased myocardial stiffness [6]. Because the distribution of the cardiac conduction system and the electrophysiological properties of dogs are similar to those of the human heart, the dog model has been widely used for electrophysiological research [4]. The Drosophila melanogaster heart has a similar molecular structure and basic physiology as the human heart. Both fly and human hearts experience age-related morphological and functional decline. Several genes in mammals that regulate oxidative stress and cardiac hypertrophy also affect the cardiac aging in a fruit fly [7]. Elderly rhesus monkeys exhibit degenerative calcifications of the aortic and mitral valves, myocardial hypertrophy, lipofuscin accumulation, interstitial
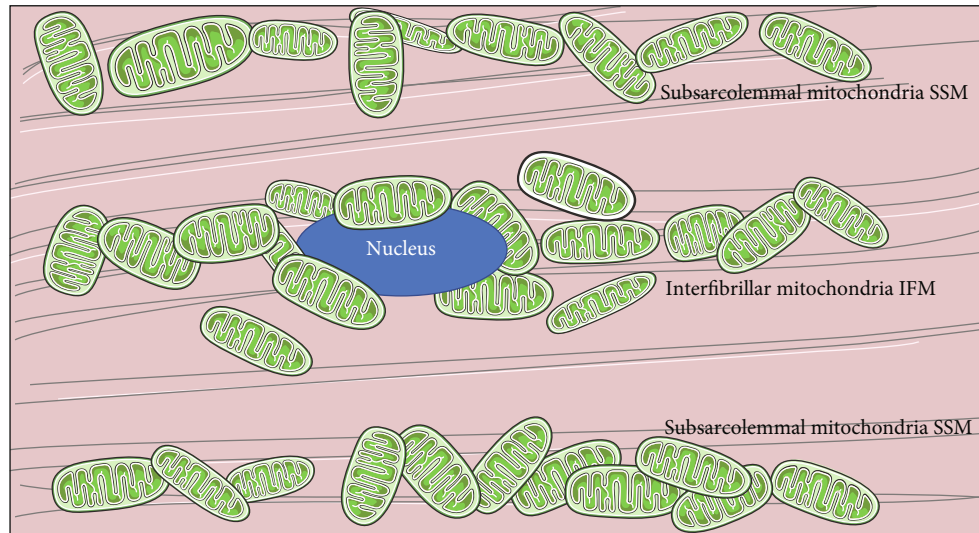
Figure 1: Schematic diagram of cardiomyocyte: the location of the subsarcolemmal mitochondria (SSM) and interfibrillar mitochondria (IFM).

fibrosis, myocardial infarction, and congestive heart failure [4]. Aged mouse hearts indicate increased fibrosis, amyloid deposition, and increased myocardial fiber size [8]. The systolic and diastolic function are also significantly impaired with age. Aged rat hearts demonstrate cardiomyocyte hypertrophy, increased LV fibrosis, and impairment of systolic and diastolic function [4].

The exact mechanisms involved in cardiac senescence are still not fully understood. Current evidence indicates that cardiac senescence is concerned with dysfunctional organelles with age [9]; meanwhile the decline in mitochondrial function during aging has been reported as a fundamental principle of aging biology for many years. As the "energy house" to fuel normal cardiac function, mitochondria research is not confined to bioenergy; new evidence has revealed unanticipated roles of mitochondria as metabolic transit points and platforms for intracellular signaling that modulate cell activities. Subsarcolemmal mitochondria (SSM) and interfibrillar mitochondria (IFM) (Figure 1) are two structurally similar but biochemically different mitochondrial populations in the heart [10]. Nevertheless, the mitochondrial defects in aging have been limited to the IFM population.

Mitochondrial-derived oxidative stress plays a vital role in cardiac aging through irreversible damage to mitochondrial DNA (mtDNA). Enzymes of the electron transport system reside on the inner mitochondrial membrane (IMM), encompassing the mitochondrial matrix containing mtDNA. Excessive mitochondrial reactive oxygen species (mtROS) can damage DNA [11, 12]. The mtDNA damage, which reduces the stabilization of adequate ATP supply during cardiac aging, disrupts the balance of cellular apoptosis, mitochondrial bioenergetics, and biogenesis.

Mitochondrial biogenesis (MB) is the underlying mechanism that controls the number of mitochondria. Mitochondrial function is strongly dependent on the morphology of the mitochondria [13]. Changes in the shape, number, and localization of the mitochondria can cause significant functional modifications. Mitochondria are dynamic entities that undergo movement, fission, and fusion processes, collectively termed the "mitochondrial dynamism"; the morphology plays critical roles in apoptosis, cell death, and development [14, 15]. The coordinated expression of the mitochondrial genome and the nuclear genes encoding mitochondrial proteins is involved in mitochondrial biogenesis. In this review, we highlight the specific mtDNA linked to mitochondrial biogenesis, oxidative metabolism, and the latent clinical utility of mtDNA in the aged heart.

2. Molecular and Cellular Mechanisms of Cardiac Aging

Aging is a complex process via many molecular and cellular mechanisms contributing to a dysfunction in organ function. Better understanding of the mechanisms involved in cardiac aging can guide us to promote healthy heart aging and mitigate the burden of CVD in the elderly. The major mechanisms involved in alterations in the heart are mitochondrial dysfunction, altered autophagy, chronic inflammation, increased mitochondrial oxidative stress, and increased mtDNA instability.

2.1. Inflammation in Cardiac Aging. Inflammation is a hallmark in the cardiac aging process. Inflammatory processes, especially those that mediate chronic low-grade inflammation, are known to lead to the development of age-related CVDs [16]. Mitochondrial dysfunction is closely associated with immune response and chronic inflammation. Studies support that mtROS contribute to the inflammation in the cardiovascular system [17]. mtROS activate the redox-sensitive mediator, nuclear factor-κB (NF-κB), which regulates the transcription of various proinflammatory cytokines

[11, 18]. As the heart ages, prolonged exposure to high levels of oxidants leads to the activation of NF-κB-mediated inflammation. Mitochondrial dysfunction leads to the leak of mtDNA in the cytoplasm or even in the circulation, which can be sensed by toll-like receptor 9 (TLR9) [19]. TLR9 is critical for the synthesis of proinflammatory cytokines. Thus, the leaking mtDNA activates caspase-1 and promotes the secretion of IL-1β and IL-18 in macrophages. In the aged heart, the increased senescent cells modulate inflammation through secreting chemokine and cytokines, such as IL-1β, IL-6, and IL-8, termed the senescence-associated secretory phenotype (SASP) [19, 20]. The cyclic GMP-AMP synthase (cGAS) is a stimulator of the interferon genes (STING). As a DNA sensor, cGAS combines with cytosolic DNA, inducing the production of cyclic GMP-AMP (cGAMP), which activates STING. Activated STING causes the interferon-regulatory factor 3 (IRF3) transcription factor to enter the nucleus, resulting in the secretion of interferon (IFN). The cGAS-STING signaling pathway has been identified as a SASP regulator [21, 22]. When mtDNA is released into the cytoplasm, inflammation is activated through the SASP program initiated by cGAS-STING [23]. Together, the activation of age-related inflammatory processes plays a key role in cardiac aging while cGAS-STING signaling regulates inflammation via multiple mechanisms, which might be a novel intervention target.

2.2. Autophagy in Cardiac Aging. Autophagy is an important cellular process involved in aging and longevity that gradually declines during cardiac aging, resulting in an increase in the sensitivity of the heart to stress [24]. Autophagy is a catabolic process involved in lifespan and aging in the cardiovascular system [25]. It plays a pivotal role in the degradation of damaged or long-lived organelles and proteins though lysosomes. Autophagy and autophagic flux are blocked in the aged heart, resulting in greater susceptibility to stress. The three known types of autophagy are chaperone-mediated autophagy (CMA), microautophagy, and macroautophagy [26]. Macroautophagy, referred to as autophagy, is the most studied autophagic process. Macroautophagy begins with a small vesicular sac, called the phagophore. The phagophore encloses long-lived cytosolic proteins and organelles, forming a double-membraned structure termed an autophagosome [27]. Then, the autophagosomes fuse with lysosomes to form autophagolysosomes, where the cargo is degraded to provide substrates for cellular metabolism to maintain cellular homeostasis. Microautophagy involves the direct capture and engulfment of cytoplasmic cargo through invaginations of the lysosomal membrane. Parts of the damaged mitochondria are degraded by microautophagy [3]. CMA is a highly selective process that specifically targets the cytosolic proteins with a KFERQ motif for degradation.

Autophagy-related genes (ATG) are required for the formation of autophagosomes in yeast. ULK1, the mammalian homologue of ATG1, performs a similar function. Serine/-threonine kinase, the mammalian target of rapamycin (mTOR) is the main regulator of autophagy negatively regulated by mTOR complex 1 (mTORC1) [28]. mTORC1 regulates autophagy induced by rapamycin and changes in nutritional and energy status through ULK1-Atg13-FIP200 complex in mammals [29]. Upon nutrient starvation, mTORC1 is inactivated, thus relieving the inhibition of phosphorylation of ULK1-Atg13-FIP200 complex. In cardiac aging, the modulation of autophagy involves AMP-activated protein kinase (AMPK) [2]. Activated AMPK turns on autophagy though the inhibition of mTOR and redirects metabolism towards increased catabolism and decreased anabolism. During aging, AMPK-mediated autophagy is reduced, suggesting cardiac dysfunction. In addition, AMPK phosphorylation of Ulk1 at a specific serine residue leads to the initiation of autophagy [30]. Rapamycin, an mTOR inhibitor and autophagy inducer, reverses cardiac remodeling and contractile dysfunction without affecting the inflammation state of the elderly heart. Rapamycin feeding for 10 weeks induces autophagy, ameliorates energy metabolism, and alters the myocardial metabolome in aged female mice [5]. As a downstream regulator of AMPK, mTOR plays a crucial role in senescence-induced cardiac remodeling. Resveratrol, an AMPK activator, inhibits mTOR with an antiaging effect. Rapamycin and resveratrol, both of which can activate autophagy, are beneficial for the treatment of cardiac remodeling and heart dysfunction [31]. This emerging evidence suggests that autophagy plays a nonnegligible cardioprotective role with clinical connotations.

3. Mitochondrial Dysfunction in Cardiac Aging

The heart has high energy demand and a high density of mitochondria. Decreased energetic capacity of the cardiac mitochondria is related to aging [32], and the heart is particularly vulnerable to mitochondrial dysfunction caused by damaged structures and increased ROS. Mechanisms contributing to disrupted bioenergetics include decreased nicotinamide adenine dinucleotide (NAD$^+$) levels [33], reduced efficacy of the respiratory chain, mutated mtDNA, leaking electrons, and dysregulated mitochondrial biogenesis. The regular action of membrane transport and barrier functions depends on cellular energy metabolism; thus, the damaged mitochondrial energy metabolism causes decreased electron transport chain (ETC) function and increased ROS generation.

Evidence suggests that the mitochondria structure is disrupted in cardiac senescence, with increased mitochondria size [34]. Electron-microscopy-based studies have demonstrated that the area of IMM obviously decreases [35], showing a loss of cristae with age in rodent heart [36]. Mitochondrial dynamics have been involved in the aging process [37], and the promotion of fusion or blockade of fission prompts cell senescence [17]. Mitofusins (MFN)-1/2 and optic atrophy protein-1 (OPA1) regulate mitochondrial morphology inside adult cardiomyocytes [38]. The deleterious effects of stress-induced OPA1 processing on myocardial function reveal the link between cardiac metabolism and mitochondrial dynamics [39]. The mitochondrial area and ultrastructure are deranged in heart failure with reduced ejection fraction (HFrEF), where the markers of mitochondrial fission dynamin-related protein-1 (DRP1) are deranged

[40]. The balance between fusion and fission is crucial to maintaining heart health [41].

An imbalance between fission and fusion is detrimental to mitochondrial homeostasis and mitochondrial quality [2]. Hence, addressing this unfavorable situation is a vital issue. Mitochondrial fragmentation and damaged mitochondria can be cleared by a form of selective autophagy-mitophagy. Mitophagy is a specific class of autophagy eliminating dysfunctional mitochondria from the heart under normal physiological conditions and pathological stresses, maintaining healthy mitochondria at a stable number [42]. Mitochondrial fusion and mitophagy were observably suppressed by ischemia-reperfusion (I/R) injury, accompanied by myocardial inflammation, infarction area expansion, heart dysfunction, and cardiomyocyte oxidative stress [43]. The mitochondrial membrane kinase, PTEN-induced kinase-1 (PINK1), and the cytosolic E3 ubiquitin ligase (Parkin) pathway are the major mitophagy pathways in mammalian cells [23, 44]. The damaged mitochondria are sensed by the decreased mitochondrial membrane potential ($\Delta\Psi$m) and transduced to Parkin via the autophosphorylation of PINK1 [45]. Ubiquitination of mitochondrial outer membrane proteins mediated by Parkin is an initial signal for autophagosome phagocytosis and subsequently progresses to lysosome degradation [42]. There were severe defects in mitochondrial homeostasis in PINK1 KO mice accompanied by changes in the mitochondrial network and an increase in ROS [46]. Parkin and PINK1 prevent inflammation by removing damaged mitochondria, thereby preventing the increase in cytosolic and circulating mtDNA and providing a new model for how mitophagy may mitigate CVDs [23]. The increase in mitochondrial damage and the decrease in mitochondrial metabolism due to impaired and deficient of mitophagy can lead to the accumulation of damaged mitochondria in cells and aggravate the process of cardiac aging.

4. Mitochondrial Oxidative Metabolism and mtDNA Mutation in Cardiac Aging

4.1. Production of Oxidants in the Aging Heart. Nohl and Hegner [47] discovered that heart mitochondria in old rats generated more H_2O_2 than did mitochondria from the young *in vivo*. Since then, a large body of studies have been published to support the role of mitochondria and cardiac mitochondrial oxidant production in the aging process, identifying that the production of intramitochondrial ROS is the major determinant of aging [48, 49]. In aging, mitochondria produce the majority of ROS during oxidative phosphorylation (OXPHOS) and ATP generation [50]. Deficient electron transport chains (ETCs) are a potential site for ROS production, including subunit complexes I and III [51, 52]. The mitochondrial free radical aging theory hypothesizes that age-related increases in mitochondrial ROS lead to mtDNA mutations and the accumulation of oxidative protein and lipid, which reduce mitochondrial respiratory efficiency [53]. Under homeostatic physiological conditions, a large amount of superoxide anion ($\bullet O^{2-}$) is generated through oxygen transformation due to the leaking of electrons mainly from complexes I and III [54, 55], and mitochondrial manga-

nese superoxide dismutase (SOD2) converts $\bullet O^{2-}$ into H_2O_2 [56]. The increased release of H_2O_2 activates NF-κB-mediated inflammatory response and mitochondrial dysfunction during aging. H_2O_2 is then catabolized by glutathione peroxidase I (GPX1) and catalase (CAT). GPX1 reduces H_2O_2 to glutathione and water. CAT is a common enzyme that catalyzes H_2O_2 to water and oxygen. CAT largely determines mitochondrial antioxidant capacity and is the enzyme most affected during aging [57].

Iron is stored in ferric (Fe^{3+}) form inside ferritin. Oxidative damage to ferritin can cause the release of redox-active ferrous (Fe^{2+}) iron. mtROS-derived mtDNA damage results in a decrease in mitochondrial membrane potential. The reduced mitochondrial membrane potential contributes to the defective transport of iron-sulfur proteins into and out of mitochondria, which is important for the assembly of the mitochondrial iron-sulfur cluster (ISC) and the maturation of iron-sulfur proteins. Defects in the mitochondrial ISC machinery lead to impaired iron homeostasis with increased iron accumulation in mitochondria [58]. In the presence of Fe^{2+}, H_2O_2 is converted into the highly reactive hydroxyl radical ($\bullet$OH) [59]. The mitochondrial iron content increases with aging in the myocardium, which accelerates the generation of $\bullet$OH and oxidative damage in aging [60]. In old rats, the rate of generation of $\bullet O^{2-}$ and $\bullet$OH anion radicals is significantly increased in heart mitochondria [61] (Figure 2).

ROS plays a pivotal role in healthy cellular and mitochondrial signaling and functionality. However, if unchecked, ROS can mediate oxidative damage to tissues and cells, leading to a vicious cycle of inflammation and more oxidative stress. Meanwhile, mitochondria, the major source of ROS, are thought to be particularly vulnerable to oxidative damage. Because of its richness in mitochondria and high oxygen demand, the heart is at high risk of oxidative damage. The most supportive evidence of the central role of mtROS in the aged heart is that overexpression of catalase targeted to mitochondria (mCAT) attenuates cardiac aging [62]. mCAT mice are resistant to fibrosis, cardiac hypertrophy, and biogenesis as well as heart failure [63]. ROS destroys myocardial energetics, leading to the decreased contractile reserve and slowed relaxation. mCAT can correct these effects preceding structural remodeling, suggesting that ROS-mediated energetic damage is sufficient to cause contractile dysfunction in the metabolic heart [64].

4.2. Mitochondrial Oxidative Stress and mtDNA Mutation in Cardiac Aging. A growing body of evidence suggests that there is increasing oxidative damage to mitochondrial DNA in cardiac aging [65, 66]. Because of the histone deficiency, limited DNA repair capabilities, and proximity of mtDNA to the site of mtROS generation, mtDNA can suffer various types of damage, including mtDNA point mutations, mtDNA point deletions, and decreased mtDNA copy number (mtDNA-CN) [67]. The oxidative damage to mtDNA has different types, including single-strand breaks (SSBs), double-strand breaks (DSBs), and oxidized bases such as 7,8-dihydro-8-oxoguanine (8oxoG). The continuous replicative state of mtDNA and existence of the nucleoid structure render mitochondria vulnerable to oxidative
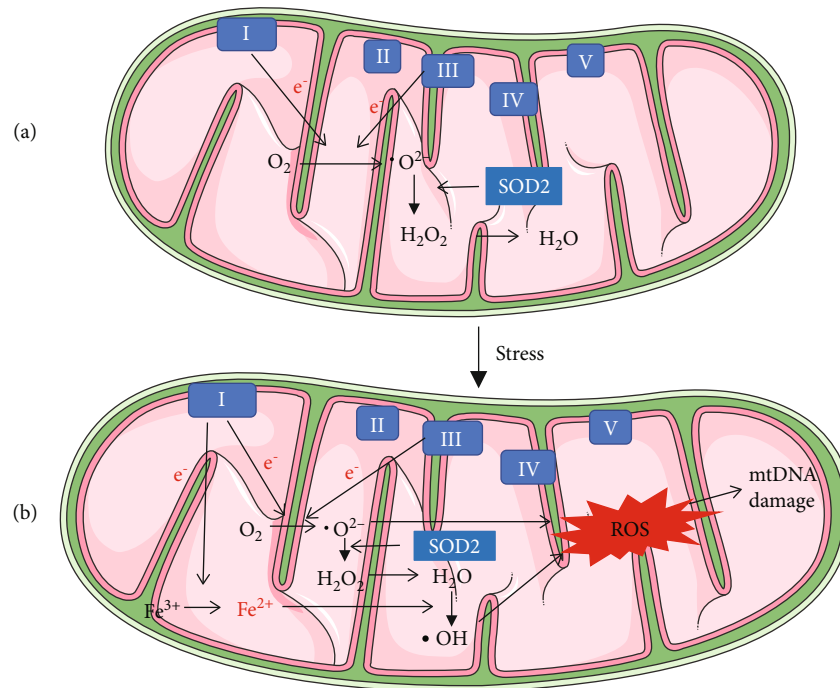
FIGURE 2: Production of oxidants. (a) Under normal physiological conditions, the leaking of electrons from complexes I and III generates highly toxic $\bullet O^{2-}$ through oxygen transformation, and $\bullet O^{2-}$ is converted into less toxic H_2O_2 by SOD2 and neutralized into O_2 and H_2O. In the presence of iron, H_2O_2 is converted into $\bullet OH$. (b) Under pathological conditions, the increase in mitochondrial iron accelerates the generation of $\bullet OH$ and ROS in mitochondria. mtROS can lead to mtDNA damage.

damage and mutations. Single-stranded DNA-binding protein (SSB), transcription factor A (TFAM), RNA polymerase (POLRMT), DNA polymerase gamma (Pol γ), and Twinkle helicase are the primary nucleoid-associated proteins in mitochondria [68, 69]. TFAM and DNA Pol γ are the two crucial metabolism-related genes. Their deletion or overexpression can promote the development of heart failure (HF) in transgenic mice [67]. Homozygous mutation of mitochondrial polymerase γ (Pol$g^{m/m}$) in mice causes cardiac hypertrophy, accelerates aging, and accumulates mutations and deletions of mtDNA [70]. 8oxoG is a common mtDNA oxidation product, and it is considered to be a cellular marker of DNA damage induced by oxidative stress [65]. Previous *in vitro* studies suggest that TFAM preferentially binds to 8oxoG to hinder the repair processes [71]. The removal of 8oxoG is a multistep process that depends on the proteins encoded by mutY DNA glycosylase (*MUTYH*) and 8oxoG DNA glycosylase (*OGG1*) genes. MUTYH excises the misincorporating adenine-inserted opposite 8oxoG [72]. In the human mitochondria, OGG1 excises 8oxoG mispaired with adenine efficiently by catalyzing the splitting of an N-glycosidic bond between the damaged 8oxoG base and a deoxyribose sugar. OGG1 is the main enzyme for base excision repair (BER) of 8oxoG lesions [73]. DNA Pol γ plays a vital role in mtDNA replication [62] simultaneously involving Twinkle helicase and SSB. DNA Pol γ has two main functions: mtDNA synthesis and proofreading. Recent studies report that ROS reduces the proofreading ability of Pol γ, causing replication errors. Thus, oxidation aggravating mtDNA mutations causes replication errors, which indirectly cause mtDNA damage [65, 74]. This proves that mtDNA mutations are largely random rather than transversional, and Pol γ oxidation is likely to account for mtDNA mutations in aging. Therefore, mtDNA mutation may be highly associated with heart aging.

4.3. *Oxidative Damage to Mitochondrial DNA Copy Number.* Altered mtDNA copy number (mtDNA-CN) and increased mutations render impaired mtDNA integrity, causing cellular dysfunction during aging [75]. A calculation of mtDNA-CN by the relative ratio of DNA from the mitochondrial gene NADH dehydrogenase subunit to the nuclear gene cytochrome P4501A1 found that mtDNA-CN decreased in angiotensin (Ang) II-induced cardiac hypertrophy mice [70]. mtDNA-CN is inversely associated with both prevalence and incidence in CVDs and sudden cardiac death (SCD) [76, 77]. mtDNA-CN can be an indirect biomarker of mitochondrial function. Its decline in cells indicates a concomitantly reduced energy metabolism, which may indicate the lack of oxidative stress response. The oxidative stress response causes damage to mtDNA replication enzymes and thus aggravates the decrease in mtDNA-CN further [78]. In pressure-overload-induced HF mice, increased mtDNA-CN induced by the overexpression of Twinkle or TFAM-alleviated fibrosis of the left ventricle, limited mitochondrial oxidative stress, and improved cardiac function [79, 80]. One study observed an inverse association between mtDNA-CN and coronary artery disease in a Chinese population, especially among smokers, and found an inverse correlation between mtDNA-CN and ROS production. This study indicates a vital relationship among mtDNA-CN,
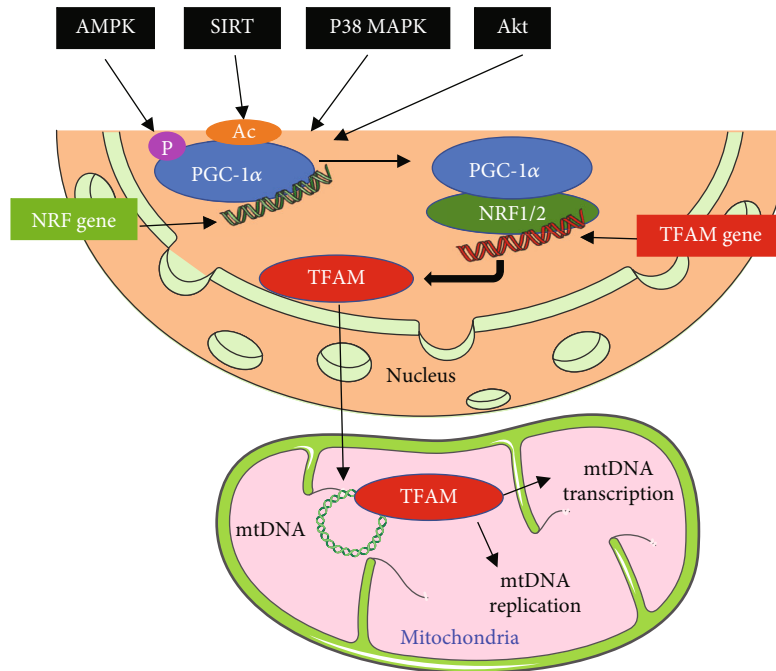
FIGURE 3: The regulation of mitochondrial biogenesis by the PGC-1α-NRF1-TFAM pathway. PGC-1α is activated via phosphorylation by AMPK, deacetylation by Sirtuin, and p38 MAPK. Activated PGC-1α and NRF1/2 result in the synthesis of TFAM. TFAM is a mitochondrial transcriptional regulator encoded by nDNA. Then, TFAM is imported into mitochondria to stabilize mtDNA and enhance the synthesis of subunits of ETC encoded by mtDNA, leading to transcription and replication of mtDNA.

oxidative stress, and coronary artery disease [81]. This evidence suggests that mtDNA-CN has potential clinical utility in improving heart damage.

5. MtDNA Homeostasis Associated with the Mitochondrial Biogenesis in Cardiac Aging

5.1. Mitochondrial Biogenesis Pathway. Mitochondrial biogenesis (MB) is the basis of the mitochondrial life cycle, including coordinated synthesis of nuclear DNA- (nDNA-) and mtDNA-encoded proteins, mtDNA replication, transcription of mitochondrial RNA (mtRNA), and translation of mitochondrial mRNAs. To ensure the proper assembly and function of a large number of proteins assembling the mitochondrial respiratory chain, MB requires the coordination of nDNA- and mtDNA-encoded gene expression [82]. The increased MB in cardiac aging is considered to be a compensatory maladaptive response to the damaged energy metabolism, which is also stimulated by age-related mtROS. Decreased MB is a vital mechanism responsible for myocardial injury and HF [83, 84]. MB alleviates mitochondrial dysfunction induced by oxidative stress and thus is considered to be a novel repair mechanism in aged heart.

Nuclear respiratory factors (NRF1/2) and the peroxisome proliferator-activated receptor gamma coactivator-1α (PGC-1α) regulate the expression of nDNA encoding mitochondrial proteins that are required for respiratory complex and biological function, including fatty acid oxidation (FAO), OXPHOS, and electron transport chain (ETC) [85, 86]. PGC-1α modulates the expression of nDNA-encoded genes, such as TFAM, by interacting with NRF1/2

in mtDNA promoters [33]. Meanwhile, TFAM works in conjunction with mtRNA polymerase to confer promoters with specificity and to increase the transcription initiation rate of mtDNA genes. This process executes replication, transcription, and translation of mtDNA [87, 88] (Figure 3). Research suggests that enalapril reduced mtROS-derived damage and cardiac hypertrophy. Following enalapril treatment, the binding of TFAM to mtDNA regions involved in transcription and replication became stronger in old rats. Mitochondrial mass, autophagy, and MB also increased in enalapril-treated rats [89]. The increased protein levels of NRF1 and TFAM, which are mitochondrial biogenesis factors, caused the restoration of mtDNA loss by oxidants [83]. Taken together, the increased MB may be a therapeutic strategy for heart injury.

5.2. Regulation of Mitochondrial Biogenesis. Many studies indicate that PGC-1α activation through genetic or drug intervention can prevent telomere shortening and age-related changes in the heart [90, 91]. Decreased PGC-1α is a common characteristic in various cardiovascular diseases in mice [92, 93]. PGC-1α has emerged as a powerful regulator of mitochondrial biology in the heart and serves as a master regulator of MB and mitochondrial function [94]. At the posttranslational level, the PGC-1α activity is regulated via phosphorylation by some signaling pathways, including Akt (protein kinase B), AMPK, deacetylation of Sirtuin (SIRT1/3) [95], and mitogen-activated protein kinase (MAPK) p38 (Figure 3).

Intracellular Ca^{2+} handling was impaired with advanced aging. Excessive accumulated Ca^{2+} in mitochondria not only leads to damage of the oxidation respiratory chain, decreased

MB, and increased mtROS but also causes mitochondrial dysfunction, cell apoptosis, and death [96]. The p38 MAPK pathway was activated and induced calcium overload during I/R, which could be relieved by SB203580 (an inhibitor of p38 MAPK) to accelerate the recovery speed of mitochondrial biogenesis and to increase the mtDNA content [97]. Reducing mitochondrial ROS by mitochondria-targeted antioxidant peptide attenuated Ang-induced mitochondrial oxidative damage, decreased MB, increased the phosphorylation of p38 MAPK, and then improved Ang-induced cardiac hypertrophy and fibrosis [98].

SIRT1 and SIRT3, located in the nuclei and mitochondria, regulate mitochondrial functions by deacetylation of nuclear proteins and mitochondrial proteins, respectively. SIRT1 is expressed abundantly in mammalian hearts. It is an NAD$^+$-dependent deacetylase and a marker of MB [99]. Activated SIRT1 improves mitochondrial dysfunction and ameliorates cardiac defects in diabetic animals. SIRT1 promotes MB though deacetylation and activation PGC-1α, thereby completing the metabolic pathway and inhibiting inflammatory signaling [100]. SIRT1-deficient primary myoblasts reduce the mtDNA content and mitochondrial membrane potential. SIRT1 deletion increases both mtROS and the rate of oxidative damage. After pressure overload, SIRT1 gene deletion mice have exhibited exacerbated cardiac dysfunction and alterations of mitochondrial properties [101]. Melatonin ameliorates myocardial I/R injury via SIRT1 activation [99]. SIRT3 has been considered a crucial mitochondrial deacetylase, playing a vital role in energy production, including the supply of intermediates for tricarboxylic acid cycle (TCA) and ETC activation [102]. Oxidative stress inactivates SIRT3 by S-glutathionylation, resulting in inactivation of SOD2 hyperacetylation and induction of mtROS. This forms a vicious cycle between mitochondrial dysfunction and mitochondrial oxidative stress [56]. The increased ROS can be reduced by SIRT3-mediated deacetylation and activation of transcription factor forkhead box O3a (Foxo3a). Deacetylated Foxo3a enhances antioxidant genes SOD2 and catalase, thereby reducing mtROS to protect cardiac function [103]. Under oxidative stress conditions, the Foxo3a existing in the nucleus induces the expression of inflammatory proteins. SIRT1 protects the cell and stabilizes nDNA by deacetylating Foxo3a and attenuating its function [104] (Figure 4). SRT1720, an activator of SIRT1, ameliorates contractile dysfunction and impaired mitophagy in cardiac aging [105]. SIRT3-deficient mice are more susceptible to age-dependent cardiac hypertrophy [106]. Doxorubicin (Doxo), a widely used clinical cancer drug, has a severe side effect on the heart. One study demonstrated that SIRT3 activation protected the heart from Doxo-induced cardiotoxicity by repairing mtDNA damage [66]. Upregulation of SIRT1/3 may improve age-induced cardiac dysfunction, suggesting the therapeutic potential of SIRT1/3 in cardiac aging.

AMPK is an essential cellular fuel sensor of cellular energy defects and controls mitochondrial biogenesis, myocardial morphology, and contractile function. AMPK deficiency may be associated with age-induced cardiac dysfunction according to the evidence that AMPK deficiency distinctly enhances age-associated ROS generation [107]. Mitochondrial
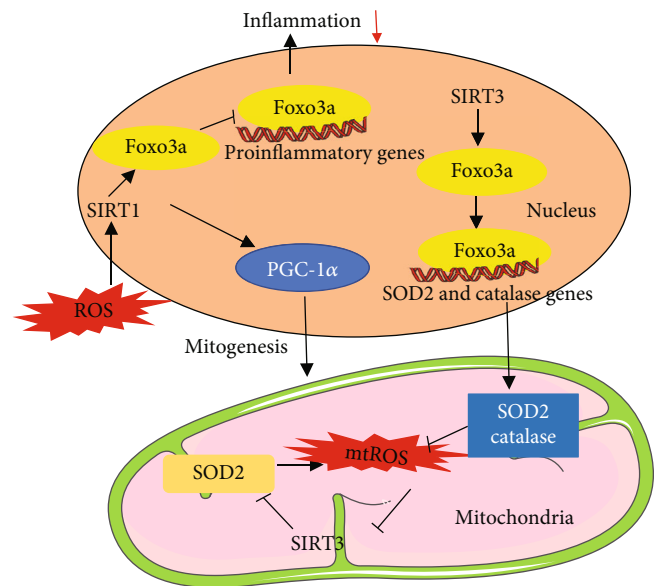
Figure 4: Crucial roles of SIRT1 and SIRT3 in regulation of mitochondrial biogenesis and oxidative stress. SIRT1 is located in the nuclei and regulates mitochondrial functions by deacetylating Foxo3a and attenuating its function to reduce the expression of inflammatory proteins. SIRT1 activates PGC-1α by deacetylating the lysine residues to induce mitochondrial biogenesis. Oxidative stress inactivates SIRT3, resulting in the inactivation of SOD2 hyperacetylation and induction of mtROS. This forms a vicious cycle between mitochondrial dysfunction and mitochondrial oxidative stress. The increased ROS can be reduced by SIRT3-mediated deacetylation and activation of Foxo3a and SOD2. Deacetylated Foxo3a enhances the expression of antioxidant genes SOD2 and catalase to reduce mtROS.

insult or defect activates AMPK, including mtDNA depletion or mutation, and impairs mitochondrial function and mitochondrial production of ATP [108]. The mitochondrial permeability transition pore (mPTP) opening is a sentinel event that triggers cell death in the early ischemic-reperfusion period. AMPK regulates MB by phosphorylating PGC-1α. The overexpression of the active AMPK γ3 subunit increased the expression of PGC-1α [109]. PGC-1α is regulated by AMPK via a variety of indirect mechanisms including p38 MAPK and SIRT1 [108]. Metformin, an AMPK activator at low dose, alleviates age-induced cardiomyocyte contractile defects via inhibition of complex I activity and activation of autophagy and leads to improved MB by increasing PGC-1α expression during I/R and heart failure [110, 111]. These studies indicate that the use of metformin should not be limited to the treatment of diabetes mellitus, and it may have potential clinical use for cardiovascular diseases.

6. Summary and Conclusions

Cardiac aging resulting in defects in cardiac mitochondrial function centers on the mtDNA damage. The mechanisms of the alterations in the aging heart mainly involve mitochondrial dysfunction, altered autophagy, chronic inflammation,

increased mitochondrial oxidative stress, and increased mtDNA instability.

Age-altered mtROS triggers accumulation of point mutations, deletion in mtDNA, and a decrease in mtDNA-CN, leading to impaired mitochondrial function and cell death. TFAM and DNA Pol γ are the two critical nucleoid-associated proteins involved mtDNA replication and repair. Oxidative Pol γ is likely to interpret mtDNA mutations in cardiac aging. Mitochondrial biogenesis is the basis of the mitochondrial life cycle, including coordinated synthesis of nDNA- and mtDNA-encoded proteins. The increased MB in cardiac aging is a compensatory maladaptive response to the mtROS-induced damaged energy metabolism. NRF1, NRF2, and PGC-1α regulate mitochondrial proteins that are essential for respiratory complex expression and biological function. PGC-1α activity is regulated via phosphorylation by some signaling pathways, including AMPK, deacetylation of Sirtuin, and MAPK p38.

A low dose of metformin, as an AMPK activator, can prolong the life span of mice without metabolic disorders. Rapamycin prevents cardiac senescence though the inhibition of mTOR. Resveratrol can induce autophagy and increase longevity. Melatonin ameliorates myocardial I/R injury via SIRT1 activation. It is worth noting that these emerging data have important theoretical and practical significance. These conventional clinical drugs can be used to prevent cardiac aging by preventing mitochondrial dysfunction and mtDNA damage. This review provides new insights into mtDNA in cardiac aging. Further research on the mechanisms of mtDNA decline in heart aging is warranted to create an opportunity to develop novel therapies to treat cardiovascular diseases and slow the rate of age-induced heart changes, thus contributing to better outcomes for longevity.

Conflicts of Interest

The authors declare that there are no commercial or financial conflicts of interest.

Authors' Contributions

Yue Quan drafted and proofread the manuscript. Xiaojing Liu edited the manuscript. Yanguo Xin, Geer Tian, and Junteng Zhou revised the manuscript. All authors have agreed upon the submission and publication of this work.

Acknowledgments

References

[1] World Health Organizationhttps://www.who.int/zh/news-room/fact-sheets/detail/cardiovascular-diseases-(cvds).

[2] N. N. Wu, Y. Zhang, and J. Ren, "Mitophagy, mitochondrial dynamics, and homeostasis in cardiovascular aging," *Oxidative Medicine and Cellular Longevity*, vol. 2019, Article ID 9825061, 15 pages, 2019.

[3] A. Shirakabe, Y. Ikeda, S. Sciarretta, D. K. Zablocki, and J. Sadoshima, "Aging and autophagy in the heart," *Circulation Research*, vol. 118, no. 10, pp. 1563–1576, 2016.

[4] E. K. Quarles, D. F. Dai, A. Tocchi, N. Basisty, L. Gitari, and P. S. Rabinovitch, "Quality control systems in cardiac aging," *Ageing Research Reviews*, vol. 23, Part A, pp. 101–115, 2015.

[5] E. J. Lesnefsky, Q. Chen, and C. L. Hoppel, "Mitochondrial metabolism in aging heart," *Circulation Research*, vol. 118, no. 10, pp. 1593–1611, 2016.

[6] A. Willems, D. Paepe, S. Marynissen et al., "Results of screening of apparently healthy senior and geriatric dogs," *Journal of Veterinary Internal Medicine*, vol. 31, no. 1, pp. 81–92, 2017.

[7] L. Cannon and R. Bodmer, "Genetic manipulation of cardiac ageing," *The Journal of Physiology*, vol. 594, no. 8, pp. 2075–2083, 2016.

[8] S. Guo, W. Deng, C. Xing, Y. Zhou, M. Ning, and E. H. Lo, "Effects of aging, hypertension and diabetes on the mouse brain and heart vasculomes," *Neurobiology of Disease*, vol. 126, pp. 117–123, 2019.

[9] T. Eisenberg, M. Abdellatif, S. Schroeder et al., "Cardioprotection and lifespan extension by the natural polyamine spermidine," *Nature Medicine*, vol. 22, no. 12, pp. 1428–1438, 2016.

[10] A. Tocchi, E. K. Quarles, N. Basisty, L. Gitari, and P. S. Rabinovitch, "Mitochondrial dysfunction in cardiac aging," *Biochimica et Biophysica Acta*, vol. 1847, no. 11, pp. 1424–1433, 2015.

[11] Z. Ungvari, S. Tarantini, A. J. Donato, V. Galvan, and A. Csiszar, "Mechanisms of vascular aging," *Circulation Research*, vol. 123, no. 7, pp. 849–867, 2018.

[12] Y. Nakada, D. C. Canseco, S. Thet et al., "Hypoxia induces heart regeneration in adult mice," *Nature*, vol. 541, no. 7636, pp. 222–227, 2017.

[13] G. Favaro, V. Romanello, T. Varanita et al., "DRP1-mediated mitochondrial shape controls calcium homeostasis and muscle mass," *Nature Communications*, vol. 10, no. 1, article 2576, 2019.

[14] N. Pfanner, B. Warscheid, and N. Wiedemann, "Mitochondrial proteins: from biogenesis to functional networks," *Nature Reviews Molecular Cell Biology*, vol. 20, no. 5, pp. 267–284, 2019.

[15] T. D. Larsen, K. H. Sabey, A. J. Knutson et al., "Diabetic pregnancy and maternal high-fat diet impair mitochondrial dynamism in the developing fetal rat heart by sex-specific mechanisms," *International Journal of Molecular Sciences*, vol. 20, no. 12, article 3090, 2019.

[16] T. J. Guzik and R. M. Touyz, "Oxidative stress, inflammation, and vascular aging in hypertension," *Hypertension*, vol. 70, no. 4, pp. 660–667, 2017.

[17] A. Picca, R. T. Mankowski, J. L. Burman et al., "Mitochondrial quality control mechanisms as molecular targets in cardiac ageing," *Nature Reviews Cardiology*, vol. 15, no. 9, pp. 543–554, 2018.

[18] H. Jiang, P. Qu, J. W. Wang, G. H. Li, and H. Y. Wang, "Effect of NF-κB inhibitor on toll-like receptor 4 expression in left ventricular myocardium in two-kidney-one-clip hypertensive rats," *European Review for Medical and Pharmacological Sciences*, vol. 22, no. 10, pp. 3224–3233, 2018.

[19] A. Mottis, S. Herzig, and J. Auwerx, "Mitocellular communication: shaping health and disease," *Science*, vol. 366, no. 6467, pp. 827–832, 2019.

[20] F. C. Lewis-McDougall, P. J. Ruchaya, E. Domenjo-Vila et al., "Aged-senescent cells contribute to impaired heart regeneration," *Aging Cell*, vol. 18, no. 3, article e12931, 2019.

[21] T. Li and Z. J. Chen, "The cGAS-cGAMP-STING pathway connects DNA damage to inflammation, senescence, and cancer," *The Journal of Experimental Medicine*, vol. 215, no. 5, pp. 1287–1299, 2018.

[22] T. M. Loo, K. Miyata, Y. Tanaka, and A. Takahashi, "Cellular senescence and senescence-associated secretory phenotype via the cGAS-STING signaling pathway in cancer," *Cancer Science*, vol. 111, no. 2, pp. 304–311, 2020.

[23] D. A. Sliter, J. Martinez, L. Hao et al., "Parkin and PINK1 mitigate STING-induced inflammation," *Nature*, vol. 561, no. 7722, pp. 258–262, 2018.

[24] J. Zhou, S. Y. Chong, A. Lim et al., "Changes in macroautophagy, chaperone-mediated autophagy, and mitochondrial metabolism in murine skeletal and cardiac muscle during aging," *Aging*, vol. 9, no. 2, pp. 583–599, 2017.

[25] S. Miyamoto, "Autophagy and cardiac aging," *Cell Death and Differentiation*, vol. 26, no. 4, pp. 653–664, 2019.

[26] S. Sciarretta, Y. Maejima, D. Zablocki, and J. Sadoshima, "The role of autophagy in the heart," *Annual Review of Physiology*, vol. 80, no. 1, pp. 1–26, 2018.

[27] R. Ghosh and J. S. Pattison, "Macroautophagy and chaperone-mediated autophagy in heart failure: the known and the unknown," *Oxidative Medicine and Cellular Longevity*, vol. 2018, Article ID 8602041, 22 pages, 2018.

[28] S. Sciarretta, M. Forte, G. Frati, and J. Sadoshima, "New insights into the role of mTOR signaling in the cardiovascular system," *Circulation Research*, vol. 122, no. 3, pp. 489–505, 2018.

[29] L. J. Leon and Å. B. Gustafsson, "Staying young at heart: autophagy and adaptation to cardiac aging," *Journal of Molecular and Cellular Cardiology*, vol. 95, pp. 78–85, 2016.

[30] X. Xu, J. Pang, Y. Chen, R. Bucala, Y. Zhang, and J. Ren, "Macrophage Migration Inhibitory Factor (MIF) Deficiency Exacerbates Aging- Induced Cardiac Remodeling and Dysfunction Despite Improved Inflammation: Role of Autophagy Regulation," *Scientific Reports*, vol. 6, no. 1, article 22488, 2016.

[31] J. Ren and Y. Zhang, "Targeting autophagy in aging and aging-related cardiovascular diseases," *Trends in Pharmacological Sciences*, vol. 39, no. 12, pp. 1064–1076, 2018.

[32] J. Y. Jang, A. Blum, J. Liu, and T. Finkel, "The role of mitochondria in aging," *The Journal of Clinical Investigation*, vol. 128, no. 9, pp. 3662–3670, 2018.

[33] A. P. Gomes, N. L. Price, A. J. Ling et al., "Declining NAD$^+$ induces a pseudohypoxic state disrupting nuclear-mitochondrial communication during aging," *Cell*, vol. 155, no. 7, pp. 1624–1638, 2013.

[34] O. M. Duicu, S. N. Mirica, D. E. Gheorgheosu, A. I. Privistirescu, O. Fira-Mladinescu, and D. M. Muntean, "Ageing-induced decrease in cardiac mitochondrial function in healthy rats," *Canadian Journal of Physiology and Pharmacology*, vol. 91, no. 8, pp. 593–600, 2013.

[35] E. L. Tate and G. H. Herbener, "A morphometric study of the density of mitochondrial cristae in heart and liver of aging mice," *Journal of Gerontology*, vol. 31, no. 2, pp. 129–134, 1976.

[36] C. M. El'darov, V. B. Vays, I. M. Vangeli, N. G. Kolosova, and L. E. Bakeeva, "Morphometric examination of mitochondrial ultrastructure in aging cardiomyocytes," *Biochemistry*, vol. 80, no. 5, pp. 604–609, 2015.

[37] Y. Ikeda, S. Sciarretta, N. Nagarajan et al., "New insights into the role of mitochondrial dynamics and autophagy during oxidative stress and aging in the heart," *Oxidative Medicine and Cellular Longevity*, vol. 2014, Article ID 210934, 13 pages, 2014.

[38] K. Faelber, L. Dietrich, J. K. Noel et al., "Structure and assembly of the mitochondrial membrane remodelling GTPase Mgm1," *Nature*, vol. 571, no. 7765, pp. 429–433, 2019.

[39] T. Wai, J. Garcia-Prieto, M. J. Baker et al., "Imbalanced OPA1 processing and mitochondrial fragmentation cause heart failure in mice," *Science*, vol. 350, no. 6265, article aad0116, 2015.

[40] A. H. Chaanine, L. D. Joyce, J. M. Stulak et al., "Mitochondrial morphology, dynamics, and function in human pressure overload or ischemic heart disease with preserved or reduced ejection fraction," *Circulation. Heart Failure*, vol. 12, no. 2, article e005131, 2019.

[41] M. Song, A. Franco, J. A. Fleischer, L. Zhang, and Dorn GW 2nd, "Abrogating mitochondrial dynamics in mouse hearts accelerates mitochondrial senescence," *Cell Metabolism*, vol. 26, no. 6, pp. 872–883.e5, 2017, e5.

[42] B. Wang, J. Nie, L. Wu et al., "AMPKα2 protects against the development of heart failure by enhancing mitophagy via PINK1 phosphorylation," *Circulation Research*, vol. 122, no. 5, pp. 712–729, 2018.

[43] Y. Zhang, Y. Wang, J. Xu et al., "Melatonin attenuates myocardial ischemia-reperfusion injury via improving mitochondrial fusion/mitophagy and activating the AMPK-OPA1 signaling pathways," *Journal of Pineal Research*, vol. 66, no. 2, article e12542, 2019.

[44] A. N. Bayne and J. F. Trempe, "Mechanisms of PINK1, ubiquitin and Parkin interactions in mitochondrial quality control and beyond," *Cellular and Molecular Life Sciences*, vol. 76, no. 23, pp. 4589–4611, 2019.

[45] G. Gong, M. Song, G. Csordas, D. P. Kelly, S. J. Matkovich, and G. W. Dorn, "Parkin-mediated mitophagy directs perinatal cardiac metabolic maturation in mice," *Science*, vol. 350, no. 6265, article aad2459, 2015.

[46] S. Matsuda, Y. Kitagishi, and M. Kobayashi, "Function and characteristics of PINK1 in mitochondria," *Oxidative Medicine and Cellular Longevity*, vol. 2013, Article ID 601587, 6 pages, 2013.

[47] H. Nohl and D. Hegner, "Do mitochondria produce oxygen radicals in vivo?," *European Journal of Biochemistry*, vol. 82, no. 2, pp. 563–567, 1978.

[48] D.-F. Dai, P. S. Rabinovitch, and Z. Ungvari, "Mitochondria and cardiovascular aging," *Circulation Research*, vol. 110, no. 8, pp. 1109–1124, 2012.

[49] T. E. S. Kauppila, J. H. K. Kauppila, and N. G. Larsson, "Mammalian mitochondria and aging: an update," *Cell Metabolism*, vol. 25, no. 1, pp. 57–71, 2017.

[50] K. Tsushima, H. Bugger, A. R. Wende et al., "Mitochondrial reactive oxygen species in lipotoxic hearts induce post-translational modifications of AKAP121, DRP1, and OPA1

that promote mitochondrial fission," *Circulation Research*, vol. 122, no. 1, pp. 58–73, 2018.

[51] M. Hu, M. A. Bogoyevitch, and D. A. Jans, "Subversion of host cell mitochondria by RSV to favor virus production is dependent on inhibition of mitochondrial complex I and ROS generation," *Cells*, vol. 8, no. 11, article 1417, 2019.

[52] E. L. Mills, B. Kelly, A. Logan et al., "Succinate dehydrogenase supports metabolic repurposing of mitochondria to drive inflammatory macrophages," *Cell*, vol. 167, no. 2, pp. 457–470.e13, 2016.

[53] E. R. Stadtman, "Protein oxidation and aging," *Science*, vol. 257, no. 5074, pp. 1220–1224, 1992.

[54] T. Cao, S. Fan, D. Zheng et al., "Increased calpain-1 in mitochondria induces dilated heart failure in mice: role of mitochondrial superoxide anion," *Basic Research in Cardiology*, vol. 114, no. 3, p. 17, 2019.

[55] W. Wang, H. Fang, L. Groom et al., "Superoxide flashes in single mitochondria," *Cell*, vol. 134, no. 2, pp. 279–290, 2008.

[56] A. E. Dikalova, H. A. Itani, R. R. Nazarewicz et al., "Sirt3 impairment and SOD2 hyperacetylation in vascular oxidative stress and hypertension," *Circulation Research*, vol. 121, no. 5, pp. 564–574, 2017.

[57] G. J. Tranah, "Mitochondrial–nuclear epistasis: implications for human aging and longevity," *Ageing Research Reviews*, vol. 10, no. 2, pp. 238–252, 2011.

[58] J. Xu, E. Marzetti, A. Y. Seo, J. S. Kim, T. A. Prolla, and C. Leeuwenburgh, "The emerging role of iron dyshomeostasis in the mitochondrial decay of aging," *Mechanisms of Ageing and Development*, vol. 131, no. 7-8, pp. 487–493, 2010.

[59] V. Mallikarjun, A. Sriram, F. Scialo, and A. Sanz, "The interplay between mitochondrial protein and iron homeostasis and its possible role in ageing," *Experimental Gerontology*, vol. 56, pp. 123–134, 2014.

[60] B. Martín-Fernández and R. Gredilla, "Mitochondria and oxidative stress in heart aging," *Age*, vol. 38, no. 4, pp. 225–238, 2016.

[61] N. A. Strutynska, A. V. Kotsiuruba, A. Y. Budko, L. A. Mys, and V. F. Sagach, "Mitochondrial dysfunction in the aging heart is accompanied by constitutive no-synthases uncoupling on the background of oxidative and nitrosative stress," *Fiziologicheskiĭ Zhurnal*, vol. 62, no. 2, pp. 3–11, 2016.

[62] D. F. Dai, L. F. Santana, M. Vermulst et al., "Overexpression of catalase targeted to mitochondria attenuates murine cardiac aging," *Circulation*, vol. 119, no. 21, pp. 2789–2797, 2009.

[63] D. F. Dai and P. Rabinovitch, "Mitochondrial oxidative stress mediates induction of autophagy and hypertrophy in angiotensin-II treated mouse hearts," *Autophagy*, vol. 7, no. 8, pp. 917-918, 2011.

[64] I. Luptak, F. Qin, A. L. Sverdlov et al., "Energetic dysfunction is mediated by mitochondrial reactive oxygen species and precedes structural remodeling in metabolic heart disease," *Antioxidants & Redox Signaling*, vol. 31, no. 7, pp. 539–549, 2019.

[65] A. P. Anderson, X. Luo, W. Russell, and Y. W. Yin, "Oxidative damage diminishes mitochondrial DNA polymerase replication fidelity," *Nucleic Acids Research*, vol. 48, no. 2, pp. 817–829, 2020.

[66] V. B. Pillai, S. Bindu, W. Sharp et al., "Sirt3 protects mitochondrial DNA damage and blocks the development of doxorubicin-induced cardiomyopathy in mice," *American Journal of Physiology-Heart and Circulatory Physiology*, vol. 310, no. 8, pp. H962–H972, 2016.

[67] J. Marín-García, "Mitochondrial DNA repair: a novel therapeutic target for heart failure," *Heart Failure Reviews*, vol. 21, no. 5, pp. 475–487, 2016.

[68] A. P. West, W. Khoury-Hanold, M. Staron et al., "Mitochondrial DNA stress primes the antiviral innate immune response," *Nature*, vol. 520, no. 7548, pp. 553–557, 2015.

[69] P. Sykora, S. Kanno, M. Akbari et al., "DNA polymerase beta participates in mitochondrial DNA repair," *Molecular and Cellular Biology*, vol. 37, no. 16, 2017.

[70] D. F. Dai, S. C. Johnson, J. J. Villarin et al., "Mitochondrial oxidative stress mediates angiotensin II-induced cardiac hypertrophy and Gαq overexpression-induced heart failure," *Circulation Research*, vol. 108, no. 7, pp. 837–846, 2011.

[71] G. Chimienti, A. Picca, F. Fracasso et al., "Differences in liver TFAM binding to mtDNA and mtDNA damage between aged and extremely aged rats," *International Journal of Molecular Sciences*, vol. 20, no. 10, article 2601, 2019.

[72] K. Scheffler, L. Rachek, P. You et al., "8-oxoguanine DNA glycosylase (Ogg1) controls hepatic gluconeogenesis," *DNA Repair*, vol. 61, pp. 56–62, 2018.

[73] K. C. Kim, M. H. S. Ruwan Kumara, K. A. Kang et al., "Exposure of keratinocytes to non-thermal dielectric barrier discharge plasma increases the level of 8-oxoguanine via inhibition of its repair enzyme," *Molecular Medicine Reports*, vol. 16, no. 5, pp. 6870–6875, 2017.

[74] A. Trifunovic, A. Wredenberg, M. Falkenberg et al., "Premature ageing in mice expressing defective mitochondrial DNA polymerase," *Nature*, vol. 429, no. 6990, pp. 417–423, 2004.

[75] K. Foote, J. Reinhold, E. P. K. Yu et al., "Restoring mitochondrial DNA copy number preserves mitochondrial function and delays vascular aging in mice," *Aging Cell*, vol. 17, no. 4, article e12773, 2018.

[76] Y. Zhang, E. Guallar, F. N. Ashar et al., "Association between mitochondrial DNA copy number and sudden cardiac death: findings from the atherosclerosis risk in communities study (ARIC)," *European Heart Journal*, vol. 38, no. 46, pp. 3443–3448, 2017.

[77] F. N. Ashar, Y. Zhang, R. J. Longchamps et al., "Association of mitochondrial DNA copy number with cardiovascular disease," *JAMA Cardiology*, vol. 2, no. 11, pp. 1247–1255, 2017.

[78] C. F. Lee, C. Y. Liu, R. H. Hsieh, and Y. H. Wei, "Oxidative stress-induced depolymerization of microtubules and alteration of mitochondrial mass in human cells," *Annals of the New York Academy of Sciences*, vol. 1042, pp. 246–254, 2005.

[79] M. Ikeda, T. Ide, T. Fujino et al., "Overexpression of TFAM or Twinkle increases mtDNA copy number and facilitates cardioprotection associated with limited mitochondrial oxidative stress," *PLoS One*, vol. 10, no. 3, article e0119687, 2015.

[80] R. Filograna, C. Koolmeister, M. Upadhyay et al., "Modulation of mtDNA copy number ameliorates the pathological consequences of a heteroplasmic mtDNA mutation in the mouse," *Science Advances*, vol. 5, no. 4, article eaav9824, 2019.

[81] X. B. Wang, N. H. Cui, S. Zhang, Z. J. Liu, J. F. Ma, and L. Ming, "Leukocyte telomere length, mitochondrial DNA copy number, and coronary artery disease risk and severity: a two-stage case-control study of 3064 Chinese subjects," *Atherosclerosis*, vol. 284, pp. 165–172, 2019.

[82] L. D. Osellame, T. S. Blacker, and M. R. Duchen, "Cellular and molecular mechanisms of mitochondrial function," *Best*

Practice & Research Clinical Endocrinology & Metabolism, vol. 26, no. 6, pp. 711–723, 2012.

[83] X. Tian, W. He, R. Yang, and Y. Liu, "Dl-3-n-butylphthalide protects the heart against ischemic injury and H9c2 cardiomyoblasts against oxidative stress: involvement of mitochondrial function and biogenesis," *Journal of Biomedical Science*, vol. 24, no. 1, p. 38, 2017.

[84] L. Tao, Y. Bei, S. Lin et al., "Exercise training protects against acute myocardial infarction via improving myocardial energy metabolism and mitochondrial biogenesis," *Cellular Physiology and Biochemistry*, vol. 37, no. 1, pp. 162–175, 2015.

[85] P. D'Aquila, D. Bellizzi, and G. Passarino, "Mitochondria in health, aging and diseases: the epigenetic perspective," *Biogerontology*, vol. 16, no. 5, pp. 569–585, 2015.

[86] R. M. Parodi-Rullán, X. R. Chapa-Dubocq, and S. Javadov, "Acetylation of mitochondrial proteins in the heart: the role of SIRT3," *Frontiers in Physiology*, vol. 9, article 1094, 2018.

[87] N. G. Larsson, "Somatic mitochondrial DNA mutations in mammalian aging," *Annual Review of Biochemistry*, vol. 79, pp. 683–706, 2010.

[88] S. C. Lewis, L. F. Uchiyama, and J. Nunnari, "ER-mitochondria contacts couple mtDNA synthesis with mitochondrial division in human cells," *Science*, vol. 353, no. 6296, article aaf5549, 2016.

[89] A. Picca, G. Sirago, V. Pesce et al., "Administration of enalapril started late in life attenuates hypertrophy and oxidative stress burden, increases mitochondrial mass, and modulates mitochondrial quality control signaling in the rat heart," *Biomolecules*, vol. 8, no. 4, p. 177, 2018.

[90] S. Garcia, N. Nissanka, E. A. Mareco et al., "Overexpression of PGC-1α in aging muscle enhances a subset of young-like molecular patterns," *Aging Cell*, vol. 17, no. 2, article e12707, 2018.

[91] E. Sahin, S. Colla, M. Liesa et al., "Telomere dysfunction induces metabolic and mitochondrial compromise," *Nature*, vol. 470, no. 7334, pp. 359–365, 2011.

[92] G. C. Rowe, A. Jiang, and Z. Arany, "PGC-1 coactivators in cardiac development and disease," *Circulation Research*, vol. 107, no. 7, pp. 825–838, 2010.

[93] G. Haemmerle, T. Moustafa, G. Woelkart et al., "ATGL-mediated fat catabolism regulates cardiac mitochondrial function via PPAR-α and PGC-1," *Nature Medicine*, vol. 17, no. 9, pp. 1076–1085, 2011.

[94] S. Din, M. H. Konstandin, B. Johnson et al., "Metabolic dysfunction consistent with premature aging results from deletion of Pim kinases," *Circulation Research*, vol. 115, no. 3, pp. 376–387, 2014.

[95] Y. Wang, X. Zhao, M. Lotz, R. Terkeltaub, and R. Liu-Bryan, "Mitochondrial biogenesis is impaired in osteoarthritis chondrocytes but reversible via peroxisome proliferator-activated receptor γ coactivator 1α," *Arthritis & Rhematology*, vol. 67, no. 8, pp. 2141–2153, 2015.

[96] S. Zhu, T. Xu, Y. Luo et al., "Luteolin enhances sarcoplasmic reticulum Ca^{2+}-ATPase activity through p38 MAPK signaling thus improving rat cardiac function after ischemia/-reperfusion," *Cellular Physiology and Biochemistry*, vol. 41, no. 3, pp. 999–1010, 2017.

[97] R. Sucher, P. Gehwolf, T. Kaier et al., "Intracellular signaling pathways control mitochondrial events associated with the development of ischemia/reperfusion-associated damage," *Transplant International*, vol. 22, no. 9, pp. 922–930, 2009.

[98] D.-F. Dai, T. Chen, H. Szeto et al., "Mitochondrial targeted antioxidant peptide ameliorates hypertensive cardiomyopathy," *Journal of the American College of Cardiology*, vol. 58, no. 1, pp. 73–82, 2011.

[99] M. Ding, N. Feng, D. Tang et al., "Melatonin prevents Drp1-mediated mitochondrial fission in diabetic hearts through SIRT1-PGC1α pathway," *Journal of Pineal Research*, vol. 65, no. 2, article e12491, 2018.

[100] S. J. Park, F. Ahmad, A. Philp et al., "Resveratrol ameliorates aging-related metabolic phenotypes by inhibiting cAMP phosphodiesterases," *Cell*, vol. 148, no. 3, pp. 421–433, 2012.

[101] M. N. Sanz, L. Grimbert, M. Moulin et al., "Inducible cardiac-specific deletion of Sirt1 in male mice reveals progressive cardiac dysfunction and sensitization of the heart to pressure overload," *International Journal of Molecular Sciences*, vol. 20, no. 20, article 5005, 2019.

[102] Y. C. Lai, D. M. Tabima, J. J. Dube et al., "SIRT3-AMP-activated protein kinase activation by nitrite and metformin improves hyperglycemia and normalizes pulmonary hypertension associated with heart failure with preserved ejection fraction," *Circulation*, vol. 133, no. 8, pp. 717–731, 2016.

[103] N. R. Sundaresan, M. Gupta, G. Kim, S. B. Rajamohan, A. Isbatan, and M. P. Gupta, "Sirt3 blocks the cardiac hypertrophic response by augmenting Foxo3a-dependent antioxidant defense mechanisms in mice," *The Journal of Clinical Investigation*, vol. 119, no. 9, pp. 2758–2771, 2009.

[104] W. K. Chen, Y. L. Tsai, M. A. Shibu et al., "Exercise training augments Sirt1-signaling and attenuates cardiac inflammation in D-galactose induced-aging rats," *Aging (Albany NY)*, vol. 10, no. 12, pp. 4166–4174, 2018.

[105] J. Ren, L. Yang, L. Zhu et al., "Akt2 ablation prolongs life span and improves myocardial contractile function with adaptive cardiac remodeling: role of Sirt1-mediated autophagy regulation," *Aging Cell*, vol. 16, no. 5, pp. 976–987, 2017.

[106] S. Winnik, J. Auwerx, D. A. Sinclair, and C. M. Matter, "Protective effects of sirtuins in cardiovascular diseases: from bench to bedside," *European Heart Journal*, vol. 36, no. 48, pp. 3404–3412, 2015.

[107] S. Turdi, X. Fan, J. Li et al., "AMP-activated protein kinase deficiency exacerbates aging-induced myocardial contractile dysfunction," *Aging Cell*, vol. 9, no. 4, pp. 592–606, 2010.

[108] S. Herzig and R. J. Shaw, "AMPK: guardian of metabolism and mitochondrial homeostasis," *Nature Reviews Molecular Cell Biology*, vol. 19, no. 2, pp. 121–135, 2018.

[109] E. N. Kim, J. H. Lim, M. Y. Kim et al., "PPARα agonist, fenofibrate, ameliorates age-related renal injury," *Experimental Gerontology*, vol. 81, pp. 42–50, 2016.

[110] C. Driver, K. D. S. Bamitale, A. Kazi, M. Olla, N. A. Nyane, and P. M. O. Owira, "Cardioprotective effects of metformin," *Journal of Cardiovascular Pharmacology*, vol. 72, no. 2, pp. 121–127, 2018.

[111] M. A. Paiva, Z. Rutter-Locher, L. M. Gonçalves et al., "Enhancing AMPK activation during ischemia protects the diabetic heart against reperfusion injury," *American Journal of Physiology-Heart and Circulatory Physiology*, vol. 300, no. 6, pp. H2123–H2134, 2011.

Review Article
The Emerging Role of Senescence in Ocular Disease

Parameswaran G. Sreekumar,[1] **David R. Hinton,**[2,3] **and Ram Kannan** [1,4]

[1]*The Stephen J. Ryan Initiative for Macular Research (RIMR), Doheny Eye Institute, Los Angeles, CA 90033, USA*
[2]*Department of Pathology, Keck School of Medicine of the University of Southern California, Los Angeles, CA 90033, USA*
[3]*Department Ophthalmology, USC Roski Eye Institute, Keck School of Medicine of the University of Southern California, Los Angeles, CA 90033, USA*
[4]*Stein Eye Institute, Geffen School of Medicine, University of California, Los Angeles, CA 90095, USA*

Correspondence should be addressed to Ram Kannan; rkannan@doheny.org

Cellular senescence is a state of irreversible cell cycle arrest in response to an array of cellular stresses. An important role for senescence has been shown for a number of pathophysiological conditions that include cardiovascular disease, pulmonary fibrosis, and diseases of the skin. However, whether senescence contributes to the progression of age-related macular degeneration (AMD) has not been studied in detail so far and the present review describes the recent research on this topic. We present an overview of the types of senescence, pathways of senescence, senescence-associated secretory phenotype (SASP), the role of mitochondria, and their functional implications along with antisenescent therapies. As a central mechanism, senescent cells can impact the surrounding tissue microenvironment via the secretion of a pool of bioactive molecules, termed the SASP. An updated summary of a number of new members of the ever-growing SASP family is presented. Further, we introduce the significance of mechanisms by which mitochondria may participate in the development of cellular senescence. Emerging evidence shows that extracellular vesicles (EVs) are important mediators of the effects of senescent cells on their microenvironment. Based on recent studies, there is reasonable evidence that senescence could be a modifiable factor, and hence, it may be possible to delay age-related diseases by modulating basic aging mechanisms using SASP inhibitors/senolytic drugs. Thus, antisenescent therapies in aging and age-related diseases appear to have a promising potential.

1. Introduction

Cellular senescence is the irreversible loss of proliferation potential of somatic cells and a variety of associated phenotypic changes that follow [1]. The concept of cellular senescence stems from pioneering studies showing that human diploid fibroblasts have a finite proliferative capacity in culture, despite the fact that they can stay metabolically active even after entering a stable, nondividing stage [2]. Subsequently, it was shown that senescence could be induced prematurely by many agents. Several independent studies have shown that senescent cells also play a role in multiple biological processes such as embryonic development, wound healing, tissue repair, tumorigenesis, aging, and age-related disease [3]. Thus, studying senescence in the eye and its association with age-related macular degeneration (AMD) will be

of great interest. Herein, the nature and role of multiple senescence inducers characterized by an array of multiple biomarkers in use as well as mechanisms of cellular senescence are reviewed. In addition, the role of mitochondria in cellular senescence with special reference to ocular diseases such as AMD is also addressed. Finally, the review summarizes available information on senolytic drugs currently used in animal models and in clinical trials.

2. Acute or Chronic Senescence

Given the involvement of the process of senescence in many activities, it raises the question whether processes of the senescent cells involved could be similar or different. Generally, senescence belongs to one of two categories: acute (transient or programmed) or chronic (damage/stress induced) [4, 5].

Such differentiation would allow understanding the dual (beneficial vs. harmful) role of senescence on normal development and regenerative processes, as well as its role in human disease and aging. Developmentally programmed senescence is a normal physiological process of the body that occurs in response to developmental events, whereas damage-/stress-induced senescence is triggered by nonphysiological stimuli or disease stages.

Acute senescence is mostly beneficial and presumably does not contribute to aging; it relies on the coordinated action of senescent cell production and subsequent elimination—the processes involved in wound healing, tissue remodeling, and embryogenesis. Senescence has been demonstrated in the endolymphatic sac and mesonephros of the mouse and human embryos followed by macrophage-mediated removal of senescence cells [4]. Further evidence of senescence was shown in the apical ectodermal ridge and the senescence-associated secretory phenotype (SASP) produced by these cells induces tissue remodeling [6]. Developmental senescence is p21 dependent, but p53 independent, and shares many common features with stress-induced senescence, including a common gene expression signature and senescence-associated β-galactosidase activity [4]. These landmark studies revealed that cellular senescence during embryonic development is a programmed, transient event that contributes to tissue remodeling via SASP or to altered cellularity through clearance, suggesting a primordial role in normal physiology.

Paradoxically, while chronic senescence can initially have beneficial effects, its long-term existence could potentially aggravate age-related diseases [7]. "Chronic" senescence develops gradually because of progressive damage over time as seen in aging and age-related diseases. During chronic senescence, the switch from temporal to persistent cell cycle arrest appears to be random, induced by the multiple inducing factors acting simultaneously on a cell. These results in arrest of proliferation and ultimately cells become dysfunctional and most importantly negatively affect local environment by a nonautonomous mechanism [8]. The differential effects of developmental versus pathological senescence on aging could be associated with their effect on other cells via the SASP. Therefore, removal of chronic senescent cells during both premature and normal aging is able to reduce the development and progression of many age-associated dysfunctions [9, 10]. However, the molecular mechanism governing the different types of senescence *in vitro* and *in vivo* is still not fully explored. It is hypothesized that the kinetics and efficiency of senescent cell clearance could be one of the key differences between acute and chronic senescence. Further research will strengthen our understanding of the relationship between acute vs. chronic senescence.

3. The Beneficial and Detrimental Role of Senescent Cells

As described earlier, senescence has been shown to have a dual role, beneficial in some contexts and detrimental in others. Senescence acts by tumor suppressor mechanisms and thus inhibits the proliferation of cancer cells and is involved in embryonic development [4, 6], wound healing [11], and tissue repair [12, 13]. Senescent cells are metabolically highly active and actively secrete an array of proinflammatory cytokines and chemokines, growth factors and extracellular matrix degrading proteins, and the SASPs [14]. It is believed that SASP molecules stimulate movement of immune cells to the senescent cells; activate and promote their clearance [12].

The beneficial process of the senescence can be compromised in aged tissues, resulting in the accumulation of senescent cells that could potentially enhance tissue dysfunction through SASP which is particularly rich in proinflamatory cytokines and matrix metalloproteinases [15–19]. Thus, senescence has been linked to aging and age-related diseases. For example, aging human skin has increased numbers of cells that are positive for SA-ß-gal [20]. In aged cells, the components of SASP has been shown to activate neighboring healthy cells to senescent cells [21]. It is of utmost interest to learn why these senescent cells in aging are not eliminated as is the case for embryonic cells and the inefficient immune system may play a role in this regard.

4. The Phenotype Associated with Cellular Senescence

Senescent cells are featured by an array of specialized features which have been extensively reviewed [3, 22, 23]. Since senescent cells are widely heterogeneous and some of their features are common in other nonsenescence cellular states, it is difficult to clearly identify senescent cells using a few markers [22, 24]. The following are some of the phenotypes associated with senescent cells:

(i) Senescence is generally accompanied by significant morphological alterations. The senescent cells become flat and enlarged more than double the size of nonsenescent cells due to rearrangement of the cytoskeleton, particularly vimentin filaments [25, 26]

(ii) Senescence-associated heterochromatin foci (SAHF) are specialized domains of facultative heterochromatin observed in the nuclei of senescent cells as punctate DNA-stained dense foci [27]. Specifically, SAHF are not associated with nonsenescent or quiescent state

(iii) *Senescent cells* normally display increased activity of the acidic *senescence*-associated *β-galactosidase* (SA-*β-gal*), which partly reflects the increase in lysosomal mass [20, 28]

(iv) Most senescent cells are characterized by the increased expression of antiproliferative molecules (p16INK4a). Increased expression of p16INK4a with age in mice and humans has been well documented [29–31]

(v) Senescent cells secrete cytokines, chemokines, extracellular matrix proteases, and growth factors, collectively known as SASP or senescence-messaging secretome [32, 33]
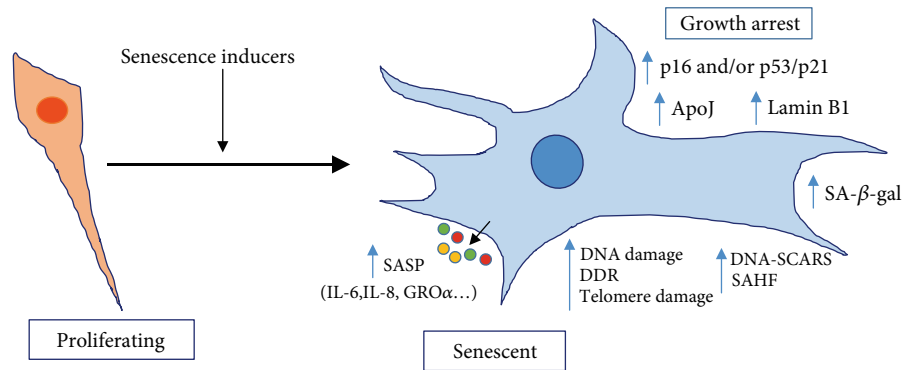
FIGURE 1: Schematic representation of senescence markers. Cellular senescence can be induced by multiple agents (senescence inducers). The senescent cell is morphologically different and bigger in size. Senescent cells also have increased levels of factors (right) which are used as markers. Senescent cells produce and secrete a complex combination of factors, collectively referred as the senescence-associated secretory phenotype (SASP). SA-β-gal: senescence-associated beta-galactosidase; ApoJ: apolipoprotein J; SAHF: senescence-associated heterochromatin foci; DDR: DNA-damage response; DNA-SCARS: DNA segments with chromatin alterations reinforcing senescence. This is adapted from [37].

(vi) Senescent cells are characterized by significant changes in mitochondrial morphology, function, and metabolism. Senescent cells remain metabolically active and have increased mitochondrial biogenesis and respiration [34]

5. Biomarkers of Senescence

As described above, no single characteristic is exclusive to the senescent state. Nor do all senescent cells display all the senescence markers identified so far. The identification of senescent cells in vivo is challenging, especially considering their diversity and heterogeneity. Therefore, senescent cells are generally identified by an array of characteristics. Though an array of senescence markers has been proposed and widely used in multiple cell types, no single one can reliably identify senescent cells either *in vitro* or *in vivo*. The most widely used markers of senescence include the senescence-associated β-galactosidase (SA-β-gal) reactivity [15, 20, 35–39], increased expression of the cyclin-dependent kinase (CDK) inhibitor p16INK4a [15, 30, 36–40], p21 (CIP1/WAF1) [36–39, 41, 42], p53 [36, 37, 41, 42], induction of SASP factors [14, 41, 43–50], mitochondrial DNA modifications [39, 50–57], and chromatin modifications [37, 47, 58, 59] (Figure 1). The limitation is that even a combination of multiple markers does not truly represent senescence but could also describe long-term cell arrest. That is one of the major reasons for intensive research in pursuit of additional robust and sensitive markers.

6. Models of Aging in *In Vitro* Systems

In response to cellular stress or damage, proliferating cells enter in a state of long-term cell cycle arrest. Senescence can be induced in cell culture by using multiple stimuli with known common agents. The known models of senescence are summarized in Table 1.

6.1. Replicative Senescence (RS).
With the exception of tumor cells and some stem cells, replicative senescence appears to be a fundamental feature of somatic cells [60]. The first formally described senescence model [2] refers to an irreversible arrest of cell proliferation and altered cell function following multiple cell divisions [61]. Telomere shortening because of multiple cell passages has been considered a plausible mechanism [23, 61]. Replicative senescence is characterized by DNA double-strand breaks, with activated ataxia telangiectasia mutated (ATM), and/or ATM and RAD3-related (ATR) mechanisms and their respective mediators, checkpoint kinase 2 (CHK2) and CHK1 [62].

6.2. Stress-Induced Premature Senescence (SIPS).
Cellular senescence can be induced by various stresses including oxidative stress. Both chronic and acute oxidative stress protocols were used to induce cellular senescence. Hydrogen peroxide or tert-butyl hydroperoxide is widely used to produce oxidative stress-induced premature senescence within a short period of time [38, 39]. Such induced premature senescent cells display markers that are similar to those from replicative senescent cells. There are many agents that could be used for SIPS, the major classes are cytokines, oxidizing agents, hyperoxia, and copper. Although oxidizing agents work partly through DNA damage, other cellular components such as mitochondria are also affected. In the acute protocol, a single stress dose will inhibit the growth of a fraction of cells with others more or less unharmed. But in the chronic protocol, cells are exposed to repeated stresses, with a dose every day or every other day, allowing to minimize unharmed cells and increasing chances of cells undergoing senescence [63–65]. Thus, SIPS could be a good model to study heterogeneity of aging at the cellular level.

6.3. DNA Damage-Induced Senescence (DDR).
Depending on the treatment protocol and dose, DNA damage response (DDR) can induce senescence [66]. Different types of DNA-damaging agents including cancer drugs such as bleomycin or doxorubicin are used to induce this

Table 1: *In vitro* senescence models.

Senescence model	Abbreviation	Method of induction	References
Replicative senescence (RS)	RS	Short telomeres, linked to excess rounds of cell division	[2, 37]
Stress-induced premature senescence (SIPS)	SIPS	H_2O_2, t-BH, cytokines, oxidizing agents, hyperoxia, copper, UV irradiation	[37–39, 64, 65]
DNA damage response- (DDR-) induced senescence	DDR	Bleomycin or doxorubicin, gamma irradiator	[37]
Oncogene-induced senescence (OIS)	OIS	Activation and/or overexpression of oncogenes	[69, 76]
Mitochondrial dysfunction-associated senescence (MiDAS)	MiDAS	Inhibiting mitochondrial SIRT3	[74]
Epigenetically induced senescence	EIS	5-Aza-2$'$-deoxycytidine, sodium butyrate, trichostatin A, curcumin, C646, BRD4770	[27, 77–79]

type of senescence. The DNA damage response is initiated by the activation of the PI(3)K- (phosphatidylinositol-3-OH-kinase-) like kinases ATM, ATR (ATM and RAD related), and DNA-PKcs (DNA-dependent protein kinase catalytic subunit) [62]. These kinases also halt progression through the stages of cell cycle by activating the effector kinases (checkpoint kinase) CHK2 and CHK1 [62]. Finally, checkpoint enforcement results from multiple signaling pathways such as p53 and the cell division cycle 25 phosphatases. Slower p53 induction upon phosphorylation by DDR kinases leads to its stabilization and enhanced ability to induce the transcription of p21 which results in a stable cell cycle arrest [62, 67].

6.4. *Oncogene-Induced Senescence (OIS).* Oncogene activation is a hallmark of cancer; however, oncogene activation in a normal cell induces cellular senescence [68]. Oncogene-evoked senescence was first discovered following expression of an oncogenic form of *Ras* in normal human fibroblasts [69]. This process resembles replicative senescence. A sustained antiproliferative response is due to oncogenic signaling resulting from mutation of an oncogene or the inactivation of a tumor-suppressor gene. The activation of oncogenes, such as Ras or B-Raf proto-oncogene, serine/threonine kinase (BRAF), or the inactivation of tumor suppressors, such as PTEN, will result in OIS [23, 70, 71]. Specifically, OIS is established independently of any telomere attrition or dysfunction [72]. So, atypical activation of signaling pathways and positive cell cycle regulators may lead to the buildup of DNA damage, and the resulting cellular senescence [72].

6.5. *Mitochondrial Dysfunction-Associated Senescence (MiDAS).* The role of mitochondrial damage in cellular senescence has been well characterized using cell cycle arrest as the main marker of senescence [73]. Very little information about the secretary phenotype in conjunction mitochondrial damage-induced senescence is available. However, a recent study describes senescence induced by multiple types of mitochondrial dysfunction lacks a wide number of cytokines secreted during canonical senescence such as IL-1α, IL-1β, IL-6, and IL-8 [74]. This secretory phenotype, controlled by NAD-AMPK-p53 axis, appears to be characteristic of this type of senescence [74]. In addition, it was demonstrated that canonical triggers of cellular senescence, when combined

with mitochondrial dysfunction, results in a senescence response that also lacks the abovementioned cytokines, suggesting that mitochondrial damage is superior to nuclear damage regarding the inhibition the cytokines [74].

6.6. *Epigenetically Induced Senescence (EIS).* DNA methylation changes and histone modification have been observed during cellular senescence. Accordingly, treating cells with epigenetic modifiers that inhibit DNA methyltransferases (5-aza-2$'$-deoxycytidine), or histone deacetylases (sodium butyrate, trichostatin A) or histone acetyltransferases (curcumin, C646), and histone methyltransferases (BRD4770) are also known to cause senescence [75].

7. Cellular Senescence during Ocular Aging and Age-Related Diseases

Aging is considered one of the most obvious predisposing factors for the development of AMD because prevalence of this disease rises in those over 60. With aging, the human retina undergoes various structural and physiologic changes [80]. Several independent studies suggest senescence contributes to the development of many ocular diseases (Table 2). Aging has been associated with fewer retinal neurons along with numerous age-related quantitative alterations such as decreased areas of dendritic and axonal arbors and decreased density of cells and synapses [81]. One study found that retinal pigment epithelium (RPE) cells were lost in large numbers in the periphery of the human retina [82] while a second study reported overall RPE to photoreceptor ratio dropped with age throughout the retina [83]. Furthermore, protein levels of canonical senescence markers such as p16, p21, and p53 were shown to increase in the RPE isolated from aged human donors (84-86 years) [84].

RPE cells show signs of senescence when grown *in vitro* for a prolonged period [85]. SA-β-gal positivity of RPE cells has also been reported in the human retina and monkey retina [86]. Neurons, but not neuroglia and blood vessels undergo cellular senescence in the aged human retina [42]. Aging causes loss of retinal neurons, including rod photoreceptors, retinal ganglion cells (RGCs), and rod bipolar cells [82, 86, 87]. In addition, intracellularly, lipofuscin deposits in the RPE, which could be a potential inducer of reactive

TABLE 2: Ocular diseases associated with cellular senescence.

Diseases	Pathology	Therapeutic strategy	References
Age-related macular degeneration (AMD)	RPE senescence is associated with the pathology	N/A	[38, 86, 100]
Wet AMD	Macrophage senescence impairs cholesterol efflux and promotes neovascular AMD	N/A	[101]
Glaucoma	Senescent cells in the outflow pathway; retinal ganglion cell senescence	N/A	[90, 95, 102]
Experimental ocular hypertension	Senescence of retinal ganglion cells		[102]
Cataracts	Senescence in lens epithelial cells	NA	[103, 104]
Retinal microaneurysm	Neurons and blood vessels undergo cellular senescence in the retina	N/A	[42]
Fuchs endothelial dystrophy (FED)	Corneal endothelial cells (HCEC) senescence	Kojic acid	[105, 106]
Birdshot Uveitis	Shortening of telomere length in peripheral leukocytes.	N/A	[107]
Diabetic retinopathy	Endothelial cell senescence	N/A	[108–110]
Hyperglycemia-induced retinal microangiopathy	Senescence of the retinal microvasculature, RPE, and ganglion cell layer (GCL) type 1 diabetic rat model	N/A	[40]

oxygen species (ROS) after exposure to oxygen and light [88]. Retinal microaneurysms overexpress canonical senescence markers, suggesting that cellular senescence is associated with the pathogenesis. Apoptosis also cooccurs with cellular senescence in old-age retinal microaneurysms [42]. The age-related decrease in the anterior segment outflow is largely responsible for the elevated intraocular pressure, one of the factors attributing to the development of glaucoma [89]. Markers of cellular senescence are found in the trabecular meshwork of patients with primary open-angle glaucoma and aging of these cells leads to their decreased function and a consequent decreased outflow facility [90]. The decreased outflow with age is also characterized by a decreased population of RGCs, neuronal cells in the retina that electrically couples the retina with the brain [90, 91]. In the mouse model of acute glaucoma, it has been shown that p53, another key player in cellular senescence [22], contributes to RGC death, as evidenced by protection of RGC in mice lacking p53 [92]. In addition, increased expression of SASP, upon acute glaucoma-induced retinal damage, was also observed suggesting that the senescence-associated cytokine network is activated in IOP-treated retinas [92]. Genome-wide association studies (GWAS) have indicated that the SIX1-SIX6 and P16/INK4A loci are among the strongest risk genes associated with primary open-angle glaucoma (POAG) [93, 94]. Deploying a combination of genetic association and functional studies, Skowronska-Krawczyk et al. [95] demonstrated that SIX6 risk variant upregulates p16/INK4A expression resulting in RGC senescence in cell culture, animal models, and human glaucoma retinas. Beyond loss of retinal cells, aging is also associated with the accumulation of both intracellular and extracellular deposits where it can generate ROS after exposure to oxygen and light [96]. The finding that $A\beta$ is also elevated in aging retina and is a component of drusen suggests that $A\beta$ may be a key factor in AMD pathology and this has opened new perspectives about the potential etiology and therapeutic approaches [97, 98]. $A\beta$ has been recently shown to induce RPE cells to enter senescence [99]. A recent study shows the role of RPE senescence in the retinal degeneration induced by $A\beta$ (1-42) peptide as characterized by upregulation of senescence markers and abnormal electroretinography (ERG) responses [100]. Hence, cellular senescence of RPE or neuronal cells induce different age-related retinal diseases and targeting them could be a viable therapeutic strategy.

8. Cell Senescence Signaling Pathways

Many molecules can work alone or in combination and make the cells senescent via p16INK4a/Rb (retinoblastoma protein), p53/p21, and likely other pathways. Cellular senescence is a state of stable cell cycle arrest and the onset and maintenance of the senescent state involve action of two major pathways, the p16Ink4a/Rb pathway and the p19Arf/p53/p21Cip1 pathway [111]. The p16Ink4 is a CDK (cyclin-dependent kinase) inhibitor that accumulates in the cell as the number of cell divisions increase. Independent of the p53/p21Cip1 pathway, the p16Ink4a/Rb pathway is considered to be the primary pathway leading to the development of senescence in cells [112]. Cellular senescence induced by oxidative stress is mainly through the p16Ink4a/Rb pathway. Oxidative stress enhanced the nuclear expression of p16 which can bind to CDK4/6, thus inhibiting the phosphorylation of the retinoblastoma protein Rb and prevent the transcription factors E2F from activating, thereby inhibiting the expression of its regulatory site genes. The mechanism of cells entering the cell cycle from G1 stage to the S stage is prevented, thus inhibiting cell proliferation, and ultimately leading to cell senescence.

Telomere-damaged senescent cells function mainly through the p53/p21Cip1 pathway. When cells are stressed, they can cause high expression of p16 protein. This can lead to the phenotype associated with cell senescence and growth arrest; formation of senescence-associated heterochromatin sites and maintenance of the p16Ink4a/Rb pathway is no longer required. p53 is a transcription factor involved in the regulation of an array of cellular processes, including metabolic adaptation, DNA repair, cell cycle arrest, apoptosis,

and senescence (see Bourgeois and Madl, [113] for a review). Several independent studies using p53 inhibitors, p53 antisense oligonucleotides, or homozygous deletion mutants demonstrated a role for p53 in cellular senescence [114]. The p53 protein in the p53/p21Cip1 pathway is a common tumor suppressor protein, which is inactivated in many tumors and upregulated in senescent cells. The ubiquitin ligase MDM2 (murine double minute 2) can promote the degradation of p53 by related proteases or directly inhibit the activity of p53 protein. The p19Arf protein can bind to and inhibit MDM2 activity. When there is damage in the DNA molecule, the upregulated p19Arf protein inhibits MDM2 and activates p53. The p53 then activates downstream p21Cip, inhibits RB phosphorylation, and thus cannot bind to E2F. Blocking cell cycle at the G1 phase makes the cells enter into the senescence state.

9. Cellular Senescence and the Role of SASPs

Multiple stressors induce senescence, some even with shared effects that can also drive multiple phenotypes and pathologies associated with aging. Many studies have provided clear evidence that an array of bioactive molecules are released by senescent cells, called SASP [14]. As mentioned earlier, these include chemokines, cytokines, metalloproteases, and growth factors which can act through both autocrine/paracrine pathways and can affect neighboring cells [115]. Although SASP is generally considered proinflammatory, the true microenvironmental impact and composition of SASP may vary according to cell types (i.e., fibroblasts/epithelial, normal/cancerous) and senescence-triggering stimuli (i.e., replicative senescence, DNA damage-induced senescence, oncogene-induced senescence) [14, 116, 117]. It is now evident that SASP functionally links senescence to various biological processes including tissue regeneration and remodeling, embryonic development, inflammation, and tumorigenesis. Based on the mechanism of action, SASP factors can be classified [118] as (1) *receptor mediated*, which includes interleukins IL-6, IL-8, and IL-1α; chemokines GROα, GROβ, CCL-2, CCL-5, CCL-16, CCL-26, and CCL-20; and the growth factors VEGF, HGF, FGF, TGF-β, and GM-CSF [119, 120]; (2) *regulatory molecules* such as tissue inhibitors of metalloproteases (TIMP), the plasminogen activator inhibitor (PAI), and insulin-like growth factor-binding proteins (IGFBP); (3) *directly acting* such as matrix metalloproteases MMP-1, MMP-10, MMP-3 and serine proteases: the tissue plasminogen activator (tPA) and urokinase plasminogen activator (uPA). Several in vitro and in vivo studies have attributed the multifunctions of the SASP to individual protein components. For example, out of the SASPs, IL-6, IL-8, and CCL2 enhance tumor cell proliferation [14, 121]; VEGF promotes angiogenesis [122]; IL-6, IL-8, IGFBP7, and PAI-1 augment senescence [119–124]. It was reported that the multifunctional cytokines such as TGF-β family ligands, CCL2, and VEGF evoke cellular senescence [125] while PDGF-AA promotes wound healing [11, 126]. In senescent cells, many of the SASP factors discussed above are activated at the transcriptional level [119, 120, 127]. However, many SASP bioactive factors are able to induce inflammation, disrupt tis-

sue architecture, and enhance malignant transformation [128, 129]. Of note, the inhibition of the SASPs such IL-6 or IL-8 only partially blocks paracrine senescence progression suggesting the involvement of alternate pathways [130, 131].

Recently, increasing evidence suggests that extracellular vesicles (EVs) released from senescent cells are unique and are involved in regulating the phenotype of recipient cells the same way as SASP bioactive molecules [132–136]. Hence, the EVs secreted from senescent cells, (senescence-associated EVs), appear to be a novel SASP factor [137–140].

There are reports demonstrating increased EV secretion and changes in the compositions of EVs with stress [141–145]. Further, the expression of the exosome markers CD63 and LAMP2 showed a significant increase in older retinal pigment epithelium tissue [146]. It is also known that the secretion of EVs increased in human RPE cells rendered senescent by the DNA-damaging agent doxorubicin [144]. However, not much is known about the role that EVs play as SASP mediators in the senescent microenvironment. The miRNA components of senescent exosomes are studied in some cell types but, aside from protumorigenic effects [134], the proteomic content and function of exosomes and small EVs secreted by senescent cells are not well studied. A comparative proteomic analysis of EVs secreted from control and DXR-induced senescent RPE cells found that EVs secreted from senescent cells showed a markedly altered protein composition [144]. Paracrine senescence via the SASP has been previously described as an important mechanism during senescence [125, 147], although these studies do not differentiate between the effect of soluble factors secreted by the cells and EVs released. Furthermore, a recent study in human primary fibroblasts provides evidence that both the soluble factors and sEVs are responsible for mediating paracrine senescence [148]. An in-depth mass spectroscopic analysis of the published protein composition of soluble factor of senescence [125] and sEV proteomics [148] shows little correlation between both fractions, suggesting that although the downstream signaling is similar, the triggers inducing senescence are diverse. A comprehensive proteomic database of soluble and exosome SASP factors (SASP Atlas), originating from multiple senescence inducers and cell types has appeared recently [149]. The protein cargo of exosomes/EVs released by senescent cells was significantly higher and many protein markers will likely be specific to cell type and originating stimulus when compared to quiescent control cells [149]. Mitsuhashi et al. [150] reported that the levels of IL-6 and IL-12 mRNAs in macrophage-derived exosomes from older subjects are higher than those from younger subjects. Furthermore, there is evidence that miRNAs that can regulate cellular senescence are contained in EVs [151, 152]. In addition, mounting evidence suggests that senescence-associated EVs are involved in pathology as well as senescent cells can impact age-related stem cell dysfunction via EVs [132, 143, 145, 153].

10. Role of Mitochondrial ROS in the Induction of Senescence

It is well known that both intracellular and extracellular ROS have been shown to contribute to the induction of

senescence. Mitochondria produce ROS as a byproduct of electron leak along the electron transport chain during cellular respiration [154]. Hydrogen peroxide (H_2O_2), which is a major endogenous ROS, is a potent inducer of cellular senescence. Work from our laboratory has documented that H_2O_2 treatment induced senescence in human RPE cells [38, 39]. ROS have also been shown to act as signaling molecules during senescence, stabilizing the cell cycle arrest. ROS contributes to initiating cellular senescence and progression by either directly damaging mitochondrial DNA (mtDNA) or in interaction with modifications of the telomerase reverse transcriptase enzyme, a catalytic subunit of the enzyme telomerase and the p53 and Ras pathways activity [21]. Dysfunctional mitochondria release multiple damage-associated molecular patterns (DAMPs), such as ATP, ROS, and mtDNA, activating the NLRP3 inflammasome, which in turn trigger the proteolytic maturation of proinflammatory cytokine precursors, such as IL-1β, and leads to the activation of the NF-κB pathway, supporting senescence biogenesis [155]. In contrast, interventions which reduce mitochondrial ROS such as nicotinamide mononucleotide (NAD) [156] and mitochondrial-targeted antioxidant MitoQ [157, 158] have been shown to prevent telomere dysfunction and prevent senescence. NAD treatment via intravitreal administration in mice also preserves NAD+ and prevents RPE senescence [156]. We have demonstrated that H_2O_2-induced senescence altered mitochondrial functions and treatment with a mitochondria-derived peptide, humanin, prevented mitochondrial ROS and delayed cellular senescence [39]. ROS also plays a role as a signaling factor in downstream senescence effector pathways [159]. In addition, canonical markers regulating major senescence pathways such as p16, p21, and p53 are elevated in response to increased ROS [39, 160] suggesting that ROS in senescent cells enhanced the cell cycle arrest characteristic of the senescence phenotype [159]. On the other hand, it is suggested that mitochondrial ROS generation may not necessarily be the primary cause of cellular senescence [161]. The senescence phenotype induced by hyperoxia was not blocked either in the mitochondrial SOD2 or catalase overexpressed human lung fibroblasts suggesting the ROS formed in the cytosol alone can induce senescence [161]. Of note, mitochondrial ROS can damage nuclear DNA and thus can induce senescence [159]. Depletion of mitochondrial DNA (mtDNA), knockdown of mitochondrial sirtuin-3 (SIRT3), or inhibition of the electron transport chain can induce mitochondrial dysfunction-associated senescence (MiDAS) [74]. It was reported that in MiDAS, pyruvate, but not an antioxidant, prevented MiDAS [74]. Further, no evidence of DNA damage was observed but rather decreased NAD+/NADH ratios caused by MiDAS [74].

11. Energy Metabolism and Cellular Senescence

Mitochondria are the principal cellular organelles responsible for ATP production, calcium regulation, biosynthetic processes, and apoptotic regulation. It is well established that not only cell size but also mitochondrial mass increases significantly in senescent cells (Table 3). Senescent cells have

been observed in the eye specifically in the neuronal, endothelial, and RPE cells [42, 86] and it is critical to understand their participation in energy metabolism during aging as well as the progression of various retinal degenerative diseases.

A strong link between mitochondrial metabolism and the senescent state has been proposed [162]. Acute oxidative stress can cause increased ROS production which is linked to mitochondrial oxidative damage, a reduction in mitochondrial copy number, and decreased mitochondrial respiration and ATP production in RPE cells [39, 163–165]. Repeated exposure stress can also induce ROS which in turn can induce and regulate cellular senescence and can cause major changes in the metabolome [166]. In particular, an increase in mitochondrial oxygen consumption and oxidative phosphorylation have been reported in oncogene-induced senescence in human fibroblasts [166, 167], oxidative stress-induced senescence [50, 168], therapy-induced senescence in lymphoma [169], and DNA damage-induced senescence [50]. However, in replicative senescence, an impairment of mitochondrial function and increased glycolysis has been described [50, 170]. Thus, it can be hypothesized that senescent cells follow different bioenergetic phenotypes, depending on the stimuli which trigger senescence induction. In particular, replicative senescence in primary human mammary epithelial cells is accompanied by a marked inhibition of nucleotide synthesis without any alteration in glycolysis. These findings demonstrate that inhibition of nucleotide synthesis plays a causative role in the establishment of replicative senescence [171].

12. Mitochondrial Retrograde Signaling and Senescence

Mitochondrial-to-nuclear signaling has gained much attention in recent years. Retrograde signaling is a mitochondrial-to-nuclear signal transduction pathway by which defective mitochondria communicate with the nuclear genetic compartment [178, 179]. When the oxidative and metabolic activities of mitochondria are altered, it communicates with the nucleus via mitochondrial retrograde signaling. An evidence for this has been reported in mitochondrial damage-associated conditions such as neurodegeneration and cardiovascular diseases [180, 181].

The retrograde signaling involves multiple factors [181] and these factors mainly activate cytosolic mediators through interactions with small molecules (e.g., Ca2+, ROS, NAD/NADH ratio) and transmit signals into the nucleus [182, 183]. These mitochondrial signals modulate the gene expression of transcription factors, (NRF1, NRF2, Sirt1, mTOR, PPARγ, Sp1, CREB) and members of the PGC-1 family of regulated coactivators (PGC-1α, PGC-1β, and PRC) [184]. These reprogrammed transcripts could restore mitochondrial function, activate alternative energy pathways, and prepare the cells for death, senescence, or proliferation [181, 185]. Thus, retrograde signaling-mediated transcriptional reprogramming could play a key role in senescence and aging. Increasing evidence indicate that mitochondrial short open reading frame- (sORF-) derived peptides are potent and evolutionarily conserved mitochondrial signals could affect

TABLE 3: Mitochondrial metabolic changes in senescence.

Cell type	Source of senescence	Mitochondrial mass	Oxidative phosphorylation	Glycolysis	Mitochondrial ATP production	References
Human MRC5 fibroblasts	RS	Increased	Increased	Increased	Decreased	[172]
Human foreskin fibroblasts	RS	Increased	Increased	Increased	Increased	[169]
Human dermal fibroblasts.	RS	No change	No change	Increased	No change	[50]
Human dermal fibroblasts.	Doxorubicin	Increased	Increased	No change	Increased	[50]
Human foreskin fibroblasts	Doxorubicin	Increased	Increased	Increased	Increased	[169]
Human diploid IMR90 fibroblasts	Oncogenic *Ras*-induced senescence (OIS)	Increased	Decreased	-	Decreased	[56
Human Dermal Fibroblasts	Oncogene-induced senescence (OIS)	NA	Increased	-	-	[167]
Human fetal lung fibroblasts	Oncogene-induced senescence (OIS)	-	Increased	-	-	[166]
Human fibroblasts	Radiation induced	-	No change	Increased	-	[173]
Mouse melanoma B16-F1 cell line	Temozolomide (genotoxic agent)	Increased	Increased	Decreased	increased	[174]
HEI-OC1 auditory cells	SIPS (H$_2$O$_2$)		Decreased	-	No change	[175]
Human lung fibroblasts	SIPS (H$_2$O$_2$)	-	Increased	-	Increased	[176]
Human lung and cardiac fibroblast cells	SIPS (nucleoside analogs)	Increased	Increased	-	Increased	[177]
Human disc cells	SIPS	Increased	Increased	-	Increased	[168]
Human fibroblasts	γ radiation	-	No change	Increased	-	[173]

RS: replicative senescence; OIS: oncogene-induced senescence; SIPS: stress-induced premature senescence.

(a)

(b)

(c)

(d)
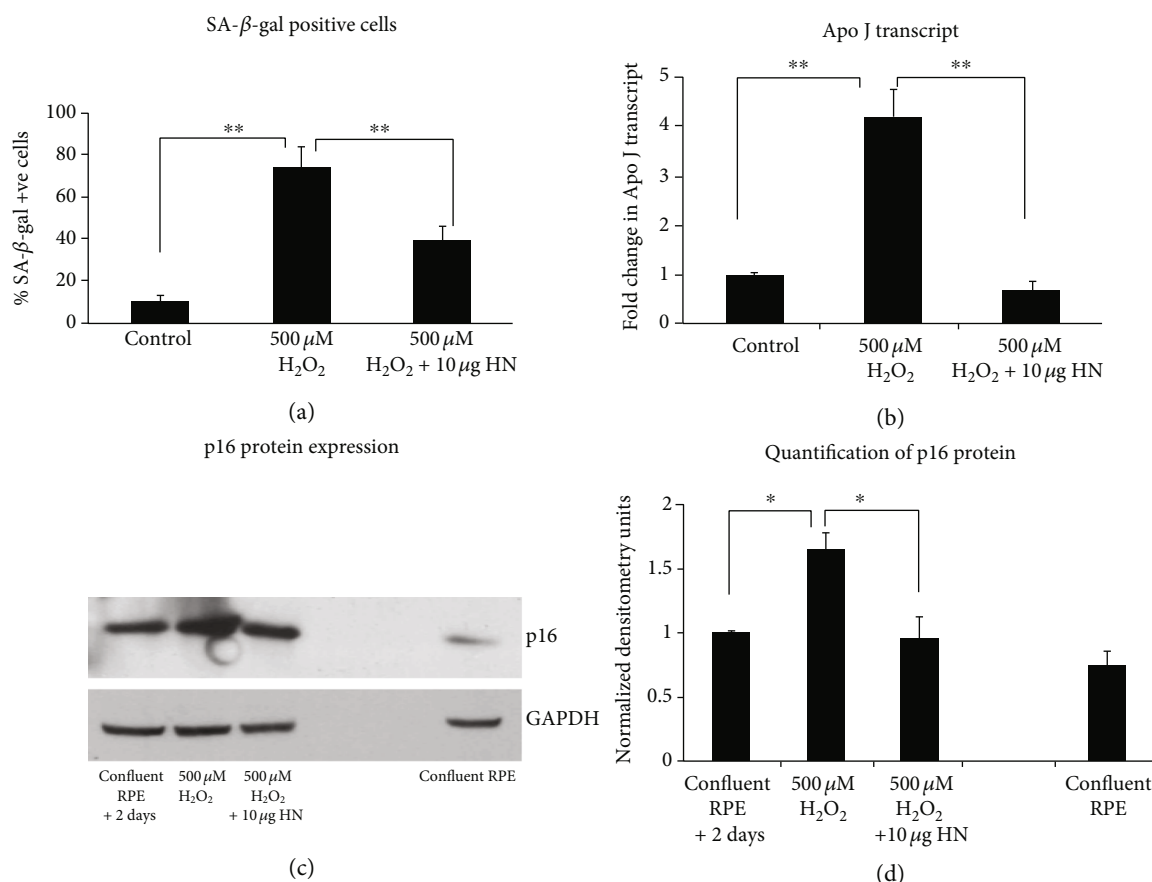
Figure 2: Evidence for increased senescence with oxidative stress and its elimination in human RPE cells with a mitochondria-derived peptide, humanin. $^*P < 0.05$, $^{**}P < 0.01$. Reproduced from [39] and is licensed under a Creative Commons Attribution-NonCommercial-NoDerivatives 4.0 International License.

various physiological processes. In support, we have demonstrated that the first mitochondria-derived peptide humanin, transcribed and translated as short ORFs from the 16S rRNA of mtDNA, delayed oxidative stress-induced senescence in RPE cells (Figure 2) [39]. Whether this MDP has a role in the regulation of nuclear factors needs to be studied. However, it has been shown that another MDP, MOTS-c, translocates to the nucleus and regulates nuclear gene expression following metabolic stress via AMPK pathway [186]. Thus, between the nucleus and the mitochondria, signaling occurs in both directions, and further studies of these pathways would provide in-depth details about senescence and organismal aging [187].

13. Mitochondrial Dynamics and Cellular Senescence

Mitochondrial dynamics, in general, include events such as fission, fusion, and mitophagy [188, 189]. Senescent cells are metabolically active and have the ability to self-integrate and remodel their morphology [189]. Fission and fusion help mitochondria to regulate cellular energy levels, and a regulated balance among these events ensure normal mitochondrial and cellular functions [190]. In particular, fusion and fission proteins MFN1, MFN2, dynamin-related protein 1

(DRP1), mitochondrial fission factor (MFF), and mitochondrial fission 1 protein (FIS1) modulate mitochondrial shape in response to cellular requirements [191]. The mitochondrial fusion is primarily regulated by Mitofusion proteins 1/2 (Mfn1/2), optic atrophy protein 1 (Opa1) [192, 193], and fission by dynamin-related protein 1 (Drp1) and fission 1 protein (Fis1). We have shown that in oxidative stress-induced RPE senescence, mitochondrial fission proteins, FIS1, and DRP1 increased significantly [194]. Altering mitochondrial dynamics including morphology can cause mitochondrial defects and dysfunction could result in cellular senescence [195, 196]. However, additional studies are required to establish the link between mitochondrial morphology, dynamics, and cellular senescence.

14. Mitochondrial Biogenesis and Senescence

It is now appreciated that senescence is accompanied by increased mitochondrial oxidative metabolism, along with increased mitochondrial mass due to increased mitochondrial biogenesis [159, 167, 194, 197, 198]. Mitochondrial biogenesis is a multifactorial process which also involves assembly as well as replication of mtDNA [199]. Despite the complexity of the different signaling pathways that potentially regulate mitochondrial biogenesis, they all use

the key component of the peroxisome proliferator-activated receptor γ coactivator-1α (PGC-1α) [200]. The gene expression of nuclear respiration factors (NRF-1 and NRF-2) and mitochondrial transcription factor A (TFAM), which are transcription factors that initiate the expression of both nuclear subunits of the respiratory chain and proteins involved in mitochondrial DNA transcription and replication, are increased by PGC-1α [162, 184, 201]. The mitochondrial mass and the mRNA levels of PGC1α and NRF-1 were found to increase during replicative senescence [202] and this could be attributed to de novo synthesis of the nuclear transcriptional factors as a compensatory response to increased ROS production and the impaired membrane potential [202]. Overexpression of the PGC-1α in human fibroblasts resulted in an increase of the mitochondrial encoded marker protein COX-II, consistent with the ability of PGC-1 to increase mitochondrial number, and accelerated the rate of cellular senescence [202, 203]. In an idiopathic pulmonary fibrosis model, mammalian target of rapamycin/peroxisome proliferator-activated receptor-γ complex 1α/β (mTOR/PGC-1α/β) axis is markedly upregulated in senescent lung epithelial cells [198]. Despite significant function of PGC-1α in mitochondrial biogenesis and senescence, only very few studies are found on its role in the retina, though some studies on its role in biogenesis exist [204, 205]. It has been also demonstrated that PGC-1α-deficient mice developed some abnormalities in RPE cells that were associated with their accelerated senescence [200, 206, 207]. A recent study using human ARPE19 cells reported that elevated PGC-1α is essential for maintaining normal autophagic flux [206]. Therefore, more detailed studies are required to establish a direct link for PGC-1α and senescence in AMD pathology.

15. Senolytic Drugs for Targeting Senescent Cells

Because of the adverse nature of senescence in the development of multiple illnesses, disrupting or preventing senescence can delay health decline during aging. The discovery of senotherapeutic drugs represents a developing and highly promising field of current research for new therapies. Inhibition of major pathways or disruption of p53 and p16, p21, have all been shown to have a significant benefit in aging phenotypes but they can increase the occurrence of cancer [208–211]. Therefore, selective removal of senescent cells could be the safer route to target senescence. Senolytics are drugs that selectively target senescent cells, not a molecule or a single biochemical pathway, by inducing apoptosis of senescent cells [212]. Effective use of potential senolytics of natural or synthetic molecules that target fundamental aging processes into clinical practice could be transformative. Age-related increase in senescent cells was reported in the skin tissue of monkeys and humans [15, 213]. The first senolytics identified were dasatinib and quercetin; their combination treatment reduced senescent cell burden in chronologically aged, radiation-exposed, and progeroid Ercc1$^{-/\Delta}$ mice (a mouse model of a human progeroid syndrome) [214]. These results demonstrated the potential of selectively target-ing senescent cells and the efficacy of senolytics for alleviating symptoms of age-related diseases and extending health span. Since then, several senolytics, such as navitoclax, 17-DMAG, and a peptide that targets the Bcl-2- and p53-related senescent cell anti-apoptotic pathways (SCAPs), have been shown to be effective in reducing senescent cells in mice as evidenced by decreasing senescent cell indicators (see reviews by Sun et al. [215] and Knoppert et al. [216] for a complete list). Following the discovery of dasatinib and quercetin, the next senolytic compound to emerge was navitoclax (ABT-263), a small molecule belonging to Bcl-2 family protein inhibitor. ABT-263 selectively binds to Bcl-2, Bcl-XL, and Bcl-w and prevents their binding to the apoptotic effectors Bax and Bak proteins [217–219]. In mouse models of atherosclerosis and neurodegeneration, ABT-263 eliminated dysfunctional senescent cells from atherosclerotic plaques and brain tissue, respectively, substantially inhibiting the progression of key disease phenotypes [220, 221]. After the discovery as a senolytic agent, ABT-263 has been extensively used to study the mechanisms of aging in several animal model systems. For example, in a model of pulmonary fibrosis, treatment of the irradiated mice with ABT-263 after persistent disease had developed reduced senescent cells and reversed the disease [222]. Fisetin [223] is another flavonoid with multipotent properties identified as a novel senolytic molecule. Acute or intermittent treatment of progeroid and old mice with fisetin reduced the biomarkers of senescence in multiple tissues, restored tissue homeostasis, reduced age-related pathology, and extended median and maximum lifespan [224]. A new class of drug candidates with senolytic properties which are inhibitors of heat-shock protein HSP90 has been discovered [225]. Multiple treatment with the HSP90 inhibitor 17-DMAG significantly delayed onset of different age-related symptoms in progeroid mice, leading to an overall health span improvement [225]. In a p16-3MR transgenic mouse model, selective depletion of senescent cells by the small-molecule chemical UBX0101 reduced the development of posttraumatic osteoarthritis by creating a proregenerative microenvironment [226]. Piperlongumine (PL) is a biologically active alkaloid and a recently identified senolytic agent which can selectively kill senescent cells by targeting oxidation resistance 1 (OXR1) to mediate PL senolytic activity [205]. The multicenter Intervention Testing Program by the National Institute for Aging has identified five drugs that increase lifespan in genetically heterogenous mice, including rapamycin, acarbose, nordihydroguaiaretic acid, 17-α-oestradiol, and aspirin [227]. Recent mechanistic studies show that stimulated by cytosolic DNA, active cyclic GMP-AMP synthase-stimulator of interferon gene (cGAS-STING) pathway triggers inflammation and plays a role in the development of senescence [228]. Based on these findings, it was hypothesized that blocking STING pathway could be a potential therapeutic strategy to prevent senescence-associated human diseases [229].

All the preclinical animal studies in different disease models with an array of senolytic agents provide confidence in bringing senolytic agents into clinical trials. In an open-label phase 1 pilot study, the first clinical trial of senolytics, dasatinib (D)+quercetin (Q) improved physical function in

patients with idiopathic pulmonary fibrosis (IPF), a fatal senescence-associated disease and diabetic kidney disease [230, 231]. D+Q decreases p16INKA, p21, and SASP factors, including IL-1α, IL-6, MMP-9, and MMP-12 [230]. The senolytic drug UBX0101 was developed to treat osteoarthritis of the knee (ClinicalTrials.gov Identifier: NCT03513016). Another drug, UBX1967, a Bcl-2 family inhibitor specifically tailored for age-related diseases of the eye, including neovascular age-related macular degeneration, proliferative diabetic retinopathy, and diabetic macular edema, is also progressing to human testing [232].

However, though the initial studies regarding senolytics show positive signs, still there are concerns regarding their effectivity as therapies. For instance, it has been reported that senescent cells reappeared after cessation of senolytic treatment in a model of osteoarthritis [226]. Although a brief disruption of prosurvival pathways is sufficient to kill senescent cells, they are very effective only when administered intermittently [214]. Further, the senescence program considerably differ among cells/tissues, increasing the possibility of finding cell-/tissue-specific senolytics. With all these, targeting senescence using senolytics or by other strategies could not only ease specific diseases but also considerably improve the general health span of aged individuals.

16. Future Directions

The body of work cited in this review implicates the role of senescent cells in tissues from aged samples as one of the contributing causes of many age-related diseases such as lung disease, cardiovascular diseases, and arthritis, but information on the role of senescent cells in ocular diseases is sparse. There is an ongoing debate whether or not senescent cells found in aged animal models contribute in a significant way to diseases. At the same time, small-molecule senolytic drugs are being developed for treatment of age-related diseases and some drugs are under testing or in clinical trials. The following issues/questions need to be considered before senolytic drug treatment becomes a valuable tool in disease prevention.

(i) Senescent cells are heterogeneous, featured by different characteristics and could follow different pathways to avoid apoptosis [233]. Further, the senescent cell phenotype is dynamic and can change at the time of senescence or various points after senescence occurs. Therefore, there is no single senolytic/SASP inhibitor that could target all the senescent cells. Characterizing those heterogeneous cells using cell-specific markers using multiple approaches, such as experimental and bioinformatics, could highly advance our understanding of senescence and provide new strategies for designing therapy

(ii) Senescent cells undergo extensive genome remodeling and changes in gene expression, which are poorly understood. Therefore, understanding the mechanisms responsible for these differences in gene expression and their role to senescence acquisition and SASPs would greatly benefit designing thera-

pies. It is also worthwhile to explore the role of key epigenetic regulators that lead to the SASP and target them directly to prevent senescence

(iii) Since senescent cells have many subpopulations in the same tissue, a single drug is unlikely to induce apoptosis to all of them. Therefore, in addition to senolytic drugs, SASP inhibitors, another group of molecules that show promise as treating age-related diseases, are also currently being tested. However, the components of the SASP vary based on the cell type from which senescent cells developed [234]. SASP components also vary in the presence of many drugs, and the regulation is segmental: not all SASP components are regulated, and hence SASPs could be modifiable [234]. Thus, it is important to learn how SASPs change at different stages of senescence, and how the SASP factors differ from tissue damage signals. Use of senolytic cocktail or combination therapy would be a better approach in fighting senescence-associated diseases in this regard

(iv) It is now widely accepted from cellular studies that mitochondrial dysfunction plays a major role in senescence. Whether stress-induced or age-related mitochondrial dysfunction cause senescence *in vivo* remains to be studied in detail. Given the complexity of mitochondria and their involvement in multiple processes and functions, it is highly likely. Therefore, it is of major importance to further investigate the molecular processes behind the role of mitochondria in aging, and their potential to serve as targets for therapeutic interventions

(v) Multiple animal models are required to test potential senolytic drugs/senolytic cocktails and to understand the off-target effects of senolytic agents [56, 95, 102]. While genetically modified mice such as p16 transgenic mice [56] or pharmacological manipulations are available for most diseases, more work on additional models is required. In other words, it is desirable that senescence-associated disease animal models are developed in which senescent cells can be tracked *in tissues of interest*, and from which senescent cells can be cleared using the potential drugs

(vi) Finally, research on understanding the mechanism of senescence from ocular cells and tissues is just beginning. IND-enabling studies of senolytic drugs for diseases such as AMD have recently been initiated [232]. The success of such investigations, although promising, will depend on a greater understanding of the mechanism of disease progression in the eye to develop optimal therapies that target the primary defect in the retina.

Conflicts of Interest

The authors declare that there is no conflict of interest regarding the publication of this paper.

Acknowledgments

References

[1] J. Campisi and F. d'Adda di Fagagna, "Cellular senescence: when bad things happen to good cells," *Nature Reviews Molecular Cell Biology*, vol. 8, no. 9, pp. 729–740, 2007.

[2] L. Hayflick and P. S. Moorhead, "The serial cultivation of human diploid cell strains," *Experimental Cell Research*, vol. 25, no. 3, pp. 585–621, 1961.

[3] B. G. Childs, M. Durik, D. J. Baker, and J. M. van Deursen, "Cellular senescence in aging and age-related disease: from mechanisms to therapy," *Nature Medicine*, vol. 21, no. 12, pp. 1424–1435, 2015.

[4] D. Muñoz-Espín, M. Cañamero, A. Maraver et al., "Programmed cell senescence during mammalian embryonic development," *Cell*, vol. 155, no. 5, pp. 1104–1118, 2013.

[5] I. Sturmlechner, M. Durik, C. J. Sieben, D. J. Baker, and J. M. van Deursen, "Cellular senescence in renal ageing and disease," *Nature Reviews Nephrology*, vol. 13, no. 2, pp. 77–89, 2017.

[6] M. Storer, A. Mas, A. Robert-Moreno et al., "Senescence is a developmental mechanism that contributes to embryonic growth and patterning," *Cell*, vol. 155, no. 5, pp. 1119–1130, 2013.

[7] J. Campisi, "CANCER: Suppressing cancer: the importance of being senescent," *Science*, vol. 309, no. 5736, pp. 886-887, 2005.

[8] D. G. A. Burton and V. Krizhanovsky, "Physiological and pathological consequences of cellular senescence," *Cellular and Molecular Life Sciences*, vol. 71, no. 22, pp. 4373–4386, 2014.

[9] D. J. Baker, T. Wijshake, T. Tchkonia et al., "Clearance of p16^{Ink4a}-positive senescent cells delays ageing-associated disorders," *Nature*, vol. 479, no. 7372, pp. 232–236, 2011.

[10] D. J. Baker, B. G. Childs, M. Durik et al., "Naturally occurring p16Ink4a-positive cells shorten healthy lifespan," *Nature*, vol. 530, no. 7589, pp. 184–189, 2016.

[11] M. Demaria, N. Ohtani, S. A. Youssef et al., "An essential role for senescent cells in optimal wound healing through secretion of PDGF-AA," *Developmental Cell*, vol. 31, no. 6, pp. 722–733, 2014.

[12] V. Krizhanovsky, M. Yon, R. A. Dickins et al., "Senescence of activated stellate cells limits liver fibrosis," *Cell*, vol. 134, no. 4, pp. 657–667, 2008.

[13] B. Ritschka, M. Storer, A. Mas et al., "The senescence-associated secretory phenotype induces cellular plasticity and tissue regeneration," *Genes & Development*, vol. 31, no. 2, pp. 172–183, 2017.

[14] J. P. Coppé, C. K. Patil, F. Rodier et al., "Senescence-associated secretory phenotypes reveal cell-nonautonomous functions of oncogenic RAS and the p53 tumor suppressor," *PLoS Biology*, vol. 6, no. 12, pp. 2853–2868, 2008.

[15] J. C. Jeyapalan, M. Ferreira, J. M. Sedivy, and U. Herbig, "Accumulation of senescent cells in mitotic tissue of aging primates," *Mechanisms of Ageing and Development*, vol. 128, no. 1, pp. 36–44, 2007.

[16] A. Biran, L. Zada, P. Abou Karam et al., "Quantitative identification of senescent cells in aging and disease," *Aging Cell*, vol. 16, no. 4, pp. 661–671, 2017.

[17] F. Rodier and J. Campisi, "Four faces of cellular senescence," *The Journal of Cell Biology*, vol. 192, no. 4, pp. 547–556, 2011.

[18] J. Birch, R. K. Anderson, C. Correia-Melo et al., "DNA damage response at telomeres contributes to lung aging and chronic obstructive pulmonary disease," *American Journal of Physiology Lung Cellular and Molecular Physiology*, vol. 309, no. 10, pp. L1124–L1137, 2015.

[19] M. Ogrodnik, S. Miwa, T. Tchkonia et al., "Cellular senescence drives age-dependent hepatic steatosis," *Nature Communications*, vol. 8, no. 1, p. 15691, 2017.

[20] G. P. Dimri, X. Lee, G. Basile et al., "A biomarker that identifies senescent human cells in culture and in aging skin in vivo," *Proceedings of the National Academy of Sciences*, vol. 92, no. 20, pp. 9363–9367, 1995.

[21] J. M. van Deursen, "The role of senescent cells in ageing," *Nature*, vol. 509, no. 7501, pp. 439–446, 2014.

[22] J. Campisi, "Aging, cellular senescence, and cancer," *Annual Review of Physiology*, vol. 75, no. 1, pp. 685–705, 2013.

[23] N. E. Sharpless and C. J. Sherr, "Forging a signature of _in vivo_ senescence," *Nature Reviews Cancer*, vol. 15, no. 7, pp. 397–408, 2015.

[24] V. Myrianthopoulos, K. Evangelou, P. V. S. Vasileiou et al., "Senescence and senotherapeutics: a new field in cancer therapy," *Pharmacology & Therapeutics*, vol. 193, pp. 31–49, 2019.

[25] A. C. Lloyd, "The regulation of cell size," *Cell*, vol. 154, no. 6, pp. 1194–1205, 2013.

[26] H. E. Walters, S. Deneka-Hannemann, and L. S. Cox, "Reversal of phenotypes of cellular senescence by pan-mTOR inhibition," *Aging*, vol. 8, no. 2, pp. 231–244, 2016.

[27] M. Narita, S. Nũnez, E. Heard et al., "Rb-mediated heterochromatin formation and silencing of E2F target genes during cellular senescence," *Cell*, vol. 113, no. 6, pp. 703–716, 2003.

[28] B. Y. Lee, J. A. Han, J. S. Im et al., "Senescence-associated beta-galactosidase is lysosomal beta-galactosidase," *Aging Cell*, vol. 5, no. 2, pp. 187–195, 2006.

[29] J. Krishnamurthy, C. Torrice, M. R. Ramsey et al., "Ink4a/Arf expression is a biomarker of aging," *The Journal of Clinical Investigation*, vol. 114, no. 9, pp. 1299–1307, 2004.

[30] S. Ressler, J. Bartkova, H. Niederegger et al., "p16INK4A is a robust in vivo biomarker of cellular aging in human skin," *Aging Cell*, vol. 5, no. 5, pp. 379–389, 2006.

[31] Y. Liu, H. K. Sanoff, H. Cho et al., "Expression of p16(INK4a) in peripheral blood T-cells is a biomarker of human aging," *Aging Cell*, vol. 8, no. 4, pp. 439–448, 2009.

[32] T. Kuilman and D. S. Peeper, "Senescence-messaging secretome: SMS-ing cellular stress," *Nature Reviews Cancer*, vol. 9, no. 2, pp. 81–94, 2009.

[33] J. P. Coppé, P. Y. Desprez, A. Krtolica, and J. Campisi, "The senescence-associated secretory phenotype: the dark side of tumor suppression," *Annual Review of Pathology*, vol. 5, no. 1, pp. 99–118, 2010.

[34] A. Helman, A. Klochendler, N. Azazmeh et al., "p16Ink4a-induced senescence of pancreatic beta cells enhances insulin secretion," *Nature Medicine*, vol. 22, no. 4, pp. 412–420, 2016.

[35] W. Chen, J. Kang, J. Xia et al., "p53-related apoptosis resistance and tumor suppression activity in UVB-induced premature senescent human skin fibroblasts," *International Journal of Molecular Medicine*, vol. 21, no. 5, pp. 645–653, 2008.

[36] P. R. Coleman, C. N. Hahn, M. Grimshaw et al., "Stress-induced premature senescence mediated by a novel gene, SENEX, results in an anti-inflammatory phenotype in endothelial cells," *Blood*, vol. 116, no. 19, pp. 4016–4024, 2010.

[37] N. Noren Hooten and M. K. Evans, "Techniques to induce and quantify cellular senescence," *Journal of Visualized Experiments*, vol. 123, no. 123, 2017.

[38] D. Zhu, J. Wu, C. Spee, S. J. Ryan, and D. R. Hinton, "BMP4 mediates oxidative stress-induced retinal pigment epithelial cell senescence and is overexpressed in age-related macular degeneration," *The Journal of Biological Chemistry*, vol. 284, no. 14, pp. 9529–9539, 2009.

[39] P. G. Sreekumar, K. Ishikawa, C. Spee et al., "The mitochondrial-derived peptide humanin protects RPE cells from oxidative stress, senescence, and mitochondrial dysfunction," *Investigative Ophthalmology & Visual Science*, vol. 57, no. 3, pp. 1238–1253, 2016.

[40] F. Lamoke, S. Shaw, J. Yuan et al., "Increased oxidative and nitrative stress accelerates aging of the retinal vasculature in the diabetic retina," *PLoS One*, vol. 10, no. 10, article e0139664, 2015.

[41] R. Lenin, P. G. Nagy, J. Gentry, and R. Gangaraju, "Featured article: deterioration of visual function mediated by senescence-associated endoplasmic reticulum stress in inflammatory tie2-TNF mice," *Experimental Biology and Medicine*, vol. 243, no. 12, pp. 976–984, 2018.

[42] M. López-Luppo, J. Catita, D. Ramos et al., "Cellular senescence is associated with human retinal microaneurysm formation during aging," *Investigative Ophthalmology & Visual Science*, vol. 58, no. 7, pp. 2832–2842, 2017.

[43] R. Bhat, E. P. Crowe, A. Bitto et al., "Astrocyte senescence as a component of Alzheimer's disease," *PLoS One*, vol. 7, no. 9, article e45069, 2012.

[44] S. Murano, R. Thweatt, R. J. Shmookler Reis, R. A. Jones, E. J. Moerman, and S. Goldstein, "Diverse gene sequences are overexpressed in Werner syndrome fibroblasts undergoing premature replicative senescence," *Molecular and Cellular Biology*, vol. 11, no. 8, pp. 3905–3914, 1991.

[45] J. I. Jun and L. F. Lau, "The matricellular protein CCN1 induces fibroblast senescence and restricts fibrosis in cutaneous wound healing," *Nature Cell Biology*, vol. 12, no. 7, pp. 676–685, 2010.

[46] K. E. Johnson, B. C. Wulff, T. M. Oberyszyn, and T. A. Wilgus, "Ultraviolet light exposure stimulates HMGB1 release by keratinocytes," *Archives of Dermatological Research*, vol. 305, no. 9, pp. 805–815, 2013.

[47] A. Chojnowski, P. F. Ong, E. S. Wong et al., "Progerin reduces LAP2α-telomere association in Hutchinson-Gilford progeria," *eLife*, vol. 4, 2015.

[48] T. Quan and G. J. Fisher, "Role of age-associated alterations of the dermal extracellular matrix microenvironment in human skin aging: a mini-review," *Gerontology*, vol. 61, no. 5, pp. 427–434, 2015.

[49] K. Ghosh and B. C. Capell, "The senescence-associated secretory phenotype: critical effector in skin cancer and aging," *The Journal of Investigative Dermatology*, vol. 136, no. 11, pp. 2133–2139, 2016.

[50] S. J. Kim, H. H. Mehta, J. Wan et al., "Mitochondrial peptides modulate mitochondrial function during cellular senescence," *Aging*, vol. 10, no. 6, pp. 1239–1256, 2018.

[51] M. Berneburg, N. Gattermann, H. Stege et al., "Chronically ultraviolet-exposed human skin shows a higher mutation frequency of mitochondrial DNA as compared to unexposed skin and the hematopoietic system," *Photochemistry and Photobiology*, vol. 66, no. 2, pp. 271–275, 1997.

[52] H. Koch, K. P. Wittern, and J. Bergemann, "In Human Keratinocytes the *Common Deletion* Reflects Donor Variabilities Rather Than Chronologic Aging and can be Induced by Ultraviolet A Irradiation," *The Journal of Investigative Dermatology*, vol. 117, no. 4, pp. 892–897, 2001.

[53] E. Hutter, K. Renner, G. Pfister, P. Stöckl, P. Jansen-Dürr, and E. Gnaiger, "Senescence-associated changes in respiration and oxidative phosphorylation in primary human fibroblasts," *The Biochemical Journal*, vol. 380, no. 3, pp. 919–928, 2004.

[54] S. Y. Park, B. Choi, H. Cheon et al., "Cellular aging of mitochondrial DNA-depleted cells," *Biochemical and Biophysical Research Communications*, vol. 325, no. 4, pp. 1399–1405, 2004.

[55] R. M. Laberge, D. Adler, M. DeMaria et al., "Mitochondrial DNA damage induces apoptosis in senescent cells," *Cell Death & Disease*, vol. 4, no. 7, article e727, 2013.

[56] O. Moiseeva, V. Bourdeau, A. Roux, X. Deschênes-Simard, and G. Ferbeyre, "Mitochondrial dysfunction contributes to oncogene-induced senescence," *Molecular and Cellular Biology*, vol. 29, no. 16, pp. 4495–4507, 2009.

[57] S. Hubackova, E. Davidova, K. Rohlenova et al., "Selective elimination of senescent cells by mitochondrial targeting is regulated by ANT2," *Cell Death and Differentiation*, vol. 26, no. 2, pp. 276–290, 2019.

[58] A. Ivanov, J. Pawlikowski, I. Manoharan et al., "Lysosome-mediated processing of chromatin in senescence," *The Journal of Cell Biology*, vol. 202, no. 1, pp. 129–143, 2013.

[59] K. Contrepois, C. Coudereau, B. A. Benayoun et al., "Histone variant H2A.J accumulates in senescent cells and promotes inflammatory gene expression," *Nature Communications*, vol. 8, no. 1, article 14995, 2017.

[60] J. Campisi, "The biology of replicative senescence," *European Journal of Cancer*, vol. 33, no. 5, pp. 703–709, 1997.

[61] J. Campisi, "Replicative senescence: an old lives' tale?," *Cell*, vol. 84, no. 4, pp. 497–500, 1996.

[62] F. d'Adda di Fagagna, "Living on a break: cellular senescence as a DNA-damage response," *Nature Reviews Cancer*, vol. 8, no. 7, pp. 512–522, 2008.

[63] P. Dumont, M. Burton, Q. M. Chen et al., "Induction of replicative senescence biomarkers by sublethal oxidative stresses in normal human fibroblast," *Free Radical Biology & Medicine*, vol. 28, no. 3, pp. 361–373, 2000.

[64] O. Toussaint, A. Houbion, and J. Remacle, "Aging as a multistep process characterized by a lowering of entropy production leading the cell to a sequence of defined stages. II. Testing some predictions on aging human fibroblasts in culture," *Mechanisms of Ageing and Development*, vol. 65, no. 1, pp. 65–83, 1992.

[65] O. Toussaint, C. Michiels, M. Raes, and J. Remacle, "Cellular aging and the importance of energetic factors," *Experimental Gerontology*, vol. 30, no. 1, pp. 1–22, 1995.

[66] A. Bielak-Zmijewska, G. Mosieniak, and E. Sikora, "Is DNA damage indispensable for stress-induced senescence?," *Mechanisms of Ageing and Development*, vol. 170, pp. 13–21, 2018.

[67] R. Salama, M. Sadaie, M. Hoare, and M. Narita, "Cellular senescence and its effector programs," *Genes & Development*, vol. 28, no. 2, pp. 99–114, 2014.

[68] A. Prieur and D. S. Peeper, "Cellular senescence _in vivo_ : a barrier to tumorigenesis," *Current Opinion in Cell Biology*, vol. 20, no. 2, pp. 150–155, 2008.

[69] M. Serrano, A. W. Lin, M. E. McCurrach, D. Beach, and S. W. Lowe, "Oncogenic _ras_ Provokes Premature Cell Senescence Associated with Accumulation of p53 and p16^{INK4a}," *Cell*, vol. 88, no. 5, pp. 593–602, 1997.

[70] W. J. Mooi and D. S. Peeper, "Oncogene-induced cell senescence–halting on the road to cancer," *The New England Journal of Medicine*, vol. 355, no. 10, pp. 1037–1046, 2006.

[71] C. Chandeck and W. J. Mooi, "Oncogene-induced cellular senescence," *Advances in Anatomic Pathology*, vol. 17, no. 1, pp. 42–48, 2010.

[72] C. J. Jones, D. Kipling, M. Morris et al., "Evidence for a telomere-independent "Clock" limiting RAS oncogene-driven proliferation of human thyroid epithelial cells," *Molecular and Cellular Biology*, vol. 20, no. 15, pp. 5690–5699, 2000.

[73] D. V. Ziegler, C. D. Wiley, and M. C. Velarde, "Mitochondrial effectors of cellular senescence: beyond the free radical theory of aging," *Aging Cell*, vol. 14, no. 1, pp. 1–7, 2015.

[74] C. D. Wiley, M. C. Velarde, P. Lecot et al., "Mitochondrial dysfunction induces senescence with a distinct secretory phenotype," *Cell Metabolism*, vol. 23, no. 2, pp. 303–314, 2016.

[75] N. V. Petrova, A. K. Velichko, S. V. Razin, and O. L. Kantidze, "Small molecule compounds that induce cellular senescence," *Aging Cell*, vol. 15, no. 6, pp. 999–1017, 2016.

[76] A. Kilbey, A. Terry, E. R. Cameron, and J. C. Neil, "Oncogene-induced senescence: an essential role for Runx," *Cell Cycle*, vol. 7, no. 15, pp. 2333–2340, 2008.

[77] W. Shi, A. Hoeflich, H. Flaswinkel, M. Stojkovic, E. Wolf, and V. Zakhartchenko, "Induction of a senescent-like phenotype does not confer the ability of bovine immortal cells to support the development of nuclear transfer Embryos1," *Biology of Reproduction*, vol. 69, no. 1, pp. 301–309, 2003.

[78] J. Munro, N. I. Barr, H. Ireland, V. Morrison, and E. K. Parkinson, "Histone deacetylase inhibitors induce a senescence-like state in human cells by a p16-dependent mechanism that is independent of a mitotic clock," *Experimental Cell Research*, vol. 295, no. 2, pp. 525–538, 2004.

[79] W. Grabowska, K. Kucharewicz, M. Wnuk et al., "Curcumin induces senescence of primary human cells building the vasculature in a DNA damage and ATM-independent manner," *Age*, vol. 37, no. 1, p. 9744, 2015.

[80] C. Cavallotti, M. Artico, N. Pescosolido, F. M. Leali, and J. Feher, "Age-related changes in the human retina," *Canadian Journal of Ophthalmology*, vol. 39, no. 1, pp. 61–68, 2004.

[81] M. A. Samuel, Y. Zhang, M. Meister, and J. R. Sanes, "Age-related alterations in neurons of the mouse retina," *The Journal of Neuroscience*, vol. 31, no. 44, pp. 16033–16044, 2011.

[82] H. Gao and J. G. Hollyfield, "Aging of the human retina. Differential loss of neurons and retinal pigment epithelial cells," *Investigative Ophthalmology & Visual Science*, vol. 33, no. 1, pp. 1–17, 1992.

[83] C. K. Dorey, G. Wu, D. Ebenstein, A. Garsd, and J. J. Weiter, "Cell loss in the aging retina. Relationship to lipofuscin accumulation and macular degeneration," *Investigative Ophthalmology & Visual Science*, vol. 30, no. 8, pp. 1691–1699, 1989.

[84] E. Chaum, C. S. Winborn, and S. Bhattacharya, "Genomic regulation of senescence and innate immunity signaling in the retinal pigment epithelium," *Mammalian Genome*, vol. 26, no. 5-6, pp. 210–221, 2015.

[85] H. Matsunaga, J. T. Handa, A. Aotaki-Keen, S. W. Sherwood, M. D. West, and L. M. Hjelmeland, "Beta-galactosidase histochemistry and telomere loss in senescent retinal pigment epithelial cells," *Investigative Ophthalmology & Visual Science*, vol. 40, no. 1, pp. 197–202, 1999.

[86] K. Mishima, J. T. Handa, A. Aotaki-Keen, G. A. Lutty, L. S. Morse, and L. M. Hjelmeland, "Senescence-associated beta-galactosidase histochemistry for the primate eye," *Investigative Ophthalmology & Visual Science*, vol. 40, no. 7, pp. 1590–1593, 1999.

[87] C. A. Curcio, C. L. Millican, K. A. Allen, and R. E. Kalina, "Aging of the human photoreceptor mosaic: evidence for selective vulnerability of rods in central retina," *Investigative Ophthalmology & Visual Science*, vol. 34, no. 12, pp. 3278–3296, 1993.

[88] J. R. Sparrow and M. Boulton, "RPE lipofuscin and its role in retinal pathobiology," *Experimental Eye Research*, vol. 80, no. 5, pp. 595–606, 2005.

[89] B. T. Gabelt and P. L. Kaufman, "Changes in aqueous humor dynamics with age and glaucoma," *Progress in Retinal and Eye Research*, vol. 24, no. 5, pp. 612–637, 2005.

[90] J. Caprioli, "Glaucoma: a disease of early cellular senescence," *Investigative Opthalmology & Visual Science*, vol. 54, no. 14, p. ORSF60, 2013.

[91] R. S. Harwerth, J. L. Wheat, and N. V. Rangaswamy, "Age-related losses of retinal ganglion cells and axons," *Investigative Ophthalmology & Visual Science*, vol. 49, no. 10, pp. 4437–4443, 2008.

[92] W. Chi, F. Li, H. Chen et al., "Caspase-8 promotes NLRP1/NLRP3 inflammasome activation and IL-1 production in acute glaucoma," *Proceedings of the National Academy of Sciences*, vol. 111, no. 30, pp. 11181–11186, 2014.

[93] J. L. Wiggs, B. L. Yaspan, M. A. Hauser et al., "Common variants at 9p21 and 8q22 are associated with increased susceptibility to optic nerve degeneration in glaucoma," *PLoS Genetics*, vol. 8, no. 4, article e1002654, 2012.

[94] K. P. Burdon, S. Macgregor, A. W. Hewitt et al., "Genome-wide association study identifies susceptibility loci for open angle glaucoma at _TMCO1_ and _CDKN2B-AS1_," *Nature Genetics*, vol. 43, no. 6, pp. 574–578, 2011.

[95] D. Skowronska-Krawczyk, L. Zhao, J. Zhu et al., "_P16INK4a_ Upregulation Mediated by _SIX6_ Defines Retinal Ganglion Cell Pathogenesis in Glaucoma," *Molecular Cell*, vol. 59, no. 6, pp. 931–940, 2015.

[96] J. Wassell, S. Davies, W. Bardsley, and M. Boulton, "The photoreactivity of the retinal age pigment lipofuscin," *The Journal of Biological Chemistry*, vol. 274, no. 34, pp. 23828–23832, 1999.

[97] L. V. Johnson, W. P. Leitner, A. J. Rivest, M. K. Staples, M. J. Radeke, and D. H. Anderson, "The Alzheimer's A beta -peptide is deposited at sites of complement activation in pathologic deposits associated with aging and age-related macular

degeneration," *Proceedings of the National Academy of Sciences*, vol. 99, no. 18, pp. 11830–11835, 2002.

[98] T. Dentchev, A. H. Milam, V. M. Lee, J. Q. Trojanowski, and J. L. Dunaief, "Amyloid-beta is found in drusen from some age-related macular degeneration retinas, but not in drusen from normal retinas," *Molecular Vision*, vol. 9, pp. 184–190, 2003.

[99] L. Cao, H. Wang, F. Wang, D. Xu, F. Liu, and C. Liu, "Aβ-induced senescent retinal pigment epithelial cells create a proinflammatory microenvironment in AMD," *Investigative Ophthalmology & Visual Science*, vol. 54, no. 5, pp. 3738–3750, 2013.

[100] C. Liu, L. Cao, S. Yang et al., "Subretinal injection of amyloid-β peptide accelerates RPE cell senescence and retinal degeneration," *International Journal of Molecular Medicine*, vol. 35, no. 1, pp. 169–176, 2015.

[101] A. Sene, A. A. Khan, D. Cox et al., "Impaired cholesterol efflux in senescent macrophages promotes age-related macular degeneration," *Cell Metabolism*, vol. 17, no. 4, pp. 549–561, 2013.

[102] R. L. Rocha, V. A. N. Huu, C. P. La Torre et al., "Early Removal of senescent cells protects retinal ganglion cells loss in experimental ocular hypertension," *Aging Cell*, vol. 19, no. 2, article e13089, 2020.

[103] Q. Fu, Z. Qin, J. Yu et al., "Effects of senescent lens epithelial cells on the severity of age-related cortical cataract in humans: a case-control study," *Medicine*, vol. 95, no. 25, article e3869, 2016.

[104] Y. Yan, H. Yu, L. Sun et al., "Laminin α4 overexpression in the anterior lens capsule may contribute to the senescence of human lens epithelial cells in age-related cataract," *Aging*, vol. 11, no. 9, pp. 2699–2723, 2019.

[105] M. Matthaei, H. Meng, A. K. Meeker, C. G. Eberhart, and A. S. Jun, "Endothelial Cdkn1a (p21) overexpression and accelerated senescence in a mouse model of Fuchs endothelial corneal dystrophy," *Investigative Ophthalmology & Visual Science*, vol. 53, no. 10, pp. 6718–6727, 2012.

[106] X. Wei, D. Luo, Y. Yan et al., "Kojic acid inhibits senescence of human corneal endothelial cells via NF-κB and p21 signaling pathways," *Experimental Eye Research*, vol. 180, pp. 174–183, 2019.

[107] N. Vazirpanah, F. H. Verhagen, A. Rothova et al., "Aberrant leukocyte telomere length in birdshot uveitis," *PLoS One*, vol. 12, no. 5, article e0176175, 2017.

[108] M. C. Thounaojam, R. N. Jadeja, M. Warren et al., "Micro-RNA-34a (miR-34a) mediates retinal endothelial cell premature senescence through mitochondrial dysfunction and loss of antioxidant activities," *Antioxidants*, vol. 8, no. 9, p. 328, 2019.

[109] M. Rojas, T. Lemtalsi, H. A. Toque et al., "NOX2-induced activation of arginase and diabetes-induced retinal endothelial cell senescence," *Antioxidants*, vol. 6, no. 2, p. 43, 2017.

[110] E. Shosha, Z. Xu, S. P. Narayanan et al., "Mechanisms of diabetes-induced endothelial cell senescence: role of arginase 1," *International Journal of Molecular Sciences*, vol. 19, no. 4, p. 1215, 2018.

[111] C. M. Beauséjour, A. Krtolica, F. Galimi et al., "Reversal of human cellular senescence: roles of the p53 and p16 pathways," *The EMBO Journal*, vol. 22, no. 16, pp. 4212–4222, 2003.

[112] T. Kuilman, C. Michaloglou, W. J. Mooi, and D. S. Peeper, "The essence of senescence," *Genes & Development*, vol. 24, no. 22, pp. 2463–2479, 2010.

[113] B. Bourgeois and T. Madl, "Regulation of cellular senescence via the FOXO4-p53 axis," *FEBS Letters*, vol. 592, no. 12, pp. 2083–2097, 2018.

[114] K. Fujita, A. M. Mondal, I. Horikawa et al., "p53 isoforms Δ133p53 and p53β are endogenous regulators of replicative cellular senescence," *Nature Cell Biology*, vol. 11, no. 9, pp. 1135–1142, 2009.

[115] M. Hoare and M. Narita, "Transmitting senescence to the cell neighbourhood," *Nature Cell Biology*, vol. 15, no. 8, pp. 887–889, 2013.

[116] A. Freund, A. V. Orjalo, P. Y. Desprez, and J. Campisi, "Inflammatory networks during cellular senescence: causes and consequences," *Trends in Molecular Medicine*, vol. 16, no. 5, pp. 238–246, 2010.

[117] N. Malaquin, V. Tu, and F. Rodier, "Assessing functional roles of the senescence-associated secretory phenotype (SASP)," *Methods in Molecular Biology*, vol. 1896, pp. 45–55, 1896.

[118] H. O. Byun, Y. K. Lee, J. M. Kim, and G. Yoon, "From cell senescence to age-related diseases: differential mechanisms of action of senescence-associated secretory phenotypes," *BMB Reports*, vol. 48, no. 10, pp. 549–558, 2015.

[119] J. C. Acosta, A. Loghlen, A. Banito, S. Raguz, and J. Gil, "Control of senescence by CXCR2 and its ligands," *Cell Cycle*, vol. 7, no. 19, pp. 2956–2959, 2008.

[120] T. Kuilman, C. Michaloglou, L. C. W. Vredeveld et al., "Oncogene-induced senescence relayed by an interleukin-dependent inflammatory network," *Cell*, vol. 133, no. 6, pp. 1019–1031, 2008.

[121] M. Ohanna, S. Giuliano, C. Bonet et al., "Senescent cells develop a PARP-1 and nuclear factor-{kappa}B-associated secretome (PNAS)," *Genes & Development*, vol. 25, no. 12, pp. 1245–1261, 2011.

[122] J. P. Coppé, K. Kauser, J. Campisi, and C. M. Beauséjour, "Secretion of vascular endothelial growth factor by primary human fibroblasts at senescence," *The Journal of Biological Chemistry*, vol. 281, no. 40, pp. 29568–29574, 2006.

[123] R. M. Kortlever, P. J. Higgins, and R. Bernards, "Plasminogen activator inhibitor-1 is a critical downstream target of p53 in the induction of replicative senescence," *Nature Cell Biology*, vol. 8, no. 8, pp. 877–884, 2006.

[124] N. Wajapeyee, R. W. Serra, X. Zhu, M. Mahalingam, and M. R. Green, "Oncogenic BRAF induces senescence and apoptosis through pathways mediated by the secreted protein IGFBP7," *Cell*, vol. 132, no. 3, pp. 363–374, 2008.

[125] J. C. Acosta, A. Banito, T. Wuestefeld et al., "A complex secretory program orchestrated by the inflammasome controls paracrine senescence," *Nature Cell Biology*, vol. 15, no. 8, pp. 978–990, 2013.

[126] M. Rhinn, B. Ritschka, and W. M. Keyes, "Cellular senescence in development, regeneration and disease," *Development*, vol. 146, no. 20, article dev151837, 2019.

[127] Y. Chien, C. Scuoppo, X. Wang et al., "Control of the senescence-associated secretory phenotype by NF-κB promotes senescence and enhances chemosensitivity," *Genes & Development*, vol. 25, no. 20, pp. 2125–2136, 2011.

[128] B. Ancrile, K. H. Lim, and C. M. Counter, "Oncogenic Ras-induced secretion of IL6 is required for tumorigenesis," *Genes & Development*, vol. 21, no. 14, pp. 1714–1719, 2007.

[129] A. Sparmann and D. Bar-Sagi, "Ras-induced interleukin-8 expression plays a critical role in tumor growth and angiogenesis," *Cancer Cell*, vol. 6, no. 5, pp. 447–458, 2004.

[130] N. Herranz, S. Gallage, M. Mellone et al., "mTOR regulates MAPKAPK2 translation to control the senescence-associated secretory phenotype," *Nature Cell Biology*, vol. 17, no. 9, pp. 1205–1217, 2015.

[131] R. M. Laberge, Y. Sun, A. V. Orjalo et al., "MTOR regulates the pro-tumorigenic senescence-associated secretory phenotype by promoting IL1A translation," *Nature Cell Biology*, vol. 17, no. 8, pp. 1049–1061, 2015.

[132] M. Abbas, L. Jesel, C. Auger et al., "Endothelial microparticles from acute coronary syndrome patients induce premature coronary artery endothelial cell aging and thrombogenicity: role of the Ang II/AT1 Receptor/NADPH oxidase-mediated activation of MAPKs and PI3-kinase pathways," *Circulation*, vol. 135, no. 3, pp. 280–296, 2017.

[133] C. Davis, A. Dukes, M. Drewry et al., "MicroRNA-183-5p increases with age in bone-derived extracellular vesicles, suppresses bone marrow stromal (stem) cell proliferation, and induces stem cell senescence," *Tissue Engineering Part A*, vol. 23, no. 21-22, pp. 1231–1240, 2017.

[134] M. Takasugi, "Emerging roles of extracellular vesicles in cellular senescence and aging," *Aging Cell*, vol. 17, no. 2, article e12734, 2018.

[135] S. Weilner, E. Schraml, M. Wieser et al., "Secreted microvesicular miR-31 inhibits osteogenic differentiation of mesenchymal stem cells," *Aging Cell*, vol. 15, no. 4, pp. 744–754, 2016.

[136] C. Borras, C. Mas-Bargues, J. Sanz-Ros et al., "Extracellular vesicles and redox modulation in aging," *Free Radical Biology and Medicine*, 2019.

[137] A. O'Loghlen, "Role for extracellular vesicles in the tumour microenvironment," *Philosophical Transactions of the Royal Society B: Biological Sciences*, vol. 373, no. 1737, p. 20160488, 2018.

[138] H. Valadi, K. Ekström, A. Bossios, M. Sjöstrand, J. J. Lee, and J. O. Lötvall, "Exosome-mediated transfer of mRNAs and microRNAs is a novel mechanism of genetic exchange between cells," *Nature Cell Biology*, vol. 9, no. 6, pp. 654–659, 2007.

[139] D. M. Pegtel, K. Cosmopoulos, D. A. Thorley-Lawson et al., "Functional delivery of viral miRNAs via exosomes," *Proceedings of the National Academy of Sciences*, vol. 107, no. 14, pp. 6328–6333, 2010.

[140] M. Pathan, P. Fonseka, S. V. Chitti et al., "Vesiclepedia 2019: a compendium of RNA, proteins, lipids and metabolites in extracellular vesicles," *Nucleic Acids Research*, vol. 47, no. D1, pp. D516–D519, 2019.

[141] L. A. Beninson and M. Fleshner, "Exosomes: an emerging factor in stress-induced immunomodulation," *Seminars in Immunology*, vol. 26, no. 5, pp. 394–401, 2014.

[142] S. Atienzar-Aroca, M. Flores-Bellver, G. Serrano-Heras et al., "Oxidative stress in retinal pigment epithelium cells increases exosome secretion and promotes angiogenesis in endothelial cells," *Journal of Cellular and Molecular Medicine*, vol. 20, no. 8, pp. 1457–1466, 2016.

[143] M. Klingeborn, W. M. Dismuke, C. Bowes Rickman, and W. D. Stamer, "Roles of exosomes in the normal and diseased eye," *Progress in Retinal and Eye Research*, vol. 59, pp. 158–177, 2017.

[144] M. Takasugi, R. Okada, A. Takahashi, D. Virya Chen, S. Watanabe, and E. Hara, "Small extracellular vesicles secreted from senescent cells promote cancer cell proliferation through EphA2," *Nature Communications*, vol. 8, no. 1, p. 15729, 2017.

[145] N. Shah, M. Ishii, C. Brandon et al., "Extracellular vesicle-mediated long-range communication in stressed retinal pigment epithelial cell monolayers," *Biochimica et Biophysica Acta - Molecular Basis of Disease*, vol. 1864, no. 8, pp. 2610–2622, 2018.

[146] A. L. Wang, T. J. Lukas, M. Yuan, N. Du, M. O. Tso, and A. H. Neufeld, "Autophagy and exosomes in the aged retinal pigment epithelium: possible relevance to drusen formation and age-related macular degeneration," *PLoS One*, vol. 4, no. 1, article e4160, 2009.

[147] M. Hoare, Y. Ito, T. W. Kang et al., "NOTCH1 mediates a switch between two distinct secretomes during senescence," *Nature Cell Biology*, vol. 18, no. 9, pp. 979–992, 2016.

[148] M. Borghesan, J. Fafián-Labora, O. Eleftheriadou et al., "Small extracellular vesicles are key regulators of non-cell autonomous intercellular communication in senescence via the interferon protein IFITM3," *Cell Reports*, vol. 27, no. 13, pp. 3956–3971.e6, 2019.

[149] N. Basisty, A. Holtz, and B. Schilling, "Accumulation of "old proteins" and the critical need for MS-based protein turnover measurements in aging and longevity," *Proteomics*, vol. 13, article e1800403, 2019.

[150] M. Mitsuhashi, D. D. Taub, D. Kapogiannis et al., "Aging enhances release of exosomal cytokine mRNAs by Aβ1-42-stimulated macrophages," *The FASEB Journal*, vol. 27, no. 12, pp. 5141–5150, 2013.

[151] B. W. van Balkom, O. G. de Jong, M. Smits et al., "Endothelial cells require miR-214 to secrete exosomes that suppress senescence and induce angiogenesis in human and mouse endothelial cells," *Blood*, vol. 121, no. 19, pp. 3997–4006, 2013.

[152] K. Weiner-Gorzel, E. Dempsey, M. Milewska et al., "Overexpression of the microRNA miR-433 promotes resistance to paclitaxel through the induction of cellular senescence in ovarian cancer cells," *Cancer Medicine*, vol. 4, no. 5, pp. 745–758, 2015.

[153] K. Okamura and K. Nohara, "Long-term arsenite exposure induces premature senescence in B cell lymphoma A20 cells," *Archives of Toxicology*, vol. 90, no. 4, pp. 793–803, 2016.

[154] M. P. Murphy, "How mitochondria produce reactive oxygen species," *The Biochemical Journal*, vol. 417, no. 1, pp. 1–13, 2009.

[155] F. Martinon, "Signaling by ROS drives inflammasome activation," *European Journal of Immunology*, vol. 40, no. 3, pp. 616–619, 2010.

[156] R. N. Jadeja, F. L. Powell, M. A. Jones et al., "Loss of NAMPT in aging retinal pigment epithelium reduces NAD$^+$ availability and promotes cellular senescence," *Aging*, vol. 10, no. 6, pp. 1306–1323, 2018.

[157] A. J. Braakhuis, R. Nagulan, and V. Somerville, "The Effect of MitoQ on Aging-Related Biomarkers: A Systematic Review and Meta- Analysis," *Oxidative Medicine and Cellular Longevity*, vol. 2018, Article ID 8575263, 12 pages, 2018.

[158] G. Saretzki, M. P. Murphy, and T. von Zglinicki, "MitoQ counteracts telomere shortening and elongates lifespan of

fibroblasts under mild oxidative stress," *Aging Cell*, vol. 2, no. 2, pp. 141–143, 2003.

[159] J. F. Passos, G. Nelson, C. Wang et al., "Feedback between p21 and reactive oxygen production is necessary for cell senescence," *Molecular Systems Biology*, vol. 6, no. 1, p. 347, 2010.

[160] A. Takahashi, N. Ohtani, K. Yamakoshi et al., "Mitogenic signalling and the p16^{INK4a}-Rb pathway cooperate to enforce irreversible cellular senescence," *Nature Cell Biology*, vol. 8, no. 11, pp. 1291–1297, 2006.

[161] T. A. Klimova, E. L. Bell, E. H. Shroff et al., "Hyperoxia-induced premature senescence requires p53 and pRb, but not mitochondrial matrix ROS," *The FASEB Journal*, vol. 23, no. 3, pp. 783–794, 2009.

[162] C. Correia-Melo and J. F. Passos, "Mitochondria: are they causal players in cellular senescence?," *Biochimica et Biophysica Acta*, vol. 1847, no. 11, pp. 1373–1379, 2015.

[163] Y. He, K. W. Leung, Y. Ren, J. Pei, J. Ge, and J. Tombran-Tink, "PEDF improves mitochondrial function in RPE cells during oxidative stress," *Investigative Ophthalmology & Visual Science*, vol. 55, no. 10, pp. 6742–6755, 2014.

[164] E. E. Brown, A. J. DeWeerd, C. J. Ildefonso, A. S. Lewin, and J. D. Ash, "Mitochondrial oxidative stress in the retinal pigment epithelium (RPE) led to metabolic dysfunction in both the RPE and retinal photoreceptors," *Redox Biology*, vol. 24, p. 101201, 2019.

[165] X. Hu, M. A. Calton, S. Tang, and D. Vollrath, "Depletion of mitochondrial DNA in differentiated retinal pigment epithelial cells," *Scientific Reports*, vol. 9, no. 1, p. 15355, 2019.

[166] C. Quijano, L. Cao, M. M. Fergusson et al., "Oncogene-induced senescence results in marked metabolic and bioenergetic alterations," *Cell Cycle*, vol. 11, no. 7, pp. 1383–1392, 2012.

[167] J. Kaplon, L. Zheng, K. Meissl et al., "A key role for mitochondrial gatekeeper pyruvate dehydrogenase in oncogene- induced senescence," *Nature*, vol. 498, no. 7452, pp. 109–112, 2013.

[168] P. Patil, M. Falabella, A. Saeed et al., "Oxidative stress-induced senescence markedly increases disc cell bioenergetics," *Mechanisms of Ageing and Development*, vol. 180, pp. 97–106, 2019.

[169] J. R. Dörr, Y. Yu, M. Milanovic et al., "Synthetic lethal metabolic targeting of cellular senescence in cancer therapy," *Nature*, vol. 501, no. 7467, pp. 421–425, 2013.

[170] F. Hariton, M. Xue, N. Rabbani, M. Fowler, and P. J. Thornalley, "Sulforaphane delays fibroblast senescence by curbing cellular glucose uptake, increased glycolysis, and oxidative damage," *Oxidative Medicine and Cellular Longevity*, vol. 2018, Article ID 5642148, 16 pages, 2018.

[171] A. Delfarah, S. Parrish, J. A. Junge et al., "Inhibition of nucleotide synthesis promotes replicative senescence of human mammary epithelial cells," *The Journal of Biological Chemistry*, vol. 294, no. 27, pp. 10564–10578, 2019.

[172] V. I. Korolchuk, S. Miwa, B. Carroll, and T. von Zglinicki, "Mitochondria in cell senescence: is mitophagy the weakest link?," *eBioMedicine*, vol. 21, pp. 7–13, 2017.

[173] E. L. James, R. D. Michalek, G. N. Pitiyage et al., "Senescent human fibroblasts show increased glycolysis and redox homeostasis with extracellular metabolomes that overlap with those of irreparable DNA damage, aging, and disease," *Journal of Proteome Research*, vol. 14, no. 4, pp. 1854–1871, 2015.

[174] J. Martínez, D. Tarallo, L. Martínez-Palma et al., "Mitofusins modulate the increase in mitochondrial length, bioenergetics and secretory phenotype in therapy-induced senescent melanoma cells," *The Biochemical Journal*, vol. 476, no. 17, pp. 2463–2486, 2019.

[175] T. Kamogashira, K. Hayashi, C. Fujimoto, S. Iwasaki, and T. Yamasoba, "Functionally and morphologically damaged mitochondria observed in auditory cells under senescence-inducing stress," *npj Aging and Mechanisms of Disease*, vol. 3, no. 1, p. 2, 2017.

[176] D. W. Waters, K. E. C. Blokland, P. S. Pathinayake et al., "STAT3 regulates the onset of oxidant-induced senescence in lung fibroblasts," *American Journal of Respiratory Cell and Molecular Biology*, vol. 61, no. 1, pp. 61–73, 2019.

[177] T. Nacarelli, A. Azar, and C. Sell, "Mitochondrial stress induces cellular senescence in an mTORC1-dependent manner," *Free Radical Biology & Medicine*, vol. 95, pp. 133–154, 2016.

[178] M. Guha and N. G. Avadhani, "Mitochondrial retrograde signaling at the crossroads of tumor bioenergetics, genetics and epigenetics," *Mitochondrion*, vol. 13, no. 6, pp. 577–591, 2013.

[179] S. M. Kwon, S. M. Hong, Y. K. Lee, S. Min, and G. Yoon, "Metabolic features and regulation in cell senescence," *BMB Reports*, vol. 52, no. 1, pp. 5–12, 2019.

[180] S. W. Ballinger, "Beyond retrograde and anterograde signalling: mitochondrial-nuclear interactions as a means for evolutionary adaptation and contemporary disease susceptibility," *Biochemical Society Transactions*, vol. 41, no. 1, pp. 111–117, 2013.

[181] M. Nam, T. E. Akie, M. Sanosaka et al., "Mitochondrial retrograde signaling connects respiratory capacity to thermogenic gene expression," *Scientific Reports*, vol. 7, no. 1, p. 2013, 2017.

[182] N. S. Chandel, "Evolution of mitochondria as signaling organelles," *Cell Metabolism*, vol. 22, no. 2, pp. 204–206, 2015.

[183] I. Bohovych and O. Khalimonchuk, "Sending out an SOS: mitochondria as a signaling hub," *Frontiers in Cell and Development Biology*, vol. 4, p. 109, 2016.

[184] R. C. Scarpulla, "Nuclear control of respiratory chain expression by nuclear respiratory factors and PGC-1-related coactivator," *Annals of the New York Academy of Sciences*, vol. 1147, no. 1, pp. 321–334, 2008.

[185] S. Chae, B. Y. Ahn, K. Byun et al., "A systems approach for decoding mitochondrial retrograde signaling pathways," *Science Signaling*, vol. 6, no. 264, p. rs4, 2013.

[186] K. H. Kim, J. M. Son, B. A. Benayoun, and C. Lee, "The mitochondrial-encoded peptide MOTS-c translocates to the nucleus to regulate nuclear gene expression in response to metabolic stress," *Cell Metabolism*, vol. 28, no. 3, pp. 516–524.e7, 2018.

[187] N. Sun, R. J. Youle, and T. Finkel, "The mitochondrial basis of aging," *Molecular Cell*, vol. 61, no. 5, pp. 654–666, 2016.

[188] R. J. Youle and D. P. Narendra, "Mechanisms of mitophagy," *Nature Reviews Molecular Cell Biology*, vol. 12, no. 1, pp. 9–14, 2011.

[189] L. Pernas and L. Scorrano, "Mito-morphosis: mitochondrial fusion, fission, and cristae remodeling as key mediators of cellular function," *Annual Review of Physiology*, vol. 78, no. 1, pp. 505–531, 2016.

[190] E. Schrepfer and L. Scorrano, "Mitofusins, from mitochondria to metabolism," *Molecular Cell*, vol. 61, no. 5, pp. 683–694, 2016.

[191] A. R. Hall, N. Burke, R. K. Dongworth, and D. J. Hausenloy, "Mitochondrial fusion and fission proteins: novel therapeutic targets for combating cardiovascular disease," *British Journal of Pharmacology*, vol. 171, no. 8, pp. 1890–1906, 2014.

[192] Y. Eura, N. Ishihara, S. Yokota, and K. Mihara, "Two mitofusin proteins, mammalian homologues of FZO, with distinct functions are both required for mitochondrial fusion," *Journal of Biochemistry*, vol. 134, no. 3, pp. 333–344, 2003.

[193] A. Olichon, L. J. Emorine, E. Descoins et al., "The human dynamin-related protein OPA1 is anchored to the mitochondrial inner membrane facing the inter-membrane space," *FEBS Letters*, vol. 523, no. 1-3, pp. 171–176, 2002.

[194] P. G. Sreekumar, D. R. Hinton, J. Campisi, S. R. Sadda, and R. Kannan, "αB crystallin chaperone peptide (mini Cry) inhibits senescence in RPE cells by modulating mitochondrial biogenesis and fission proteins," *Investigative Ophthalmology & Visual Science*, vol. 60, p. 1950, 2019.

[195] Y. Y. Park, S. Lee, M. Karbowski, A. Neutzner, R. J. Youle, and H. Cho, "Loss of MARCH5 mitochondrial E3 ubiquitin ligase induces cellular senescence through dynamin-related protein 1 and mitofusin 1," *Journal of Cell Science*, vol. 123, no. 4, pp. 619–626, 2010.

[196] H. Hara, J. Araya, S. Ito et al., "Mitochondrial fragmentation in cigarette smoke-induced bronchial epithelial cell senescence," *American Journal of Physiology Lung Cellular and Molecular Physiology*, vol. 305, no. 10, pp. L737–L746, 2013.

[197] C. Correia-Melo, F. D. Marques, R. Anderson et al., "Mitochondria are required for pro-ageing features of the senescent phenotype," *The EMBO Journal*, vol. 35, no. 7, pp. 724–742, 2016.

[198] R. Summer, H. Shaghaghi, D. Schriner et al., "Activation of the mTORC1/PGC-1 axis promotes mitochondrial biogenesis and induces cellular senescence in the lung epithelium," *American Journal of Physiology Lung Cellular and Molecular Physiology*, vol. 316, no. 6, pp. L1049–L1060, 2019.

[199] J. Zhu, K. Z. Q. Wang, and C. T. Chu, "After the banquet: mitochondrial biogenesis, mitophagy, and cell survival," *Autophagy*, vol. 9, no. 11, pp. 1663–1676, 2013.

[200] K. Kaarniranta, J. Kajdanek, J. Morawiec, E. Pawlowska, and J. Blasiak, "PGC-1α protects RPE cells of the aging retina against oxidative stress-induced degeneration through the regulation of senescence and mitochondrial quality control. The significance for AMD pathogenesis," *International Journal of Molecular Sciences*, vol. 19, no. 8, p. 2317, 2018.

[201] C. Kukat and N. G. Larsson, "mtDNA makes a U-turn for the mitochondrial nucleoid," *Trends in Cell Biology*, vol. 23, no. 9, pp. 457–463, 2013.

[202] H. C. Lee, P. H. Yin, C. W. Chi, and Y. H. Wei, "Increase in mitochondrial mass in human fibroblasts under oxidative stress and during replicative cell senescence," *Journal of Biomedical Science*, vol. 9, no. 6, pp. 517–526, 2002.

[203] P. V. S. Vasileiou, K. Evangelou, K. Vlasis et al., "Mitochondrial homeostasis and cellular senescence," *Cells*, vol. 8, no. 7, p. 686, 2019.

[204] A. Egger, M. Samardzija, V. Sothilingam et al., "PGC-1α determines light damage susceptibility of the murine retina," *PLoS One*, vol. 7, no. 2, article e31272, 2012.

[205] X. Zhang, S. Zhang, X. Liu et al., "Oxidation resistance 1 is a novel senolytic target," *Aging Cell*, vol. 17, no. 4, article e12780, 2018.

[206] M. A. B. Rosales, D. Y. Shu, J. Iacovelli, and M. Saint-Geniez, "Loss of PGC-1α in RPE induces mesenchymal transition and promotes retinal degeneration," *Life Science Alliance*, vol. 2, no. 3, article e201800212, 2019.

[207] S. Felszeghy, J. Viiri, J. J. Paterno et al., "Loss of NRF-2 and PGC-1 α genes leads to retinal pigment epithelium damage resembling dry age-related macular degeneration," *Redox Biology*, vol. 20, pp. 1–12, 2019.

[208] N. E. Sharpless, N. Bardeesy, K. H. Lee et al., "Loss of p16^{Ink4a} with retention of p19^{Arf} predisposes mice to tumorigenesis," *Nature*, vol. 413, no. 6851, pp. 86–91, 2001.

[209] K. Ito, A. Hirao, F. Arai et al., "Reactive oxygen species act through p38 MAPK to limit the lifespan of hematopoietic stem cells," *Nature Medicine*, vol. 12, no. 4, pp. 446–451, 2006.

[210] V. Janzen, R. Forkert, H. E. Fleming et al., "Stem-cell ageing modified by the cyclin-dependent kinase inhibitor p16INK4a," *Nature*, vol. 443, no. 7110, pp. 421–426, 2006.

[211] J. W. Shay, "Role of telomeres and telomerase in aging and cancer," *Cancer Discovery*, vol. 6, no. 6, pp. 584–593, 2016.

[212] J. L. Kirkland, T. Tchkonia, Y. Zhu, L. J. Niedernhofer, and P. D. Robbins, "The clinical potential of senolytic drugs," *Journal of the American Geriatrics Society*, vol. 65, no. 10, pp. 2297–2301, 2017.

[213] M. E. Waaijer, W. E. Parish, B. H. Strongitharm et al., "The number of p16INK4a positive cells in human skin reflects biological age," *Aging Cell*, vol. 11, no. 4, pp. 722–725, 2012.

[214] Y. Zhu, T. Tchkonia, T. Pirtskhalava et al., "The Achilles' heel of senescent cells: from transcriptome to senolytic drugs," *Aging Cell*, vol. 14, no. 4, pp. 644–658, 2015.

[215] Y. Sun, J. P. Coppé, and E. W. F. Lam, "Cellular senescence: the sought or the unwanted?," *Trends in Molecular Medicine*, vol. 24, no. 10, pp. 871–885, 2018.

[216] S. N. Knoppert, F. A. Valentijn, T. Q. Nguyen, R. Goldschmeding, and L. L. Falke, "Cellular senescence and the kidney: potential therapeutic targets and tools," *Frontiers in Pharmacology*, vol. 10, p. 770, 2019.

[217] C. Tse, A. R. Shoemaker, J. Adickes et al., "ABT-263: a potent and orally bioavailable Bcl-2 family inhibitor," *Cancer Research*, vol. 68, no. 9, pp. 3421–3428, 2008.

[218] J. Chang, Y. Wang, L. Shao et al., "Clearance of senescent cells by ABT263 rejuvenates aged hematopoietic stem cells in mice," *Nature Medicine*, vol. 22, no. 1, pp. 78–83, 2016.

[219] Y. Zhu, T. Tchkonia, H. Fuhrmann-Stroissnigg et al., "Identification of a novel senolytic agent, navitoclax, targeting the Bcl-2 family of anti-apoptotic factors," *Aging Cell*, vol. 15, no. 3, pp. 428–435, 2016.

[220] T. J. Bussian, A. Aziz, C. F. Meyer, B. L. Swenson, J. M. van Deursen, and D. J. Baker, "Clearance of senescent glial cells prevents tau-dependent pathology and cognitive decline," *Nature*, vol. 562, no. 7728, pp. 578–582, 2018.

[221] B. G. Childs, D. J. Baker, T. Wijshake, C. A. Conover, J. Campisi, and J. M. van Deursen, "Senescent intimal foam cells are deleterious at all stages of atherosclerosis," *Science*, vol. 354, no. 6311, pp. 472–477, 2016.

[222] J. Pan, D. Li, Y. Xu et al., "Inhibition of Bcl-2/xl with ABT-263 selectively kills senescent type II pneumocytes and

reverses persistent pulmonary fibrosis induced by ionizing radiation in mice," *International Journal of Radiation Oncology, Biology, Physics*, vol. 99, no. 2, pp. 353–361, 2017.

[223] Y. Zhu, E. J. Doornebal, T. Pirtskhalava et al., "New agents that target senescent cells: the flavone, fisetin, and the BCL-X$_L$ inhibitors, A1331852 and A1155463," *Aging*, vol. 9, no. 3, pp. 955–963, 2017.

[224] M. J. Yousefzadeh, Y. Zhu, S. J. McGowan et al., "Fisetin is a senotherapeutic that extends health and lifespan," *eBioMedicine*, vol. 36, pp. 18–28, 2018.

[225] H. Fuhrmann-Stroissnigg, Y. Y. Ling, J. Zhao et al., "Identification of HSP90 inhibitors as a novel class of senolytics," *Nature Communications*, vol. 8, no. 1, p. 422, 2017.

[226] O. H. Jeon, C. Kim, R. M. Laberge et al., "Local clearance of senescent cells attenuates the development of post- traumatic osteoarthritis and creates a pro-regenerative environment," *Nature Medicine*, vol. 23, no. 6, pp. 775–781, 2017.

[227] J. Campisi, P. Kapahi, G. J. Lithgow, S. Melov, J. C. Newman, and E. Verdin, "From discoveries in ageing research to therapeutics for healthy ageing," *Nature*, vol. 571, no. 7764, pp. 183–192, 2019.

[228] H. Yang, H. Wang, J. Ren, Q. Chen, and Z. J. Chen, "cGAS is essential for cellular senescence," *Proceedings of the National Academy of Sciences*, vol. 114, no. 23, pp. E4612–E4620, 2017.

[229] Y. Wu, Q. Wei, and J. Yu, "The cGAS/STING pathway: a sensor of senescence-associated DNA damage and trigger of inflammation in early age-related macular degeneration," *Clinical Interventions in Aging*, vol. Volume 14, pp. 1277–1283, 2019.

[230] L. J. Hickson, L. P. LGP, S. A. Bobart et al., "Senolytics decrease senescent cells in humans: preliminary report from a clinical trial of dasatinib plus quercetin in individuals with diabetic kidney disease," *EBioMedicine*, vol. 47, pp. 446–456, 2019.

[231] J. N. Justice, A. M. Nambiar, T. Tchkonia et al., "Senolytics in idiopathic pulmonary fibrosis: results from a first-in-human, open-label, pilot study," *eBioMedicine*, vol. 40, pp. 554–563, 2019.

[232] J. M. van Deursen, "Senolytic therapies for healthy longevity," *Science*, vol. 364, no. 6441, pp. 636-637, 2019.

[233] A. Hernandez-Segura, T. V. de Jong, S. Melov, V. Guryev, J. Campisi, and M. Demaria, "Unmasking transcriptional heterogeneity in senescent cells," *Current Biology*, vol. 27, no. 17, pp. 2652–2660.e4, 2017.

[234] J. L. Kirkland and T. Tchkonia, "Cellular senescence: a translational perspective," *eBioMedicine*, vol. 21, pp. 21–28, 2017.

Research Article

Capsaicin Alleviates the Deteriorative Mitochondrial Function by Upregulating 14-3-3η in Anoxic or Anoxic/Reoxygenated Cardiomyocytes

Yang Qiao,[1,2] **Tianhong Hu,**[2] **Bin Yang,**[2] **Hongwei Li,**[2] **Tianpeng Chen,**[2] **Dong Yin** ![ORCID],[3] **Huan He** ![ORCID],[2] **and Ming He** ![ORCID][1]

[1]*Jiangxi Provincial Institute of Hypertension, The First Affiliated Hospital of Nanchang University, Nanchang 330006, China*
[2]*Jiangxi Provincial Key Laboratory of Basic Pharmacology, Nanchang University School of Pharmaceutical Science,*
Nanchang 330006, China
[3]*Jiangxi Provincial Key Laboratory of Molecular Medicine, The Second Affiliated Hospital of Nanchang University,*
Nanchang 330006, China

Correspondence should be addressed to Huan He; hehuan0118@ncu.edu.cn and Ming He; jxhm56@hotmail.com

Reactive oxygen species (ROS) are byproducts of a defective electron transport chain (ETC). The redox couples, GSH/GSSG and NAD$^+$/NADH, play an essential role in physiology as internal defenses against excessive ROS generation by facilitating intracellular/mitochondrial (mt) redox homeostasis. Anoxia alone and anoxia/reoxygenation (A/R) are dissimilar pathological processes. In this study, we measured the impact of capsaicin (Cap) on these pathological processes using a primary cultured neonatal rat cardiomyocyte in vitro model. The results showed that overproduction of ROS was tightly associated with disturbed GSH/GSSG and NAD$^+$/NADH suppressed mt complex I and III activities, decreased oxygen consumption rates, and elevated extracellular acidification rates. During anoxia or A/R period, these indices interact with each other causing the mitochondrial function to worsen. Cap protected cardiomyocytes against the different stages of A/R injury by rescuing NAD$^+$/NADH, GSH/GSSG, and mt complex I/III activities and cellular energy metabolism. Importantly, Cap-mediated upregulation of 14-3-3η, a protective phosphoserine-binding protein in cardiomyocytes, ameliorated mt function caused by a disruptive redox status and an impaired ETC. In conclusion, redox pair, mt complex I/III, and metabolic equilibrium were significantly different in anoxia alone and A/R injury; Cap through upregulating 14-3-3η plays a protection against the above injury in cardiomyocyte.

1. Introduction

Aging, hypoxia, ischemia, and ischemia/reperfusion (I/R) are the primary causes of cardiovascular disease [1, 2]. Ischemia (anoxia) and I/R (anoxia/reoxygenation, A/R) injury can be generally divided into two stages: anoxia alone and A/R [3]. Reactive oxygen species (ROS) participate in several pathophysiologic processes (e.g., cellular damage, aging, and apoptosis) during the above injury [4–6]. This injury causes excessive ROS generation, resulting in severe myocardial damage [3–9]. However, ignoring the close relationship between redox balance and ROS in cellular pathological con-

ditions often prevents clinical trials from recognizing the significance of decreasing disease risk and progression.

Glutathione (GSH) converts into glutathione disulfide (GSSG) under oxidative stress. GSH/GSSG ratio sustains the redox homeostasis in cardiomyocyte by decreasing elevated ROS generation [10–12]. An equilibrium between nicotine adenine dinucleotide (NAD$^+$, oxidized) and NADH (reduced) is also an essential regulator of the redox system under the pathologic condition of anoxia or A/R; however, the imbalance of NAD$^+$ and NADH can also influence oxygen radical levels at the site of complex I on the mitochondrial (mt) electron transport chain (ETC) [13–15]. mt

complexes I and III are a major source of ROS in cardiomyocytes [4, 16, 17]. Previous studies documented that decreased complex I/III activities result in excessive ROS accumulation and influence energy metabolism [18–21]. A metabolic disorder is closely associated with the mitochondrial dysfunction of cardiomyocytes during A/R injury [22, 23]. During anoxia, insufficient oxygen supply decreases in oxygen consumption rates (OCR) and adenosine triphosphate (ATP) production inhibiting the ability to meet the demands of energy metabolism and ultimately inducing an irreversible injury on cardiomyocytes [24]. Although oxygen restoration is necessary for salvaging anoxic cell death, it also induces cellular injury due to excessive ROS generation and Ca^{2+} overload [25].

Capsaicin (trans-8-methyl-N-vanillyl-6-nonenamide, $C_{18}H_{27}NO$, Cap) is the main active ingredient in plants of the genus Capsicum. Cap has been widely studied as a potential therapeutic agent in diseases such as conjunctivitis, cancer, obesity, and cardiovascular disease [26–29]. Cap is known to have antimicrobial, analgesic, and antioxidant, among other effects [30]. Our recent studies showed that Cap upregulated 14-3-3η (a dimeric phospho-serine-binding protein involved in cardiac protection) and SIRT1 (NAD^+-dependent proteins that act as gatekeepers against oxidative stress and cardiovascular injury) expression in cardiomyocytes in response to A/R injury [7, 8]. The pathologic process of A/R remains unexplored. Cap could have differential modulatory effects on the anoxia and A/R stage.

We performed Cap pretreatments prior to anoxia or A/R injury to test the following: (1) impact of A/R injury on NAD^+/NADH, GSH/GSSG, mt complexes I/III, and energy metabolism and (2) Cap-mediated effects on redox couples, complex I/III, and energy metabolism.

2. Materials and Methods

2.1. Reagents. Cap (purity ≥ 98%) was purchased from the National Institutes for Food and Drug Control (Beijing, China). Adenovirus pAD/14-3-3η-shRNA was obtained from GeneChem Co., Ltd (Shanghai, China). Antibodies directed against 14-3-3η, cytochrome c (cyt C), cleaved caspase-3, Cox4, and β-actin were obtained from Cell Signaling Technology (Beverly, MA, USA). Antibodies against NADH dehydrogenase [ubiquinone] 1 beta subcomplex subunit 8 (NDUFB8) and cytochrome b-c1 complex subunit 2 (UQCRC2) were obtained from Abcam (Cambridge, UK). Horseradish peroxidase-conjugated IgG secondary antibody was purchased from Zsbio (Beijing, China).

2.2. Primary Cardiomyocyte Culture and Anoxia Alone or Anoxia/Reoxygenation Injury. All experimental protocols were conducted according to the *Guide for the Care and Use of Laboratory Animals* published by the US National Institutes of Health (NIH Publication no. 85-23, revised 1996) and approved by the Ethics Committee of Nanchang University (no. 2019-0036). Cardiomyocytes from 0-3 days old Sprague-Dawley rats (the Animal Center of Nanchang University, Nanchang, China) were prepared as published [7]. Briefly, hearts from neonatal rats were removed and placed in precooling D-Hank's balanced salt solution. The

ventricles were digested with 0.1% trypsin and then harvested repeatedly by centrifugation at 600 × g for 5 min. The cells were resuspended in plating medium (80% Dulbecco's Minimal Essential Medium (DMEM), 20% Fetal Bovine Serum (FBS), and 100 U/ml of penicillin and streptomycin) and plated in culture dishes that were incubated 37°C for 30 min to remove nonmyocytes. The suspended cells were plated on 60 mm gelatin-coated culture dishes at 1×10^6 cells per dish and incubated at 37°C in a standard humidity incubator with 95% O_2 and 5% CO_2. After 18 hours, cardiomyocytes were washed and plates in fresh medium and incubated for an additional 3 days at 37°C in a standard humidity incubator with 95% O_2 and 5% CO_2 before the experiment.

Cardiomyocytes were exposed to three hours of anoxia alone or three hours of anoxia followed by two hours of reoxygenation. Anoxic conditions were generated by incubating the culture plates in an air-tight anoxic chamber placed in a humidified 37°C incubator and passing a mixture of 95% N_2 and 5% CO_2. Reoxygenation was provided by placing the cultured plates in a standard humidified 37°C incubator and passing a mixture of 95% O_2 and 5% CO_2 [31].

2.3. Experimental Grouping and Reagent Treatment. The experimental groups were as follows: during anoxia stage: (1) control group: incubation under normal growth conditions; (2) anoxia group: exposure to anoxic injury; (3) Cap +anoxia group: pretreatment with 10 μM Cap for 36 hours prior to anoxic injury; and (d) pAD/14-3-3η-shRNA+Cap +anoxia group: pretreatment with adenovirus pAD/14-3-3η-shRNA for 5 hours prior to preconditioning with Cap (36 hours) and anoxic injury.

During the A/R stage, cardiomyocytes were distributed into experimental groups as follows: (a) control group; (b) A/R group: exposure to A/R injury; (c) Cap+A/R group: pretreatment with 10 μM Cap for 36 hours before A/R; and (d) pAD/14-3-3η-shRNA+Cap+A/R group: pretreatment with pAD/14-3-3η-shRNA for 5 hours prior to preconditioning with Cap (36 hours) and A/R injury.

2.4. Measurement of Cell Viability and Biochemical Parameters. Cell viability was measured using a colorimetric assay using the tetrazolium salt WST-8 (TransGen Biotech, Beijing, China). Cardiomyocytes were seeded in 96-well plates at a density of 4×10^3 cells/well. Cells were incubated with 20 μl WST-8 (5 mg/ml) per 100 μl medium for 2 hours at 37°C, and absorbance was measured at 490 nm using a microplate reader (Bio-Rad 680, Hercules, CA, USA). Data was expressed as the ratio between experimental and control groups.

Culture medium after anoxia or A/R treatment was collected to evaluate the activities of lactate dehydrogenase (LDH) and creatine phosphate kinase (CK) using commercially available assay kits (Jiancheng, Nanjing, China) according to the manufacturer's instructions [7].

2.5. Preparation of Mitochondrial Fractions and Assessment of NAD$^+$/NADH and GSH/GSSG Level. Mitochondrial fractions of cardiomyocytes were prepared using the mitochondria isolation kit (Thermo Fisher, USA). Cells were

harvested and centrifuged at $700 \times g$ for 5 min, with the addition of 800 μl ice-cold reagent A and 10 μl precooling reagent B, and incubated for 5 min on ice. Following this, 800 μl of reagent C was added and incubated for 10 min at 4°C. The sample was then centrifuged at $700 \times g$ for 10 min to remove the undissolved protein and debris. The supernatant was collected and centrifuged at $12000 \times g$ for 15 min at 4°C. Then, removed the supernatant and washed the pellet (mitochondria) in 500 μl of reagent C and centrifuged at $12000 \times g$ for 5 min at 4°C. The final pellet was resuspended in lysis buffer containing a protease inhibitor, and the homogenate was designated as the mitochondrial fraction.

NAD+, NADH, and NAD+/NADH ratios of the mitochondrial fraction were measured using the NAD+/NADH Quantification Kit (Sigma-Aldrich, St. Louis, MO, USA). GSH, GSSG, and GSH/GSSG ratios were examined using the GSH and GSSG Assay Kit (Beyotime, Shanghai, China) consistent with the manufacturer's instructions.

2.6. Measurement of OCR and ECAR.

OCR and extracellular acidification rate (ECAR) were assayed using commercially available assay kits by the Seahorse XFe[24] Extracellular Flux analyzer (Agilent Technologies, Santa Clara, CA, USA) [32]. Cardiomyocytes were seeded in Seahorse XF Cell Culture Microplate at a density of 4×10^3 cells/well in DMEM supplemented with 10% (v/v) FBS. A sensor cartridge was added to Seahorse XF Calibrant solution and incubated at 37°C in a non-CO$_2$ incubator overnight. Cells were incubated with XF Base Medium (Agilent Technologies) at 37°C in a non-CO$_2$ incubator for 45 min prior to the assay. OCR values were assayed under basal/resting conditions and after adding oligomycin, FCCP, rotenone, and antimycin A. Meanwhile, ECAR was measured under basal conditions and with glucose, oligomycin, and 2-DG. The results of OCR and ECAR were calculated from Wave.

2.7. Flow Cytometry Assay.

ROS levels were assessed with oxidation-sensitive fluorescent probe DCFH-DA (Beyotime, Shanghai, China) [7]. Cells were harvested after treatment as described in Section 2.3 and incubated with DCFH-DA at 37°C for 30 min in darkness. The cells were then centrifuged, washed with ice-cold 1x phosphate-buffered saline (PBS), and detected (excitation (Ex) = 488 nm, emission (Em) = 525 nm) immediately using Cytomics FC500 flow cytometer (Beckman Coulter, Brea, CA, USA).

Mitochondrial Membrane Potential (MMP) was measured using the fluorescent dye JC-1 (BestBio, Shanghai, China) [7]. In brief, cardiomyocytes were incubated with JC-1 for 30 min at 37°C in darkness, centrifuged, and washed to remove the excess reagents. Fluorescence was assessed using Cytomics FC500 flow cytometer at wavelengths of 530/580 nm (red) and 485/530 nm (green). The ratio of the red to green fluorescence intensity of the cells reflected the level of MMP.

Mitochondrial permeability transition pores (mPTP) were assessed utilizing the fluorescent probe BbcellProbe™ M61 (BestBio, Shanghai, China) [33]. Cells were co-incubated with BbcellProbe™ M61 and quenching agent at 37°C for 15 min in darkness and centrifuged at $600 \times g$ for

5 min followed by washing with Hank's balanced salt solution (HBSS). The fluorescence intensity of the dissociated cells was analyzed by a Cytomics FC500 flow cytometer (Ex = 488 nm; Em = 558 nm).

Cells apoptosis was measured according to a method described previously [7]. Cells were collected and resuspended in 1x Annexin V binding buffer. Cell suspension was incubated with 5 μl Annexin V-FITC and 10 μl PI and detected (Ex = 488 nm, Em = 578 nm) directly using Cytomics FC500 flow cytometer.

2.8. Western Blot Analysis.

Cardiomyocytes were harvested and lysed with RIPA lysis buffer supplemented with a protease inhibitor (phenylmethanesulfonyl fluoride (PMSF)) and incubated for 30 min at 4°C. Protein extracts were centrifuged at 4°C for 15 min to remove insoluble substances. The protein concentration was measured using a bicinchoninic acid (BCA) protein assay kit (Thermo Fisher, USA). Equal amounts of protein (30 μg) were separated by denaturing sodium dodecyl sulfonate polyacrylamide gel electrophoresis (SDS-PAGE) using a gel apparatus and later transferred to a polyvinylidene fluoride (PVDF) membrane. The membrane was blocked with 5% bull serum albumin, washed, and saturated with primary antibodies (14-3-3η, 1 : 1000; cleaved caspase-3, 1 : 1000; cyt C, 1 : 1000; NDUFB8, 1 : 500; UQCRC2, 1 : 500; Cox4, 1 : 1000; and β-actin, 1 : 1000) overnight at 4°C and then blotted with horseradish peroxidase- (HRP-) conjugated secondary antibody. Subsequently, the membrane was incubated with an enhanced chemiluminescence substrate for 1 min, and protein bands were visualized and analyzed with the Quantity One software (Bio-Rad, USA).

2.9. Terminal Deoxynucleotidyl Transferase-Mediated Nick-End Labeling (TUNEL) Assay.

Apoptosis was determined using the DeadEnd™ Colorimetric TUNEL System (Promega, USA) and visualized using a fluorescence microscope (Olympus, Tokyo, Japan). Cardiomyocytes were added to microscope slides and fixed with 4% methanol-free formaldehyde at 25°C for 25 min, washed twice with PBS, and permeabilized with 0.2% Triton X-100 at 25°C for 5 min. After washing with PBS, incubation buffer (equilibration buffer, biotinylated nucleotide mix, and recombinant terminal deoxynucleotidyl transferase) was added, and the sample was covered with a plastic coverslip and incubated at 37°C for 1 hour. Subsequently, the slides were immersed in 2x SSC, blocked with 0.3% H$_2$O$_2$ for 5 min, and incubated with 100 μl HRP for 30 min. Finally, 100 μl of a diaminobenzidine (DAB) solution was added, and the sample was incubated for 5 min in the dark. Next, the sample was rinsed with deionized water and stained with hematoxylin for 1 min. Microscopic analysis was performed as described [7].

2.10. Statistical Analysis.

Values were represented as mean ± standard error of mean (SEM) from at least six independent experiments. The significance of biochemical data across each group was tested by one-way ANOVA, and the individual differences were tested by least significant difference (LSD) testing. The results were considered statistically significant at a value of $P < 0.05$.

(a)

(b)

(c)

(d)
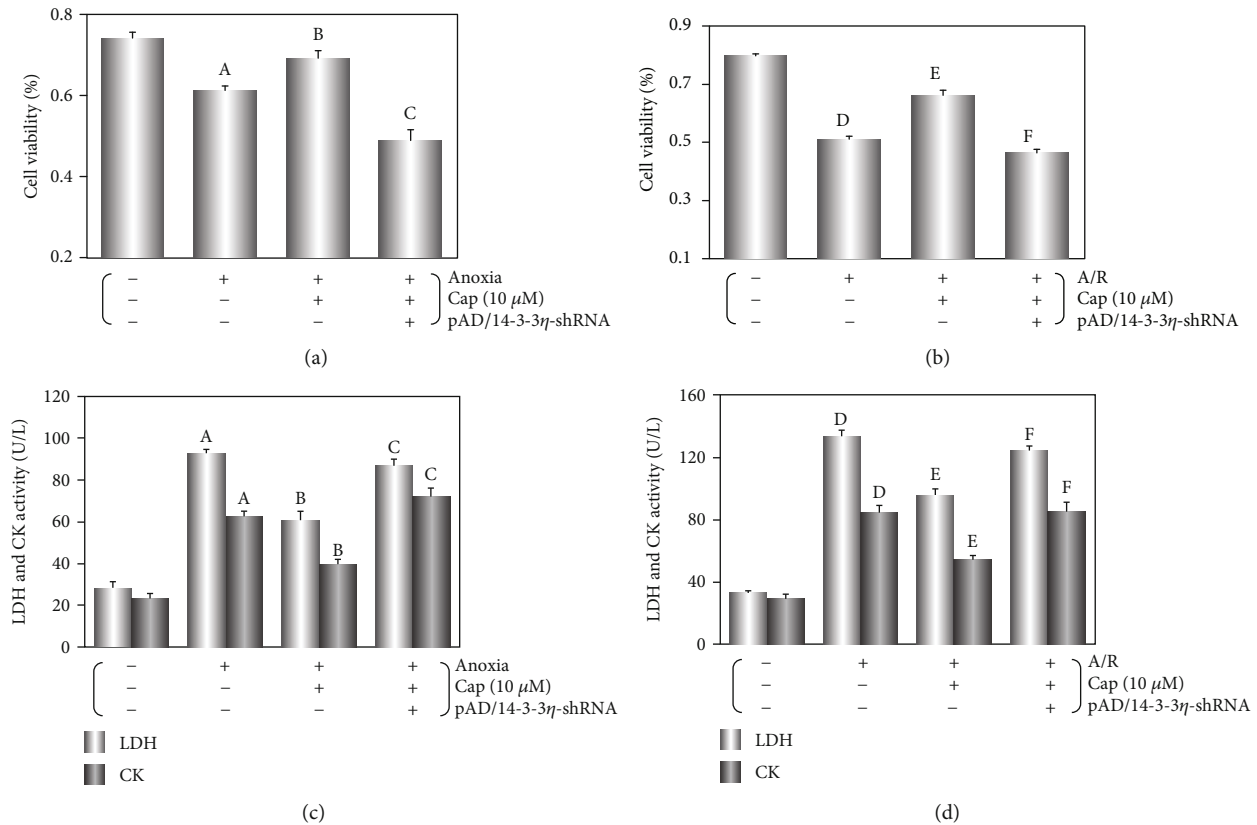
Figure 1: Cap protects cardiomyocytes against anoxia or A/R injury. (a, b) Cell viability of cardiomyocytes. (c, d) LDH and CK activity in culture media. Data are presented as mean ± SEM ($n = 6$). A: $P < 0.01$ vs. control group (anoxia); B: $P < 0.01$ vs. anoxia group; C: $P < 0.01$ vs. Cap+anoxia group; D: $P < 0.01$ vs. control group (A/R); E: $P < 0.01$ vs. A/R group; F: $P < 0.01$ vs. Cap+A/R group.

3. Results

3.1. Cap Protects Cardiomyocytes against Anoxia Alone or A/R Injury.
Cell viability, LDH, and CK activities served as the indicators of cytotoxicity [7]. Following anoxia alone, cell viability decreased, LDH and CK activities increased as compared with the control group ($P < 0.01$), while pretreatment with 10 μM Cap improved cell viability and LDH and CK activities ($P < 0.05$, Figures 1(a) and 1(c)).

Compared with anoxia alone, reoxygenation following anoxia further decreased cell viability (from 61.2 ± 3.2% to 54.1 ± 2.8%, $P < 0.01$, Figures 1(a) and 1(b)) and increased LDH and CK activities ($P < 0.01$, Figures 1(c) and 1(d)), suggesting that reoxygenation stage is an exacerbation period in cardiomyocytes. After treatment with 10 μM Cap, cell viability was similar to the Cap+anoxia group (69.2 ± 3.7% to 71.8 ± 3.6%, $P > 0.05$, Figures 1(a) and 1(b)), and LDH and CK activities were also similar ($P > 0.05$, Figures 1(c) and 1(d)). This could indicate that Cap is able to alleviate cardiomyocyte deterioration. However, the protection of Cap on cardiomyocyte was abrogated by the addition of pAD/14-3-3η-shRNA under conditions of anoxia alone or A/R injury ($P < 0.01$, Figure 1).

3.2. Cap Upregulates 14-3-3η Expression in Cardiomyocytes following Anoxia or A/R Injury.
14-3-3η expression was downregulated by anoxia alone or A/R injury ($P < 0.01$, Figure 2). Following anoxia alone, Cap-pretreated cardiomyocytes slightly increased 14-3-3η level ($P < 0.05$, Figure 2(a)), whereas Cap significantly upregulated 14-3-3η expression after undergoing AR injury ($P < 0.01$, Figure 2(b)).

3.3. Cap Decreases ROS Generation by Maintaining the Redox Balance and Changing Electron Transport in Cardiomyocytes following Anoxia or A/R Injury.
As shown in Figures 3(a) and 3(b), ROS generation increased overall during anoxia or A/R injury when compared with the control group. A/R injury significantly increased ROS generation compared with anoxia alone (from 2.05 (anoxia) to 3.88 (A/R) times, vs. the control group, $P < 0.01$). However, Cap significantly inhibited ROS generation caused by the two treatments (0.61 (anoxia); 0.41 (A/R), vs. the respective injury group, $P > 0.01$). NAD$^+$, GSSG, and NAD$^+$/NADH increased significantly, while NADH, GSH, and GSH/GSSG decreased significantly after anoxia alone or A/R injury (Figures 3(c)–3(f), $P > 0.01$). The NAD$^+$/NADH ratio increased from 5.22 (anoxia) to 9.07 (A/R) (vs. the control group, $P < 0.01$), and the GSH/GSSG ratio decreased from 0.31 (anoxia) to 0.24 (A/R) (vs. the control group, $P < 0.01$). Cap reversed the effects, especially in NAD$^+$/NADH and GSH/GSSG ratio (NAD$^+$/NADH ratio: 0.28 (anoxia) to 0.18 (A/R), vs. the respective injury group, $P < 0.01$; GSH/GSSG ratio: 1.89
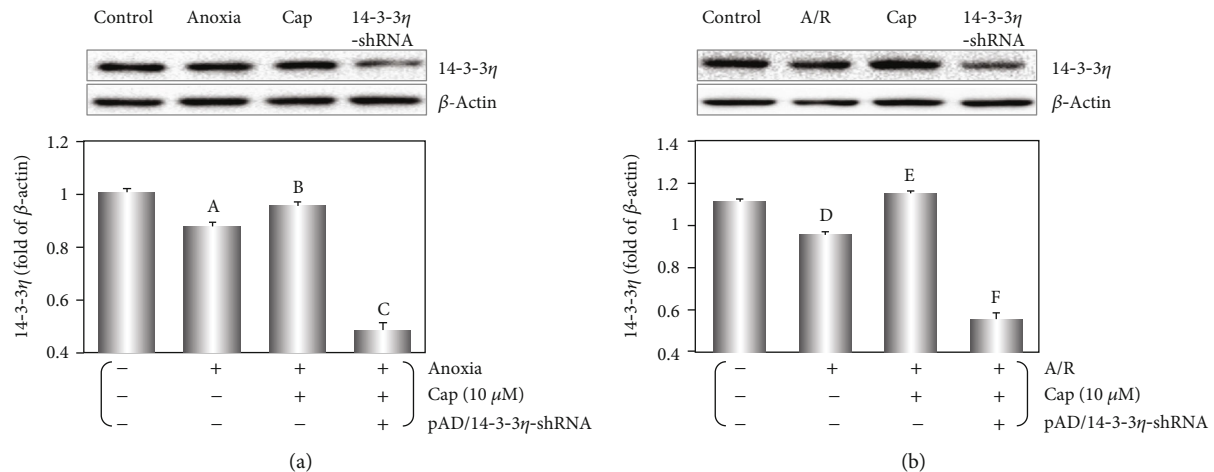
Figure 2: Cap upregulates 14-3-3η on cardiomyocytes exposed to anoxia or A/R injury. (a) Western blot and graphic of 14-3-3η expression during anoxia treatment. (b) Western blot and graphic of 14-3-3η expression during A/R treatment. Data are presented as mean ± SEM ($n = 6$). A: $P < 0.01$ vs. control group (anoxia); B: $P < 0.01$ vs. anoxia group; C: $P < 0.01$ vs. Cap+anoxia group; D: $P < 0.01$ vs. control group (A/R); E: $P < 0.01$ vs. A/R group; F: $P < 0.01$ vs. Cap+A/R group.

(anoxia) to 2.74 (A/R), vs. the respective injury group, $P < 0.01$). The results showed that A/R injury could activate ROS generation and redox status more than anoxia alone and Cap could rescue the related cellular deterioration.

The levels of NDUFB8 (a subunit of mt complex I) and UQCRC2 (a subunit of mt complex III) were determined by Western blot. NDUFB8 and UQCRC2 levels decreased during the anoxia or A/R exposure ($P < 0.01$, Figures 4(a) and 4(b)), indicating an inhibition of the mitochondrial respiratory chain of cardiomyocyte. This result could partially explain the measured ROS burst and perturbation of mitochondrial redox status including changes in NAD$^+$/NADH and GSH/GSSG ratios. The Cap pretreatment significantly increased the mitochondrial complexes of ETC ($P < 0.01$).

Furthermore, OCR measurements showed a significant decrease in basal oxygen consumption, ATP-linked OCR, and spare respiratory capacity over the normoxic control cells ($P < 0.01$, Figures 4(c) and 4(d)). Collectively, these observations indicated that mitochondrial vitality was significantly inhibited following anoxia or A/R injury. ECAR measurements indicated that glycolysis increased significantly after anoxia or A/R injury resulting in lactate accumulation and increased extracellular acidification ($P < 0.01$, Figures 4(e) and 4(f)). As expected, Cap increased OCR and decreased the concentration of extracellular H$^+$ in cardiomyocytes during the different types of injury ($P < 0.01$) with a prominent effect in the context of A/R injury. These results corroborate in the data on ROS generation, GSH/GSSG and NAD$^+$/NADH ratio, and mt complex I/III activities. The Cap-mediated beneficial effects were abrogated by coincubating with pAD/14-3-3η-shRNA ($P < 0.01$).

3.4. Cap Improves Mitochondrial Function in Cardiomyocytes Exposed to Anoxia or A/R Injury.

A major characteristic of

early apoptotic cells is loss of plasma membrane potential [34]. In living cells, the fluorescent dye JC-1 accumulates in the mitochondrial matrix and emits a red fluorescence. However, in apoptotic and dead cells, JC-1 exists as a monomer and emits a green fluorescence. We utilized the red/green fluorescence ratio to express the loss of MMP potential [7]. Both anoxia and A/R exposure induced a loss of MMP ($P < 0.01$) that was rescued by treatment with Cap ($P < 0.01$, Figures 5(a) and 5(b)).

Increased mPTP opening causes the early functional changes of apoptosis [35] with a release of cyt C from mitochondria into the cytosol [36]. As illustrated in Figures 5(c)–5(f), cyt C levels in the cytosol were higher in the A/R group than these in the anoxia alone group ($P < 0.01$), indicating an aggravated mitochondrial malfunction caused by A/R injury. Cap rescue of this effect was significantly stronger in A/R injury stage compared with anoxia alone. As demonstrated in other results, the inhibition of 14-3-3η using pAD/14-3-3η-shRNA could reverse the effects of Cap ($P < 0.01$).

3.5. Cap Decreases Apoptosis of Cardiomyocyte Induced by Anoxia Alone or A/R Injury.

Cleaved caspase-3 is an activated form of caspase-3 [7]. Cleaved caspase-3 expression increased significantly following anoxia or A/R injury ($P < 0.01$, Figures 6(c) and 6(d)). The addition of Cap significantly decreased cleaved caspase-3 expression following injury with anoxia or A/R ($P < 0.01$).

Furthermore, apoptosis was measured by flow cytometry [7]. Apoptotic ratio in the anoxia and A/R groups compared with the control group ($P < 0.01$, Figures 6(a) and 6(b)). Cap treatment decreased the apoptotic ratio induced by anoxia or A/R injury ($P < 0.01$). The results of TUNEL staining corroborated the above findings. Varying degrees of accumulation of TUNEL positive cells were identified in anoxia or A/R injury and this was decreased following Cap treatment

(a)

(b)

(c)

(d)

Figure 3: Continued.

(e)

(f)
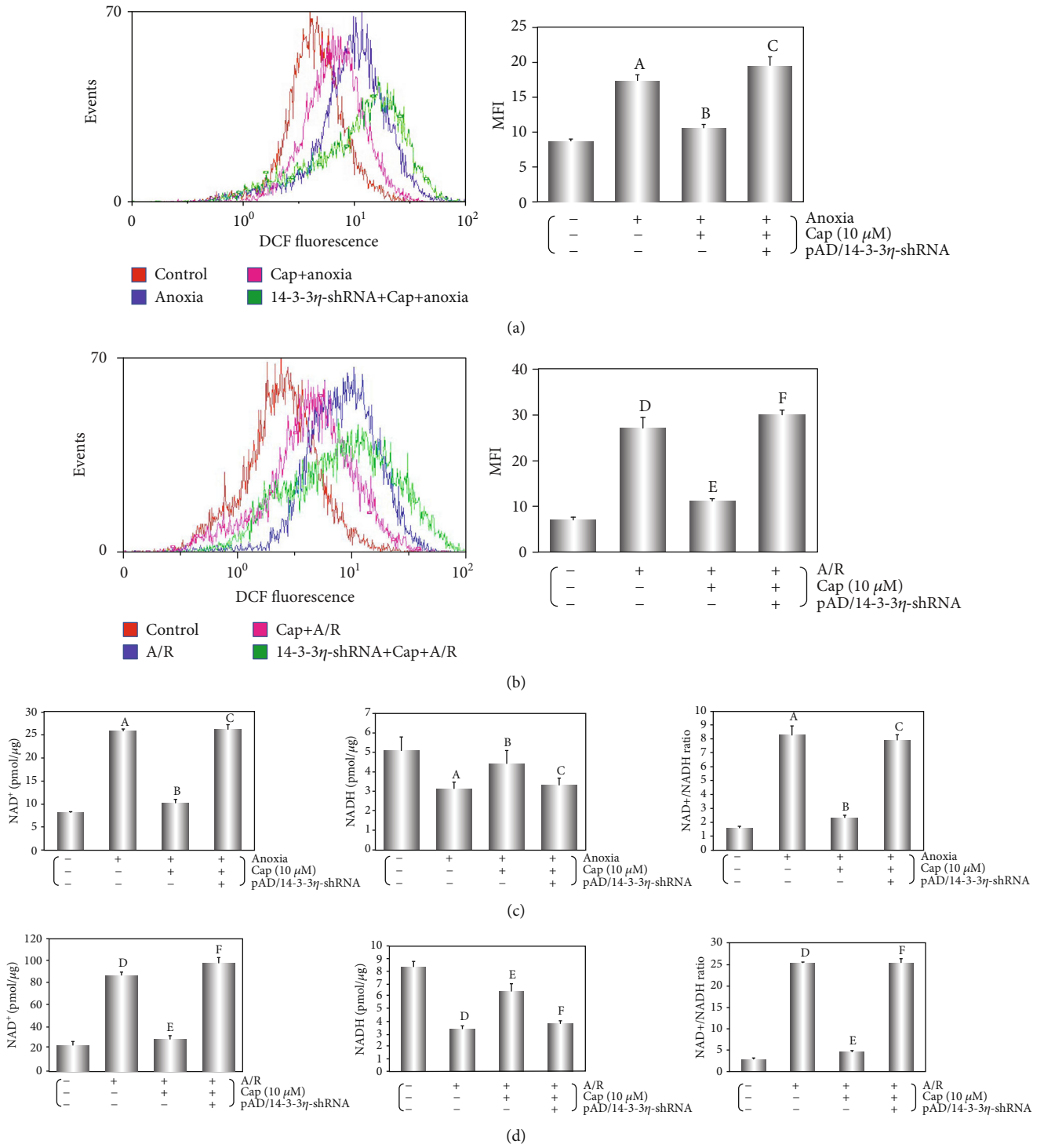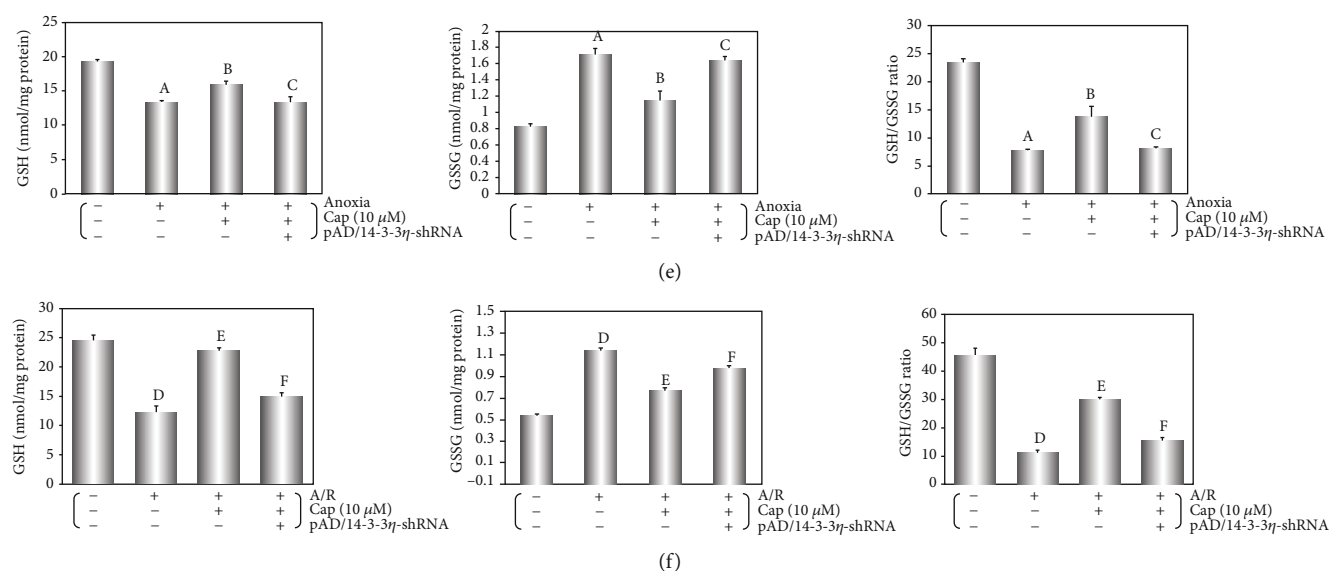
FIGURE 3: Cap reduces ROS generation by maintaining the redox balance following anoxia or A/R injury. (a, b) Fluorescent probe DCFH-DA indicating ROS level was detected by flow cytometry and column chart of average fluorescence intensity values during A/R exposure. (c, d) Mitochondrial NAD levels in cardiomyocytes after different treatments. Left: histogram of mitochondrial NAD$^+$ levels; middle: histogram of mitochondrial NADH levels; right: histogram of mitochondrial NAD$^+$/NADH ratio. (e, f) Intracellular glutathione levels of cardiomyocyte after different treatments. Left: histogram of intracellular GSH levels; middle: histogram of intracellular GSSG levels; right: histogram of intracellular GSH/GSSG ratio. Data are presented as mean ± SEM ($n = 6$). A: $P < 0.01$ vs. control group (anoxia); B: $P < 0.01$ vs. anoxia group; C: $P < 0.01$ vs. Cap+anoxia group; D: $P < 0.01$ vs. control group (A/R); E: $P < 0.01$ vs. A/R group; F: $P < 0.01$ vs. Cap+A/R group.

(Figure 7). Treatment with pAD/14-3-3η-shRNA reversed the Cap-mediated rescue of apoptosis ($P < 0.01$).

4. Discussion

Anoxia leads to the disorder of energy metabolism in cells, induces oxidative stress, and interferes with the synthesis and function of a large number of proteins [3]. After reoxygenation, cellular function further deteriorates as well studied in cardiomyocyte [24, 25]. In the current study, decreased cell viability and increased LDH and CK activity, cleaved caspase-3 expression, and apoptotic ratio in cardiomyocytes following anoxia or A/R stage (Figures 1, 6, and 7) indicated damage in cardiomyocytes. The impact of A/R injury was stronger compared with anoxia alone in keeping with previously published work [3–9, 24, 25]. Interestingly, Cap significantly blocked the inhibitory effects of anoxia or A/R injury (Figures 1, 6, and 7), suggesting a protective effect on cardiomyocytes following injury, supporting previously published work [7, 8].

As a phytochemical compound with multiple targets and mechanisms of action, Cap regulates the expression and activity of a variety of proteins, further affecting downstream signaling pathways resulting in a biological effect [26, 30]. Cap significantly upregulated 14-3-3η and SIRT1 expression, thus promoting translocation of Bcl-2 to mitochondria in cardiomyocytes in response to A/R injury [7, 8]. In this study, we identified that Cap-mediated rescue of cardiomyocytes was linked to 14-3-3η expression. This was corroborated by the shRNA-mediated downregulation of 14-3-3η

expression, which reversed the protective effects of Cap (Figures 1–7).

There are seven known isoforms (β, γ, ε, η, ζ, σ, and τ/θ) of 14-3-3 family proteins in mammals. Functionally, together with partner proteins, 14-3-3 regulates phosphorylation and dephosphorylation, kinase activity, and cellular location of proteins that may participate in cell proliferation, differentiation, survival, transformation, and apoptosis [37, 38]. Our previous study demonstrated that 14-3-3η is activated in ischemia/hypoxia injury while 14-3-3γ activation is linked to infectious/inflammatory lesions [7–9, 39]. 14-3-3 is the molecular target of many active ingredients of plants. We have confirmed that 14-3-3 assists PKCε, Bcl-2, and other functional proteins to locate to mitochondria and protect cardiomyocytes and vascular endothelial cells against multiple injuries [7, 9, 40–43]. Further studies are needed to define specific mechanism(s) of action for Cap-activated 14-3-3η in anoxia and A/R injured cardiomyocytes.

Mitochondrial dysfunction, a major hallmark of anoxia injury in cardiomyocyte, is exacerbated through reoxygenation to severely affect ROS production and impede cardiomyocyte survival [44, 45]. In this study, we found that ROS generation increased following anoxia alone but was excessive following A/R injury (Figures 3(a) and 3(b)). Mitochondria are furnished with endogenous defense mechanisms against excessive ROS generation [46]. The mechanism of internal defense mainly contains several antioxidant defense systems, among them, GSH/GSSG and NAD$^+$/NADH play an important role in maintaining the cellular redox status [47, 48]. Additionally, the balance of ROS and redox states

(a)

(b)

(c)

(d)
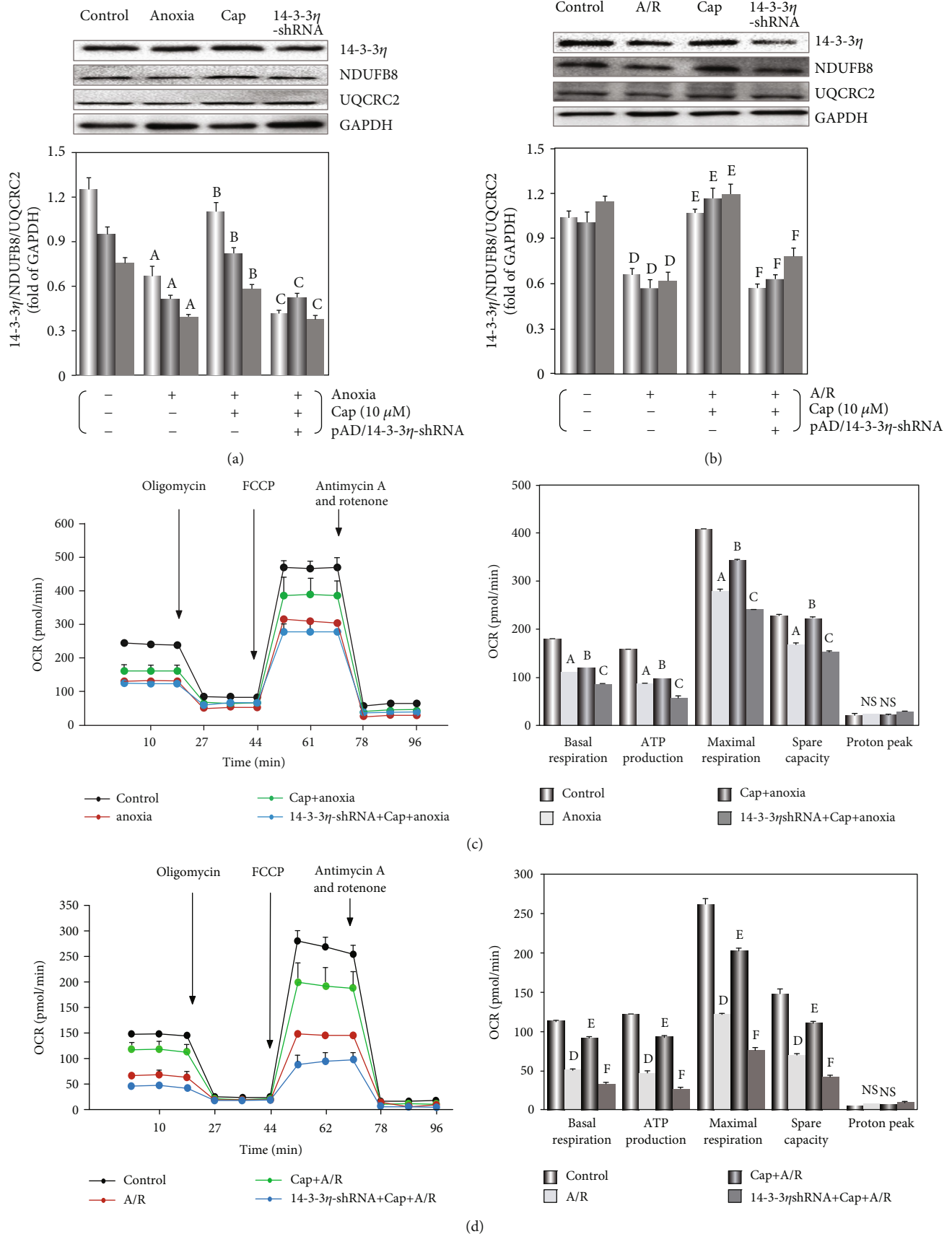
Figure 4: Continued.
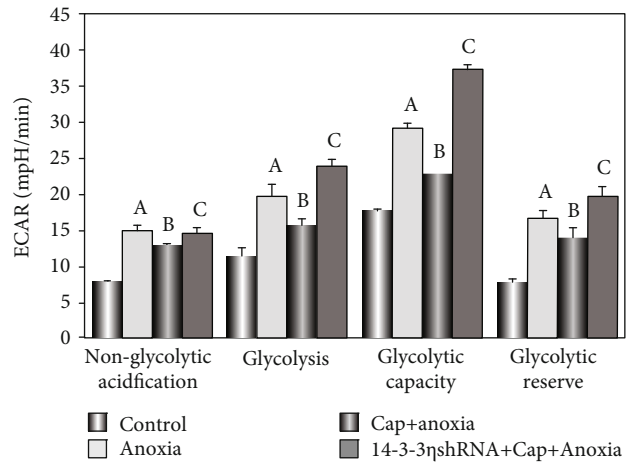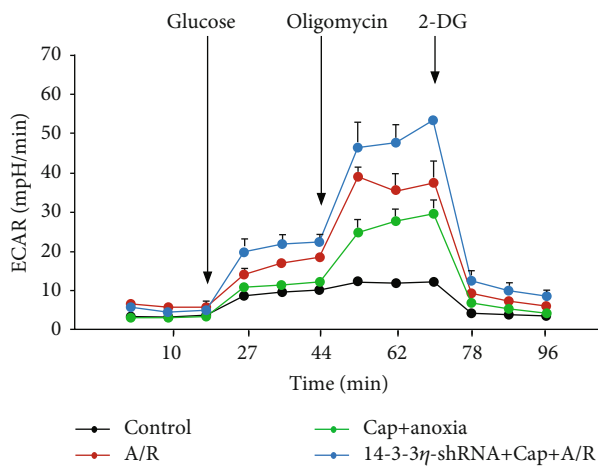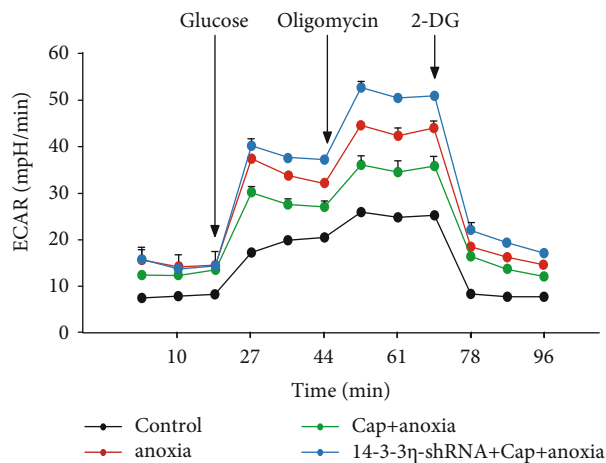
(e)
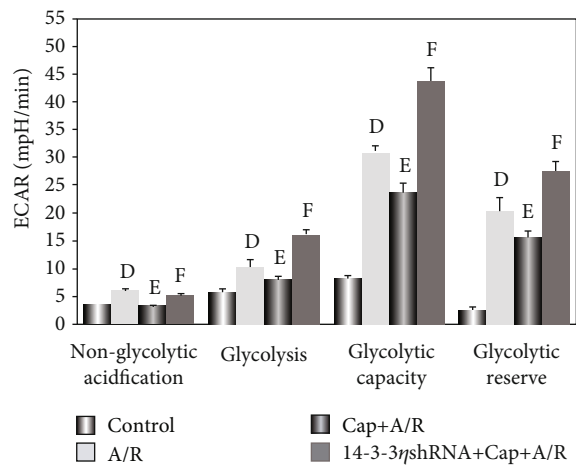
(f)

FIGURE 4: Effects of Cap treatment on mitochondrial bioenergetics and glycolytic activity of cardiomyocytes during A/R injury. (a, b) Western blot and graphic of 14-3-3η, NDUFB8, and UQCRC2. (c, d) Effects of Cap on OCR. Cap pretreatment increased mitochondrial respiration following injury. (e, f) Effects of Cap on ECAR. Cap pretreatment decreased lactate accumulation and extracellular acidification. Data are presented as mean ± SEM ($n = 6$). A: $P < 0.01$ vs. control group (anoxia); B: $P < 0.01$ vs. anoxia group; C: $P < 0.01$ vs. Cap+anoxia group; D: $P < 0.01$ vs. control group (A/R); E: $P < 0.01$ vs. A/R group; F: $P < 0.01$ vs. Cap+A/R group.

could maintain cellular homeostasis by modulating ion channels, conditioning transports, and regulating enzyme activity [49, 50]. Compared with anoxia alone, GSH/GSSG ratio was dramatically decreased and NAD$^+$/NADH ratio was significantly increased by A/R injury. The disruption of antioxidant homeostasis therefore could explain the excessive production of ROS (Figures 3(c)–3(f)).

It is well known that inhibition of activities of mt complexes I and III can result in inducing ROS overproduction and perturbation of the NAD$^+$/NADH ratio [51–53]. In the present study, the expression of NDUFB8 and UQCRC2 were decreased in cardiomyocytes after undergoing anoxia or A/R injury (Figures 4(a) and 4(b)). Complexes I/III are inhibited by rotenone and antimycin A, respectively, which leads to the inhibition of the flow of electrons along the respiratory chain and the formation of ATP [54, 55]. Accumulating evidence indicated that the anoxic cardiomyocyte

mainly produces ATP by the anaerobic glycolytic pathways [56, 57]. However, accelerated glycolysis of cardiomyocyte in response to impaired pyruvate oxidation could lead to lactate accumulation during anoxia stage [58, 59]. In anoxia or A/R injury, ATP suppression and damaged mitochondrial respiration result from a metabolic flux in cardiomyocytes under pathological conditions (Figures 4(c) and 4(d)). Accordingly, the cardiomyocyte accounted for higher index of glycolytic reserves thus indicating towards mitochondrial malfunction was aggravated during the pathological process (Figures 4(e) and 4(f)). Remarkably, these findings were in keeping with the changes in the redox couples mentioned above, likely because inhibition of mt complexes I/III activity could disturb the redox balance and the homeostasis of cellular energy metabolism during A/R injury.

We found that Cap treatment could increase NADH, GSH, and GSH/GSSG ratio and inhibit NAD$^+$, GSSG, and

(a)

(b)

(c)

FIGURE 5: Continued.

(d)

(e)

(f)
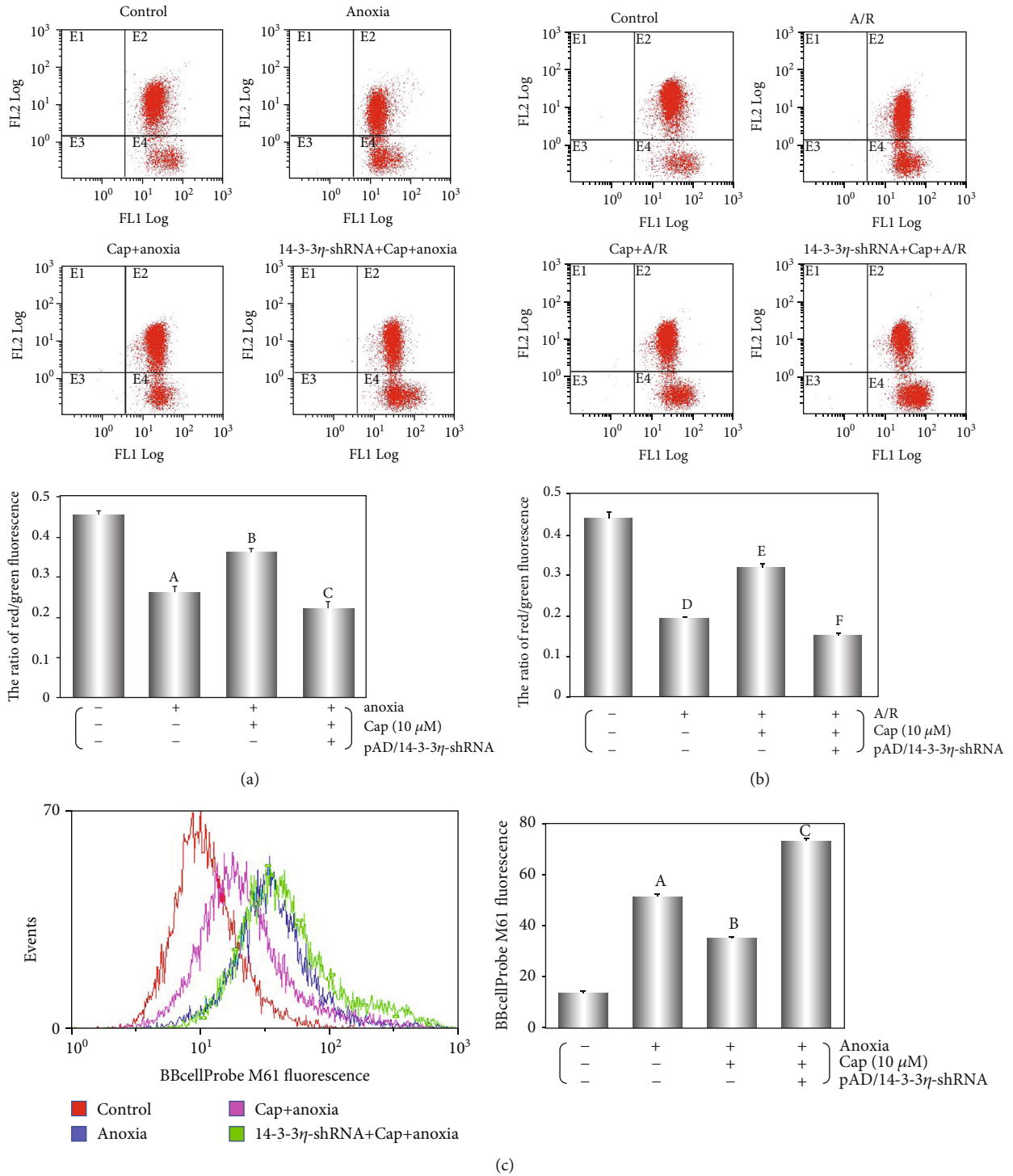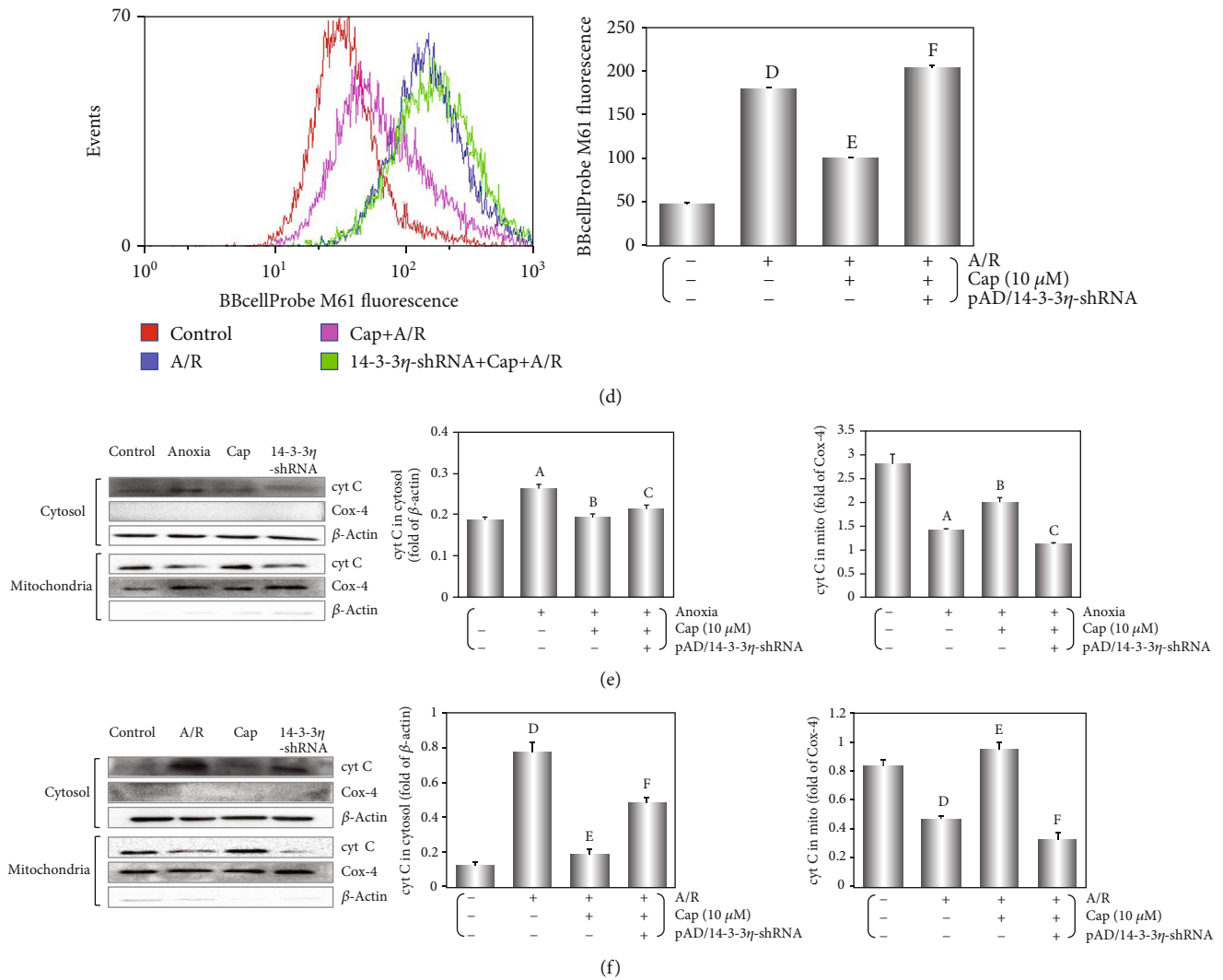
FIGURE 5: Cap improves mitochondrial function in cardiomyocytes exposed to anoxia or A/R injury. (a, b) Fluorescent dye JC-1 indicating MMP level was detected by flow cytometry, and the ratio of red/green fluorescence is represented. (c, d) Fluorescent probe BBcellProbe M61 indicating mPTP opening was detected by flow cytometry, and column chart of average fluorescence intensity values is shown. (e, f) Western blot and graphic of cyt C level in the cytosol/mitochondria. Data are presented as mean ± SEM ($n = 6$). A: $P < 0.01$ vs. control group (anoxia); B: $P < 0.01$ vs. anoxia group; C: $P < 0.01$ vs. Cap+anoxia group; D: $P < 0.01$ vs. control group (A/R); E: $P < 0.01$ vs. A/R group; F: $P < 0.01$ vs. Cap+A/R group.

NAD$^+$/NADH ratio after anoxia or A/R injury in cardiomyocytes. Contrasted with the results caused by anoxia alone, the doubling ratio of NAD$^+$/NADH and GSH/GSSG implied that the ability of Cap to protect cardiomyocyte against external injury was more effective during the A/R period (Figures 3(c)–3(f)). Moreover, Cap treatment could elevate complex I/III expression on cardiomyocyte (Figures 4(a) and 4(b)), increase ATP production-associated mitochondrial respiration, and reduce lactate accumulation (Figures 4(c)–4(f)), while cotreatment with pAD/14-3-3η-shRNA could invert effects mentioned above. Therefore, it is difficult to explain the effects as mentioned earlier of Cap just by its antioxidant capacity; the role of Cap upregulating 14-3-3η expression and its effects on downstream related pathways are more important. Furthermore, myocardial mitochondrial dysfunction

was worse caused by A/R injury than that by anoxia alone. On the contrary, Cap showed a benign protective effect during the gradual deterioration of pathology, which was reflected in redox balance, complexes of ETC, OCR, and ECAR.

Mitochondria are the primary organelle that generates ROS in cardiomyocyte [60]. The excessive ROS generation stimulated MMP and further caused mPTP openness in the inner mitochondrial membrane leading to severe mitochondrial swelling, rupture, and the release of apoptogenic factors [61, 62]. Consistently, pretreatment with Cap stabilized MMP (Figures 5(a) and 5(b)), closed mPTP (Figures 5(c) and 5(d)), and decreased the release of cyt C into the cytoplasm in cardiomyocytes during A/R injury (Figures 5(e) and 5(f)). These responses increased cell viability (Figure 1),
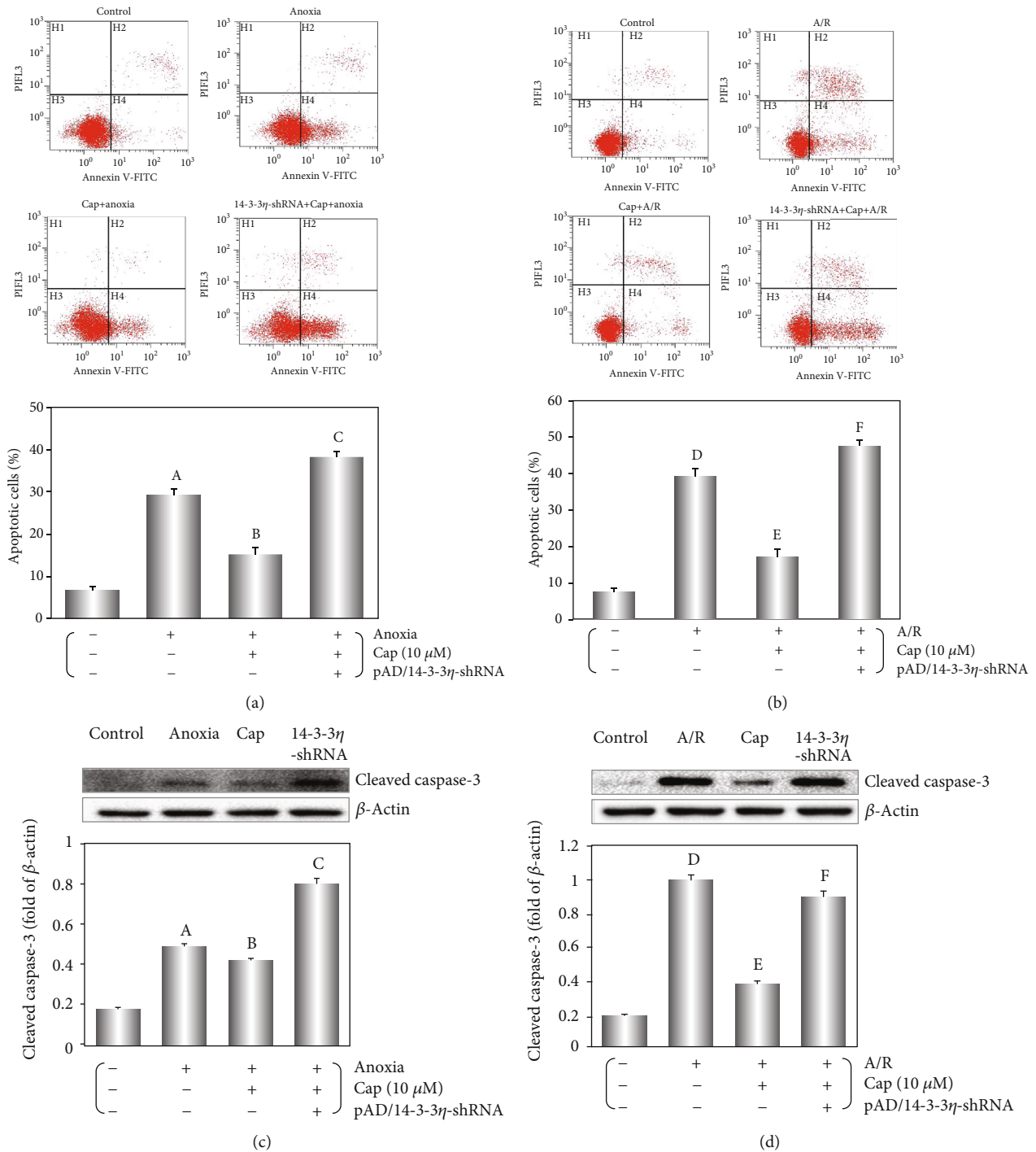
Figure 6: Cap decreases the apoptosis of cardiomyocyte induced by anoxia or A/R. (a, b) Dot plots of Annexin V-FITC/PI detected by flow cytometry and the apoptosis analyzed with the CXP analysis software. (c, d) Western blot and graphic of cleaved caspase-3 levels in cardiomyocytes. Data are presented as mean ± SEM ($n = 6$). A: $P < 0.01$ vs. control group (anoxia); B: $P < 0.01$ vs. anoxia group; C: $P < 0.01$ vs. Cap+anoxia group; D: $P < 0.01$ vs. control group (A/R); E: $P < 0.01$ vs. A/R group; F: $P < 0.01$ vs. Cap+A/R group.

decreased cleaved caspase 3 expression (Figures 6(a) and 6(b)), and inhibited apoptosis (Figures 6 and 7).

5. Conclusions

Taken together, by comparing the damage from anoxia or reoxygenation, we found that reoxygenation following anoxia could further abrogate the tolerance and adaptability of cardiomyocytes as evidenced by increased ROS generation, inhibited complex I/III activities, and disturbed redox status and homeostasis of cellular energy metabolism. Cap rescued these effects in cardiomyocytes likely through the upregulation of 14-3-3η. Cap-treated cardiomyocytes showed improved mitochondrial functioning resulting in apoptosis inhibition.

(a)

(b)
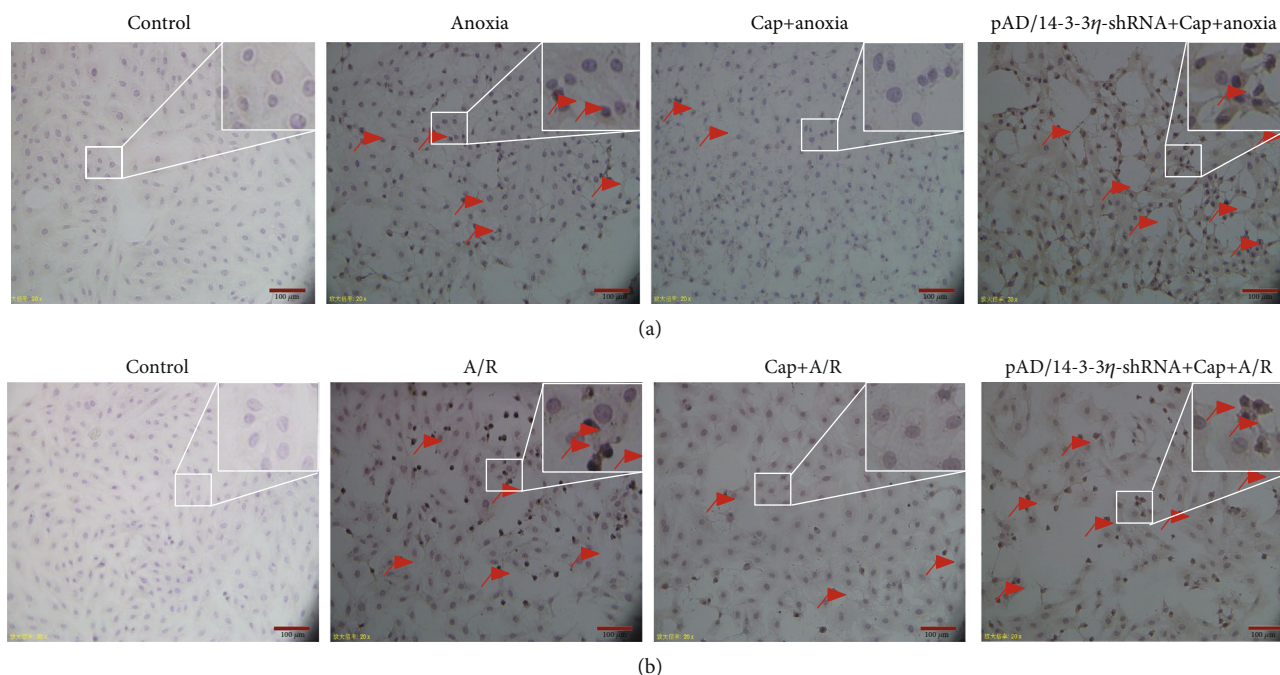
Figure 7: TUNEL assay for apoptotic cells induced by anoxia or A/R injury. Red arrows indicate TUNEL-positive (apoptotic) cardiomyocytes.

Abbreviations

ANOVA:	Analysis of variance
A/R:	Anoxia/reoxygenation
ATP:	Adenosine triphosphate
BCA:	Bicinchoninic acid
Cap:	Capsaicin
CK:	Creatine kinase
cyt C:	Cytochrome C
DAB:	Diaminobenzidine
DCFH-DA:	6-Carboxy-2′-7′-dichlorodihydro-fluorescein diacetate
DMEM:	Dulbecco's modified Eagle medium
ECAR:	Extracellular acidification rate
ETC:	Electron transport chain
FBS:	Fetal bovine serum
GSH:	Reduced glutathione
GSSG:	Oxidized glutathione
HBSS:	Hank's balanced salt solution
I/R:	Ischemia/reperfusion
JC-1:	5,5′,6,6′-Tetrachloro-1,1′,3,3′-tetraethyl-benzimidazolo carbocyanine iodide
LDH:	Lactate dehydrogenase
LSD:	Least significant difference
mPTP:	Mitochondrial permeability transition pore
MMP:	Mitochondrial membrane potential
NAD^+:	Oxidized nicotinamide adenine dinucleotide
NADH:	Reduced nicotinamide adenine dinucleotide
NDUFB8:	NADH dehydrogenase [ubiquinone] 1 beta subcomplex subunit 8
OCR:	Oxygen consumption rate
PBS:	Phosphate-buffered saline
PI:	Propidium iodide
PMSF:	Phenylmethanesulfonyl fluoride
ROS:	Reactive oxygen species
SEM:	Standard error of mean
TUNEL:	Terminal deoxynucleotidyl transferase dUTP nick-end labeling
UQCRC2:	Cytochrome b-c1 complex subunit 2
WST-8:	2-(2-Methoxy-4-nitrophenyl)-3-(4-nitrophenyl)-5-(2,4-disulfophenyl)-2H-tetrazolium, monosodium salt.

Data Availability

The data used to support the findings of this study are included within the article.

Conflicts of Interest

The authors declare that there is no conflict of interest regarding the publication of this paper.

Acknowledgments

References

[1] M. Christoffersen and A. Tybjaerg-Hansen, "Visible aging signs as risk markers for ischemic heart disease: epidemiology, pathogenesis and clinical implications," *Ageing Research Reviews*, vol. 25, pp. 24–41, 2016.

[2] J. Roh, J. Rhee, V. Chaudhari, and A. Rosenzweig, "The role of exercise in cardiac aging: from physiology to molecular mechanisms," *Circulation Research*, vol. 118, no. 2, pp. 279–295, 2016.

[3] G. Heusch, "Molecular basis of cardioprotection: signal transduction in ischemic pre-, post-, and remote conditioning," *Circulation Research*, vol. 116, no. 4, pp. 674–699, 2015.

[4] Q. Chen, E. J. Vazquez, S. Moghaddas, C. L. Hoppel, and E. J. Lesnefsky, "Production of reactive oxygen species by mitochondria central role of complex III," *Journal of Biological Chemistry*, vol. 278, no. 38, pp. 36027–36031, 2003.

[5] E. T. Chouchani, V. R. Pell, E. Gaude et al., "Ischaemic accumulation of succinate controls reperfusion injury through mitochondrial ROS," *Nature*, vol. 515, no. 7527, pp. 431–435, 2014.

[6] D. F. Dai and P. S. Rabinovitch, "Cardiac aging in mice and humans: the role of mitochondrial oxidative stress," *Trends in Cardiovascular Medicine*, vol. 19, no. 7, pp. 213–220, 2009.

[7] H. He, Y. Zhou, J. Huang et al., "Capsaicin protects cardiomyocytes against anoxia/reoxygenation injury via preventing mitochondrial dysfunction mediated by SIRT1," *Oxidative Medicine and Cellular Longevity*, vol. 2017, Article ID 1035702, 14 pages, 2017.

[8] J. Huang, Z. Liu, P. Xu et al., "Capsaicin prevents mitochondrial damage, protects cardiomyocytes subjected to anoxia/reoxygenation injury mediated by 14-3-3η/Bcl-2," *European Journal of Pharmacology*, vol. 819, pp. 43–50, 2018.

[9] Z. Zhang, H. He, Y. Qiao et al., "Tanshinone IIA pretreatment protects H9c2 cells against anoxia/reoxygenation injury: involvement of the translocation of Bcl-2 to mitochondria mediated by 14-3-3η," *Oxidative Medicine and Cellular Longevity*, vol. 2018, Article ID 3583921, 13 pages, 2018.

[10] D. Giustarini, D. Tsikas, G. Colombo et al., "Pitfalls in the analysis of the physiological antioxidant glutathione (GSH) and its disulfide (GSSG) in biological samples: an elephant in the room," *Journal of Chromatography B*, vol. 1019, pp. 21–28, 2016.

[11] J. J. Soldevila-Barreda and N. Metzler-Nolte, "Intracellular catalysis with selected metal complexes and metallic nanoparticles: advances toward the development of catalytic metallodrugs," *Chemical Reviews*, vol. 119, no. 2, pp. 829–869, 2019.

[12] P. K. Prasai, B. Shrestha, A. W. Orr, and C. B. Pattillo, "Decreases in GSH:GSSG activate vascular endothelial growth factor receptor 2 (VEGFR2) in human aortic endothelial cells," *Redox Biology*, vol. 19, pp. 22–27, 2018.

[13] J. Li, Y.-L. Yang, L.-Z. Li et al., "Succinate accumulation impairs cardiac pyruvate dehydrogenase activity through GRP91-dependent and independent signaling pathways: therapeutic effects of ginsenoside Rb1," *Biochimica et Biophysica Acta (BBA)-Molecular Basis of Disease*, vol. 1863, no. 11, pp. 2835–2847, 2017.

[14] C. F. Lee, J. D. Chavez, L. Garcia-Menendez et al., "Normalization of NAD$^+$ redox balance as a therapy for heart failure," *Circulation*, vol. 134, no. 12, pp. 883–894, 2016.

[15] S. Lim and P. Barter, "Antioxidant effects of statins in the management of cardiometabolic disorders," *Journal of Atherosclerosis and Thrombosis*, vol. 21, no. 10, pp. 997–1010, 2014.

[16] S. M. Kilbride and J. H. M. Prehn, "Central roles of apoptotic proteins in mitochondrial function," *Oncogene*, vol. 32, no. 22, pp. 2703–2711, 2013.

[17] M. P. Murphy, "How mitochondria produce reactive oxygen species," *Biochemical Journal*, vol. 417, no. 1, pp. 1–13, 2009.

[18] J. Hirst, "Mitochondrial complex I," *Annual Review of Biochemistry*, vol. 82, no. 1, pp. 551–575, 2013.

[19] C. W. Davis, B. J. Hawkins, S. Ramasamy et al., "Nitration of the mitochondrial complex I subunit NDUFB8 elicits RIP1- and RIP3-mediated necrosis," *Free Radical Biology and Medicine*, vol. 48, no. 2, pp. 306–317, 2010.

[20] Q. Sun, W. Zhong, W. Zhang, and Z. Zhou, "Defect of mitochondrial respiratory chain is a mechanism of ROS overproduction in a rat model of alcoholic liver disease: role of zinc deficiency," *American Journal of Physiology-Gastrointestinal and Liver Physiology*, vol. 310, no. 3, pp. G205–G214, 2016.

[21] R. D. Guzy and P. T. Schumacker, "Oxygen sensing by mitochondria at complex III: the paradox of increased reactive oxygen species during hypoxia," *Experimental Physiology*, vol. 91, no. 5, pp. 807–819, 2006.

[22] H. El Hadi, R. Vettor, and M. Rossato, "Cardiomyocyte mitochondrial dysfunction in diabetes and its contribution in cardiac arrhythmogenesis," *Mitochondrion*, vol. 46, pp. 6–14, 2019.

[23] K. K. Upadhyay, R. N. Jadeja, H. S. Vyas et al., "Carbon monoxide releasing molecule-A1 improves nonalcoholic steatohepatitis via Nrf2 activation mediated improvement in oxidative stress and mitochondrial function," *Redox Biology*, vol. 28, article 101314, 2020.

[24] S. C. Kolwicz Jr., S. Purohit, and R. Tian, "Cardiac metabolism and its interactions with contraction, growth, and survival of cardiomyocytes," *Circulation Research*, vol. 113, no. 5, pp. 603–616, 2013.

[25] D. J. Hausenloy and D. M. Yellon, "Myocardial ischemia-reperfusion injury: a neglected therapeutic target," *The Journal of Clinical Investigation*, vol. 123, no. 1, pp. 92–100, 2013.

[26] H. Krishnatreyya, H. Hazarika, A. Saha, and P. Chattopadhyay, "Capsaicin, the primary constituent of pepper sprays and its pharmacological effects on mammalian ocular tissues," *European Journal of Pharmacology*, vol. 819, pp. 114–121, 2018.

[27] C. H. Choi, Y. K. Jung, and S. H. Oh, "Autophagy induction by capsaicin in malignant human breast cells is modulated by p38 and extracellular signal-regulated mitogen-activated protein kinases and retards cell death by suppressing endoplasmic reticulum stress-mediated apoptosis," *Molecular Pharmacology*, vol. 78, no. 1, pp. 114–125, 2010.

[28] P. Patowary, M. P. Pathak, K. Zaman, P. S. Raju, and P. Chattopadhyay, "Research progress of capsaicin responses to various pharmacological challenges," *Biomedicine & Pharmacotherapy*, vol. 96, pp. 1501–1512, 2017.

[29] A. J. D'Alonzo, G. J. Grover, R. B. Darbenzio et al., "In vitro effects of capsaicin: antiarrhythmic and antiischemic activity,"

European Journal of Pharmacology, vol. 272, no. 2-3, pp. 269–278, 1995.

[30] W. Gerber, D. Steyn, A. Kotzé, H. Svitina, C. Weldon, and J. Hamman, "Capsaicin and piperine as functional excipients for improved drug delivery across nasal epithelial models," *Planta Medica*, vol. 85, no. 13, pp. 1114–1123, 2019.

[31] M. Xu, Y. Wang, K. Hirai, A. Ayub, and M. Ashraf, "Calcium preconditioning inhibits mitochondrial permeability transition and apoptosis," *American Journal of Physiology-Heart and Circulatory Physiology*, vol. 280, no. 2, pp. H899–H908, 2001.

[32] Y. Pan, W. Zhao, D. Zhao et al., "Salvianolic acid B improves mitochondrial function in 3T3-L1 adipocytes through a pathway involving PPARγ coactivator-1α (PGC-1α)," *Frontiers in Pharmacology*, vol. 9, article 671, 2018.

[33] X. Li, R. Zhang, L. Guo et al., "Colocalization coefficients of a target-switchable fluorescent probe can serve as an indicator of mitochondrial membrane potential," *Analytical Chemistry*, vol. 91, no. 4, pp. 2672–2677, 2019.

[34] S. De Biasi, L. Gibellini, and A. Cossarizza, "Uncompensated polychromatic analysis of mitochondrial membrane potential using JC-1 and multilaser excitation," *Current Protocols in Cytometry*, vol. 72, no. 1, pp. 7.32.1–7.32.11, 2015.

[35] K. W. Kinnally, P. M. Peixoto, S. Y. Ryu, and L. M. Dejean, "Is mPTP the gatekeeper for necrosis, apoptosis, or both?," *Biochimica et Biophysica Acta (BBA)-Molecular Cell Research*, vol. 1813, no. 4, pp. 616–622, 2011.

[36] C. Garrido, L. Galluzzi, M. Brunet, P. E. Puig, C. Didelot, and G. Kroemer, "Mechanisms of cytochrome c release from mitochondria," *Cell Death and Differentiation*, vol. 13, no. 9, pp. 1423–1433, 2006.

[37] M. B. Yaffe, K. Rittinger, S. Volinia et al., "The structural basis for 14-3-3: phosphopeptide binding specificity," *Cell*, vol. 91, no. 7, pp. 961–971, 1997.

[38] P. Mhawech, "14-3-3 proteins–an update," *Cell Research*, vol. 15, no. 4, pp. 228–236, 2005.

[39] M. He, J. Zhang, L. Shao et al., "Upregulation of 14-3-3 isoforms in acute rat myocardial injuries induced by burn and lipopolysaccharide," *Clinical and Experimental Pharmacology and Physiology*, vol. 33, no. 4, pp. 374–380, 2006.

[40] Z. Liu, L. Yang, J. Huang et al., "Luteoloside attenuates anoxia/reoxygenation-induced cardiomyocytes injury via mitochondrial pathway mediated by 14-3-3η protein," *Phytotherapy Research*, vol. 32, no. 6, pp. 1126–1134, 2018.

[41] B. Huang, J. You, Y. Qiao et al., "Tetramethylpyrazine attenuates lipopolysaccharide-induced cardiomyocyte injury via improving mitochondrial function mediated by 14-3-3γ," *European Journal of Pharmacology*, vol. 832, pp. 67–74, 2018.

[42] Y. Luo, Q. Wan, M. Xu et al., "Nutritional preconditioning induced by astragaloside IV on isolated hearts and cardiomyocytes against myocardial ischemia injury via improving Bcl-2-mediated mitochondrial function," *Chemico-Biological Interactions*, vol. 309, p. 108723, 2019.

[43] B. Yang, H. Li, Y. Qiao et al., "Tetramethylpyrazine attenuates the endotheliotoxicity and the mitochondrial dysfunction by doxorubicin via 14-3-3γ/Bcl-2," *Oxidative Medicine and Cellular Longevity*, vol. 2019, Article ID 5820415, 20 pages, 2019.

[44] E. J. Lesnefsky and C. L. Hoppel, "Ischemia-reperfusion injury in the aged heart: role of mitochondria," *Archives of Biochemistry and Biophysics*, vol. 420, no. 2, pp. 287–297, 2003.

[45] B. Shin, D. B. Cowan, S. M. Emani, J. Pedro, and J. D. McCully, "Mitochondrial transplantation in myocardial ischemia and reperfusion injury," in *Advances in Experimental Medicine and Biology*, vol. 982, pp. 595–619, Springer, Cham, 2017.

[46] J. R. Burgoyne, H. Mongue-Din, P. Eaton, and A. M. Shah, "Redox signaling in cardiac physiology and pathology," *Circulation Research*, vol. 111, no. 8, pp. 1091–1106, 2012.

[47] M. Valko, D. Leibfritz, J. Moncol, M. T. D. Cronin, M. Mazur, and J. Telser, "Free radicals and antioxidants in normal physiological functions and human disease," *The International Journal of Biochemistry & Cell Biology*, vol. 39, no. 1, pp. 44–84, 2007.

[48] N. T. Aggarwal and J. C. Makielski, "Redox control of cardiac excitability," *Antioxidants & Redox Signaling*, vol. 18, no. 4, pp. 432–468, 2013.

[49] K. J. Dunham-Snary, Z. G. Hong, P. Y. Xiong et al., "A mitochondrial redox oxygen sensor in the pulmonary vasculature and ductus arteriosus," *Pflugers Archiv-European Journal of Physiology*, vol. 468, no. 1, pp. 43–58, 2016.

[50] A. V. Kuznetsov, S. Javadov, R. Margreiter, M. Grimm, J. Hagenbuchner, and M. J. Ausserlechner, "The role of mitochondria in the mechanisms of cardiac ischemia-reperfusion injury," *Antioxidants*, vol. 8, no. 10, article 454, 2019.

[51] H. Pei, Y. Yang, H. Zhao et al., "The role of mitochondrial functional proteins in ROS production in ischemic heart diseases," *Oxidative Medicine and Cellular Longevity*, vol. 2016, Article ID 5470457, 8 pages, 2016.

[52] M. Mimaki, X. Wang, M. McKenzie, D. R. Thorburn, and M. T. Ryan, "Understanding mitochondrial complex I assembly in health and disease," *Biochimica et Biophysica Acta (BBA)-Bioenergetics*, vol. 1817, no. 6, pp. 851–862, 2012.

[53] D. Jarreta, J. Orus, A. Barrientos et al., "Mitochondrial function in heart muscle from patients with idiopathic dilated cardiomyopathy," *Cardiovascular Research*, vol. 45, no. 4, pp. 860–865, 2000.

[54] N. Raimundo, "Mitochondrial pathology: stress signals from the energy factory," *Trends in Molecular Medicine*, vol. 20, no. 5, pp. 282–292, 2014.

[55] H. X. Wang, J. T. Luo, W. X. Tian et al., "γ-Tocotrienol inhibits oxidative phosphorylation and triggers apoptosis by inhibiting mitochondrial complex I subunit NDUFB8 and complex II subunit SDHB," *Toxicology*, vol. 417, pp. 42–53, 2019.

[56] T. Miyata, S. Takizawa, and C. van Ypersele de Strihou, "Hypoxia. 1. Intracellular sensors for oxygen and oxidative stress: novel therapeutic targets," *American Journal of Physiology-Cell Physiology*, vol. 300, no. 2, pp. C226–C231, 2011.

[57] G. M. Rosano, M. Fini, G. Caminiti, and G. Barbaro, "Cardiac Metabolism in Myocardial Ischemia," *Current Pharmaceutical Design*, vol. 14, no. 25, pp. 2551–2562, 2008.

[58] W. C. Stanley, F. A. Recchia, and G. D. Lopaschuk, "Myocardial substrate metabolism in the normal and failing heart," *Physiological Reviews*, vol. 85, no. 3, pp. 1093–1129, 2005.

[59] W. C. Stanley, G. D. Lopaschuk, J. L. Hall, and J. G. McCormack, "Regulation of myocardial carbohydrate metabolism under normal and ischaemic conditions: potential for pharmacological interventions," *Cardiovascular Research*, vol. 33, no. 2, pp. 243–257, 1997.

[60] S. W. Ballinger, C. Patterson, C. A. Knight-Lozano et al., "Mitochondrial integrity and function in atherogenesis," *Circulation*, vol. 106, no. 5, pp. 544–549, 2002.

[61] H. Tsutsui, S. Kinugawa, and S. Matsushima, "Oxidative stress and mitochondrial DNA damage in heart failure," *Circulation Journal*, vol. 72, Supplement A, pp. A31–A37, 2008.

[62] G. Petrosillo, F. M. Ruggiero, M. Pistolese, and G. Paradies, "Reactive oxygen species generated from the mitochondrial electron transport chain induce cytochrome c dissociation from beef-heart submitochondrial particles via cardiolipin peroxidation. Possible role in the apoptosis," *FEBS Letters*, vol. 509, no. 3, pp. 435–438, 2001.

Research Article

The Reduced Oligomerization of MAVS Mediated by ROS Enhances the Cellular Radioresistance

Yarong Du,[1,2] Dong Pan,[1] Rong Jia,[1,3] Yaxiong Chen,[1] Cong Jia,[2] Jufang Wang,[1,3] and Burong Hu [1,3]

[1]*Key Laboratory of Space Radiobiology of Gansu Province & CAS Key Laboratory of Heavy Ion Radiation Biology and Medicine, Institute of Modern Physics, Chinese Academy of Sciences, Lanzhou 730000, China*
[2]*College of Life Science, Northwest Normal University, Lanzhou 730070, China*
[3]*School of Nuclear Science and Technology, University of Chinese Academy of Sciences, Beijing 100039, China*

Correspondence should be addressed to Burong Hu; hubr@impcas.ac.cn

Although the mitochondrial antiviral signaling protein (MAVS), located in the mitochondrial outmembrane, is believed to be a signaling adaptor with antiviral feature firstly, it has been shown that suppression of MAVS enhanced radioresistance. The mechanisms underlying this radioresistance remain unclear. Our current study demonstrated that knockdown of MAVS alleviated the radiation-induced mitochondrial dysfunction (mitochondrial membrane potential disruption and ATP production), downregulated the expressions of proapoptotic proteins, and reduced the generation of ROS in cells after irradiation. Furthermore, inhibition of mitochondrial ROS by the mitochondria-targeted antioxidant MitoQ reduced amounts of oligomerized MAVS after irradiation compared with the control group and also prevented the incidence of MN and increased the survival fraction of normal A549 cells after irradiation. To our knowledge, it is the first report to indicate that MAVS, an innate immune signaling molecule, is involved in radiation response via its oligomerization mediated by radiation-induced ROS, which may be a potential target for the precise radiotherapy or radioprotection.

1. Introduction

Mitochondrial antiviral signaling protein (MAVS), a signaling adaptor with antiviral feature in the mitochondrial membrane, is critical for host defenses against viral infection. The homeotypic interaction between the domains of a caspase recruitment domain (CARD) of MAVS and the CARD of RIG-I forms protein aggregates on the surface of the mitochondria that can further activate MAVS proteins to form functional clusters to propagate antiviral innate immune response [1]. These high molecular weight MAVS complexes then recruit the IKK and TBK1/IKKi complexes to induce transcriptional expression of type I interferon (IFN) by promoting the nuclear translocation of the NF-κB and IRF3/7 transcription factors, respectively, and thus elicit the innate antiviral response (F. [2, 3]). Radiation-mediated NF-κB activation can directly induce expression of several proinflam-

matory cytokines including TNF, IL-1α, and IL-1β [4–6]. Thereby, radiotherapy can also activate innate and adaptive immune responses against tumors [7–10]. MAVS is involved in IFN-beta and IFN-stimulated gene expression in the response to ionizing radiation (IR). It was reported that physiologic responses to radio-/chemotherapy converge on an antiviral program in recruitment of the RLR pathway by a sncRNA- (small nuclear RNAs U1 and U2-) dependent activation of RIG-I which commences cytotoxic IFN signaling, and suppression of MAVS conferred radioresistance in normal and cancer cells [11]. However, the underlying mechanisms on MAVS suppression resulting in radioresistance remain poorly understood.

Mitochondria are involved in many important cell processes including cell respiration, reactive oxygen species (ROS) production, and apoptosis induction. Accumulating data indicate that IR damages the mitochondrial structure

(mass, morphology) and induces the dysfunctions of mitochondria in cells, such as the disorder of cellular respiration, changes of calcium balance and membrane potential, and elevation of ROS level, which result in the radiosensitivity [12–14]. MAVS is predominantly localized and executes its functions at the outer membrane of the mitochondria. It is not clear whether the change of MAVS expression influences the mitochondrial functions responding to IR and results in the radiosensitivity. Hou et al. reported that increased cellular ROS promoted MAVS forming functional prion-like aggregates to activate and propagate antiviral innate immune response [1, 15]. Conversely, repression of mitochondrial ROS (mtROS) production by cytochrome C oxidase complex subunit 5 inhibits MAVS aggregation and the downstream NF-κB and IRF3/7 signaling pathway [16]. IR can induce the generation of ROS. Whether and how did the increase of radiosenstivity partially via the activation of MAVS aggregation by radiation induce ROS?

In the present work, we attempted to investigate the mechanisms of radioresistance in cells after MAVS suppression. Our results demonstrated that suppression of MAVS alleviated the radiation-induced mitochondrial dysfunction and reduced the generation of ROS, compared to the normal cells. We also observed that more large aggregates of MAVS formed after IR and these MAVS aggregates lead to a gain of function in activating downstream factors. Radiation-induced MAVS oligomerization was inhibited by the addition of MitoQ, a mitochondria-targeted antioxidant, and decreased the radiosensitivity. Our results suggest a mechanism that MAVS oligomerization induced by radiation plays a role in the induction of radiosenstivity.

2. Materials and Methods

2.1. Cell Culture. A549 and BEAS-2B cells were obtained from Chinese Center for Disease Control and Prevention and cultured in RPMI 1640 medium (Gibco, USA) supplemented with 10% fetal bovine serum (Hyclone, USA) and 1% penicillin/streptomycin (Amresco, USA). HepG2 and MCF7 cells were purchased from Shanghai Cell Bank. Cells were cultured in DMEM medium (Gibco, USA) supplemented with 10% fetal bovine serum (Hyclone, USA) and 1% penicillin/streptomycin (Amresco, USA) at 37°C in a humidified atmosphere containing 5% CO_2. MitoQ was purchased from MedChemExpress.

2.2. Radiation. For X-ray irradiation, an X-ray facility (target: W, Faxitron Bioptics, USA) was used. The dose rate was ~0.78 Gy/min.

2.3. Gene Transfection. A549 cells were transfected with siRNA oligos at a final concentration of 50 nM. siRNA that targets MAVS and its negative control were purchased from RiboBio (Guangzhou, China). MAVS siRNAs (sense: 5′CCACCUUGAUGCCUGUGAATT-3′, antisense: 5′ UU CACAGGCAUCAAGGUGGTT-3′) were constructed as described [17]. Cells on the day before transfection were at a 70% of confluence and then, transfection was performed with Lipofectamine 2000 (Invitrogen, USA)

according to the manufacturer's instructions. The medium was exchanged for new culture medium 6 h posttransfection. The cells at 48 h after transfection were used in the following experiments.

2.4. Micronuclei (MN) Scoring. MN formation analysis is another generally used biological endpoint for the study of radiation effect. In brief, the cells in the slides were irradiated and continuously cultured for 48 h. The cells were fixed with Carnoy's solution for 20 min at room temperature and then stained with 20 μL of acridine orange in an aqueous solution (10 μg/mL). The cellular images were taken under the fluorescence microscope (Axio Imager. Z2) at 20x magnification, and 500 cells at least for each sample were scored, and cells with MN were calculated. Each experiment was repeated three times independently at least.

2.5. Colony Formation Assay. Briefly, the cells were trypsinized immediately after irradiation treatment and resuspended in RPMI 1640 medium with 10% FBS. A549 or BEAS-2B cells in appropriate amount were plated into each 60 mm dish to produce colonies. After being cultured for 14 days, the medium were removed and cells were stained with 0.5% crystal violet for 30 min. Colonies with more than 50 cells were manually counted. Plating efficiencies (PE) were calculated as follows: numbers of colonies formed/numbers of cells plated. Surviving fractions were calculated as follows: PE (irradiated)/PE (unirradiated).

2.6. Western Blot Assay. Cells were lysed in RIPA buffer (Beyotime, China) with Protease Inhibitor Cocktail Tablets (Roche, Switzerland). The protein concentration was quantified using a BCA protein assay kit (Thermo Scientific, USA). Equal amounts of protein were denatured with loading buffer (Beyotime, China) at 100°C for 10 min, subjected to 12% SDS-PAGE, and then blotted to a methanol-activated PVDF membrane (Millipore, USA). After blocked with 5% bovine serum albumin (ABCONE, China) in tris-buffered saline (TBS) for 1 h at room temperature, the membranes were respectively incubated overnight with the following antibodies at 4°C: MAVS (1 : 1000, Abcam, USA); pho-IRF3 (1 : 1000, Abcam, USA); caspase-3 (1 : 1000, Cell Signaling Technology, USA); IFN-I, IRF3, cyto C, Bax, and Bcl2 (1 : 1000, Affinity Biosciences, USA); and beta-actin (1 : 1000, ZSGB-BIO, China). After being washed for three times with TBS, the membranes were incubated with the horseradish peroxidase- (HRP-) labeled secondary antibody (1 : 2500, ZSGB-BIO, China) for 1 h at room temperature.

2.7. Mitochondrial Membrane Potential (MMP) Measurement. The status of the cellular mitochondrial membrane potential ($\Delta\Psi$m) was evaluated using JC-1 (BD Biosciences) and was quantified by the microplate reader (Tecan Infinite 200 M) [18]. Briefly, after being transfected with MAVS siRNA oligos for 48 h and followed by 2 Gy X-ray irradiation for 24 h, the cells (~1×10^6 cells/mL) were washed once with PBS and harvested into a centrifuge tube. Cells were resuspended in 500 μL JC-1 working solution, incubated at 37°C for 15 min, then washed twice with 1x assay buffer, and resuspended each cell pellet in 500 μL of 1x assay

buffer. Microplate reader and immunofluorescence microscopy (Axio Imager Z2) analysis at 10x magnification were performed after staining.

2.8. Cellular ATP Content. The intracellular ATP content was evaluated by measuring the luminescence with an ATP determination kit (Thermo Fisher, USA) according to the manufacturer's protocol. Briefly, the MAVS knockdown cells were irradiated by 0 and 2 Gy X-rays and then incubated for 1, 12, and 24 h. The cells were lysed in RIPA buffer on ice (Beyotime, China), and then, the supernatants were collected into 1.5 mL tubes. The chemiluminescence from each well was measured with an Infinite 200 Microplate Reader (Tecan, Switzerland) set at 25°C. The standard curve for a series of ATP concentrations was confirmed. ATP concentrations of sample were calculated from the standard curve. To eliminate errors caused by differences in sample content, we use a Bradford protein assay kit to normalize protein quantity. The amount of ATP was expressed as mmol/g of protein.

2.9. Apoptosis Assays. At the end of all interventions, A549 ($>1 \times 10^5$) cells were collected and stained with Annexin V-FITC/propidium iodide (PI) Kit (BD, USA) according to the manufacturer's protocol. The apoptosis of A549 was measured by a flow cytometer FlowSight (Amnis, USA).

2.10. ROS Level Measurement. The fluorescent probe, $2'7'$-dichlorofluorescin (DCFH-DA, Sigma, USA), was employed to quantify the level of ROS as described [19]. The medium of the cells to be detected was removed at the designed time points. Cells were washed once with 1x PBS solution and then stained with $10 \mu M$ DCFH-DA for 30 min at 37°C in the dark. The fluorescence images were taken under the fluorescence microscopy (Axio Imager Z2), and the relative fluorescence intensity for each treatment was quantified by means of ImageJ software.

2.11. Semidenaturing Detergent Agarose Gel Electrophoresis (SDD-AGE). SDD-AGE was performed according to a published protocol with minor modifications [20]. Briefly, equal amounts of the whole cell lysate were resuspended in one-third volume of 4x loading buffer consisting of 20% glycerol, 8% SDS, and 0.01% bromophenol blue in 2x TAE. Samples were incubated for 5 min at room temperature and loaded onto a vertical 1.5% agarose gel containing a final concentration of 0.1% SDS. Migration was performed for 35 min with a constant voltage of 100 V at 4°C. Proteins were transferred to PVDF membranes using a liquid transfer system in preparation for western blotting analysis. In order to confirm the consistency of the sample amounts, save half of the sample volume and boil it for western blotting analysis.

2.12. Level of Cytokine Measurement by ELISA Analysis. The cellular media of each treated group were collected at the indicated time points, and the levels of IL6, TNF-α, and IL-1β in the media were measured using ELISA kits (eBioscience) following the manufacturer's instructions. The fold changes of IL-6, TNF-α, and IL-1β levels were analyzed among different treatment group.

2.13. Statistical Analysis. The data were presented as mean ± SD of three independent experiments at least. The statistical significance (P value) was determined using Student's t-test for single comparisons and analysis of variance (ANOVA) for statistical comparison between different groups. If the P value < 0.05 was considered statistically significant between two sample comparison.

3. Results

3.1. MAVS Is Involved in Radiation Response. The levels of MAVS expression in different cell lines (A549, BEAS-2B, HepG2, and MCF7) were also analyzed. Figure 1(a) shows that the expressions of MAVS in BEAS-2B and MCF7 cells were lower. The expressions of MAVS were upregulated in both A549 (Figure 1(b)) and BEAS-2B (Figure 1(c)) cells at 1 h after X-ray radiation and then decreased. After being transfected with siRNA, the expression of MAVS in two cell lines was silenced and the upregulations of MAVS expressions induced by radiation were suppressed effectively, compared to the normal irradiated cells. Further, colony formation assays revealed that knockdown of MAVS gene increased the survival fraction of A549 (Figure 1(d)) and BEAS-2B (Figure 1(e)) after irradiation, compared to the normal control (NC) irradiation group. Consistently, knockdown of MAVS gene greatly diminished the incidence of MN in A549 and BEAS-2B cells after irradiation, compared to those NC cells after radiation (Figure 1(f)). These results confirm that MAVS responds to radiation and knockdown of MAVS increases the radioresistance.

3.2. Knockdown of MAVS Attenuates Radiation-Triggered MMP Disruption. MMP is a key indicator of mitochondrial function and activity because it reflects the process of elector transport and oxidative phosphorylation and is the driving force for mitochondrial ATP synthesis. Consequently, mitochondrial depolarization exhibited decreased red fluorescence and enhanced green fluorescence, and a collapse in the $\Delta\Psi$m is indicated by a reduction in the red/green fluorescence intensity ratio [21]. To investigate the effects of MAVS suppression on mitochondrial functions after irradiation, we carried out the measurement of MMP. Figure 2(a) shows that the states of JC-1 monomers (green color cell) and JC-1 aggregates (red color cell) in normal or MAVS knockdown cell lines after irradiation. Figure 2(b) shows the knockdown of MAVS prevented the radiation-induced decrease in the red-to-green fluorescence intensity ratio of JC-1 staining measured by the microplate reader. After irradiation, the fluorescence ratio of JC-1 aggregates dramatically decreased in the irradiated normal A549 cell lines at 24 h time point, while these ratios did not change obviously in the irradiated cells with MAVS knockdown, compared to their control cells. These results suggest that knockdown of MAVS attenuates radiation-triggered MMP disruption.

3.3. Knockdown of MAVS Alleviates the Reduction of ATP Production of Cells after Irradiation. Mitochondrial ATP content is a classic indicator of mitochondrial respiration

(a)

(b)

(c)

(d)

(e)

(f)
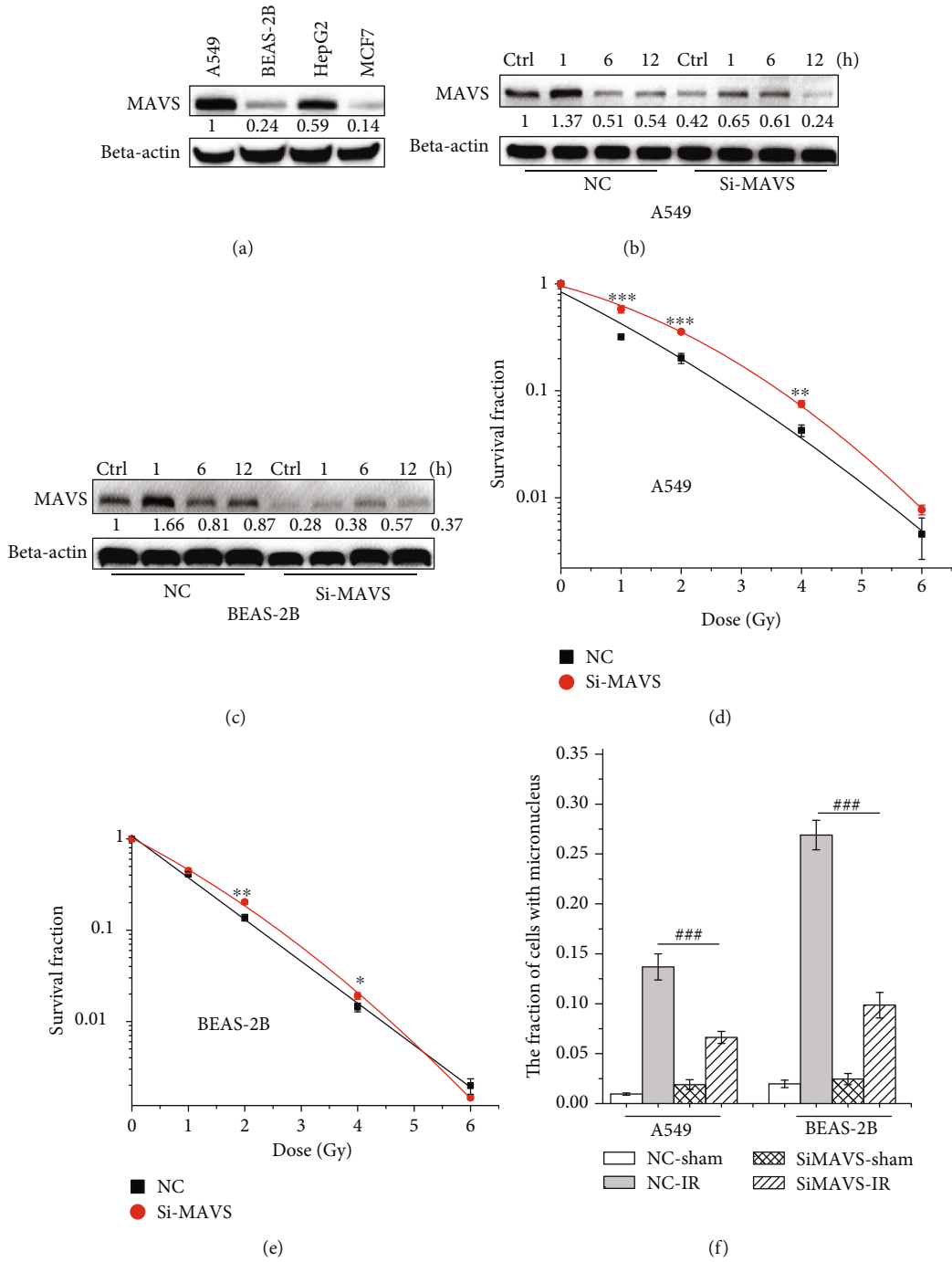
Figure 1: MAVS knockdown is resistant to radiation response. (a) The comparison of MAVS expression among A549, BEAS-2B, HepG2, and MCF7 cells. The expressions of MAVS at the indicated time points after 2 Gy X-rays in negative vector or MAVS-silenced A549 cells (b) and BEAS-2B cells (c) by western blot assay. Survival in A549 cells (d) and BEAS-2B cells (e) transfected with siRNA-MAVS or negative vector and then exposed to 0, 1, 2, 4, or 6 Gy X-rays measured by colony formation assay. (f) The fraction analysis of MN in negative vector and MAVS silenced in A549 and BEAS-2B cells after 2 Gy X-ray irradiation. Data are presented as mean ± SD. $^*P < 0.05$, $^{**}P < 0.01$, and $^{***}P < 0.001$ vs. the control group; $^{###}P < 0.001$ vs. the irradiation group.

function. We wanted to know whether the knockdown of MAVS influenced the ATP production and what would happen in the MAVS knockdown cells after irradiation. The levels of cellular ATP in the cells were measured using a luciferin/luciferase kit. As shown in Figure 2(c), the cellular ATP

content remained unchanged in both normal and knockdown cells at 1 h after irradiation. Interestingly, the content of ATP in the normal irradiated cells at 24 h postirradiation dramatically decreased, compared to that in MAVS knockdown cells. These data suggest that irradiation

(a)

(b)

(c)
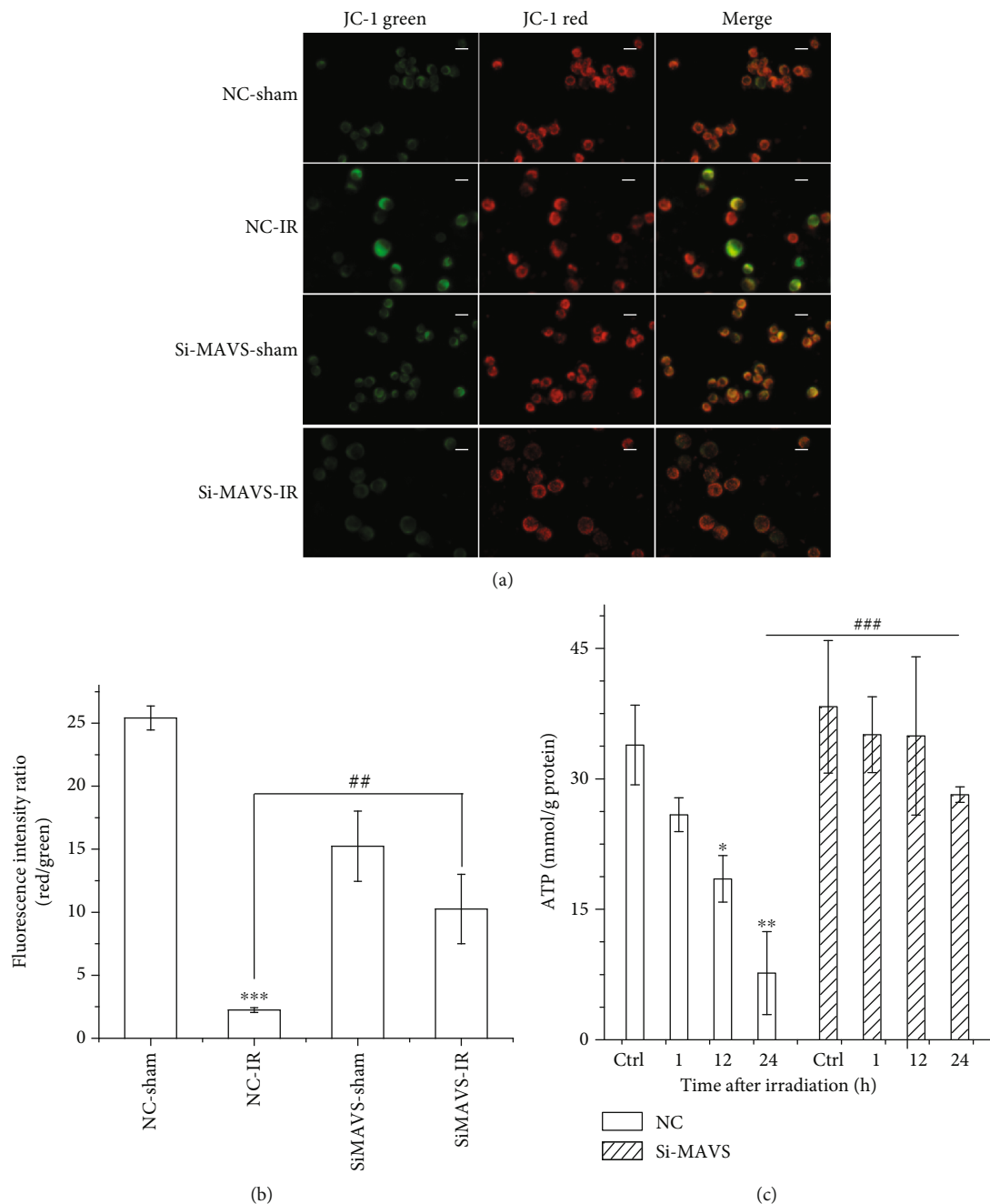
FIGURE 2: The impact of MAVS silencing combined with irradiation on the MMP and the mitochondrial ATP production of cells. The MMP of negative vector or MAVS-silenced cells at 24 h after 2 Gy X-ray irradiation was assessed by fluorescence microscope (a) and quantified by the microplate reader (b). Scale bar represents 10 μm. (c) The content of ATP was detected by ATP assay kit in negative vector and MAVS-silenced cells after irradiation. Data are presented as mean $\pm$ SD. $***P < 0.001$ vs. the control group; $^{\#\#}P < 0.01$ vs. the irradiation group. Red fluorescent represents intact MMP, and green fluorescent represents dissipation of MMP.

stimulation decreases the process of mitochondrial energy metabolism of cell and MAVS knockdown partially recovers the production of mitochondrial energy under the condition of stress stimulation.

3.4. Knockdown of MAVS Downregulates the Expressions of Apoptosis-Related Protein. Mitochondrial damage facilitates cytochrome C (cyto C) release from mitochondria into the cytoplasm and activates Bcl-2 family proteins, which leads to activation of the caspase cascade (apoptotic markers) and cellular apoptosis [22]. Our above results showed that knockdown of MAVS led to the alleviation of radiation-triggered MMP disruption. Thus, the expression levels of mitochondrial apoptosis-associated proteins, such as cyto C, caspase-3, Bax, and Bcl-2, were determined by western blot to deduce the role of MAVS suppression in the radiation-induced cell apoptosis. Figure 3(a) shows that MAVS knockdown suppressed the expression of cyto C,

(a)

(b)

(c)
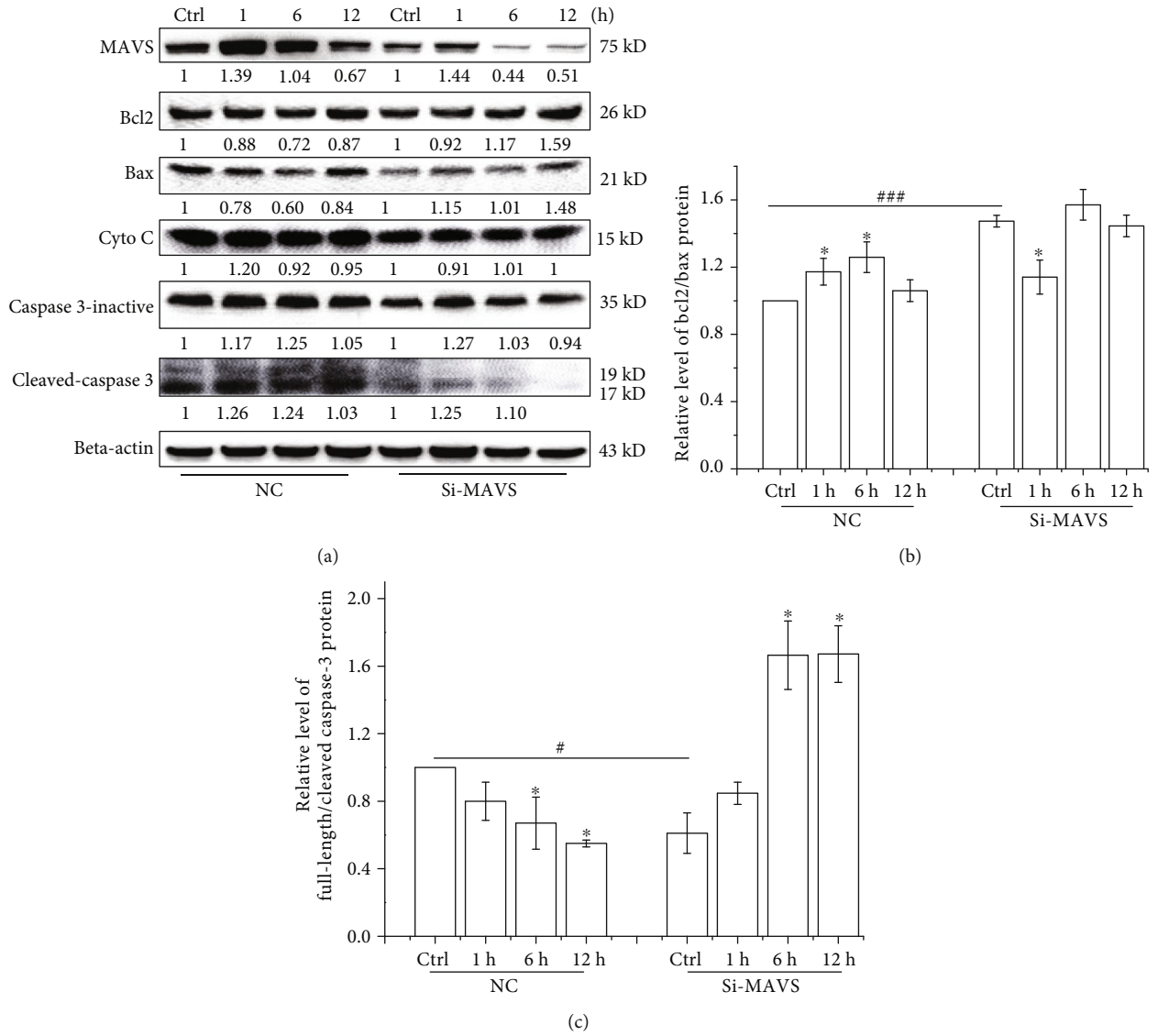
Figure 3: Continued.
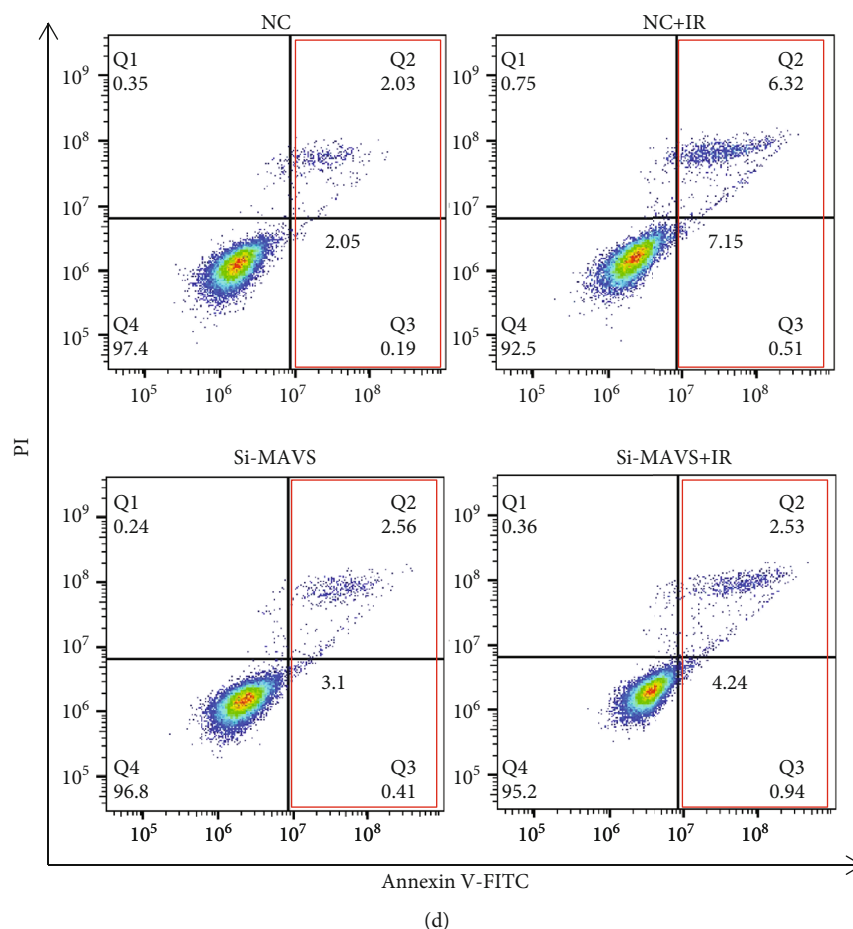
FIGURE 3: Effects of MAVS ectopic expression on cell apoptosis and the changes in regulatory proteins induced in negative vector and MAVS-silenced cells after irradiation. (a) The expression of apoptosis-related proteins was assessed and quantified in negative vector or MAVS-silenced A549 cells after 2 Gy X-ray irradiation by western blotting. (b) Value of Bcl2/Bax protein expression quantified using ImageJ software was presented. (c) Value of full length/cleaved caspase-3 protein expression quantified using ImageJ software was presented. (d) Apoptosis was quantified by the combined staining of Annexin V and PI, and fluorescence was analyzed using flow cytometry in negative vector and MAVS-silenced A549 cells after irradiation. Each data point represents the mean of three separate experiments. Values are presented as mean ± SD. $^{*}P < 0.05$, $^{**}P < 0.01$, and $^{***}P < 0.001$ vs. the control group; $^{\#}P < 0.05$, $^{\#\#}P < 0.01$, and $^{\#\#\#}P < 0.001$ vs. the irradiation group.

caspase-3-inactive (total caspase-3 protein), cleaved-caspase-3, and Bax. Cyto C expression increased in normal A549 cells at 1 h after irradiation, while kept relatively constant in MAVS knockdown cells after irradiation. The total caspase-3 expression increased at 1-6 h and then decreased at 12 h in the normal A549 cell after irradiation, while only increased at 1 h and then decreased at 6 h in the irradiated MAVS knockdown cells. However, the expression of activated caspase-3 (cleaved caspase-3) significantly increased in normal cells at 1-6 h after irradiation, while there is no obvious change in the MAVS knockdown A549 cells. Compared to the respective control, the expressions of activated caspase-3 were blunted in the irradiated MAVS knockdown cells. Overexpression of Bcl2 promotes cellular survival, and over-expression of Bax enhances the cellular apoptosis. Thus, the higher the ratio of Bcl2/Bax, the more cellular survival it reflects [23]. In comparison to the normal A549, the ratio of Bcl2/Bax is slightly higher in MAVS knockdown A549 cells at 6 and 12 h after irradiation (Figure 3(b)). These results

indicate that knockdown of MAVS suppresses the expressions of apoptosis-associated proteins and protect the cells from the radiation-induced death. Meanwhile, our results from flow cytometry confirmed that knockdown of MAVS inhibited cell apoptosis after X-ray radiation (Figure 3(c)).

3.5. Knockdown of MAVS Inhibits the Generation of Radiation-Induced ROS. Generation of higher level of ROS in cells is related to cell apoptosis [24]. To determine the relationship between the knockdown of MAVS and the level of ROS after irradiation, we measured the ROS level in cells at 15 min, 1, and 6 h after exposed to 2 Gy X-rays. Figure 4 shows that the ROS level increased in normal A549 cells at 15 min after irradiation, while it remained relatively constant in the MAVS knockdown cells after irradiation. Compared to the irradiated MAVS knockdown A549 cells, the ROS level in the normal cells increased by 3.0-fold at 15 min after irradiation. There were no big differences between normal and MAVS knockdown A549 cells at 1 and 6 h after irradiation.
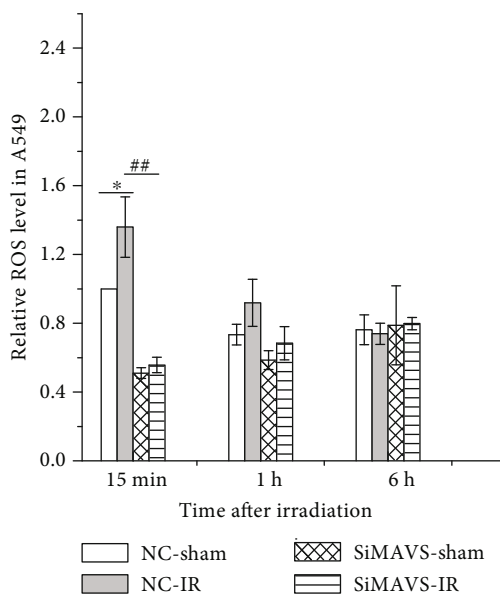
FIGURE 4: The relative levels of ROS induced by 2 Gy X-ray radiation in negative vector and MAVS-silenced A549 cells. Data are presented as mean ± SD. $^*P < 0.05$ vs. the control group; $^{##}P < 0.01$ vs. the irradiation group.

3.6. The Mitochondria-Targeted Antioxidant MitoQ Reduces MAVS Oligomerization.

Study demonstrated that increased cellular ROS promoted MAVS aggregates to activate the downstream signaling response [1]. To evaluate the influence of radiation or radiation-induced ROS on MAVS oligomerization, we adapted a SDD-AGE system to detect MAVS aggregates after irradiation. MitoQ is a mitochondria-targeted antioxidant, which contains ubiquinol as the active antioxidant component [25]. Cells pretreated with $1 \mu m$ MitoQ for 2 h dramatically reduced MAVS oligomerization, compared to the X-ray radiation alone group, which is at least a 75% of decrease in the amount of MAVS oligomers (Figure 5), while there is no increase of MAVS oligomers in MAVS knockdown A549 cells after irradiation. These results suggest that radiation-induced ROS activate the oligomerization of MAVS and the phenomenon will be reduced if the MAVS is suppressed.

3.7. The Pretreatment of MitoQ Reduces the Cellular Radiosensitivity.

Figure 6(a) shows that the incidence of MN was greatly diminished in A549 cells pretreated with MitoQ, compared to the knockdown of MAVS after 1 Gy or 2 Gy X-ray irradiation. Further, survival fraction of A549 cells pretreated with MitoQ and then irradiation was increased, compared to the irradiated cells alone (Figure 6(b)). MitoQ did not affect the biological effect of MAVS knockdown cell lines after irradiation.

3.8. Knockdown of MAVS Inhibits the Generation of IL6 and Expression of IFN.

Cytokines, such as IL6, TGFα, and IL1β, are the downstream of MAVS signaling pathway and involve in radiation induced sensitivity. Thus, we detected the relative level of these cytokines in normal and MAVS knockdown cells after irradiation. Irradiation stimulation reduced

the level of IL6 at early time (15 min after) then induced the upregulation of level of IL6 at 6 h time point. Knockdown of MAVS suppressed the level of IL6 after irradiation, compared to the irradiated normal cells (Figure 7(a)). The levels of TGFα and IL1β were not obviously different between the normal and MAVS knockdown cells after irradiation (data not shown). Figure 7(b) shows that knockdown of MAVS suppressed the expression of IFN and also inhibited the expression of total IRF3 (IFN regulatory factor-3) and pho-IRF3, suggesting that MAVS knockdown suppresses the inflammation signaling pathway and may contribute to the radioresistance.

4. Discussion

IR, because of its cell killing capability, has been utilized to therapy cancers, and radiotherapy is one of the three main therapies (surgery, chemotherapy, and radiotherapy) for many types of tumor [26]. Radiotherapy can increase innate and adaptive immune responses against tumors, and the type I IFN signaling pathway is involved in this process [27]. It was reported that MAVS is necessary for IFN-beta induction and interferon-stimulated gene expression in the response to IR and suppression of MAVS conferred radioresistance in normal and cancer cells [11]. However, the mechanisms underlying this process are largely unknown.

In the current study, we first verified the phenomenon of suppression of MAVS conferring radioresistance by means of clone survival and MN assay. Further, because MAVS is a protein which localized the outer membrane of mitochondrial, we attempted to investigate the influences of suppression of MAVS on mitochondrial functions to probe the potential mechanisms. Although we also observed a slight changes of MMP in MAVS-silenced cells, the cellular collapse of the $\Delta\Psi m$ in the irradiated normal cells was dramatically more than that in the irradiated MAVS-silenced cells at 24 h after irradiation. The content of ATP in normal cells after irradiation dramatically decreased, but the decrease was relieved in the MAVS-silenced cells after irradiation. Mitochondrial dysfunction can lead to the release of Cyto C and cell apoptosis. Our results demonstrated that the expressions of apoptosis protein Cyto C and active caspase-3 in the irradiated MAVS knockdown cell line were lower and the ratio of Bcl2/Bax proteins was higher than that of the irradiated normal cells, indicating that apoptosis decreased in MAVS knockdown cells after irradiation. These data suggest that knockdown of MAVS not only inhibit the radiation-induced mitochondrial dysfunction but also block the transmission of cellular apoptosis signaling pathway, which results in the subsequent radioresistance and may also indicate one of mechanisms on radioresistance.

In general case, except for the direct damage to DNA and other cellular components, IR also instantaneously causes the formation of water radiolysis products that contain ROS (chemical process occurred in the extremely early stage of radiation). ROS are also suggested to be released from biological sources in irradiated cells [28]. In our study, we observed that generation of radiation-induced ROS in MAVS knockdown cells decreased by 3.0-fold at 15 min after irradiation.
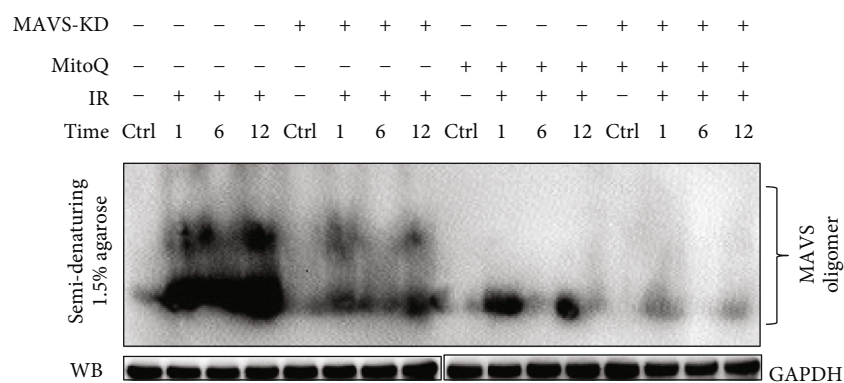
FIGURE 5: MAVS oligomerization was detected in negative vector or MAVS-silenced A549 cells at the indicated times after X-ray radiation by nonreducing gels and western blotting analysis. To define the role of ROS in MAVS oligomerization, MitoQ was used as scavenging mitochondria ROS agent.

(a)

(b)
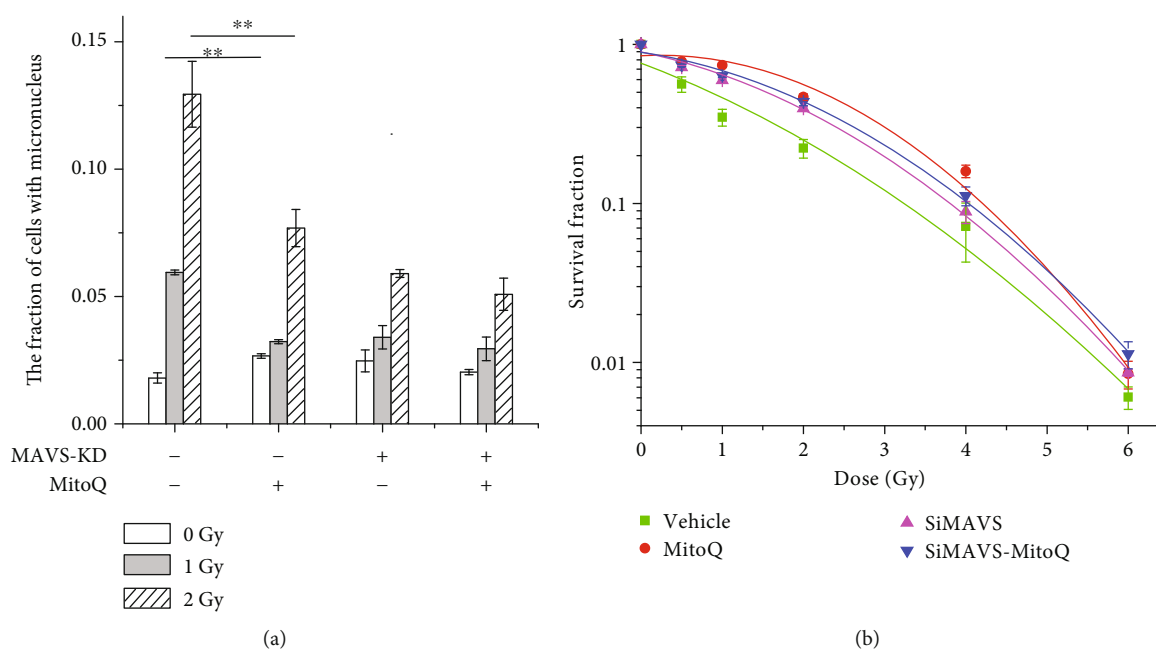
FIGURE 6: Biological effect changes in negative vector and MAVS-silenced A549 cells after being pretreated with MitoQ and X-ray irradiation. (a) The fraction analysis of MN in negative vector and MAVS-silenced A549 cells pretreated with MitoQ for 2 h and then radiated with 1 Gy and 2 Gy X-ray. (b) The survival analysis of negative vector and MAVS-silenced A549 cells pretreated with MitoQ after exposed to 0, 1, 2, 4, and 6 Gy X-rays. Data are presented as mean ± SD. $^*P < 0.05$, $^{**}P < 0.01$, and $^{***}P < 0.001$ vs. the irradiation group.

Buskiewicz et al. reported that chemically generated oxidative stress (using glucose oxidase) stimulated the formation of MAVS oligomers, which led to mitochondrial hyperpolarization and decreased ATP production and spare respiratory capacity [29]. MAVS oligomerization directly suppresses the function of mitochondrial complexes I to IV and trigger the deficiency of ATP and the effusion of Cyto C [30]. Based on their findings, we speculate that MAVS involves in radiosensitivity through its oligomerization mediated by ROS.

According to their measure method, we first observed that the irradiation increased the oligomerization of MAVS in A549, which was significantly inhibited by MitoQ pretreatment, and there was no increased oligomer of MAVS in the knockdown cell. MitoQ pretreatment also decreased the radiation-induced fractions of MN and increased the survival of normal A549 cells. Additionally, knockdown of MAVS also suppressed the expression of IRF3, type I IFNs, and almost eliminated pho-IRF3. Radiation stimulation induced the upregulation of IL6 level at 6 h after IR. Knockdown of MAVS suppressed the increase of the level of IL6 after IR. These results suggest that oligomerization of MAVS mediated by radiation-induced ROS form prion-like aggregates to induce the mitochondrial dysfunction and the activation NF-κB and IFN-type I. Suppression of MAVS reduces MAVS oligomer, thus decreasing radiation-induced mitochondrial dysfunction and inhibiting the pathway of cell apoptosis and the release of part of proinflammation cytokines, as well as the generation of mtROS again,

(a)

(b)
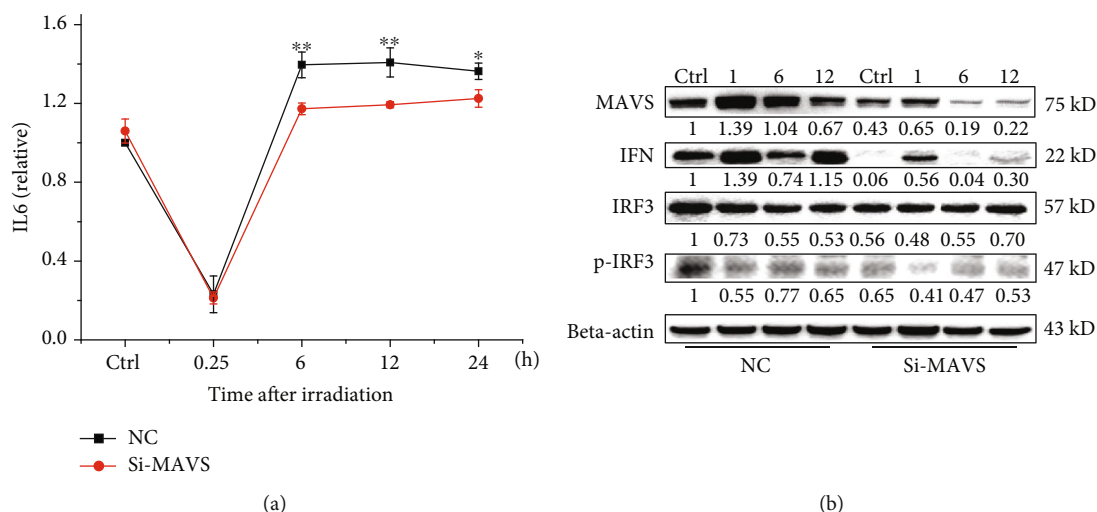
FIGURE 7: Associated immune factor was detected by ELISA assay (a) and western blotting (b) in negative vector and MAVS-silenced A549 cells at the indicated times after X-ray radiation. Data are presented as mean ± SD. $^*P < 0.05$, $^{**}P < 0.01$, and $^{***}P < 0.001$ vs. the irradiation group.

resulting in the radioresistance. These findings imply a model that ROS generation during initial chemical progress after irradiation could be an initial upstream signaling factor of MAVS responding to radiation, and then this kind of ROS-mediating initial MAVS oligomerization induces the increase of mtROS, which in turn induces more oligomers of MAVS and expand the radiation-induced damage (Figure 8). In order to confirm the conclusion, we also constructed the overexpression MAVS plasmid and transfected to A549 or BEAS-2B cell lines but unfortunately could not get stable over expression cell lines. From previous experiment results, we speculated the occurrence of mitochondrial dysfunction and apoptosis in MAVS overexpression, resulting to apoptosis or necrosis in the MAVS overexpression cell lines.

5. Conclusions

MAVS, an innate immune signaling molecule, is involved in radiation response via its oligomerization mediated by radiation-induced ROS. Knockdown of MAVS alleviates the radiation-induced mitochondrial dysfunction and decreases the expressions of proapoptotic proteins in cells after irradiation, which results in the radioresistance. Our study implies that MAVS may be a potential target for the precise radiotherapy or radioprotection.

Data Availability

The data used to support the findings of this study are available from the corresponding authors upon request.

Disclosure

Dong Pan's present address is Department of Dermatology, Duke University Medical Center, Durham, NC 27710, USA.
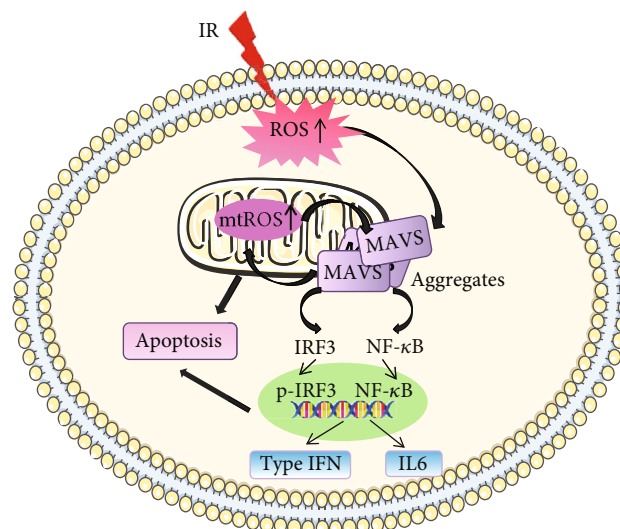
FIGURE 8: The speculated model of ROS-mediated MAVS oligomerization resulting in the radioresistance.

Conflicts of Interest

The authors do not have any conflicts of interest.

Authors' Contributions

Yarong Du designed and performed experiments, analyzed the results, and wrote the manuscript. Dong Pan, Rong Jia, Yaxiong Chen, and Cong Jia helped with the experiments, data interpretation, and manuscript preparation. Jufang Wang and Burong Hu involved in the experimental design, data analysis, and manuscript revise. All authors read and approved the final manuscript.

Acknowledgments

References

[1] F. Hou, L. Sun, H. Zheng, B. Skaug, Q. X. Jiang, and Z. J. Chen, "MAVS forms functional prion-like aggregates to activate and propagate antiviral innate immune response," *Cell*, vol. 146, no. 3, pp. 448–461, 2011.

[2] F. Liu and J. Gu, "Retinoic acid inducible gene-I, more than a virus sensor," *Protein & Cell*, vol. 2, no. 5, pp. 351–357, 2011.

[3] M. Yoneyama, M. Kikuchi, T. Natsukawa et al., "The RNA helicase RIG-I has an essential function in double-stranded RNA- induced innate antiviral responses," *Nature Immunology*, vol. 5, no. 7, pp. 730–737, 2004.

[4] D. E. Hallahan, D. R. Spriggs, M. A. Beckett, D. W. Kufe, and R. R. Weichselbaum, "Increased tumor necrosis factor alpha mRNA after cellular exposure to ionizing radiation," *Proceedings of the National Academy of Sciences of the United States of America*, vol. 86, no. 24, pp. 10104–10107, 1989.

[5] J.-H. Hong, C. S. Chiang, C. Y. Tsao, P. Y. Lin, W. H. McBride, and C. J. Wu, "Rapid induction of cytokine gene expression in the lung after single and fractionated doses of radiation," *International Journal of Radiation Biology*, vol. 75, no. 11, pp. 1421–1427, 1999.

[6] A. O'Brien-Ladner, M. E. Nelson, B. F. Kimler, and L. J. Wesselius, "Release of interleukin-1 by human alveolar macrophages after in vitro irradiation," *Radiation Research*, vol. 136, no. 1, pp. 37–41, 1993.

[7] B. Burnette, Y. X. Fu, and R. R. Weichselbaum, "The confluence of radiotherapy and immunotherapy," *Frontiers in Oncology*, vol. 2, p. 143, 2012.

[8] B. Burnette and R. R. Weichselbaum, "Radiation as an immune modulator," *Seminars in Radiation Oncology*, vol. 23, no. 4, pp. 273–280, 2013.

[9] L. Deng, H. Liang, B. Burnette et al., "Irradiation and anti-PD-L1 treatment synergistically promote antitumor immunity in mice," *The Journal of Clinical Investigation*, vol. 124, no. 2, pp. 687–695, 2014.

[10] B. Frey, Y. Rubner, R. Wunderlich et al., "Induction of abscopal anti-tumor immunity and immunogenic tumor cell death by ionizing irradiation - implications for cancer therapies," *Current Medicinal Chemistry*, vol. 19, no. 12, pp. 1751–1764, 2012.

[11] D. R. E. Ranoa, A. D. Parekh, S. P. Pitroda et al., "Cancer therapies activate RIG-I-like receptor pathway through endogenous non-coding RNAs," *Oncotarget*, vol. 7, no. 18, pp. 26496–26515, 2016.

[12] J. K. Leach, G. Van Tuyle, P. S. Lin, R. Schmidt-Ullrich, and R. B. Mikkelsen, "Ionizing radiation-induced, mitochondria-dependent generation of reactive oxygen/nitrogen," *Cancer Research*, vol. 61, no. 10, pp. 3894–3901, 2001.

[13] S. M. Nugent, C. E. Mothersill, C. Seymour, B. McClean, F. M. Lyng, and J. E. Murphy, "Increased mitochondrial mass in cells with functionally compromised mitochondria after exposure to both direct gamma radiation and bystander factors," *Radiation Research*, vol. 168, no. 1, pp. 134–142, 2007.

[14] A. Ogura, S. Oowada, Y. Kon et al., "Redox regulation in radiation-induced cytochrome *c* release from mitochondria of human lung carcinoma A549 cells," *Cancer Letters*, vol. 277, no. 1, pp. 64–71, 2009.

[15] M. C. Tal, M. Sasai, H. K. Lee, B. Yordy, G. S. Shadel, and A. Iwasaki, "Absence of autophagy results in reactive oxygen species-dependent amplification of RLR signaling," *Proceedings of the National Academy of Sciences of the United States of America*, vol. 106, no. 8, pp. 2770–2775, 2009.

[16] Y. Zhao, X. Sun, X. Nie et al., "COX5B regulates MAVS-mediated antiviral signaling through interaction with ATG5 and repressing ROS production," *PLoS Pathogens*, vol. 8, no. 12, article e1003086, 2012.

[17] Y. Huang, H. Liu, S. Li et al., "MAVS-MKK7-JNK2 defines a novel apoptotic signaling pathway during viral infection," *PLoS Pathogens*, vol. 10, no. 3, article e1004020, 2014.

[18] S. Salvioli, A. Ardizzoni, C. Franceschi, and A. Cossarizza, "JC-1, but not $DiOC_6(3)$ or rhodamine 123, is a reliable fluorescent probe to assess $\Delta\Psi$ changes in intact cells: implications for studies on mitochondrial functionality during apoptosis," *FEBS Letters*, vol. 411, no. 1, pp. 77–82, 1997.

[19] X. S. Wan, Z. Zhou, J. H. Ware, and A. R. Kennedy, "Standardization of a fluorometric assay for measuring oxidative stress in irradiated cells," *Radiation Research*, vol. 163, no. 2, pp. 232–240, 2005.

[20] R. Halfmann and S. Lindquist, "Screening for amyloid aggregation by semi-denaturing detergent-agarose gel electrophoresis," *Journal of Visualized Experiments*, vol. 17, no. 17, 2008.

[21] Y. Liu, J. Yan, C. Sun et al., "Ameliorating mitochondrial dysfunction restores carbon ion-induced cognitive deficits via co-activation of NRF2 and PINK1 signaling pathway," *Redox Biology*, vol. 17, pp. 143–157, 2018.

[22] A. Hamaï, C. Richon, F. Meslin et al., "Imatinib enhances human melanoma cell susceptibility to TRAIL-induced cell death: relationship to Bcl-2 family and caspase activation," *Oncogene*, vol. 25, no. 58, pp. 7618–7634, 2006.

[23] F. Pettersson, A. G. Dalgleish, R. P. Bissonnette, and K. W. Colston, "Retinoids cause apoptosis in pancreatic cancer cells via activation of RAR-γ and altered expression of Bcl-2/Bax," *British Journal of Cancer*, vol. 87, no. 5, pp. 555–561, 2002.

[24] X. Wang, J. Zhang, J. Fu et al., "Role of ROS-mediated autophagy in radiation-induced bystander effect of hepatoma cells," *International Journal of Radiation Biology*, vol. 91, no. 5, pp. 452–458, 2015.

[25] G. F. Kelso, C. M. Porteous, C. V. Coulter et al., "Selective targeting of a redox-active ubiquinone to mitochondria within cells: antioxidant and antiapoptotic properties," *The Journal of Biological Chemistry*, vol. 276, no. 7, pp. 4588–4596, 2001.

[26] J. Thariat, J. M. Hannoun-Levi, A. Sun Myint, T. Vuong, and J. P. Gerard, "Past, present, and future of radiotherapy for the benefit of patients," *Nature Reviews Clinical Oncology*, vol. 10, no. 1, pp. 52–60, 2013.

[27] M. C. Boelens, T. J. Wu, B. Y. Nabet et al., "Exosome transfer from stromal to breast cancer cells regulates therapy resistance pathways," *Cell*, vol. 159, no. 3, pp. 499–513, 2014.

[28] M. A. Kang, E. Y. So, A. L. Simons, D. R. Spitz, and T. Ouchi, "DNA damage induces reactive oxygen species generation through the H2AX- Nox1/Rac1 pathway," *Cell Death & Disease*, vol. 3, no. 1, article e249, 2012.

[29] I. A. Buskiewicz, T. Montgomery, E. C. Yasewicz et al., "Reactive oxygen species induce virus-independent MAVS oligomerization in systemic lupus erythematosus," *Science Signaling*, vol. 9, no. 456, article ra115, 2016.

[30] M. S. Hwang, J. Boulanger, J. D. Howe et al., "MAVS polymers smaller than 80 nm induce mitochondrial membrane remodeling and interferon signaling," *The FEBS Journal*, vol. 286, no. 8, pp. 1543–1560, 2019.

Review Article

A Review of Adropin as the Medium of Dialogue between Energy Regulation and Immune Regulation

Shuyu Zhang,[1] **Qingquan Chen,**[1] **Xuchen Lin,**[1] **Min Chen** ⑩**,**[1] **and Qicai Liu** ⑩[2]

[1]*Department of Laboratory Medicine, Fujian Medical University, 350004 Fuzhou, China*
[2]*Center for Reproductive Medicine, 1st Affiliated Hospital, Fujian Medical University, 350004 Fuzhou, China*

Correspondence should be addressed to Min Chen; cmjy503@163.com and Qicai Liu; lqc673673673@163.com

Adropin is a secretory protein encoded by the energy balance gene and is closely associated with regulation of energy metabolism and insulin resistance. The clinical findings demonstrated its decreased expression in various inflammatory diseases, its negative correlation with the expression levels of inflammatory cytokines, and its potential anti-inflammatory effects. We speculate that adropin plays a pivotal regulatory role in immune cells and inflammatory factors. In this study, we reviewed the advances in researches concentrated on immunological effects of adropin.

1. Introduction

Adropin is a peptide hormone encoded by the energy homeostasis-associated (ENHO) gene. The nomenclature of adropin is derived from the Latin roots "aduro" and "pinquis," meaning "promoting fat burning," with identical amino acid sequences in humans and mice [1]. At present, the half-life of adropin has still remained elusive, and its half-life may last from several minutes to half an hour, which is similar to other secretory proteins [2]. The biological effects of adropin are mediated through activation of the orphan G protein-coupled receptor 19 (GPR19) [3, 4]. In 2008, Kumar et al. [1] found that the ENHO gene was localized on chromosome 9p13.3 in obese mice model and consisted of 25 exons. They also reported that adropin is consisted of 76 amino acids, and it was originally described as a secreted peptide, with residues 1-33 encoding a secretory signal peptide sequence. Besides, it was mainly expressed in tissues, such as liver, brain, heart, kidney, pancreas, coronary artery, and umbilical vein, and its expression was the highest in the brain. Simultaneously, the expression of ENHO gene in mouse brain by means of autoradiography and their results revealed that ENHO was highly expressed in the regions controlling complex behaviors, such as circadian rhythm and stress response. Similarly, serum adropin levels

are regulated by metabolic status and diet. In the study of K. Ganesh [5], adropin levels were high in chow-fed conditions and were low in fasting, and serum adropin levels were significantly higher in mice fed a high-fat low-carbohydrate diet than in mice fed a low-fat high-carbohydrate diet. Meanwhile, diet-induced obesity (DIO) suppressed the serum adropin levels of mice. However, human serum adropin levels are not affected by acute signals such as fasting or meal, but by obesity and dietary preferences. There is a positive association between human serum adropin levels and fat intake and a negative association with carbohydrate intake [6–8].

The expression level of adropin in normal human plasma is 1-10 μg/L, in which its expression level in males is slightly higher than that in females [6]. Meanwhile, the expression level of adropin is reduced with increase of age [9].

2. Overview on Functions of Adropin

A number of scholars studied functions of adropin, while they have mainly concentrated on metabolic disorders and cardiovascular diseases. Adropin enhances glucose oxidation and ameliorates metabolic inflexibility of utilizing glucose in obese and insulin-resistant mice. The underlying mechanisms appear to involve suppressions of carnitine

palmitoyltransferase-1B (CPT-1B) and CD36, two key enzymes in fatty acid utilization. Adropin treatment activates pyruvate dehydrogenase (PDH), a rate-limiting enzyme in glucose oxidation, and downregulates PDH kinase-4 (PDK-4) that inhibits PDH [10]. Adropin can up-regulate the endothelial nitric oxide synthase (eNOS) expression through VEGFR2-PI3K-Akt or VEGFR2-ERK1/2 pathway, increase the release of NO, improve endothelial cell function, and promote the neovascularization, thereby protecting the cardiovascular system [11]. In recent years, the role of adropin in the central nervous system (CNS) has also been studied. It has been shown that adropin acts as a plasma membrane-binding protein in CNS, interacts with brain-specific Notch1 ligand NB3, regulates physical activity and motor coordination through the NB3/Notch signaling pathway, and plays a pivotal role in cerebellum development in mice [12]. It also exerts neuroprotective effects by reducing oxidative damage [9]. In studies of the association of adropin with atherosclerosis and insulin resistance, in addition to its role in regulating metabolism and improving functions of endothelial cells, the immunological effects of adropin have gradually attracted scholars' attention.

3. Metabolic Disorders Caused by the Immune Regulation of Adropin

Obesity intervention results from a persistent energy imbalance. Adipose tissue is increasingly considered as a key regulator of energy balance and is a "crossroad" of energy homeostasis, inflammation, and atherosclerosis [13]. If the number of free fatty acid (FFA) exceeds the storage capacity of the adipose tissue, it may overflow and may be accumulated in metabolic tissues, such as skeletal muscle, liver, and pancreas; excessive FFA can activate inflammatory pathways and damage immune system and adipose tissues, thereby leading to cell dysfunction [14, 15]. Therefore, fatty acid can regulate the function and inflammation phenotype of immune cells, playing a substantial role in causing metabolic disorders, such as insulin resistance and type 2 diabetes.

Numerous studies demonstrated that visceral adipose tissue is associated with macrophages in chronic inflammatory conditions around the adipocytes, and infiltration of visceral adipose tissues by proinflammatory macrophages is a key event driving adipose-tissue inflammation and insulin resistance [14]. The macrophages in the adipose tissue are the main source of inflammatory cytokines, such as tumor necrosis factor α (TNF-α), a multifunctional proinflammatory cytokine that plays a significant role in the inflammatory process [16, 17]. The fat content is positively correlated with the number of macrophages, and the ablation of adipose tissues leads to a decrease in systemic inflammation [18]. Adropin can regulate the expressions of lipogenic genes and peroxisome proliferator-activated receptor γ (PPAR-γ) in the adipose tissues and liver, and is a main regulator of lipogenesis as well. Besides, PPAR-γ was found to be significantly decreased in mice with overexpression of adropin [1]. A recently conducted study demonstrated that adropin promotes the proliferation of 3T3-L1 preadipocyte via mediating ERK1/2 and AKT (Figure 1), and inhibits differentiation of preadipocytes into mature adipocytes by reducing lipid accumulation and expressions of adipogenic genes in 3T3-L1 cells and rat preadipocytes [19]. Thus, adropin can reduce macrophage infiltration by decreasing fat accumulation, thereby improving inflammation.

Treg cells are involved in controlling the inflammatory state of adipose tissues. Treg cells are the main cells responsible for the negative regulation of immune-mediated inflammation. It is involved in the negative regulation of autoimmune diseases, allergies, acute, and chronic infections, cancer, and metabolic inflammation. In obese mice, the number of Treg cells in adipose tissue is strikingly reduced, and the imbalance of immune cells leads to fat inflammation. Meanwhile, the decrease of Treg cells in adipose tissue also leads to the occurrence of insulin resistance, so it is believed that Treg cells play an important role in metabolic regulation [20, 21]. Additionally, a previous research reported that adropin deficiency associates with loss of Treg cells and leads to autoimmune diseases [22].

PPAR-γ is highly expressed in adipose tissues and plays an irreplaceable role in adipocyte differentiation, and is involved in fatty acid metabolism. In addition, activation of PPAR-γ has potential effects on the expressions and secretions of numerous factors, including reducing expressions and secretions of adipokines, such as adiponectin and resisting, and proinflammatory cytokines (e.g., interleukin 6 (IL-6), TNF-α, and monocyte chemotactic protein-1 (MCP-1)); MCP-1 and TNF-α can induce macrophage infiltration and inflammation [23]. Therefore, activation of PPAR-γ may reduce macrophage infiltration and inflammation of adipose tissues. The study demonstrated that adropin regulates the anti-inflammatory or proinflammatory phenotypes of macrophages by up-regulating the expression of PPAR-γ [24]. Although, in current research, the reason for the tissue-specific effects of adropin on PPAR-γ expression is often unclear, PPAR-γ may be an important target for adropin to exert anti-inflammatory effects (Figure 2). Another study showed that M1 macrophages use aerobic glycolysis to provide energy for rapid, transient bactericidal effect or proinflammatory responses. Conversely, M2 macrophages depend on the energy provided by fatty acid oxidation (FAO) to exert anti-inflammatory effects for a long period of time [25]. The change in the polarization of macrophages varies according to the diversity of cytokines present in the microenvironment or by the stimuli of an antigen. It involves interferon-regulatory factors, such as PPARs, hypoxia-inducible factors (HIFs), and signal transducers and activators of transcription [26]. It also has been reported that in macrophages, PPAR-γ has been shown to play critical roles in inflammation and metabolism [27]. However, further research is required to indicate whether adropin can alter the macrophage phenotype by regulating cell metabolism.

Adropin plays a significant role in other metabolic disorders, such as diabetic nephropathy, polycystic ovary syndrome (PCOS), etc. Studies indicated that adropin can significantly reduce the expressions of TNF-α, IL-6, and inducible NOS (iNOS) at the mRNA level in pancreatic tissues of diabetic rats [28, 29]. Furthermore, decreased level of adropin is associated with an increase in the
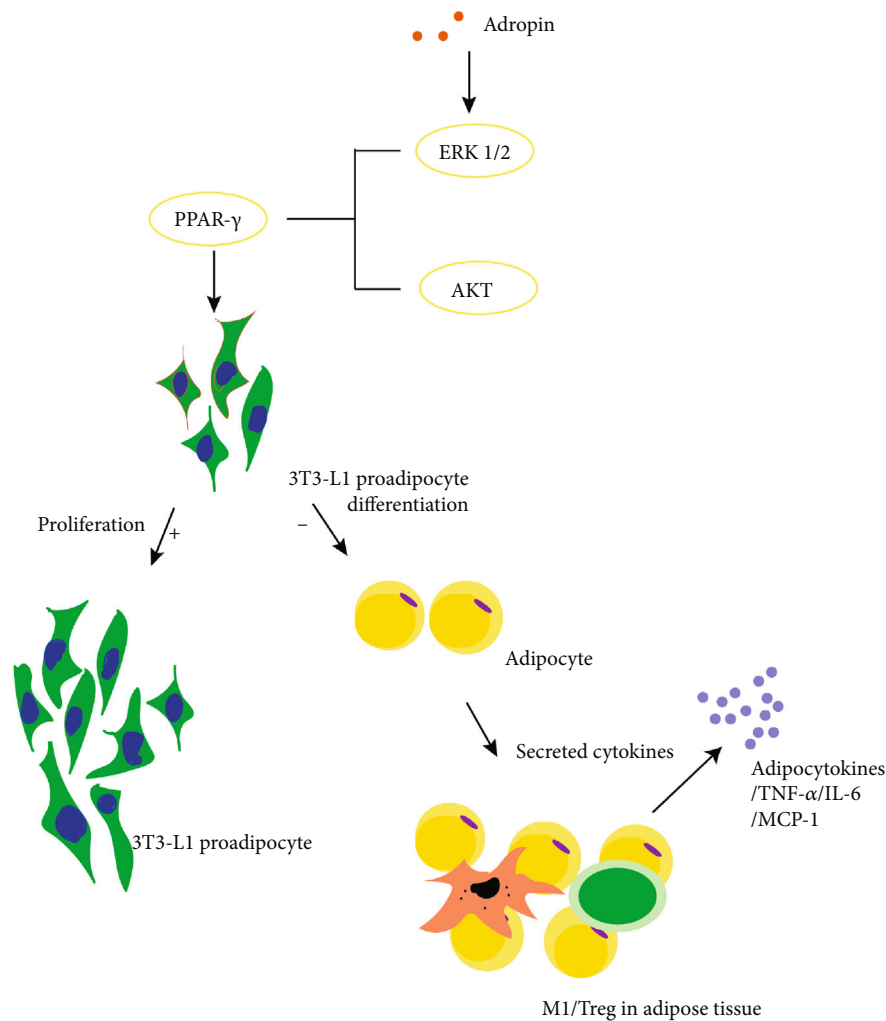
FIGURE 1: Infiltration of macrophages in adipose tissues causes chronic inflammation. Adipocytes are able to secrete cytokines such as TNF-α and MCP-1 that attract macrophages and Treg cells, leading to fat inflammation. Adropin regulates the expression of PPAR-γ by activating EK1/2 and AKT pathways, thus promoting the proliferation of 3T3-L1 preadipocytes and inhibiting the differentiation of 3T3-L1 preadipocytes into mature adipocytes and thus reducing fat accumulation and fat inflammation.

inflammatory marker (TNF-α) in women with PCOS [30]. The above-mentioned findings demonstrated that the expression level of adropin can be reduced in various inflammatory metabolic diseases.

4. Correlation between Inhibition of Inflammation by Adropin and Cardiovascular Diseases

Studies on the correlation between adropin and pathogenesis of cardiovascular diseases mainly concentrated on the protection and regulation of function of endothelial cells by adropin. Adropin can also upregulate the expression level of eNOS by upregulating PI3K/Akt and extracellular signal-regulated kinase (ERK) signal transduction pathways in vitro and in vivo, thereby increasing bioavailability of NO [11]. On the one hand, as an endogenous vasodilator, NO plays a substantial role in maintaining the homeostasis of endothelial cells [31]; on the other hand, NO can exert

immunomodulatory influences in inhibiting adhesion of monocytes and leukocytes to the endothelia [32]. Sato et al. [24] demonstrated that adropin can inhibit TNF-α-induced adhesion of THP1 monocytes to endothelial cells in the process of atherosclerosis. With impeding monocyte-endothelial cell interactions, it can inhibit the inflammatory response of endothelial cells and monocytes/macrophages. With regulation of the phenotype of macrophages, it exerts proinflammatory or anti-inflammatory effects on atherosclerosis. In terms of energy metabolism, metabolic disorders caused by insulin resistance or inflammation leads to activations of inflammatory transcription factor nuclear factor kB (NF-κB) and inflammatory signaling system, as well as elevated levels of cytokines, thereby accelerating the damage to function of endothelial cells and formation of atherosclerotic plaques [22]. As a regulator of energy metabolism, adropin may exert its potential anti-inflammatory effects through regulation of energy metabolism.

Additionally, in studies on cardiovascular diseases, such as coronary artery disease (CAD) and atherosclerosis,
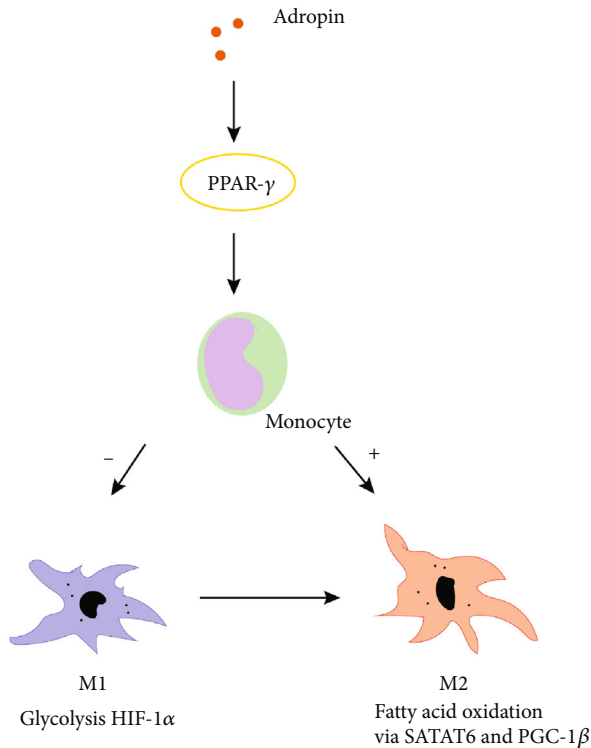
FIGURE 2: Regulatory mechanisms of adropin for immune cells. M1 macrophages use the energy provided by aerobic glycolysis for proinflammatory responses, while M2 macrophages depend on the energy provided by fatty acid oxidation for anti-inflammatory responses. Adropin regulates macrophage polarization by regulating the expression of PPAR-γ, a gene related to fatty acid metabolism.

scholars found that adropin has a significant negative correlation with homocysteine (Hcy), hypersensitive C-reactive protein (hs-CRP), and levels of cytokines. (1) Hcy: Hcy is known to mediate cardiovascular problems by its adverse effects on cardiovascular endothelium and smooth muscle cells with resultant alterations in subclinical arterial structure and function. Serum Hcy level is negatively correlated with serum adropin level in CAD patients [33]. Hyperhomocysteinemia activates c-Jun N-terminal kinase by inducing endoplasmic reticulum stress, which can stimulate the production of proinflammatory cytokines and promote macrophage infiltration, thereby promoting insulin resistance [34]. (2) Inflammatory cytokines: studies conducted by Sato et al. [24] showed that adropin could reduce the expressions of TNF-α and IL-6 at the mRNA level by regulating the expression of iNOS, thereby exerting anti-inflammatory effects on the atherosclerosis. (3) CD36: CD36, which can be downregulated by adropin, is a multi-ligand and multifunctional inflammatory receptor that induces inflammatory responses through activation of various ligands and cellular responses; for example, the interaction with fibrillar β-amyloid (fAβ)/integrin can induce an inflammatory response by increasing expressions of proinflammatory cytokines and chemokines; CD36 receptor for oxidized low-density lipoprotein (oxLDL) can alter cytoskeletal dynamics, enhance macrophage spreading, and inhibit

migration. This may result in macrophages being captured in the endarterium, as well as further promoting atherosclerosis [10, 35, 36]. (4) hs-CRP: adropin is negatively correlated with acute inflammatory marker (hs-CRP), which can also provide strong evidence for the anti-inflammatory effect of adropin.

5. Association between Adropin and Other Inflammatory Diseases

In addition to metabolic disorders and cardiovascular diseases, adropin has been shown as a potential anti-inflammatory factor in other inflammatory diseases. Gao et al. [37] demonstrated that ENHO-/- mice showed MPO-ANCA-related pulmonary vasculitis, which is an autoimmune disease. It is well known that Treg cell is a subset of T cells that control autoimmune reactivity, and their deficiency can lead to autoimmune diseases. In the lung tissues of AdrKO mice, the number and ratio of Treg cells were found to be significantly reduced. At the same time, there was a sharp increase in CD3, CD20, and CD38 positive cells in the lung tissues of AdrKO mice. The neutrophil recruitment and neutrophil-endothelial cell interactions caused by ENHO mutation/adropin deficiency were associated with lung injury related to MPO-ANCA.

It was previously revealed that adropin can inhibit hepatic cell inflammation in hyperlipidemia rats [38]. In AdrKO mice, the more the accumulation of hepatic lipid, the more severe the inflammatory response, and the expressions of inflammation-related genes (Il1b, Il6, and Tnf) were remarkably elevated [39]. This may be attributed to the regulatory effects of adropin on the accumulation of hepatic lipid. However, it also suggested that in a variety of inflammations, various tissues, and even blood, the level of adropin is associated with inflammation-related genes (especially Il6 and Tnf). In patients with knee osteoarthritis, the level of adropin is negatively correlated with TNF-α level, white blood cell (WBC) count, and neutrophil-lymphocyte ratio (NLR) [40]. The underlying mechanism may be related to the upregulation of eNOS activity by adropin, and the produced NO can negatively regulate inflammatory mediators. Furthermore, it can impede the leukocyte extravasation and movement process regulated by TNF-α, thereby applying its anti-inflammatory effects [41].

Adropin has the effect of antioxidative stress. Study has shown that adropin deficiency correlates with increased oxidative stress associated with endothelial dysfunction in the brain of rats [9]. Meanwhile, adropin can activate ERK 1/2 through VEGFR2, and ERK 1/2 activation induces Nrf2 and protect neurons from oxidative stress [42]. Inhibition of ERK 1/2 may reduce DNA repairing ability, accelerate cell apoptosis, and aggravate neuron loss [43]. The antioxidative stress effect of adropin is also related to its immune regulation function. Adropin activates Nrf2 signaling in nonalcoholic steatohepatitis (NASH) and plays a role in decreasing reactive oxygen species (ROS) production from liver mitochondria. So, it may protect mitochondrial function to alleviate oxidative stress and apoptosis and thus protect against liver injury and prevent the NASH progression [44].
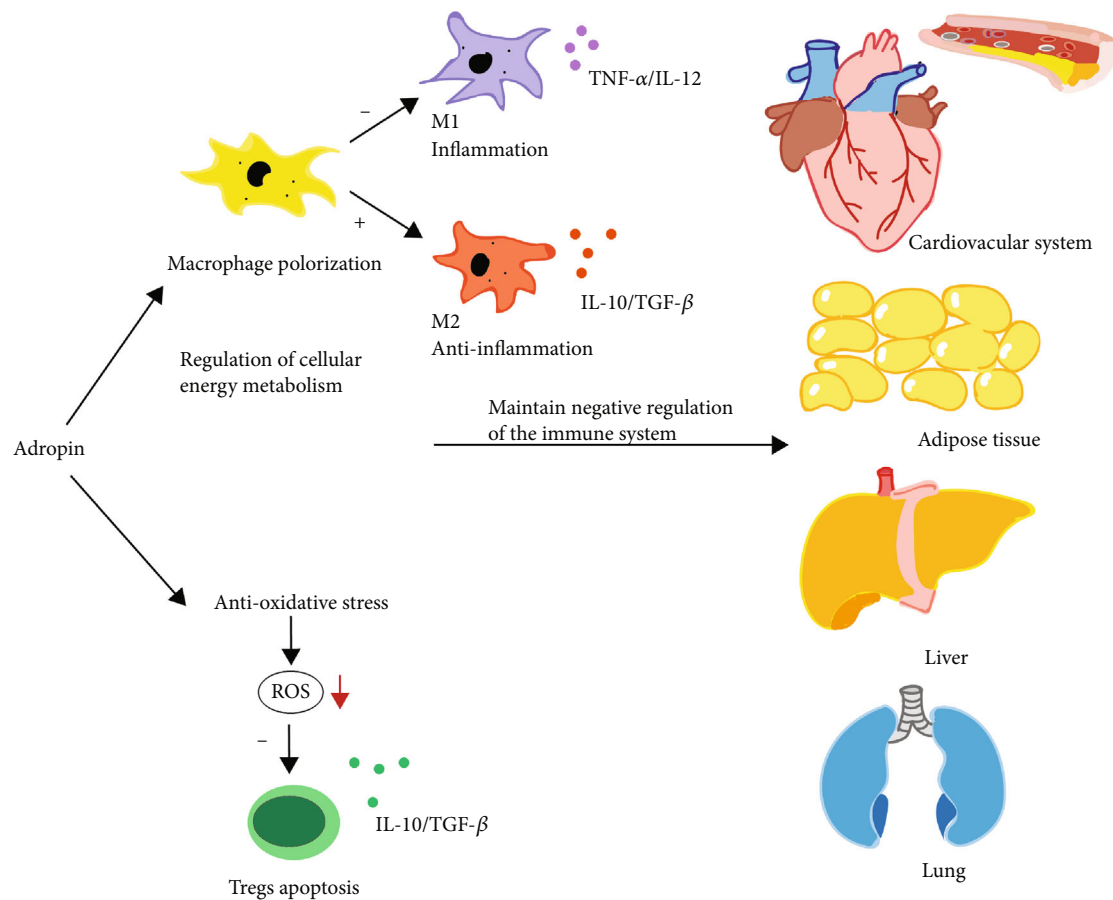
FIGURE 3: Adropin plays an anti-inflammatory role in a variety of tissues. Adropin can affect macrophage polarization by regulating cell energy metabolism and prevent ROS-induced apoptosis of Tregs through antioxidant stress. Thus, it can maintain the negative regulation of the immune system and play an anti-inflammatory role in atherosclerosis, fat inflammation, fatty liver, nonalcoholic hepatitis, and pulmonary vasculitis. Adropin deficiency can lead to imbalance of immune cells and inflammatory cytokines, which will destroy the negative regulation of the immune system and result in inflammation.

Excessive reactive oxygen production can cause inflammation [45]. The study indicated that the increase of oxidative stress in a fatty liver caused the apoptosis of Tregs, reduced the number of hepatic Tregs, and led to a lowered suppression of inflammatory responses. This is because increased fatty acid metabolism leads to increased mitochondrial respiratory activity and excessive production of mitochondrial ROS in the liver, which can reduce the expression of bcl-2 in Tregs and selectively affected a subpopulation of T lymphocytes (Tregs) (Figure 3) [46, 47].

6. Prospect

At present, studies concentrated on adropin protein and its functions are still in the preliminary stage. However, there is increasing evidence that adropin is highly associated with various inflammatory diseases, and is also involved in the inflammatory process of different diseases. Moreover, it plays a substantial role in regulating the phenotype and biological behavior of immune cells, in addition to the secretion of inflammatory cytokines. The specific mechanisms have not been fully and systematically elucidated, and a larger sample size is also required to confirm the immunomodulatory effects of adropin. Nevertheless, as a potential anti-inflammatory protein, its immunological effects should be investigated in the future researches.

Conflicts of Interest

The authors have no competing interests to declare.

Acknowledgments

References

[1] K. G. Kumar, J. L. Trevaskis, D. D. Lam et al., "Identification of adropin as a secreted factor linking dietary macronutrient intake with energy homeostasis and lipid metabolism," *Cell Metabolism*, vol. 8, no. 6, pp. 468–481, 2008.

[2] W. Han, C. Zhang, H. Wang et al., "Alterations of irisin, adropin, preptin and BDNF concentrations in coronary heart

disease patients comorbid with depression," *Annals of Translational Medicine*, vol. 7, no. 14, p. 298, 2019.

[3] L. M. Stein, G. L. C. Yosten, and W. K. Samson, "Adropin acts in brain to inhibit water drinking: potential interaction with the orphan G protein-coupled receptor, GPR19," *American Journal of Physiology-Regulatory, Integrative and Comparative Physiology*, vol. 310, no. 6, pp. R476–R480, 2016.

[4] D. Thapa, M. W. Stoner, M. Zhang et al., "Adropin regulates pyruvate dehydrogenase in cardiac cells via a novel GPCR-MAPK-PDK4 signaling pathway," *Redox Biology*, vol. 18, pp. 25–32, 2018.

[5] K. Ganesh Kumar, J. Zhang, S. Gao et al., "Adropin deficiency is associated with increased adiposity and insulin resistance," *Obesity*, vol. 20, no. 7, pp. 1394–1402, 2012.

[6] A. A. Butler, C. S. Tam, K. L. Stanhope et al., "Low circulating adropin concentrations with obesity and aging correlate with risk factors for metabolic disease and increase after gastric bypass surgery in humans," *The Journal of Clinical Endocrinology & Metabolism*, vol. 97, no. 10, pp. 3783–3791, 2012.

[7] J. R. Stevens, M. L. Kearney, M. P. St-Onge et al., "Inverse association between carbohydrate consumption and plasma adropin concentrations in humans," *Obesity*, vol. 24, no. 8, pp. 1731–1740, 2016.

[8] M. P. St-Onge, A. Shechter, J. Shlisky et al., "Fasting plasma adropin concentrations correlate with fat consumption in human females," *Obesity*, vol. 22, no. 4, pp. 1056–1063, 2014.

[9] C. Yang, K. M. DeMars, and E. Candelario-Jalil, "Age-dependent decrease in adropin is associated with reduced levels of endothelial nitric oxide synthase and increased oxidative stress in the rat brain," *Aging and Disease*, vol. 9, no. 2, pp. 322–330, 2018.

[10] S. Gao, R. P. McMillan, Q. Zhu, G. D. Lopaschuk, M. W. Hulver, and A. A. Butler, "Therapeutic effects of adropin on glucose tolerance and substrate utilization in diet-induced obese mice with insulin resistance," *Molecular Metabolism*, vol. 4, no. 4, pp. 310–324, 2015.

[11] F. Lovren, Y. Pan, A. Quan et al., "Adropin is a novel regulator of endothelial function," *Circulation*, vol. 122, 11 Suppl, pp. S185–S192, 2010.

[12] C.-M. Wong, Y. Wang, J. T. H. Lee et al., "Adropin is a brain membrane-bound protein regulating physical activity via the NB-3/Notch signaling pathway in mice," *The Journal of Biological Chemistry*, vol. 289, no. 37, pp. 25976–25986, 2014.

[13] M. W. Rajala and P. E. Scherer, "Minireview: the adipocyte-at the crossroads of energy homeostasis, inflammation, and atherosclerosis," *Endocrinology*, vol. 144, no. 9, pp. 3765–3773, 2003.

[14] D. Cipolletta, M. Feuerer, A. Li et al., "PPAR-γ is a major driver of the accumulation and phenotype of adipose tissue Treg cells," *Nature*, vol. 486, no. 7404, pp. 549–553, 2012.

[15] N. Krahmer, R. V. Farese Jr., and T. C. Walther, "Balancing the fat: lipid droplets and human disease," *EMBO Molecular Medicine*, vol. 5, no. 7, pp. 973–983, 2013.

[16] J. R. Bradley, "TNF-mediated inflammatory disease," *The Journal of Pathology*, vol. 214, no. 2, pp. 149–160, 2008.

[17] V. Bourlier, A. Zakaroff-Girard, A. Miranville et al., "Remodeling phenotype of human subcutaneous adipose tissue macrophages," *Circulation*, vol. 117, no. 6, pp. 806–815, 2008.

[18] P. E. Scherer, "Adipose tissue: from lipid storage compartment to endocrine organ," *Diabetes*, vol. 55, no. 6, pp. 1537–1545, 2006.

[19] M. Jasaszwili, T. Wojciechowicz, M. Billert, M. Z. Strowski, K. W. Nowak, and M. Skrzypski, "Effects of adropin on proliferation and differentiation of 3T3-L1 cells and rat primary preadipocytes," *Molecular and Cellular Endocrinology*, vol. 496, article 110532, 2019.

[20] M. Feuerer, L. Herrero, D. Cipolletta et al., "Lean, but not obese, fat is enriched for a unique population of regulatory T cells that affect metabolic parameters," *Nature Medicine*, vol. 15, no. 8, pp. 930–939, 2009.

[21] K. Eller, A. Kirsch, A. M. Wolf et al., "Potential role of regulatory T cells in reversing obesity-linked insulin resistance and diabetic nephropathy," *Diabetes*, vol. 60, no. 11, pp. 2954–2962, 2011.

[22] S. Chen, K. Zeng, Q. C. Liu et al., "Adropin deficiency worsens HFD-induced metabolic defects," *Cell Death & Disease*, vol. 8, no. 8, article e3008, 2017.

[23] A. M. Sharma and B. Staels, "Review: peroxisome proliferator-activated receptor gamma and adipose tissue-understanding obesity-related changes in regulation of lipid and glucose metabolism," *The Journal of Clinical Endocrinology and Metabolism*, vol. 92, no. 2, pp. 386–395, 2007.

[24] K. Sato, T. Yamashita, R. Shirai et al., "Adropin contributes to anti-atherosclerosis by suppressing monocyte-endothelial cell adhesion and smooth muscle cell proliferation," *International Journal of Molecular Sciences*, vol. 19, no. 5, p. 1293, 2018.

[25] M. Ouimet, H. N. Ediriweera, U. M. Gundra et al., "Micro-RNA-33-dependent regulation of macrophage metabolism directs immune cell polarization in atherosclerosis," *The Journal of Clinical Investigation*, vol. 125, no. 12, pp. 4334–4348, 2015.

[26] D. Vats, L. Mukundan, J. I. Odegaard et al., "Oxidative metabolism and PGC-1beta attenuate macrophage-mediated inflammation," *Cell Metabolism*, vol. 4, no. 1, pp. 13–24, 2006.

[27] S. Galván-Peña and L. A. J. O'Neill, "Metabolic reprograming in macrophage polarization," *Frontiers in Immunology*, vol. 5, p. 420, 2014.

[28] W. Hu and L. Chen, "Association of serum adropin concentrations with diabetic nephropathy," *Mediators of Inflammation*, vol. 2016, Article ID 6038261, 5 pages, 2016.

[29] T. Kuloglu and S. Aydin, "Immunohistochemical expressions of adropin and ınducible nitric oxide synthase in renal tissues of rats with streptozotocin-ınduced experimental diabetes," *Biotechnic & Histochemistry*, vol. 89, no. 2, pp. 104–110, 2014.

[30] T. Kume, M. Calan, O. Yilmaz et al., "A possible connection between tumor necrosis factor alpha and adropin levels in polycystic ovary syndrome," *Journal of Endocrinological Investigation*, vol. 39, no. 7, pp. 747–754, 2016.

[31] A. Celik, M. Balin, M. A. Kobat et al., "Deficiency of a new protein associated with cardiac syndrome X; called adropin," *Cardiovascular Therapeutics*, vol. 31, no. 3, pp. 174–178, 2013.

[32] P. Kubes, M. Suzuki, and D. N. Granger, "Nitric oxide: an endogenous modulator of leukocyte adhesion," *Proceedings of the National Academy of Sciences of the United States of America*, vol. 88, no. 11, pp. 4651–4655, 1991.

[33] L. P. Zhao, T. You, S. P. Chan, J. C. Chen, and W. T. Xu, "Adropin is associated with hyperhomocysteine and coronary atherosclerosis," *Experimental and Therapeutic Medicine*, vol. 11, no. 3, pp. 1065–1070, 2016.

[34] Y. Li, H. Zhang, C. Jiang et al., "Hyperhomocysteinemia promotes insulin resistance by inducing endoplasmic reticulum stress in adipose tissue," *The Journal of Biological Chemistry*, vol. 288, no. 14, pp. 9583–9592, 2013.

[35] S. Cho, E. M. Park, M. Febbraio et al., "The class B scavenger receptor CD36 mediates free radical production and tissue injury in cerebral ischemia," *The Journal of Neuroscience*, vol. 25, no. 10, pp. 2504–2512, 2005.

[36] Y. M. Park, M. Febbraio, and R. L. Silverstein, "CD36 modulates migration of mouse and human macrophages in response to oxidized LDL and may contribute to macrophage trapping in the arterial intima," *The Journal of Clinical Investigation*, vol. 119, no. 1, pp. 136–145, 2009.

[37] F. Gao, J. Fang, F. Chen et al., "*Enho* mutations causing low adropin: a possible pathomechanism of MPO-ANCA associated lung injury," *EBioMedicine*, vol. 9, pp. 324–335, 2016.

[38] R. Akcılar, F. Emel Koçak, H. Şimşek et al., "The effect of adropin on lipid and glucose metabolism in rats with hyperlipidemia," *Iranian Journal of Basic Medical Sciences*, vol. 19, no. 3, pp. 245–251, 2016.

[39] O. Sayın, Y. Tokgöz, and N. Arslan, "Investigation of adropin and leptin levels in pediatric obesity-related nonalcoholic fatty liver disease," *Journal of Pediatric Endocrinology and Metabolism*, vol. 27, no. 5–6, pp. 479–484, 2014.

[40] G. Gundogdu and K. Gundogdu, "A novel biomarker in patients with knee osteoarthritis: adropin," *Clinical Rheumatology*, vol. 37, no. 8, pp. 2179–2186, 2018.

[41] J. Bozic, J. A. Borovac, T. Galic, T. T. Kurir, D. Supe-Domic, and Z. Dogas, "Adropin and inflammation biomarker levels in male patients with obstructive sleep apnea: a link with glucose metabolism and sleep parameters," *Journal of Clinical Sleep Medicine*, vol. 14, no. 7, pp. 1109–1118, 2018.

[42] N. Kweider, A. Fragoulis, C. Rosen et al., "Interplay between vascular endothelial growth factor (VEGF) and nuclear factor erythroid 2-related factor-2 (Nrf2): implications for preeclampsia," *Journal of Biological Chemistry*, vol. 286, no. 50, pp. 42863–42872, 2011.

[43] Y. Zhao, J. Li, Q. Tang et al., "Regulation of extracellular signal-regulated kinase 1/2 influences hippocampal neuronal survival in a rat model of diabetic cerebral ischemia," *Neural Regeneration Research*, vol. 9, no. 7, pp. 749–756, 2014.

[44] X. Chen, H. Xue, W. Fang et al., "Adropin protects against liver injury in nonalcoholic steatohepatitis via the Nrf2 mediated antioxidant capacity," *Redox Biology*, vol. 21, article 101068, 2019.

[45] D. Damgaard, M. E. Bjørn, P. Ø. Jensen, and C. H. Nielsen, "Reactive oxygen species inhibit catalytic activity of peptidylarginine deiminase," *Journal of Enzyme Inhibition and Medicinal Chemistry*, vol. 32, no. 1, pp. 1203–1208, 2017.

[46] X. Ma, J. Hua, A. R. Mohamood, A. R. Hamad, R. Ravi, and Z. Li, "A high-fat diet and regulatory T cells influence susceptibility to endotoxin-induced liver injury," *Hepatology*, vol. 46, no. 5, pp. 1519–1529, 2007.

[47] M. L.-H. Huang, S. Chiang, D. S. Kalinowski, D.-H. Bae, S. Sahni, and D. R. Richardson, "The role of the antioxidant response in mitochondrial dysfunction in degenerative diseases: cross-talk between antioxidant defense, autophagy, and apoptosis," *Oxidative Medicine and Cellular Longevity*, vol. 2019, Article ID 6392763, 26 pages, 2019.

Research Article

The Inhibition of Aldose Reductase Accelerates Liver Regeneration through Regulating Energy Metabolism

Chang Xian Li [ID], Hong Wei Wang, Wang Jie Jiang, Gao Chao Li, Yao Dong Zhang [ID], Chen Huan Luo, and Xiang Cheng Li [ID]

Hepatobiliary Center, The First Affiliated Hospital of Nanjing Medical University, Key Laboratory of Living Donor Liver Transplantation, Nanjing, Jiangsu Province, China

Correspondence should be addressed to Chang Xian Li; doclicx20@163.com and Xiang Cheng Li; drxcli@njmu.edu.cn

Objectives. Our previous study showed that aldose reductase (AR) played key roles in fatty liver ischemia-reperfusion (IR) injury by regulating inflammatory response and energy metabolism. Here, we aim to investigate the role and mechanism of AR in the regeneration of normal and fatty livers after liver surgery. *Methods*. The association of AR expression with liver regeneration was studied in the rat small-for-size liver transplantation model and the mice major hepatectomy and hepatic IR injury model with or without fatty change. The direct role and mechanism of AR in liver regeneration was explored in the AR knockout mouse model. *Results*. Delayed regeneration was detected in fatty liver after liver surgery in both rat and mouse models. Furthermore, the expression of AR was increased in liver after liver surgery, especially in fatty liver. In a functional study, the knockout of AR promoted liver regeneration at day 2 after major hepatectomy and IR injury. Compared to wild-type groups, the expressions of cyclins were increased in normal and fatty livers of AR knockout mice. AR inhibition increased the expressions of PPAR-α and PPAR-γ in both normal liver and fatty liver groups after major hepatectomy and IR injury. In addition, the knockout of AR promoted the expressions of SDHB, AMPK, SIRT1, and PGC1-α in liver, which regulated mitochondrial biogenesis and energy metabolism. *Conclusions*. The knockout of AR promoted the regeneration of normal and fatty livers through regulating energy metabolism. AR may be a new potential therapeutic target to accelerate liver regeneration after surgery.

1. Introduction

Hepatectomy and liver transplantation are effective treatments for all kinds of liver diseases. Nonalcoholic fatty liver disease (NAFLD) is a common cause of chronic liver disease, and its worldwide prevalence continues to increase with the growing epidemic of obesity and diabetes [1]. It is reported that more than 20% of the patients planned for liver resection have some degree of steatosis, which is associated with increased risk of postoperative complications and death [2, 3]. Furthermore, steatotic liver graft also increased the risk of primary nonfunction or dysfunction after transplantation compared to normal graft [2, 3]. Research showed that fatty liver is more vulnerable to ischemia-reperfusion (IR) injury and then impaired liver regeneration and recovery, resulting in an amplified postoperative morbidity and mortality of

patients [4, 5]. Therefore, clarifying the mechanism of fatty liver regeneration after an operation and finding effective intervention methods to promote fatty liver regeneration are very important for the recovery of liver function and improvement of long-term survival.

Aldose reductase (AR), a member of the aldo-keto reductase super family, is the first enzyme in the polyol pathway and converts glucose to sorbitol in the presence of NADPH as cofactor. AR plays important roles in the pathogenesis of diabetic complications such as cataractogenesis, retinopathy, neuropathy, and cardiovascular disease [6]. The inhibition of AR has been an attractive approach for the treatment and management of diabetic complications. Furthermore, more evidence showed that AR is upregulated and plays key roles in a number of inflammatory diseases [6–8]. The inhibition of AR suppressed the activation of transcription factors

NF-κB and inflammatory cytokine expression in macrophages [9, 10]. AR has been reported to be involved in the development of NAFLD. AR inhibitors may improve NAFLD through attenuating oxidative stress and inflammatory cytokine expression [11]. Moreover, experimental studies have demonstrated that AR was overexpressed in ischemic myocardium and mediated myocardial IR injury by opening the mitochondrial permeability transition pore [12]. Our previous study showed that AR played key roles in hepatic IR injury [13–15]. AR was overexpressed in ischemic liver, especially in fatty liver, and its deficiency attenuated hepatic IR injury in both normal and fatty livers by reducing liver inflammatory responses [13]. Furthermore, AR inhibition also attenuated steatotic liver injury by maintaining the homeostasis of NAD(P)(H) contents and regulating energy metabolism [14, 15]. Recently, research showed that the inhibition of AR enhanced lens regeneration by regulating the response of lens epithelial cells [16]. However, the role and mechanism of AR in the regeneration of normal liver and fatty liver after liver surgery are still unknown.

In this study, we aimed to explore the effect and mechanism of AR in the regeneration of normal and fatty livers. Firstly, the association of AR expression with liver regeneration was studied in the rat liver transplantation model and in the mice model with or without fatty change. The direct role of AR in liver regeneration was explored in the AR knockout mouse major hepatectomy and hepatic IR injury model. Together, our study found that the inhibition of AR accelerated the regeneration of normal and fatty livers through regulating energy metabolism.

2. Materials and Methods

2.1. Animal Models. Male Sprague-Dawley rats (6-8 weeks) were used as donors and recipients. C57BL/6 (6-8 weeks) mice and AR knockout mice were applied in the mouse model. Fatty livers of rats and mice were induced by feeding with a high-fat diet (TestDiet, USA) for 2 weeks. Animals were allowed free access to food and water in a room with a 12-hour light, 12-hour dark cycle. The experimental protocol was approved by the Committee on the Use of Live Animals in Teaching and Research, Nanjing Medical University.

Rat orthotopic liver transplantation was established using small-for-size liver graft with or with fatty change [13]. The median lobe, right lobe, and triangle lobe of the liver were selected to be small-for-size grafts, and the median ratio of graft weight to recipient liver weight was about 50%. Rat orthotopic liver transplantation was conducted in 2 groups: (I) normal graft group and (II) fatty graft group. Liver samples were sampled at days 2, 4, 7, and 14 after transplantation for further studies. To mimic the clinical situation, AR knockout and wild-type mice models with major hepatectomy and hepatic IR injury were applied. The branches of the hepatic artery and portal vein to the right and triangle lobes were clamped for 45 minutes by microvessel clamps followed by reperfusion. Major hepatectomy of the left and caudate lobes were performed during the ischemia duration.

Liver samples and blood were collected at days 1, 2, 4, and 7 after reperfusion.

2.2. Immunohistochemical Staining. The expression of PCNA was detected by immunohistochemical staining (IHC). The detail of IHC staining was described in our previous paper [17].

2.3. Detection of Gene Expression by Real-Time RT-PCR. Each 1 μg of total RNA from different samples was used to synthesize 22 μl of cDNA using the High-Capacity cDNA Kit (Applied Biosystems, Foster City, CA). RT-PCR was done with a modified version of a previous method [13]. All samples were detected in triplicate, and the readings from each sample and its internal control were used to calculate the gene expression level. After normalization with the internal control, the gene expression levels were expressed as folds relative to the control liver.

2.4. Measurement of Protein Levels by Western Blotting. Western blotting was done with a modified version of a previous method. β-Actin, anti-p-AMPK, and anti-SIRT1 antibodies were purchased from Cell Signaling Technology and Abcam.

2.5. ATP Assay. In order to investigate the role of AR in energy metabolism, the content of ATP was detected by an ATP assay. The ATP assay (Sigma-Aldrich) was performed according to the manufacturer's instructions.

2.6. Statistics and Data Analyses. Continuous variables were expressed as average with standard deviation (SD). The Mann-Whitney U test was used for statistical comparison. Significance was defined as $P < 0.05$. Calculations were performed by using the SPSS computer software version 16. (SPSS Inc., Chicago, IL, USA).

3. Results

3.1. Regeneration of Fatty Liver Was Inhibited after Liver Surgery. In order to investigate the effect of steatosis on liver graft regeneration after transplantation, the rat orthotopic transplantation model was established using the small-for-size fatty graft and the small-for-size normal graft. The IHC-staining data showed that hepatocyte regeneration with PCNA staining was markedly reduced in the small-for-size fatty graft compared with the small-for-size-normal graft at days 2, 4, 7, and 14 after transplantation (Figure 1(a)). The number of PCNA-positive cells were significantly lower in the small-for-size fatty graft than those in the small-for-size normal graft (Figure 1(b)). The q-PCR data also confirmed that the mRNA expression level of PCNA was decreased in the small-for-size fatty graft compared to the small-for-size normal graft (Figure 1(c)). The levels of AST and ALT were increased in the small-for-size fatty graft compared to the small-for-size normal graft (Figures 1(d) and 1(e)). Furthermore, low expressions of PPAR-γ, cyclin D1, and cyclin E1 were found in the small-for-size fatty graft (Figures 1(f)–1(h)). These results were also confirmed in the mouse major hepatectomy and IR injury model (Figure 2(a)). These results suggested that regeneration of fatty liver was inhibited after liver surgery.
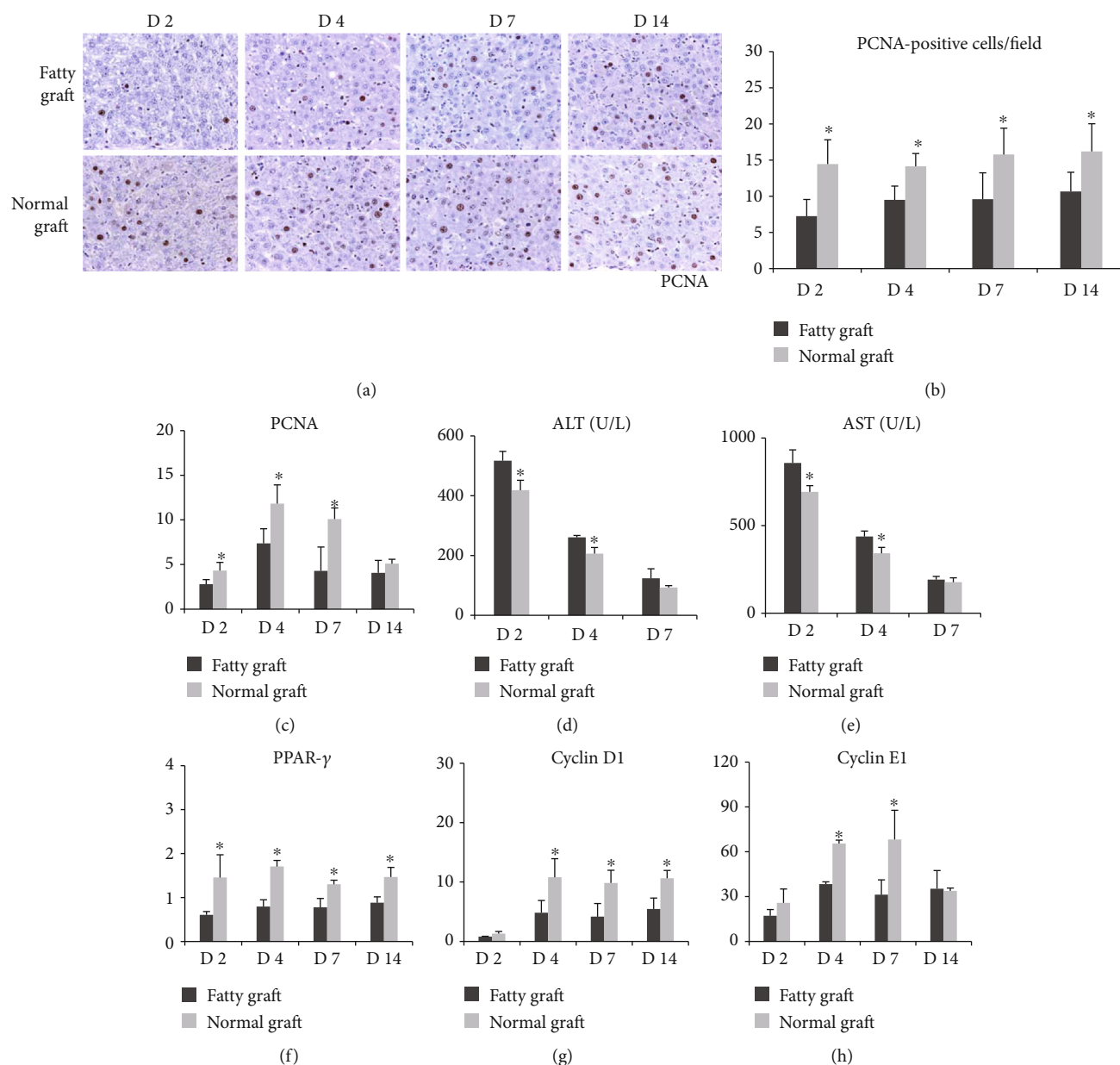
FIGURE 1: Regeneration of fatty liver was inhibited after liver surgery. (a–c) Liver regeneration was delayed in the small-for-size fatty liver graft after transplantation. (d–e) The levels of AST and ALT were increased in the small-for-size fatty graft compared with the small-for-size normal graft. (f–h) The mRNA expressions of PCNA, PPAR-γ, cyclin D1, and cyclin E1 in the fatty liver graft were decreased after transplantation ($^*P < 0.05$, $N = 3$-6/group).

3.2. AR Was Upregulated in Fatty Liver after Liver Surgery.

In order to explore the mechanism of fatty liver graft delayed regeneration after surgery, we firstly detected the expression profile of genes in the liver graft after liver transplantation. The cDNA screening showed that AR was upregulated in the small-for-size fatty graft compared to the small-for-size normal graft. The real-time PCR confirmed that the expression of AR was increased in the liver graft at days 2, 4, 7, and 14 after transplantation, especially in the small-for-size fatty graft (Figure 2(b)). We further detected the expression of AR in the mouse major hepatectomy and partial I/R injury model. Similar to the results in rat transplantation, the expression of AR was higher in fatty liver after major

hepatectomy and partial I/R injury compared to normal liver (Figure 2(c)).

3.3. The Knockout of AR Attenuated Hepatic Injury and Increased the Weight Ratio of Liver to Body after Hepatectomy and IR Injury.

Our previous data showed that compared with wild-type groups, hepatic lobular architecture and portal tracts were well preserved in both the N-KO and F-KO groups after reperfusion [13]. In this study, our data showed that the levels of AST and ALT were decreased in the KO groups after hepatectomy and IR injury compared with the wild-type groups (Figures 3(a) and 3(b)). We also compared the weight ratio of liver to body at different time

(a)

(b)

(c)
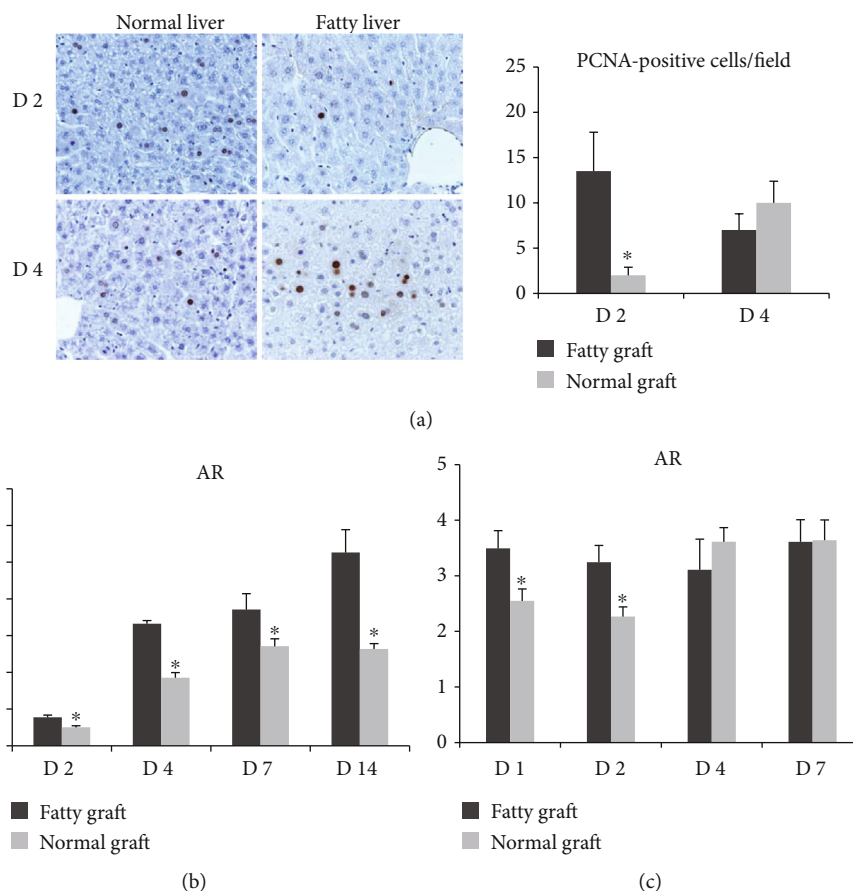
FIGURE 2: The expression of AR was upregulated in fatty liver after liver surgery. (a) Liver regeneration was delayed in mouse fatty liver after hepatectomy and IR injury. (b) The expression of AR was upregulated in the fatty liver graft after liver transplantation compared to normal liver. (c) The expression of AR was upregulated in fatty liver after hepatectomy and IR injury compared to normal liver ($^*P < 0.05$, $N = 3$-6/group).

points after IRI. The results showed that the knockout of AR increased the weight ratio of liver to body in normal liver at day 4 after hepatectomy and IR injury (Figure 3(c)). Similar results were also found in fatty liver: a higher weight ratio of liver to body was found in the fatty KO group at day 4 after hepatectomy and IR injury compared to the wild-type fatty group (Figure 3(d)).

3.4. The Knockout of AR Promoted Liver Regeneration after Major Hepatectomy and IR Injury. In order to explore the role of AR in liver regeneration, the mouse major hepatectomy and IR injury model was established in AR knockout or wild-type mice with or without fatty change. In normal liver groups, our results showed that AR deficiency significantly promoted hepatocyte regeneration with PCNA staining compared with the wild-type group at day 2 after major hepatectomy and IR injury (Figure 4(a)). Compared to the wild-type group, the knockout of AR exhibited more PCNA-positive nuclei and higher mRNA expression levels of PCNA and ki-67 in normal liver (Figures 4(a)–4(d)). A similar result was also found in the fatty liver group: more PCNA-positive cells and higher mRNA expression levels of PCNA and ki-67 were found in knockout mice (Figures 4(b)–4(d)). These data indicated that the knockout

of AR promoted liver generation after major hepatectomy and IR injury in both normal liver and fatty liver.

3.5. The Knockout of AR Increased the Cyclin Expressions in Liver after Major Hepatectomy and IR Injury. In order to further explore the mechanism of AR in liver regeneration, we detected the expressions of several cyclins such as cyclin A2, B, D1, and E1. Cyclins are important downstream effectors of diverse proliferative and transforming signaling pathways. In the normal liver group, the expressions of cyclin A2, B, D1, and E1 in liver were found to be more elevated in the N-KO group after major hepatectomy and IR injury compared to the N-WT group (Figure 5(a)). Consistent with the results of normal livers, the knockout of AR also upregulated the mRNA levels of cyclin A2, B, D1, and E1 in fatty liver after major hepatectomy and IR injury compared with the F-WT group (Figure 5(b)).

3.6. The Knockout of AR Promoted Mitochondrial Biogenesis and Energy Metabolism in Liver after Major Hepatectomy and IR Injury. PPARs (peroxisome-proliferator-activated receptors) represent a group of nuclear receptors that plays pivotal roles in the regulation of energy metabolism. Our research showed that the knockout of AR increased the

(a)

(b)

(c)   (d)
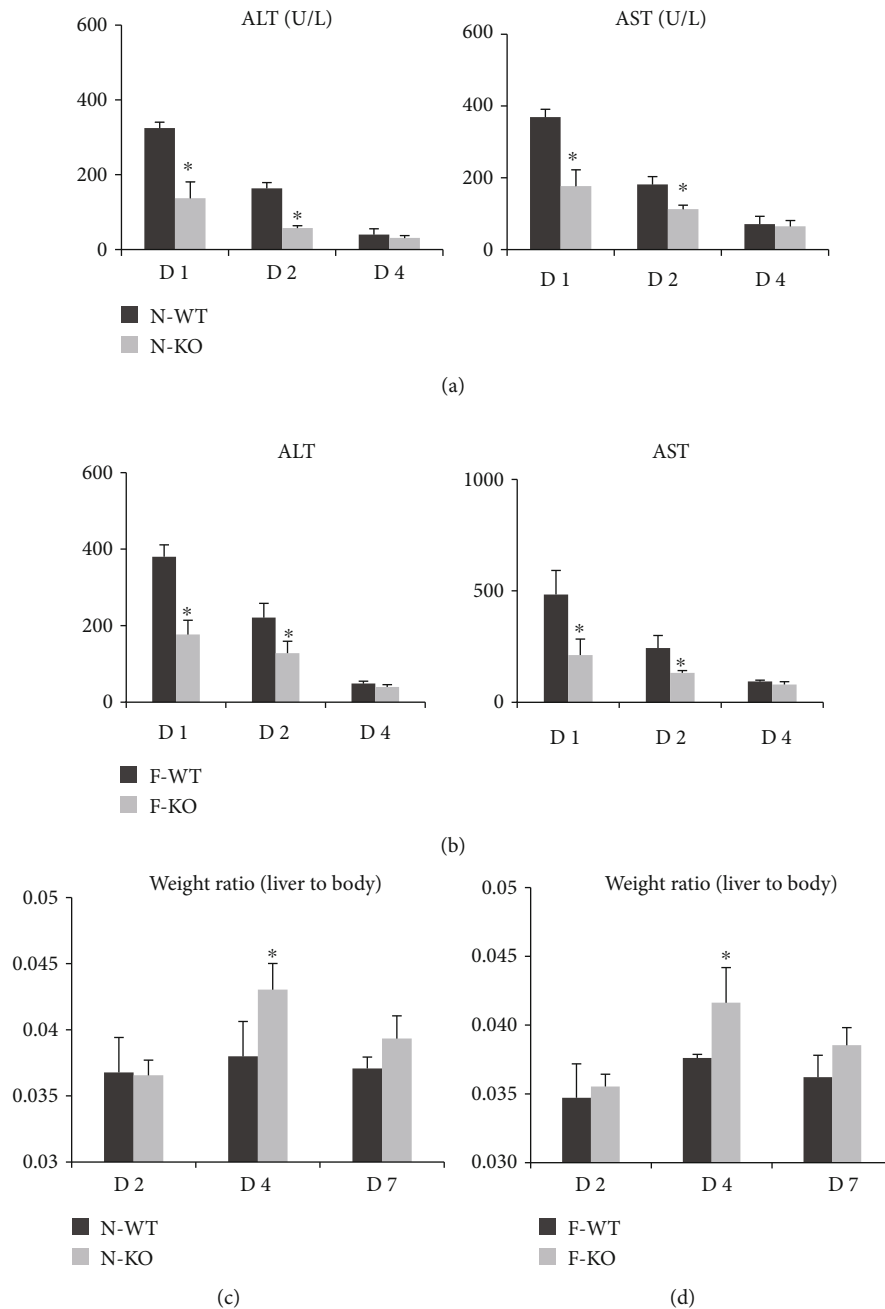
FIGURE 3: The knockout of AR attenuated hepatic injury and increased the weight ratio of liver to body after hepatectomy and IR injury. (a–b) The levels of AST and ALT were decreased in the KO groups after hepatectomy and IR injury compared to the wild-type groups. (c–d) The knockout of AR increased the weight ratio of liver to body at day 4 after hepatectomy and IR injury compared to the wild-type group ($^{*}P < 0.05$, $N = 4$-6/group).

expression of PPAR-α in both the normal liver and fatty liver groups after major hepatectomy and IR injury compared to that of the wild-type groups (Figures 6(a) and 6(b)). Furthermore, the expression of PPAR-γ was higher in the N-KO and F-KO groups than those in the corresponding wild-type groups (Figures 6(a) and 6(b)).

Mitochondria are important organelles for the energy metabolism of hepatocytes, while AMPK signaling is a key regulator of bioenergy metabolism. To further investigate the effect of AR in AMPK signaling during liver regeneration,

the expressions of AMPK signaling such as AMPK, SIRT1, and PGC1-α in liver were detected by q-PCR. In normal liver, the mRNA expressions of AMPK, SIRT1, and PGC1-α were increased in AR knockout mice compared to wild-type mice (Figure 6(a)). The western blot data also confirmed that the knockout of AR increased the expression of p-AMPK and SIRT1 in liver after major hepatectomy and IR injury compared to the wild-type group (Figure 7(a)). Similar data were also found in fatty liver (Figure 6(b)). Furthermore, we also detected the levels of succinate dehydrogenase complex iron
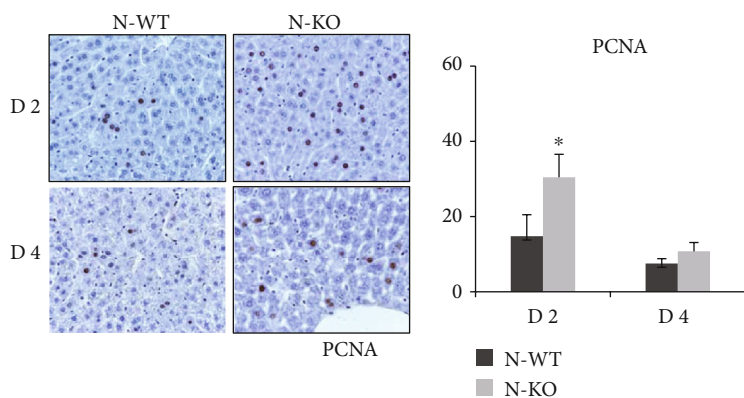
(a)
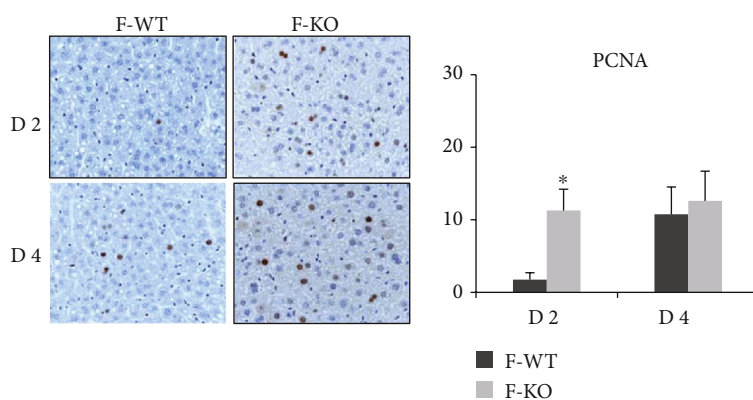
(b)
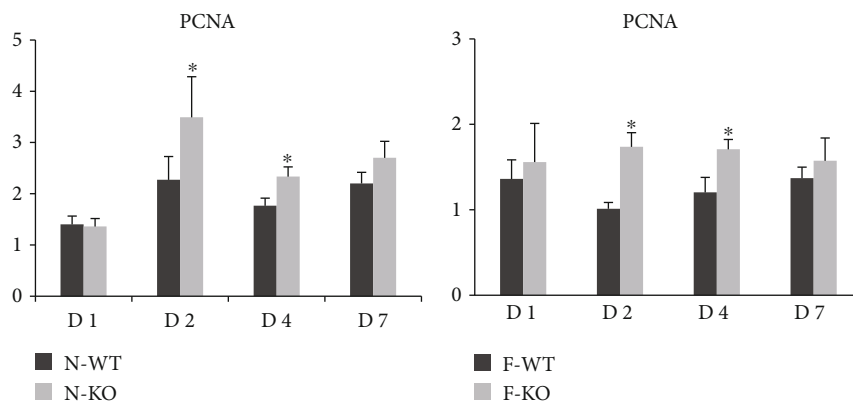
(c)

FIGURE 4: Continued.

(d)
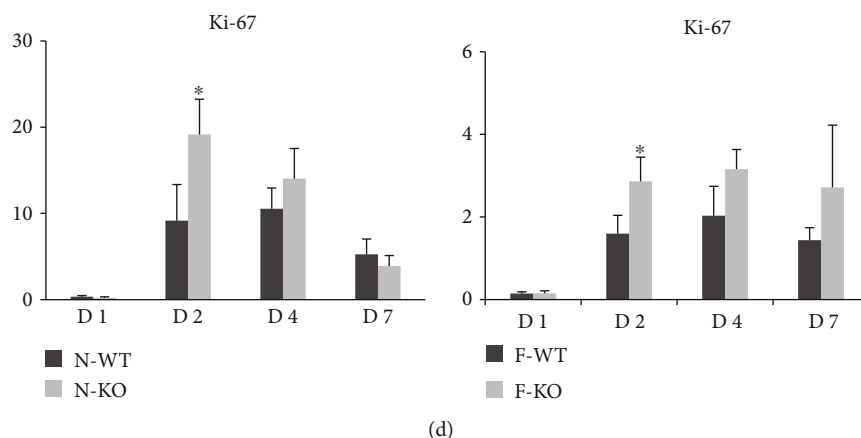
FIGURE 4: The knockout of AR accelerated liver regeneration in the mouse model. (a–b) AR deficiency significantly promoted hepatocyte regeneration with PCNA staining compared with the wild-type group at day 2 and after major hepatectomy and IR injury. (c–d) Compared to control group, the knockout of AR exhibited higher mRNA expression levels of PCNA and ki-67 in liver ($^{*}P < 0.05$, $N = 4$-6/group).

sulfur subunit B (SDHB) and ATP. The data showed that the expression of SDHB was upregulated in both the N-KO and F-KO groups (Figures 6(a) and 6(b)). More importantly, the knockout of AR increased the content of ATP in both normal and fatty livers after major hepatectomy and IR injury compared to the wild-type group (Figure 7(b)).

4. Discussion

Liver regeneration is a highly coordinated process involving complex networks of interactions between various cellular, cytokine, and growth factors [18]. Remnant liver can restore the original hepatic mass after liver surgery through hepatocyte proliferation or oval cell transformation. A variety of cytokines and growth factors have been implicated in regulating liver regeneration [19]. It has been reported that the regeneration capacity of fatty liver was significantly decreased and the risk of postoperative liver failure and graft failure was increased [4, 5, 20]. Our results also confirmed that fatty liver regeneration was delayed in the rat transplantation model and the mouse major hepatectomy and partial IR injury model. Some evidence suggested that impaired fatty liver regeneration maybe due to oxidative stress and metabolism disorder, which resulted in mitochondrial dysfunction and decreased adenosine triphosphate (ATP) production [4, 5, 20]. Therefore, it was worthwhile to clarify the mechanism of fatty liver regeneration and find effective intervention methods to promote fatty liver regeneration.

To our knowledge, this is the first report on the role and mechanism of AR in liver regeneration. In this study, our results demonstrated that the expression of AR was increased in liver after rat liver transplantation and mouse major hepatectomy and IR injury, especially in fatty liver. Furthermore, overexpression of AR in fatty liver was associated with impaired regeneration of fatty liver. The knockout of AR promoted the regeneration of normal and fatty livers in the mouse model. Our data also showed that AR knockout increased the expressions of cyclin A2, B, D1, and E after

hepatectomy and IR injury. Cyclins are important downstream effectors of cell cycle and transforming signaling pathways, which play central roles in cell proliferation [21, 22]. Collectively, these data suggested that the inhibition of AR accelerated liver regeneration and could be a potential therapeutic target.

PPARs are nuclear receptor ligand-dependent transcription factors that regulate gene expression, and they are composed of three types: PPAR-α, PPAR-β, and PPAR-γ. Increasing evidence showed that PPARs play important roles in liver generation. A deficiency of PPAR-α impaired liver regeneration after partial hepatectomy through regulating gene expression involved in cell cycle control, cytokine signaling, and fat metabolism [23, 24]. There are some papers suggesting that PPAR-β was involved in the progression of liver regeneration by regulating PDK1/Akt and E2f signaling-controlled metabolism and proliferation [25, 26]. Moreover, regeneration was impaired in liver-specific PPAR-γ null mice with diet-induced hepatic steatosis after hepatectomy. These data suggested that augmenting liver PPAR activity might promote the regeneration of liver after surgery. Recent research showed that AR overexpression caused strong suppression of PPAR-α activity by regulating ERK1/2 signaling [27]. In this project, our data showed that the knockout of AR increased the expressions of PPAR-α and PPAR-γ in both the normal liver and fatty liver groups after major hepatectomy and IR injury compared to the wild-type groups. These data demonstrated that AR negatively regulated the progression of liver regeneration maybe through regulating expressions of PPAR-α and PPAR-γ.

Mitochondria are significant organelles for hepatocyte energy metabolism. ATP is critical not only for energy supply to maintain cell functions and survival but is also a significant factor in controlling regenerative signaling [28–30]. Decreased ATP production was associated with severe injury, impaired liver regeneration, and increased mortality after transplantation with the small-for-size liver graft [31, 32]. AMP-activated protein kinase (AMPK) is an

(a)
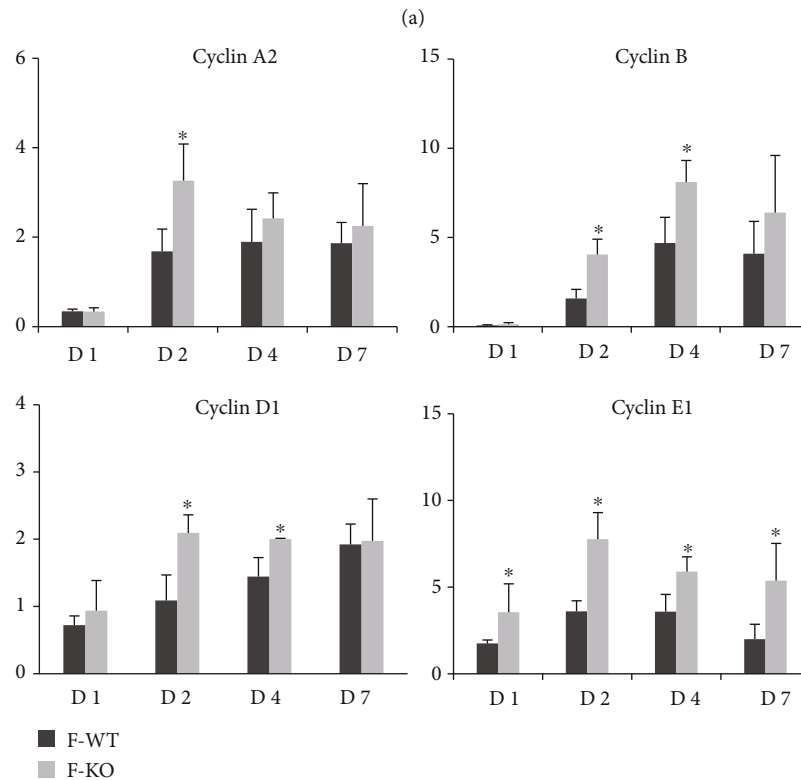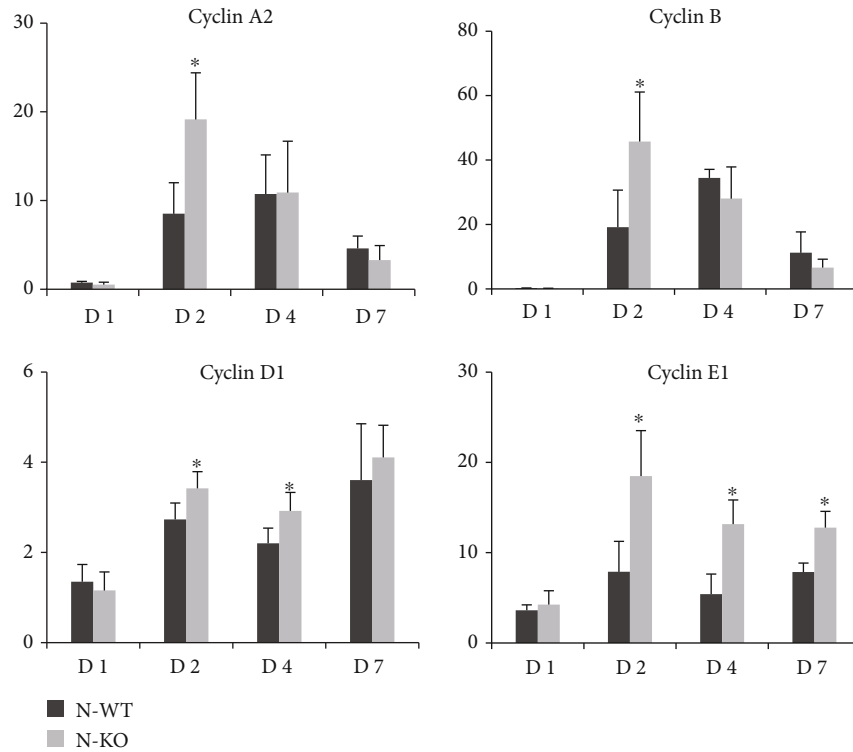
(b)

FIGURE 5: The knockout of AR increased the cyclin expressions in liver after major hepatectomy and IR injury. (a) The expressions of cyclin A2, B, D1, and E1 in normal liver were found to be increased in the N-KO group after major hepatectomy and IR injury. (b) The knockout of AR increased the mRNA levels of cyclin A2, B, D1, and E1 in fatty liver after major hepatectomy and IR injury ($*P < 0.05$, $N = 4$-6/group).
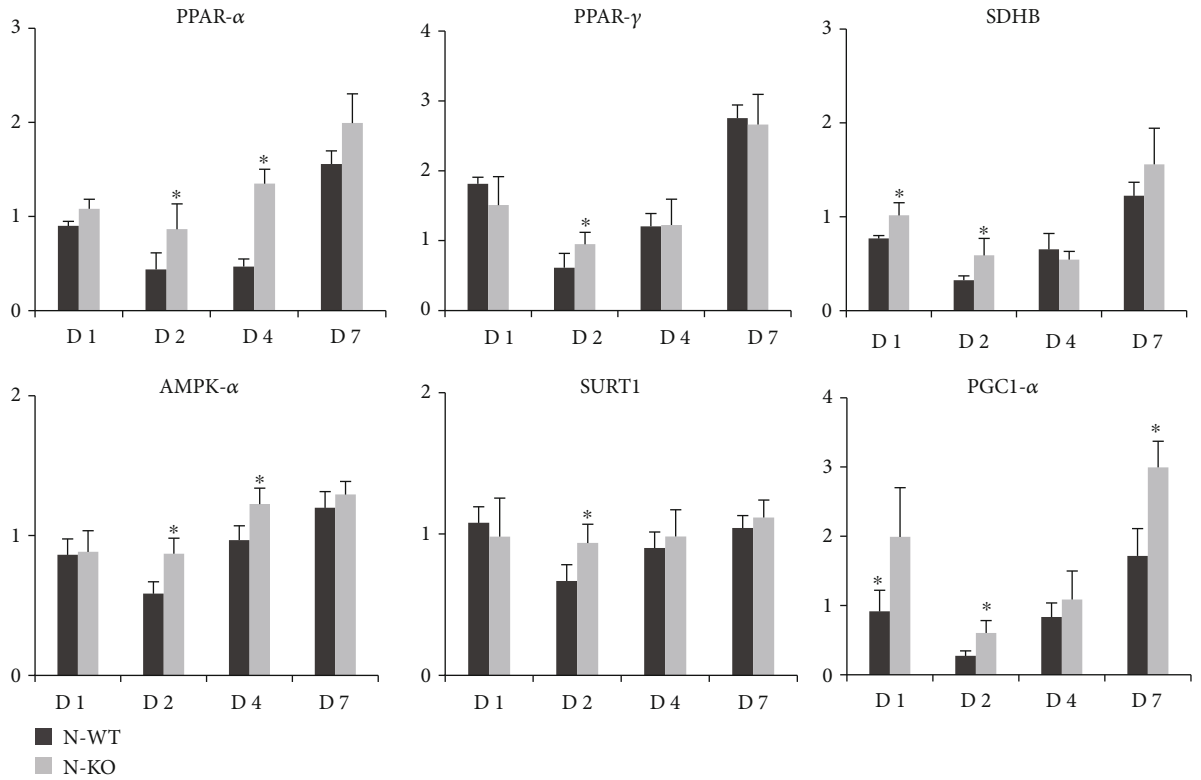
(a)
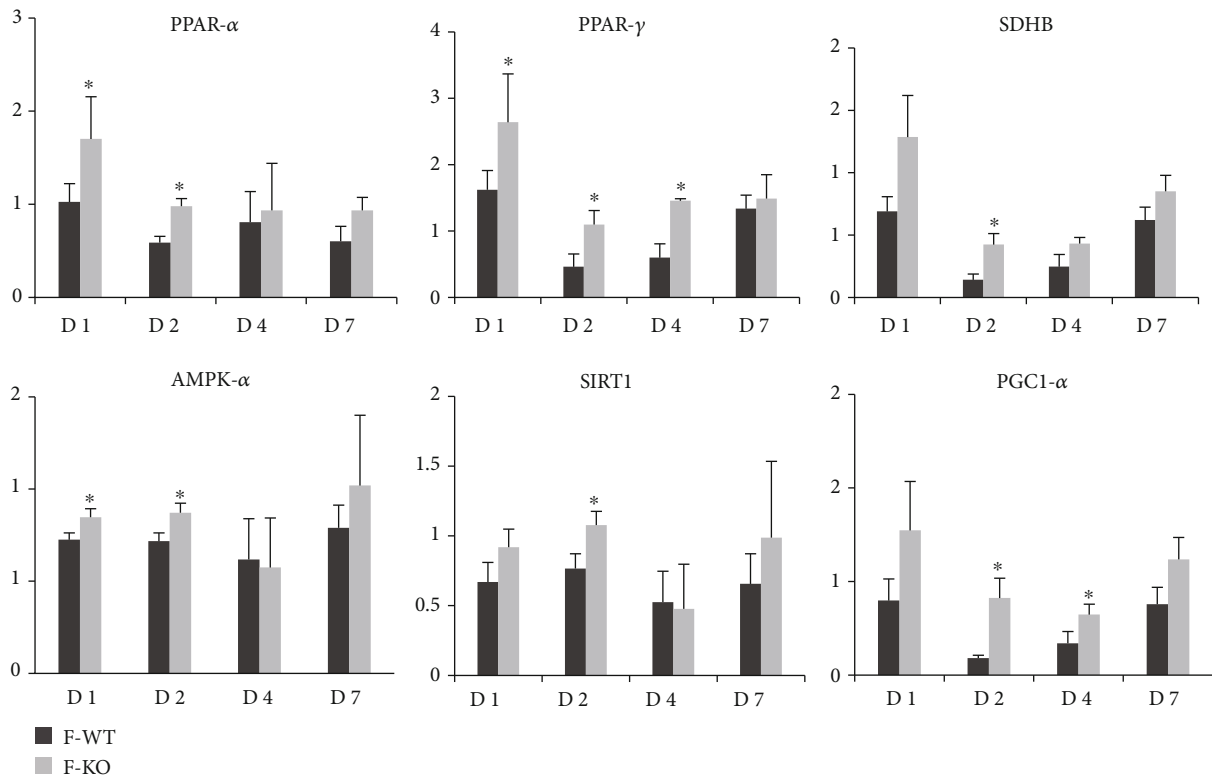
(b)

FIGURE 6: The knockout of AR promoted mitochondrial biogenesis and energy metabolism in liver after major hepatectomy and IR injury. (a) The expressions of PPAR-α, PPAR-β, SDHB, AMPK, SIRT1, and PGC1 in normal liver were found to be increased in the N-KO group after major hepatectomy and IR injury. (b) The knockout of AR increased the mRNA levels of PPAR-α, PPAR-β, SDHB, AMPK, SIRT1, and PGC1 in fatty liver after major hepatectomy and IR injury ($^*P < 0.05$, $N = 4$-6/group).
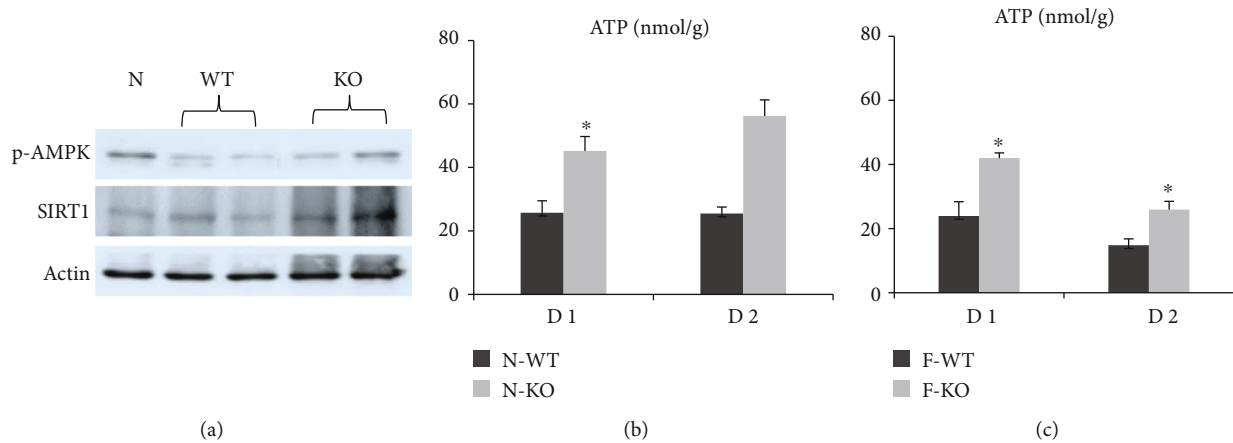
FIGURE 7: The knockout of AR increased ATP content in liver after major hepatectomy and IR injury. (a) The knockout of AR increased the expression of p-AMPK and SIRT1 in liver after major hepatectomy and IR injury compared to the wild-type group. (b) The knockout of AR increased the content of ATP in both normal and fatty livers after major hepatectomy and IR injury compared to the wild-type group ($^*P < 0.05$, $N = 4$-6/group).

evolutionarily conserved sensor of cellular energy status that contributes to the restoration of energy homeostasis. AMPK is critical for energy-demanding situations such as liver regeneration by controlling the balance between hepatocyte metabolic adaptation [33]. Deletion of AMPK-α delayed liver regeneration after partial hepatectomy by impacting on the G1/S transition phase [34]. PGC1-α, as the coactivator of PPAR-γ, has been reported to play important roles in mitochondrial biogenesis and energy metabolism. The AR inhibitor increased mitochondrial biogenesis via increasing the expression of Nrf2/HO-1/AMPK/p53 and decreasing the mitochondrial DNA damage in colon cancer cells [35]. In addition, the inhibition of AR also attenuated alcoholic liver disease by activating AMPK and modulating oxidative stress [36]. In this study, our results showed that the knockout of AR increased the expressions of AMPK, SIRT1, PGC1-α, SDHB, and ATP content in both normal and fatty livers after major hepatectomy and IR injury. These data indicated that AR inhibition accelerated fatty liver regeneration maybe through regulating mitochondrial biogenesis and energy metabolism. The precise mechanism of AR in regulating energy metabolism during liver regeneration needs to be further studied.

In summary, we demonstrated the role and underlying mechanism of AR in the regeneration of normal and fatty livers after liver surgery. The knockout of AR promoted the regeneration of normal and fatty livers through regulating energy metabolism. The effect of AR in liver regeneration may provide a new potential therapeutic target to accelerate postoperative liver regeneration and decrease the incidence of mobility and mortality.

Data Availability

The datasets used and/or analyzed during the current study are available from the corresponding author on reasonable request.

Conflicts of Interest

The authors declare that there is no conflict of interests regarding the publication of this paper.

Acknowledgments

Supplementary Materials

Supplementary Table 1: sequences of the primer pairs. (Supplementary Materials)

References

[1] G. Vernon, A. Baranova, and Z. M. Younossi, "Systematic review: the epidemiology and natural history of non-alcoholic fatty liver disease and non-alcoholic steatohepatitis in adults," *Alimentary Pharmacology & Therapeutics*, vol. 34, no. 3, pp. 274–285, 2011.

[2] V. E. de Meijer, B. T. Kalish, M. Puder, and J. N. M. IJzermans, "Systematic review and meta-analysis of steatosis as a risk factor in major hepatic resection," *The British Journal of Surgery*, vol. 97, no. 9, pp. 1331–1339, 2010.

[3] R. Veteläinen, A.??. van Vliet, D. J. Gouma, and T. M. van Gulik, "Steatosis as a risk factor in liver surgery," *Annals of Surgery*, vol. 245, no. 1, pp. 20–30, 2007.

[4] Y. Inaba, T. Furutani, K. Kimura et al., "Growth arrest and DNA damage-inducible 34 regulates liver regeneration in hepatic steatosis in mice," *Hepatology*, vol. 61, no. 4, pp. 1343–1356, 2015.

[5] H. Kato, N. Kuriyama, S. Duarte, P. A. Clavien, R. W. Busuttil, and A. J. Coito, "MMP-9 deficiency shelters endothelial PECAM-1 expression and enhances regeneration of steatotic

livers after ischemia and reperfusion injury," *Journal of Hepatology*, vol. 60, no. 5, pp. 1032–1039, 2014.

[6] A. S. Grewal, S. Bhardwaj, D. Pandita, V. Lather, and B. S. Sekhon, "Updates on aldose reductase inhibitors for management of diabetic complications and non-diabetic diseases," *Mini Reviews in Medicinal Chemistry*, vol. 16, no. 2, pp. 120–162, 2016.

[7] S. K. Srivastava, U. C. S. Yadav, A. B. M. Reddy et al., "Aldose reductase inhibition suppresses oxidative stress-induced inflammatory disorders," *Chemico-Biological Interactions*, vol. 191, no. 1-3, pp. 330–338, 2011.

[8] Y. Y. Wang, L. N. Qi, J. H. Zhong et al., "High expression of AKR1B10 predicts low risk of early tumor recurrence in patients with hepatitis B virus-related hepatocellular carcinoma," *Scientific Reports*, vol. 7, no. 1, article 42199, 2017.

[9] K. V. Ramana, B. Friedrich, A. Bhatnagar, and S. K. Srivastava, "Aldose reductase mediates cytotoxic signals of hyperglycemia and TNF-α in human lens epithelial cells," *The FASEB Journal*, vol. 17, no. 2, pp. 315–317, 2003.

[10] K. V. Ramana, A. Bhatnagar, and S. K. Srivastava, "Inhibition of aldose reductase attenuates TNF-α-induced expression of adhesion molecules in endothelial cells," *The FASEB Journal*, vol. 18, no. 11, pp. 1209–1218, 2004.

[11] L. Qiu and C. Guo, "Natural aldose reductase inhibitor: a potential therapeutic agent for non-alcoholic fatty liver disease," *Current Drug Targets*, vol. 20, 2019.

[12] R. Ananthakrishnan, M. Kaneko, Y. C. Hwang et al., "Aldose reductase mediates myocardial ischemia-reperfusion injury in part by opening mitochondrial permeability transition pore," *American Journal of Physiology. Heart and Circulatory Physiology*, vol. 296, no. 2, pp. H333–H341, 2009.

[13] C. X. Li, K. T. P. Ng, Y. Shao et al., "The inhibition of aldose reductase attenuates hepatic ischemia-reperfusion injury through reducing inflammatory response," *Annals of Surgery*, vol. 260, no. 2, pp. 317–328, 2014.

[14] C. Zhang, C. Huang, Y. Tian, and X. Li, "Polyol pathway exacerbated ischemia/reperfusion-induced injury in steatotic liver," *Oxidative Medicine and Cellular Longevity*, vol. 2014, Article ID 963629, 9 pages, 2014.

[15] C. Zhang, X. Li, and Q. Liu, "Sorbitol dehydrogenase inhibitor protects the liver from ischemia/reperfusion-induced injury via elevated glycolytic flux and enhanced sirtuin 1 activity," *Molecular Medicine Reports*, vol. 11, no. 1, pp. 283–288, 2015.

[16] L. M. Zukin, M. G. Pedler, K. Chyung et al., "Aldose reductase inhibition enhances lens regeneration in mice," *Chemico-Biological Interactions*, vol. 307, pp. 58–62, 2019.

[17] C. X. Li, L. L. Chen, X. C. Li et al., "ApoA-1 accelerates regeneration of small-for-size fatty liver graft after transplantation," *Life Sciences*, vol. 215, pp. 128–135, 2018.

[18] N. Fausto, J. S. Campbell, and K. J. Riehle, "Liver regeneration," *Hepatology*, vol. 43, Supplement 1, pp. S45–S53, 2006.

[19] R. Taub, "Liver regeneration: from myth to mechanism," *Nature Reviews Molecular Cell Biology*, vol. 5, no. 10, pp. 836–847, 2004.

[20] S. Q. Yang, H. Z. Lin, A. K. Mandal, J. Huang, and A. M. Diehl, "Disrupted signaling and inhibited regeneration in obese mice with fatty livers: implications for nonalcoholic fatty liver disease pathophysiology," *Hepatology*, vol. 34, no. 4, pp. 694–706, 2001.

[21] R. A. Woo and R. Y. Poon, "Cyclin-dependent kinases and S phase control in mammalian cells," *Cell Cycle*, vol. 2, no. 4, pp. 316–324, 2003.

[22] C. H. Yam, T. K. Fung, and R. Y. C. Poon, "Cyclin A in cell cycle control and cancer," *Cellular and Molecular Life Sciences*, vol. 59, no. 8, pp. 1317–1326, 2002.

[23] S. P. Anderson, L. Yoon, E. B. Richard, C. S. Dunn, R. C. Cattley, and J. C. Corton, "Delayed liver regeneration in peroxisome proliferator-activated receptor-α-null mice," *Hepatology*, vol. 36, no. 3, pp. 544–554, 2002.

[24] M. S. Rao, J. M. Peters, F. J. Gonzalez, and J. K. Reddy, "Hepatic regeneration in peroxisome proliferator-activated receptor α-null mice after partial hepatectomy," *Hepatology Research*, vol. 22, no. 1, pp. 52–57, 2002.

[25] H. X. Liu, Y. Fang, Y. Hu, F. J. Gonzalez, J. Fang, and Y. J. Y. Wan, "PPARβ regulates liver regeneration by modulating Akt and E2f signaling," *PLoS One*, vol. 8, no. 6, article e65644, 2013.

[26] A. Magadum and F. B. Engel, "PPARβ/δ: linking metabolism to regeneration," *International Journal of Molecular Sciences*, vol. 19, no. 7, p. 2013, 2018.

[27] L. Qiu, X. Wu, J. F. L. Chau et al., "Aldose reductase regulates hepatic peroxisome proliferator-activated receptor α phosphorylation and activity to impact lipid homeostasis," *The Journal of Biological Chemistry*, vol. 283, no. 25, pp. 17175–17183, 2008.

[28] E. Gonzales, B. Julien, V. Serrière-Lanneau et al., "ATP release after partial hepatectomy regulates liver regeneration in the rat," *Journal of Hepatology*, vol. 52, no. 1, pp. 54–62, 2010.

[29] S. Crumm, M. Cofan, E. Juskeviciute, and J. B. Hoek, "Adenine nucleotide changes in the remnant liver: an early signal for regeneration after partial hepatectomy," *Hepatology*, vol. 48, no. 3, pp. 898–908, 2008.

[30] S. Thevananther, H. Sun, D. Li et al., "Extracellular ATP activates c-Jun N-terminal kinase signaling and cell cycle progression in hepatocytes," *Hepatology*, vol. 39, no. 2, pp. 393–402, 2004.

[31] Z. Zhong, H. Connor, M. Froh et al., "Free radical-dependent dysfunction of small-for-size rat liver grafts: prevention by plant polyphenols," *Gastroenterology*, vol. 129, no. 2, pp. 652–664, 2005.

[32] Z. Zhong, R. F. Schwabe, Y. Kai et al., "Liver regeneration is suppressed in small-for-size liver grafts after transplantation: involvement of c-Jun N-terminal kinase, cyclin D1, and defective energy supply," *Transplantation*, vol. 82, no. 2, pp. 241–250, 2006.

[33] M. Varela-Rey, N. Beraza, S. C. Lu, J. M. Mato, and M. L. Martínez-Chantar, "Role of AMP-activated protein kinase in the control of hepatocyte priming and proliferation during liver regeneration," *Experimental Biology and Medicine (Maywood, N.J.)*, vol. 236, no. 4, pp. 402–408, 2011.

[34] G. Merlen, G. Gentric, S. Celton-Morizur et al., "AMPKα1 controls hepatocyte proliferation independently of energy balance by regulating Cyclin A2 expression," *Journal of Hepatology*, vol. 60, no. 1, pp. 152–159, 2014.

[35] K. Shukla, H. Sonowal, A. Saxena, K. V. Ramana, and S. K. Srivastava, "Aldose reductase inhibitor, fidarestat regulates mitochondrial biogenesis via Nrf2/HO-1/AMPK pathway in colon cancer cells," *Cancer Letters*, vol. 411, pp. 57–63, 2017.

[36] C. Shi, Y. Wang, J. Gao et al., "Inhibition of aldose reductase ameliorates alcoholic liver disease by activating AMPK and modulating oxidative stress and inflammatory cytokines," *Molecular Medicine Reports*, vol. 16, no. 3, pp. 2767–2772, 2017.

Research Article

Inhibition of Mitochondrial ROS by MitoQ Alleviates White Matter Injury and Improves Outcomes after Intracerebral Haemorrhage in Mice

Weixiang Chen, Chao Guo, Zhengcai Jia, Jie Wang, Min Xia, Chengcheng Li, Mingxi Li, Yi Yin, Xiaoqin Tang, Tunan Chen, Rong Hu, Yujie Chen (ID), Xin Liu (ID), and Hua Feng (ID)

Department of Neurosurgery, Southwest Hospital, Third Military Medical University (Army Medical University), 29 Gaotanyan Street, Shapingba District, Chongqing 400038, China

Correspondence should be addressed to Xin Liu; shenwai@tmmu.edu.cn and Hua Feng; fenghua8888@vip.163.com

White matter injury (WMI) is an important cause of high disability after intracerebral haemorrhage (ICH). It is widely accepted that reactive oxygen species (ROS) contributes to WMI, but there is still no evidence-based treatment. Here, mitoquinone (MitoQ), a newly developed selective mitochondrial ROS scavenger, was used to test its neuroprotective potential. The data showed that MitoQ attenuated motor function deficits and motor-evoked potential (MEP) latency prolongation. Further research found that MitoQ blunted the loss of oligodendrocytes and oligodendrocyte precursor cells, therefore reduced demyelination and axon swelling after ICH. In the in vitro experiments, MitoQ, but not the nonselective antioxidant, almost completely attenuated the iron-induced membrane potential decrease and cell death. Mechanistically, MitoQ blocked the ATP deletion and mitochondrial ROS overproduction. The present study demonstrates that the selective mitochondrial ROS scavenger MitoQ may improve the efficacy of antioxidant treatment of ICH by white matter injury alleviation.

1. Introduction

The prevalence rate of intracerebral haemorrhage (ICH) is approximately 120/100000 [1]. Fifty-eight percent of ICH patients die within one year, and two-thirds of survivors remain moderately or even severely disabled [2, 3]. Serious secondary brain injury (SBI) is the major cause of the poor prognosis of the patient after ICH, which includes white matter injury, inflammation, and neuronal death [4]. Among these processes, white matter injury- (WMI-) induced motor function deficit is a serious complication affecting the quality of life of patients after ICH [5]. However, there is still no medicine available for WMI after intracerebral haemorrhage.

Reactive oxygen species (ROS) are the primary inducement of secondary injury after ICH [6]. Excessive accumulation of ROS can induce significant cell death and tissue damage [7]. Since the mitochondria are the main source of ROS, mitochondria enrichment and hyperoxia consumption in the central nervous system lead to the tissue being suscep-

tible to oxidative stress injury [8, 9]. Oligodendrocyte is rich in lipids and is prone to oxidative stress damage, which leads to white matter injury [10]. Several antioxidants showed promising results but failed in the clinical trial of intracerebral haemorrhage [11, 12]. ROS are mainly produced by the Fenton reaction induced by iron overload after ICH, which occurs primarily in the mitochondria [13–15]. And the selective mitochondrial ROS scavengers are reported superior to nonselective ROS scavengers in the treatment of many redox diseases involving mitochondrial dysfunction [16–18]. Therefore, it is urgent to explore the protective effect of selective mitochondrial ROS scavenger on secondary injury of ICH.

Mitoquinone (MitoQ) is a selective mitochondrial antioxidant that accumulates in high concentrations in the mitochondria. The compound which passes easily through the blood-brain barrier rapidly accumulates in the brain [19, 20]. Although the administration of MitoQ can reduce mitochondrial oxidative damage in in vitro experiments

such as erastin-mediated ferroptosis and in vivo experiments such as myocardial injury models [21, 22], it still needs to be investigated after induction after ICH. To explore the role of selective targeting mitochondrial ROS in white matter damage of ICH and its related mechanisms, MitoQ was administrated and demyelination, white matter injury, and neurological deficits were explored after ICH in this study.

2. Materials and Methods

2.1. Animal Model. All animal procedures were approved by the Animal Care and Use Committee of the National Institute on Aging Intramural Research Program. Seven-week-old C57BL/6N mice weighing 23–26 g were purchased from Army Medical University. The animals were randomly divided into different experimental groups.

The animals were anesthetized with halothane (70% N_2O and 30% O_2; 4% induction, 2% maintenance, China), immobilized on a stereotactic instrument (RWD Life Sciences Ltd. China), and injected with 25 μl of autologous blood into the right caudate nucleus. The following coordinates were used, as described previously, from bregma: 0.8 mm anteriorly, 2.5 mm laterally, and 3.0 mm deep [23]. The craniotomy was finished with bone wax, and sutures were applied to the scalp. During the entire experiment and recovery, the body temperature of the animals was maintained at $37 \pm 0.5°C$. Sham-operated mice were subjected to needle insertion only.

MitoQ was purchased from BioVision (B1309, USA, dissolved in a 1 : 1 ratio of ethanol to water and dissolved in 1 mL 0.9% sterile NaCl at a final concentration of 1 mg/mL) and administered intraperitoneally (i.p.) 1 hour and 24 hours after ICH (4 mg/kg). The ICH+vehicle group received an equal volume of solvent at the corresponding time point as the ICH+MitoQ group [20, 24].

2.2. Immunohistochemistry. The brains were removed after perfusion with the fixative 4% paraformaldehyde and then immersed in 30% sucrose in phosphate-buffered saline (PBS). Serial sections were cut on a freezing microtome, blocked, and incubated in the following primary antibodies: goat anti-MBP (diluted 1 : 500, Santa Cruz, sc-13914, USA), rabbit anti-Neurofilament 200 (NF200) (1 : 200; Sigma-Aldrich, N4142, USA), mouse anti-APC (or Ab-7, CC-1) (1 : 500; Merck Millipore, OP80, USA), and rat anti-NG-2 (NG2 chondroitin sulfate proteoglycan; 1 : 200; Millipore; AB5320, USA). After washing, the sections were incubated with the appropriate fluorescent secondary Alexa Fluor 488- or Alexa Fluor 555-conjugated antibody (diluted 1 : 1000, Invitrogen, USA) and counterstained with DAPI. Images of the perihematomal region in each section were captured by a Zeiss microscope (LSM780; Zeiss, Germany). Randomly selected microscopic fields on each of the three consecutive sections from each brain were analyzed by a blinded investigator.

2.3. Transmission Electron Microscopy. For the transmission electron microscopy (TEM), the animals were perfused with 1.25% glutaraldehyde and 2% paraformaldehyde in 0.1 M PB

after an initial flush with isotonic saline. Then, the brains were rapidly removed and fixed for at least three days at 4°C. The tissues were rinsed and post fixed with 1% OsO_4 in PB for two hours, counterstained with uranyl acetate, dehydrated in a graded series of acetone, infiltrated with propylene oxide, and embedded in Epon. Ultrathin sections (~60 nm) were cut by an ultramicrotome (LKB-V, LKB Produkter AB, Bromma, Germany) and observed under a transmission electron microscope (Tecnai 10; Philips, Netherlands) [25]. Random images of 12 different fields of view were selected for each animal for the statistical analysis of myelinated axons. The *g*-ratios of the myelinated fibers were calculated as the ratio of the diameter of the axon to the diameter of the axon and myelin sheath using ImageJ software (ImageJ 1.8; NIH, Bethesda, MD, USA), and at least 60 myelinated fibers from each animal were analyzed [26].

2.4. Behavioral Tests

2.4.1. Beam Walking Test. The mouse was allowed to cross a round wooden beam with a diameter of 1.5 cm and a length of 70 cm. The mice were required to completely cross the beam to obtain a corresponding score. The test was repeated three times, and the score (0–4) was decided by the walking distance. The average score of three consecutive trials was calculated. Higher scores indicated better test performance. The scores are as follows: 0 point: the mouse cannot grasp or sit on the wooden pole and falls immediately; 1 point: the mouse can grasp or sit on the wooden pole and cannot move, but can remain on the pole for 1 minute; 2 points: the mouse can maintain its balance on the wooden pole, carry out small activities, and remain on the pole for 1 minute; 3 points: the mouse can walk from one end of the pole to the other end, but foot faults occur; and 4 points: the mouse can freely walk from one end of the wooden pole to the other [27].

2.4.2. Basso Mouse Scale (BMS). This open-field locomotor scoring system ranges from 0 (no ankle movement) to 9 (frequent or consistent plantar stepping that is mostly coordinated, parallel paws during the initial contact and lifting of the paws, normal trunk stability, and a constantly raised tail) [28, 29].

All the behavioral tests were randomly assigned, and the investigator was blinded to the tests.

2.5. Electrophysiological Assessment. In each recording session, the mice were anesthetized with halothane (70% N_2O and 30% O_2; 4% induction, 2% maintenance). Motor-evoked potentials (MEPs) were elicited with a pair of needle monopolar electrodes placed over the intact scalp and implanted into the skull above the primary motor cortex. The cathode was placed at the midpoint of an imaginary line connecting the two ears, and the anode was placed at the base of the nose. A needle electrode was inserted into the contralateral gastrocnemius muscle to record MEPs. Electrical stimulation was applied with a stimulator to excite the brain (Keypoint, Medtronic, USA). A single pulse of stimulation (7.8 mA, 0.1 ms, 1 Hz) was delivered via a single electrode

(DSN1620, Medtronic, USA). A single pulse of stimulation ($100 \mu s$, 350 V) was delivered via a modified E5-9S ear electrode (Electro-Cap Inc., Eaton, OH, China). The electrical stimulation was repeated five times in each mouse with an interval of 15 seconds. An activity that was two standard deviations above the baseline activity in response to transcranial stimulation was regarded as the MEPs. The MEP latency was recorded for analysis.

Clampfit software was used to analyze MEP data. Events that occurred within 4–8 ms after TMS and had the peak amplitude that was two standard deviations above the baseline activity were regarded as MEPs.

2.6. Immunoblot Analysis. Cultured cells or tissues were solubilized in sample buffer, and the protein concentration of each sample was determined using a Beyotime protein assay kit with bovine serum albumin as the standard. Immunoblot analysis ($30 \mu g$ of protein per lane) was conducted using a 4–10% SDS gradient polyacrylamide gel followed by a standard blotting procedure. Primary antibodies that selectively recognize goat anti-MBP (1 : 250; Santa Cruz; Cat: sc-13914, USA) and actin (1 : 2000, Santa Cruz, USA) were used. Images of the blots were analyzed using ImageJ software (NIH, USA).

2.7. Cell Cultures and In Vitro Study

2.7.1. Cell Cultures. OLI-neu, an immortalized oligodendrocyte cell line, was kindly gifted by Professor Lan Xiao (Department of Histology and Embryology, Chongqing Key Laboratory of Neurobiology, Third Military Medical University) and cultured in DMEM (Gibco, USA) with 10% fetal calf serum (FCS; Gibco, USA), N2 supplement (Gibco, USA), and insulin (Sigma, USA). For the cell death experiment and mitochondrial membrane potential, the OLI-neu cells were exposed to $250 \mu M$ $FeCl_2$ for 48 hours with or without 400 nM MitoQ and 1 mM NAC (N-acetyl-L-cysteine; Sigma, USA). For ATP and mitochondrial ROS assays, OLI-neu cells from each group were treated as described above for 24 hours.

2.7.2. Mitochondrial Membrane Potential and Cell Death Assay. The mitochondrial membrane potential ($\Delta \Psi m$) was measured using TMRM (Life Technology, USA) following the manufacturer's instructions. The OLI-neu cells were plated at a concentration of 1×10^5 cells/ml. The cells were then stained with TMRM at a final concentration of 25 nM in the culture medium at room temperature. TMRM staining was analyzed using the Auto Live-Cell Imaging Station (Invitrogen™, USA), with excitation and emission wavelengths of 535 nm and 610/620 nm, respectively [7]. Cell death analysis was performed using a propidium iodide (PI; Thermo, USA) detection kit (R37108, Thermo, USA); at the end of the experiment, the medium was removed, and the cells were washed with PBS and stained with 500 nM PI for 20 min in a humidified atmosphere of 5% CO_2 at 37°C. After washing with PBS, the cell sampling was performed using flow cytometry (Beckman MoFlo XDP, USA).

2.7.3. Mitochondrial ROS and ATP Content Detection. Mitochondrial ROS were measured by MitoSOX Red (Molecular Probes, Eugene, OR, USA), which is a fluorogenic indicator of superoxide generated specifically by the mitochondria. At the end of the experiment, the medium was removed, and the cells were washed with PBS and stained with $5 \mu M$ MitoSOX Red for 10 min in a humidified atmosphere of 5% CO_2 at 37°C. After washing with PBS, the cell sampling was performed using confocal microscopy (Zeiss LSM 780, Germany) or flow cytometry (Beckman MoFlo XDP, USA) and analyzed by FlowJo. For in vivo Mito-ROS (mitochondrial ROS) analysis, perihematomal tissues were homogenized in mitochondria isolation buffer reagent A (Mitochondria Isolation Kit, 89874, Thermo, USA) and centrifuged at $850g$ for 5 min at 4°C. The pellet was discarded, and the supernatant was centrifuged a second time at $13,500g$ for 10 min. The pellet was resuspended in isolation buffer reagent C, and the mixture was centrifuged again at $13,500g$ for 10 min. This step was repeated once, and the final pellet was resuspended in isolation buffer without EDTA, then washed with mitochondrial solution and stained with $5 \mu M$ MitoSOX Red for 10 min in a humidified atmosphere of 5% CO_2 at 37°C. After washing with PBS, the cell sampling was performed using confocal microscopy.

OLI-neu cells were lysed in RIPA buffer and homogenized by passing through a 25-gauge syringe needle multiple times. The samples were then centrifuged at 10000 rcf (g) for 10 min at 4°C, and then ATP levels in the supernatants were measured using a bioluminescence detection kit (Beyotime, China). In brief, $30 \mu l$ (cells) of supernatant was transferred into one well of a black 96-well plate, and $150 \mu l$ reaction buffer was added to each well. The luminescence was determined as relative luminescent units using a Varioskan Flash (Thermo, USA). Experiments were performed with two replicates of each sample. The determined protein concentrations of each sample were used to normalize the ATP level.

2.8. Statistical Analysis. The values are presented as the mean ± SEM, and SPSS 19 (SPSS Inc., Chicago, USA) was used for statistical analysis. If the data were not normally distributed even with log transformation, the Kruskal-Wallis test followed by Dunn's post hoc test was used for statistics, and the median and interquartile range are used to express this data. The Mann–Whitney U test was used to compare behavioral and activity scores among the groups. Other data were analyzed by one-way ANOVA followed by the Scheffé F test for post hoc analysis or by Student's t test. $P < 0.05$ was considered statistically significant.

3. Results

3.1. MitoQ Attenuated Neurological Deficits after ICH. The Basso Mouse Scale (BMS) and the beam walking test indicated neurological function impairments in the ICH+vehicle group compared to the sham group (Figures 1(a) and 1(b)). The MitoQ treatment group exhibited improved neurological scores compared to those of the ICH+vehicle group (BMS, $P < 0.05$ on days 1, 2, 3, 5, and 7; beam walking, $P < 0.05$ on days 1, 2, 3, 5, and 28; Figures 1(c) and 1(d)).

(a)

(b)

(c)

(d)
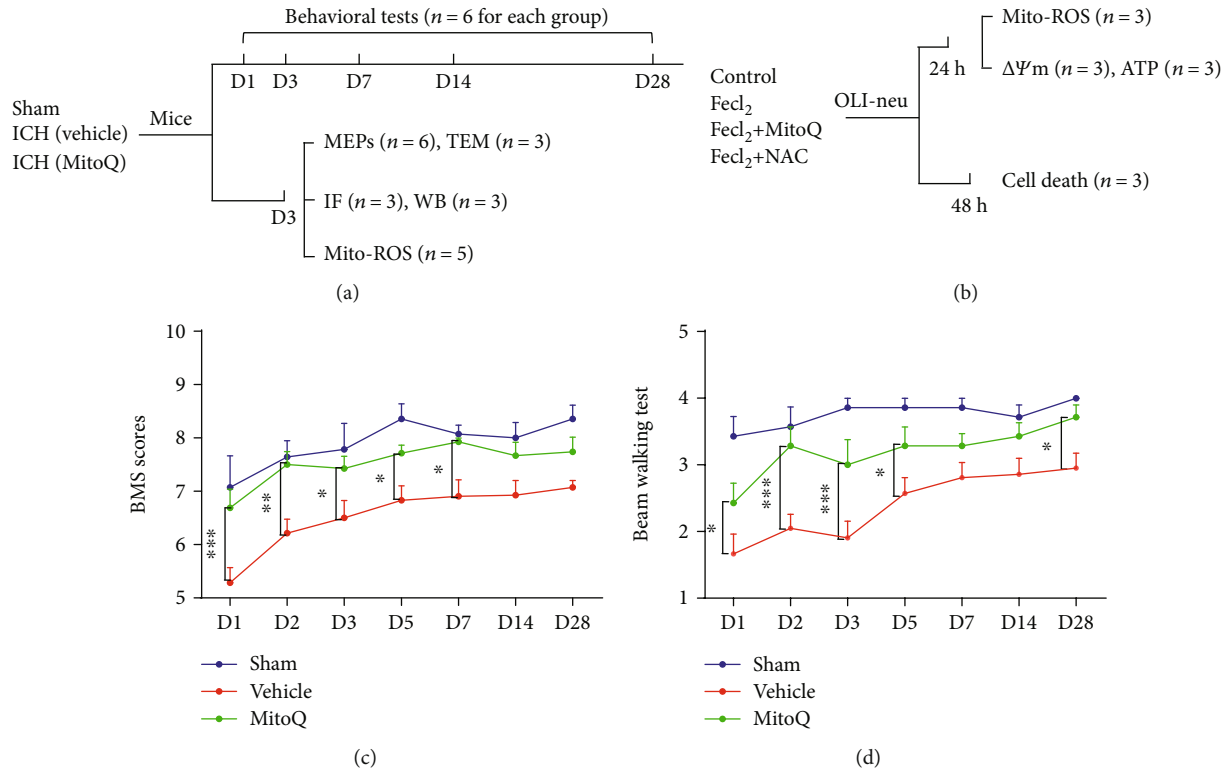
FIGURE 1: Mitoquinone (MitoQ) attenuated neurological deficits after ICH. (a) In vivo experimental design. IF: immunofluorescence; WB: western blotting. The "n" means the number of mice in each group. (b) In vitro experimental design. (c) Basso Mouse scale. (d) Beam walking test. The neurological score data is expressed as the median and the interquartile range and were analyzed using the Kruskal–Wallis test followed by Dunn's post hoc test. $^{*}P < 0.05$; $^{**}P < 0.01$; $^{***}P < 0.001$.

3.2. MitoQ Alleviated MEP Latency Prolongation and White Matter Damage after ICH.

Our results and other research groups found that the neurological behavior and electrophysiological conductivity of mice after ICH was significant impaired after three days. In addition, the pathological results of previous studies also showed that the inflammatory reaction and white matter damage around the hematoma were the most serious on the third day [30, 31]. So we chose the third day after bleeding as the main time to study the physiological changes. The motor-evoked potential (MEP) latency, which indicated the transduction of cortical spinal tracts, was significantly prolonged on the third day after ICH (23.56 ± 1.74 ms in the vehicle group versus 14.84 ± 0.67 ms in the sham group, $P < 0.001$; Figures 2(a) and 2(b)), and MitoQ treatment reduced the MEP latency prolongation (15.84 ± 0.78 ms in the MitoQ group versus the vehicle group, $P < 0.001$; Figures 2(a) and 2(b)). The g-ratio of the nerve conduction tracts was calculated in the internal capsule around the hematoma and an increased g-ratio indicated thinning of the myelin sheath (sham, 0.61 ± 0.037; vehicle, 0.76 ± 0.031; MitoQ, 0.66 ± 0.019; Figures 2(c) and 2(d)). The diameter of the axons is listed in each group, and an increase in the diameter of axon indicates the axon edema (sham, 0.74 ± 0.009; vehicle, 0.82 ± 0.008; MitoQ, 0.73 ± 0.010; Figure 2(e)). The results showed that the g-ratio of the tracts and the diameter of the axons were significantly increased in the

ICH+vehicle group compared with the sham group (diameter of the axons, $P < 0.01$; g-ratio, $P < 0.001$; Figures 2(c)–2(e)). Compared with vehicle treatment, MitoQ treatment resulted in a significant increase in the g-ratio of the tracts and the diameter of the axons when compared with the ICH+vehicle group (diameter of the axons, $P < 0.05$; g-ratio, $P < 0.001$; Figures 2(c)–2(e)).

3.3. MitoQ Reduced Demyelination after ICH.

The intensity of myelin basic protein (MBP) staining in the vehicle group was decreased on day 3 compared with that in the sham group ($P < 0.01$) (Figures 3(a) and 3(b)), which indicated the degradation of myelin. Western blotting confirmed a significant decrease in the expression of MBP in the ICH+vehicle group compared with the sham group ($P < 0.05$; Figures 3(c) and 3(d)). And compared to vehicle treatment, the administration of MitoQ after ICH resulted in a significant increase in MBP expression compared with the ICH+vehicle group ($P < 0.05$; Figures 3(c) and 3(d)).

3.4. MitoQ Decreased the Loss of Oligodendrocyte Precursor Cells and Oligodendrocytes after ICH.

Three days after ICH, the mice were euthanized, and their brains were processed for the analysis of cell survival in the regions around the hematoma of the internal capsule. The brain sections were stained with DAPI to label all of the cells and with NG-2 and APC antibodies to label oligodendrocyte precursor

(a)

(b)

(c)

(d)

(e)
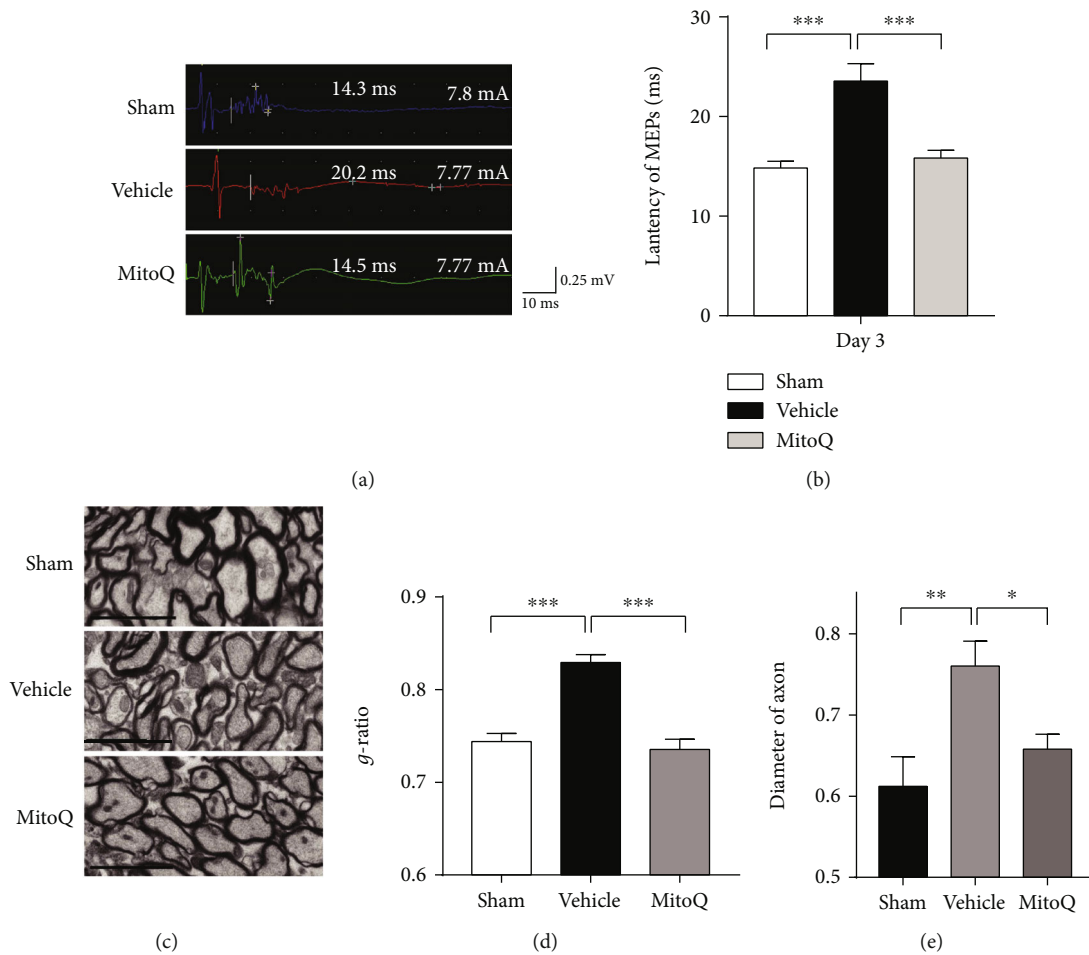
FIGURE 2: Mitoquinone (MitoQ) attenuated latency prolongation and white matter injury after ICH. (a) Motor-evoked potential latency. The scale bar is shown adjacent to the image. (b) The results of the latency of MEPs were analyzed; $n = 6$ per group. (c) Transmission electron microscopy showing axons and myelin sheaths around the hematoma on the third day after ICH; scale bars: 2 nm (inset column). (d) The g-ratios of the different groups; $n = 60$, 3 mice. (e) The diameters of the axons; $n = 60$, 3 mice. The values represent the mean ± SEM when using ANOVA followed by Tukey's post hoc test. $^*P < 0.05$; $^{**}P < 0.01$; $^{***}P < 0.001$.

cells (OPCs) and oligodendrocytes (OLs), respectively (Figure 4(a)). The results of the cell counts revealed that significantly more OLs and OPCs loss in the ICH+vehicle group mice compared to the sham group mice (OPCs, $P < 0.001$; OLs, $P < 0.001$; Figures 4(a) and 4(b)). MitoQ treatment attenuated the loss of both cell types (OPCs, $P < 0.05$; OLs, $P < 0.05$; Figures 4(a) and 4(b)). The level of perihematomal mitochondrial ROS increased 3 days after ICH injury in mice. MitoQ, a selective mitochondrial ROS scavenger, significantly reduced the level of mitochondrial ROS (Figures 4(c) and 4(d)).

3.5. MitoQ Blocked Iron Overload-Induced Loss of Mitochondrial Membrane Potential and Death of OLI-Neu Cells.
Cell death caused by oxidative stress is one of the mechanisms of secondary injury after ICH, and mitochondrial dysfunction is the important target of cell death caused by oxidative stress. To verify the protective effect of selective mitochondria ROS scavengers on oxidative stress after ICH, iron, which is released from hematoma after ICH, was used

to simulate oxidative stress injury. TMRM was used to detect mitochondrial membrane potential and NAC as a nonselective ROS scavenger as control.

The real-time detection of living cells showed that MitoQ, but not NAC, could reduce the mitochondrial membrane potential decline and cell death induced by $250\,\mu m$ $FeCl_2$ in OLI-neu cells (cell death rate: $3.67 \pm 0.34\%$ in the control group versus $15.13 \pm 1.57\%$ in the $FeCl_2$ group, $P < 0.05$; $6.07 \pm 0.80\%$ in the $FeCl_2$+MitoQ group versus $15.03 \pm 3.38\%$ in the $FeCl_2$+NAC group, $P < 0.05$; Figures 5(a)–5(d)).

3.6. MitoQ Inhibited Mitochondrial ROS and ATP Deletion in OLI-Neu Cells.
In order to investigate the protective effect of selective mitochondrial antioxidants, mitochondrial ROS in OLI-Neu cells was detected with MitoSOX after 24 hours of ferrous ion treatment. Results showed that the fluorescence intensity of MitoSOX was significantly enhanced which indicated the increasing of mitochondrial ROS in the OLI-neu cells after treatment with $250\,\mu M$ $Fecl_2$. MitoQ, rather than

(a)

(b)

(c)

(d)
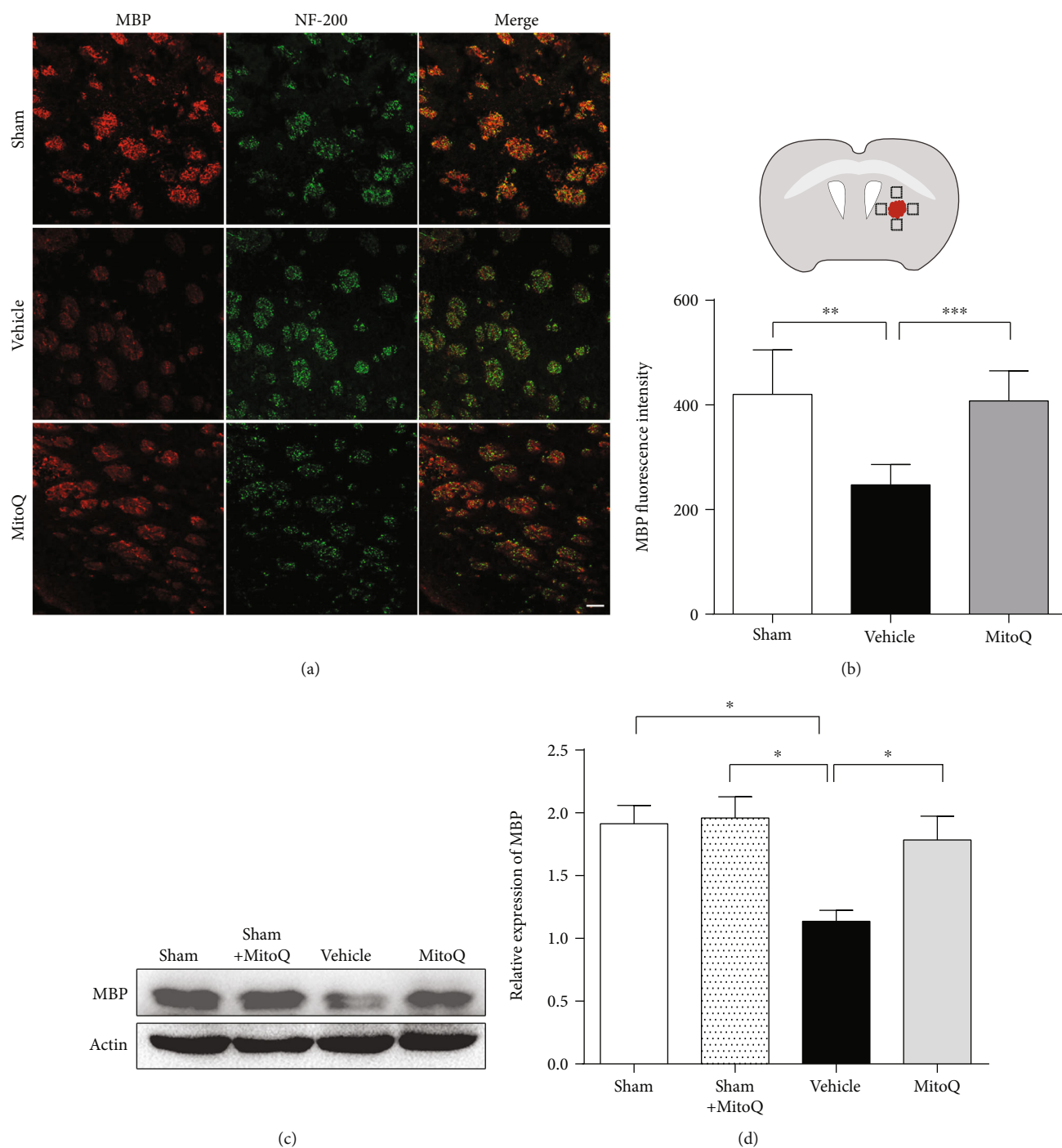
FIGURE 3: Mitoquinone (MitoQ) reduced myelin degradation after ICH. (a) Representative images of double immunofluorescence staining for MBP and NF-200 on the third day after ICH. Scale bars: 50 μm (inset column). (b) The quantification of MBP staining (right); $n = 3$ mice and 6 pictures. (c) Representative western blot images. Quantitative analyses of (d) MBP expression; $n = 5$ per group. The values represent the mean ± SEM; $^{*}P < 0.05$; $^{**}P < 0.01$; $^{***}P < 0.001$. The black box in panel (b) shows the region of interest in the brain.

NAC, can reduce the content of mitochondrial ROS of OLI-neu cells under high ferrous environment (Figures 6(a)–6(d)). The ATP content of OLI-neu cells decreased after treatment with 250 μM Fe^{2+}. MitoQ, rather than NAC, increased the content of ATP in OLI-neu cells under high ferrous environment (Figure 6(e)).

4. Discussion

The human brain accounts for 20% of the total oxygen consumption of the human body and it has strong oxidative respiration. Brain tissue is rich in polyunsaturated fatty acids, which are sensitive to oxidation, making it most vulnerable to

(a)

(b)

(c)

(d)
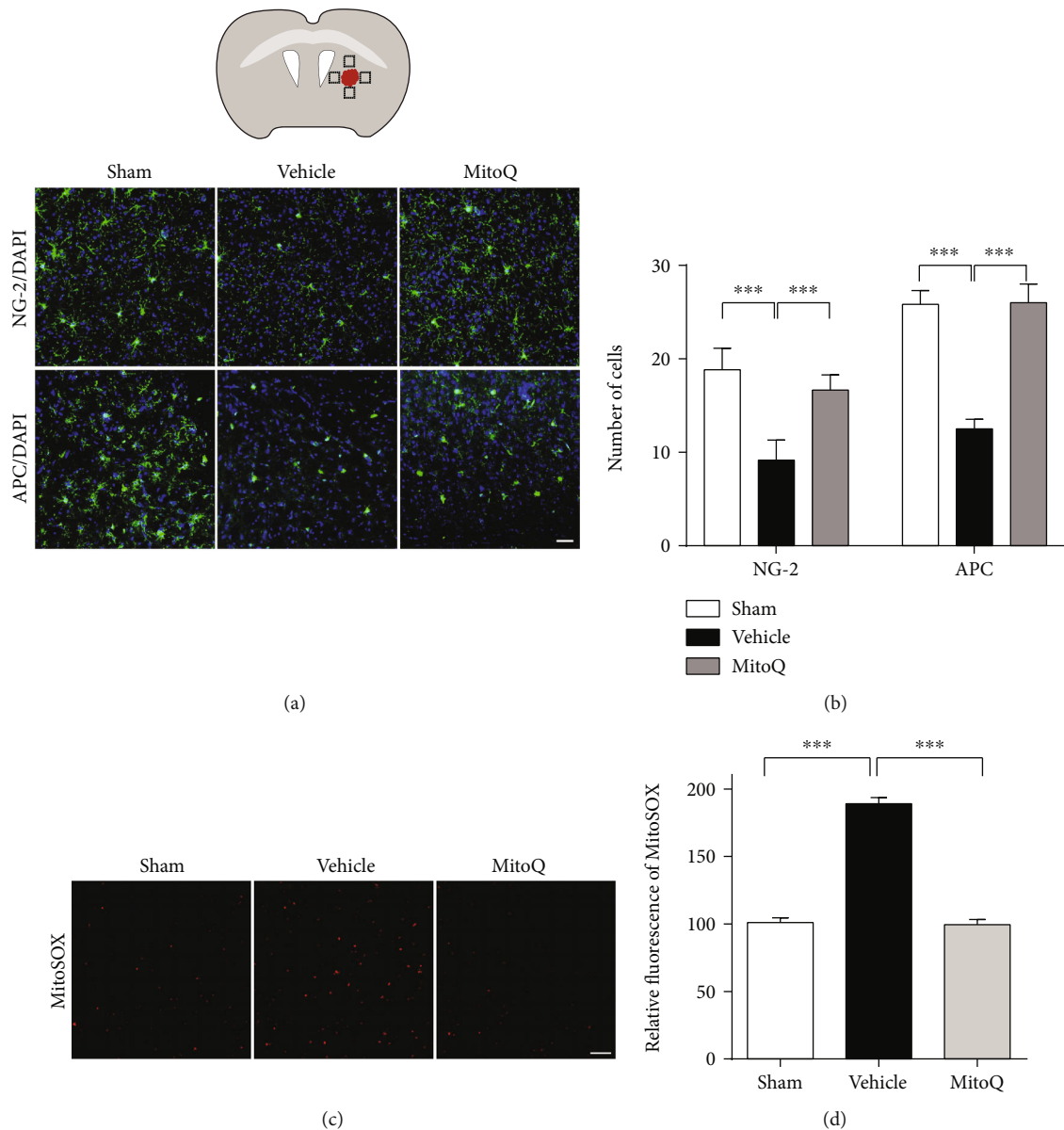
Figure 4: MitoQ decreased the loss of oligodendrocyte precursor cells (OPCs) and oligodendrocytes 3 days after ICH. (a) Images showing NG-2 or APC immunostaining (green) with DAPI (blue) in the internal capsule of the mice after ICH. (b) The results of the quantitative analysis of the number of APC-positive and NG-2 positive cells in bin areas of the internal capsule; $n = 6$ sections, 3 mice per group. (c) The mitochondrial ROS around hematoma were detected by MitoSOX Red 3 days after ICH. (d) The intensity of MitoSOX Red was analyzed show in histogram; $n = 5$ mice. The values represent the mean ± SEM. Scale bar: (a) 50 μm, (c) 20 μm. $^*P < 0.05$; $^{**}P < 0.01$; $^{***}P < 0.001$. The black box in panel (a) shows the region of interest in the brain.

ROS damage [32, 33]. Such as in Parkinson's disease (PD) and amyotrophic lateral sclerosis, the lipid peroxidation marker 4-hydroxysterol (4-HNE) and carbonylated proteins increased significantly in the patient's brain lesion area [34–36]. Therefore, antioxidant therapy is indispensable in the treatment of central nervous system diseases. But so far, there is no clinical evidence to show the intervention in this process can effectively reduce damage [37].

In the progress of antioxidant research, the first thing to consider is the different damage mechanism of specific ROS in different diseases. For example, diabetic nephropathy is characterized by hyperactive NADPH oxidase. Therefore,

GKT137831 is a promising specific NADPH oxidase inhibitor, which is currently in phase II clinical trials of diabetic nephropathy [38]. Second is the proposed intervention for selective subcellular localization. Mitochondria are ROS-producing and primary oxidative stress-damaging organelles [17, 39]. Clinical trial reported that CoQ10-targeted mitochondrial ROS therapy to reduce major adverse cardiovascular events, hospitalization rates, and mortality. [40]. Iron overload after ICH was observed in patients as well as in animal models and was associated with excessive ROS production around the hematoma [41, 42]. Although clinical studies of the nonselective reactive oxygen scavenger

(a)

(b)

(c)

(d)
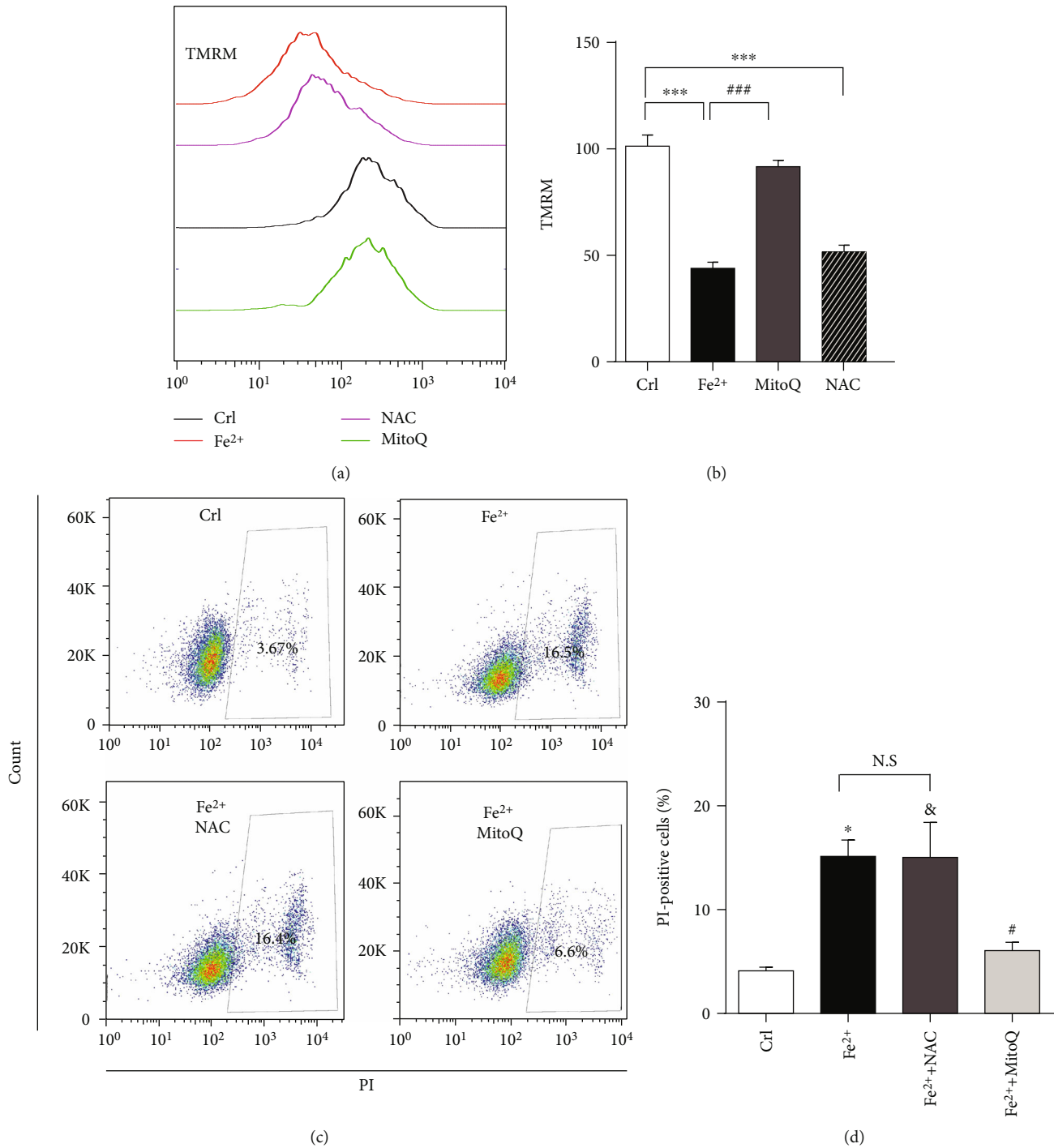
FIGURE 5: MitoQ protected OLI-neu cells from mitochondrial membrane potential decrease and cell death caused by FeCl$_2$. (a) After 24 hours of treatment with FeCl$_2$ (250 μM) and cotreatment with or without NAC (1 mM) or MitoQ (200 μM), TMRM fluorescence was detected in OLI-neu cells by flow cytometry. (b) Quantitative analyses of TMRM fluorescence; $n = 6$. Scale bars: 20 μm. The data are expressed as means and SEM and were analyzed using ANOVA followed by Tukey's post hoc test. (c) OLI-neu cells were treated with FeCl$_2$ and with or without NAC (1 mM) or MitoQ (200 μM). Cell death was detected by propodium iodide staining and flow cytometry after 48 hours. (d) Quantitative analyses of PI-positive cells, $n = 3$. The data are expressed as mean and SEM and were analyzed using 2-way ANOVA followed by Tukey's multiple comparisons test. $^{*}P < 0.05$; $^{***}P < 0.001$ represents Fe^{2+} versus control; $^{\#}P < 0.05$, $^{\#\#\#}P < 0.001$ represents Fe^{2+} versus Fe^{2+}+MitoQ; $^{\&}P < 0.05$, $^{\&\&\&}P < 0.001$ represents Fe^{2+}+NAC versus control.

edaravone have failed [11, 12], interventions that selectively target mitochondrial ROS or specific oxidants are still promising treatments for ICH.

$^{\bullet}$OH is the most oxidative damaging molecule, a key molecule of mitochondria and cell damage caused by iron overload after ICH [43]. It is known that mitoquinone (MitoQ)

(a)

(b)

(c)
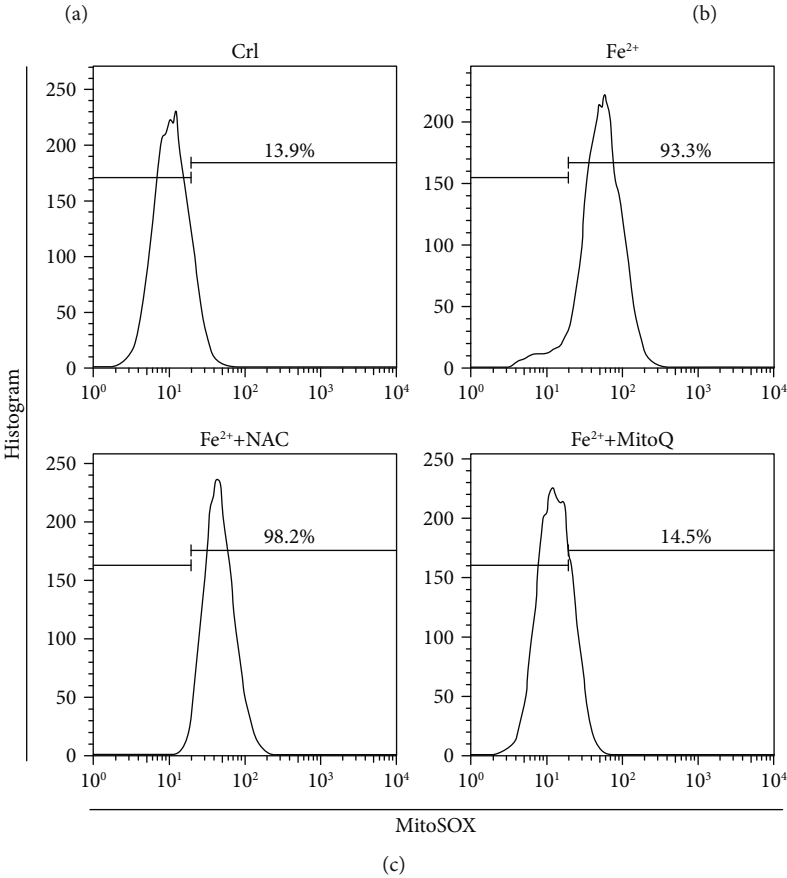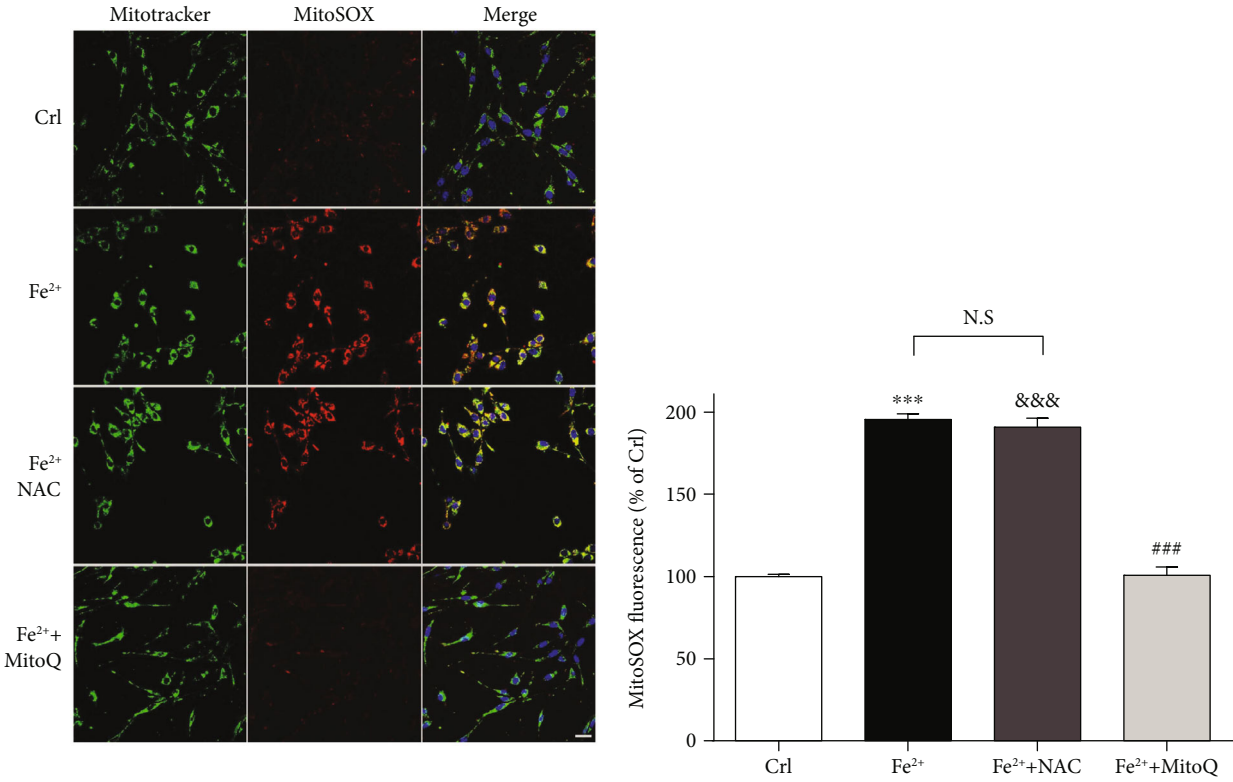
FIGURE 6: Continued.

(d)

(e)
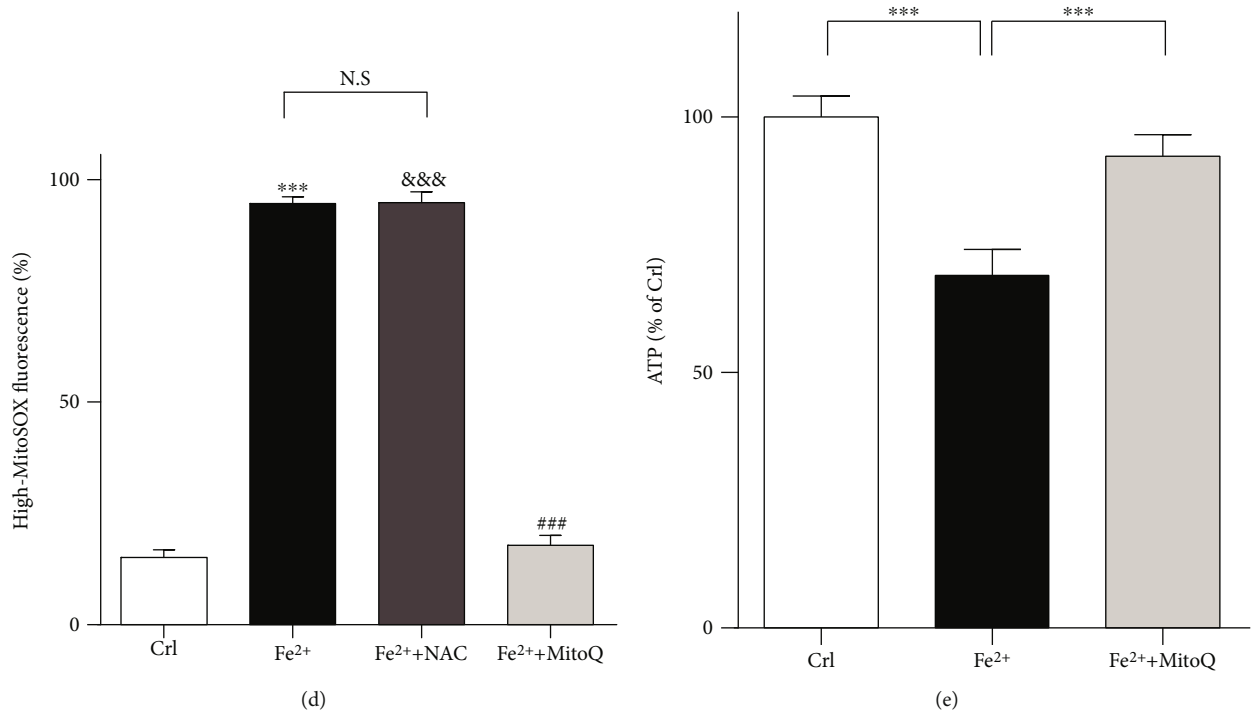
Figure 6: MitoQ decreased the $FeCl_2$ insult-induced accumulation of mitochondrial ROS and ATP deletion in OLI-neu cells. The level of mitochondrial ROS accumulation (red) in the OLI-neu cells was examined using MitoSox Red staining 24 hours after $FeCl_2$ (250 μM) treatment and treatment with or without NAC (1 mM) or MitoQ (200 μM). The staining was analyzed by microscopy (a) and flow cytometry (c). The data were analyzed in (b) and (d). (e) ATP content was analyzed using in OLI-neu cells after 24 hours of $FeCl_2$ treatment and treatment with or without NAC (1 mM) or MitoQ (200 μM). Scale bars in (a) and (c): 20 μm. The data are expressed as mean and SEM and were analyzed using 2-way ANOVA. ***$P < 0.001$ represents Fe^{2+} versus control; ###$P < 0.001$ represents Fe^{2+} versus Fe^{2+}+MitoQ; &$P < 0.05$, &&&$P < 0.001$ represents Fe^{2+}+NAC versus control.

inhibits the final step of lipid peroxidation by blocking •OH attack and continuously circulates through the return of the mitochondrial respiratory chain complex II to the active panthenol form [19]. MitoQ is a mitochondria-targeting antioxidant that acts as a lipophilic conjugated compound that readily accumulates high concentrations in the mitochondria, where the ubiquinone is reduced to its active antioxidant ubiquinol form [20, 44]. The biological properties of MitoQ not only allow it to cross the mitochondrial membrane but also better access to brain tissue through the blood-brain barrier, which is used in central nervous system diseases [45]. Interventions that selectively target mitochondrial ROS and specific hydroxyl radical damage may make MitoQ suitable for the treatment of oxidative stress damage in intracerebral haemorrhage. Our results showed that the mitochondrial antioxidant MitoQ, but not the nonselective antioxidant NAC, can reduce mitochondrial ROS levels and attenuate the mitochondrial membrane potential loss and cell death induced by ferrous overload in OLI-neu cells. In addition, in vivo data proved that MitoQ can inhibit loss of oligodendrocyte precursor cells and oligodendrocytes after ICH.

The basal ganglia haemorrhage accounts for more than 80% in all the intracerebral parenchymal haemorrhage [46]. The basal ganglia is full with corticospinal tracts, so WMI-induced motor deficit is a serious complication [2, 47]. Demyelination severely impairs white matter conduction
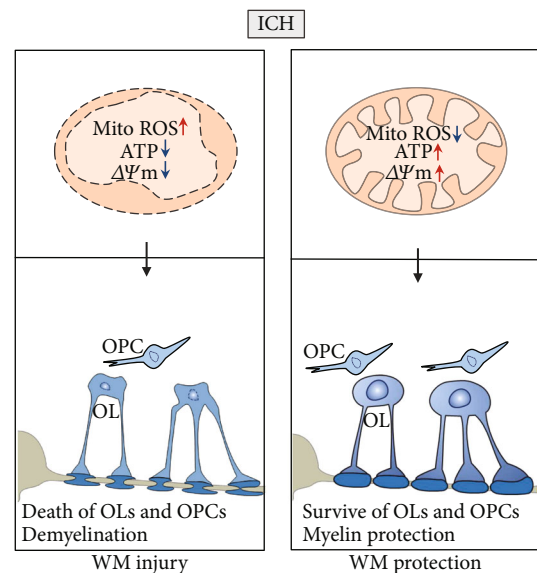
Figure 7: Intracerebral haemorrhage was accompanied demyelination and loss of oligodendrocytes (OLs) and oligodendrocyte precursor cells (OPCs), which resulted in white matter injury. MitoQ treatment reduced OL and OPC death by blocking iron overload-induced mitochondrial damage, which include the increase of mitochondrial ROS and decrease of ATP and mitochondrial membrane potential ($\Delta\Psi m$). Finally, rescuing white matter injury improved the outcomes after intracerebral haemorrhage.

and is considered to underline the long-term neurological deficits in central nervous system diseases such as intracerebral hemorrhage (ICH) and multiple sclerosis [30, 48]. The mechanism of WMI after ICH has not been elucidated and there is no specific intervention. The relationship between WMI and mitochondrial ROS after ICH is unclear [49]. It was reported that myelin degradation may be involved in WMI after ICH [50]. Our results showed that severe myelin degradation, axon swelling, and motor-evoked potential (MEP) latency prolongation occurred on the third day after ICH, which correspond to behavioral impairment. And the present data illustrated that MitoQ significantly reduced the myelin loss and oligodendrocyte loss, and ultimately promoted the integrity of myelin-axon in the white matter after intracerebral hemorrhage in the basal ganglia, thereby improving conduction velocity of the corticospinal tract and neurological function in mice. To our knowledge, this study is the first to reveal the protective effect and the underlining of MitoQ on white matter injury after ICH.

In summary, we demonstrated that selective mitochondrial ROS scavenger MitoQ can attenuate white matter injury and improve neurological impairment after ICH. This may due to MitoQ administration-reduced oligodendrocyte death and demyelination after ICH through the inhibition of mitochondrial injury after ICH. Therefore, MitoQ can be used as a therapeutic agent for neuroprotection after ICH (Figure 7).

Data Availability

We can provide the data if needed.

Conflicts of Interest

No relevant conflicts of interest.

Acknowledgments

References

[1] V. L. Feigin, R. V. Krishnamurthi, P. Parmar et al., "Update on the global burden of ischemic and hemorrhagic stroke in 1990-2013: the GBD 2013 study," *Neuroepidemiology*, vol. 45, no. 3, pp. 161–176, 2015.

[2] J. S. Balami and A. M. Buchan, "Complications of intracerebral haemorrhage," *Lancet Neurology*, vol. 11, no. 1, pp. 101–118, 2012.

[3] S. Kumar, M. Selim, S. Marchina, and L. R. Caplan, "Transient neurological symptoms in patients with intracerebral hemorrhage," *JAMA Neurology*, vol. 73, no. 3, pp. 316–320, 2016.

[4] J. Aronowski and X. Zhao, "Molecular pathophysiology of cerebral hemorrhage: secondary brain injury," *Stroke*, vol. 42, no. 6, pp. 1781–1786, 2011.

[5] S. H. Lee, B. J. Kim, W. S. Ryu et al., "White matter lesions and poor outcome after intracerebral hemorrhage: a nationwide cohort study," *Neurology*, vol. 74, no. 19, pp. 1502–1510, 2010.

[6] J. Qu, W. Chen, R. Hu, and H. Feng, "The injury and therapy of reactive oxygen species in intracerebral hemorrhage looking at mitochondria," *Oxidative Medicine and Cellular Longevity*, vol. 2016, Article ID 2592935, 9 pages, 2016.

[7] A. V. Vaseva, N. D. Marchenko, K. Ji, S. E. Tsirka, S. Holzmann, and U. M. Moll, "p53 opens the mitochondrial permeability transition pore to trigger necrosis," *Cell*, vol. 149, no. 7, pp. 1536–1548, 2012.

[8] M. M. Essa, M. Moghadas, T. Ba-Omar et al., "Protective effects of antioxidants in Huntington's disease: an extensive review," *Neurotoxicity Research*, vol. 35, no. 3, pp. 739–774, 2019.

[9] J. D. Guo, X. Zhao, Y. Li, G. R. Li, and X. L. Liu, "Damage to dopaminergic neurons by oxidative stress in Parkinson's disease (review)," *International Journal of Molecular Medicine*, vol. 41, no. 4, pp. 1817–1825, 2018.

[10] Z. Bagi, D. D. Brandner, P. le et al., "Vasodilator dysfunction and oligodendrocyte dysmaturation in aging white matter," *Annals of Neurology*, vol. 83, no. 1, pp. 142–152, 2018.

[11] J. Yang, M. Liu, J. Zhou, S. Zhang, S. Lin, and H. Zhao, "Edaravone for acute intracerebral haemorrhage," *Cochrane Database of Systematic Reviews*, no. 2, article Cd007755, 2011.

[12] J. Yang, X. Cui, J. Li, C. Zhang, J. Zhang, and M. Liu, "Edaravone for acute stroke: meta-analyses of data from randomized controlled trials," *Developmental Neurorehabilitation*, vol. 18, no. 5, pp. 330–335, 2015.

[13] L. Leanza, M. Romio, K. A. Becker et al., "Direct pharmacological targeting of a mitochondrial ion channel selectively kills tumor cells in vivo," *Cancer Cell*, vol. 31, no. 4, pp. 516–531.e10, 2017.

[14] Q. Ma, S. Chen, Q. Hu, H. Feng, J. H. Zhang, and J. Tang, "NLRP3 inflammasome contributes to inflammation after intracerebral hemorrhage," *Annals of Neurology*, vol. 75, no. 2, pp. 209–219, 2014.

[15] A. Thangaraj, P. Periyasamy, K. Liao et al., "HIV-1 TAT-mediated microglial activation: role of mitochondrial dysfunction and defective mitophagy," *Autophagy*, vol. 14, no. 9, pp. 1596–1619, 2018.

[16] K. Du, A. Farhood, and H. Jaeschke, "Mitochondria-targeted antioxidant Mito-tempo protects against acetaminophen hepatotoxicity," *Archives of Toxicology*, vol. 91, no. 2, pp. 761–773, 2017.

[17] E. Sidlauskaite, J. W. Gibson, I. L. Megson et al., "Mitochondrial ROS cause motor deficits induced by synaptic inactivity: implications for synapse pruning," *Redox Biology*, vol. 16, pp. 344–351, 2018.

[18] B. Wang, J. Fu, T. Yu et al., "Contradictory effects of mitochondria- and non-mitochondria-targeted antioxidants on hepatocarcinogenesis by altering DNA repair in mice," *Hepatology*, vol. 67, no. 2, pp. 623–635, 2018.

[19] M. P. Murphy and R. A. J. Smith, "Targeting antioxidants to mitochondria by conjugation to lipophilic cations," *Annual Review of Pharmacology and Toxicology*, vol. 47, no. 1, pp. 629–656, 2007.

[20] R. A. J. Smith and M. P. Murphy, "Animal and human studies with the mitochondria-targeted antioxidant MitoQ," *Annals of the New York Academy of Sciences*, vol. 1201, no. 1, pp. 96–103, 2010.

[21] K. Y. Goh, L. He, J. Song et al., "Mitoquinone ameliorates pressure overload-induced cardiac fibrosis and left ventricular dysfunction in mice," *Redox Biology*, vol. 21, article 101100, 2019.

[22] A. Jelinek, L. Heyder, M. Daude et al., "Mitochondrial rescue prevents glutathione peroxidase-dependent ferroptosis," *Free Radical Biology & Medicine*, vol. 117, pp. 45–57, 2018.

[23] X. Y. Xiong, L. Liu, F. X. Wang et al., "Toll-like receptor 4/MyD88-mediated signaling of hepcidin expression causing brain Iron accumulation, oxidative injury, and cognitive impairment after intracerebral hemorrhage," *Circulation*, vol. 134, no. 14, pp. 1025–1038, 2016.

[24] J. Zhou, H. Wang, R. Shen et al., "Mitochondrial-targeted antioxidant MitoQ provides neuroprotection and reduces neuronal apoptosis in experimental traumatic brain injury possibly via the Nrf2-ARE pathway," *American Journal of Translational Research*, vol. 10, no. 6, pp. 1887–1899, 2018.

[25] F. Wang, Y. J. Yang, N. Yang et al., "Enhancing oligodendrocyte myelination rescues synaptic loss and improves functional recovery after chronic hypoxia," *Neuron*, vol. 99, no. 4, pp. 689–701.e5, 2018.

[26] S. Doyle, D. B. Hansen, J. Vella et al., "Vesicular glutamate release from central axons contributes to myelin damage," *Nature Communications*, vol. 9, article 1032, 2018.

[27] S. Schneider, A. Gruart, S. Grade et al., "Decrease in newly generated oligodendrocytes leads to motor dysfunctions and changed myelin structures that can be rescued by transplanted cells," *Glia*, vol. 64, no. 12, pp. 2201–2218, 2016.

[28] D. M. Basso, L. C. Fisher, A. J. Anderson, L. B. Jakeman, D. M. McTigue, and P. G. Popovich, "Basso mouse scale for locomotion detects differences in recovery after spinal cord injury in five common mouse strains," *Journal of Neurotrauma*, vol. 23, no. 5, pp. 635–659, 2006.

[29] W. Wu, W. Xiong, P. Zhang et al., "Increased threshold of short-latency motor evoked potentials in transgenic mice expressing channel rhodopsin-2," *PLoS One*, vol. 12, no. 5, article e0178803, 2017.

[30] M. Xia, W. Chen, J. Wang et al., "TRPA1 activation-induced myelin degradation plays a key role in motor dysfunction after intracerebral hemorrhage," *Frontiers in Molecular Neuroscience*, vol. 12, p. 98, 2019.

[31] J. Yang, Q. Li, Z. Wang et al., "Multimodality MRI assessment of grey and white matter injury and blood-brain barrier disruption after intracerebral haemorrhage in mice," *Scientific Reports*, vol. 7, no. 1, article 40358, 2017.

[32] M. Belanger, I. Allaman, and P. J. Magistretti, "Brain energy metabolism: focus on astrocyte-neuron metabolic cooperation," *Cell Metabolism*, vol. 14, no. 6, pp. 724–738, 2011.

[33] E. Mariani, M. C. Polidori, A. Cherubini, and P. Mecocci, "Oxidative stress in brain aging, neurodegenerative and vascular diseases: an overview," *Journal of Chromatography B*, vol. 827, no. 1, pp. 65–75, 2005.

[34] V. Bonet-Costa, L. C.-D. Pomatto, and K. J. A. Davies, "The proteasome and oxidative stress in Alzheimer's disease," *Antioxidants & Redox Signaling*, vol. 25, no. 16, pp. 886–901, 2016.

[35] E. P. Simpson, Y. K. Henry, J. S. Henkel, R. G. Smith, and S. H. Appel, "Increased lipid peroxidation in sera of ALS patients: a

[36] A. Yoritaka, N. Hattori, K. Uchida, M. Tanaka, E. R. Stadtman, and Y. Mizuno, "Immunohistochemical detection of 4-hydroxynonenal protein adducts in Parkinson disease," *Proceedings of the National Academy of Sciences of the United States of America*, vol. 93, no. 7, pp. 2696–2701, 1996.

[37] H. Sies, C. Berndt, and D. P. Jones, "Oxidative stress," *Annual Review of Biochemistry*, vol. 86, no. 1, pp. 715–748, 2017.

[38] G. Teixeira, C. Szyndralewiez, S. Molango et al., "Therapeutic potential of NADPH oxidase 1/4 inhibitors," *British Journal of Pharmacology*, vol. 174, no. 12, pp. 1647–1669, 2017.

[39] M. D. Brand, "The sites and topology of mitochondrial superoxide production," *Experimental Gerontology*, vol. 45, no. 7-8, pp. 466–472, 2010.

[40] S. A. Mortensen, F. Rosenfeldt, A. Kumar et al., "The effect of coenzyme Q_{10} on morbidity and mortality in chronic heart failure: results from Q-SYMBIO: a randomized double-blind trial," *JACC: Heart Failure*, vol. 2, no. 6, pp. 641–649, 2014.

[41] M. Lou, K. Lieb, and M. Selim, "The relationship between hematoma iron content and perihematoma edema: an MRI study," *Cerebrovascular Diseases*, vol. 27, no. 3, pp. 266–271, 2009.

[42] J. Wu, Y. Hua, R. F. Keep, T. Nakamura, J. T. Hoff, and G. Xi, "Iron and iron-handling proteins in the brain after intracerebral hemorrhage," *Stroke*, vol. 34, no. 12, pp. 2964–2969, 2003.

[43] N. P. Mena, P. J. Urrutia, F. Lourido, C. M. Carrasco, and M. T. Nunez, "Mitochondrial iron homeostasis and its dysfunctions in neurodegenerative disorders," *Mitochondrion*, vol. 21, pp. 92–105, 2015.

[44] A. M. James, M. S. Sharpley, A. R. B. Manas et al., "Interaction of the mitochondria-targeted antioxidant MitoQ with phospholipid bilayers and ubiquinone oxidoreductases," *The Journal of Biological Chemistry*, vol. 282, no. 20, pp. 14708–14718, 2007.

[45] L. F. Ng, J. Gruber, I. K. Cheah et al., "The mitochondria-targeted antioxidant MitoQ extends lifespan and improves healthspan of a transgenic *Caenorhabditis elegans* model of Alzheimer disease," *Free Radical Biology & Medicine*, vol. 71, pp. 390–401, 2014.

[46] S. Gotoh, J. Hata, T. Ninomiya et al., "Trends in the incidence and survival of intracerebral hemorrhage by its location in a Japanese community," *Circulation Journal*, vol. 78, no. 2, pp. 403–409, 2014.

[47] Y. Kusano, T. Seguchi, T. Horiuchi et al., "Prediction of functional outcome in acute cerebral hemorrhage using diffusion tensor imaging at 3T: a prospective study," *American Journal of Neuroradiology*, vol. 30, no. 8, pp. 1561–1565, 2009.

[48] R. A. Desai, A. L. Davies, M. Tachrount et al., "Cause and prevention of demyelination in a model multiple sclerosis lesion," *Annals of Neurology*, vol. 79, no. 4, pp. 591–604, 2016.

[49] S. Zuo, P. Pan, Q. Li, Y. Chen, and H. Feng, "White matter injury and recovery after hypertensive intracerebral hemorrhage," *BioMed Research International*, vol. 2017, Article ID 6138424, 11 pages, 2017.

[50] M. J. E. Joseph, J. Caliaperumal, and L. C. Schlichter, "After intracerebral hemorrhage, oligodendrocyte precursors proliferate and differentiate inside white-matter tracts in the rat striatum," *Translational Stroke Research*, vol. 7, no. 3, pp. 192–208, 2016.

Research Article

Autophagy Deficiency Leads to Impaired Antioxidant Defense via p62-FOXO1/3 Axis

Lin Zhao [ID],[1] Hao Li [ID],[1] Yan Wang,[1] Adi Zheng,[1] Liu Cao,[2] and Jiankang Liu [ID][1]

[1]*Institute of Mitochondrial Biology and Medicine, The Key Laboratory of Biomedical Information Engineering of Ministry of Education, School of Life Science and Technology and Frontier Institute of Science and Technology, Xi'an Jiaotong University, Xi'an 710049, China*
[2]*Key Laboratory of Medical Cell Biology, China Medical University, Shenyang 110001, China*

Correspondence should be addressed to Jiankang Liu; j.liu@mail.xjtu.edu.cn

Autophagy, an intracellular degradation mechanism eliminating unused or damaged cytoplasmic components for recycling, is often activated in response to diverse types of stress, profoundly influencing cellular physiology or pathophysiology. Upon encountering oxidative stress, autophagy acts rapidly and effectively to remove oxidized proteins or organelles, including damaged mitochondria that generate more ROS, thereby indirectly contributing to the maintenance of redox homeostasis. Emerging studies are shedding light on the crosstalks among autophagy, mitochondria, and oxidative stress; however, whether and how autophagy could directly modulate antioxidant defense and redox homeostasis remains unaddressed. Here, we showed mitochondrial dysfunction, elevated ROS level, impaired antioxidant enzymes, and loss of FOXO1/3 in autophagy deficiency cellular models established by either chemical inhibitors or knocking down/out key molecules implementing autophagy, and overexpression of FOXO1/3 restored antioxidant enzymes hence suppressed elevated ROS; knockdown of p62 increased protein level of FOXO1/3 and recovered FOXO1 in Atg5-knockdown cells. Our data demonstrates that the loss of FOXO1/3 is responsible for the impairment of antioxidant enzymes and the consequent elevation of ROS, and accumulation of p62 under condition of autophagy deficiency might be mediating the loss of FOXO1/3. Furthermore, we found in an animal model that the p62-FOXO1/3 axis could be dominant in aging liver but not in type 2 diabetic liver. Together, these evidences uncover the p62-FOXO1/3 axis as the molecular cue that underlies the impairment of antioxidant defense in autophagy deficiency and suggest its potential involvement in aging, substantiating the impact of inadequate autophagy on mitochondria and redox homeostasis.

1. Introduction

Autophagy is an intrinsic process that disassembles and degrades unused or damaged cellular components including organelles like mitochondria, macromolecules like proteins or lipids, and other cytoplasmic materials. In contrast to the other two defined types of autophagy, microautophagy and chaperone-mediated autophagy, macroautophagy (hereafter referred to as autophagy) is a highly regulated process characterized by the formation of the intermediary autophagosome that later fuses with the lysosome to deliver cytoplasmic cargo, and it is the one getting intensive attention in the past two decades [1–3]. A cohort of ATG proteins composing autophagy machinery and the mechanisms of the four major

steps of autophagy have been characterized in detail from yeasts to the mammalian system [4], and the quest for the diverse cellular roles of autophagy and the complex impact of the deregulated autophagy pathway on health and disease, as well as the potential of therapeutically manipulating autophagy, both induction and inhibition, in clinical applications is still ongoing [5–12].

Autophagy, with an essential role in homeostasis and normal physiology, has been linked with longevity, aging [13], and multiple age-related diseases like neurodegenerative disorders, cancer, cardiovascular disease, and metabolic diseases [10, 13–15], and emerging data suggest that most components of the molecular machinery for autophagy have autophagy-independent roles [16]. However, the relation

between autophagy and diseases remains elusive. Autophagy is often recognized as a double-edged sword having competing or opposing effects even in the same pathophysiological scenario, and only with better understanding of the detailed molecular mechanisms in play can we develop worthwhile translational and clinical studies [17].

Meanwhile, the progressive accumulation of dysfunctional mitochondria and oxidative damage is widely recognized to play a causal role in aging and in a wide variety of age-associated diseases according to the mitochondrial free-radical theory of aging [18], which was prevalent for more than half a century and developed into the redox theory of aging recently [19]. Indeed, major causes of human morbidity and mortality are associated with oxidative stress, which occurs with a high amount of oxidants and ineffective antioxidant defense, leading to a disruption of a repertoire of redox signalings and consequently impacting fundamental cellular activities like bioenergetics, formation of metabolite and macromolecule structure, and spatial and temporal activation/deactivation of protein switches, eventually expediting cellular senescence and death [19]. It should be pointed out that antioxidant enzymes fulfill a major role in antioxidant defense rather than small-molecule antioxidant compounds in the endeavor of maintaining redox balance [20].

There exists an intricate crosstalk between autophagy and oxidative stress, intimately involving mitochondria and redox signaling ([21, 22]). Oxidative stress acts as the converging point of various types of stimuli for autophagy, with reactive oxygen species (ROS) being an important signal transducer mediated by macromolecule damage and reversible modifications of thiol-containing proteins [23]. ROS activate autophagy flux ([24]), and ROS elimination by antioxidant treatment or overexpression of antioxidant enzymes has been shown to inhibit autophagy in many models ([25, 26]). On the other side of the autophagy-oxidative stress interconnection, evidences are also emerging. Autophagic clearance of diverse damaged molecules may serve as an essential cellular antioxidant pathway [14]; autophagy-deficient models exhibit oxidative stress, probably due to the accumulation of dysfunctional mitochondria and the consequent increase of ROS generation [27–29]. Nevertheless, besides clearing oxidized cellular components and protecting mitochondrial state for less generation of ROS at source, whether autophagy affects redox homeostasis by regulating antioxidant enzymes, the key player in maintaining redox balance, arises as a key question to be addressed; if so, the mediating molecular mechanisms also need to be elucidated.

It has been reported that p62 could sequester Kelch-like ECH-associated protein 1 (Keap1) for degradation via autophagy and detach nuclear factor erythroid 2-related factor 2(Nrf2) from Keap1, leading to nuclear translocation of Nrf2 and the subsequent transcriptional activation of antioxidant and detoxifying genes ([23, 30–32]). The Forkhead Box O family of transcription factors (FOXOs) serve as the central regulator of cellular homeostasis encompassing cell cycle arrest, cell death, stress resistance, and cellular metabolism ([33–35]). FOXOs not only participate in the regulation of the transcription of antioxidant enzymes such as catalase,

Cu-ZnSOD, and MnSOD [36–38], but also control the process of autophagy by modulating the transcription of autophagy-related genes such as LC3, Gabarapl1, Atg12, Vps34, Bnip3, and Bnip3l [39–41] or by directly interacting with Atg7 to regulate the induction of autophagy ([42]). Besides the wide range of downstream effects, FOXOs' activities are under tight control at multiple levels by diverse upstream regulators and have been recently proposed to be signaling integrators coordinating cellular homeostasis and response to environmental changes over time; redox status modulates FOXOs directly by reversible Cys oxidation on FOXOs or indirectly by affecting FOXO regulators [33]. However, whether autophagy is among the many upstream regulators for FOXOs or whether autophagy can conversely regulate FOXOs and exert influence on cellular homeostasis especially redox homeostasis remains uninvestigated.

In the current study, we reported that the expression of FOXO1/3 transcription factors as well as antioxidant enzymes including Cu-ZnSOD, MnSOD, and catalase significantly decreased in response to the inhibition of autophagy and loss of FOXO1/3 caused by accumulated p62 was responsible for the impairment of the antioxidant system; hence, we propose that the p62-FOXO1/3 axis is the underlying pathway by which antioxidant defense is impaired in the condition of autophagy deficiency. Furthermore, observations in animal liver tissue imply the involvement of this regulatory axis in aging but not in a type 2 diabetic context. Our results further strengthened p62 as an autophagy-related signaling molecule. Our data, which uncovers the p62-FOXO1/3 axis, contribute to the depiction of a more comprehensive molecular basis by which p62 downregulates the antioxidant defense system in addition to the already reported p62/keap1/Nrf2 pathway which upregulates the antioxidant defense system. These findings promote our understanding of the modulation of the expression of antioxidant enzymes mediated by p62 and FOXO1/3, help decode the role of autophagy and redox homeostasis in diseases, and hint towards potential therapeutic opportunities related to the p62-FOXO1/3 axis.

2. Materials and Methods

2.1. Cell Culture and Chemicals. Wild-type (WT) and Atg7-deficient (Atg7-/-) MEFs (mouse embryonic fibroblasts) have been described ([29, 43]) and were maintained in H-DMEM (Gibco) supplemented with 15% fetal bovine serum (Biological Industries), 100 U/mL penicillin, and 100 g/mL streptomycin (Sigma-Aldrich). HEK293T cells were purchased from the American Type Culture Collection and maintained in H-DMEM supplemented with 10% fetal bovine serum. Cells were maintained at 37°C in a humidified atmosphere of 5% CO_2 and 95% air. All plastic ware was from Corning Life Sciences. The inhibitors N-acetyl-L-cysteine (Klotz et al., 2015), chloroquine diphosphate salt (CQ), bafilomycin A1 (bafi A1), 3-methyladenine (3-MA), and other reagents were bought from Sigma-Aldrich and prepared as stock solutions and stored at -20°C until use.

2.2. *Animals.* Sprague-Dawley (SD) male rats were purchased from a commercial breeder (SLAC, Shanghai, China). The rats were housed in temperature- (24-26°C) and humidity- (60%) controlled animal rooms and maintained on a 12 h light/12 h dark cycle (light on from 08:00 a.m. to 08:00 p.m.) with free access to food and water throughout the experiments. Four-week-old male rats weighing 180–200 g were used to start the experiments, and after reaching 25 months and 5 months of age (old and young groups, respectively), the animals were sacrificed and then liver samples were collected. The C57 mice, B6-OB/Nju (B6/JNju-Lep^{em1Cd25}/Nju) mice, and BKS-*db* (BSK-Lepr^{em2Cd479}/Nju) mice at 18 weeks of age were provided by the Model Animal Research Center of Nanjing University. The animals were sacrificed after adaptation to the environment, and then liver samples were collected. All of the procedures were performed in accordance with the United States Public Health Services Guide for the Care and Use of Laboratory Animals, and all efforts were made to minimize the suffering and the number of animals used in this study.

2.3. *Transfection.* siRNA targeting Atg5, Beclin1, and p62 were purchased from GenePharma (Shanghai, China) and were transfected into HEK293T cells using Lipofectamine 2000 (Invitrogen) with Opti-MEM® I Reduced Serum Medium (Gibco) according to the manufacturer's instructions. The siRNA sequences could be found in Table S1. pcDNA3-Flag-FOXO1 and GFP-FOXO3 constructs were kind gifts from Dr. Kun-Liang Guan (University of California, San Diego) and Dr. Mien-Chie Hung (MD Anderson Cancer Center), respectively, and have been previously described [44, 45]. The plasmids were transfected into HEK293T cells with empty vectors as the negative control using X-tremeGENE HP DNA Transfection Reagent (Roche) according to the manufacturer's instructions.

2.4. *Western Blotting.* Cells were lysed and centrifuged at 13,000 g for 15 min at 4°C. The supernatants were collected, and protein concentrations were determined with the BCA Protein Assay Kit (Pierce). Equal amounts of protein samples were applied to sodium dodecyl sulfate polyacrylamide gel electrophoresis (SDS-PAGE) gels, transferred to pure nitrocellulose membranes (PerkinElmer), and blocked with 5% nonfat milk for 2 hours. The membranes were then incubated with the indicated primary antibodies at 4°C overnight. Primary antibodies used in this study were β-actin from Sigma-Aldrich; Atg7, Atg5, Beclin1, and FOXO1 from Cell Signaling Technology; FOXO3 from Sigma-Aldrich; p62, Cu-ZnSOD, MnSOD, and catalase from Santa Cruz Biotechnology; Complex I Ndufs3, Complex I Ndufa9, Complex II subunit 30 kDa Ip, Complex III subunit Core 1, Complex IV Subunit I, and ATP Synthase Subunit Alpha from Invitrogen; and LC3B from Abcam. The membranes were incubated with secondary peroxidase-conjugated antibodies (Jackson ImmunoResearch) at room temperature for 1 h. Chemiluminescent detection was performed by ECL (Pierce). The results were analyzed and quantified by Quantity One Software (Bio-Rad) to obtain the optical density ratio of the target protein to β-actin. One representative result was shown from at least three independent experiments.

2.5. *Quantitative RT-PCR.* Total RNA was extracted from cells using Tripure (Roche) according to the manufacturer's protocol. Reverse transcription was performed using the PrimeScript RT-PCR Kit (TaKaRa) followed by semiquantitative real-time PCR with specific primers described in Table S2 using SYBR Premix Ex Taq (TaKaRa). Real-time PCR was performed on a real-time PCR system (Eppendorf, Germany) with an initial step of 10 min at 95°C, followed by 40 cycles of 30 s denaturation at 95°C, 30 s annealing at 60°C, and 20 s extension at 72°C. Melting curves were assessed over the range 60-99°C to ensure specific DNA amplification. Target gene expression was normalized to β-actin expression and is shown as levels relative to control samples.

2.6. *Activity Assays for Mitochondrial Electron Transport Chain Complexes.* Activities of NADH-ubiquinone oxidoreductase (Complex I) and succinate-CoQ oxidoreductase (Complex II) were measured spectrometrically using conventional assays as described [46, 47].

2.7. *Assays for Mitochondrial Membrane Potential and ROS Generation.* Mitochondrial membrane potential was assessed in cells using a mitochondria-specific cationic probe JC-1 (Invitrogen). Intracellular ROS levels were determined by using of DCFDA. The assays have been described [48].

2.8. *Total DNA Isolation and mtDNA Copy Number Detection.* Total DNA was extracted using the QIAamp DNA Mini Kit (Qiagen), and quantitative PCR was performed using mitochondrial DNA and genomic DNA-specific primers described in Table S2. Final results were expressed as changes relative to control samples in mitochondrial D-loop levels relative to the 18S rRNA gene.

2.9. *Assay for Oxygen Consumption Capacity.* Cellular mitochondrial respiration rates (oxygen consumption rates (OCR)) of certain numbers of cells (30,000 for 293T and 20,000 for MEFs) were investigated using the Seahorse Extracellular Flux Analyzer (Seahorse Bioscience, North Billerica, MA) according to the manufacturer's instructions ([49]). Resulting rates were adjusted to the number of cells per well after detection.

2.10. *Intracellular Superoxide Dismutase and Catalase Activity Measurements.* Superoxide dismutase and catalase activity were measured using commercially available kits (Jiancheng Biochemical Research, Inc.) following the instructions provided by the manufacturer. The activities of antioxidant enzymes were expressed as changes relative to control samples.

2.11. *Cell Viability.* MEFs were plated in 24-well plates and incubated overnight. Cells were treated with 1 mM tBHP (*tert*-butyl hydroperoxide) for the indicated time periods and then incubated with 0.5 mg/mL MTT (3-(4,5-dimethyl-thiazol-2-yl)-2,5-diphenyltetrazolium bromide) medium.

The optical density was determined by a microplate spectrophotometer at a wavelength of 550 nm.

2.12. Protein Carbonylation Assay. Protein carbonyls in soluble proteins were assayed using the OxyBlot protein oxidation detection kit (Cell Biolabs, USA). Protein carbonyls were labeled with 2,4-dinitrophenylhydrazine and detected by Western blot. As a negative loading control, equal amounts of samples were subjected to 10% SDS-PAGE and stained with Coomassie brilliant blue.

2.13. Statistical Analysis. All data are expressed as the means ± SEM. Immunoblots are representative results of at least three independent experiments. Statistical significance was analyzed by unpaired two-tailed Student's *t*-test or ANOVA. A *p* value of less than 0.05 was considered statistically significant.

3. Results

3.1. Mitochondrial Dysfunction, Increased ROS, and Impairment of Antioxidant Enzymes Occur in Response to Chemical Inhibitors of Autophagy or under Circumstance of Atg7 Knockout or Knockdown of Other Autophagy Components. To determine the impact of autophagy inhibition on cellular mitochondrial homeostasis and redox balance, we first measured mitochondrial alterations and ROS level in HEK293T cells or MEF cells treated with three different chemical inhibitors of autophagy, Bafi A1 (bafilomycin A1, a widely used inhibitor disrupting autophagosome-lysosome fusion), CQ (chloroquine diphosphate salt, reported to inhibit autophagy), and 3-MA (3-methyladenine, a selective PI3K inhibitor that also blocks autophagosome formation). CQ treatment results in a time-responsive decline in mRNA levels of key autophagy components Atg12, Bnip3, and LC3, indicating the inhibition of autophagy (Figures S1A–S1C). All three inhibitors induced a more than a two-fold increase in mitochondrial DNA copy number (Figure 1(a)) as well as a robust decrease to less than one half in mitochondrial membrane potential (MMP) (Figure 1(b)) in HEK293T cells, and CQ significantly reduced oxygen consumption rate (OCR) in MEF cells (Figure 1(c)). These data indicate that inhibition of autophagy results in increased mitochondrial number but impaired mitochondrial function, which make sense as damaged mitochondria accumulate in the cell due to a lack of degradation through mitophagy, an important mitochondrial quality control mechanism. Concurrently, these inhibitors also increased ROS level significantly and 3-MA was found to boost ROS in a time-dependent manner, especially with prolonged time (Figure 1(d)). Since ROS generated in the mitochondria as a byproduct of the electron transport chain accounts for the majority of cellular ROS, accumulated dysfunctional mitochondria would release more ROS and eventually enhance intracellular oxidative stress if the endogenous antioxidant defense remains poor. We then went on to check the expression of the most important antioxidant enzymes Cu-ZnSOD, MnSOD, and catalase and detected a significant

decrease in their protein levels when cells were treated with any of the three different autophagy inhibitors (Figure 1(e)), and the reduction of their mRNA levels by CQ treatment exhibited time-dependence (Figure 1(f)). So, inhibition of autophagy can trigger oxidative stress by paralyzing mitochondria to generate more ROS on the one hand, on the other sabotaging endogenous antioxidant defense.

We further corroborated our findings employing Atg7-/- and WT MEF cells. The mRNA levels of key autophagy components Atg5, Atg12, Bnip3, gaparapl1, LC3, and vps34 were universally decreased in Atg7-/- MEF cells compared with WT (Figure S1D); the protein level of Atg5 was decreased as much as Atg7; LC3II was almost absent; and p62 was increased in Atg7-/- MEF cells (Figure S2C), indicating an obvious state of autophagy deficiency in Atg7-/- MEF cells. MMP was significantly lowered in Atg7-/- MEF cells than WT (Figure 2(a)). With deeper investigation, we found that several subunits of the mitochondrial electron transport chain (ETC) complexes exhibited a substantial decrease in both mRNA transcript and protein levels, especially subunits of Complexes I and V, and the activity of ETC Complex I dropped significantly in Atg7-/- MEF cells compared with WT MEF cells (Figure 2(b)). In addition, we used siRNA to knockdown other components of autophagy, Atg5 or Beclin1 in particular, to exclude the specific effect of Atg7, and as expected OCR dropped substantially in HEK293T cells (Figure 2(c)). Clearly, these findings verify the adverse impact of autophagy deficiency on mitochondrial function. Since the mitochondrial rate of reactive oxygen species (mitROS) production is recently considered of more importance than overall ROS level, we next examined ROS level with two different fluorescent probes, one indicating for intracellular ROS, the other targeting for mitochondrial superoxide, and both intracellular ROS and mitochondrial superoxide increased in Atg7-/- MEF cells compared with WT MEF cells (Figure 2(d)). Besides, Atg7-/- MEF cells showed higher vulnerability than WT MEF cells when challenged with tBHP (*tert*-butyl hydroperoxide), an exogenous inducer of oxidative stress (Figure 2(e)). Underneath the increased ROS level and higher vulnerability to oxidative stress of Atg7-/- MEF cells, we observed a drastic decrease in both mRNA levels and protein levels of key antioxidant enzymes, Cu-ZnSOD, MnSOD, and catalase; moreover, even their enzymatic activities were found to be universally reduced in Atg7-/- MEF cells compared with WT MEF cells (Figure 2(f)). Likewise, Atg5 or Beclin1 knockdown by siRNA also led to decreased protein levels of all three antioxidant enzymes in HEK293T cells (Figure 2(f)). These data demonstrate that autophagy deficiency can cause the impairment of antioxidant defense. Together, Atg7 knockout or knockdown of other autophagy components simultaneously destroyed mitochondrial homeostasis and endogenous antioxidant defense, which is consistent with the findings with autophagy inhibitors.

From the above results we can see that in general, inhibition of autophagy or autophagy deficiency leads to the accumulation of dysfunctional mitochondria, which release more ROS and in turn cause further damage to one of its major
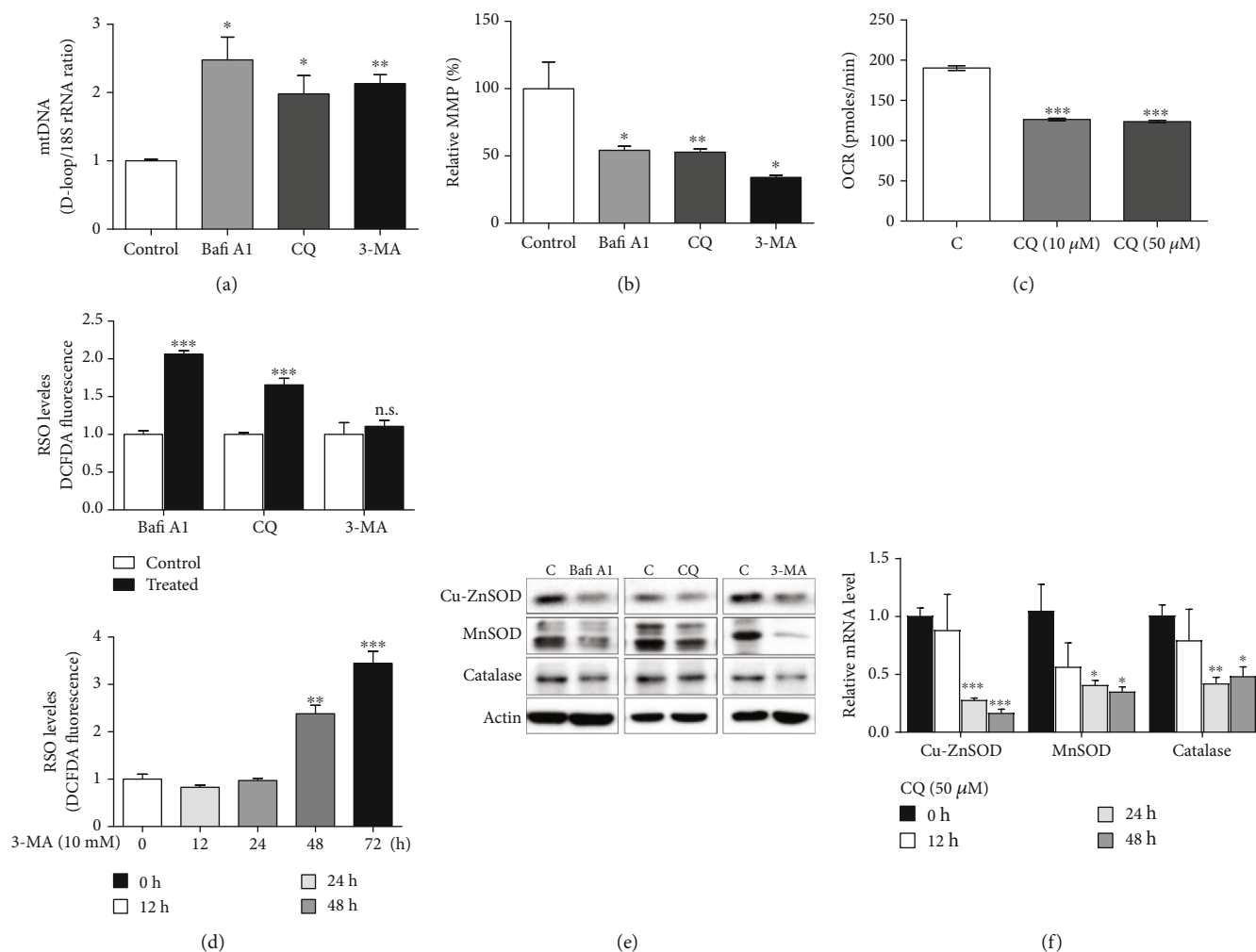
Figure 1: Mitochondrial dysfunction, increased ROS, and impairment of antioxidant enzymes occur in response to chemical inhibitors of autophagy. (a, b, d, and e) HEK293T cells were treated with autophagy inhibitors Bafi A1 (100 nM), CQ (50 μM), or 3-MA (10 mM) for 24 hours or with 10 mM 3-MA in a time course within 72 hours before harvest. Then, mitochondrial DNA (as D-loop DNA) copy number was detected by real-time PCR ($n = 3$) (a), mitochondrial membrane potential (MMP) was detected with the JC-1 fluorescent probe ($n > 9$) (b), ROS level alterations were determined by a fluorescence microplate reader after staining with DCFDA ($n = 3$) (d), and protein levels of antioxidant enzymes were determined by W.B. (e). (c and f) WT MEF cells were treated with CQ at indicated concentrations for 24 hours or with 50 μM CQ for the indicated time period before harvest, then oxygen consumption rate (OCR) was determined using the Seahorse XF24 Analyzer ($n = 6$-7) (c) and mRNA levels of antioxidant enzymes were determined by q-RT-PCR ($n = 3$) (f). Values are represented as mean ± SEM. $^*p < 0.05$; $^{**}p < 0.01$; $^{***}p < 0.001$; * vs. control group.

target mitochondria, thus establishing a vicious cycle between mitochondrial malfunction and cellular redox imbalance. Cells possess an innate powerful antioxidant system capable of attenuating intracellular free radicals to protect against their attack, among which an array of antioxidant enzymes play the key role. In condition of autophagy inhibition, mitochondrial dysfunction and the consequent intracellular oxidative stress could only be left exacerbated with the downregulation of antioxidant enzymes and decrease of enzymatic activities, and the lack of mitophagy eliminating damaged mitochondria.

3.2. Impairment of Antioxidant Enzymes and Elevation of ROS in Condition of Autophagy Deficiency Is Mediated by the Decrease of FOXO1/3 Transcription Factors. We next sought to investigate the mechanism underlying the down-

regulation of antioxidant enzymes in condition of autophagy deficiency. Since the amounts of mRNA transcripts of antioxidant enzymes were dramatically reduced in various autophagy deficiency models (Figures 1(f) and 2(f)), we focused on transcriptional regulation and looked into related transcription factors. Nrf2 (nuclear factor erythroid 2-related factor 2), the master regulator of the total antioxidant system or phase II detoxifying enzymes, is a transcription factor that bonds to ARE (Antioxidant Response Element) and activate the expression of cytoprotective enzymes, playing important role in adaptive response to oxidative stress. We found that the protein level of Nrf2 was dramatically higher in Atg7-/- MEF cells than in WT MEF cells (Figure S2A), and the expression of NQO1 (NAD (P) H quinone dehydrogenase 1), one of Nrf2's downstream target genes, exhibited higher induction as manifested by higher levels of both mRNA

(a)

(b)

(c)

(d)

Figure 2: Continued.

(e)

(f)
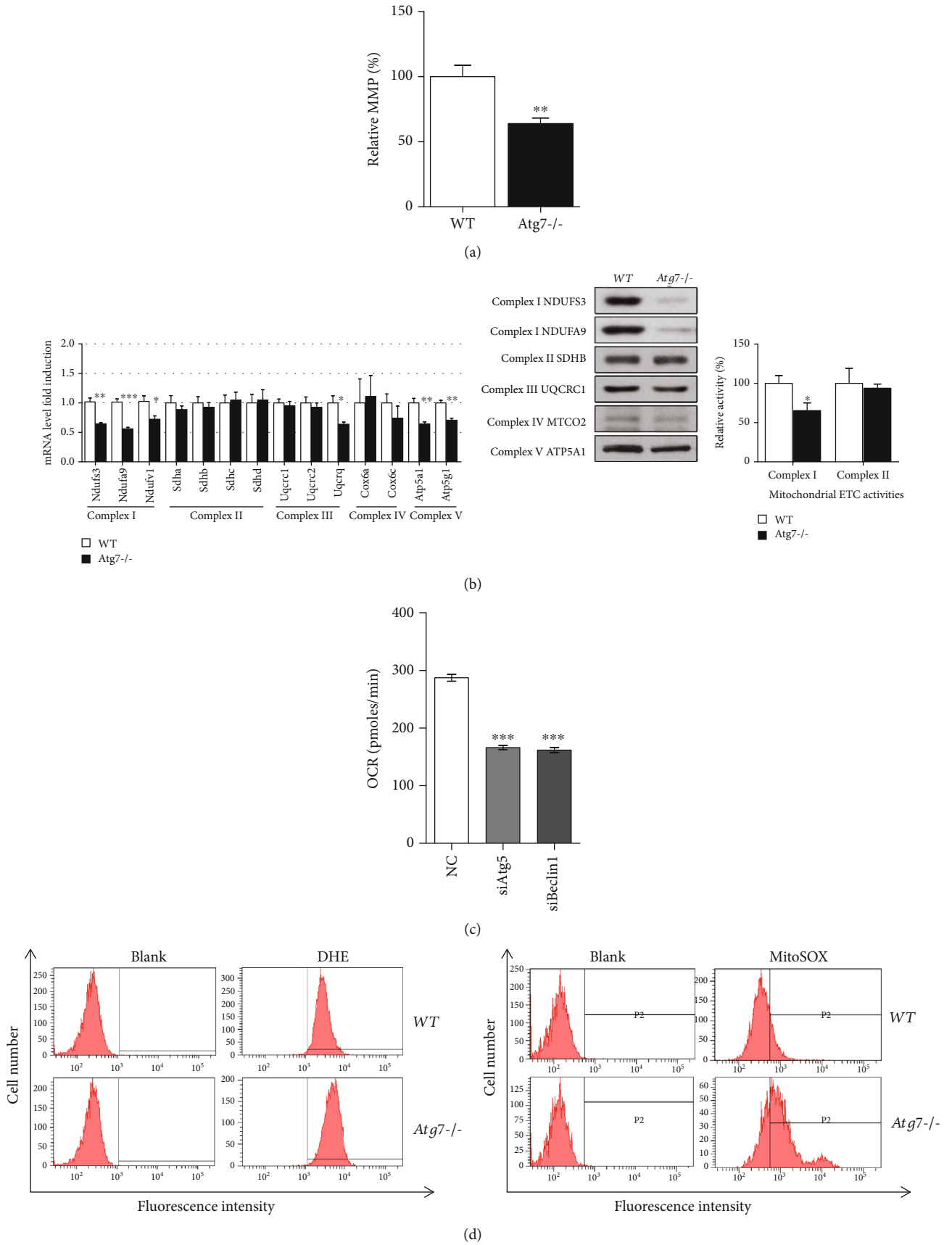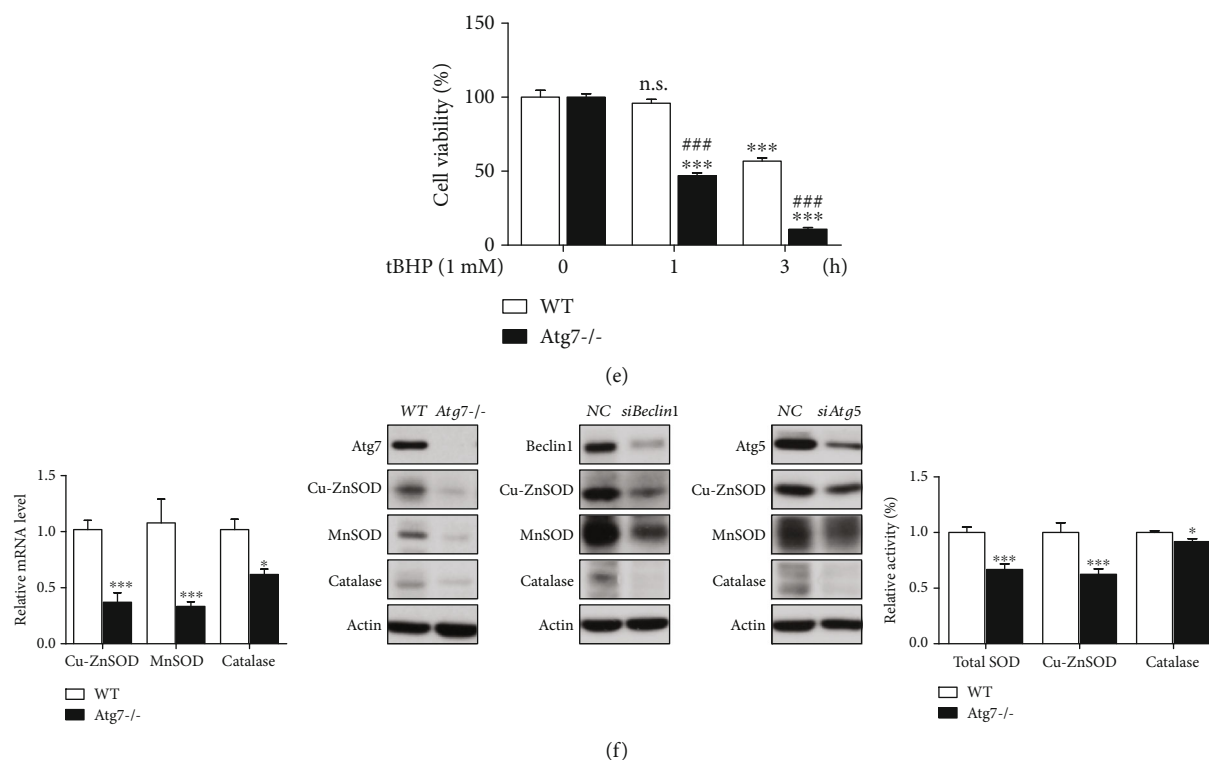
FIGURE 2: Mitochondrial dysfunction, increased ROS, decreased capacity to survive oxidative stress, and impairment of antioxidant enzymes also occur when Atg7 is deleted or other autophagy components are knocked down by siRNA. (a) Mitochondrial membrane potential (MMP) in WT and Atg7-/- MEF cells ($n > 9$) was detected with the JC-1 probe. (b) Relative mRNA levels of subunits of mitochondrial respiratory complexes were determined by quantitative RT-PCR ($n = 4$), relative protein levels of subunits of mitochondrial respiratory complexes were determined by W.B., and relative activities of mitochondrial respiratory complexes I and II were measured in isolated mitochondria from WT and Atg7-/- MEF cells ($n=8$). (c) HEK293T cells were transfected with negative control siRNA, siAtg5, or siBeclin1, then OCR was determined using the Seahorse XF24 Analyzer ($n = 6$-7). (d) ROS level changes and mitochondrial superoxide level changes in WT and Atg7-/- MEF cells were detected by flow cytometry using 5 μM DHE or 5 μM MitoSOX Red Mitochondrial Superoxide Indicator. (e) WT and Atg7-/- MEFs were treated with 1 mM tBHP for the indicated time period, and their cell viability was determined by MTT ($n = 10$). (f) mRNA levels of Cu-ZnSOD, MnSOD, and catalase in WT and Atg7-/- MEF cells were determined by q-RT-PCR ($n = 6$); protein levels of antioxidant enzymes in Atg7-/- MEF cells in comparison to WT or siBeclin1- or siAtg5-transfected HEK293T cells in comparison to negative control siRNA were determined by W.B.; relative enzymatic activities of antioxidant enzymes were measured in WT and Atg7-/- MEF cells ($n = 6$). Values are represented as mean ± SEM. $^*p < 0.05$; $^{**}p < 0.01$; $^{***,\#\#\#}p < 0.001$; * vs. control group or WT MEF cells, $^\#$ vs. WT MEF cells with the same treatment time period.

and protein in Atg7-/- MEF cells than in WT MEF cells (Figures S2A and S2B). The fact that the Nrf2/ARE pathway is activated probably responding to oxidative stress but failing to induce the expression of antioxidant enzymes in the condition of autophagy deficiency suggests the involvement of other players downregulating antioxidant enzymes.

We continued to search for the molecules that are held accountable for the decrease of the mRNA levels and the protein levels of antioxidant enzymes in autophagy deficiency models. Because FOXO (Forkhead Box O) transcription factors are also known to regulate the expression of MnSOD, catalase [36], and Cu-ZnSOD [37, 50] through transcriptional control, we examined the protein levels of FOXO1 and FOXO3 in HEK293T cells treated with three different autophagy inhibitors and found both FOXO1 and FOXO3 decreased robustly, and both molecules along with antioxidant enzymes Cu-ZnSOD, MnSOD, and catalase showed a time-dependent decrease in response to a 48-hour time

course of CQ treatment (Figure 3(a)). To find out the role that FOXO1/3 plays in impaired antioxidant defense and enhanced oxidative stress in an autophagy deficiency condition, we overexpressed FOXO1 or FOXO3 in CQ-treated HEK293T cells and the recovery of Cu-ZnSOD, MnSOD, and catalase was confirmed in both protein and mRNA levels (Figure 3(b)). Besides, the simultaneous overexpression of FOXO1 and FOXO3 could further induce the increase in mRNA transcripts of antioxidant enzymes (Figure S3A). Moreover, as expected, overexpression of FOXO1 or FOXO3 also relieved the intracellular oxidative stress in CQ-treated HEK293T cells, represented by ROS level (Figure 3(c)). We also checked the expression of FOXO1/3 in other autophagy-deficient models. Both protein levels and mRNA levels of FOXO1/3 were dramatically decreased in Atg7-/- MEF cells in comparison to WT MEF cells (Figures S2C and S2D; Figure 3(d)), and protein levels of both FOXO1 and FOXO3 were substantially decreased in siAtg5- or siBeclin1-transfected HEK293T cells in comparison to negative

control siRNA-transfected ones (Figure 3(d)). Collectively, these data verify that it is the downregulation of FOXO1/3 transcription factors by autophagy deficiency that subsequently reduces the transcription of antioxidant enzymes and further exacerbates oxidative stress already existing due to mitochondrial dysfunction induced by inhibition of autophagy.

FOXOs are also considered as an upstream modulator of autophagy; for instance, conditional deletion of FOXOs strongly impairs autophagic flux in adult neurogenesis [51]. This prompted us to examine the impact of FOXO1/3 overexpression on transcription of genes participating in autophagy, and we found that the decreased mRNA levels of Atg12, Bnip3, and LC3 in CQ-treated HEK293T cells were restored by FOXO1/3 overexpression (Figure S3B). Therefore, it can be inferred that FOXO1/3 overexpression would alleviate oxidative stress in autophagy-deficient models through simultaneously inducing expression of antioxidant enzymes and restoring expression of genes participating autophagy, while on the other side it can be conjectured that the negative regulation of FOXO1/3 by autophagy deficiency would have exerted additional inhibition on autophagy, forming a feedforward loop resulting in retarded autophagy and the following oxidative stress.

3.3. Scavenging ROS by NAC Not Only Fails to Rescue the Loss of FOXOs and Antioxidant Enzymes but Even Exacerbates Their Loss in Autophagy Deficient Condition.

Now we know that FOXO1/3 sits at the pivot linking autophagy deficiency to redox imbalance, but what leads to the decrease of FOXO1/3 in a condition of autophagy deficiency emerges as the key question to be addressed. It has already been reported that ROS could modulate not only the transcriptional and posttranscriptional control of FOXO expression but also the activity of FOXO at multiple levels including posttranslational modifications of FOXOs (such as phosphorylation and acetylation), interaction with coregulators, alterations in FOXO subcellular localization, protein synthesis, and stability [52]. As shown in Figure 3(e), NAC (N-acetyl-L-cysteine), a commonly used ROS scavenger, not only failed to recover the loss of FOXO1/3 as well as antioxidant enzymes but even exacerbates their loss in both Atg7-/- MEF cells and CQ-treated HEK293T cells. These findings suggest that the elevation of ROS level in autophagy-deficient cellular models not only made no contribution to the decrease of FOXO1/3 and the impairment of antioxidant enzymes but quite on the contrary had also made its efforts to upregulate or maybe also to activate FOXO1/3 and subsequently to increase the expression of antioxidant enzymes, hence promoting cellular resistance to oxidative stress.

3.4. Accumulated p62 under Autophagy Deficiency Condition Is Responsible for the Loss of FOXO1/3.

p62 (p62/SQSTM1 or Sequestosome 1) serves as a scaffold by binding with ubiquitinated cellular cargoes and autophagosomal membrane protein LC3, facilitating substrate degradation of autophagy. Protein aggregates formed by p62 are often used as reporters of retarded autophagy activity. More importantly, it is a multifunctional protein involved in many signal transduction pathways and has been linked to oxidative stress. It prompts us to investigate whether the accumulation of p62 under an autophagy inhibition condition has anything to do with the loss of FOXO1/3. We observed that the protein levels of both FOXO1 and FOXO3 increased when p62 was knocked down by siRNA in HEK293T cells (Figure 4(a)), indicating a negative regulation of FOXO1/3 by p62. More interestingly, knocking down the accumulated p62 in siAtg5-transfected HEK293T cells by sip62 did partially restore the expression of FOXO1/3 (Figure 4(b)), demonstrating that the accumulation of p62 plays an essential role in mediating autophagy deficiency-induced loss of FOXO1/3. Considering the increased p62 protein level and decreased FOXO1/3 mRNA levels in Atg7-/- MEF cells (Figure S2D), transcriptional modulation might be involved in the downregulation of FOXO1/3 by p62, though other possibilities could not be ruled out; further studies are needed to elucidate the regulating mechanisms. Altogether, the above results reveal the existence of a negative regulatory axis pointing from p62 to FOXO1/3 and show that autophagy deficiency impairs antioxidant defense via the newly uncovered p62-FOXO1/3 axis. Moreover, these findings also substantiate the existence of a crosstalk between autophagy and FOXO1/3 which is of significance in health and disease.

3.5. Decline of Autophagy, Accumulation of p62, Loss of FOXO1/3, and Oxidative Stress Suggest the Involvement of p62-FOXO1/3 Axis in Aging.

Autophagy has long been proposed and demonstrated to be involved in aging as it degrades dysfunctional organelles and macromolecules, and autophagy defect could accelerate the aging process maybe due to the accumulation of damaged organelles or molecules [53]. By far, there are many postulated theories of aging including the widespread free-radical and mitochondrial theories of aging. However, aging remains to be an intricate phenomenon with a largely elusive underlying mechanism. We detected increased protein carbonylation levels in aged rat livers compared to young ones (Figure 4(c)), demonstrating increased oxidative damage and oxidative stress in aged liver. We also observed an increased expression of p62 and NQO1 accompanied by a decreased expression of FOXO1 and FOXO3 in those aged rat livers in comparison to young ones (Figure 4(d)), indicating the inhibition of autophagy activity in aged liver. These findings suggest that the p62-FOXO1/3 axis we uncovered in the current study is involved in liver aging, and it provides us a possible interpretative perspective to the aging process which starts from declining autophagy, the driving force, to accumulation of p62, then loss of FOXO1/3, followed by impairment of antioxidant defense leading to oxidative stress and irreversible damage, eventually contributing to the progression of aging.

3.6. Decline of Autophagy and Accumulation of p62 but Upregulation of FOXO1/3 and Reduced ROS Level Show That p62-FOXO1/3 Axis Is Not Dominant in Type 2 Diabetes Animal Models.

Autophagy was recently identified to be closely associated with obesity and type 2 diabetes by regulating lipid homeostasis and insulin sensitivity, as defective autophagy promotes ER stress, hepatic steatosis,
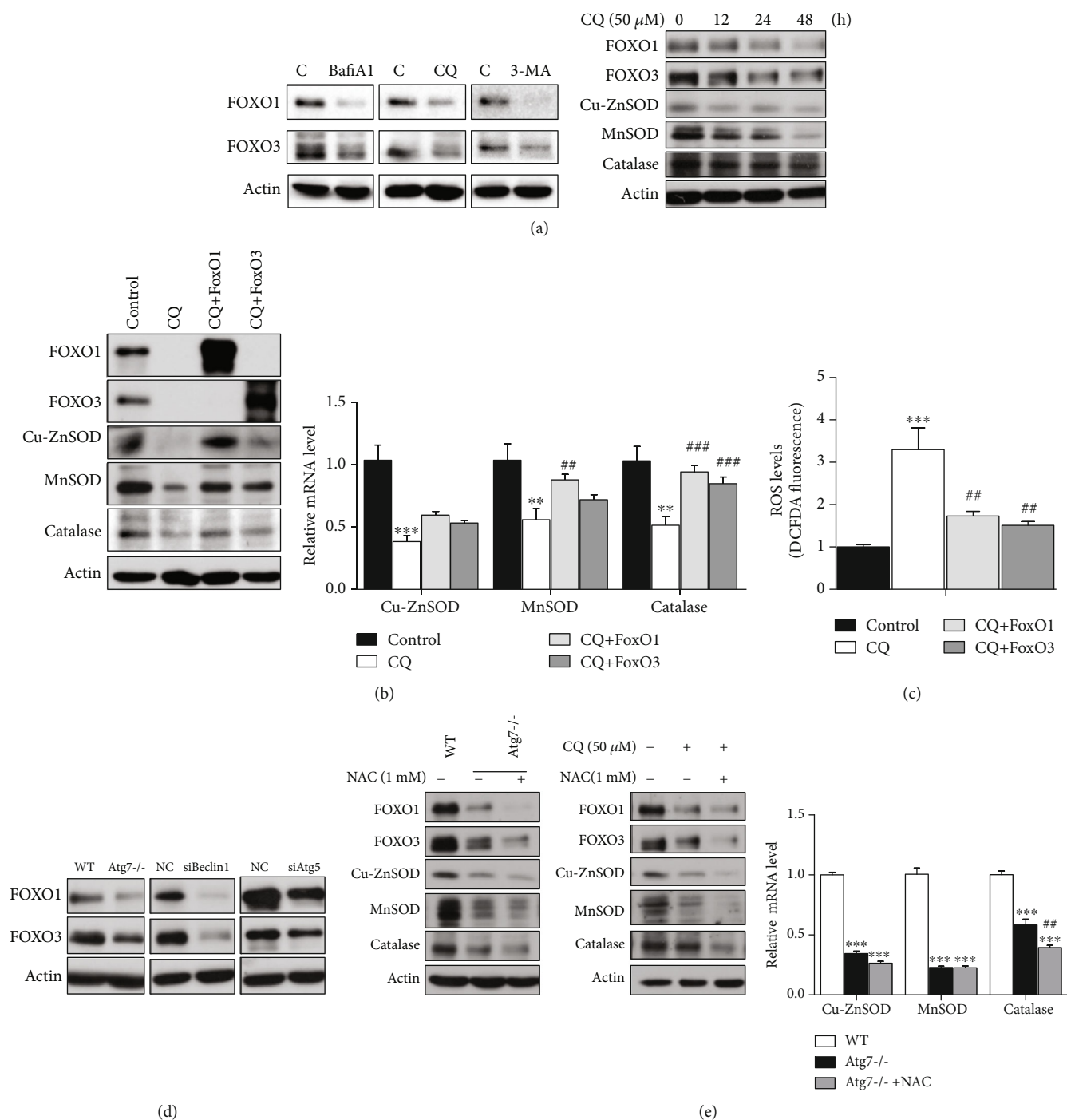
Figure 3: Impairment of antioxidant enzymes and elevation of ROS in a condition of inhibited autophagy is mediated by the decrease of FOXO1/3 transcription factors, and scavenging ROS by NAC not only fails to rescue the loss of FOXOs or antioxidant enzymes but even exacerbates their loss. (a) HEK293T cells were treated with autophagy inhibitors Bafi A1 (100 nM), CQ (50 μM), or 3-MA (10 mM) for 24 h or with 50 μM CQ for 0, 12, 24, or 48 hours before harvest, then protein levels of FOXO transcription factors and antioxidant enzymes were determined by W.B. (b and c) HEK293T cells were treated with 50 μM CQ for 24 hours before transfection with FOXO1 or FOXO3 plasmids, then followed by treatment with 50 μM CQ for another 48 hours before harvest, and then protein and mRNA levels of FOXOs and antioxidant enzymes were relatively determined by W.B. and q-RT-PCR ($n = 6$) (b), and intracellular ROS levels were measured with a DCFDA probe (c) ($n = 12$). (d) Protein levels of FOXO1 and FOXO3 in Atg7-/- MEF cells compared with WT MEF cells, in siAtg5- or siBeclin1-transfected HEK293T cells compared with negative control siRNA transfected ones were determined by W.B. (e) Atg7-/- MEF cells were treated with 1 mM NAC for 48 hours before harvest, HEK293T cells were treated with 1 mM NAC for 48 hours and/or CQ for 24 hours before harvest, then protein levels of FOXOs and antioxidant enzymes were determined by W.B. in both cells, and mRNA levels of antioxidant enzymes were determined by q-RT-PCR ($n = 6$) in MEF cells. Values are represented as mean ± SEM. $^{*,\#}p < 0.05$; $^{**,\#\#}p < 0.01$; $^{***,\#\#\#}p < 0.001$; * vs. control group or WT MEF cells, $^{\#}$ vs. treatment with CQ alone or Atg7-/- MEF cells.
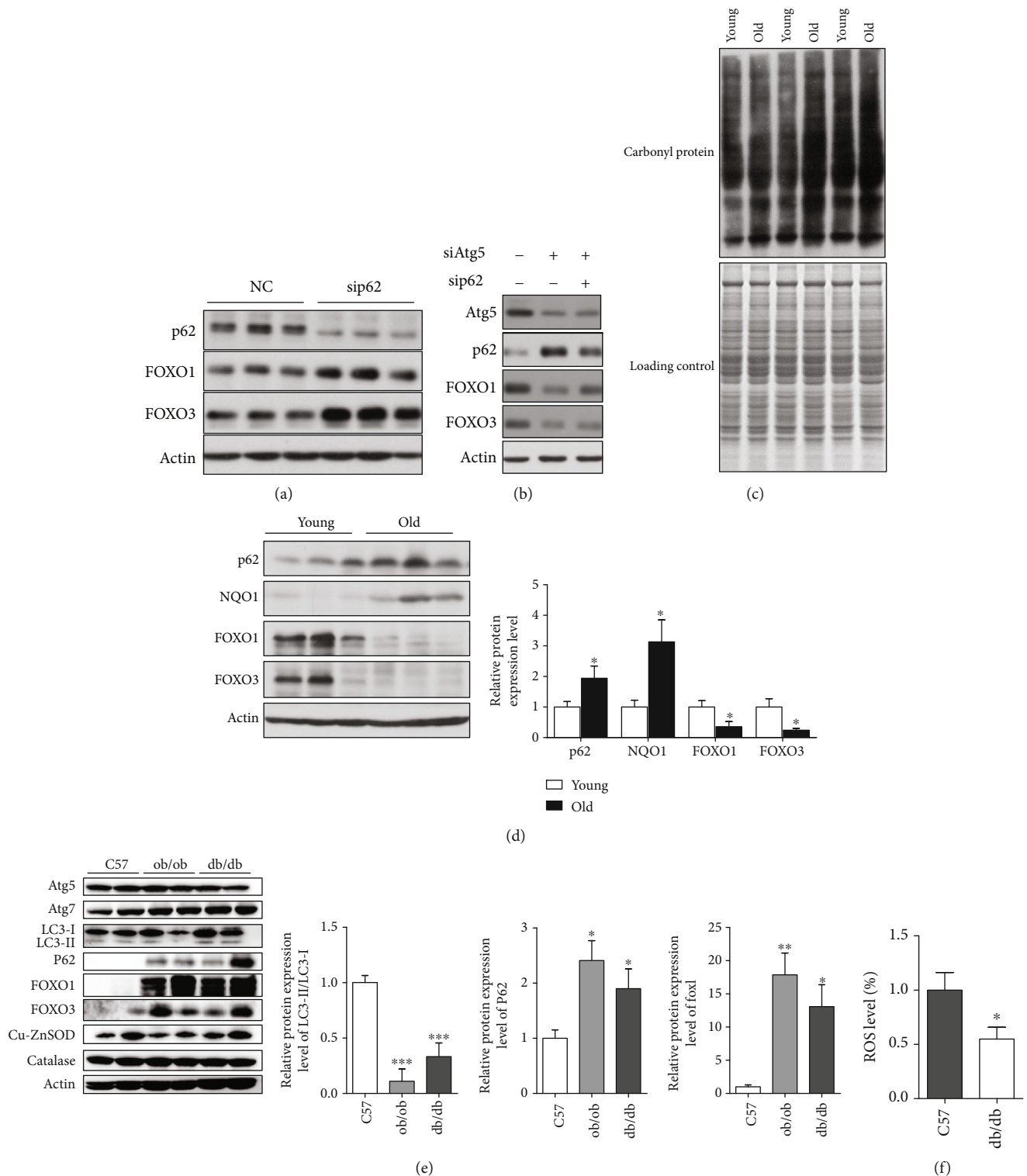
FIGURE 4: Accumulated p62 in a condition of inhibited autophagy is responsible for the loss of FOXO1/3, which is involved in aging but not dominant in type 2 diabetes mellitus animal models. (a and b) HEK293T cells were transfected with sip62 or negative control siRNA or with sip62 and/or siAtg5 for 48 hours before harvest; indicated protein levels were determined by W.B. (c and d) Liver tissues from SD rats aged five months (young) and 25 months (old) were homogenized to yield lysates, protein carbonylation levels were detected with a commercially available kit, Coomassie brilliant blue staining was used to monitor equal loading control (c), and indicated protein levels were determined by W.B. and densitometry analysis ($n = 9$) (d). (e and f) Liver tissues from 18-week-old ob/ob (B6/JNju-Lep^{em1Cd25}/Nju), db/db (BSK-Lepr^{em2Cd479}/Nju), and C57 mice were homogenized to yield lysates, indicated protein levels were determined by W.B. and densitometry analysis ($n = 6$) (e), and ROS levels were measured with a DCFDA probe ($n = 6$) (f). Values are represented as mean ± SEM, and statistical analysis were conducted using t-test. $^*p < 0.05$; $^{**}p < 0.01$; $^{***}p < 0.001$; vs. young or C57.

and insulin resistance [54, 55]. We observed increased p62 along with a decreased ratio of LC3II to LC3I in the liver of ob/ob or db/db mice compared with those in the liver of c57 mice (Figures 4(e) and 4(f); Figure S4), indicating the attenuation of autophagy activity in the liver of both type 2 diabetes mice models, which could have contributed to the exacerbation of hepatic steatosis and insulin resistance. The role oxidative stress plays in type 2 diabetes could be bidirectional [56], as it is reported that increased ROS level is an important trigger for insulin resistance [57] and there is also evidence indicating the enhancement of insulin sensitivity by ROS [58]. To help disentangle the complex knot involving autophagy and ROS in type 2 diabetes, we attempted to check whether the potential p62-FOXO1/3 axis takes any effect in type 2 diabetes animal models. We found reduced ROS level but higher expression of FOXO1/3 in the liver of ob/ob or db/db mice compared with the liver of c57 mice (Figures 4(e) and 4(f); Figure S4). Consistently, it has been reported that the hyperactivation of FOXOs is associated with hyperglycemia, hypertriglyceridemia, and insulin resistance [52]. The fact that accumulated p62, upregulated FOXO1/3, and reduced ROS levels coexist in the liver of type 2 diabetes animal models indicate that the p62-FOXO1/3 axis is not dominant in diabetic liver and suggest that there are other mechanisms underlying the upregulation of FOXO1/3 in diabetic liver which could have suppressed the downregulating effect of accumulated p62 on FOXO1/3 level.

4. Discussion

Autophagy contributes to redox homeostasis in an antioxidative fashion not only by the clearance of oxidized cellular components as classically recognized but also by promoting antioxidant defense capacity via the p62/keap1/Nrf2 pathway in recent discoveries. In this study, we reported mitochondrial dysfunction and decrease of both expression and enzymatic activities of the antioxidant enzymes, the key components of the antioxidant defense system, in different autophagy deficiency cellular models, and revealed the p62-FOXO1/3 axis that mediates the influence of autophagy deficiency on redox balance. Our findings clearly show that inhibition of autophagy injures antioxidant enzymes which leads to oxidative stress, suggesting that autophagy deficiency impacts redox homeostasis in a prooxidant fashion by sabotaging antioxidant defense capacity besides the well-recognized insufficient clearance of oxidized cellular materials. This deepens our understanding of the regulation of redox homeostasis by autophagy to a more comprehensive sense. Furthermore, our story implicates autophagy deficiency in the etiology of aging and possibly age-related disease, too, where oxidative stress and mitochondrial dysfunction is a signature, and offers the p62-FOXO1/3 axis as potential therapeutic targeting directions in diseases involving autophagy defects.

Emerging evidences are demonstrating multifaceted roles of autophagy, especially the dynamic role of autophagy in regulating cell signaling [27, 59, 60]. p62, conventionally

known as a selective autophagy receptor for the degradation of ubiquitinated substrates, has recently been proposed to function as a signaling hub for diverse cellular events [61]. Our results further corroborate the notion of p62 being an important signaling molecule as its accumulation downregulates the protein level of FOXO1/3 transcription factor that plays vital roles in coordinating metabolism and stress response in pathophysiological conditions. FOXOs serve as a converging point where numerous signaling converge and integrate to maintain homeostasis ([33, 62]). This study demonstrated the negative regulation of FOXO1/3 protein abundance by p62, indicating that FOXOs could also sense signals transduced by p62 level that integrates information derived from various cellular processes including autophagy activity. Nonetheless, the detailed molecular mechanisms by which FOXO1/3 gets downregulated in response to p62 accumulation, either through directly altering posttranslational modification of FOXO1/3 to modulating its stability or via indirect mediations of other players acting at multiple regulatory levels such as transcriptional/posttranscriptional level, warrants further investigations to elaborate. Transcriptional modulation of FOXO1/3 by p62, either directly or indirectly, should at least play a part, as mRNA levels of FOXO1/3 were lower in Atg7-/- MEF cells than in WT MEF cells (Figure S2D). More interestingly, treatment with antioxidants such as N-acetyl-L-cysteine has shown benefits in circumstances related to oxidative stress or autophagy defect, like mitochondrial dysfunction and DNA damage [27], whereas NAC treatment of Atg7-/- MEFs and autophagy inhibitor-treated cells not only failed to restore protein levels of FOXO1/3 and antioxidant enzymes but even aggravated the losses. Since FOXO gene expression itself is sensitive to redox state [52], we infer that FOXO1/3 is the pivot where redox balance and autophagy activity crosstalk with each other, and the net result of FOXO1/3's integration of signals from both sources and possibly other sources orchestrate in cooperation with cofactors the expression of FOXO1/3's target genes including autophagy machinery and antioxidant enzymes. Our results imply that NAC treatment has a dark side as a therapeutic approach because quenching ROS by NAC might downregulate the FOXO-antioxidant pathway and most likely autophagy activity too, which could in turn weaken the endogenous cellular antioxidant capacity. Therefore, pharmacological approaches activating FOXO activity might be promising strategies for treating diseases induced by autophagy defects.

The predominant role of FOXOs is to respond to and counteract stress conditions for the maintenance of cellular homeostasis, and it can be activated by metabolic and oxidative stress [33]. Autophagy-deficient cells are known to suffer from severe oxidative stress and DNA damage due to the well-characterized defects in the clearance of damaged and aberrant organelles such as mitochondria, and accumulation of dysfunctional mitochondria due to absent autophagy results in the generation of more reactive species that would further harm mitochondria, feeding a vicious cycle [27]. Our results show that FOXOs fail to respond to the enhanced

oxidative stress present in an autophagy deficiency condition by upregulating antioxidant enzymes as the accumulation of p62 negatively regulates the protein levels of FOXO1/3, suggesting that autophagy deficiency represents a severe disturbance of homeostasis where stress response depending on FOXO1/3 is wrecked and homeostasis can no longer be recovered. Therefore, autophagy-deficient cells are much more vulnerable to cellular oxidative damage, implying that enhancing autophagy could have therapeutic potential in oxidative stress-associated pathologies and increasing antioxidant power could render benefits for diseases implicating autophagy deficiency. Indeed, increasing basal autophagy levels could extend lifespan and enhance resistance to oxidative stress in adult *Drosophila* [63] and in mice [64]; treatment with antioxidants rescued the defects of intestinal stem cell-dependent intestinal recovery after irradiation in mice lacking Atg5 [65], and NAC treatment ameliorated the impairment of glucose tolerance in pancreatic β cells in autophagy-deficient models by reducing continuous oxidative stress ([29]).

The probable cause-and-effect relationship between autophagy and aging has been investigated and discussed intensively in the past decade. Generally, autophagy diminishes with both normal and pathological aging, autophagy inhibition leads to premature aging, and autophagy defect accelerates the aging process while stimulating autophagy delays aging and extends longevity [53]. We infer from our observations with aged and young rat liver and cellular studies that autophagy activity abates while oxidative damage heightens during rat liver aging, and the p62-FOXO1/3 axis regulating antioxidant defense might play an important role in liver aging process. Specifically, FOXO1/3 loss and the impaired antioxidant enzymes might accelerate aging or increase incidence of age-associated diseases in a condition of autophagy deficiency; therefore, targeting p62, FOXOs, or antioxidant defense might be considered in developing potential therapeutic strategies for diseases implicated with autophagy defects.

In addition, we also detected increased expression of NQO1, one of the phase II detoxifying enzymes, in aged rat liver, and increased expression of NQO1 as well as its upstream regulator Nrf2 in Atg7-/- MEF cells (Figure 4(d); Figures S2A and S2B). NQO1 is a highly inducible detoxification enzyme regulated by the Keap1/Nrf2/ARE pathway; it promotes 2/4-electron reductions of quinones and can minimize reactive oxygen intermediate generation from redox cycling and reserve intracellular thiol pools; its important antioxidant function in combating oxidative stress has been well substantiated [66]. Our results are consistent with previous findings that autophagy-deficient models exhibit hyperactivated Nrf2 transcription activity and enhanced induction of Nrf2 target genes such as NQO1, possibly due to the competitive inhibition of Nrf2-Keap1 interactions by accumulated p62 which can bind to Keap1 and mediate its degradation [32]. These findings suggest that upregulation or activation of the Nrf2/ARE/NQO1 pathway might occur in aged liver, which the abated autophagy activity in aged liver is probably partly accountable for. Meanwhile, the overall increase of

oxidative damage in aged rat liver implies that the activation of the Nrf2/ARE/NQO1 pathway is not sufficient to confer enough antioxidant capacity to protect against oxidative stress induced by autophagy decline during aging. The downregulation of more vital antioxidant enzymes like Cu-ZnSOD, MnSOD, and catalase by the p62-FOXO1/3 axis is probably more decisive in overall output of antioxidant defense capacity in aged rat liver. As can be seen, the regulation of antioxidant enzymes during aging involves versatile transcription factors like Nrf2 and FOXO1/3, which integrates a wide spectrum of upstream signals including information delivered by p62 which together produce the actual net outcome. In addition, NQO1's cytoprotective roles unrelated to enzymatic activities have been demonstrated; for instance, it selectively binds to and hence stabilizes specific proteins like p53, a well-known tumor suppressor, against proteasomal degradation [66]. This suggests that the increase of NQO1 expression in aged rat liver might have other significances beyond its antioxidant function, which might involve regulation of the degradative fate of certain important proteins, and contribute to the prevention and protection against tumorigenesis during aging. Further studies are warranted to fully decipher the roles of NQO1 in aging.

Autophagy plays intricate roles in type 2 diabetes. There are paradoxical reports that autophagy defect promotes insulin resistance, the core of type 2 diabetes ([55]), and autophagy deficiency leads to protection from obesity and insulin resistance by inducing mitokine [67]. Taken together with our observations, we can see that the driving force is derived from the lack of leptin or leptin receptor as in ob/ob or db/db mice; the attenuation of autophagy activity eventually occurs and could further contribute to the progression of type 2 diabetes or act as a protective response against the exacerbation of insulin resistance. FOXO proteins are crucial in diabetes as they are highly expressed in the major insulin target tissues and play multiple and complex roles as both overexpression of constitutively active FOXO1α and knockdown of FOXO1/3α could lead to diabetes or hypertriglyceridemia [52]. In our results, FOXO1/3 exhibits higher expression levels in the liver of ob/ob or db/db mice in comparison to those of c57 mice. FOXOs also have beneficial effects in the context of diabetes, as FOXO-dependent transcription of antioxidant enzymes may counteract oxidative stress-induced cellular damage [52], which agrees with our findings that overall ROS level is lower in liver homogenates of db/db mice compared to those of c57, though expression of Cu-ZnSOD and catalase in the liver of ob/ob or db/db mice is similar to that of c57 mice. These findings suggest that the p62 accumulation due to diminished autophagy in diabetic liver was not able to decrease FOXO1/3 which is hyperactivated by other mechanisms and yields an overall decrease in ROS level despite that hyperglycemia typically induces oxidative stress. In fact, the relationship between autophagy and antioxidant defense is neither simple nor straightforward, depending on specific contexts. A study of the intestinal epithelial cell-specific Atg5 knockout mice model showed that activation of the ERK/Nrf2/HO-1 pathway by oxidative stress in a condition of autophagy deficiency led

to diminished indomethacin-induced intestinal epithelial cell damage because of the stronger resistance to oxidative stress [68]. Yu et al. [69] demonstrated that catalase could be selectively degraded by autophagy in caspase inhibition conditions, thus leading to programmed cell death induced by abnormal ROS accumulation. To fully unravel the interplay of autophagy, FOXOs, and redox balance in a diabetic setting and lay groundwork for potential therapeutic strategies, further studies are called to dissect more molecular events.

In conclusion, the present study demonstrates that inhibition of autophagy by either chemical or genetic approaches leads to mitochondrial dysfunction, oxidative stress, and impaired expressions and enzymatic activities of the antioxidant enzymes; the p62-FOXO1/3 axis underlies the impairment of antioxidant defense in an autophagy deficiency condition. We propose that autophagy deficiency could disrupt intracellular homeostasis through injuring the antioxidant system besides the incapability of clearing damaged components; and accumulation of damaged mitochondria and the impaired antioxidant defense enhance oxidative stress together in a condition of autophagy deficiency. The newly uncovered p62-FOXO1/3 axis is probably linking autophagy decline to oxidative stress in liver aging, which provides a perspective to help reveal the mystery of aging. Hopefully, our study could shed light on the path elucidating the interplay between autophagy and oxidative stress and the quest for the mechanisms of aging and pathophysiology of autophagy-defect-related diseases, and could lay ground for potential therapeutic strategies.

Data Availability

The biochemical data, gene expression data, and Western blot data used to support the findings of this study are included within the article and the supplementary figures. Any additional data used to support the findings of this study are available upon request.

Additional Points

Highlights. (i) Inhibition of autophagy by chemical inhibitors, knockdown of Atg5 or Beclin-1, or Atg7 knockout leads to mitochondrial dysfunction, elevated ROS level, impaired antioxidant defense, and downregulated FOXO1/3 transcription factors. (ii) Overexpression of FOXO1/3 rescues the impairment of antioxidant enzymes and reduces the elevation of ROS level under an autophagy deficiency condition. (iii) p62 knockdown increases the expression of FOXO1/3, and p62 knockdown reverses the downregulation of FOXO1 in a condition of Atg5 knockdown where p62 accumulates. (iv) Accumulated p62, loss of FOXO1/3, and increased oxidative damage occur in aged rat liver, whereas accumulated p62, upregulated FOXO1/3, and reduced ROS level coexist in the liver of a type 2 diabetes mice model, suggesting that the p62-FOXO1/3 axis is involved in liver aging but not dominant in diabetic liver

Supplementary Materials

Figure S1: CQ treatment results in decreased mRNA levels of autophagy components in WT MEF cells in a dose-dependent manner, and mRNA levels of autophagy components decrease in Atg7-/- MEF cells compared with WT. Figure S2: Nrf2 and NQO1 expression is upregulated in Atg7-/- MEF cells compared with WT. Figure S3: over-expression of FOXOs restores mRNA levels of antioxidant enzymes as well as autophagy components. Figure S4: expression levels of indicated proteins in the liver tissues of 18-week-old ob/ob (B6/JNju-Lepem1Cd25/Nju), db/db (BSK-Leprem2Cd479 889/Nju), and C57 mice were determined by W.B. ($n = 6$). *(Supplementary Materials)*

References

[1] C. F. Bento, M. Renna, G. Ghislat et al., "Mammalian autophagy: how does it work?," *Annual Review of Biochemistry*, vol. 85, pp. 685–713, 2016.

[2] D. Gatica, V. Lahiri, and D. J. Klionsky, "Cargo recognition and degradation by selective autophagy," *Nature Cell Biology*, vol. 20, no. 3, pp. 233–242, 2018.

[3] D. Glick, S. Barth, and K. F. Macleod, "Autophagy: cellular and molecular mechanisms," *The Journal of Pathology*, vol. 221, no. 1, pp. 3–12, 2010.

[4] L. Yu, Y. Chen, and S. A. Tooze, "Autophagy pathway: cellular and molecular mechanisms," *Autophagy*, vol. 14, no. 2, pp. 207–215, 2018.

[5] A. Benedetto and D. Gems, "Autophagy promotes visceral aging in wild-type *C. elegans*," *Autophagy*, vol. 15, no. 4, pp. 731-732, 2019.

[6] I. Dikic and Z. Elazar, "Mechanism and medical implications of mammalian autophagy," *Nature Reviews Molecular Cell Biology*, vol. 19, no. 6, pp. 349–364, 2018.

[7] J. Doherty and E. H. Baehrecke, "Life, death and autophagy," *Nature Cell Biology*, vol. 20, no. 10, pp. 1110–1117, 2018.

[8] P. Jiang and N. Mizushima, "Autophagy and human diseases," *Cell Research*, vol. 24, no. 1, pp. 69–79, 2014.

[9] G. Kroemer, "Autophagy: a druggable process that is deregulated in aging and human disease," *The Journal of Clinical Investigation*, vol. 125, no. 1, pp. 1–4, 2015.

[10] B. Levine and G. Kroemer, "Biological functions of autophagy genes: a disease perspective," *Cell*, vol. 176, no. 1-2, pp. 11–42, 2019.

[11] C. Lopez-Otin and G. Kroemer, "Decelerating ageing and biological clocks by autophagy," *Nature Reviews Molecular Cell Biology*, vol. 20, no. 7, pp. 385-386, 2019.

[12] H. Morishita and N. Mizushima, "Diverse cellular roles of autophagy," *Annual Review of Cell and Developmental Biology*, vol. 35, no. 1, pp. 453–475, 2019.

[13] S. Q. Wong, A. V. Kumar, J. Mills, and L. R. Lapierre, "Autophagy in aging and longevity," *Human Genetics*, pp. 1–14, 2019.

[14] S. Giordano, V. Darley-Usmar, and J. Zhang, "Autophagy as an essential cellular antioxidant pathway in neurodegenerative disease," *Redox Biology*, vol. 2, pp. 82–90, 2014.

[15] J. Ren and Y. Zhang, "Targeting autophagy in aging and aging-related cardiovascular diseases," *Trends in Pharmacological Sciences*, vol. 39, no. 12, pp. 1064–1076, 2018.

[16] L. Galluzzi and D. R. Green, "Autophagy-independent functions of the autophagy machinery," *Cell*, vol. 177, no. 7, pp. 1682–1699, 2019.

[17] A. Thorburn, "Autophagy and disease," *The Journal of Biological Chemistry*, vol. 293, no. 15, pp. 5425–5430, 2018.

[18] Y. Kong, S. E. Trabucco, and H. Zhang, "Oxidative stress, mitochondrial dysfunction and the mitochondria theory of aging," *Interdisciplinary Topics in Gerontology*, vol. 39, pp. 86–107, 2014.

[19] Y. M. Go and D. P. Jones, "Redox theory of aging: implications for health and disease," *Clinical Science*, vol. 131, no. 14, pp. 1669–1688, 2017.

[20] H. Sies, "Oxidative stress: a concept in redox biology and medicine," *Redox Biology*, vol. 4, pp. 180–183, 2015.

[21] J. Lee, S. Giordano, and J. Zhang, "Autophagy, mitochondria and oxidative stress: cross-talk and redox signalling," *The Biochemical Journal*, vol. 441, no. 2, pp. 523–540, 2012.

[22] R. Scherz-Shouval and Z. Elazar, "ROS, mitochondria and the regulation of autophagy," *Trends in Cell Biology*, vol. 17, no. 9, pp. 422–427, 2007.

[23] G. Filomeni, D. De Zio, and F. Cecconi, "Oxidative stress and autophagy: the clash between damage and metabolic needs," *Cell Death and Differentiation*, vol. 22, no. 3, pp. 377–388, 2015.

[24] R. Scherz-Shouval and Z. Elazar, "Regulation of autophagy by ROS: physiology and pathology," *Trends in Biochemical Sciences*, vol. 36, no. 1, pp. 30–38, 2011.

[25] R. Scherz-Shouval and Z. Elazar, "Chapter 8 Monitoring starvation-induced reactive oxygen species formation," *Methods in Enzymology*, vol. 452, pp. 119–130, 2009.

[26] B. R. Underwood, S. Imarisio, A. Fleming et al., "Antioxidants can inhibit basal autophagy and enhance neurodegeneration in models of polyglutamine disease," *Human Molecular Genetics*, vol. 19, no. 17, pp. 3413–3429, 2010.

[27] I. H. Lee, Y. Kawai, M. M. Fergusson et al., "Atg7 modulates p53 activity to regulate cell cycle and survival during metabolic stress," *Science*, vol. 336, no. 6078, pp. 225–228, 2012.

[28] M. C. Tal, M. Sasai, H. K. Lee, B. Yordy, G. S. Shadel, and A. Iwasaki, "Absence of autophagy results in reactive oxygen species-dependent amplification of RLR signaling," *Proceedings of the National Academy of Sciences of the United States of America*, vol. 106, no. 8, pp. 2770–2775, 2009.

[29] J. J. Wu, C. Quijano, E. Chen et al., "Mitochondrial dysfunction and oxidative stress mediate the physiological impairment induced by the disruption of autophagy," *Aging*, vol. 1, no. 4, pp. 425–437, 2009.

[30] Y. Inami, S. Waguri, A. Sakamoto et al., "Persistent activation of Nrf2 through p62 in hepatocellular carcinoma cells," *The Journal of Cell Biology*, vol. 193, no. 2, pp. 275–284, 2011.

[31] M. Komatsu, H. Kurokawa, S. Waguri et al., "The selective autophagy substrate p62 activates the stress responsive transcription factor Nrf2 through inactivation of Keap1," *Nature Cell Biology*, vol. 12, no. 3, pp. 213–223, 2010.

[32] A. Lau, X.-J. Wang, F. Zhao et al., "A noncanonical mechanism of Nrf2 activation by autophagy deficiency: direct interaction between Keap1 and p62," *Molecular and Cellular Biology*, vol. 30, no. 13, pp. 3275–3285, 2010.

[33] A. Eijkelenboom and B. M. T. Burgering, "FOXOs: signalling integrators for homeostasis maintenance," *Nature Reviews Molecular Cell Biology*, vol. 14, no. 2, pp. 83–97, 2013.

[34] R. Martins, G. J. Lithgow, and W. Link, "Long live FOXO: unraveling the role of FOXO proteins in aging and longevity," *Aging Cell*, vol. 15, no. 2, pp. 196–207, 2016.

[35] A. van der Horst and B. M. T. Burgering, "Stressing the role of FoxO proteins in lifespan and disease," *Nature Reviews Molecular Cell Biology*, vol. 8, no. 6, pp. 440–450, 2007.

[36] G. J. P. L. Kops, T. B. Dansen, P. E. Polderman et al., "Forkhead transcription factor FOXO3a protects quiescent cells from oxidative stress," *Nature*, vol. 419, no. 6904, pp. 316–321, 2002.

[37] D. Marinkovic, X. Zhang, S. Yalcin et al., "Foxo3 is required for the regulation of oxidative stress in erythropoiesis," *The Journal of Clinical Investigation*, vol. 117, no. 8, pp. 2133–2144, 2007.

[38] S. Nemoto and T. Finkel, "Redox regulation of forkhead proteins through a p66shc-dependent signaling pathway," *Science*, vol. 295, no. 5564, pp. 2450–2452, 2002.

[39] C. Mammucari, G. Milan, V. Romanello et al., "FoxO3 controls autophagy in skeletal muscle in vivo," *Cell Metabolism*, vol. 6, no. 6, pp. 458–471, 2007.

[40] A. Sengupta, J. D. Molkentin, and K. E. Yutzey, "FoxO transcription factors promote autophagy in cardiomyocytes," *The Journal of Biological Chemistry*, vol. 284, no. 41, pp. 28319–28331, 2009.

[41] J. Zhao, J. J. Brault, A. Schild et al., "FoxO3 coordinately activates protein degradation by the autophagic/lysosomal and proteasomal pathways in atrophying muscle cells," *Cell Metabolism*, vol. 6, no. 6, pp. 472–483, 2007.

[42] Y. Zhao, J. Yang, W. Liao et al., "Cytosolic FoxO1 is essential for the induction of autophagy and tumour suppressor activity," *Nature Cell Biology*, vol. 12, no. 7, pp. 665–675, 2010.

[43] M. Komatsu, S. Waguri, T. Ueno et al., "Impairment of starvation-induced and constitutive autophagy in Atg7-deficient mice," *Journal of Cell Biology*, vol. 169, no. 3, pp. 425–434, 2005.

[44] E. D. Tang, G. Nunez, F. G. Barr, and K. L. Guan, "Negative regulation of the forkhead transcription factor FKHR by Akt," *The Journal of Biological Chemistry*, vol. 274, no. 24, pp. 16741–16746, 1999.

[45] J.-Y. Yang, C. S. Zong, W. Xia et al., "ERK promotes tumorigenesis by inhibiting FOXO3a via MDM2-mediated degradation," *Nature Cell Biology*, vol. 10, no. 2, pp. 138–148, 2008.

[46] J. Long, X. Wang, H. Gao et al., "Malonaldehyde acts as a mitochondrial toxin: inhibitory effects on respiratory function and enzyme activities in isolated rat liver mitochondria," *Life Sciences*, vol. 79, no. 15, pp. 1466–1472, 2006.

[47] L. Sun, C. Luo, J. Long, D. Wei, and J. Liu, "Acrolein is a mitochondrial toxin: effects on respiratory function and enzyme activities in isolated rat liver mitochondria," *Mitochondrion*, vol. 6, no. 3, pp. 136–142, 2006.

[48] X. Wang, H. Li, A. Zheng et al., "Mitochondrial dysfunction-associated OPA1 cleavage contributes to muscle degeneration: preventative effect of hydroxytyrosol acetate," *Cell Death & Disease*, vol. 5, article e1521, 2014.

[49] M. Wu, A. Neilson, A. L. Swift et al., "Multiparameter metabolic analysis reveals a close link between attenuated mitochondrial bioenergetic function and enhanced glycolysis dependency in human tumor cells," *American Journal of Physiology-Cell Physiology*, vol. 292, no. 1, pp. C125–C136, 2007.

[50] S. Yalcin, X. Zhang, J. P. Luciano et al., "Foxo3 is essential for the regulation of ataxia telangiectasia mutated and oxidative stress-mediated homeostasis of hematopoietic stem cells," *The Journal of Biological Chemistry*, vol. 283, no. 37, pp. 25692–25705, 2008.

[51] I. Schäffner, G. Minakaki, M. A. Khan et al., "FoxO function is essential for maintenance of autophagic flux and neuronal morphogenesis in adult neurogenesis," *Neuron*, vol. 99, no. 6, pp. 1188–1203.e6, 2018.

[52] L.-O. Klotz, C. Sánchez-Ramos, I. Prieto-Arroyo, P. Urbánek, H. Steinbrenner, and M. Monsalve, "Redox regulation of FoxO transcription factors," *Redox Biology*, vol. 6, pp. 51–72, 2015.

[53] D. C. Rubinsztein, G. Mariño, and G. Kroemer, "Autophagy and aging," *Cell*, vol. 146, no. 5, pp. 682–695, 2011.

[54] Q. Qian, Z. Zhang, A. Orwig et al., "S-Nitrosoglutathione reductase dysfunction contributes to obesity-associated hepatic insulin resistance via regulating autophagy," *Diabetes*, vol. 67, no. 2, pp. 193–207, 2018.

[55] L. Yang, P. Li, S. Fu, E. S. Calay, and G. S. Hotamisligil, "Defective hepatic autophagy in obesity promotes ER stress and causes insulin resistance," *Cell Metabolism*, vol. 11, no. 6, pp. 467–478, 2010.

[56] X. G. Lei and M. Z. Vatamaniuk, "Two tales of antioxidant enzymes on β cells and diabetes," *Antioxidants & Redox Signaling*, vol. 14, no. 3, pp. 489–503, 2011.

[57] N. Houstis, E. D. Rosen, and E. S. Lander, "Reactive oxygen species have a causal role in multiple forms of insulin resistance," *Nature*, vol. 440, no. 7086, pp. 944–948, 2006.

[58] K. Loh, H. Deng, A. Fukushima et al., "Reactive oxygen species enhance insulin sensitivity," *Cell Metabolism*, vol. 10, no. 4, pp. 260–272, 2009.

[59] C. Gao, W. Cao, L. Bao et al., "Autophagy negatively regulates Wnt signalling by promoting Dishevelled degradation," *Nature Cell Biology*, vol. 12, no. 8, pp. 781–790, 2010.

[60] N. Martinez-Lopez, D. Athonvarangkul, P. Mishall, S. Sahu, and R. Singh, "Autophagy proteins regulate ERK phosphorylation," *Nature Communications*, vol. 4, no. 1, 2013.

[61] Y. Katsuragi, Y. Ichimura, and M. Komatsu, "p62/SQSTM1 functions as a signaling hub and an autophagy adaptor," *The FEBS Journal*, vol. 282, no. 24, pp. 4672–4678, 2015.

[62] S. Lee and H. H. Dong, "FoxO integration of insulin signaling with glucose and lipid metabolism," *The Journal of Endocrinology*, vol. 233, no. 2, pp. R67–r79, 2017.

[63] A. Simonsen, R. C. Cumming, A. Brech, P. Isakson, D. R. Schubert, and K. D. Finley, "Promoting basal levels of autophagy in the nervous system enhances longevity and oxidant resistance in adult *Drosophila*," *Autophagy*, vol. 4, no. 2, pp. 176–184, 2008.

[64] J.-O. Pyo, S. M. Yoo, H. H. Ahn et al., "Overexpression of Atg5 in mice activates autophagy and extends lifespan," *Nature Communications*, vol. 4, no. 1, 2013.

[65] J. Asano, T. Sato, S. Ichinose et al., "Intrinsic autophagy is required for the maintenance of intestinal stem cells and for irradiation-induced intestinal regeneration," *Cell Reports*, vol. 20, no. 5, pp. 1050–1060, 2017.

[66] A. T. Dinkova-Kostova and P. Talalay, "NAD(P)H: quinone acceptor oxidoreductase 1 (NQO1), a multifunctional antioxidant enzyme and exceptionally versatile cytoprotector," *Archives of Biochemistry and Biophysics*, vol. 501, no. 1, pp. 116–123, 2010.

[67] K. H. Kim, Y. T. Jeong, H. Oh et al., "Autophagy deficiency leads to protection from obesity and insulin resistance by inducing Fgf21 as a mitokine," *Nature Medicine*, vol. 19, no. 1, pp. 83–92, 2013.

[68] S. Harada, T. Nakagawa, S. Yokoe et al., "Autophagy deficiency diminishes indomethacin-induced intestinal epithelial cell damage through activation of the ERK/Nrf2/HO-1 pathway," *The Journal of Pharmacology and Experimental Therapeutics*, vol. 355, no. 3, pp. 353–361, 2015.

[69] L. Yu, F. Wan, S. Dutta et al., "Autophagic programmed cell death by selective catalase degradation," *Proceedings of the National Academy of Sciences of the United States of America*, vol. 103, no. 13, pp. 4952–4957, 2006.

Research Article

Phosphocreatine Improves Cardiac Dysfunction by Normalizing Mitochondrial Respiratory Function through JAK2/STAT3 Signaling Pathway *In Vivo* and *In Vitro*

Eskandar Qaed,[1] **Jiaqi Wang,**[2] **Marwan Almoiliqy,**[1] **Yanlin Song,**[1] **Wu Liu,**[1] **Peng Chu,**[1] **Sawsan Alademi,**[3] **Maria Alademi,**[3] **Hailong Li,**[1] **Mohammed Alshwmi,**[1] **Mahmoud Al-Azab,**[4] **Anil Ahsan,**[1] **Samar Mahdi,**[1] **Guozhu Han,**[1] **Mengyue Niu,**[1] **Amr Ali,**[1] **Abdullah Shopit,**[1] **Hongyan Wang** [1] **Xiaodong Li,**[1] **Abdullah Qaid,**[5] **Xiaodong Ma,**[1] **Tong Li,**[1] **Jinyong Peng,**[1] **Jing Ma,**[1] **Jianbin Zhang** [1] **and Zeyao Tang** [1]

[1]*Department of Pharmacology, Dalian Medical University, Dalian, Liaoning 116044, China*
[2]*Department of Plastic and Reconstructive Surgery, The First Hospital of Jilin University, 1500 Qinghua Road, Changchun 130021, China*
[3]*College of Medical Sciences, Taiz University, Yemen*
[4]*Department of Immunology Guangzhou Institute Pediatrics, Guangzhou Woman and Childrens Medical Center, Guangzhou Medical University, Guangzhou, 510623, China*
[5]*N.I. Pirogov Russian National Research Medical University, Russia*

Correspondence should be addressed to Jianbin Zhang; zhangjb@dmu.edu.cn and Zeyao Tang; zeyaotang@163.com

Diabetic cardiomyopathy (DCM) is one of the common cardiovascular complications in patients with diabetes. Accumulating evidence has demonstrated that DCM is thoroughly related to mitochondrial energy impairment and increases the generation of reactive oxygen species (ROS). Therefore, an ongoing study is developing strategies to protect cardiac mitochondria from diabetic complications, especially from hyperglycemia. Phosphocreatine (PCr) plays a major metabolic role in cardiac muscular cells including intracellular concentration of ATP which affects the activity of the myocardium. We hypothesized that PCr might improve oxidative phosphorylation and electron transport capacity in mitochondria impaired by hyperglycemia in vivo and in vitro. Also, we aimed to evaluate the protective effect of PCr against DCM through the JAK2/STAT3 signaling pathway. The mitochondrial respiratory capacity from rats and H9C2 cells was measured by high-resolution respirometry (HRR). Expressions of proteins Bax, Bcl-2, caspase 3, caspase 9, cleaved caspase 3, and cleaved caspase 9, as well as JAK2/STAT3 signaling pathways, were determined by western blotting. ROS generation and mitochondrial membrane potential (MMP) were measured with fluorescent probes. Type 1 diabetes mellitus was induced in Wistar male rats by a single intraperitoneal injection of streptozotocin (STZ) (80 mg/kg body weight). Our results revealed that PCr possessed protective effects against DCM injury by improving the mitochondrial bioenergetics and by positively exerting protective effects against DCM in vivo and in vitro, not only improving diabetes symptom, resulting in changes of cardiac tissue using hematoxylin and eosin (H&E) stain, but also ameliorating biochemical changes. Moreover, PCr increased Bcl-2, caspase 3, and caspase 9 protein expressions and decreased Bax, cleaved caspase 3, and cleaved caspase 9 expressions as well as the JAK2/STAT3 signaling pathway. In conclusion, PCr improves mitochondrial functions and exerts an antiapoptotic effect in vivo and in vitro exposed to oxidative stress by hyperglycemia through the JAK2/STAT3 signaling pathway. Our findings suggest that PCr medication is a possible therapeutic strategy for cardioprotection.

1. Introduction

Recent studies have demonstrated that diabetic cardiomyopathy (DCM) is the main sequence of diabetes mellitus (DM). DCM is characterized with inconsistent increase in left ventricular (LV) muscle [1–4]. Moreover, recent researches have showed that mitochondrial energy metabolism variation is one of the common causes of heart disease including DCM [5]. In addition, mitochondria are essential and important regulators of cellular bioenergetics to provide the normal heart its daily need of ATP. In fact, about 40% of the cytoplasmic space in adult cardiac myocyte is employed by mitochondria. Mitochondrial oxidative phosphorylation (OXPHOS) in the respiratory chain (RC) complexes locates in their inner membrane occupying the majority of high demand for ATP [6]. Therefore, myocardial mitochondria are highly responsive to any injury through high energy demand substrate accessibility which plays a very important role in heart stability. On the other hand, clinical studies have indicated that mitochondrial dysfunction contributes to cardiomyopathy with several clinical indicators. Moreover, mitochondrial dysfunction and diminished energy creation have been detected in various formulas of heart illnesses including DCM [7]. Likewise, the revelation of a novel helpful procedure for the advancement and upkeep of a mitochondrial work is of extraordinary logical significance in the treatment of DCM [8]. High generation of reactive oxygen species (ROS) is the main cause of progression to cardiac brokenness when mitochondrial vitality is impaired [9]. Recently, oxidative stress has been recognized as a risk factor in the progressing of diabetic cardiovascular complications [10]. Oxidative stress caused by higher production or reduced degradation of ROS is involved crucially in physiological and pathological processes of cell life and death decisions [11, 12], for example, apoptosis. It has been accounted for that apoptosis of cardiomyocytes is one of the fundamental outcomes of hyperglycemia-actuated oxidative stress in the myocardium [13]. Cardiomyocyte apoptosis in diabetic creature models and patients is expanded because of the loss of contractile tissues, rebuilding, and at last brokenness [14, 15]. It has been known that cardiomyocyte apoptosis is related to a few pathways like extrinsic pathway induced by ligands fixed to death receptors and the intrinsic pathway managed by the arrival of a few genius apoptotic proteins from the mitochondria [16].

Phosphocreatine (PCr) is a high vitality phosphate compound which goes as a vitality provider and has the double capacity of stacking and dispatching ATP in vitality digestion [17]. Though exogenous PCr offers vitality straightforwardly to the cell through the creatine transport, different investigations have suggested that PCr is essential for supporting the vitality digestion of apoptotic cells which is through keeping up picture dependability [18]. Currently, PCr can be synthesized artificially. Exogenous PCr has recently been used as a cardioprotective drug due to its superior efficacy in the protection of the myocardium against hypoxia injury and its significant improvement [19]. PCr has been added to the cardioplegia arrangement and conveyed before the start of a cardiopulmonary detour by means of intravenously [20]. The Janus kinase/signal transducer and activator of transcription (JAK/STAT) signaling pathway is an intracellular pathway which accepts a key part in cell improvement, sur-

vival, and directing quality articulation [21, 22]. Upon phosphorylation by JAK/STAT, proteins translocate into the nucleus to muddle to the sponsor area of target genes and control their transcription. In the heart, STATs adjust the appearance of genes encoding proteins concerned in development, extracellular matrix composition, inflammation, apoptosis, and cellular signaling. In addition, JAK/STAT plays a serious role in the expansion of heart failure and cardiac hypertrophy [23]. Inhibition of JAK2 may offer a novel helpful methodology in the treatment of diabetic inconvenience in the vasculature of the STZ-actuated diabetic rats. JAK2 phosphorylation is a basic stage in the enhancement of diabetic vascular complexities [24]. Hyperglycemia is a key clinical indication of diabetes mellitus which has been found to expand the age of ROS [25].

Based on the above considerations, we proposed a speculation that PCr might have the defensive impact of diabetic cardiomyocytes against a dangerous effect of hyperglycemia by the regulation of heart mitochondrial respirometric states through the JAK2/STAT3 signaling pathway. Moreover, we supposed the therapeutic activity of PCr through reducing ROS subsequently decreasing apoptosis. What we are concerned with our test drug, PCr, could protect against DCM and whether it is related to the mitochondrial respiratory chain and signal conduction pathway. In any case, the issues of an inclusion of the JAK2/STAT3 pathway tweak in the defensive impacts of PCr against DCM have not been accounted yet after we have reviewed the cardioprotective effect of PCr in vivo and in vitro hyperglycemia-prompted concentration on its impact on the JAK2/STAT3 signaling pathway.

2. Materials and Methods

2.1. In Vivo Experimental Design

2.1.1. Animal.
In the present experiment, forty Wistar male rats (4~6 weeks old and 150~200 g) were used. The approval to conduct this study was granted by the ethical committee of human and animal research of the Dalian Medical University. The study was conducted in accordance with Guide for the Care and Use of Laboratory Animals [26]. The rats were kept in steady situations at room temperature (21~23°C) with a 12/12 light/dark cycle. After three weeks of adaptation, the rats were divided into four groups: (1) healthy rats, (2) diabetic rats, (3) diabetic rats injected with low-dose PCr (20 mM), and (4) diabetic rats injected with high-dose PCr (50 mM).

2.1.2. Induction of Diabetes.
STZ is a glucosamine-nitrosourea compound that shows particular cytotoxicity to pancreatic cells. It is utilized to actuate trial creature diabetes. Type 1 diabetes was instigated in Wistar male rats (4~6 weeks old and 150~200 g body/weight). The rats were given an intraperitoneal freshly prepared solution of STZ (80 mg/kg body weight) dissolved in sodium citrate buffer (0.1 M, pH 4.2; Sigma-Aldrich, USA). The rats were housed in a steadied domain kept up in the research center with a consistent temperature from the start of our examination. Accordingly, rats were divided into the following groups: (1)

control—nondiabetic rats simply accepting water, (2) STZ—diabetic rats that have been presented to STZ and given fresh water, (3) treatment-PCr—diabetic rats accepting low-dose PCr (20 mM) intravenously once daily over the span of the investigation, and (4) treatment-PCr—diabetic rats accepting high-dose PCr (50 mM) intravenously once daily for 12-week treatment over the span of the investigation. The measurement of fasting blood glucose was measured using a blood glucose meter (OneTouch UltraEasy, Edina, MN, USA) (centralization higher than 16.7 mmol/L).

2.1.3. Blood Glucose and Cardiac Marker Measurement. Fasting blood glucose (stately dependably at 08:00~9:00 AM) was estimated once in nondiabetic rats and watched weekly in all STZ group as well as treatment with the PCr group. We utilized exceptional needle prick to collect the blood from tail vessels. The last assurance of blood glucose was recorded utilizing glucose strips at a time going before the basic event (weekly) and alluded correspondingly to terminal glucose. Moreover, the myocardial catalyst markers such as malondialdehyde (MDA), superoxide dismutase (SOD), and glutathione (GSH) from tissues were estimated as indicated by the manufacturer's instructions (Nanjing Jiancheng Bioengineering Institute, China).

2.1.4. Tissue Accumulation and Histology. At the end of the analysis, the hearts of the rats were extracted and weighed, and we have taken a photograph of the heart size to evaluate the difference that happened in the estimation; after that, left ventricles were fixed in 4% supported paraformaldehyde and paraffin and separated. In each group, not less than 5 arbitrarily chosen areas were recolored with hematoxylin and eosin (H&E) according to the manufacturer's instructions and photographed using a light microscope (Nikon Eclipse TE2000-U, NIKON, Japan).

2.1.5. Immunofluorescence Staining. Tissue area slides were settled with 4% paraformaldehyde for 20 min at room temperature and after that flushed with PBS (phosphate-buffered saline) for 5 min and incubated in a permeabilization with 0.4% TritonX-100 for 10 min. The slides were washed with PBS three times for 5 min each time and then blocked with 15% bovine serum albumin (BSA) for 30 min in PBS, then washed three times with PBS and incubated with a p-STAT3 counteracting agent at 4°C overnight; after being washed with PBS three times for 10 min, fluorescein-conjugated secondary antibody was added in 1% solution of blocking and incubated for 1 h each. Subsequently, cell nuclei were stained with DAPI (1 μg/mL for 10 min). The samples were examined using a fluorescence microscope (CKX4, OLYMPUS, Japan).

2.1.6. TUNEL Assay. The measurement of in vivo apoptotic cell death was performed using TUNEL assay as indicated according to the manufacturer's instructions (Roche, Germany). DAPI was incorporated in the unit, as DNA pieces could be stained by TUNEL particularly and delivered green fluorescence. Quickly, tissue sections were settled with 4% paraformaldehyde at room temperature and afterwards were washed with PBS for 5 min and hatched in permeabilization with 0.4% TritonX-100 for 10 min and washed with PBS three times. The TUNEL response blend was included, and the samples were incubated with CO_2 at 37°C for 1 h. The sections were stained with 1 μg/mL DAPI for 10 min. The apoptotic rate was demonstrated by TUNEL-positive cell number against the aggregate cell number with DAPI under a fluorescence microscope (CKX4, OLYMPUS, Japan).

2.1.7. High-Resolution Respirometry. Oxygen consumption was estimated by high-resolution respirometry utilizing Oxygraph 2k (Oroboros Instruments GmbH, Innsbruck, Austria) according to the manufacturer's instructions [27]. All substrates and inhibitors were included as portrayed in Figure 1. Investigations utilizing heart tissue homogenate and isolated heart mitochondria were performed in MiR05 (110 mM sucrose, 60 mM K-lactobionate, 0.5 mM EGTA, 3 mM ($MgCl_2$), 20 mM taurine, 10 mM (KH_2PO_4), 20 mM (HEPES), and 1 g/L BSA pH 7.1). Data were dissected using Oroboros DatLab 5.1 software. O2k instruments (two chambers) were used. All the investigations were performed at 37°C.

2.1.8. Isolation of Cardiac Mitochondria. Rats were anesthetised by intraperitoneal infusion of thiopental (0.1 g/kg). Heart tissue for each group was homogenized gently, and heart mitochondria were separated from the treated group and diabetes rats individually. Mitochondria were isolated according to the standard protocol [28]. With a little alteration, the left ventricle was quickly removed from euthanized rats [2.5 mg/g wet weight (heart)]. Then it was immediately placed in small volume of ice-cold isolation solution (containing 250 mM sucrose, 2 mM EDTA, 10 mM Tris, and 1 g/L BSA, pH 7.4) and was cut into small pieces with scissors and left together with 10 mL of isolation solution with the addition of dispase II (Sigma-Aldrich, D 4693). Then, the pieces of the heart were transferred to a teflon/glass homogenizer and homogenized gently for 2~3 min. After centrifugation of the homogenized sample at 800× g for 10 min at 4°C, the protease containing supernatant with a part of mitochondria which were in a direct contact with the protease was centrifuged at 4800× g for 10 min, at 4°C. Then, the pellet was resuspended in the same volume of isolation solution, but without protease, and was again homogenized and spun down at 4800× g for 10 min at 4°C. The last centrifugation of the pellet was done at the same conditions as described above. Finally, the pellet containing mitochondria was again resuspended in the ice-cold isolation solution (buffer, pH 7.4). Mitochondrial protein content was determined by the bicinchoninic acid (BCA) (Bio-Rad, Hercules, CA, USA). The respiration of isolated mitochondria from rat heart and heart tissue homogenate were determined using substrate-uncoupler inhibitor titration (SUIT) protocols with modifications, then transferred to mitochondrial respiration medium (MiR05) [0.5 mM EGTA, 3 mM $MgCl_2$, 60 mM K-lactobionate, 20 mM taurine, 10 mM KH_2PO_4, 20 mM HEPES, 110 mM D-sucrose, and 1 g/L BSA (Sigma-Aldrich; A3803) changed in accordance with pH 7.1]. The following are used: pyruvate (P) (5 mM), glutamate (G) (10 mM), and malate (M) (2 mM), which were first added as substrates for

(a)

(b)

(c)

(d)

(e)

(f)

(g)

(h)
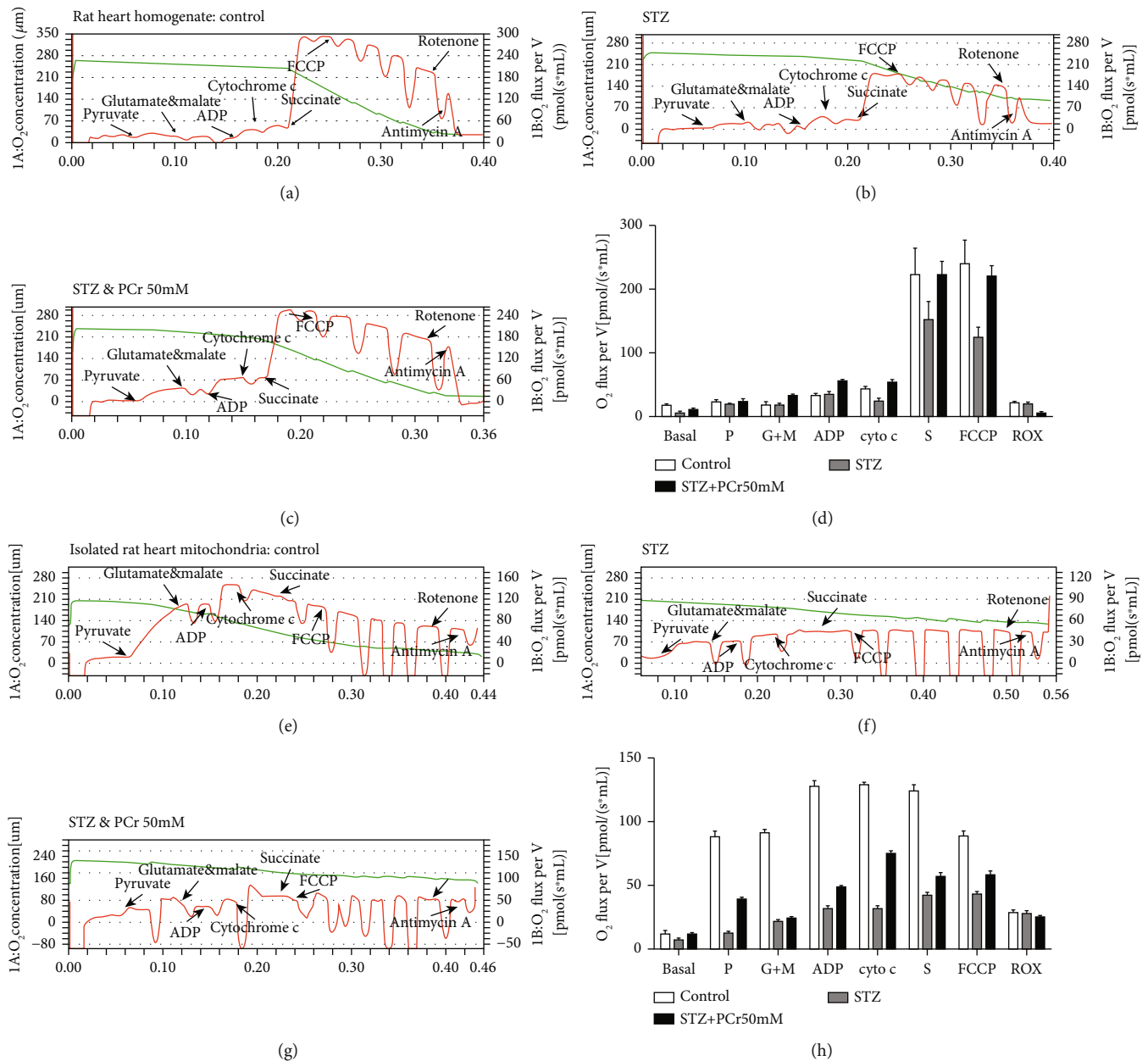
FIGURE 1: Mitochondrial respiration in heart tissue homogenate and isolated heart mitochondria of rats. (a) Healthy heart rat tissue homogenate and the mitochondrial respiration were detected using Oxygraph-2k. Red lines indicate the oxygen consumption rate in response to sequential loading of mitochondrial effectors (indicated by arrows above the graphs). (b) STZ group. (c) The treatment group with PCr (50 mM). (d) Quantitative examinations of oxygen utilization rate in light of effectors. Correlations were performed utilizing data lab programming. (e) Isolated heart mitochondria from healthy rats. (f) STZ group. (g) The treatment group with PCr (50 mM). (h) Quantitative examinations of oxygen utilization rate in light of effectors. The following are added: P: pyruvate (5 mM); G: glutamate (10 mM); M: malate (2 mM); ADP: adenosine diphosphate (5 mM); Cyt C: cytochrome c (10 μM); S: succinate (10 mM); FCCP (0.5 μM steps); rotenone (0.5 μM); antimycin A (2.5 μM). Data are displayed as the mean ± SE (n = 3 per group), and comparisons were performed using DatLab software.

mitochondrial respiration; adenosine diphosphate (ADP) (5 mM) was added to induce state 3 respiration; Cyt C (cytochrome c) (10 μM) was added to test the integrity of the outer mitochondrial membrane; succinate (S) (10 mM) was added for electron transfer to complex II; then FCCP (0.5 μM steps), a mitochondrial respiration uncoupler, was added to obtain maximal oxygen consumption rate; rotenone (0.5 μM) was added to inhibit complex I; antimycin A (2.5 μM) to inhibit complex III was added for the determination of residual oxygen consumption (ROX).

2.1.9. Protein Extraction and Western Blot Analysis. Heart tissue homogenate was lysed. The proteins were separated on (10~ 15%) sodium dodecyl sulfate-polyacrylamide gel

electrophoresis (SDS-PAGE) and then electrically transferred onto a polyvinylidene difluoride (PVDF) membrane. The protein concentrations of the samples were determined by BCA. The membranes were visualized using enhanced chemiluminescence reagent with LabWorks software (UVP, Upland, CA, USA). The analogous experiments were performed at least three times.

2.2. In Vitro Experimental Design

2.2.1. Cell Culture and Treatment.
H9C2 cardiomyoblast was bought from the Organization of Natural Chemistry Cell Biology (Shanghai, China). Phosphocreatine (PCr) was bought from Harbin Laiboten Pharmaceutical Co., Ltd. Methylglyoxal (MGO), 3-(4,5-dimethylthiazol-2-yl)-2,5-diphenyltetrazolium bromide (MTT), streptomycin, and penicillin were obtained from Sigma-Aldrich (St. Louis, MO, USA). The MDA, SOD, and GSH kits were acquired from Nanjing Jiancheng Bioengineering Institute (Nanjing, China). 5,58,6,68-Tetraethyl benzimidazol carbocyanine iodide (JC-1) were purchased from Fanbo Biochemicals. $2'$,$7'$-Dichlorodihydrofluorescein diacetate (DCFH-DA) was acquired from Beyotime (Jiangsu, China). The antibodies such as JAK2, STAT3, anti-phospho-STAT3, and anti-phospho-JAK2 were obtained from Bioworld Technology (USA). Anti-Bax, anti-Bcl-2, anti-caspase 3, anti-caspase 9, cytochrome c (mitochondria), lamin B1, and β-actin were obtained from Proteintech Group, Inc. (Chicago, IL, USA). In the present study, we utilized Dulbecco's modified Eagle medium (DMEM) which contains 10% fetal bovine serum (FBS), 100 U/mL of penicillin, and 100 U/mL of streptomycin. H9C2 cells were cultured and treated with different concentrations (5~40 mM) of PCr and then incubated with CO_2 at 37°C. PCr-pretreated cells were gradually stimulated with MGO (0.2~1.2 mM). Furthermore, a solution of different concentrations of PCr was diluted with DMEM to give a final concentration of 20 mM. PCr concentration was subjected to a test to identify the toxic effect. Also, the final concentration of MGO was 1 mM. For high-resolution respirometry and O2k-Fluorometry, all the materials such as pyruvate, glutamate, malate, succinate, cytochrome c, rotenone, oligomycin, FCCP, digitonin, antimycin A, and ADP were obtained from Sigma-Aldrich. All the reagents and solvents used in this study were of the highest analytical reagent grade.

2.2.2. MTT Assay.
The H9C2 cells were plated in 96-well plates for 24 h at a density of 1×10^6 cells/mL and treated with different concentrations of PCr (5~20 mM) and N-acetyl cysteine (NAC) (2 mM) for 2 h, then stimulated for 24 h with MGO (1 mM). The reasonability of cells was evaluated by the MTT method. Additionally, for morphological appearance examination, the cells were plated in 6-well plates and pretreated with or without PCr (5~20 mM) and NAC (2 mM) for 2 h, individually, then stimulated with MGO (1 mM) for 24 h. The images were obtained by using an inverted microscope (Nikon, Japan).

2.2.3. DAPI Staining.
The H9C2 cells (1×10^6 cells/mL) were seeded in 6-well plates and incubated at 37°C for 24 h. Then, the cells were treated with PCr (5~20 mM) or NAC (2 mM) concentrations of test compounds for 2 h, then stimulated with MGO (1 mM) for 24 h. Once the incubation time was done, the cells were washed two times with PBS (phosphate-buffered saline). The cells were stained with DAPI (1 μg/mL) diluted in asepsis water. The pictures were evaluated by a fluorescence microscope (OLYMPUS, Japan).

2.2.4. Detection of Cell Apoptosis.
After the indicated treatments, the treated H9C2 cells were harvested, washed three times with ice-cold PBS, and assessed for apoptosis using an Annexin V-fluorescein isothiocyanate (FITC) and propidium iodide (PI) double staining kit according to the manufacturer's instructions (Nanjing KeyGen Biotech. Co. Ltd., Nanjing, China). The percentages of apoptotic cells were investigated by flow cytometry (Becton Dickinson, USA).

2.2.5. Detection of Mitochondrial Membrane Potential.
The H9C2 cells (1×10^6 cells/mL) were seeded overnight in 6-well plates and pretreated for 2 h with and without PCr (5~20 mM) individually, then stimulated with MGO (1 mM) for 24 h. The cells were flushed with the DMEM, incubated with JC-1 (10 μg/mL) for 15 min at 37°C. After that, cells were washed two times with PBS. The samples were measured using a fluorescence microscope (CKX4, OLYMPUS, Japan).

2.2.6. Determination of Cellular Respiration.
Oxygen consumption was estimated by high-resolution respirometry utilizing Oxygraph 2k (Oroboros Instruments GmbH, Innsbruck, Austria) according to the manufacturer's instructions. The H9C2 cells (1×10^6 cells/mL) were seeded overnight in 6-well plates and pretreated for 2 h with and without PCr (20 mM) individually, then stimulated with MGO (1 mM) for 24 h; after the incubation time, the cells were harvested and loaded with MiR05 in addition to 1 mg/mL cells suspended in 2.2 mL warm MiR05 and moved to chambers in the O2K. The following are used: digitonin (8.1 μM, 10 μg/10^6 cells) to permeabilize the plasma membranes completely only affecting mitochondrial membranes at higher concentrations, pyruvate (P) (5 mM), glutamate (G) (10 mM), and malate (M) (2 mM) which were first added as substrates for mitochondrial respiration; adenosine diphosphate (ADP) (5 mM) which was added to induce state 3 respiration; succinate (S) (10 mM) which was added for electron transfer to complex II; FCCP (0.5 μM steps), a mitochondrial respiration uncoupler, which was added to obtain maximal oxygen consumption rate; rotenone (0.5 μM) which was added to inhibit complex I; and antimycin A (2.5 μM) to inhibit complex III added for the determination of residual oxygen consumption (ROX). Additionally, the intact H9C2 cells (1×10^6 cells/mL) were seeded overnight in 6-well plates and pretreated with and without PCr 20 mM individually for 2 h, then stimulated with MGO (1 mM) for 24 h. The cells were harvested and loaded with DMEM, then moved to chambers in the O2K. The following are used: after adjustment of ROUTINE respiration, the ATP-synthase inhibitor oligomycin (2.5 μM) added to get a measure of LEAK respiration, then FCCP (0.5 μM steps); rotenone (0.5 μM); and antimycin A (2.5 μM) added for the determination of

residual oxygen consumption (ROX). All the investigations were performed at 37°C.

2.2.7. Detection of Intracellular ROS Production. The H9C2 cells (1×10^6 cells/mL) were seeded overnight in 6-well plates and pretreated with and without PCr (20 mM) individually for 2 h, then stimulated with MGO (1 mM) for 24 h. The cells were gathered and after that stacked with 500 μL of DCFH diacetate (10 mM) at 37°C for 20 min, subsequent to washing twice with PBS. The samples were investigated by flow cytometry (Becton Dickinson, USA).

2.2.8. Immunofluorescence Staining. The effect of PCr on the nuclear translocation of p-STAT3 was examined by immunofluorescence staining. For the immunofluorescence staining of p-STAT3, the formalin-fixed H9C2 cells were incubated with anti-p-STAT3 antibodies overnight at 4°C. Then, after being washed with PBS three times for 10 min, the fluorescein-conjugated secondary antibody was added in 1% blocking solutions and incubated for 1 h. Subsequently, cell nuclei were stained with DAPI (1 μg/mL for 10 min). The samples were examined using a fluorescence microscope (CKX4, OLYMPUS, Japan).

2.2.9. Protein Extraction and Western Blot Analysis. The H9C2 cells (1×10^6 cells/ml) were cultured in 6-well plates and pretreated with PCr (5~20 mM) for 2 h, respectively, then stimulated with MGO (1 mM) for 24 h. Total cytosolic proteins were extracted with a cold lysis buffer (100 μM PMSF) for 10 min on ice; then the mixtures were centrifuged at $12000 \times g$ for 15 min at 4°C, and the supernatant was collected. Proteins were separated using SDS-PAGE and then electrically transferred onto a polyvinylidene difluoride (PVDF) membrane. The protein concentrations of the samples were determined by BCA. The membranes were visualized using enhanced chemiluminescence reagent with LabWorks software (UVP, Upland, CA, USA). The analogous experiments were performed at least three times.

2.3. Statistical Analysis. Data were analyzed using GraphPad Prism 5 (Graph Pad Software, Inc., San Diego, CA) and expressed as the mean and standard deviation. Statistical evaluations of post hoc multiple group comparisons were conducted using one-way ANOVA. A Bonferroni test was used for statistical analysis. P value < 0.05 was considered statistically significant.

3. Results

3.1. In Vivo Experiments

3.1.1. PCr Lightens Histopathologic Changes in the Myocardium of DCM. Heart weight was higher in diabetic rats than control and treated rats as shown in (Figure 2(a)). Also, we confirmed our result using western blot for ANP and BNP as shown in (Figures 2(g)–2(i)). Additionally, H&E staining as shown in (Figure 2(b)) was performed to illuminate the impact of PCr on the histopathologic changes in the myocardium. It was resolved that the cardiomyocytes were obviously striated and routinely showed in the control

rats, while confused and central rot cells were exhibited in the STZ rats. This was enhanced after treatment with the low and high portion of PCr. Surely, the histopathologic changes in the high portion PCr assemble enhanced to a more noteworthy degree than the low portion in the treatment gathered with PCr, demonstrating that PCr offers a defensive impact against the DCM.

3.1.2. Effects of PCr on Blood Glucose. Blood glucose, water charge, and sustenance utilization body weight (72 h after STZ infusion) of the rats extraordinarily expanded, and the rats additionally showed traditional side effects of diabetes, including expanded water charge and nourishment utilization and polyuria. High glucose builds the osmotic weight of the pee because of expanded liquid misfortune, causing drying out and expanded thirst; the body cannot make full utilization of glucose because of insulin inadequacy, which prompts absence of vitality and results in polyphagia for the whole investigation. The outcomes demonstrated that PCr had an impact on blood glucose or nourishment utilization of the rats; i.e., PCr treatment diminished blood glucose level essentially as shown in Figure 2(c), compared with the diabetes group. Moreover, the body weights (BWs) of rats in the diabetic group were lower than those in the control group, while BWs were higher in diabetic rats with PCr treatment compared with the diabetes group.

3.1.3. Effects of PCr on Myocardial Markers. The antioxidant activities of PCr were determined by MDA, SOD, and GSH assays using ELISA technique as shown in Figures 2(d)–2(f). These reflect the release of MDA, which was inhibited under the influence of PCr in the treated groups when compared with the STZ group, while SOD and GSH release was diminished in the STZ group when compared with the PCr-treated groups. This indicates that PCr has an antioxidant capacity.

3.1.4. PCr Enhances Mitochondrial Respiration in Isolated Heart Mitochondria and Tissue Homogenate. PCr has a substrate-autonomous enhancement in the respiratory capacity as exhibited by the expansion in every respiratory parameter (state 2, OXPHOS, state 4, and electron transport system (ETS)). In fact, incitement of respiration was watched for complex I and complex II substrates, pyruvate, glutamate, malate, and succinate, individually. The integrity of the mitochondrial layer was evaluated in those examinations by including cytochrome c. In our grasp, the outcomes demonstrated that PCr enhanced ADP-animated respiration, as shown in Figures 1(c) and 1(g), by an expansion in OXPHOS for the two substrates, most presumably by filling in as an extra wellspring of electrons for the ETS similar to the control group. Additionally, PCr expanded OXPHOS in mitochondria empowered with pyruvate, glutamate, and malate. The mitochondria were stimulated with succinate, and its ETS was enhanced compared to the STZ group. A comparable inclination is seen in Figures 1(a), 1(b), 1(e), and 1(f). A comparable result was seen in the group treated with PCr (Figures 1(c) and 1(g)). Additionally, quantitative
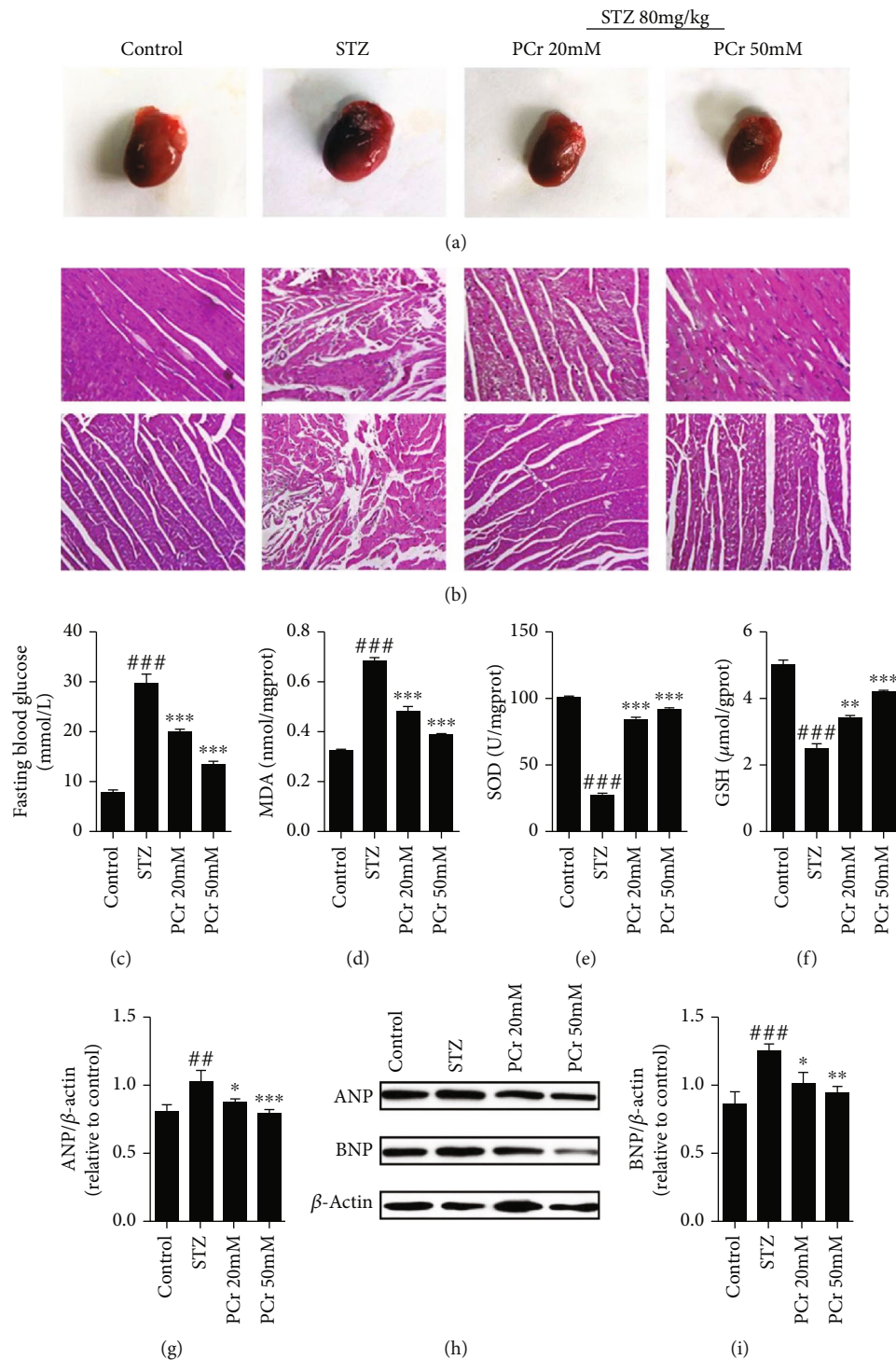
FIGURE 2: PCr decreased pathological changes in diabetic hearts. (a) Effects of PCr on heart size were reduced significantly in treated groups than the diabetic group. (b) Hematoxylin and eosin (H&E) staining of the heart tissue showed that PCr improved the striation of myocardial fibers arranged regularly in treated groups. (c) Effects of PCr on blood glucose levels were reduced remarkably in the treated groups than the STZ group. (d) Effects of PCr on myocardial and antioxidative enzyme activities: MDA level was decreased significantly in the PCr group than in the diabetic group; (e, f) SOD and GSH were increased in treated groups compared with diabetic groups indicating the antioxidant capacity agent was endangered in the diabetic myocardium. (g, h, i) Western blot investigation of atrial natriuretic peptide (ANP) and brain natriuretic peptide (BNP). Data are introduced as the mean ± SD ($n = 3$). $^{###}P < 0.01$ vs. control; $^{**}P < 0.01$ and $^{***}P < 0.01$ vs. the STZ group.

examinations of oxygen respiration rate in light of effectors are shown in Figures 1(d) and 1(h).

3.1.5. PCr Modulation on a JAK2/STAT3 Signaling Pathway.
p-STAT3 phosphorylation in STZ assemble was expanded. PCr pretreatment specifically reversed the expanded phosphorylation of p-STAT3 in a dose-dependent manner. The immunofluorescence investigation demonstrated that p-STAT3 nuclear translocation was restrained by PCr as shown in Figure 3(a). Moreover, our results demonstrated that the protein expression of p-STAT3 was essentially expanded in a rat's myocardium after STZ infusion, while PCr treatment further diminished the declaration of p-STAT3 (Figures 3(b)–3(d)). A comparable propensity was seen in the protein expression of p-JAK. The outcomes showed that the mitochondrial pathway of apoptosis may be engaged with the pathogenesis of diabetic cardiomyopathy.

3.1.6. Effects of PCr on STZ-Actuated Apoptosis in DCM.
Apoptosis actuated by STZ rats was identified utilizing TUNEL recoloring which demonstrated that STZ groups have fundamentally expanded apoptosis. Our results demonstrated that pretreatment with PCr essentially reversed the expanded apoptosis by decreasing the TUNEL-positive cells as shown in Figures 4(a) and 4(b). Furthermore, the impact of PCr on apoptosis identified with Bcl-2 family in diabetic rat hearts was examined by western blot investigation. Bcl-2 protein level was diminished, and Bax level was expanded in diabetic rats. The expression of Bcl-2 was increased, and Bax was decreased in the PCr group (Figure 4(c)). Results demonstrated that the protein expressions of caspase 3 and caspase 9 were fundamentally diminished in a rat's myocardium after STZ infusion, while being expanded after PCr treatment. Moreover, the cleaved caspase 3 and cleaved caspase 9 were altogether expanded in a rat's myocardium after STZ infusion, while being diminished after PCr treatment (Figures 4(c)–4(j)). Likewise, cytochrome c (mitochondria) was diminished in a rat's myocardium after STZ infusion while being expanded after PCr treatment. The results have shown that the mitochondrial pathway of apoptosis may be engaged with the pathogenesis of diabetic cardiomyopathy.

3.2. In Vitro Experiments

3.2.1. PCr Lessened MGO-Incited Cell Damage in H9C2 Cells.
First of all, the chemical structure of phosphocreatine is shown in Figure 5(a). Then the cell viability test of H9C2 cell line was performed as shown in Figures 5(d)–5(f). The results indicated that PCr at different concentrations (5~40 mM) has no lethality on normal H9C2 cells. Additionally, PCr has shown protective effects on the same cell-induced injury with MGO. H9C2 cell injury was done by gradual exposure to different concentrations of MGO (0.2~1.2 mM) to induce the hyperglycemia. PCr was found to provide a significant protective effect in H9C2 cells injured by exposure to MGO.

3.2.2. Improvement of Morphological Changes by PCr.
As appeared in (Figure 5(b)), pretreatment with PCr for 2 h fundamentally reestablished the morphological changes of

H9C2 cells including nuclear pyknosis. Through DAPI fluorescent recoloring, changes in apoptotic cells were watched. Pretreatment with PCr for 2 h portion conditionally stifled apoptosis in H9C2, as shown in (Figure 5(c)).

3.2.3. PCr Inhibits MGO-Induced Apoptosis.
The apoptosis induced by MGO in H9C2 cells was obstructed by PCr as shown in Figures 6(a) and 6(b); it demonstrated that PCr has a defensive impact that diminished apoptosis in early and late apoptosis, showing that the concealment of apoptotic cells was diminished by PCr in a dose-dependent manner. This impact had been researched with Annexin V-FITC and PI double recoloring and was performed by utilizing flow cytometry investigation.

3.2.4. Effects of PCr on the Expression of Proteins Associated with DCM.
The impacts of PCr on apoptosis-related Bcl-2 family and the JAK2/STAT3 pathway actuated by MGO were studied by western blot investigation. Bcl-2 protein level was diminished, and Bax level was expanded in the MGO group, bringing about a higher distinction, contrasting in the treatment groups. Additionally, cytochrome c (mitochondria) was diminished in the MGO group while being expanded after PCr treatment. The outcomes have shown that the mitochondrial pathway of apoptosis may be associated with the pathogenesis of DCM. PCr treatment fundamentally expanded Bcl-2 expression and diminished Bax expression (Figures 6(c)–6(i)). Results demonstrated that the protein expression of p-JAK was essentially expanded in the MGO-instigated group, while PCr treatment further diminished the outflow of p-JAK. A comparable propensity was seen in the protein expression of p-STAT3 (Figures 6(c), 6(j), and 6(k)).

3.2.5. PCr Improves Mitochondrial Respiration.
In an ordinary cell culture, mitochondrion gives the greater part of the vitality produced under typical conditions. The generation of energy in mitochondria can be estimated by mitochondrial oxidative phosphorylation limit (oxygen flux or oxygen consumption rate (OCR)) and oxygen concentration (Figures 7(a) and 7(e)). OCR was assessed utilizing high-goal respirometry. After a standard OCR was recorded, oligomycin was included and the oligomycin safe respiration rate or nonphosphorylating respiration was resolved. Maximal respiratory capacity (MRC) alludes to the most extreme animated respiration of the electron transport chain (ETC) (complex I~V incorporated movement) by FCCP. The control group had higher OCR of basal, hole, and FCCP than the MGO-actuated damage group as shown in Figures 7(b) and 7(f). Nevertheless, the PCr pretreatment had higher OCR essentially extraordinary in contrast with the MGO group. Also, the coupling proficiency was like the control (Figures 7(a) and 7(c)). The rate of oligomycin-safe respiration is frequently optional to proton leak, while in the ATP blend, proton leak also impacts substrate oxidation on the baseline OCR. Undoubtedly, our result indicated that oligomycin-safe OCR in the MGO group was significantly lower compared with that in the control group and the PCr pretreatment group showed significantly increased OCR

(a)

(b) (c) (d)
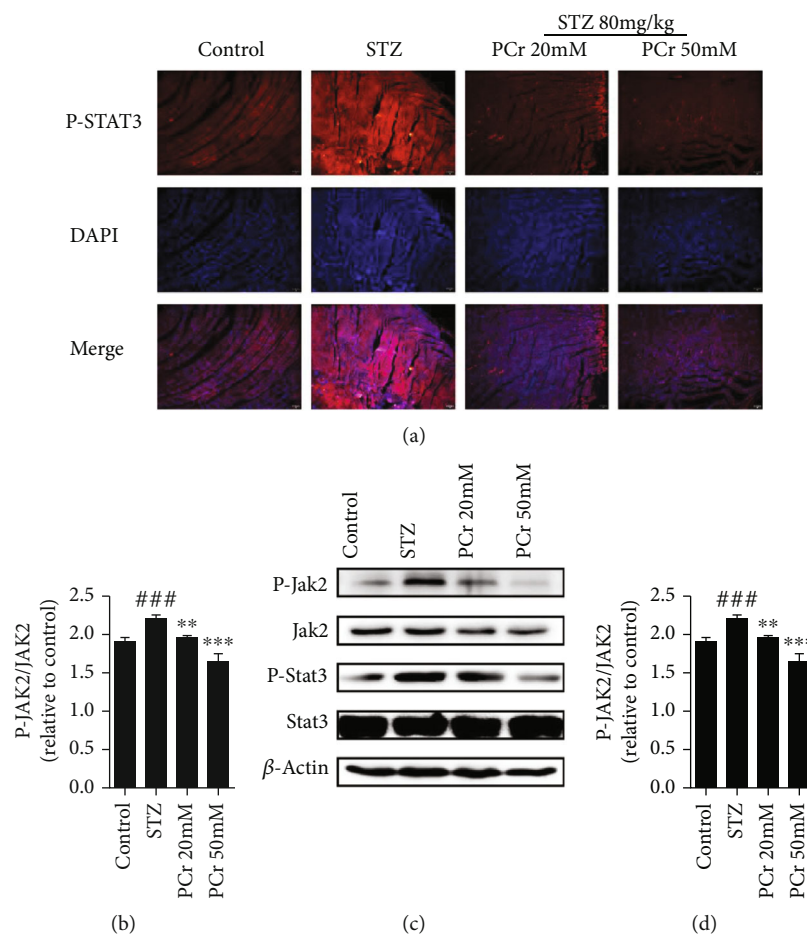
FIGURE 3: PCr modulation on the JAK2/STAT3 signaling pathway. (a) Effects of PCr on p-STAT3 translocation in ordinary and STZ conditions (original magnification 200). (b, c, d) Effects of PCr on the declaration of p-JAK2, JAK2, p-STAT3, and STAT3 in STZ and treatment as well as healthy rats ($n = 3$). Qualities are expressed as the mean ± SEM. $^{\#\#}P < 0.001$ and $^{\#\#\#}P < 0.005$ *vs.* the control group. $^{**}P < 0.01$ and $^{***}P < 0.001$ *vs.* the STZ group.

compared with the MGO group. It was recommended that there was an expansion in ATP combination by complex V in these cells. Recommending there was an expansion in ATP combination by complex V in these cells. Besides, the proof in help of expanded mitochondrial capacity can be found in the reality the save control group and PCr group likewise had higher ETC than MGO amass recommending that MGO group capacity closer to their bioenergetics potential at instrument when looked with expanding needs was not ready to enlarge vitality creation. Overall, this information recommends that PCr demonstrations fortify mitochondrial and oxidative limit. Likewise, in permeabilization of H9C2 cells, PCr possessed a substrate-autonomous enhancement in the respiratory capacity as shown by the expansion in every single respiratory parameter (state 2, OXPHOS, state 4, and ETS) in both control and treated groups with PCr (Figures 7(e) and 7(g)). The incitement of respiration was observed for complex I and complex II substrates, i.e., pyruvate, glutamate, malate, and succinate, separately. PCr enhanced ADP-animated respiration, as shown by an expansion in OXPHOS for the two substrates, most likely by filling in as an extra wellspring of electrons for the ETS. Similar to

the control group, PCr expanded OXPHOS in mitochondria empowered with pyruvate, glutamate, and malate. The mitochondria were invigorated with succinate contrasted with the MGO-actuated group. Also, a comparable propensity was seen in both intact and permeabilized H9C2 cells as shown in Figures 7(d) and 7(h).

3.2.6. Improvement of Mitochondrial Membrane Permeability ($\Delta\Psi m$) by PCr on the MGO-Harmed H9C2 Cells. We assessed MMP utilizing the JC-1 test to test the counter apoptotic impacts of PCr (Figures 8(c) and 8(d)). Suitable cells were shown with red fluorescence, implying a high MMP while apoptotic cells show green fluorescence implying a low MMP ($\Delta\psi m$). After the H9C2 cells applied with MGO for 24 h, MMP was depolarized in MGO-treated cells as shown by the increase in green fluorescence, while pretreatment of PCr kept the condition in $\Delta\psi m$ as shown by the decrease in red fluorescence.

3.2.7. Suppression of Intracellular ROS Generation. To analyze whether the expanded oxidative pressure is related to MGO-prompted apoptosis in H9C2, flow cytometry

(a)

(b)

(c)

(d)

(e)

(f)

(g)

(h)

(i)

(j)
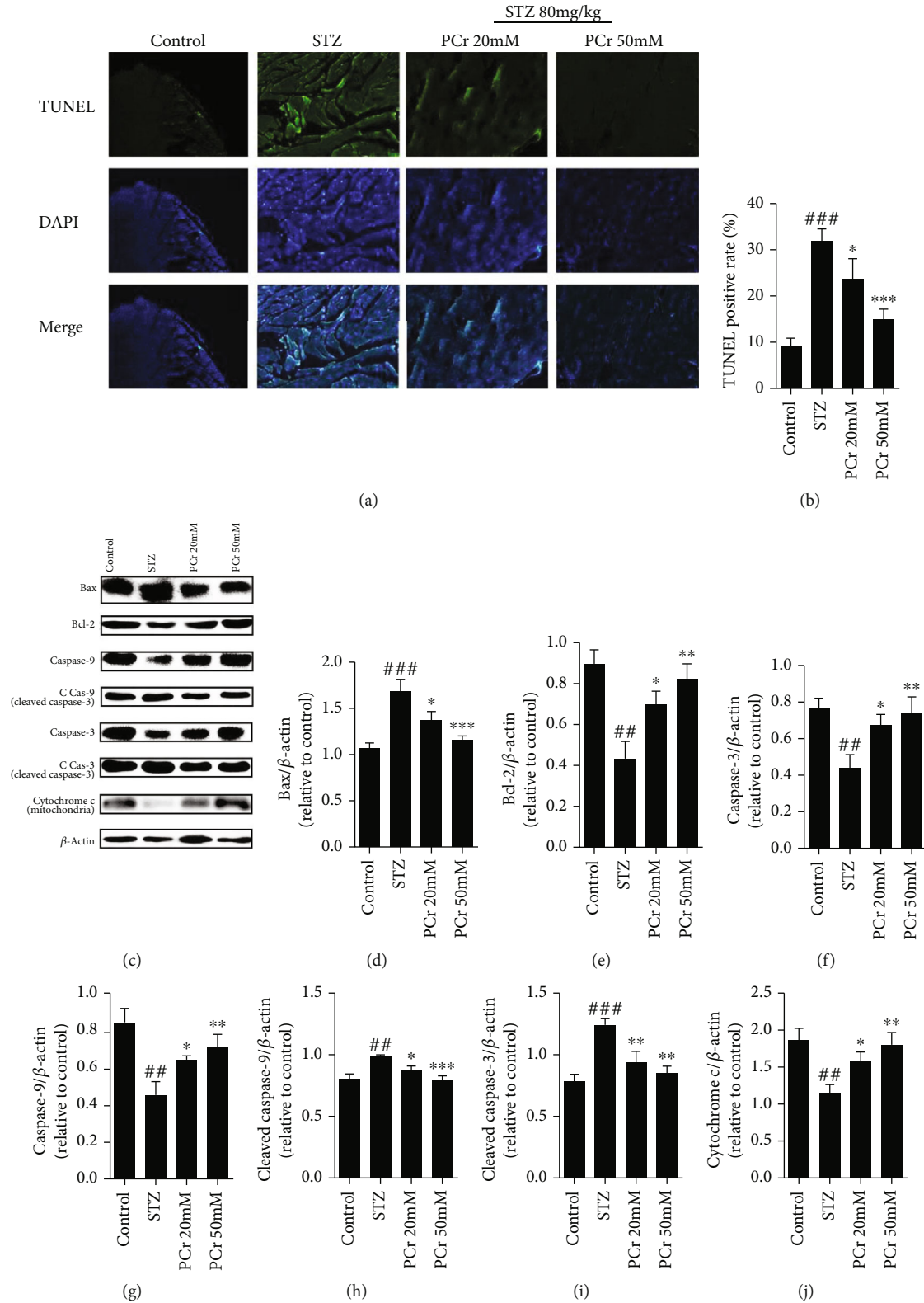
FIGURE 4: Effects of PCr on STZ-instigated apoptosis in DCM. (a) The TUNEL and DAPI recoloring on the myocardium. The nuclei of TUNEL-positive cells are shown utilizing green fluorescence. (b) Quantification of TUNEL-positive cells. (c) The protein dimensions of Bcl-2, Bax, caspase 3, caspase 9, cleaved caspase 3, cleaved caspase 9, and cytochrome c (mitochondria) were recognized by western blot in tissue homogenate. (d, e, f, g, h, i) Quantifications of western blot. Data are exhibited as the mean ± SD ($n = 3$). $^{##}P < 0.05$ and $^{###}P < 0.01$ vs. the control group. $^{*}P < 0.05$, $^{**}P < 0.01$, and $^{***}P < 0.01$ vs. the STZ group.

(a)

(b)

MGO (mM)	0	1	1	1	1	1
PCr (mM)	0	0	5	10	20	0
NAC (mM)	0	0	0	0	0	2

(c)

MGO (mM)	0	0.2	0.4	0.6	0.8	1.0	1.2
PCr (mM)	0	0	0	0	0	0	0
NAC (mM)	0	0	0	0	0	0	0

(d)

MGO (mM)	0	1	1	1	1	1
PCr (mM)	0	0	5	10	20	0
NAC (mM)	0	0	0	0	0	2

(e)

MGO (mM)	0	0	0	0	0
PCr (mM)	0	5	10	20	40
NAC (mM)	0	0	0	0	0

(f)
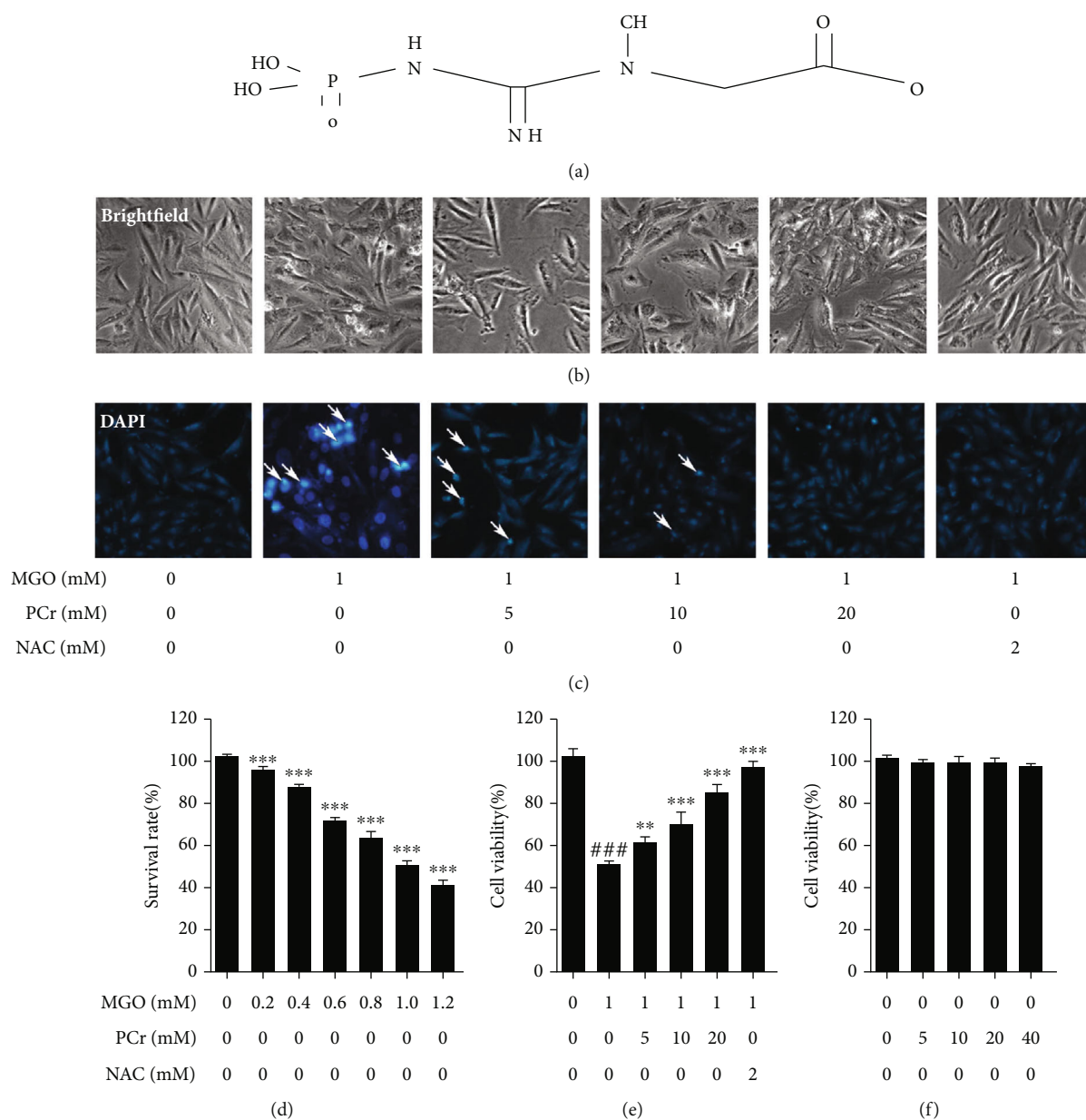
FIGURE 5: Protective impacts of PCr against MGO-actuated damage and apoptosis in H9C2 cells. (a) Chemical structure of phosphocreatine. (b) Effect of pretreatment with PCr (5~20 mM) for 2 h, on the cell morphology and structure of H9C2 cells by bright image (100x magnification) examination. (c) The apoptosis occurrences of H9C2 were stained by DAPI observed by fluorescence images for (200x final magnification). (d) MGO-induced toxicity (0.2~1.2 mM) on H9C2 cell. (e) Effect of PCr (5~20 mM) on induced MGO H9C2. (f) Cytotoxicity of PCr on H9C2 cells. The effects of PCr on the loss of cell practicality, initiated by MGO. Data are displayed as the mean ± SD ($n = 3$). $^{\#\#\#}P < 0.05$ vs. the control group. $^{**}P < 0.05$ and $^{***}P < 0.01$ vs. the MGO group.

examination by DCFH-DA recoloring was affirmed (Figures 8(a) and 8(b)). The H9C2 cells with MGO (1 mM) for 24 h notably caused ROS generation compared with control, while treatment with PCr for 2 h conditionally smothered ROS creation in the H9C2 cells.

3.2.8. Modulation of PCr on the p-STAT3 Pathway in H9C2 Cells. We have analyzed the phosphorylated and aggregate expression dimension of p-STAT3, after being treated with PCr in H9C2 cells initiated by MGO using immunofluorescence recoloring and western blot. As shown in Figure 9(a),

the pretreatment with PCr (10 and 20 mM) for 2 h essentially diminished the nuclear translocation of p-STAT3. In Figure 9(a), p-STAT3 was dominatingly situated in the cytoplasm of H9C2 cells in the model group. What is more, the fluorescence force of the nuclear p-STAT3 was diminished essentially in a dose-dependet manner after PCr treatment individually; in contrast with the model group, as shown in Figure 9(a), pretreatment of PCr (20 mM) clearly is reliable with the outcome that the nuclear p-STAT3 levels were diminished in the cytoplasm by western blot test as shown in Figures 9(b) and 9(c).

(a)   (b)

(c)   (d)   (e)   (f)

(g)   (h)   (i)   (j)   (k)
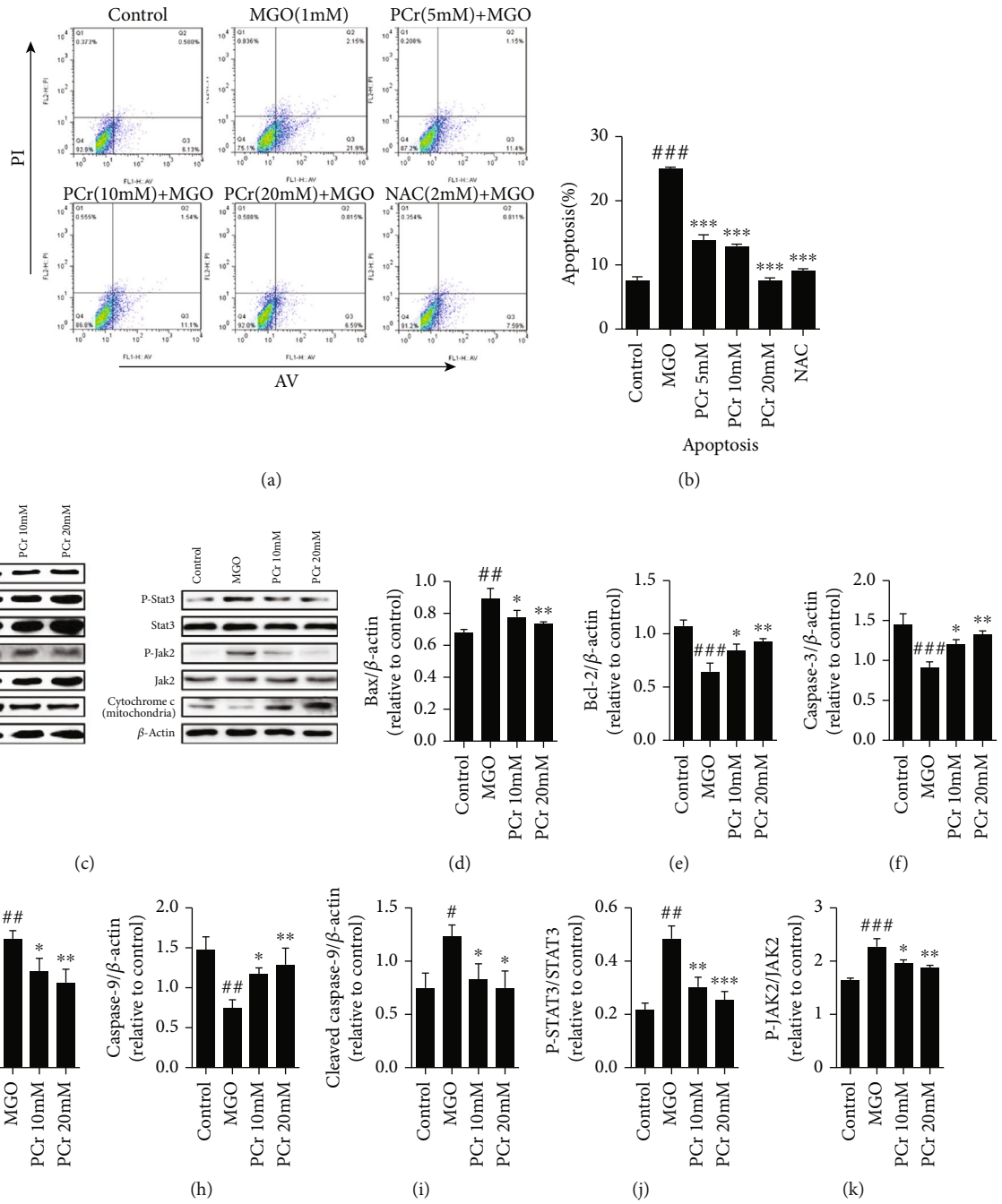
FIGURE 6: PCr inhibits MGO-induced apoptosis by modulating Bax, Bcl-2, caspase 3, caspase 9, cleaved caspase 3, cleaved caspase 9, and cytochrome c (mitochondria) in H9C2 cells. (a) Cells were treated with PCr (5~20 mM) for 2 h preceding being presented to 1 mM MGO for 24 h. Cell apoptosis was estimated by flow cytometry. (b) Apoptotic cells represent the percentage of Annexin V single positive and Annexin V/PI twofold positive cells. (c) The protein dimensions of Bcl-2, Bax, caspase 3, caspase 9, cleaved caspase 3, cleaved caspase 9, and cytochrome c (mitochondria) were recognized by western blot in cells. (d, e, f, g, h, i, j, k) Quantifications of western blot. Data are exhibited as the mean ± SD ($n = 3$). $^{\#\#\#}P < 0.05$, $^{\#\#}P < 0.01$, and $^{\#}P < 0.05$ vs. the control group. $^{*}P < 0.05$, $^{**}P < 0.01$, and $^{***}P < 0.05$ vs. the MGO group.

4. Discussion

DCM, one of the most severe cardiovascular complications, can cause cardiac dysfunction in diabetic patients [29]. DCM is characterized with cardiac functional and structural changes, such as cardiac hypertrophy, oxidative stress, apoptosis, and myocardial interstitial fibrosis, which are the principal features of DCM [1, 30, 31]. Our histopathological study has shown markedly structural changes such as abnormal striation in myocardium tissue in the untreated group compared with the treated group, with a clear improvement of the myocardium striation as well as a reduction of heart size in treated groups, indicating that PCr is a novel therapeutic choice against the major features of DCM, while the

(a)

(b)

(c)

(d)

(e)

(f)

(g)

(h)
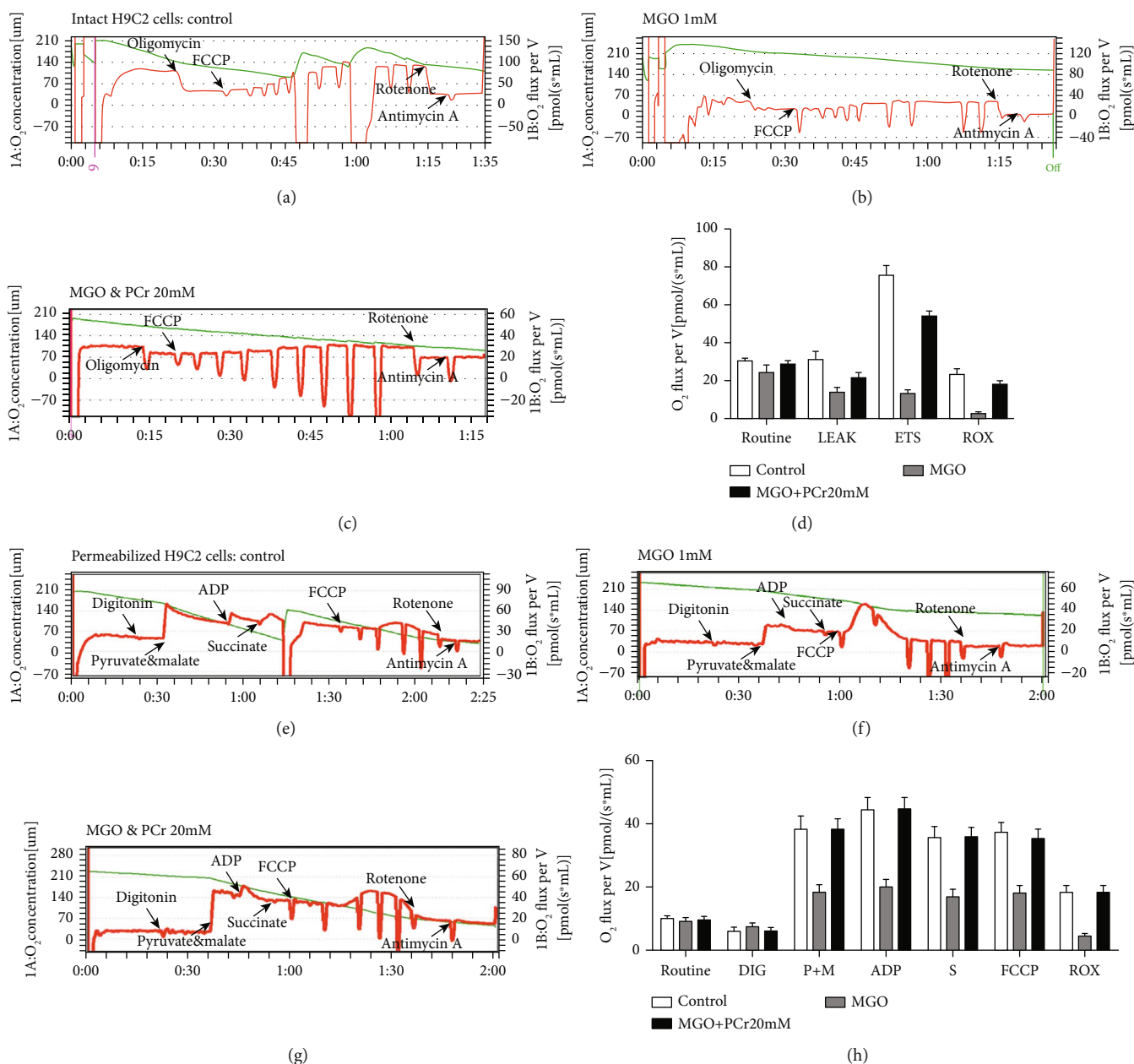
FIGURE 7: PCr enhances mitochondrial respiration. (a) Effects of PCr on mitochondrial respiration in intact H9C2 cells. Agent respiratory explore different avenues regarding control H9C2 cells. (b) MGO-incited H9C2 cells. (c) PCr (20 mM) pretreated with MGO (1 mM) invigorated cells. (d) Quantification for all groups in intact H9C2 cells. The respirometry convention for intact cells included the ROUTINE state which was estimated when a steady oxygen transition had been gotten following expansion of cells into the test chamber. Uncoupled respiration in the LEAK state was estimated when a consistent oxygen motion had been accomplished after the expansion of oligomycin (2.5 μM), FCCP (0.5 μM steps), rotenone (0.5 μM), and antimycin A (2.5 μM). (e) Effect of PCr on permeabilized H9C2 cells in control. (f) MGO-induced H9C2 cells. (g) PCr (20 mM) pretreated with MGO-stimulated cells. (h) Quantification for all the groups in permeabilized H9C2 cells. The following are added: digitonin (8.1 μM, 10 μg/10^6 cells); P: pyruvate (5 mM); G: glutamate (10 mM); M: malate (2 mM); ADP (5 mM); S: succinate (10 mM); FCCP (0.5 μM steps); rotenone (0.5 μM); antimycin A (2.5 μM). Data are presented as the mean ± SD ($n = 3$).

morphology of H9C2 has also been improved in the treated group rather than the MGO-induced group.

Treatment with PCr (20~50 mM) in rats shows that PCr effectively reduced the blood glucose level and improved diabetes symptoms slightly, suggesting that the reduction of blood glucose level by PCr may be one of the mechanisms of improving heart morphology and function in diabetes.

Impressive proof proposes that overproduction of ROS actuated by hyperglycemia is an unequivocal factor in the improvement of DCM [32, 33]. Ongoing investigations have recommended that hyperglycemia-induced oxidative damage plays an important role in the early stage of DCM [34]. Our present study showed that PCr could create a protective effect against ROS as well as MGO-induced H9C2 cell injury

(a)

(b)

(c)

(d)
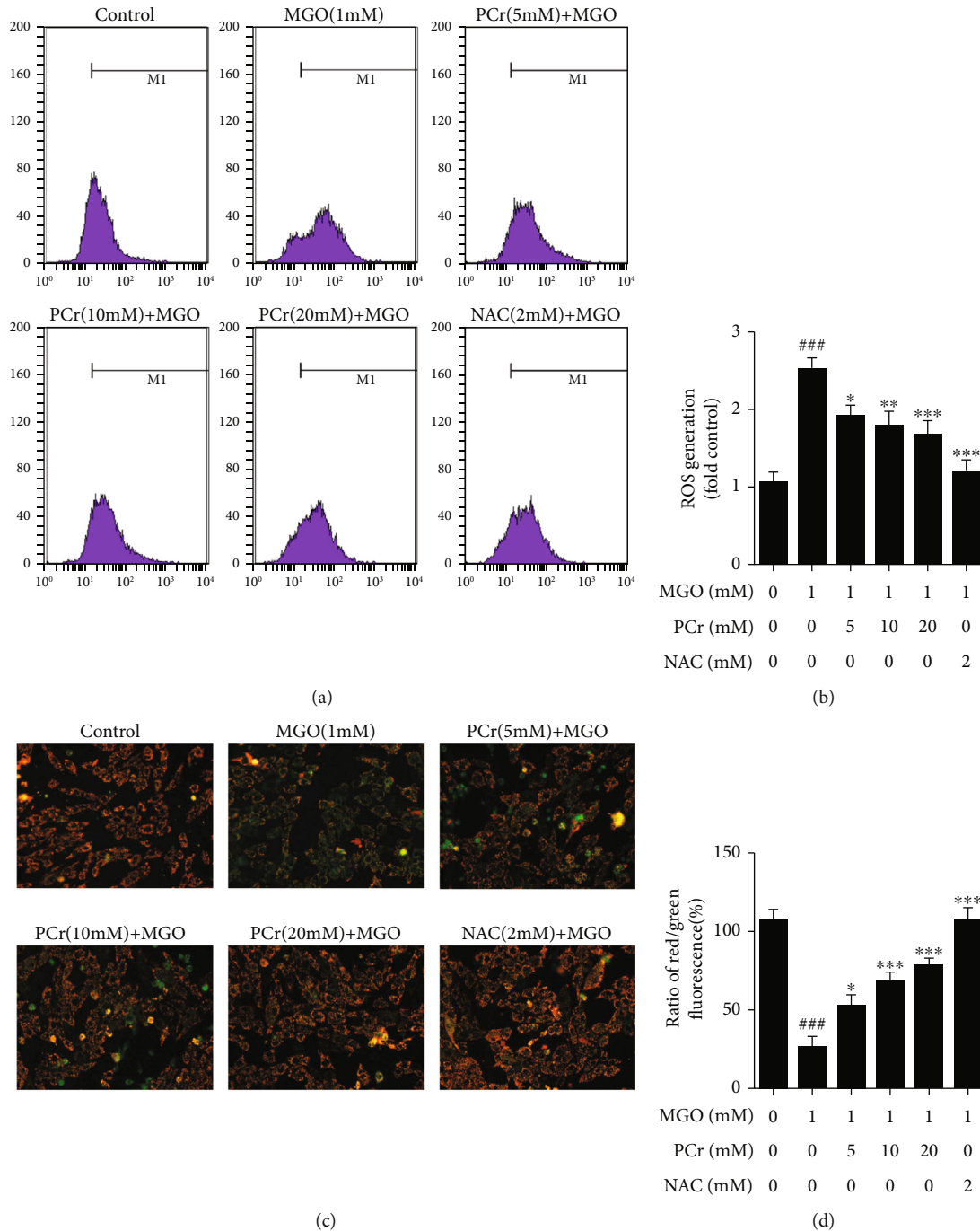
FIGURE 8: Inhibitory impacts of PCr on MGO-actuated H9C2 ROS overproduction. (a) Cells were treated with convergences of (5~20 mM) PCr or 2 mM NAC for 2 h before being animated with (1 mM) MGO for 24 h. (b) Quantification ROS age. (c) Protective impacts of PCr against MGO-initiated mitochondrial brokenness in H9C2 cells. The impact of PCr on mitochondrial membrane potential. The $\Delta\psi$m in each group was computed as the proportion of red to green fluorescence. (d) Data are presented as the mean ± SD ($n = 3$). $^{\#\#\#}P < 0.05$vs. the control group. $^{*}P < 0.05$, $^{**}P < 0.01$, and $^{***}P < 0.01$vs. the MGO group.

by antioxidant activities, which was consistent with our previous study regarding the antioxidant activities of PCr in MGO-induced endothelial cells [35, 36].

Augmented myocardial cell apoptosis is an imperative occasion in the improvement of DCM [4]. Recent studies have described the role of STAT3 in apoptosis, demonstrating that inhibition of STAT3 suppresses cleaved caspase 3

[43]. In our present examination, the after effects in vivo and in vitro demonstrated that PCr likewise bolstered the report, i.e., the inhibition of STAT3 stifled caspase-3. In addition, we found that PCr could improve the cardiomyopathy by repressing oxidative pressure and balancing the mitochondrial pathway through the decreased apoptosis pathway. These discoveries demonstrated that PCr may be a

(a)   (b)   (c)
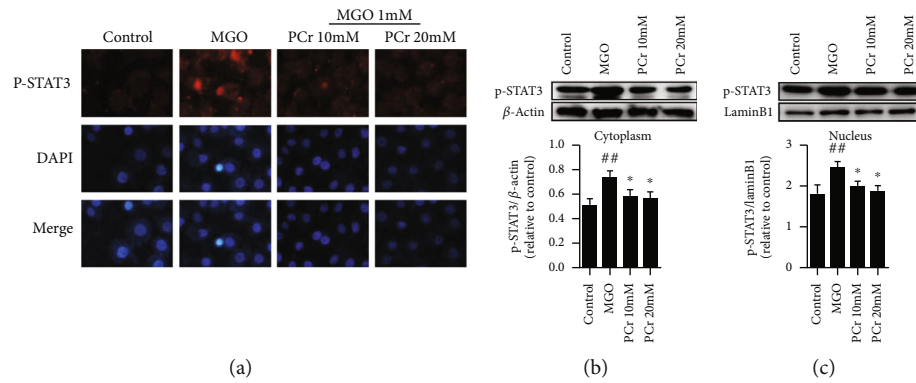
FIGURE 9: Effects of PCr on the expression level of pSTAT signaling pathway. (a) Immunofluorescence recoloring examination of pSTAT confinement. The H9C2 cells were named with pSTAT (red), and the nuclei were recolored with DAPI (blue). (b, c, d) Western blot examination of pSTAT in the cytoplasm and nucleus. Data are introduced as the mean ± SD ($n = 3$). $^*P < 0.05$ and $^{**}P < 0.01$ significantly different from the control group.

plausibility in the improvement of diabetic cardiomyopathy. Our study proposes new aspects to the signal transduction pathway of this PCr-mediated protection and emphasized the involvement of mitochondrial signaling pathways (Figure 10).

Moreover, SOD, MDA, and GSH are enzymatic prevention agents that assume a fundamental job in keeping cells from being presented to oxidative harm in diabetes mellitus [37]. Our results showed that significant impacts of PCr on SOD, MDA, and GSH reveal potent antioxidant activity. In addition, an in vitro study showed that ROS was markedly increased in the MGO group compared with the treated group in different concentrations of PCr in a dose-dependent manner. The rising proof proposes that DCM is connected to adjustments in myocardial fuel and energy metabolism. Diverse trial reports have shown that the mitochondria assume an essential job in the pathogenesis of diabetes [38]. It is known that diabetic cardiomyopathy (DCM) is involved in glucose and lipid metabolism disorder, oxidative stress, inflammation, apoptosis, and so on. Our results showed that mitochondrial dysfunction was closely related to multiple pathogenic links of DCM. Mitochondria are important sites of energy metabolism in cells, compared with other muscle cells. The heart is rich in mitochondria. The activity of mitochondrial respiratory chain-related enzymes in rats was significantly decreased [44]. Type 2 diabetes' mitochondrial respiratory function was impaired in ob/ob and db/db mice [45, 46]. We are sure that our clinical advances will enlighten clinical doctors to explore effective prevention and treatment measures targeting the mitochondria. In addition, mitochondrial brokenness is for all intents and purposes at the center of every single cardiovascular issue and associated with the maturing procedure. Besides, it has been accounted for that keeping mitochondria in a solid state is a confounded procedure and must be firmly managed by means of mitochondrial quality control instruments and complex transaction between mitochondrial biogenesis and degradation [39]. Despite the mitochondria being the primary generator of ROS, they are likewise helpless to the harming impact of ROS. In the mix, the changes in diabetes-actuated mitochondria are very much depicted;

the changes in the primary parameters of mitochondrial respiration would thus prompt the confinement of ATP generation and most likely the expansion in the ROS arrangement. In this manner, the capacity of mitochondria is closely linked to the maintenance of redox [40]. Our results indicated that the application of the measurement of mitochondrial respiration could be a potential sensitive assay for cellular dysfunction from STZ and MGO poisoning. These recommended that decreased effectiveness of mitochondrial respiration by PCr has been exhibited in diabetes, especially for the exceptional need in tissues. Our results additionally showed that this recuperation of mitochondrial respiration by PCr diminished unsettling influences of mitochondrial works because of the increase of the electron transport chain action and ATP creation. It is shown that the estimation of mitochondrial respiration may hold more noteworthy utility in this regard [41]. In the current study, we further found that the mitochondrial respiration function in the isolated heart mitochondria or heart tissue homogenated groups treated with PCr-induced STZ could be elevated to recover the same with the control group, showing a normal response similar to the control group, which means they expired from STZ poisoning. We also found that ETS, which represents the mitochondrial bioenergetics reserve, was significantly decreased in the STZ group. For the supporting evidence of this notion in both tissue homogenated and isolated heart mitochondria, we observed that the rats treated with the highest PCr dose (50 mM/day) displayed a huge propensity to have the most astounding substrate affectability in contrast with the STZ group and control subject. Moreover, the past examination has demonstrated that the depolarization in mitochondrial film potential (MMP) is an element of apoptosis. Intracellular ROS creation has been shown to prompt apoptosis by uncontrollable MMP [42]. Exorbitant intracellular ROS creation has been shown to prompt apoptosis by boisterous MMP. Our outcome affirmed that the counter apoptotic activity of PCr was intervened by the concealment of mitochondrial layer potential condition in order to hinder the mitochondrial apoptotic pathway and to additionally forestall DCM. Moreover, our results demonstrated that the apoptosis pathway significantly reduced as depicted in flow
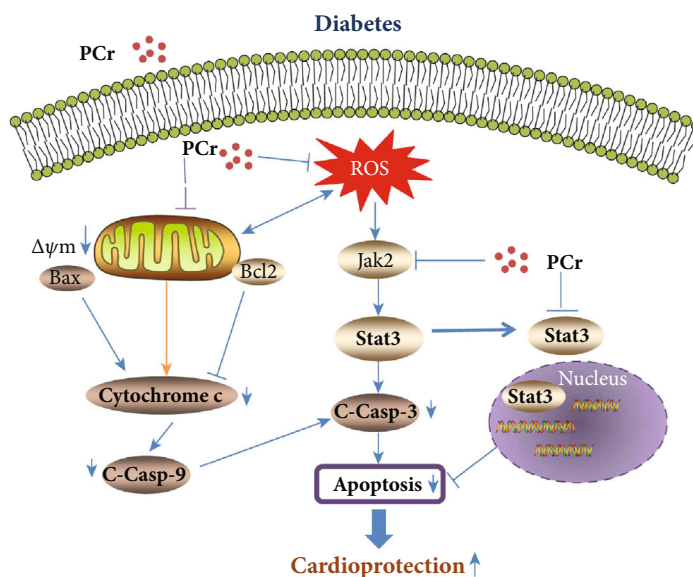
FIGURE 10: Schematic representation influence of PCr against DCM on Bcl-2 family members and other mitochondrial apoptotic and metabolic proteins in cardiomyocytes under various pathological conditions.

cytometry as well as TUNEL assay. Moreover, PCr possesses the antiapoptotic effect *in vivo* and *in vitro* when using western blot in changing the protein expression of apoptotic proteins such as Bcl-2, which was decreased in the model group and increased in the treatment groups compared with the control group. In addition, Bax was expanded in the model group and diminished in the treatment group in contrast with the control group. Furthermore, caspase 3 and caspase 9 were diminished in the model group and expanded in the treatment group, and also cleaved caspase 3 and cleaved caspase 9 were expanded in the model group and diminished in the treatment group with PCr. Moreover, the nuclear translocation of p-STAT3 was detected to be higher in the STZ group than that of the PCr group, reflecting the improvement of PCr against DCM.

5. Conclusion

The simultaneous measurement of respiration greatly enhances the informative potential of studies of mitochondria. Our outcomes are given proof that PCr can avoid hyperglycemia-initiated myocardial oxidative pressure, mitochondrial brokenness, and protected cardiovascular dysfunction. The pretreatment with PCr is an effective protective agent against the complications associated with diabetes in H9C2 and in cardiac tissue from rats, being treated with STZ to induce experimental diabetes. More specifically, pretreatment with PCr has been found to arrest apoptosis triggered by hyperglycemia. Although, PCr preserved the normal morphology of cardiac cells exposed to MGO through the restraint of the JAK2/STAT3 signaling pathway. Besides, PCr may fill in as a novel restorative methodology for enhancing and balancing out mitochondrial work and a defensive impact against DCM.

Abbreviations

ROS: Reactive oxygen species
JAK/STAT: Janus kinase/signal transducer and activator of transcription.

Data Availability

All data are preserved by Eskandar Qaed and Zeyao Tang.

Conflicts of Interest

The authors declare that they have no conflict of interest.

Authors' Contributions

Eskandar Qaed, Jiaqi Wang, Marwan Almoiliqy, and Yanlin Song are equal contributors. Jianbin Zhang and Zeyao Tang contributed equally.

Acknowledgments

References

[1] Q. Liu, S. Wang, and L. Cai, "Diabetic cardiomyopathy and its mechanisms: role of oxidative stress and damage," *Journal of Diabetes Investigation*, vol. 5, no. 6, pp. 623–634, 2014.

[2] Y. Lei, Q. Xu, B. Zeng et al., "Angiotensin-(1–7) protects cardiomyocytes against high glucose-induced injuries through inhibiting reactive oxygen species-activated leptin–p38 mitogen-activated protein kinase/extracellular signal-regulated protein kinase 1/2 pathways, but not the leptin–c-Jun N-terminal

kinase pathway *in vitro*," *Journal of Diabetes Investigation*, vol. 8, no. 4, pp. 434–445, 2017.

[3] P. V. Dludla, C. J. Muller, E. Joubert et al., "Aspalathin protects the heart against hyperglycemia-induced oxidative damage by up-regulating *Nrf2* expression," *Molecules*, vol. 22, no. 1, p. 129, 2017.

[4] X. M. Wang, Y. C. Wang, X. J. Liu et al., "BRD7 mediates hyperglycaemia-induced myocardial apoptosis *via* endoplasmic reticulum stress signalling pathway," *Journal of Cellular and Molecular Medicine*, vol. 21, no. 6, pp. 1094–1105, 2017.

[5] J. M. Huss and D. P. Kelly, "Mitochondrial energy metabolism in heart failure: a question of balance," *The Journal of Clinical Investigation*, vol. 115, no. 3, pp. 547–555, 2005.

[6] X. Huang, L. Sun, S. Ji et al., "Kissing and nanotunneling mediate intermitochondrial communication in the heart," *Proceedings of the National Academy of Sciences of the United States of America*, vol. 110, no. 8, pp. 2846–2851, 2013.

[7] N. Fillmore, J. Mori, and G. D. Lopaschuk, "Mitochondrial fatty acid oxidation alterations in heart failure, ischaemic heart disease and diabetic cardiomyopathy," *British Journal of Pharmacology*, vol. 171, no. 8, pp. 2080–2090, 2014.

[8] S. Lin, X. Wu, L. Tao et al., "The metabolic effects of traditional Chinese medication Qiliqiangxin on H9C2 cardiomyocytes," *Cellular Physiology and Biochemistry*, vol. 37, no. 6, pp. 2246–2256, 2015.

[9] O. M. Duicu, A. Privistirescu, A. Wolf et al., "Methylene blue improves mitochondrial respiration and decreases oxidative stress in a substrate-dependent manner in diabetic rat hearts," *Canadian Journal of Physiology and Pharmacology*, vol. 95, no. 11, pp. 1376–1382, 2017.

[10] G. V. Sangle, S. K. R. Chowdhury, X. Xie, G. L. Stelmack, A. J. Halayko, and G. X. Shen, "Impairment of mitochondrial respiratory chain activity in aortic endothelial cells induced by glycated low-density lipoprotein," *Free Radical Biology and Medicine*, vol. 48, no. 6, pp. 781–790, 2010.

[11] M. Makrecka-Kuka, G. Krumschnabel, and E. Gnaiger, "High-resolution respirometry for simultaneous measurement of oxygen and hydrogen peroxide fluxes in permeabilized cells, tissue homogenate and isolated mitochondria," *Biomolecules*, vol. 5, no. 3, pp. 1319–1338, 2015.

[12] R. M. Perez-Gutierrez, A. H. Garcia-Campoy, and A. Muñiz-Ramirez, "Properties of flavonoids isolated from the bark of *Eysenhardtia polystachya* and their effect on oxidative stress in streptozotocin-induced diabetes mellitus in mice," *Oxidative Medicine and Cellular Longevity*, vol. 2016, Article ID 9156510, 13 pages, 2016.

[13] W. Li, Q. Wang, M. du et al., "Effects of overexpressing FoxO1 on apoptosis in glomeruli of diabetic mice and in podocytes cultured in high glucose medium," *Biochemical and Biophysical Research Communications*, vol. 478, no. 2, pp. 612–617, 2016.

[14] L. Cai, W. Li, G. Wang, L. Guo, Y. Jiang, and Y. J. Kang, "Hyperglycemia-induced apoptosis in mouse myocardium: mitochondrial cytochrome C-mediated caspase-3 activation pathway," *Diabetes*, vol. 51, no. 6, pp. 1938–1948, 2002.

[15] L. Cai, Y. Wang, G. Zhou et al., "Attenuation by metallothionein of early cardiac cell death via suppression of mitochondrial oxidative stress results in a prevention of diabetic cardiomyopathy," *Journal of the American College of Cardiology*, vol. 48, no. 8, pp. 1688–1697, 2006.

[16] Y. Pan, Y. Wang, Y. Zhao et al., "Inhibition of JNK phosphorylation by a novel curcumin analog prevents high glucose–induced inflammation and apoptosis in cardiomyocytes and the development of diabetic cardiomyopathy," *Diabetes*, vol. 63, no. 10, pp. 3497–3511, 2014.

[17] M. Wyss and R. Kaddurah-Daouk, "Creatine and creatinine metabolism," *Physiological Reviews*, vol. 80, no. 3, pp. 1107–1213, 2000.

[18] Z. Sun, X. Lan, A. Ahsan et al., "Erratum to: Phosphocreatine protects against LPS-induced human umbilical vein endothelial cell apoptosis by regulating mitochondrial oxidative phosphorylation," *Apoptosis*, vol. 21, no. 4, pp. 514-515, 2016.

[19] L. Xu, C. Y. Wang, L. Lv, K. X. Liu, H. J. Sun, and G. Z. Han, "Pharmacokinetics of phosphocreatine and its active metabolite creatine in the mouse plasma and myocardium," *Pharmacological Reports*, vol. 66, no. 5, pp. 908–914, 2014.

[20] G. Landoni, A. Zangrillo, V. V. Lomivorotov et al., "Cardiac protection with phosphocreatine: a meta-analysis," *Interactive Cardiovascular and Thoracic Surgery*, vol. 23, no. 4, pp. 637–646, 2016.

[21] H. Kiu and S. E. Nicholson, "Biology and significance of the JAK/STAT signalling pathways," *Growth Factors*, vol. 30, no. 2, pp. 88–106, 2012.

[22] R. P. Soebiyanto, S. N. Sreenath, C. K. Qu, K. A. Loparo, and K. D. Bunting, "Complex systems biology approach to understanding coordination of JAK-STAT signaling," *Biosystems*, vol. 90, no. 3, pp. 830–842, 2007.

[23] N. Al-Rasheed, N. Al-Rasheed, I. Hasan, M. Al-Amin, H. Al-Ajmi, and A. Mahmoud, "Sitagliptin attenuates cardiomyopathy by modulating the JAK/STAT signaling pathway in experimental diabetic rats," *Drug Design, Development and Therapy*, vol. 10, pp. 2095–2107, 2016.

[24] A. K. L. Banes-Berceli, P. Ketsawatsomkron, S. Ogbi, B. Patel, D. M. Pollock, and M. B. Marrero, "Angiotensin II and endothelin-1 augment the vascular complications of diabetes via JAK2 activation," *American Journal of Physiology-Heart and Circulatory Physiology*, vol. 293, no. 2, pp. H1291–H1299, 2007.

[25] N. H. Ugochukwu and M. K. Cobourne, "Modification of renal oxidative stress and lipid peroxidation in streptozotocin-induced diabetic rats treated with extracts from *Gongronema latifolium* leaves," *Clinica Chimica Acta*, vol. 336, no. 1-2, pp. 73–81, 2003.

[26] J. Mujkosova, M. Ferko, P. Humenik, I. Waczulikova, and A. Ziegelhoffer, "Seasonal variations in properties of healthy and diabetic rat heart mitochondria: Mg^{2+}-ATPase activity, content of conjugated dienes and membrane fluidity," *Physiological Research*, vol. 57, Supplement 2, pp. S75–S82, 2008.

[27] D. Pesta and E. Gnaiger, "High-resolution respirometry: OXPHOS protocols for human cells and permeabilized fibers from small biopsies of human muscle," *Methods in Molecular Biology*, vol. 810, pp. 25–58, 2012.

[28] M. Ferko, D. Habodászová, I. Waczulíková et al., "Endogenous protective mechanisms in remodeling of rat heart mitochondrial membranes in the acute phase of streptozotocin-induced diabetes," *Physiological Research*, vol. 57, Supplement 2, pp. S67–S73, 2008.

[29] X. Liu, C. Liu, J. Li, X. Zhang, F. Song, and J. Xu, "Urocortin attenuates myocardial fibrosis in diabetic rats via the Akt/GSK-3β signaling pathway," *Endocrine Research*, vol. 41, no. 2, pp. 148–157, 2016.

[30] N. M. Al-Rasheed, N. M. Al-Rasheed, I. H. Hasan et al., "Simvastatin ameliorates diabetic cardiomyopathy by attenuating

oxidative stress and inflammation in rats," *Oxidative Medicine and Cellular Longevity*, vol. 2017, Article ID 1092015, 13 pages, 2017.

[31] P. K. Battiprolu, B. Hojayev, N. Jiang et al., "Metabolic stress-induced activation of FoxO1 triggers diabetic cardiomyopathy in mice," *The Journal of Clinical Investigation*, vol. 122, no. 3, pp. 1109–1118, 2012.

[32] X. Sun, R. C. Chen, Z. H. Yang et al., "Taxifolin prevents diabetic cardiomyopathy in vivo and in vitro by inhibition of oxidative stress and cell apoptosis," *Food and Chemical Toxicology*, vol. 63, pp. 221–232, 2014.

[33] W. J. Fang, C. J. Wang, Y. He, Y. L. Zhou, X. D. Peng, and S. K. Liu, "Resveratrol alleviates diabetic cardiomyopathy in rats by improving mitochondrial function through PGC-1α deacetylation," *Acta Pharmacologica Sinica*, vol. 39, no. 1, pp. 59–73, 2018.

[34] P. Ristic, I. Srejovic, T. Nikolic et al., "The effects of zofenopril on cardiac function and pro-oxidative parameters in the streptozotocin-induced diabetic rat heart," *Molecular and Cellular Biochemistry*, vol. 426, no. 1-2, pp. 183–193, 2017.

[35] P. Chu, G. Han, A. Ahsan et al., "Phosphocreatine protects endothelial cells from Methylglyoxal induced oxidative stress and apoptosis via the regulation of PI3K/Akt/eNOS and NF-κB pathway," *Vascular Pharmacology*, vol. 91, pp. 26–35, 2017.

[36] A. Ahsan, G. Han, J. Pan et al., "Phosphocreatine protects endothelial cells from oxidized low-density lipoprotein-induced apoptosis by modulating the PI3K/Akt/eNOS pathway," *Apoptosis*, vol. 20, no. 12, pp. 1563–1576, 2015.

[37] K. A. S. Silva, J. Dong, Y. Dong et al., "Inhibition of Stat3 activation suppresses caspase-3 and the ubiquitin-proteasome system, leading to preservation of muscle mass in cancer cachexia," *The Journal of Biological Chemistry*, vol. 290, no. 17, pp. 11177–11187, 2015.

[38] R. Chandran, T. Parimelazhagan, S. Shanmugam, and S. Thankarajan, "Antidiabetic activity of *Syzygium calophyllifolium* in streptozotocin- nicotinamide induced type-2 diabetic rats," *Biomedicine & Pharmacotherapy*, vol. 82, pp. 547–554, 2016.

[39] P. J. Oliveira, A. P. Rolo, R. Seica, M. S. Santos, C. M. Palmeira, and A. J. Moreno, "Reduction in cardiac mitochondrial calcium loading capacity is observable during α-naphthylisothiocyanate-induced acute cholestasis: a clue for hepatic-derived cardiomyopathies?," *Biochimica et Biophysica Acta (BBA) - Molecular Basis of Disease*, vol. 1637, no. 1, pp. 39–45, 2003.

[40] A. S. Benischke, S. Vasanth, T. Miyai et al., "Activation of mitophagy leads to decline in Mfn2 and loss of mitochondrial mass in Fuchs endothelial corneal dystrophy," *Scientific Reports*, vol. 7, no. 1, article 6656, 2017.

[41] K. Li, Y. C. Cui, H. Zhang et al., "Glutamine reduces the apoptosis of H9C2 cells treated with high-glucose and reperfusion through an oxidation-related mechanism," *PLoS One*, vol. 10, no. 7, article e0132402, 2015.

[42] J. Chen and K. M. Ko, "Ursolic-acid-enriched Herba Cynomorii extract protects against oxidant injury in H9c2 cells and rat myocardium by increasing mitochondrial ATP generation capacity and enhancing cellular glutathione redox cycling, possibly through mitochondrial uncoupling," *Evidence-Based Complementary and Alternative Medicine*, vol. 2013, Article ID 924128, 14 pages, 2013.

[43] B. D. Follstad, D. I. C. Wang, and G. Stephanopoulos, "Mitochondrial membrane potential differentiates cells resistant to

apoptosis in hybridoma cultures," *European Journal of Biochemistry*, vol. 267, no. 22, pp. 6534–6540, 2000.

[44] H. Raza, A. John, and F. Howarth, "Alterations in glutathione redox metabolism, oxidative stress, and mitochondrial function in the left ventricle of elderly zucker diabetic fatty rat heart," *International Journal of Molecular Sciences*, vol. 13, no. 12, pp. 16241–16254, 2012.

[45] T. Pham, D. Loiselle, A. Power, and A. J. R. Hickey, "Mitochondrial inefficiencies and anoxic ATP hydrolysis capacities in diabetic rat heart," *American Journal of Physiology-Cell Physiology*, vol. 307, no. 6, pp. C499–C507, 2014.

[46] C. Sloan, J. Tuinei, K. Nemetz et al., "Central leptin signaling is required to normalize myocardial fatty acid oxidation rates in caloric-restricted *ob/ob* mice," *Diabetes*, vol. 60, no. 5, pp. 1424–1434, 2011.

Research Article

Mitochondrial Oxidative Stress Impairs Energy Metabolism and Reduces Stress Resistance and Longevity of *C. elegans*

Benjamin Dilberger,[1] Stefan Baumanns,[2] Fabian Schmitt,[1] Tommy Schmiedl,[1] Martin Hardt,[3] Uwe Wenzel,[2] and Gunter P. Eckert [1]

[1]*Institute of Nutritional Sciences, Laboratory for Nutrition in Prevention and Therapy, Biomedical Research Center Seltersberg (BFS), Justus Liebig University Giessen, Schubertstrasse 81, 35392 Giessen, Germany*
[2]*Molecular Nutrition Research, Interdisciplinary Research Center, Justus Liebig University Giessen, Heinrich-Buff-Ring 26-32, 35392 Giessen, Germany*
[3]*Imaging Unit, Biomedical Research Center Seltersberg (BFS), Justus Liebig University Giessen, Schubertstrasse 81, 35392 Giessen, Germany*

Correspondence should be addressed to Gunter P. Eckert; eckert@uni-giessen.de

Introduction. Mitochondria supply cellular energy and are key regulators of intrinsic cell death and consequently affect longevity. The nematode *Caenorhabditis elegans* is frequently used for lifespan assays. Using paraquat (PQ) as a generator of reactive oxygen species, we here describe its effects on the acceleration of aging and the associated dysfunctions at the level of mitochondria. *Methods*. Nematodes were incubated with various concentrations of paraquat in a heat-stress resistance assay (37°C) using nucleic staining. The most effective concentration was validated under physiological conditions, and chemotaxis was assayed. Mitochondrial membrane potential ($\Delta\Psi m$) was measured using rhodamine 123, and activity of respiratory chain complexes determined using a Clark-type electrode in isolated mitochondria. Energetic metabolites in the form of pyruvate, lactate, and ATP were determined using commercial kits. Mitochondrial integrity and structure was investigated using transmission electron microscopy. Live imaging after staining with fluorescent dyes was used to measure mitochondrial and cytosolic ROS. Expression of longevity- and mitogenesis-related genes were evaluated using qRT-PCR. *Results*. PQ (5 mM) significantly increased ROS formation in nematodes and reduced the chemotaxis, the physiological lifespan, and the survival in assays for heat-stress resistance. The number of fragmented mitochondria significantly increased. The $\Delta\Psi m$, the activities of complexes I-IV of the mitochondrial respiratory chain, and the levels of pyruvate and lactate were significantly reduced, whereas ATP production was not affected. Transcript levels of genetic marker genes, *atfs-1*, *atp-2*, *skn-1*, and *sir-2.1*, were significantly upregulated after PQ incubation, which implicates a close connection between mitochondrial dysfunction and oxidative stress response. Expression levels of *aak-2* and *daf-16* were unchanged. *Conclusion*. Using paraquat as a stressor, we here describe the association of oxidative stress, restricted energy metabolism, and reduced stress resistance and longevity in the nematode *Caenorhabditis elegans* making it a readily accessible *in vivo* model for mitochondrial dysfunction.

1. Introduction

Mitochondria supply cellular energy and are key regulators of intrinsic cell death and consequently affect longevity [1, 2]. A link between aging and mitochondrial dysfunction has been well established [2–7]. The "free radical theory" of aging, first proposed by Harman et al., explains aging as a result of the accumulation of cellular damage caused by reactive oxygen species (ROS) [2, 8, 9]. Since mitochondria are the primary source of ROS, Harman himself extended his theory to the "mitochondrial theory of aging" [3, 10]. An imbalance between ROS and cellular stress defence mechanisms accordingly causes a vicious cycle of further mitochondrial dysfunction leading to more ROS, which in turn

promotes more damage, an energetic imbalance, and finally triggers cell death and thereby aging. The importance of an equilibrium between ROS and defence mechanism is evidenced by the fact that low concentrations of ROS lead to hormesis with a higher state of stress resistance [11–14].

Investigations on isolated mitochondria in aging nematodes are scarce. Several organisms, ranging from yeast to mice [13, 15–18], have been used to study the effect of alterations within the mitochondrial electron chain (ETC) and longevity [5]. However, *C. elegans* offers distinct advantages compared to other model organisms. Especially its ability as a hermaphrodite to produce identical offspring and its short lifespan make it a powerful tool that has been widely used to investigate longevity-related questions [19, 20]. Since molecular and functional processes associated with mitochondria are highly conserved in species over long evolutionary distances, *C. elegans* represents an outstanding model for aging mechanisms with mitochondria [20]. Specific transcription factors, including *skn-1* (Nrf-2 ortholog), *aak-2* (AMPK ortholog), *atfs-1*, and *sir-2.1* (Sirt1 ortholog), involved in crucial metabolic pathways [21–24], have been identified, connecting alterations in longevity to mitochondrial dysfunction and mitochondrial biogenesis [25, 26].

Compared to *in situ* studies, investigating isolated mitochondria in the context of aging, however, appears to be crucial since it offers clear advantages [27] in an environment free from interfering organelles or reactions [28].

In the present study, paraquat (1,1'-dimethyl-4'4-bipyridinium dichloride; PQ) was used as a well-known stressor of the mitochondrial respiration chain in order to assess the effects of mitochondrial dysfunction on stress resistance and aging. Life span and health span of nematodes, generation of mitochondrial and cytosolic ROS, energy metabolites (ATP, lactate, and pyruvate), and expression of key genes were investigated in whole animals. Mitochondrial integrity and structure as well as activities of ETC complexes and membrane potential ($\Delta\Psi$m) were evaluated in isolated mitochondria putting the close relation between mitochondrial dysfunction and longevity into a broader context.

2. Material and Methods

2.1. Chemicals. Chemicals used were of the highest available purity and standard from Sigma-Aldrich (St. Louis, MO, USA) or Merck (Darmstadt, Germany).

2.2. Nematode and Bacterial Strain. *C. elegans* wild-type strain N2 was obtained from the Caenorhabditis Genetics Center (University of Minnesota, MN, US). Nematodes were maintained on nematode growth medium (NGM) agar plates seeded with *E. coli* OP50 at 20°C according to standard protocols [29]. For all experiments, synchronous populations were generated through a standard bleaching protocol [30].

2.3. Cultivation and Treatment. Synchronous larvae were washed twice in M9 buffer, counted, and adjusted to 10 larvae per 10 μL. Depending on the experiment and on the number needed, nematodes were either raised in 96-well plates (Greiner Bio-One, Frickenhausen, Germany), cell culture flasks (Sarstedt, Nümbrecht, Germany), or OP50 spread NGM plates. For 96-well plates and flasks, OP50-NGM was added as a standardized food source with a volume 4.4-fold of the larvae containing M9 solution. L1 larvae were maintained under shaking at 20°C reaching adulthood within 3 days.

Unless otherwise stated, paraquat was dissolved in M9 and added after reaching young adulthood, 48 h prior to the experiment. M9 was used as control.

2.4. Lifespan Assay. To determine the nematode's lifespan at 20°C, a modified protocol from Amrit et al. was applied [31] and synchronized larvae, obtained from egg preparation as stated above, were raised on NGM agar plates spread with standard OP50 *E. coli* culture. After completing the L4 larval stage, 60 healthy animals per group were transferred to fresh NGM *E. coli* containing plates with a sterilized platinum wire. Effectors were incorporated into the OP50 culture with the concentration as needed. Nematodes were transferred to new plates every two days to distinguish between offspring until egg-laying stopped. In line with the separation from eggs and larvae, nematodes were checked for vital signs using a hot platinum wire held next to the animals' heads. Worms showing no reaction to the heat stimulus were considered dead. The lifespan curves were statistically compared using the log-rank test.

2.5. Heat-Shock Survival Assay. Approximately 10 nematodes were raised per well in a 96-well microplate as mentioned above. After 48 h of incubation with effectors, time till death was determined using a microplate thermotolerance assay [32]. In brief, nematodes were washed off the wells with M9-buffer into 15 mL tubes followed by three additional washing steps. Each well of a black 384-well low-volume microtiter plate (Greiner Bio-One, Frickenhausen, Germany) was prefilled with 6.5 μL M9 buffer/Tween® 20 (1%*v/v*). Subsequently, one nematode was immersed into 1 μL M9 buffer under a stereomicroscope (Breukhoven Microscope Systems, Netherlands). A volume of 7.5 μL SYTOX™ Green (final concentration 1 μM; Life Technologies, Karlsruhe, Germany), which penetrates only into cells with compromised plasma membrane and gets fluorescent after binding to DNA, was added for fluorescent detection. To prevent water evaporation, the plates were sealed with a Rotilabo sealing film (Greiner Bio-One, Frickenhausen, Germany). Heat shock (37°C) was applied and fluorescence measured with a ClarioStar Plate Reader (BMG, Ortenberg, Germany) every 30 min over the course of 17 h. The excitation wavelength was set at 485 nm, and the emission detected at 538 nm.

2.6. Chemotaxis Assay. Chemotaxis was assessed using a previously published method [33]. Briefly, agar plates were divided into four quadrants. Sodium acid (0.5 M) was mixed in the same parts with ethanol (95%) as control, or diacetyl (0.5%) as attractant. Either 2 μL of control or attractant solution was added to the center of two opposite quadrants with the same distance to the middle of the plate. Nematodes were washed and separated from larvae as stated above, and a number of approximately 150 animals placed in the plates'

center. After 1 h, each quadrant was counted, and a chemotaxis index calculated ((number of attractant − number of control)/number total).

2.7. Mitochondrial and Cytosolic ROS Measurement. To determine mitochondrial ROS levels, young adult nematodes were incubated for 48 h with 0.5μM MitoTracker® Red CM-H$_2$XRos (Fisher Scientific, Schwerte, Germany). Mito-Tracker® Red accumulates to a high extend at the inner mitochondrial membrane showing an increased fluorescence upon elevated ROS mainly associated with mitochondria. To detect cytosolic ROS, nematodes were incubated for 4 h with 25μM fluorescent probe $2',7'$-dichlorofluorescein diacetate (CM-H$_2$DCFDA) (Fisher Scientific, Schwerte, Germany). The probe passively diffuses into cells where it is oxidized by cytosolic reactive oxygen species into its fluorescent form. Paraquat (5 mM) was added 4 h prior to the experiment for both parameters. For epifluorescence microscopy (EVOS FL digital fluorescence microscope, AMG, Bothell, USA), worms were washed with M9-buffer/Tween®20 (1% v/v) solution and anesthetized by addition of 2 mM levamisole. Nematodes were transferred onto a labelled glass slide and covered with a cover slip. The dye was visualized using the EVOS LED Light Cube RFP, with an excitation at 531 ± 40 nm and an emission at 593 ± 40 nm for MitoTracker® Red and an excitation at 470 ± 22 nm and an emission at 525 ± 50 nm for CM-H$_2$DCFDA. Images were taken at a tenfold magnification. For each group, at least 20 nematodes were photographed. The quantification of fluorescence intensity was done using ImageJ (National Institute of Health (NIH)).

2.8. Isolation of Mitochondria. To isolate functional mitochondria, nematode populations ranging from 5,000 to 10,000 per group were needed. Nematodes were raised in liquid OP50-NGM culture medium and incubated with effectors as stated above under standardized conditions.

Two-day-old gravid adults were separated from larvae and washed to remove residual bacteria using a self-made separation device with a nylon mesh (Dr. Fill®, Giessen, Germany) before being transferred to ice-cold isolation buffer (300 mM sucrose, 5 mM TES, 200μM EGTA, pH 7.2) [34].

To obtain a mitochondria-enriched fraction, a Balch Homogenizer (Isobiotec, Heidelberg, Germany) was used [35]. Nematodes were gently passed through the homogenizer chamber with 1 mL glass syringes (SGE Syringe, Trajan, Australia) fitted with a metal luer lock for 5 times. To fracture nematode cuticle, a 12μm ball clearance was applied. The homogenate was centrifuged at 800 g for 5 minutes at 4°C (Heraeus Fresco 21, Thermo Scientific, Langenselbold, Germany) to sediment debris and larger worm fragments. The mitochondria-containing supernatant was collected and centrifuged at 9,000 g for 10 minutes at 4°C. The crude mitochondria-containing pellet was resuspended in 70μL swelling buffer (SWB) (0.2 M sucrose, 10 mM MOPS-Tris, 5 mM succinat, 1 mM H$_3$PO$_4$, 10μM EGTA, 2μM rotenone) for measurement of membrane potential ($\Delta\Psi$m) [34] or 200μL of mitochondrial respiration medium MirO5 (0.5 mM EGTA, 3 mM MgCl$_2$, 60 mM K-lactobionate, 20 mM taurine, 10 mM KH$_2$PO$_4$, 20 mM HEPES, 110 mM

sucrose, 1 g/L BSA, pH 7.1; developed by Oroboros) for high-resolution respiratory experiments [36]. For $\Delta\Psi$m and respiration measurements, fresh mitochondria were immediately used after preparation. Aliquots were shock frozen in liquid nitrogen for determination of citrate synthase activity and protein content.

2.9. Transmission Electron Microscopy. For fixation, 200μL of fixative (glutaraldehyde (5%) in 0.1 M cacodylate buffer) was added in 200μL immersed mitochondria, incubated for 30 minutes at room temperature, centrifuged at 9,000 g for 10 minutes, and replaced with fresh fixative (glutaraldehyde (2.5%) in 0.1 M cacodylate buffer). Samples were stored under constant movement overnight at 4°C. Probes were postfixed in 1% OsO$_4$ in 0.1 M cacodylate buffer for 45 minutes at room temperature. Before staining with 1% uranyl acetate overnight at 4°C, samples were embedded in low melting temperature gelatine. The gelatine blocks were dehydrated in an ethanol series (10-20 minutes each in 30%, 50%, 70%, 80%, 90%, 96%, 99%, and 99% over molecular sieve) on ice followed by propylene oxide before embedding in Epon and hardened at 60°C for 24 hours. Probes were cut into 80 nm slices, transferred on copper mesh grids and stained with aqueous uranyl acetate followed by lead citrate. Grids were examined with a Leo 912 AB Omega Electron Microscope (Carl Zeiss, Oberkochen, Germany).

To exclude eventual bias, ten pictures for every investigated parameter were taken by a third party and randomized before evaluation. For determination of integrity, mitochondria were divided into four categories ("intact," outer membrane appears intact and crista structure is visible (a); "mildly fractured," slight fractures of outer membrane are visible but mitochondria appear overall in a good state (b); "heavily fractured," outer membrane and crista structure appears damaged (c); "fragmented," mitochondria are torn in parts or only fragments of former mitochondria are visible (d)). Categorization was conducted by two independent investigators.

2.10. Mitochondrial Membrane Potential ($\Delta\Psi$m). To determine the mitochondrial membrane potential, a modified protocol of Schmitt et al. was applied [34]. The fluorescent dye rhodamine 123 (Rh123) was used to assess the $\Delta\Psi$m of 25μL swelling buffer-resuspended isolated mitochondria in a black 96 well-plate with a ClarioStar Plate Reader (BMG, Ortenberg, Germany). To ensure mitochondrial integrity, the membrane potential was measured for 30 minutes, and after reaching equilibrium, 500 nM FCCP was added to evaluate the $\Delta\Psi$m-dependent effect on the quenching of Rh123. Results were normalized to protein content.

2.11. High-Resolution Respirometry. Respiration experiments were conducted at 20°C using a Clark-type electrode (O2k Oxygraph, Oroboros Instruments, Austria). For each measurement, an aliquot of 80μL in MirO5-resuspended mitochondria, as described preciously, was inserted into 2 mL of air-saturated MirO5-containing electrode chamber. For analysis, the provided DatLab software (Version 7.0.0.2) was used. To determine mitochondrial function, a

complex protocol (developed by Prof. Erich Gnaiger, Oroboros, Innsbruck, Austria) was applied, as previously stated [37].

2.12. Citrate-Synthase Activity. Frozen and at -80°C, stored samples were slowly thawed, and a reaction mix containing 0.5 mM oxaloacetate, 0.1 mM 5,5′-dithio-bis-2-nitrobenzoic acid (DTNB), 0.31 mM acetyl coenzyme A, 50 μM EDTA, 5 mM triethanolamine hydrochloride, and 0.1 M Tris-HCl was prepared and pre-heated for 5 minutes at 30°C. To determine citrate synthase (CS) activity, 10 μL of mitochondrial suspension was added, and the resulting complex of DNTB with CoA-SH was measured photospectrometrically at 412 nm [38, 39]. Measurements were performed in triplicate.

2.13. Nematode Homogenization. To assess energetic metabolites such as ATP, lactate, and pyruvate, a nematode homogenate was generated. In brief, 4,000 synchronized nematodes were harvested, thoroughly washed, shock frozen, and boiled for 15 minutes prior to sonication to denature degrading proteins. After centrifugation at 15,000 g for 10 minutes, supernatants were collected. ATP content was assessed immediately and aliquots stored at -80°C for determination of lactate, pyruvate, and protein content.

2.14. ATP Measurement. Intracellular ATP levels were determined using the ATPlite luminescence assay system (Perkin Elmer, Waltham, MA, USA). Luminescence was measured in triplicate following the manufacturer's guidelines with a ClarioStar Plate Reader (BMG, Ortenberg, Germany). Aliquots were stored at -80°C for determination of protein content.

2.15. Colorimetric Assessment of Lactate and Pyruvate Content. Frozen homogenate samples were slowly thawed until reaching room temperature. Concentrations of lactate and pyruvate were detected by changes in the NADH content using two colorimetric assay kits from Sigma-Aldrich following the manufacturer's guidelines (Sigma-Aldrich, St. Louis, MO, USA) using a ClarioStar Plate Reader (BMG, Ortenberg, Germany).

2.16. Protein Quantification. Protein contents were assessed according to the Pierce™ BCA Protein Assay Kit (Thermo Fisher Scientific, Waltham, MA, USA). Bovine serum albumin was used as a standard.

2.17. Quantitative Real-Time PCR. Total RNA was isolated using the RNeasy Mini Kit (Qiagen, Hilden, Germany) according to the manufacturer's guidelines after fracturing the nematodes' cuticle using a Balch Homogenizer with 10 μM clearance. The concentration of RNA was quantified by measuring the absorbance at 260 and 280 nm using a NanoDrop™ 2000c spectrophotometer (Thermo Fisher Scientific, Waltham, MA, USA). RNA purity was assessed with the ratio of absorbance at 260/280 nm and 260/230 nm, respectively. Subsequently, samples were treated with a TURBO DNA-free Kit™ (Thermo Fisher Scientific, Waltham, MA, USA) to remove residual genomic DNA. According to the manufacturer's guidelines, complementary DNA was

TABLE 1: Oligonucleotide primer sequences and product sizes for quantitative real-time PCR. Concentration was 0.1 μM for all primers.

Primer	Sequence	Product size (bp)
Aak-2	5′-tgcttcaccatatgctctgc-3′ 5′-gtggatcatctcccagcaat-3′	219
Ama-1	5′-ccaggaacttcggctcagta-3′ 5′-tgtatgatggtgaagctggcg-3′	85
Act-2	5′-cccactcaatccaaaggcta-3′ 5′-gggactgtgtgggraacacc-3′	168
Atfs-1	5′-tcggcgatcgatcagctaac-3′ 5′-agaatcagttcttggattaggggga-3′	75
Atp-2	5′-tccaagtcgctgaggtgttc-3′ 5′-aggtggtcgagttctcctga-3′	151
Daf-16	5′-tcctcattcactcccgattc-3′ 5′-ccggtgtattcatgaacgtg-3′	175
Sir-2.1	5′-tggctgacgattcgatggat-3′ 5′-atgagcagaaatcgcgacac-3′	179
Skn-1	5′-acagggtggaaaaagcaagg-3′ 5′-caggccaaacgccaatgac-3′	246

bp: base pairs; Conc: concentration.

synthesized from 1 μg total RNA using an iScript cDNA Synthesis Kit (Bio-Rad, Munich, Germany) and temporarily stored at -80°C. qRT-PCR was conducted using a CfX 96 Connect™ system (Bio-Rad, Munich, Germany). Primers were purchased from BioMers (Ulm, Germany). Oligonucleotide primer sequences, primer concentrations, and product sizes are listed in Table 1. All cDNA samples were performed in triplicate after a 1 : 10 dilution with RNase-free water (Quiagen, Hilden, Germany). PCR cycling conditions were an initial denaturation at 95°C for 3 min, followed by 45 cycles of 95°C for 10 s, 58°C for 45 s (with the exception of *aak-2* at 62°C), and extension at 72°C for 29 s. Gene expression levels were analysed by applying the $-(2\Delta\Delta C_q)$ method using Bio-Rad CfX manager software and normalized to the expression levels of amanitin resistant (*ama-1*) and actin (*act-2*).

2.18. Statistics. Values are presented as mean ± standard error of means (SEM). Statistical analyses were performed by applying Student's t-test (Prism 8.0 GraphPad Software, San Diego, CA, USA). Statistical significance was defined for p values $^*p < 0.05$, $^{**}p < 0.01$, $^{***}p < 0.001$, and $^{****}p < 0.0001$.

3. Results

3.1. Paraquat Reduces the Survival under Heat-Stress and Lifespan at 20°C. A screening of various paraquat concentrations showed a dose-dependent decline in heat-stress resistance of nematodes (Figure 1(a)). Exposure to 5 mM paraquat, a concentration which caused a significant

(a)

(b)
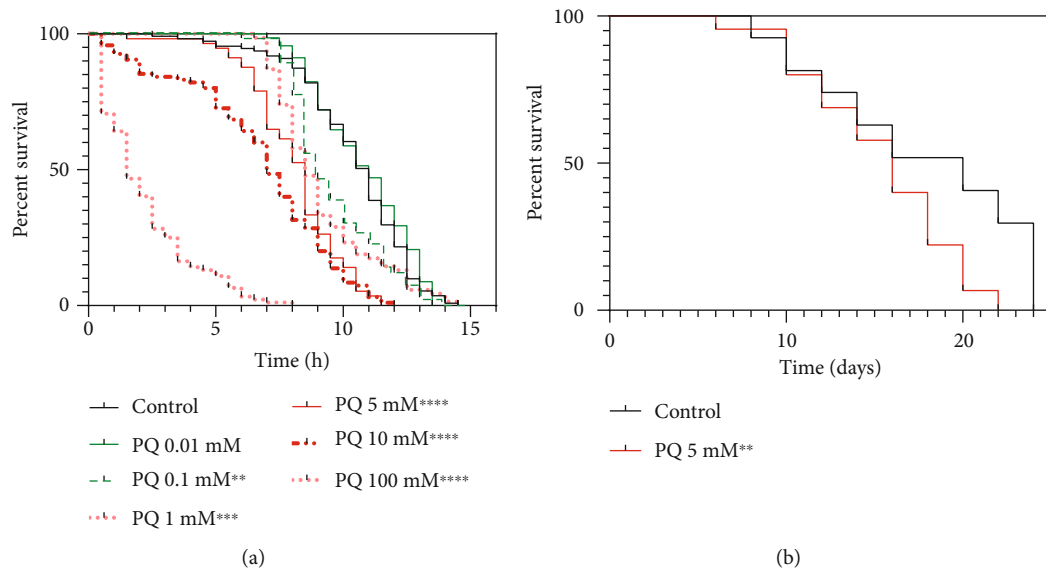
FIGURE 1: Heat-stress resistance and lifespan of C. elegans are reduced under paraquat exposure. (a) Survival at 37°C was assessed due to the penetration of SYTOX™ Green nucleic acid stain into dead cells. (b) Survival of wild-type C. elegans N2 at 20°C was assessed in the absence and presence of 5 mM paraquat. Log-rank (Mantel-Cox) test; $^{**}p < 0.01$, $^{***}p < 0.001$, and $^{****}p < 0.0001$.
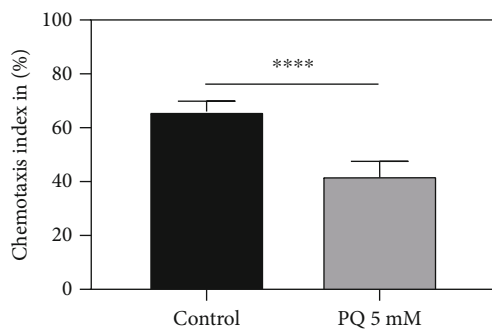
FIGURE 2: Chemotaxis index after treatment with 5 mM PQ for 48 h. $n = 5$; mean ± SEM; Student's t-test; $^{****}p < 0.0001$.

reduction of stress resistance, also caused a significant reduction in the nematode survival rate at 20°C (Figure 1(b)).

3.2. PQ Reduces Chemotaxis.
PQ significantly reduced nematode chemotaxis, resulting in a decreased ability to locate food. Animals insulted with 5 mM PQ appeared 24% less likely to locate the attractant diacetyl compared to control ($^{****}p < 0.0001$) (Figure 2).

3.3. Mitochondrial and Cytosolic ROS Measurement.
To evaluate the effect of PQ on ROS production in the cytosol and mitochondria, especially, of wild-type nematodes, they were stained with two fluorescent markers. MitoTracker® Red was applied to evaluate mitochondrial site of ROS generation and CM-H$_2$DCFDA for determination of cytosolic ROS (Figure 3).

PQ treatment increases mitochondrial ROS level significantly by 31.5% ($^{****}p < 0.0001$) and cytosolic ROS level by 19.4% ($^{****}p < 0.0001$) (Figure 4).

3.4. Effects of PQ on the Integrity of Mitochondria.
To elucidate the quality of mitochondria after Balch homogenization as well as the damaging impact of PQ (5 mM) on mitochondrial integrity, we conducted transmission electron mircospy. Figure 5 shows two representative pictures of mitochondria from control nematodes and those treated with 5 mM. As visualized, PQ causes a significant damage of mitochondria, as evidenced by disrupted membranes and loss of crista structure. Exemplary pointers indicate the different degrees of damage as described in Material and Methods. In brief, "intact" (a), mildly "fractured" (b), "heavily fractured" (c), and "fractured" (d) (Figure 5).

Treatment with PQ resulted in a significantly lower number of fully intact and mildly fractured mitochondria compared to the control. For the heavily fractured category, no significant differences could be observed between the two groups, while the number of fragmented mitochondria significantly increased (Figure 6).

3.5. Effect of PQ on Mitochondrial Function.
To ensure mitochondrial integrity, its membrane potential ($\Delta\Psi$m) was measured over the course of 130 minutes after isolation with fluorescent dye rhodamine 123 (Rh123). Addition of 500 nM carbonyl cyanide-4-(trifluoromethoxy)phenylhydrazone (FCCP), at three different time points to aliquots of the same isolation, was used to depolarize the inner mitochondrial membrane and to abolish $\Delta\Psi$m, after 30, 60, and 120 minutes [34]. Figure 7(a) shows a maximum fluorescence of Rh123 alone and a constant signal after quenching of the fluorescent dye in intact mitochondria beyond the time point of 60 minutes and slowly increasing afterwards. Addition of FCCP depolarizes $\Delta\Psi$m resulting in an increased Rh123 signal after all time points to the same level.

PQ (5 mM) significantly decreased $\Delta\Psi$m by 49% compared to the control (Figure 7(b)). PQ impaired the
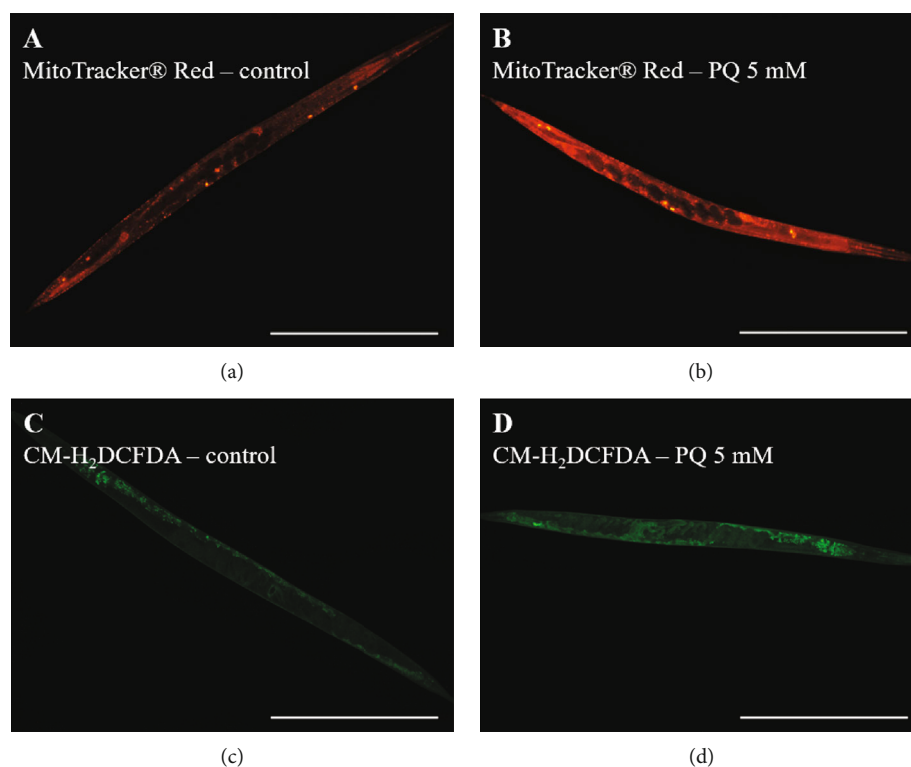
FIGURE 3: Nematodes, stained with MitoTracker® Red (a, b) for mitochondrial and with CM-H$_2$DCFDA (c, d) for cytosolic site of ROS generation, treated for 4 h in the absence (control) or presence of 5 mM PQ. Scaling bar is 400 μM.
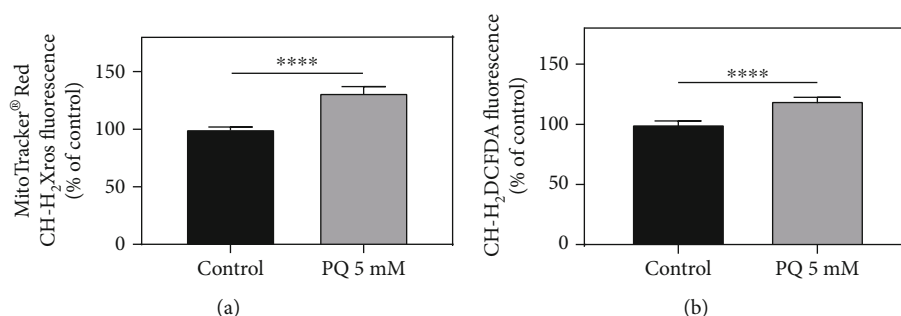
FIGURE 4: Paraquat (5 mM) increases mitochondrial and cytosolic ROS level in wild-type nematodes after 4 h of exposure. (a) MitoTracker® Red (CM-H$_2$Xros) was used to determine mitochondrial and (b) CM-H$_2$DCFDA for cytosolic ROS production. Mean ± SEM; Student's t-test; ****$p < 0.0001$.

mitochondrial respiratory chain and significantly reduced the activity of CI, CII, and CIV (Figure 7(c)).

The ratio between ETS and leak respiration after oligomycin addition, known as respiratory control ratio (RCR), is an accepted indicator of an increased proton gradient for ATP synthesis via complex V [37]. RCR was not altered after PQ incubation (data not shown).

The activity of citrate synthase (CS), as part of the Krebs cycle, is an established mitochondrial matrix marker [40]. PQ significantly reduced CS activity (Figure 7(d)) indicating a reduced mitochondrial mass [41].

3.6. PQ Decreases the Levels of Pyruvate and Lactate. Next, effects on energy metabolites were determined. Although

PQ significantly impaired $\Delta\Psi$m, respiratory chain, and mitochondrial integrity, ATP levels were not significantly reduced (Figure 8(a)). The energetic metabolites pyruvate and lactate were significantly decreased (Figures 8(b) and 8(c)). The decline of lactate was stronger than the reduction of pyruvate, resulting in a significantly decreased lactate/pyruvate ratio after PQ treatment (Figure 8(d)), indicating a lower glycolytic turnover [42].

3.7. PQ Causes an Upregulation of Genes Relevant for Longevity and Mitochondrial Biogenesis. PQ affected the expression levels of several longevity- and mitochondrial biogenesis-related genes in *C. elegans*. The ortholog of human forkhead box O1 *daf-16* known to be relevant for

(a)   (b)
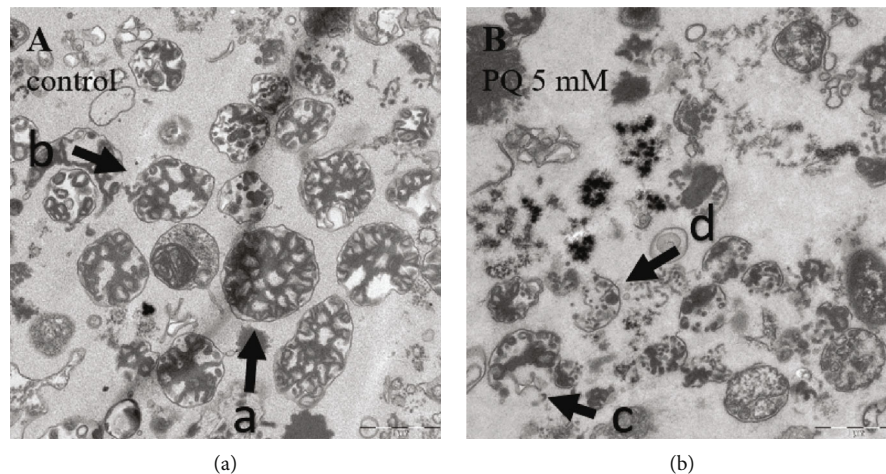
Figure 5: Transmission electron microscopic pictures of isolated mitochondria from C. elegans treated for 48 h in the absence (a; control) or presence of 5 mM PQ (b). Degrees of damage are indicated by exemplary pointers (A = "intact"; B = "mildly fractured"; C = "heavily fractured"; and D = "fractured").
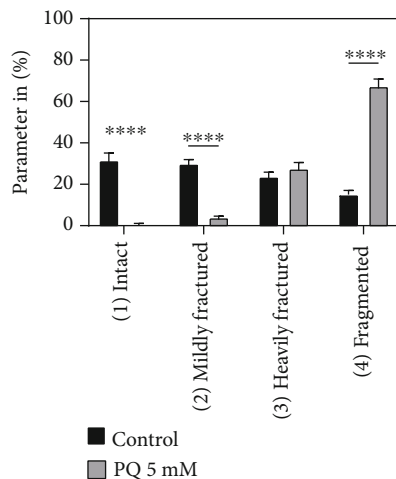
Figure 6: Mitochondria isolated from nematodes after a 48 h incubation in the absence (control) or presence of 5 mM PQ were assessed by transmission electron microscopy and categorized into four categories (intact, mildly fractured, heavily fractured, and fragmented) as described in Material and Methods. Mean ± SEM; Student's t-test; $****p < 0.0001$.

stress resistance, was insignificantly increased by 7%, likewise to *aak-2* (AMP-activated kinase) which was increased by 17% at its transcript level. *Sir-2.1*, which also plays a prominent role for longevity and stress-resistance and encodes an ortholog of human Sirtuin 1, was significantly increased by 73%. Marker genes for mitochondrial biogenesis, i.e., *skn-1*, *atfs-1*, and *atp-2*, were all significantly upregulated at the mRNA level by paraquat (Figure 9).

4. Discussion

C. elegans represents a well-established model especially for investigations of longevity and genetic variations [43–46]. Mitochondria have been unravelled as organelles with a great

impact on longevity and stress resistance [47]. While mitochondrial investigations in nematodes are conducted predominantly using fluorescent staining methods [48–50], mitochondrial isolation protocols are scarce [43]. In this study, we not only present data supporting the connection between mitochondrial function and longevity but also an easy and suitable way to isolate functional mitochondria. Questions concerned with the organelles' function are more distinct in a cell-free environment, free from intervening influences [28].

Paraquat (PQ) was used to induce oxidative stress resulting in mitochondrial dysfunction to display significant effects on the nematodes' lifespan and their respiratory chain capacity. PQ represents a known stress inducer impairing all respiratory chain complexes but most prominently complex I. In a reduced state, it uses oxygen as an oxidant producing the radical superoxide, mediating PQ toxicity [51]. PQ has been commonly used to trigger mitochondrial stress and dysfunction in *C. elegans* [52], as well as to reduce lifespan [53], and was therefore preferred over other known inducers of oxidative stress, as for example juglone, creating ROS through an increased apoptosis [54], or rotenone which specifically blocks complex I and therefore is commonly used for Parkinson's disease models [55].

Our goal was to identify links and causalities between mitochondrial dysfunction and a reduced lifespan and healthspan, as well as to establish a platform for future investigations concerned with potentially beneficial effects of nutrients or pharmaceuticals. We used a Balch Homogenizer and confirmed that the use of this technique represents a highly efficient and powerful tool to isolate mitochondrial fractions with a high quality [34].

4.1. Linking Longevity and Mitochondrial Function. In different experimental settings, various concentrations of PQ ranging from 0.2 to 25 mM were used [56–59]. Thus, identifying an optimal concentration for our investigations was the initial step. In a heat-stress resistance assay, we tested PQ

(a)

(b)

(c)

(d)
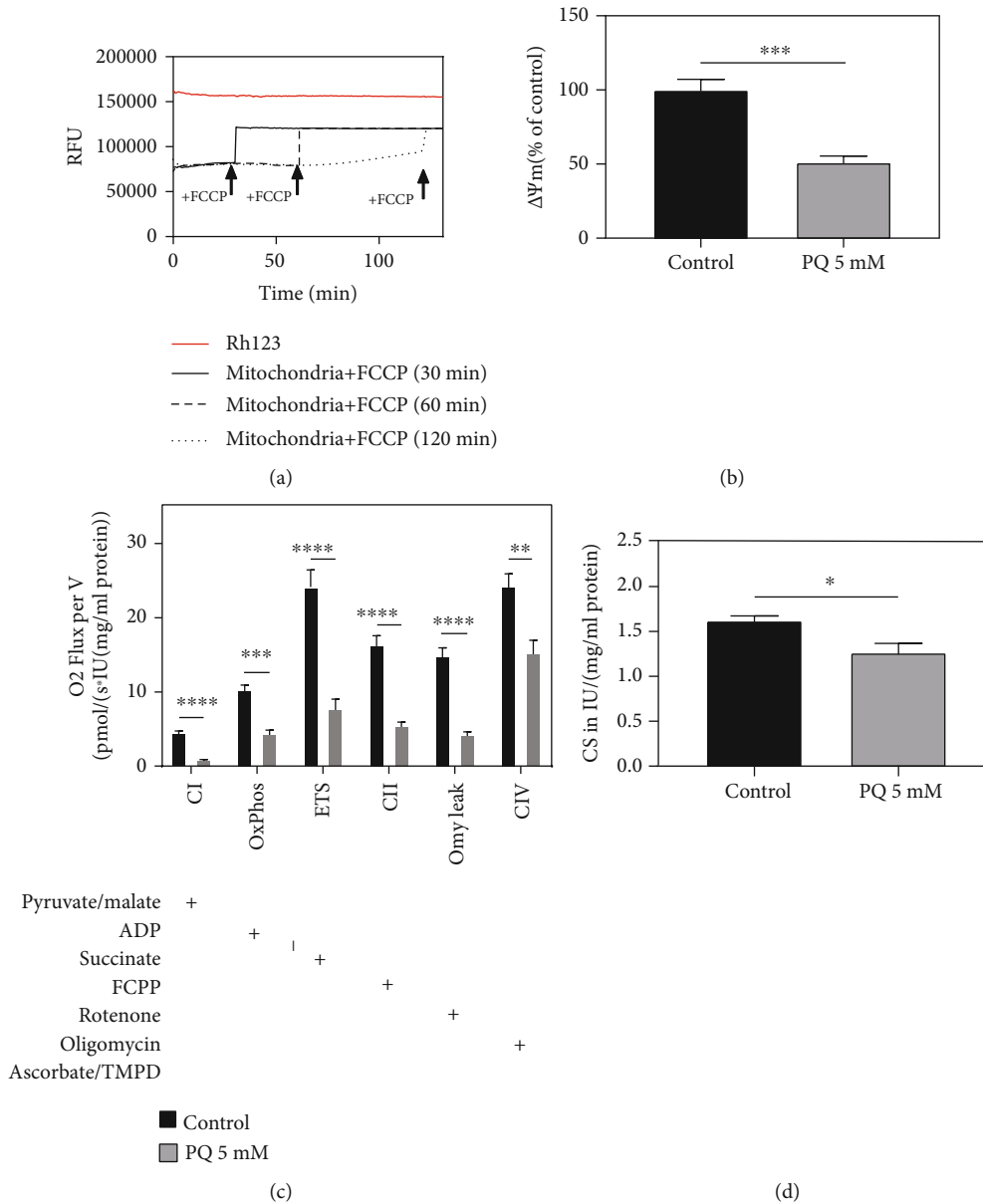
FIGURE 7: (a) Mitochondrial membrane potential ($\Delta\Psi$m) over 130 minutes assessed by fluorescent dye rhodamine 123 (Rh123). Short circuit of $\Delta\Psi$m was achieved by the addition of FCCP after 30, 60, and 120 minutes. (b) $\Delta\Psi$m (MMP), assessed by mitochondria-dependent increase of Rh123 fluorescence in percentage, after PQ treatment (5 mM) for 48 h, detected with a ClarioStar Plate Reader (BMG, Ortenberg, Germany). (c) Respiration of isolated mitochondria from C. elegans normalized to (d) citrate synthase activity in international units IU/(mg/mL protein). Activity of respiration complexes was measured using an O2k Oxygraph (Oroboros, Innsbruck, Austria). Addition of substances into the Oxygraph's chambers is indicated with a plus sign (+). Mean ± SEM; Student's t-test; $^*p < 0.05$, $^{**}p < 0.01$, $^{***}p < 0.001$, and $^{****}p < 0.0001$.

concentrations ranging from 0.01 mM to 100 mM to establish their effects on the nematodes' survival at 37°C. A concentration-dependent decline in the nematodes' ability to tolerate heat stress of 37°C could be observed. In our experiments, a concentration of 5 mM PQ was the lowest to reach a level of significance of $^{****}p < 0.0001$, lowering the median survival from 11 h to 8.5 h and was therefore selected for the following investigations. Interestingly, even though not significant, PQ at a concentration of 0.01 mM led to a slightly increased tolerance of heat stress in wild-type nematodes. To validate PQ 5 mM, as a concentration high enough

to alter the nematodes' lifespan, supposedly through mitochondrial stress, we tested this concentration in a survival experiment under physiological conditions. Again, PQ significantly decreased the nematodes' survival by 20% ($^{**}p = 0.0026$) compared to control.

Similar to our results, Wu et al. used PQ as an oxidative stressor in an thermotolerance assay, resulting in a reduced survival time of nematodes [59]. While PQ is often used to generate oxidative stress [60], to our best knowledge, the effect of sole PQ exposure on nematode survival under physiological conditions has only been investigated with a
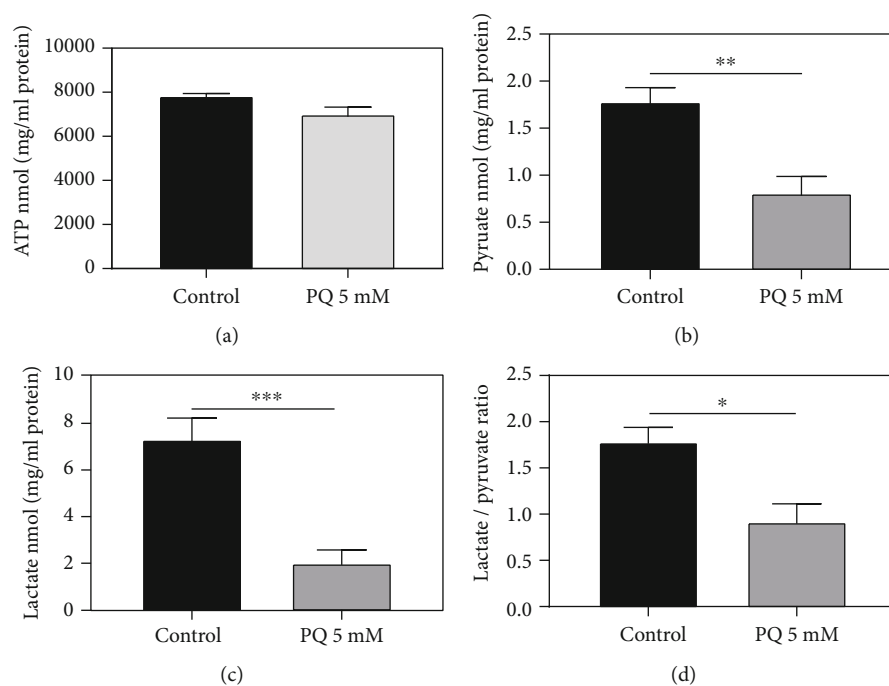
FIGURE 8: Determination of intracellular ATP levels (a), pyruvate (b), lactate (c), and lactate/pyruvate ratio (d) of wild-type C. elegans exposed to PQ (5 mM) or not (control). ATP levels were assessed using an ATPlite luminescence assay, and lactate and pyruvate using two colorimetric assay kits. Values were normalized to protein concentrations. $n = 8$; Mean ± SEM; Student's t-test; $^*p < 0.05$, $^{**}p < 0.01$, and $^{***}p < 0.001$.

concentration of 0.25 mM [58]. This low-dose exposure resulted in an extended lifespan, comparable to our heat-stress survival assay, showing a slightly increased stress resistance after 0.01 mM PQ exposure, suggesting a mitohormetic effect [61, 62]. Generally, a close relation between elevated reactive oxygen species and shortened lifespan expectancy can be drawn throughout investigations and species [63, 64], which is in line with our findings.

Nematodes retrieve their food through chemotaxis [33, 65]. Mitochondrial dysfunction not only effects longevity as such but also impairs neuronal function and consequently the animals' sensory ability of tracking food. This closely links chemotaxis and longevity through cellular and neuronal impairment caused by oxidative stress [66]. PQ significantly decreased chemotaxis in *C. elegans*, thus further strengthening the connection between mitochondrial dysfunction and longevity from another point of view. To our best knowledge, the effect of PQ on chemotaxis has never been invested but fits our previous findings and is coherent with the results of Wu et al. showing chemotaxis deficits caused through Aβ-mediated oxidative stress [67].

4.2. Isolation and Qualification of Isolated Nematode Mitochondria.
Mitochondrial investigations in *C. elegans* so far have mostly been restricted to measuring overall oxygen consumption, using, for example, an O2k Oxygraph from Oroboros, or fluorescent staining of whole cells or nematodes targeting ROS generation or membrane potentials [68–71]. Studies focusing on isolated mitochondria, however, have been scarce [43, 71]. Isolated mitochondria have distinct

advantages compared to whole cell or organism systems, since they allow investigations free from interfering organelles or cellular reactions and make it possible to draw direct causalities [27, 28]. A challenge is the nematodes' resilient cuticle making it hard to gather sufficient and especially efficient mitochondria. Several techniques have been described, ranging from grinding worms with a pestle after snap freezing in liquid nitrogen, "bead beating" with glass beads, to mechanically disrupting the nematodes' cuticle, or sonication. Nonetheless, each method suffers from one or more limitations. Grinding requires relatively large sample sizes, which are easily lost [72]. When applying "bead beating" or sonication, samples are prone to denaturation as samples heat up during the process and potentially damaging mitochondria [73]. Furthermore, sonication is unable to produce intact nucleic acids.

Balch homogenization is able to effectively break *C. elegans* cuticles of any stages [72]. The system is able to produce functional proteins, qRT-PCR quality mRNA, and intact mitochondria of a high quality and intactness. Through changeable ball clearance sizes, or number of syringe passes, homogenization roughness can be controlled [34, 74].

Mitochondria isolated with a 12 μm ball clearance appear more intact, after electron microscopy, compared to isolates gathered with a ball clearance leaving only a 6 μm gap (see Supp. 1). A semiquantitative and double-blinded counting validates the first impression and shows that especially percentage numbers in the "heavily fractured" (32%) and "fragmented" (25%) categories are higher for mitochondria isolated with a 6 μm ball clearance, compared to 12 μm. Here,
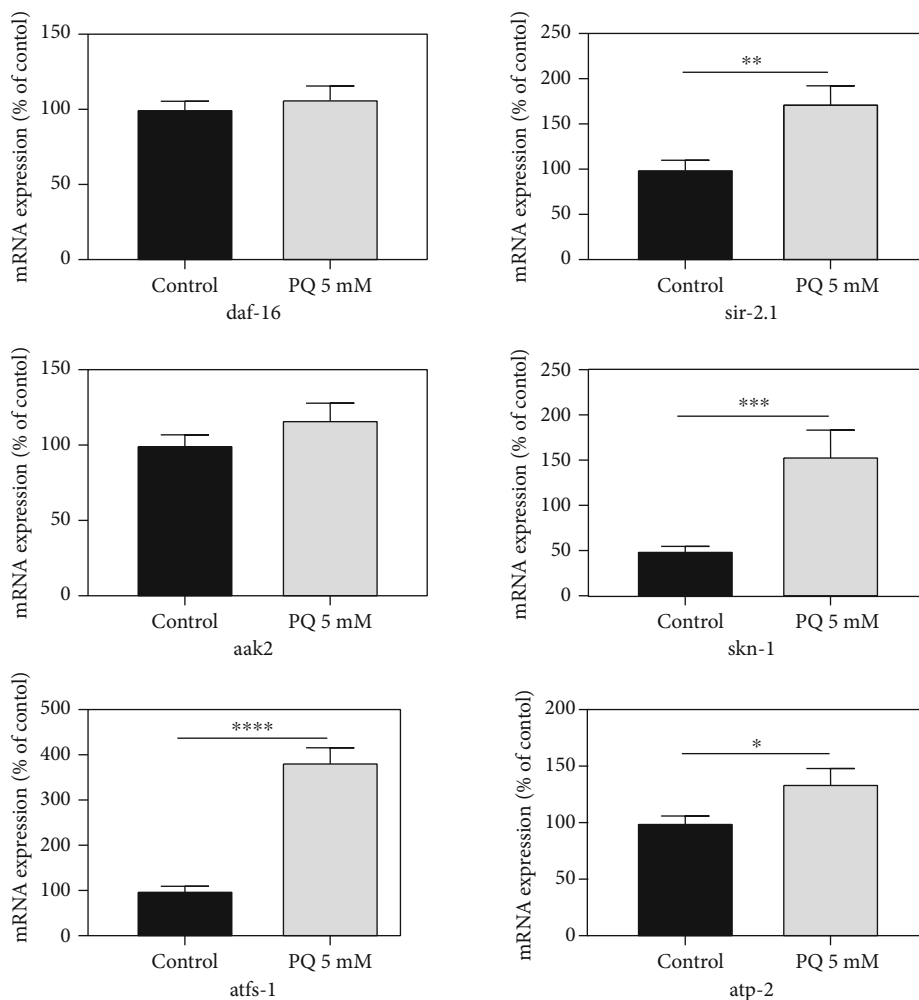
FIGURE 9: Relative normalized mRNA expression levels of longevity- and mitochondrial biogenesis-related genes daf-16, sir-2.1, aak-2, skn-1, atfs-1, and atp-2 in C. elegans in the absence or presence of PQ (5 mM); Mean ± SEM; Student's t-test; $^*p < 0.05$, $^{**}p < 0.01$, $^{***}p < 0.001$, and $^{****}p < 0.0001$; Results are normalized to the mRNA expression levels of amanitin resistant (ama-1) and actin (act-2).

only 24% was "heavily fractured" and 15% fragmented. Rougher homogenization using a $6\,\mu$m clearance results in only 15% fully intact mitochondria compared to 32% for a $12\,\mu$m clearance (see Supp. 2).

The applicability of isolation of mitochondria with a $12\,\mu$m clearance was further evidenced by addition of cytochrome c which would enter, if fractured, the outer mitochondrial membrane resulting in an increased respiration rate [75]. No changes of respiration, however, could be observed after isolation with a $12\,\mu$m clearance, supporting the integrity of the outer membrane, whereas a significant increase in respirational flux was measured after isolation with a $6\,\mu$m clearance (see Supp. 3).

Since none of our described experimental procedures takes more than 30 minutes after isolation, mitochondrial stability over that time period needed to be ensured. We could demonstrate a stable $\Delta\Psi$m over more than 60 minutes giving more than twice the time needed for all the experiments described. Furthermore, this verifies the $12\,\mu$m ball clearance and 5 strokes applied, as valid parameters to generate a sufficient and intact mitochondrial fraction, as

evidenced by transmission electron microscopy. Treatment of nematodes with 5 mM PQ, however, caused a significant increase in heavily fractured and fragmented mitochondria characterized by membrane rupture and damaged crista structure.

4.3. Impact of Paraquat on Mitochondrial Function. Paraquat at a concentration of 5 mM was identified to reduce significantly the stress resistance as well as longevity in wild-type nematodes. This was associated with a significantly reduced mitochondrial membrane potential ($\Delta\Psi$m) after 48 h. A similar decrease in $\Delta\Psi$m, after PQ treatment, was observed by Zhang et al. and Wu et al., while the latter also described a decreased expression of complex I, II, and III genes of the mitochondrial respiratory chain (ETC) [76, 77]. The latter findings are in line with the results of our respiration experiments, where PQ significantly decreased respiration rates of complex I and II. A decreased activity could be observed in our experiments also for the respiratory complexes CI and CII as well as for the OxPhos, ETS, and OmyLeak. Interestingly, complex IV was not altered in its activity. Citrate

synthase activity (CS) represents an established indicator for the mitochondrial mass [40]. Thus, the decreased CS activity in our experiments indicates that PQ reduced the mitochondrial mass. These results fit to reports describing a reduced respiratory capacity and a reduced mitochondrial mass after 4 mM PQ exposure in a PC12 cell model [78] or decreased respiration rates in zebra fish [79].

To validate an increased ROS generation by PQ as the reason for mitochondrial dysfunction, we investigated mitochondrial and also cytosolic ROS levels. Since PQ treatment for 48 h decreased intestinal pumping of nematodes causing an insufficient uptake of both fluorescent markers (data not shown), we had to decrease the time of exposure to 4 h. Nevertheless, also after this short incubation period, ROS levels at both locations were significantly increased which is in line with previous findings [14, 58, 59, 80, 81].

According to the observed dysfunction of mitochondria, it appeared reasonable to suggest that PQ causes limitations in the generation of ATP and by the accumulation of substrates also reduces the glycolytic flux. Interestingly, only slightly decreased ATP concentrations were found. This might be explained by the increased ATP synthase activity as a consequence of enhanced *atp-2* mRNA levels observed here. Significant ATP depletion of approximately 20% was found, however, at higher concentrations of 10 mM PQ in nematodes [76]. Pyruvate and lactate levels, however, were significantly decreased after PQ insult in our studies. Similar results have already been shown for glycolytic metabolites after PQ exposure in SK-N-SH cells [82].

To elaborate genetic pathways affected by PQ exposure, we assessed the mRNA levels of *daf-16*, *aak-2*, and *sir-2.1*, three genes with relevance for longevity and stress-resistance longevity [70, 77, 78]. While *daf-16* and *aak-2* were only slightly elevated due to PQ, expression of the human Sirtuin 1 ortholog *sir-2.1* was significantly increased by 73%. *Daf-16* as key modulator of longevity in *C. elegans*, is activated, amongst others, by *sir-2.1* and *aak-2* [83]. The lack of enhanced expression of *daf-16* lets us suggest that the enhanced expression of *sir-2.1* is not sufficient to activate *daf-16* expression in the presence of PQ. However, another gene important for stress resistance and also for mitogenesis, which was found to be significantly upregulated, is the *nrf-2* homolog *skn-1*. *Skn-1* upregulation was also found to increase the activity of PGC1α, the mammalian key regulator of mitogenesis, which, however, has no direct homolog in the nematode [50, 84]. Adaptations to compensate for the PQ-induced stress are evident finally also by enhanced expression of *atfs-1*, a key regulator of mitochondrial unfolded protein response (UPR^{mt}).

5. Conclusions

Using paraquat as a stressor, we here describe the close association of oxidative stress, restricted energy metabolism, reduced stress resistance, and longevity in the nematode *Caenorhabditis elegans*, focusing on isolated mitochondria, making it a readily accessible *in vivo* model for mitochondrial dysfunction.

Data Availability

The dataset generated during this study is available from the corresponding author on reasonable request.

Conflicts of Interest

The authors declare that they have no conflict of interest.

Acknowledgments

Supplementary Materials

Supp.1: transmission electron microscopic pictures of mitochondria from C. elegans isolated with a 12 μm (A) or 6 μm ball clearance (B). Degrees of damage are indicated by exemplary pointers (a = "intact"; b = "mildly fractured"; c = "heavily fractured"; and d = "fractured"). Supp. 2: mitochondria isolated from nematodes with 12 μm or 6 μm clearance were assessed by transmission electron microscopy and categorized into four categories (intact, mildly fractured, heavily fractured, and fragmented) as described in Material and Methods. Isolation with 6 μm ball clearance resulted in significantly less intact as well as more fragmented mitochondria. Mean ± SEM; Student's *t*-test; $^*p < 0.05$, $^{**}p < 0.01$. Supp. 3: cytochrome c addition, as a marker for intactness of the outer mitochondrial membrane, increases respiration after isolation with a 6 μm compared to a 12 μm clearance, indicating a fractured outer membrane. $n = 5$; Mean ± SEM; Students *t*-test; $^{***}p < 0.001$. *(Supplementary Materials)*

References

[1] P.-P. Tan, B.-H. Zhou, W.-P. Zhao, L. S. Jia, J. Liu, and H. W. Wang, "Mitochondria-mediated pathway regulates C2C12 cell apoptosis induced by fluoride," *Biological Trace Element Research*, vol. 185, no. 2, pp. 440–447, 2018.

[2] J. L. Aguilar-Lopez, R. Laboy, F. Jaimes-Miranda, E. Garay, A. DeLuna, and S. Funes, "Slm35 links mitochondrial stress response and longevity through TOR signaling pathway," *Aging*, vol. 8, no. 12, pp. 3255–3271, 2016.

[3] A. Raffaello and R. Rizzuto, "Mitochondrial longevity pathways," *Biochimica et Biophysica Acta*, vol. 1813, no. 1, pp. 260–268, 2011.

[4] T. Finkel, "The metabolic regulation of aging," *Nature Medicine*, vol. 21, no. 12, pp. 1416–1423, 2015.

[5] H.-W. Chang, S. Pisano, A. Chaturbedi et al., "Transcription factors CEP-1/p53 and CEH-23 collaborate with AAK-2/AMPK to modulate longevity in Caenorhabditis elegans.," *Aging Cell*, vol. 16, no. 4, pp. 814–824, 2017.

[6] Y. Wang and S. Hekimi, "Mitochondrial dysfunction and longevity in animals: untangling the knot," *Science*, vol. 350, no. 6265, pp. 1204–1207, 2015.

[7] B. Dilberger, M. Passon, H. Asseburg et al., "Polyphenols and metabolites enhance survival in rodents and nematodes-impact of mitochondria," *Nutrients*, vol. 11, no. 8, p. 1886, 2019.

[8] D. Harman, "Aging: a theory based on free radical and radiation chemistry," *Journal of Gerontology*, vol. 11, no. 3, pp. 298–300, 1956.

[9] A. Y. Seo, A. M. Joseph, D. Dutta, J. C. Y. Hwang, J. P. Aris, and C. Leeuwenburgh, "New insights into the role of mitochondria in aging: mitochondrial dynamics and more," *Journal of Cell Science*, vol. 123, no. 15, pp. 2533–2542, 2010.

[10] D. Harman, "The biologic clock: the mitochondria?," *Journal of the American Geriatrics Society*, vol. 20, no. 4, pp. 145–147, 1972.

[11] R. S. Balaban, S. Nemoto, and T. Finkel, "Mitochondria, oxidants, and aging," *Cell*, vol. 120, no. 4, pp. 483–495, 2005.

[12] W. Yang and S. Hekimi, "A mitochondrial superoxide signal triggers increased longevity in Caenorhabditis elegans," *PLoS Biology*, vol. 8, no. 12, p. e1000556, 2010.

[13] J. M. Copeland, J. Cho, T. Lo Jr. et al., "Extension of _Drosophila_ Life Span by RNAi of the Mitochondrial Respiratory Chain," *Current Biology*, vol. 19, no. 19, pp. 1591–1598, 2009.

[14] S. W. Smith, L. C. Latta, D. R. Denver, and S. Estes, "Endogenous ROS levels in C. elegans under exogenous stress support revision of oxidative stress theory of life-history tradeoffs," *BMC Evolutionary Biology*, vol. 14, no. 1, p. 161, 2014.

[15] A. Dillin, A. L. Hsu, N. Arantes-Oliveira et al., "Rates of behavior and aging specified by mitochondrial function during development," *Science*, vol. 298, no. 5602, pp. 2398–2401, 2002.

[16] P. A. Kirchman, S. Kim, C. Y. Lai, and S. M. Jazwinski, "Interorganelle signaling is a determinant of longevity in Saccharomyces cerevisiae," *Genetics*, vol. 152, no. 1, pp. 179–190, 1999.

[17] S. S. Lee, R. Y. N. Lee, A. G. Fraser, R. S. Kamath, J. Ahringer, and G. Ruvkun, "A systematic RNAi screen identifies a critical role for mitochondria in _C. elegans_ longevity," *Nature Genetics*, vol. 33, no. 1, pp. 40–48, 2003.

[18] X. Liu, N. Jiang, B. Hughes, E. Bigras, E. Shoubridge, and S. Hekimi, "Evolutionary conservation of the clk-1-dependent mechanism of longevity: loss of mclk1 increases cellular fitness and lifespan in mice," *Genes & Development*, vol. 19, no. 20, pp. 2424–2434, 2005.

[19] W. B. Wood, *The Nematode Caenorhabditis Elegans*, Cold Spring Harbor Laboratory, Cold Spring Harbor, N.Y, 1988.

[20] J. Gruber, C. B. Chen, S. Fong, L. F. Ng, E. Teo, and B. Halliwell, "Caenorhabditis elegans: what we can and cannot learn from aging worms," *Antioxidants & Redox Signaling*, vol. 23, no. 3, pp. 256–279, 2015.

[21] S. Schmeisser, K. Schmeisser, S. Weimer et al., "Mitochondrial hormesis links low-dose arsenite exposure to lifespan extension," *Aging Cell*, vol. 12, no. 3, pp. 508–517, 2013.

[22] K. Burkewitz, Y. Zhang, and W. B. Mair, "AMPK at the nexus of energetics and aging," *Cell Metabolism*, vol. 20, no. 1, pp. 10–25, 2014.

[23] A. M. Nargund, M. W. Pellegrino, C. J. Fiorese, B. M. Baker, and C. M. Haynes, "Mitochondrial import efficiency of ATFS-1 regulates mitochondrial UPR activation," *Science*, vol. 337, no. 6094, pp. 587–590, 2012.

[24] T. J. Schulz, K. Zarse, A. Voigt, N. Urban, M. Birringer, and M. Ristow, "Glucose restriction extends _Caenorhabditis elegans_ life span by inducing mitochondrial respiration and increasing oxidative stress," *Cell Metabolism*, vol. 6, no. 4, pp. 280–293, 2007.

[25] N. Ventura, S. L. Rea, A. Schiavi, A. Torgovnick, R. Testi, and T. E. Johnson, "p53/CEP-1 increases or decreases lifespan, depending on level of mitochondrial bioenergetic stress," *Aging Cell*, vol. 8, no. 4, pp. 380–393, 2009.

[26] L. Walter, A. Baruah, H. W. Chang, H. M. Pace, and S. S. Lee, "The homeobox protein CEH-23 mediates prolonged longevity in response to impaired mitochondrial electron transport chain in C. elegans," *PLoS Biology*, vol. 9, no. 6, p. e1001084, 2011.

[27] C. Frezza, S. Cipolat, and L. Scorrano, "Organelle isolation: functional mitochondria from mouse liver, muscle and cultured filroblasts," *Nature Protocols*, vol. 2, no. 2, pp. 287–295, 2007.

[28] K.-M. Debatin, D. Poncet, and G. Kroemer, "Chemotherapy: targeting the mitochondrial cell death pathway," *Oncogene*, vol. 21, no. 57, pp. 8786–8803, 2002.

[29] S. Brenner, "The genetics of Caenorhabditis elegans," *Genetics*, vol. 77, no. 1, pp. 71–94, 1974.

[30] T. Stiernagle, "Maintenance of C. elegans," *C. elegans*, vol. 2, pp. 51–67, 1999.

[31] F. R. G. Amrit, R. Ratnappan, S. A. Keith, and A. Ghazi, "The _C. elegans_ lifespan assay toolkit," *Methods*, vol. 68, no. 3, pp. 465–475, 2014.

[32] E. Fitzenberger, D. J. Deusing, C. Marx, M. Boll, K. Lüersen, and U. Wenzel, "The polyphenol quercetin protects the mev-1 mutant of Caenorhabditis elegans from glucose-induced reduction of survival under heat-stress depending on SIR-2.1, DAF-12, and proteasomal activity," *Molecular Nutrition & Food Research*, vol. 58, no. 5, pp. 984–994, 2014.

[33] O. Margie, C. Palmer, and I. Chin-Sang, "C. elegans chemotaxis assay," *JoVE (Journal of Visualized Experiments)*, vol. 74, article e50069, 2013.

[34] S. Schmitt, F. Saathoff, L. Meissner et al., "A semi-automated method for isolating functionally intact mitochondria from cultured cells and tissue biopsies," *Analytical Biochemistry*, vol. 443, no. 1, pp. 66–74, 2013.

[35] W. E. Balch and J. E. Rothman, "Characterization of protein transport between successive compartments of the Golgi apparatus: asymmetric properties of donor and acceptor activities in a cell-free system," *Archives of Biochemistry and Biophysics*, vol. 240, no. 1, pp. 413–425, 1985.

[36] S. Stadlmann, K. Renner, J. Pollheimer et al., "Preserved coupling of oxidative phosphorylation but decreased mitochondrial respiratory capacity in IL-1beta-treated human peritoneal mesothelial cells," *Cell Biochemistry and Biophysics*, vol. 44, no. 2, pp. 179–186, 2006.

[37] S. Hagl, A. Kocher, C. Schiborr et al., "Rice bran extract protects from mitochondrial dysfunction in guinea pig brains," *Pharmacological Research*, vol. 76, pp. 17–27, 2013.

[38] E. Hutter, K. Renner, G. Pfister, P. Stöckl, P. Jansen-Dürr, and E. Gnaiger, "Senescence-associated changes in respiration and oxidative phosphorylation in primary human fibroblasts," *The Biochemical Journal*, vol. 380, pp. 919–928, 2004.

[39] A. V. Kuznetsov, D. Strobl, E. Ruttmann, A. Königsrainer, R. Margreiter, and E. Gnaiger, "Evaluation of mitochondrial respiratory function in small biopsies of liver," *Analytical Biochemistry*, vol. 305, no. 2, pp. 186–194, 2002.

[40] S. Larsen, J. Nielsen, C. N. Hansen et al., "Biomarkers of mitochondrial content in skeletal muscle of healthy young human

subjects," *The Journal of Physiology*, vol. 590, no. 14, pp. 3349–3360, 2012.

[41] R. Rabøl, S. Larsen, P. M. V. Højberg et al., "Regional anatomic differences in skeletal muscle mitochondrial respiration in type 2 diabetes and obesity," *The Journal of Clinical Endocrinology and Metabolism*, vol. 95, no. 2, pp. 857–863, 2010.

[42] S. Yanase, H. Suda, K. Yasuda, and N. Ishii, "Impaired p53/CEP-1 is associated with lifespan extension through an age-related imbalance in the energy metabolism of C. elegans," *Genes to Cells*, vol. 22, no. 12, pp. 1004–1010, 2017.

[43] N. Castelein, M. Muschol, I. Dhondt et al., "Mitochondrial efficiency is increased in axenically cultured _Caenorhabditis elegans_," *Experimental Gerontology*, vol. 56, pp. 26–36, 2014.

[44] E. Fitzenberger, D. J. Deusing, A. Wittkop et al., "Effects of plant extracts on the reversal of glucose-induced impairment of stress-resistance in Caenorhabditis elegans," *Plant Foods for Human Nutrition*, vol. 69, no. 1, pp. 78–84, 2014.

[45] H. J. Weir, P. Yao, F. K. Huynh et al., "Dietary restriction and AMPK increase lifespan via mitochondrial network and peroxisome remodeling," *Cell Metabolism*, vol. 26, no. 6, pp. 884–896.e5, 2017.

[46] The C elegans Sequencing Consortium, "Genome sequence of the nematode C. elegans: a platform for investigating biology," *Science*, vol. 282, no. 5, pp. 2012–2018, 1998.

[47] S. Tan and E. Wong, "Mitophagy transcriptome: mechanistic insights into polyphenol-mediated mitophagy," *Oxidative Medicine and Cellular Longevity*, vol. 2017, Article ID 9028435, 2017.

[48] E. F. Fang, T. B. Waltz, H. Kassahun et al., "Tomatidine enhances lifespan and healthspan in C. elegans through mitophagy induction via the SKN-1/Nrf2 pathway," *Scientific reports*, vol. 7, 2017.

[49] T. Heidler, K. Hartwig, H. Daniel, and U. Wenzel, "Caenorhabditis elegans lifespan extension caused by treatment with an orally active ROS-generator is dependent on DAF-16 and SIR-2.1," *Biogerontology*, vol. 11, no. 2, pp. 183–195, 2010.

[50] K. Palikaras, E. Lionaki, and N. Tavernarakis, "Coordination of mitophagy and mitochondrial biogenesis during ageing in _C. elegans_," *Nature*, vol. 521, no. 7553, pp. 525–528, 2015.

[51] H. M. Cocheme and M. P. Murphy, "Complex I is the major site of mitochondrial superoxide production by paraquat," *The Journal of Biological Chemistry*, vol. 283, no. 4, pp. 1786–1798, 2008.

[52] R. J. Mockett, A. C. V. Bayne, L. K. Kwong, W. C. Orr, and R. S. Sohal, "Ectopic expression of catalase in _Drosophila_ mitochondria increases stress resistance but not longevity," *Free Radical Biology & Medicine*, vol. 34, no. 2, pp. 207–217, 2003.

[53] J. N. Sampayo, A. Olsen, and G. J. Lithgow, "Oxidative stress in Caenorhabditis elegans: protective effects of superoxide dismutase/catalase mimetics," *Aging Cell*, vol. 2, no. 6, pp. 319–326, 2003.

[54] J. Wu, H. Zhang, Y. Xu et al., "Juglone induces apoptosis of tumor stem-like cells through ROS-p38 pathway in glioblastoma," *BMC Neurology*, vol. 17, no. 1, 2017.

[55] M. Maulik, S. Mitra, A. Bult-Ito, B. E. Taylor, and E. M. Vayndorf, "Behavioral phenotyping and pathological indicators of Parkinson's disease in C. elegans models," *Frontiers in Genetics*, vol. 8, 2017.

[56] M. E. Lima, A. C. Colpo, W. G. Salgueiro, G. E. Sardinha, D. S. Avila, and V. Folmer, "Ilex paraguariensis extract increases lifespan and protects against the toxic effects caused by para-quat in Caenorhabditis elegans," *International Journal of Environmental Research and Public Health*, vol. 11, no. 10, pp. 10091–10104, 2014.

[57] M. Fujii, N. Tanaka, K. Miki, M. N. Hossain, M. Endoh, and D. Ayusawa, "Uncoupling of longevity and paraquat resistance in mutants of the NematodeCaenorhabditis elegans," *Bioscience, Biotechnology, and Biochemistry*, vol. 69, no. 10, pp. 2015–2018, 2005.

[58] A. B. Hwang, E.-A. Ryu, M. Artan et al., "Feedback regulation via AMPK and HIF-1 mediates ROS-dependent longevity in Caenorhabditis elegans," *Proceedings of the National Academy of Sciences of the United States of America*, vol. 111, no. 42, pp. E4458–E4467, 2014.

[59] M. Wu, X. Kang, Q. Wang, C. Zhou, C. Mohan, and A. Peng, "Regulator of G protein signaling-1 modulates paraquat-induced oxidative stress and longevity via the insulin like signaling pathway in _Caenorhabditis elegans_," *Toxicology Letters*, vol. 273, pp. 97–105, 2017.

[60] S.-I. Oh, J.-K. Park, and S.-K. Park, "Lifespan extension and increased resistance to environmental stressors by N-acetyl-L-cysteine in Caenorhabditis elegans," *Clinics*, vol. 70, no. 5, pp. 380–386, 2015.

[61] E. J. Calabrese, V. Calabrese, and J. Giordano, "The role of hormesis in the functional performance and protection of neural systems," *Brain Circulation*, vol. 3, no. 1, pp. 1–13, 2017.

[62] V. Calabrese, C. Cornelius, A. T. Dinkova-Kostova, E. J. Calabrese, and M. P. Mattson, "Cellular stress responses, the hormesis paradigm, and vitagenes: novel targets for therapeutic intervention in neurodegenerative disorders," *Antioxidants & Redox Signaling*, vol. 13, no. 11, pp. 1763–1811, 2010.

[63] A. Vikram, R. Anish, A. Kumar, D. N. Tripathi, and R. K. Kaundal, "Oxidative stress and autophagy in metabolism and longevity," *Oxidative Medicine and Cellular Longevity*, vol. 2017, Article ID 3451528, 3 pages, 2017.

[64] V. Marasco, A. Stier, W. Boner, K. Griffiths, B. Heidinger, and P. Monaghan, "Environmental conditions can modulate the links among oxidative stress, age, and longevity," *Mechanisms of Ageing and Development*, vol. 164, pp. 100–107, 2017.

[65] C. I. Bargmann, "Chemosensation in C. elegans," in *WormBook: The Online Review of C. elegans Biology*, WormBook, 2006.

[66] S. Maglioni, A. Schiavi, A. Runci, A. Shaik, and N. Ventura, "Mitochondrial stress extends lifespan in _C. elegans_ through neuronal hormesis," *Experimental Gerontology*, vol. 56, pp. 89–98, 2014.

[67] Y. Wu, Z. Wu, P. Butko et al., "Amyloid-beta-induced pathological behaviors are suppressed by Ginkgo biloba extract EGb 761 and ginkgolides in transgenic Caenorhabditis elegans," *The Journal of neuroscience : the official journal of the Society for Neuroscience*, vol. 26, no. 50, pp. 13102–13113, 2006.

[68] Y. J. Kwon, S. Guha, F. Tuluc, and M. J. Falk, "High-throughput BioSorter quantification of relative mitochondrial content and membrane potential in living _Caenorhabditis elegans_," *Mitochondrion*, vol. 40, pp. 42–50, 2018.

[69] B. P. Braeckman, A. Smolders, P. Back, and S. de Henau, "In vivo detection of reactive oxygen species and redox status in Caenorhabditis elegans," *Antioxidants & Redox Signaling*, vol. 25, no. 10, pp. 577–592, 2016.

[70] P. Gubert, B. Puntel, T. Lehmen et al., "Metabolic effects of manganese in the nematode _Caenorhabditis elegans_

through DAergic pathway and transcription factors activation," *Neurotoxicology*, vol. 67, pp. 65–72, 2018.

[71] J. R. Daniele, K. Heydari, E. A. Arriaga, and A. Dillin, "Identification and characterization of mitochondrial subtypes in Caenorhabditis elegans via analysis of individual mitochondria by flow cytometry," *Analytical Chemistry*, vol. 88, no. 12, pp. 6309–6316, 2016.

[72] S. Bhaskaran, J. A. Butler, S. Becerra, V. Fassio, M. Girotti, and S. L. Rea, "Breaking _Caenorhabditis elegans_ the easy way using the Balch homogenizer: an old tool for a new application," *Analytical Biochemistry*, vol. 413, no. 2, pp. 123–132, 2011.

[73] N. J. Szewczyk, R. L. Mancinelli, W. McLamb, D. Reed, B. S. Blumberg, and C. A. Conley, "Caenorhabditis elegans survives atmospheric breakup of STS-107, space shuttle Columbia," *Astrobiology*, vol. 5, no. 6, pp. 690–705, 2005.

[74] S. Schmitt, C. Eberhagen, S. Weber, M. Aichler, and H. Zischka, "Isolation of mitochondria from cultured cells and liver tissue biopsies for molecular and biochemical analyses," *Methods in Molecular Biology*, vol. 1295, pp. 87–97, 2015.

[75] M. Wikstrom and R. Casey, "The oxidation of exogenous cytochrome c by mitochondria," *FEBS Letters*, vol. 183, no. 2, pp. 293–298, 1985.

[76] J. Zhang, R. Shi, H. Li et al., "Antioxidant and neuroprotective effects of _Dictyophora indusiata_ polysaccharide in _Caenorhabditis elegans_," *Journal of Ethnopharmacology*, vol. 192, pp. 413–422, 2016.

[77] S. Wu, L. Lei, Y. Song et al., "Mutation of _hop-1_ and _pink-1_ attenuates vulnerability of neurotoxicity in _C. elegans_ : the role of mitochondria-associated membrane proteins in Parkinsonism," *Experimental Neurology*, vol. 309, pp. 67–78, 2018.

[78] Q. Zhou, H. Zhang, Q. Wu, J. Shi, and S. Zhou, "Pharmacological manipulations of autophagy modulate paraquat-induced cytotoxicity in PC12 cells," *International Journal of Biochemistry and Molecular Biology*, vol. 8, no. 2, pp. 13–22, 2017.

[79] X. H. Wang, C. L. Souders, Y. H. Zhao, and C. J. Martyniuk, "Paraquat affects mitochondrial bioenergetics, dopamine system expression, and locomotor activity in zebrafish (*Danio rerio*)," *Chemosphere*, vol. 191, pp. 106–117, 2018.

[80] K. Wang, S. Chen, C. Zhang et al., "Enhanced ROS production leads to excessive fat accumulation through DAF-16 in _Caenorhabditis elegans_," *Experimental Gerontology*, vol. 112, pp. 20–29, 2018.

[81] C. E. Schaar, D. J. Dues, K. K. Spielbauer et al., "Mitochondrial and cytoplasmic ROS have opposing effects on lifespan," *PLoS Genetics*, vol. 11, no. 2, p. e1004972, 2015.

[82] S. Lei, L. Zavala-Flores, A. Garcia-Garcia et al., "Alterations in energy/redox metabolism induced by mitochondrial and environmental toxins: a specific role for glucose-6-phosphate-dehydrogenase and the pentose phosphate pathway in paraquat toxicity," *ACS Chemical Biology*, vol. 9, no. 9, pp. 2032–2048, 2014.

[83] C. T. Murphy and P. J. Hu, "Insulin/insulin-like growth factor signaling in C. elegans," *WormBook: The Online Review of C. elegans Biology*, WormBook, 2005.

[84] J. R. Friedman and J. Nunnari, "Mitochondrial form and function," *Nature*, vol. 505, no. 7483, pp. 335–343, 2014.

Review Article

Mitophagy, Mitochondrial Dynamics, and Homeostasis in Cardiovascular Aging

Ne N. Wu [ID],[1,2] **Yingmei Zhang** [ID],[1,2] **and Jun Ren** [ID] [1,2,3]

[1]*Department of Cardiology, Zhongshan Hospital, Fudan University, China*
[2]*Shanghai Institute of Cardiovascular Diseases, Shanghai 200032, China*
[3]*Center for Cardiovascular Research and Alternative Medicine, University of Wyoming College of Health Sciences, Laramie, WY 82071, USA*

Correspondence should be addressed to Yingmei Zhang; zhangym197951@126.com and Jun Ren; jren@uwyo.edu

Biological aging is an inevitable and independent risk factor for a wide array of chronic diseases including cardiovascular and metabolic diseases. Ample evidence has established a pivotal role for interrupted mitochondrial homeostasis in the onset and development of aging-related cardiovascular anomalies. A number of culprit factors have been suggested in aging-associated mitochondrial anomalies including oxidative stress, lipid toxicity, telomere shortening, metabolic disturbance, and DNA damage, with recent findings revealing a likely role for compromised mitochondrial dynamics and mitochondrial quality control machinery such as autophagy. Mitochondria undergo consistent fusion and fission, which are crucial for mitochondrial homeostasis and energy adaptation. Autophagy, in particular, mitochondria-selective autophagy, namely, mitophagy, refers to a highly conservative cellular process to degrade and clear long-lived or damaged cellular organelles including mitochondria, the function of which gradually deteriorates with increased age. Mitochondrial homeostasis could be achieved through a cascade of independent but closely related processes including fusion, fission, mitophagy, and mitochondrial biogenesis. With improved health care and increased human longevity, the ever-rising aging society has imposed a high cardiovascular disease prevalence. It is thus imperative to understand the role of mitochondrial homeostasis in the regulation of lifespan and healthspan. Targeting mitochondrial homeostasis should offer promising novel therapeutic strategies against aging-related complications, particularly cardiovascular diseases.

1. Background

Biological aging is associated with a gradual decline in the organismal reproductive and regenerative capacity although a dramatic individual variation exists in the rate of decline [1]. To this end, chronological age may not be the best and authentic index for the prediction of individual health status. Healthspan offers an overlapping albeit distinct aging phenotype and is considered the ultimate goal for the elderly [2–4]. Maneuvers targeting the biological aging process are expected to ameliorate aging-related complications and improve well-being in the elderly [5]. According to the 2019 Statistical Update from the America Heart Association, cardiovascular disease (CVD) remains the leading cause of disability and death (17.6 million mortality in 2016, a 14.5% rise from

2006) with an expense predicted at $1.1 trillion in 2035 in the United States [6]. From a physiological perspective, intrinsic functional decline over time is expected to render the cardiovascular system more vulnerable to pathological stresses, resulting in a disproportionate prevalence of cardiovascular diseases with advanced age [7].

Cardiovascular aging refers to age-related deterioration of cardiovascular function and is manifested as the loss of myocardial contractile capacity including increased left ventricular (LV) wall thickness and chamber size, prolonged diastole [8, 9], as well as loss of compliance in LV wall and coronary vasculature, arterial stiffness, and endothelial dysfunction [8, 10–12]. Up to date, a number of theories have been postulated for the pathogenesis of aging-related cardiovascular dysfunction including oxidative stress, DNA damage, telomere
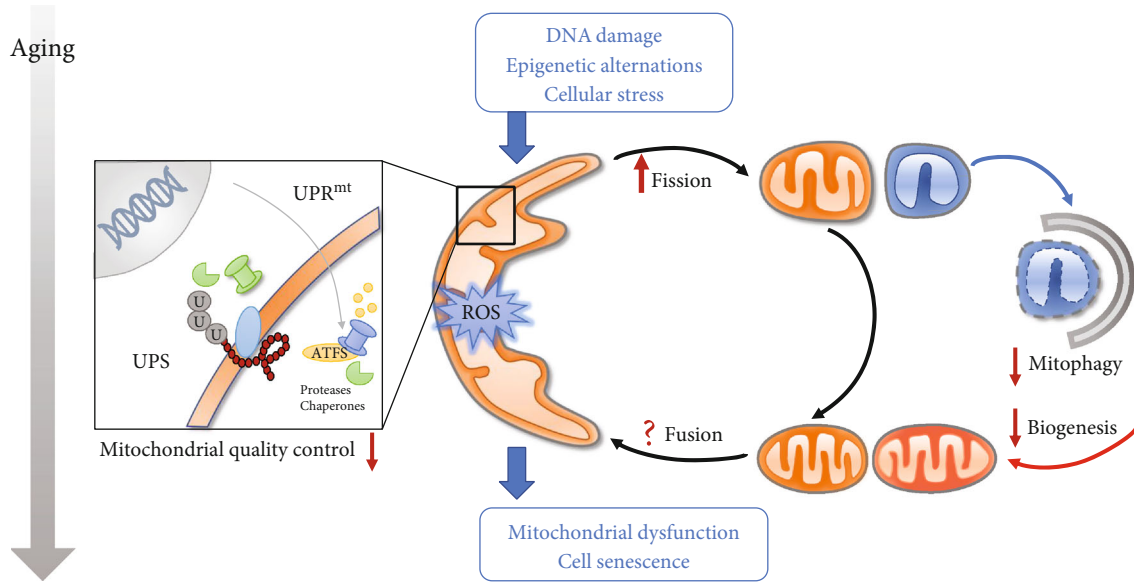
FIGURE 1: Unbalanced mitochondrial dynamics and turnover during aging. Mitochondrial homeostasis is maintained by a series of protective mechanisms. There is an overall decline of mitochondrial function with aging. A mitochondrial quality control system fails to repair mitochondrial defects. A mitochondrial network is progressively compromised due to loss of balanced mitochondrial fission and fusion. Inefficient mitophagy finally leads to buildup of dysfunctional mitochondria. UPS: ubiquitin-proteasome system; UPRmt: mitochondrial unfolded protein response.

shortening, genomic instability, epigenetic and metabolic disarray, inflammation, apoptosis, lipotoxicity, and mitochondrial injury [13–15], among which mitochondrial injury has received close attention over the past decades. Mitochondria are double-membraned organelles found in eukaryotic cells capable of producing adenosine triphosphate (ATP) utilized for nearly all of the biological processes. Mitochondria are entangled in multitasks beyond energy production, such as susceptibility to cell stress and cell fate determination [16]. With aging, mitochondria usually display a gradual although dramatic decline in abundance, integrity, dynamics, purging, and bioenergetic efficiency [17]. Defects in mitochondria are commonly reflected as accumulated mtDNA mutation, impaired metabolism, inflammatory responses, deformation (swelling and shrinkage), and cell senescence [17–21], thus contributing to a myriad of aging-related disease phenotypes, such as neurodegenerative diseases, metabolic disorders, cancer, and cardiovascular diseases [22–26]. Mitochondria make up nearly 1/3 of cellular volume and are vital for all cellular processes including metabolism, energy, intracellular Ca^{2+} handling, and redox homeostasis [27]. Disturbance in mitochondrial homeostasis under pathological stress leads to reactive oxygen species (ROS) production and energetic insufficiency, which further disrupt mitochondrial and cellular homeostasis into a vicious cycle [28]. The precise control of mitochondrial homeostasis through a well-orchestrated yet complex network of antioxidants, DNA repair, and mitochondrial quality control systems helps to maintain a pool of healthy and functional mitochondria [29]. Furthermore, mitochondria are highly dynamic and constantly undergo morphological changes between fission (division) and fusion in response to various metabolic and environmental cues. A fusion process assists to homogenize the contents of damaged

mitochondria resulting in mitochondrial elongation. Fission, on the other hand, leads to mitochondrial fragmentation and promotes clearance of damaged mitochondria through a form of selective autophagy-mitophagy [30]. Excessive or untimely fission or fusion may be detrimental to mitochondrial quality and mitochondrial homeostasis (Figure 1). The identification and manipulation of molecules involved in mitochondrial dynamics such as dynamin-related protein 1 (DRP1) and Fis1 have greatly added breadth to our understanding for mitochondria in biological particularly cardiovascular aging [31]. Intriguingly, an organism seems to be much more tolerant to poor mitochondrial efficiency than one would expect, and certain mitochondria-related deviations and modulations are proven to benefit healthspan [32]. In this minireview, we will highlight key components of mitochondrial fission-fusion, mitophagy, and mitochondrial homeostasis and their roles in the biology of aging and aging-related cardiovascular diseases. We used the key terms of "aging," "mitochondria," "quality control," and "mitophagy" as the key terms to search PubMed over the last 5 years.

2. Overview of Mitochondrial Fission-Fusion

Fission-fusion processes play a vital role in the dynamic regulation of mitochondria. In mammals, several dynamin-related GTPases participate in the mitochondrial fusion process: the mitofusins (Mfn1 and Mfn2) for the fusion of the outer mitochondrial membrane (OMM) and optic atrophy 1 (OPA1) for the inner membrane fusion [33]. Constitutive processing of OPA1 at proteolytic cleavage sites generates two isoforms of OPA1 [34]: long-OPA1 (L-OPA1) and short-OPA1 (S-OPA1), which cooperatively modulate the mitochondrial fusion state. Several proteases such as

OMA1, YME1L (an i-AAA protease), and AFG3L2 (an m-AAA protease) regulate OPA1 variants [35]. More recent findings suggested that L-OPA1 is sufficient for mitochondrial fusion through its binding with cardiolipin (CL) on the opposite membrane and homotypic interaction of OPA1 mediates IMM tethering and formation of cristae [36]. Stress-induced rapid proteolytic cleavage of OPA1 into short forms participates in mitochondrial fragmentation [37]. These mitochondrial fusion proteins may be ubiquitination by several E3 ligases such as Parkin and MARCH5/MITOL and then get degraded by proteases, leading to decreased mitochondrial fusion and autophagic degradation of mitochondrial organelles [38, 39]. It was reported that overexpression of appoptosin, a mitochondrial carrier protein located on IMM, compromised the interaction between Mfn1 and Mfn2, resulting in mitochondrial fragmentation [40].

For mitochondrial fission, dynamin-related protein 1 (Drp1) plays a paramount role. Drp1 adaptors such as mitochondrial fission 1 (Fis1), mitochondrial dynamics proteins of 49 and 51 kDa (MiD49/51), and mitochondrial fusion factor (Mff) cooperatively or independently form fission sites where Drp1 gathers to assemble the higher-ordered spiral complexes that constrict mitochondria for division [41]. Drp1 may constantly oligomerize on mitochondria although such process does not sufficiently trigger fission. The presence of certain fission factors, such as actin filaments, promotes the progressive maturation of Drp1 oligomers and uneven division due to unequal membrane potential [42]. Drp1 is also regulated by posttranslational modifications and metabolic signals [43]. Mdivi-1 is known to inhibit Drp1-dependent fission, while recent studies indicated that Mdivi-1 may not be a specific inhibitor of Drp1 and can reversibly inhibit mitochondrial complex I [44]. The presence of mitophagy and mitochondrial division in the Drp1-defective cells prompted the recognition of several novel mediators of fission, such as Tmem135 [45]. For instance, phagophores could emerge and elongate on a budded portion of mitochondria. Mitochondria are divided when the phagophore is closed without Atg5/Agt3 [46]. These data suggest the possible presence of atypical mitochondrial fission. A work reported by Fonseca and coworkers reconfirmed the crucial role of Drp1 in fission while dynamins (DNM1-3) are dispensable [47].

3. Mitochondrial Dynamics and Aging

Historically, mitochondrial dynamics resides in bioenergetic adaption to favor integrated or fragmented morphology of organelles. Mitochondrial dynamics was at one time difficult to capture in cultured cardiomyocytes, where proteins essential to these processes are abundant [48]. With the advancement of modern imaging technology, scientists have captured robust mitochondrial fusion and fission in healthy cardiomyocytes promptly after isolation. It has been suggested that well-functioning transition through fusion and fission is crucial for normal cardiomyocytes. Emerging evidence suggests that disrupted mitochondrial dynamics negatively impacts mitochondrial function and myocardial survival, resulting in the aging-induced buildup of dysfunctional mitochondria [49]. Table 1 summarizes evidence of mitochondrial dynamics in longevity and cardiovascular diseases.

Given the constant high-energy demand for cardiac contractility, a broadly connected mitochondrial network is essential for cardiomyocytes [50]. Studies from C. elegans revealed the role of increased mitochondrial fusion as a potent avenue to reconstitute a productive mitochondrial network [51]. Wai and associates found that ablation of Yme1L in a mouse heart activated OMA1 and OPA1 proteolysis, which induced mitochondrial fragmentation, dilated cardiomyopathy, and heart failure [52]. Furthermore, mitochondrial fusion could possibly preserve mitochondrial mass against pathological insults such as aging [53]. Mitochondrial fusion under the regulation by CAND-1 and SCF$^{\text{LIN-23}}$ is responsible for increased elongation of mitochondria and is required in longevity signaling such as insulin/IGF-1 signaling inactivation, physical exertion, caloric restriction, TOR (LET-363) inactivation, activation of sirtuin (SIR-2.1), and AMPK [54]. All these long-lived animal models presented an elongated mitochondrial network and generated less mitochondrial ROS [54]. The extended lifespan was significantly shortened upon the treatment with *eat-3* RNAi to interrupt mitochondrial fusion [54]. Consistent with this notion, Byrne and coworkers reported that lack of fusion (*eat-3*, *foz-1*) or fission proteins (*drp-1*) in C. elegans impacted movement and neuronal function and significantly reduced median lifespan without affecting the maximal lifespan. Moreover, interruption of fusion displayed a potent impact on median lifespan (12, 13, and 15.6 days for *eat-3* mutants, *foz-1* mutants, and *drp-1* mutants, respectively) in comparison with the wild type (20 days) [55]. Despite the fact that mitochondrial fusion is required for longevity, a fine balance between fusion and fission is vital for pathological changes including cardiovascular diseases. Defects in one process could be temporarily alleviated by a concomitant suppression of other processes in a compensatory manner [56]. Concomitant disruption of mitochondrial fission diminishes mitochondrial fragment and improves mitochondrial function triggered by lessened fusion, indicating an essential role for the maintenance fission-fusion balanced in the face of disrupted mitochondrial fusion under pathological stresses [55, 57].

In physiological conditions, Drp1-mediated fission may set a "strict" threshold for mitophagy and protect healthy mitochondria from "unchecked" mitophagy. Coronado and colleagues suggested that physiological fission is required for cardiac adaptation in response to normal energy stress, such as exercise [58]. It is also reported that Drp1 deletion in normal conditions with low levels of Parkin provoked hypermitophagy through upregulating Parkin and contributed to mitochondrial depletion and lethal cardiomyopathy [59]. Paradigms have held that segregation of depolarized portions of mitochondria via fission facilitates mitophagy to remove damaged or long-lived mitochondria, preserving mitochondrial homeostasis under stresses. Shirakabe and colleagues proposed that upregulation of fission and autophagy in acute settings may protect the mitochondria and heart from pressure overload, while suppression of Drp1-

TABLE 1: Alterations in mitochondrial dynamics and turnover for aging and CVD.

Protein	Alteration	Age-related disease/phenotype	Organism/model	References
Mfn2	Reduced expression	Hyperproliferation of vascular smooth muscle cells	Rats or mice: hypertensive and atherosclerotic arteries	[159]
	Increased expression	Accelerated cardiac hypertrophy and cardiomyopathy	Mouse heart	[38, 160, 161]
Mfn1	Reduced expression	Decreased glycolysis, increased oxygen consumption rate, and ATP levels	Old normal human fibroblasts	[162]
		Accelerated heart failure	Heart from humans, rats, and mice	[52, 163, 164]
Opa1	Increased expression	Protection from ischemia-reperfusion (I/R) injury	Mouse heart	[165]
	Increased expression	Decreased glycolysis, increased oxygen consumption rate, and ATP levels	Old normal human fibroblasts	[162]
	Reduced expression	Development of cardiac dysfunction	Mouse heart	[166, 167]
		Attenuated diabetes-induced cardiac dysfunction	Streptozotocin- (STZ-) induced diabetic mice	[66]
		Protection against posttraumatic/diabetes-induced cardiac dysfunction	Adult rats	[168]
Drp1	Inhibition	Protection from cardiac hypertrophy and function after I/R injury or myocardial infarction	Mouse heart	[169, 170]
		Improved LV functions, reduced MI size	Mouse heart	[64]
		Protection from Dox-induced cardiac damage	H9c2	[65]
	Short-term induction in midlife	Prolonged lifespan	Drosophila melanogaster	[62]
	Increased expression	Increased cell senescence	Neonatal rat cardiomyocytes	[125]
PINK1	Activation	Improved mitochondrial function, decreased ROS production, decreased apoptosis	Mouse heart	[124]
Parkin	Increased expression	Prolonged lifespan	Drosophila melanogaster	[171]
		Decayed aging	Mouse	[172]
	Reduced expression	Impaired recovery of cardiac contractility	Mouse heart	[173]
	Abrogation	Sustained mitochondrial fission, cell death, and heart failure	Adult mice cardiac progenitor cells (CPCs)	[104]
FUNDC1	Increased expression	Increased mitophagy and reduced platelet activity, protection from I/R injury	Mouse	[125]
	Increased expression	Infarction area expansion and cardiac dysfunction following acute cardiac IR injury	Mouse	[85]
BNIP3	Suppressed activity	Stressed cardiomyocytes	Human heart	[174]
	Increased expression	Attenuated heart failure	Mouse heart	[60]
BECN1/Beclin1	Deceased interaction with BCL-2	Improved healthspan, prolonged longevity	Mutant mice	[175]
PCG-1α	Overexpression	Suppressed aging-induced mitophagy, improved mitochondria	Mouse skeletal muscle	[129]

dependent mitochondrial autophagy could be responsible for cardiac pathology. They found that nonselective autophagy (within 24 hours), Drp-1 mediated fission [2-3 days after transverse aortic constriction (TAC)], and mitochondrial autophagy (3-5 days after TAC) were transiently activated in mouse hearts after TAC. Interestingly, autophagy and fission were significantly suppressed below physiological levels during the second phase (after 5-7 days for autophagy and after 14 days for Drp1). Heart failure developed after mitochondrial fragmentation, whereas Drp1 may return to normal levels along with suppressed autophagy. Haploinsufficiency of Drp1 abolished mitophagy and exacerbated heart failure, while protective mitophagy elicited by Tat-Beclin was abrogated by removal of Drp1 [60].

However, the regulation of mitochondrial fission declines during aging. This notion may be echoed by diminished mitophagy in aging, in concert with mitochondrial fission. D'amico and associates showed that RNA-binding protein Pumilio2 (PUM2), a translation repressor, decreased with age and downregulated translation of Mff, which hampered mitochondrial fission and mitophagy and promoted age-related mitochondrial dysfunction [61]. Moderately sustained stimulation of fission could protect against aging by unidentified mechanism(s). Rana and colleagues reported that short-term induction of Drp1 in midlife, but not earlier, extended both the lifespan and healthspan of Drosophila melanogaster. Midlife induction of Drp1 resulted in a decrease of p62 accumulation to mitochondria, while lack of Atg1 in midlife eliminated the benefits of Drp1, indicating that mitophagy may play a role in the beneficial effects of Drp1 [62].

A shift was noted from fusion to fission under multiple pathological conditions, indicating a possible role for mitochondrial fission in cardiovascular diseases [63]. Several studies suggested that unchecked fission and mitophagy are, at least in part, responsible for the development of cardiac aging, while interventions that limit excessive mitochondrial fission were suggested to offer cardioprotective effects in such pathological processes. Mdivi-1 treatment given prior to ischemia significantly improved cardiac function and reduced infarction size and arrhythmia [64]. Doxorubicin-treated H9c2 myocytes exhibited mitochondrial fragmentation and accelerated mitophagy, while RNA-mediated knockdown of Drp1 decreased cell death and attenuated cardiac damage [65]. It was reported that melatonin could prevent myopathy by inhibiting diabetes-induced activation of Drp-1 and fission through a Sirt1-PCG1α-dependent manner [66]. A novel regulator of mitochondrial fission Tmem135 has also been noted in cardiovascular diseases. It was reported that overexpression of Tmem135 induced mitochondrial fragmentation and exaggerated collagen accumulation and hypertrophy, which exhibited similar gene expression patterns and disease phenotypes to those found in aging [67]. Furthermore, mitochondrial fission may induce cellular death in extreme conditions. Excessive mitochondrial fission is induced in cardiac ischemic injury and leads to a higher susceptibility to mitochondrial permeability transition pore (mPTP) opening and apoptosis during reperfusion phase [68]. In addition, fission may indirectly

attenuate the aging process. Increased mitochondrial fission is also associated with high proliferation in some cancer cells and with low differentiation in stem cells [69]. Drp1-mediated mitochondrial fission is required to remove apoptotic cells by phagocytes, resulting in alleviation of postapoptotic necrosis and inflammation [70]. Whether fission-mediated anti-inflammation benefits cardiac aging has not been well understood. Despite ample evidence consolidating the benefit of inhibiting Drp1-mediated fission in pathological conditions, its effectiveness may be model-dependent. Using a large animal (pig) model of acute myocardial infarction, Mdivi-1 treatment given at the onset of reperfusion failed to preserve LV function or reduce myocardial infarction size. Furthermore, these authors revealed little change in fission after Mdivi-1 treatment, suggesting the necessity of more specific Drp1 inhibitors [71].

4. Mitochondrial Quality Control

More than 1000 proteins encoded by nuclear genes reside in mitochondria to integrate the network that governs mitochondrial biogenesis, morphology, and function [72]. Proper folding, translocation, and assembly of proteins are fundamental to mitochondrial homeostasis. In addition, mitochondria constantly produce energy in response to metabolic alternations and environmental cues at the cost of erosion by metabolic byproducts, such as ROS [73]. Failure to achieve structural integrity leads to accumulation of protein aggregates and dysfunctional organelles with aging [4]. To counter these culprits, several mechanisms may emerge as follows: (1) Dedicated chaperones and proteases degrade aberrant proteins within the matrix and intermembrane space (IMS) [74]. (2) A cytosolic ubiquitin-proteasome system (UPS) ubiquitinated proteins for subsequent destruction by the 26S proteasome in a p97-dependent manner [75]. (3) The mitochondrial unfolded protein response (UPRmt) relays stress signals retrograde to the nucleus and transcriptionally upregulates mitochondrial chaperones and proteases, such as ClpP (protease) and mtHsp60 (chaperone) to promote folding and degradation capacity [76]. (4) Mitochondria-derived vesicles (MDVs) transport damaged portions to the late endosome/lysosome and even to neighboring cells for degradation in hopes of preserving the undamaged part [77]. (5) Mitochondrial dynamics, biogenesis, and clearance of damaged mitochondria by mitophagy cooperate with each other to conserve mitochondrial fitness and cellular homeostasis [78]. Mitochondria also support quality control systems in extramitochondrial compartments through interconnected processes. It has been found in yeast that cytosolic aggregation-prone proteins are imported into mitochondria for degradation with the help of a chaperone protein Hsp104 to dissociate aggregates [79]. Mitochondria may act as a transient disposal unit in cells, where the wastes is sorted and destroyed [80].

High-energy stress imposes mitochondria more prone to injury. Such high-energy demand tissues such as the myocardium are also more sensitive to mitochondrial dysregulation, where slight tinkering is not enough. Thus, selective degradation of mitochondria is imperative here to recycle useful

constituents and then restore the fidelity of mitochondria. Mitophagy specifically recognizes and removes defective mitochondrial units that would otherwise be detrimental to organismal health. Given the high-energy demand of cardiomyocytes, here, we mainly talk about the role of mitophagy in cardiac aging rather than other cellular stress responses.

4.1. Molecular Mechanisms of Mitophagy and Biogenesis.
Mitophagy is one kind of selective autophagy, which targets long-lived or damaged mitochondria to degradation. In mammals, the molecular mechanism of mitophagy was first elucidated in mitochondrial clearance during erythropoiesis, which requires Nip3-like protein X (NIX/BNIP3L) [81]. The transmembrane mitophagy receptors, such as NIX, BNIP3, and FUNDC1, harbor a LC3-interacting region (LIR) motif, allowing formation of a bridge between ligands on the OMM with LC3/GABARAP, the mammalian autophagy-related 8 (Atg8) homologs attached to the autophagosomes [82, 83]. Receptor-mediated mitophagy is generally activated in response to cellular differentiation cues (NIX) [84] and some acute stresses, such as hypoxia (BNIP3, NIX and FUNDC1), nutrient stress (BNIP3), and ischemia-reperfusion [85]. For instance, FUNDC1 promotes mitophagy in response to hypoxia upon dephosphorylation by PGAM5, while casein kinase 2 (CK2) reverses the FUNDC1 activation process by phosphorylating FUNDC1 at Ser^{13} [86]. BcL2L1/Bcl-xL suppresses mitophagy through binding to PGAM5 and preventing the dephosphorylation of FUNDC1 [87].

PINK1 (PTEN-induced putative kinase protein 1), a more well-known mitophagy mediator, accumulates on the depolarized mitochondria, where PINK1 proteolysis is compromised, and phosphorylates the E3 ubiquitin ligase Parkin. Parkin tags proteins embedded in the OMM with PINK1-generated phosphoubiquitin, which then become substrates of PINK1, feeding back to amplify autophagic signals [88]. Cytosolic autophagy receptors, such as optineurin (OPTN), nuclear dot protein 52 kDa (NDP52), and (to a lesser degree) TAXBP1, but not p62, bind ubiquitin chains on the targeted mitochondria to processed LC3/GABARAP [89], whereas more recent studies suggested that LC3-II is not mandatory for autophagosome formation in PINK1-Parkin-mediated mitophagy or starvation-induced autophagy [90]. Consistent with this notion, it was reported that OPTN and NDP52 induce local recruitment and activation of autophagy factors like ULK1, DFCP1 (double FYVE domain-containing protein 1), and WIPI1 (WD repeat domain phosphoinositide-interacting protein 1) proximal to mitochondria, which likely contributes to autophagosomal formation de novo on injured mitochondria or lysosomal targeting to damaged mitochondria.

Alternatively, mitophagy may be regulated differently from how general autophagy is regulated such as in the absence of Atg5 or Atg7 (alternative autophagy) and thus cannot be evaluated with conventional markers such as LC3-II. The ATG5/ATG7-independent autophagy, which depends on the ULK (Unc-51-like kinase) and Beclin1 complexes, plays a prominent role in mitophagy induction [91]. Cardiolipin (CL) on the OMM could also bind to another Atg8 human ortholog LC3B and induce mitophagy

[92]. Endoplasmic reticulum (ER) and mitochondria form tight functional contacts that regulate several cellular processes. PINK1 and Beclin1 translocate to specific regions of ER-mitochondria contact, namely, mitochondria-associated membranes (MAM) and promote the formation of autophagosomes [93]. Autophagosome could also form from other sources, such as Golgi vesicles in a GTPase Rab9-dependent manner [94]. It was reported that mitochondria may be sequestered into the early Rab5-positive endosomes through the ESCRT machinery before being delivered to lysosomes for degradation [95]. Intriguingly, the lost or unuse of Parkin does not block mitophagy [96], but that does not imply Parkin has no part to play because Parkin dramatically increases mitophagy through ubiquitylating many proteins on OMM directly or indirectly involved in mitophagy, including Mfn1/Mfn2, PGC-1α, and NIX [97, 98].

To rejuvenate mitochondrial mass, mitochondrial biogenesis is also required to provide new and healthy "new blood" to the mitochondrial pools [99]. Mitochondria are semiautonomous organelles. Mitochondrial DNA (mtDNA) encodes 13 essential subunits of the oxidative phosphorylation (OXPHOS) system, with their levels depending on spatiotemporal coordination with nucleus genes [100]. Thus, identification of a single particular regulator of mitochondrial biogenesis is difficult. In general, peroxisome proliferator-activated receptor gamma coactivator 1-α (PGC-1α) is thought to act as a central hub in fine-tuned crosstalk between mitophagy and mitochondrial biogenesis. PGC-1α may interact with transcription factors, such as peroxisome proliferator-activated receptor (PPARβ), nuclear respiratory factor (NRF), and estrogen-related receptors (ERR) to orchestrate the overlapping gene expression in mitochondrial biogenesis. PGC-1α can also promote mitochondrial fusion and inhibit mitochondrial fission through regulating Mfn2 and Drp1 [101].

4.2. Role of Mitophagy in Cardiac Aging.
Defective segments of mitochondria are segregated from the rest of the mitochondrial network through fission for elimination by mitophagy. Fragmented mitochondria and decreased baseline of mitophagy have been noted in aging hearts [102]. Several proteins involved in mitochondrial turnover such as PINK1 and PGC-1α tend to decrease in old animals. These data indicated a decline in the function and regulation of mitophagy during aging [103]. Recent studies suggested that aging-related mtDNA mutations may disrupt the receptor- (NIX and FUNDC1) mediated mitophagy in the differentiation process in adult cardiac progenitor cells (CPCs), which resulted in sustained fission and less functional fragmented mitochondria [104]. Therefore, some activators of mitophagy have been used in aging models and showed some beneficial effects. For instance, urolithin A has been widely reported to extend lifespan in C. elegans and improve physical exercise capacity in rodents through upregulating mitophagy [105]. However, why and how mitophagy declines during aging have not been well defined. Several hypotheses were speculated thus far. Rizza and colleagues reported S-nitrosoglutathione reductase (GSNOR/ADH5), a protein denitrosylase that regulates S-nitrosylation, was

downregulated with aging in mice and humans [106]. Accumulation of S-nitrosylation severely impaired mitophagy, rather than autophagy, leading to hyperactivated mitochondrial fission by targeting Drp-1 in GSNOR$^{-/-}$ mice and cells [106]. It is noteworthy that expression of ADH5 is sustained in long-lived individuals, indicating the potential of ADH5 and S-nitrosylation as targets in the aging process through selectively modulating mitophagy [107]. Manzella and associates observed that ROS produced by mitochondrial enzyme monoamine oxidase-A (MAO-A) resulted in cytosolic accumulation of p53, one of the classic markers for cellular senescence. p53 further suppressed Parkin and therefore inhibited mitophagy, leading to mitochondrial dysfunction, which suggested a possible mechanism of MAO-A-induced oxidative stress in an age-related process [108]. Certain mitophagy proteins are directly or indirectly involved in the aging process. Parkin enhances transmission and replication of mtDNA in the presence of TFAM (mitochondrial transcription factor A) in proliferating cells [109]. TFAM is known to promote mtDNA through packaging mtDNA into mitochondrial nucleoids [110]. Chimienti and coworkers examined TFAM binding to mtDNA in aged (28 months) and extremely aged rats (32 months) and revealed a significant drop in TFAM binding in the extremely aged rats [111].

In essence, mitophagy is considered a self-defense and garbage removal process that maintains mitochondrial homeostasis and cellular health, in the face of pathological stimuli. Knuppertz and coworkers found that a PaSOD3 (P. anserine mitochondrial superoxide dismutase) deletion strain of ascomycete Podospora anserine surprisingly displayed similar lifespan as wild type, though superoxide accumulated and respiratory chain was impaired. They noted that mitophagy was predominantly induced by superoxide in the old PaSOD3 deletion strain. To verify whether autophagy is permissive to maintain the deficient strain healthy, they concomitantly ablated PaATG1 (ULK1 in mammals) and PaSOD3 and found a significant decrease in lifespan. They also elaborated the double sides of autophagy and mitophagy—with mild stress triggering protective level of autophagy and severe stress prompting excessive mitophagy, therefore provoking predeath pathways and accelerating aging [112], whereas the optimum state of mitophagy remains controversial and the impact of mitophagy may differ depending on pathological conditions. Both positive and negative effects of mitophagy in ischemia-reperfusion (IR) have been reported among various organs including the hearts, brains, and kidneys. Relatively, more evidence supported the positive side of mitophagy in cardiac IR. Zhou and coworkers found that NR4A1 was markedly increased following IR injury, accompanied with facilitated Mff-mediated fission and suppressed FUNDC1 mitophagy through a CK2α-mediated mechanism, leading to mitochondrial damage and microvascular collapse [113]. These authors suggested that increased Ripk3 may induce mitochondria-mediated apoptosis in cardiac IR via suppressing mitophagy, while Ripk3 deficiency reduced apoptosis and protected mitochondrial against IR damage in a mitophagy-dependent manner [114]. It was reported that melatonin could prevent cardiac IR injury through activating AMPK-OPA1-mediated fusion

and mitophagy [115]. Mammalian STE20-like kinase 1 (Mst1) significantly increased in a reperfused heart, which suppressed FUDC1-mediated mitophagy and induced proapoptosis signals. Mst1 knockout mice could reverse FUNDC1 expression and markedly reduced the myocardial infarction (MI) size [116]. Besides acute activation of protective mitophagy mentioned above, it should be noted that mitophagy also plays a role in chronic cardiac diseases. A recent study reconfirmed that mitophagy is crucial for mitochondrial homeostasis and cellular health in mice in response to a high-fat diet. Inhibition of mitophagy enhanced mitochondrial defect and lipid accumulation and thus deteriorated diabetic cardiomyopathy [117]. Moreover, Mst1 possibly participated in the development of diabetic cardiomyopathy through inhibiting Sirt3-related mitophagy [118]. It was demonstrated that simvastatin may prevent angiotensin II-induced heart failure through promoting autophagy and mitophagy and increasing lipid droplets in cardiomyocytes, contributing to the maintenance of mitochondrial quality and function [119]. Mitophagy has also been reported to combat against drug-induced cardiotoxicity. A mouse model of doxorubicin-induced cardiotoxicity showed decreased Rubicon expression and mitophagy 16 hours after intraperitoneal injection. Therefore, targeting doxorubicin-induced inhibition of mitophagy, autophagy flux, and mitochondrial dynamics may represent a novel avenue for doxorubicin cardiomyopathy [120].

On the contrary, mitophagy may also provide unfavorable effects on the heart. Feng and associates reported GPER (G protein-coupled estrogen receptor 1) protects a mouse heart from IR injury at the onset reperfusion through downregulating mitophagy [121]. Advanced glycation end products (AGEs) significantly increased the number of senescent cells in neonatal rat cardiomyocytes, coinciding with activation of PINK1/Parkin-mediated mitophagy [122]. These different effects shown above may result from the different levels, types, and duration of mitophagy; the method and time points of treatments; and the intrinsic differences of different models in these studies. In addition, two phases of IR exhibit different features, including the basal mitophagy, which we will talk about later. Despite much work has been done to clarify why autophagy could be harmful, more studies are still needed to clarify the underlying mechanism of mitophagy-induced damage. Zhou and coworkers recently reported that increased mitochondrial permeability is attributed to switching autophagy into a harmful force in mammals. Serum/glucocorticoid regulated kinase-1 (SGK-1) is required for degradation of mPTP component VDAC1 in both C. elegans and mammalian cells [123]. They found that C. elegans lacking SGK-1 presented overly activated mTORC2-induced autophagy and short lifespan [123].

Dozens of species have depicted a unique protective role of mitophagy in aging and cardiovascular diseases, an effect consistent with suppressed mitophagy in multiple pathways. The baseline of mitophagy in different cardiac diseases may help understand the complex effects of mitophagy. The presence of a switch from AMPKα2 to AMPKα1 in failing hearts has been well documented, leading to a decrease of

AMPKα2-mediated mitophagy and development of heart failure [124]. In another independent study, upregulated CK2α following acute cardiac IR injury was found to suppress FUNDC1-mediated mitophagy, leading to infarct area expansion and cardiac dysfunction [85]. Furthermore, ischemia activated FUNDC1-mediated mitophagy while reperfusion suppressed mitophagy possibly through activating Ripk3 [114]. Not surprisingly, interventions that restored mitophagy to normal levels, but not above normal levels, in these conditions should help to maintain mitochondrial homeostasis and cellular function. For instance, hypoxic precondition was recognized to suppress the activation of platelets and I/R injury in the heart through increasing FUNDC1-mediated mitophagy [125]. Exercise was reported to restore autophagic flux and mitochondrial oxidative capacity after myocardial infarction [126]. Table 1 summarizes evidence from a cadre of mitophagy in longevity and cardiovascular diseases.

Generation of new mitochondria through mitochondrial biogenesis plays a vital role in populating mitochondrial pool with adequate numbers and mass [127]. There has been some evidence to suggest the benefits of mitochondrial biogenesis during aging. PGC-1α overexpression improves lysosomal capacity and autophagy but reduces aging-associated mitophagy and ameliorates a mitochondrial defect [128, 129]. Several studies tried to associate the loss of PCG-1α with aging-related diseases, while its effects in cardiovascular diseases are less known. PCG-1$\alpha^{+/-}$ mice fed a high-fat diet for 4 months presented age-related macular degeneration- (AMD-) like abnormalities in retinal pigment epithelium (RPE) as well as decreased mitochondrial activity and increased ROS [130]. Muscle-specific upregulation and downregulation of PCG-1α, respectively, alleviated and exacerbated age-related muscle loss in mice. PCG-1α is also required for the muscle benefits of endurance exercise training [131].

5. Mitochondrial Adaptation and Metabolic Signals

Mitochondrial adaptation is partially established by metabolic signal molecules and epigenetic mechanisms that orchestrate gene expression underlying the generation and the removal of mitochondria. Several nutritional sensors, such as mTOR (mechanistic target of rapamycin), AMPK (AMP-activated protein kinase), and sirtuins, are involved in the processes that link environmental and intracellular stimuli to mitochondrial morphology and turnover. Generally, mTORC1 is recognized as a negative regulator of autophagy, while AMPK and SIRT1 facilitate autophagy and induce PGC-1α-mediated biogenesis [132]. AMPK extended lifespan through reviving the youthful mitochondrial homeostasis via both fusion and fission [133]. A novel stress-induced protein, sestrin2, declines with aging, which hampered the activation of AMPK, leading to reduced substrate metabolism and increased sensitivity to ischemia injury [134]. mTORC1 may promote fission in high caloric intake conditions through upregulating the translation of mitochondrial fission process 1 (MTFP1), which is coupled with the activation and recruit-

ment of Drp1 [135]. Lang and colleagues detected increased autophagy flux and significantly decreased Parkin-induced mitophagy under stress conditions in HEK293 cells with stable expression of Sirt4 [136]. Sirt4 tilted the mitochondrial dynamic balance towards fusion and counteracted fission as well as mitophagy possibly via interacting with L-OPA1 [136]. Sirt3 has been intensively discussed given its protective role in cardiac IR injury through multiple mechanisms. Sirt3 may either activate or inhibit autophagy, which may be used to maintain an optimal range of autophagy in different phases of IR [137]. Chen and colleagues reported that sustained exercise improved Sirt1, AMPKα1, and PCG-1α and attenuated aging-associated cardiac inflammation in D-galactose-induced aging mice [138]. Not surprisingly, the sirtuin cofactor NAD+ activates Sirt1 and a range of transcription factors that may decelerate aging, making it an emerging focus in the field of aging. Mitochondria control the concentration of NAD+ in cellular [139]. Katsyuba and coworkers showed that α-amino-β-carboxymuconate-ε-semialdehyde decarboxylase (ACMSD) limits de novo NAD+ biosynthetic pathway across species, including C. elegans, rats, and human [140]. Inhibition of ACMSD boosted NAD+ synthesis, prolonged lifespan in worms, and prompted a more extensive and interconnected mitochondrial network in C. elegans [140]. On the contrary, ablation of ACMSD was reported to enhance mitochondrial functions in human hepatocytes, indicating the complexity of NAD+ biosynthesis in organ function [140]. eNAMPT, one of the rate-limiting enzymes in the NAD+ biosynthetic pathway, declines with age in mammals, including human. A more recent study demonstrated that genetic supplementation or extracellular vesicle-mediated supplementation of eNAMPT could extend lifespan in mice, which prompted to the scrutiny of mitochondria in the longevity-defining processes outside mitochondria itself [141]. In C. elegans, SKN-1 (the nematode NRF) senses metabolic signaling and initiates a retrograde response towards the mitophagy-related DCT-1 (NIX/BNIP3L homolog) [142]. It was reported that autophagy and lysosomal biogenesis-related gene transcription factor EB (TFEB) exhibit parallel changes with that of PGC-1α. The putative nutrient-sensing regulator GCN5L1 (general control of amino acid synthesis 5-like 1) may restrain both mitochondrial biogenesis and degradation through direct transcriptional suppression of TFEB [143].

5.1. From Middle Age to Old Ages. Mitochondrial adaptation could be either beneficial or detrimental throughout life; the effects of mitochondrial dynamics and mitophagy largely depend on the type, level, and duration of stresses and the overall condition of individuals. Here, we are trying to depict a simplified picture about how mitochondria adapt throughout the entire life, which may imply some possible strategies to prolong healthspan. There is a transition from neonatal glycolysis to mitochondrial oxidative mechanism that mainly utilizes fatty acids in adulthood. Parkin-mediated mitophagy, through interaction with mitochondrial biogenesis, contributes to this metabolic remodeling by way of replacing old mitochondria with new ones that contain different enzymes and substrates [144]. Mild stress could make mitochondria more tolerant and adaptable. Senchuk and colleagues studied

three C. elegans and mitochondrial mutants and found that increased ROS activated FOXO transcription factor DAF-16 and contributed to their longevity [145]. Moreover, a set of molecules released from mitochondria, such as NAD+, NADPH, ROS, iron-sulfur cluster, and Ca^{2+}, has been determined as "second messengers" that affect the efficiency of some aging or antiaging processes throughout the lifetime [139]. However, both cellular homeostasis and mitochondrial functions are crucial, while mitochondria would sometimes sacrifice their own quality and integrity to accomplish its mission. Li and associates reported that the MOM protein FUNDC1 interacted with HSC70 to promote the unfolded protein response, but excessive accumulation of unfolded protein on the mitochondria impaired mitochondria and fatally evoked the pathways leading to cell senescence [146].

Accumulating observations have suggested a biphasic model of mitochondria wherein the metabolic rate is increased from youth to middle age and then drops again at older ages [147]. Rana and colleagues observed a decline of Drp-1 in the midlife of Drosophila, which may contribute to the more elongated mitochondria and then a decline in mitophagy [62]. On the one side, a midlife shift toward mitochondria fusion in response to relatively mild stress seemed to benefit temporarily but turned out to be potential threats later in life since reduced fission and accompanying deficiency of mitophagy resulted in the accumulation of dysfunctional mitochondria [62]. Byrne and coworkers performed several behavioral assays in C. elegans and revealed that disruption of mitochondrial fission progressively reduced animal movement in older drp-1 mutants, but displayed fewer defects in early adulthood than that of fusion mutants, which provided further support to the notion that fission is crucial in late life in response to severe stressors [55]. On the other hand, midlife promotion of mitochondrial capacity may link to the chronic cell senescence [148]. Cell senescence is another hallmark of aging, a stage of terminal cell cycle arrest characterized by high metabolic activity and hypersecretion of proinflammatory and prooxidant signals, termed senescence-associated secretory phenotype (SASP), which requires massive activation of mitochondria and interacts with senescent-associated mitochondrial dysfunction (SAMD) [149]. Some observations indirectly support the postulation that mitochondria excessively fused for abundant energy at the cost of reduced fission and mitochondrial quality: early intervention of caloric restriction is sufficient to expand lifespan and preemptively reduce age-related diseases in diverse species [150], while higher energy expenditure increases the risk of premature death in human life [151].

From the "struggling" middle age to the "difficult" old age, resources are exhausted, where cellular stress responses are no longer robust. Mitochondrial defects progressively accumulate and ultimately become unrepairable by a mitochondrial quality control system. There is a progressive loss of mitochondrial network connectivity and a reduction in mitochondrial mass in aging cells of C. elegans [133]. The overt decline of mitochondria depresses ATP-linked respiration and exacerbates superoxide generation, which results in a compensatory higher oxygen consumption rate (OCR) to meet energetic requirements. Under certain pathological

stress, mitochondria could switch from the key player in cell adaptive survival to the final executor of cell death through Bcl-2 family interaction-mediated proton leak and release of proapoptotic factors such as cytochrome C [152]. Recent studies in cancer cells revealed mitochondria-modulated apoptotic protein expression [153]. Likewise, mitochondrial dynamics and mitophagy could conversely act as maladaptive processes that amplify mitochondrial damage and apoptotic signaling [154]. Autosis, a form of cell death triggered by high levels of autophagy in response to stimulus-like pharmacological treatment, starvation, and ischemia, is mediated by the Na^+-K^+-ATPase pump and featured by increased autophagosomes/autolysosomes [155]. Starvation-induced abrogation of PGC-1α leads to p53-mediated apoptosis, indicating a possible link to cell fate determination [156]. Selective organelle clearance and cell death are not distinct processes; they perform hierarchically at the level of organelle or cell [157].

6. Conclusion and Future Perspectives

Mitochondria constitute a dynamic network interacting with other cellular compartments to orchestrate various physiological processes and cellular stress responses. Alterations in mitochondrial functions are proven to be a major contributor to aging and aging-related diseases, especially cardiovascular diseases. Mitochondrial dynamics, biogenesis, and turnover are essential for mitochondrial and cellular homeostasis. Aging is potentially malleable via metabolic and genetic interventions, such as caloric restriction and exercise [158]. Dietary supplements such as antioxidants offer limited benefit. Physiological and pharmacological inducers of mitophagy as well as modulators of mitochondrial dynamics improve mitochondrial function and healthspan in various model organisms [4]. Further progress in preserving and attenuating aging-induced pathologies should come from a better understanding of the causal mechanisms underlying aging itself and hopefully from targeting the mechanisms implicated in the regulation of mitochondrial homeostasis to counteract mitochondrial damage at an early stage. Perhaps, the way we fight aging lies in the way we treat with midlife.

Ethical Approval

Work conducted in our laboratories has been approved by the institutional ethics committees at the Zhongshan Hospital Fudan University (Shanghai) and the University of Wyoming (Laramie, WY). No human studies were involved.

Conflicts of Interest

The authors declare that they have no conflicts of interest.

Authors' Contributions

NW and JR drafted and proofed the manuscript. YZ edited the manuscript. All authors have agreed upon the submission and publication of this work.

Acknowledgments

References

[1] S. S. Khan, B. D. Singer, and D. E. Vaughan, "Molecular and physiological manifestations and measurement of aging in humans," *Aging Cell*, vol. 16, no. 4, pp. 624–633, 2017.

[2] J. R. Beard, I. Araujo de Carvalho, Y. Sumi, A. Officer, and J. A. Thiyagarajan, "Healthy ageing: moving forward," *Bulletin of the World Health Organization*, vol. 95, no. 11, pp. 730–730a, 2017.

[3] G. A. Erikson, D. L. Bodian, M. Rueda et al., "Whole-genome sequencing of a healthy aging cohort," *Cell*, vol. 165, no. 4, pp. 1002–1011, 2016.

[4] J. Ren and Y. Zhang, "Targeting autophagy in aging and aging-related cardiovascular diseases," *Trends in Pharmacological Sciences*, vol. 39, no. 12, pp. 1064–1076, 2018.

[5] N. Barzilai, A. M. Cuervo, and S. Austad, "Aging as a biological target for prevention and therapy," *Jama*, vol. 320, no. 13, pp. 1321-1322, 2018.

[6] E. J. Benjamin, P. Muntner, A. Alonso et al., "Heart disease and stroke statistics-2019 update: a report from the American Heart Association," *Circulation*, vol. 139, no. 10, pp. e56–e528, 2019.

[7] F. Paneni, C. Diaz Canestro, P. Libby, T. F. Luscher, and G. G. Camici, "The aging cardiovascular system: understanding it at the cellular and clinical levels," *Journal of the American College of Cardiology*, vol. 69, no. 15, pp. 1952–1967, 2017.

[8] V. Obas and R. S. Vasan, "The aging heart," *Clinical Science*, vol. 132, no. 13, pp. 1367–1382, 2018.

[9] I. Liguori, G. Russo, F. Curcio et al., "Oxidative stress, aging, and diseases," *Clinical Interventions in Aging*, vol. 13, pp. 757–772, 2018.

[10] I. Alfaras, C. Di Germanio, M. Bernier et al., "Pharmacological strategies to retard cardiovascular aging," *Circulation Research*, vol. 118, no. 10, pp. 1626–1642, 2016.

[11] T. W. Buford, "Hypertension and aging," *Ageing Research Reviews*, vol. 26, pp. 96–111, 2016.

[12] A. Picca, R. T. Mankowski, J. L. Burman et al., "Mitochondrial quality control mechanisms as molecular targets in cardiac ageing," *Nature Reviews Cardiology*, vol. 15, no. 9, pp. 543–554, 2018.

[13] A. Calcinotto, J. Kohli, E. Zagato, L. Pellegrini, M. Demaria, and A. Alimonti, "Cellular senescence: Aging, Cancer, and Injury," *Physiological Reviews*, vol. 99, no. 2, pp. 1047–1078, 2019.

[14] N. Kubben and T. Misteli, "Shared molecular and cellular mechanisms of premature ageing and ageing- associated diseases," *Nature Reviews Molecular Cell Biology*, vol. 18, no. 10, pp. 595–609, 2017.

[15] P. Sen, P. P. Shah, R. Nativio, and S. L. Berger, "Epigenetic mechanisms of longevity and aging," *Cell*, vol. 166, no. 4, pp. 822–839, 2016.

[16] J. R. Friedman and J. Nunnari, "Mitochondrial form and function," *Nature*, vol. 505, no. 7483, pp. 335–343, 2014.

[17] K. Boengler, M. Kosiol, M. Mayr, R. Schulz, and S. Rohrbach, "Mitochondria and ageing: role in heart, skeletal muscle and adipose tissue," *Journal of Cachexia, Sarcopenia and Muscle*, vol. 8, no. 3, pp. 349–369, 2017.

[18] T. E. S. Kauppila, J. H. K. Kauppila, and N. G. Larsson, "Mammalian mitochondria and aging: an update," *Cell Metabolism*, vol. 25, no. 1, pp. 57–71, 2017.

[19] C. Franceschi, P. Garagnani, G. Vitale, M. Capri, and S. Salvioli, "Inflammaging and 'Garb-aging'," *Trends in Endocrinology & Metabolism*, vol. 28, no. 3, pp. 199–212, 2017.

[20] C. Lopez-Otin, L. Galluzzi, J. M. P. Freije, F. Madeo, and G. Kroemer, "Metabolic control of longevity," *Cell*, vol. 166, no. 4, pp. 802–821, 2016.

[21] J. Y. Jang, A. Blum, J. Liu, and T. Finkel, "The role of mitochondria in aging," *Journal of Clinical Investigation*, vol. 128, no. 9, pp. 3662–3670, 2018.

[22] S. M. Raefsky and M. P. Mattson, "Adaptive responses of neuronal mitochondria to bioenergetic challenges: roles in neuroplasticity and disease resistance," *Free Radical Biology and Medicine*, vol. 102, pp. 203–216, 2017.

[23] A. H. de Mello, A. B. Costa, J. D. G. Engel, and G. T. Rezin, "Mitochondrial dysfunction in obesity," *Life Sciences*, vol. 192, pp. 26–32, 2018.

[24] J. Zhang, M. L. Culp, J. G. Craver, and V. Darley-Usmar, "Mitochondrial function and autophagy: integrating proteotoxic, redox, and metabolic stress in Parkinson's disease," *Journal of Neurochemistry*, vol. 144, no. 6, pp. 691–709, 2018.

[25] G. R. Anderson, S. E. Wardell, M. Cakir et al., "Dysregulation of mitochondrial dynamics proteins are a targetable feature of human tumors," *Nature Communications*, vol. 9, no. 1, p. 1677, 2018.

[26] M. Bonora, M. R. Wieckowski, D. A. Sinclair, G. Kroemer, P. Pinton, and L. Galluzzi, "Targeting mitochondria for cardiovascular disorders: therapeutic potential and obstacles," *Nature Reviews Cardiology*, vol. 16, no. 1, pp. 33–55, 2019.

[27] M. N. Sack, F. Y. Fyhrquist, O. J. Saijonmaa, V. Fuster, and J. C. Kovacic, "Basic biology of oxidative stress and the cardiovascular system: part 1 of a 3-part series," *Journal of the American College of Cardiology*, vol. 70, no. 2, pp. 196–211, 2017.

[28] F. G. Tahrir, D. Langford, S. Amini, T. Mohseni Ahooyi, and K. Khalili, "Mitochondrial quality control in cardiac cells: mechanisms and role in cardiac cell injury and disease," *Journal of Cellular Physiology*, vol. 234, no. 6, pp. 8122–8133, 2018.

[29] S. Pickles, P. Vigie, and R. J. Youle, "Mitophagy and quality control mechanisms in mitochondrial maintenance," *Current Biology*, vol. 28, no. 4, pp. R170–r185, 2018.

[30] R. J. Youle and A. M. van der Bliek, "Mitochondrial fission, fusion, and stress," *Science*, vol. 337, no. 6098, pp. 1062–1065, 2012.

[31] M. Gonzalez-Freire, R. de Cabo, M. Bernier et al., "Reconsidering the role of mitochondria in aging," *The Journals of Gerontology Series A: Biological Sciences and Medical Sciences*, vol. 70, no. 11, pp. 1334–1342, 2015.

[32] Y. Wang and S. Hekimi, "Mitochondrial dysfunction and longevity in animals: untangling the knot," *Science*, vol. 350, no. 6265, pp. 1204–1207, 2015.

[33] A. Santel and M. T. Fuller, "Control of mitochondrial morphology by a human mitofusin," *Journal of Cell Science*, vol. 114, Part 5, pp. 867–874, 2001.

[34] N. Ishihara, Y. Fujita, T. Oka, and K. Mihara, "Regulation of mitochondrial morphology through proteolytic cleavage of OPA1," *The EMBO Journal*, vol. 25, no. 13, pp. 2966–2977, 2006.

[35] F. Consolato, F. Maltecca, S. Tulli, I. Sambri, and G. Casari, "m-AAA and i-AAA complexes coordinate to regulate OMA1, the stress-activated supervisor of mitochondrial dynamics," *Journal of Cell Science*, vol. 131, no. 7, article jcs213546, 2018.

[36] T. Ban, T. Ishihara, H. Kohno et al., "Molecular basis of selective mitochondrial fusion by heterotypic action between OPA1 and cardiolipin," *Nature Cell Biology*, vol. 19, no. 7, pp. 856–863, 2017.

[37] R. Anand, T. Wai, M. J. Baker et al., "The i-AAA protease YME1L and OMA1 cleave OPA1 to balance mitochondrial fusion and fission," *The Journal of Cell Biology*, vol. 204, no. 6, pp. 919–929, 2014.

[38] Y. Chen and G. W. Dorn II, "PINK1-phosphorylated mitofusin 2 is a Parkin receptor for culling damaged mitochondria," *Science*, vol. 340, no. 6131, pp. 471–475, 2013.

[39] N. Nakamura, Y. Kimura, M. Tokuda, S. Honda, and S. Hirose, "MARCH-V is a novel mitofusin 2- and Drp1-binding protein able to change mitochondrial morphology," *EMBO reports*, vol. 7, no. 10, pp. 1019–1022, 2006.

[40] C. Zhang, Z. Shi, L. Zhang et al., "Appoptosin interacts with mitochondrial outer-membrane fusion proteins and regulates mitochondrial morphology," *Journal of Cell Science*, vol. 129, no. 5, pp. 994–1002, 2016.

[41] L. D. Osellame, A. P. Singh, D. A. Stroud et al., "Cooperative and independent roles of the Drp1 adaptors Mff, MiD49 and MiD51 in mitochondrial fission," *Journal of Cell Science*, vol. 129, no. 11, pp. 2170–2181, 2016.

[42] W. K. Ji, A. L. Hatch, R. A. Merrill, S. Strack, and H. N. Higgs, "Actin filaments target the oligomeric maturation of the dynamin GTPase Drp1 to mitochondrial fission sites," *Elife*, vol. 4, article e11553, 2015.

[43] C. Hu, Y. Huang, and L. Li, "Drp1-dependent mitochondrial fission plays critical roles in physiological and pathological progresses in mammals," *International Journal of Molecular Sciences*, vol. 18, no. 1, p. 144, 2017.

[44] E. A. Bordt, P. Clerc, B. A. Roelofs et al., "The putative Drp1 inhibitor mdivi-1 is a reversible mitochondrial complex I inhibitor that modulates reactive oxygen species," *Developmental Cell*, vol. 40, no. 6, pp. 583–594.e6, 2017.

[45] W. H. Lee, H. Higuchi, S. Ikeda et al., "Mouse Tmem135 mutation reveals a mechanism involving mitochondrial dynamics that leads to age-dependent retinal pathologies," *eLife*, vol. 5, 2016.

[46] S. I. Yamashita and T. Kanki, "How autophagy eats large mitochondria: autophagosome formation coupled with mitochondrial fragmentation," *Autophagy*, vol. 13, no. 5, pp. 980-981, 2017.

[47] T. B. Fonseca, A. Sanchez-Guerrero, I. Milosevic, and N. Raimundo, "Mitochondrial fission requires DRP1 but not dynamins," *Nature*, vol. 570, no. 7761, pp. E34–e42, 2019.

[48] A. Sivakumar, R. Subbiah, R. Balakrishnan, and J. Rajendhran, "Cardiac mitochondrial dynamics: miR-mediated regulation during cardiac injury," *Journal of Molecular and Cellular Cardiology*, vol. 110, pp. 26–34, 2017.

[49] D. Sebastian, M. Palacin, and A. Zorzano, "Mitochondrial dynamics: coupling mitochondrial fitness with healthy aging," *Trends in Molecular Medicine*, vol. 23, no. 3, pp. 201–215, 2017.

[50] C. Blackstone and C. R. Chang, "Mitochondria unite to survive," *Nature Cell Biology*, vol. 13, no. 5, pp. 521-522, 2011.

[51] S. N. Chaudhari and E. T. Kipreos, "The energy maintenance theory of aging: maintaining energy metabolism to allow longevity," *Bioessays*, vol. 40, no. 8, article e1800005, 2018.

[52] T. Wai, J. Garcia-Prieto, M. J. Baker et al., "Imbalanced OPA1 processing and mitochondrial fragmentation cause heart failure in mice," *Science*, vol. 350, no. 6265, p. aad0116, 2015.

[53] R. Higuchi-Sanabria, P. A. Frankino, J. W. Paul III, S. U. Tronnes, and A. Dillin, "A Futile Battle? Protein Quality Control and the Stress of Aging," *Developmental Cell*, vol. 44, no. 2, pp. 139–163, 2018.

[54] S. N. Chaudhari and E. T. Kipreos, "Increased mitochondrial fusion allows the survival of older animals in diverse *C. elegans* longevity pathways," *Nature Communications*, vol. 8, no. 1, p. 182, 2017.

[55] J. J. Byrne, M. S. Soh, G. Chandhok et al., "Disruption of mitochondrial dynamics affects behaviour and lifespan in Caenorhabditis elegans," *Cellular and Molecular Life Sciences*, vol. 76, no. 10, pp. 1967–1985, 2019.

[56] M. Song, A. Franco, J. A. Fleischer, L. Zhang, and G. W. Dorn II, "Abrogating mitochondrial dynamics in mouse hearts accelerates mitochondrial senescence," *Cell Metabolism*, vol. 26, no. 6, pp. 872–883.e5, 2017.

[57] H. Chen, S. Ren, C. Clish et al., "Titration of mitochondrial fusion rescues Mff-deficient cardiomyopathy," *Journal Of Cell Biology*, vol. 211, no. 4, pp. 795–805, 2015.

[58] M. Coronado, G. Fajardo, K. Nguyen et al., "Physiological mitochondrial fragmentation is a normal cardiac adaptation to increased energy demand," *Circulation Research*, vol. 122, no. 2, pp. 282–295, 2018.

[59] M. Song, G. Gong, Y. Burelle et al., "Interdependence of Parkin-mediated mitophagy and mitochondrial fission in adult mouse hearts," *Circulation Research*, vol. 117, no. 4, pp. 346–351, 2015.

[60] A. Shirakabe, P. Zhai, Y. Ikeda et al., "Drp1-dependent mitochondrial autophagy plays a protective role against pressure overload-induced mitochondrial dysfunction and heart failure," *Circulation*, vol. 133, no. 13, pp. 1249–1263, 2016.

[61] D. D'Amico, A. Mottis, F. Potenza et al., "The RNA-binding protein PUM2 impairs mitochondrial dynamics and mitophagy during aging," *Molecular Cell*, vol. 73, no. 4, pp. 775–787.e10, 2019.

[62] A. Rana, M. P. Oliveira, A. V. Khamoui et al., "Promoting Drp1-mediated mitochondrial fission in midlife prolongs healthy lifespan of *Drosophila melanogaster*.," *Nature Communications*, vol. 8, no. 1, p. 448, 2017.

[63] V. Eisner, R. R. Cupo, E. Gao et al., "Mitochondrial fusion dynamics is robust in the heart and depends on calcium oscillations and contractile activity," *Proceedings of the National Academy of Sciences*, vol. 114, no. 5, pp. E859–e868, 2017.

[64] C. Maneechote, S. Palee, S. Kerdphoo, T. Jaiwongkam, S. C. Chattipakorn, and N. Chattipakorn, "Differential temporal inhibition of mitochondrial fission by Mdivi-1 exerts effective cardioprotection in cardiac ischemia/reperfusion injury," *Clinical Science*, vol. 132, no. 15, pp. 1669–1683, 2018.

[65] M. P. Catanzaro, A. Weiner, A. Kaminaris et al., "Doxorubicin-induced cardiomyocyte death is mediated by unchecked

mitochondrial fission and mitophagy," *The FASEB Journal*, vol. 33, no. 10, pp. 11096–11108, 2019.

[66] M. Ding, N. Feng, D. Tang et al., "Melatonin prevents Drp1-mediated mitochondrial fission in diabetic hearts through SIRT1-PGC1α pathway," *Journal of Pineal Research*, vol. 65, no. 2, article e12491, 2018.

[67] S. A. Lewis, T. Takimoto, S. Mehrvar et al., "The effect of Tmem135 overexpression on the mouse heart," *PLoS One*, vol. 13, no. 8, article e0201986, 2018.

[68] C. Maneechote, S. Palee, S. C. Chattipakorn, and N. Chattipakorn, "Roles of mitochondrial dynamics modulators in cardiac ischaemia/reperfusion injury," *Journal of Cellular and Molecular Medicine*, vol. 21, no. 11, pp. 2643–2653, 2017.

[69] H. Chen and D. C. Chan, "Mitochondrial dynamics in regulating the unique phenotypes of cancer and stem cells," *Cell Metabolism*, vol. 26, no. 1, pp. 39–48, 2017.

[70] Y. Wang, M. Subramanian, A. Yurdagul Jr. et al., "Mitochondrial fission promotes the continued clearance of apoptotic cells by macrophages," *Cell*, vol. 171, no. 2, pp. 331–345.e22, 2017.

[71] S. B. Ong, X. Y. Kwek, K. Katwadi et al., "Targeting mitochondrial fission using Mdivi-1 in a clinically relevant large animal model of acute myocardial infarction: a pilot study," *International Journal of Molecular Sciences*, vol. 20, no. 16, p. 3972, 2019.

[72] N. Wiedemann and N. Pfanner, "Mitochondrial machineries for protein import and assembly," *Annual Review of Biochemistry*, vol. 86, no. 1, pp. 685–714, 2017.

[73] P. Kramer and P. Bressan, "Our (mother's) mitochondria and our mind," *Perspectives on Psychological Science*, vol. 13, no. 1, pp. 88–100, 2018.

[74] M. J. Baker, T. Tatsuta, and T. Langer, "Quality control of mitochondrial proteostasis," *Cold Spring Harbor Perspectives in Biology*, vol. 3, no. 7, article a007559, 2011.

[75] R. J. Braun and B. Westermann, "With the help of MOM: mitochondrial contributions to cellular quality control," *Trends in Cell Biology*, vol. 27, no. 6, pp. 441–452, 2017.

[76] T. Arnould, S. Michel, and P. Renard, "Mitochondria retrograde signaling and the UPR mt: where are we in mammals?," *International Journal of Molecular Sciences*, vol. 16, no. 8, pp. 18224–18251, 2015.

[77] T. G. McWilliams and M. M. Muqit, "PINK1 and Parkin: emerging themes in mitochondrial homeostasis," *Current Opinion in Cell Biology*, vol. 45, pp. 83–91, 2017.

[78] G. Ashrafi and T. L. Schwarz, "The pathways of mitophagy for quality control and clearance of mitochondria," *Cell Death & Differentiation*, vol. 20, no. 1, pp. 31–42, 2013.

[79] L. Ruan, C. Zhou, E. Jin et al., "Cytosolic proteostasis through importing of misfolded proteins into mitochondria," *Nature*, vol. 543, no. 7645, pp. 443–446, 2017.

[80] M. A. Eldeeb and R. P. Fahlman, "Does too much MAGIC lead to mitophagy?," *Trends in Biochemical Sciences*, vol. 43, no. 7, pp. 485–487, 2018.

[81] S. Rikka, M. N. Quinsay, R. L. Thomas et al., "Bnip3 impairs mitochondrial bioenergetics and stimulates mitochondrial turnover," *Cell Death & Differentiation*, vol. 18, no. 4, pp. 721–731, 2011.

[82] R. L. Schweers, J. Zhang, M. S. Randall et al., "NIX is required for programmed mitochondrial clearance during reticulocyte maturation," *Proceedings of the National Academy of Sciences*, vol. 104, no. 49, pp. 19500–19505, 2007.

[83] L. Liu, K. Sakakibara, Q. Chen, and K. Okamoto, "Receptor-mediated mitophagy in yeast and mammalian systems," *Cell Research*, vol. 24, no. 7, pp. 787–795, 2014.

[84] L. E. Drake, M. Z. Springer, L. P. Poole, C. J. Kim, and K. F. Macleod, "Expanding perspectives on the significance of mitophagy in cancer," *Semin Cancer Biol*, vol. 47, pp. 110–124, 2017.

[85] H. Zhou, P. Zhu, J. Wang, H. Zhu, J. Ren, and Y. Chen, "Pathogenesis of cardiac ischemia reperfusion injury is associated with CK2α-disturbed mitochondrial homeostasis via suppression of FUNDC1-related mitophagy," *Cell Death & Differentiation*, vol. 25, no. 6, pp. 1080–1093, 2018.

[86] G. Chen, Z. Han, D. Feng et al., "A regulatory signaling loop comprising the PGAM5 phosphatase and CK2 controls receptor-mediated mitophagy," *Molecular Cell*, vol. 54, no. 3, pp. 362–377, 2014.

[87] H. Wu, D. Xue, G. Chen et al., "The BCL2L1 and PGAM5 axis defines hypoxia-induced receptor-mediated mitophagy," *Autophagy*, vol. 10, no. 10, pp. 1712–1725, 2014.

[88] T. N. Nguyen, B. S. Padman, and M. Lazarou, "Deciphering the molecular signals of PINK1/Parkin mitophagy," *Trends in Cell Biology*, vol. 26, no. 10, pp. 733–744, 2016.

[89] M. Lazarou, D. A. Sliter, L. A. Kane et al., "The ubiquitin kinase PINK1 recruits autophagy receptors to induce mitophagy," *Nature*, vol. 524, no. 7565, pp. 309–314, 2015.

[90] B. S. Padman, T. N. Nguyen, and M. Lazarou, "Autophagosome formation and cargo sequestration in the absence of LC3/GABARAPs," *Autophagy*, vol. 13, no. 4, pp. 772–774, 2017.

[91] Y. Hirota, S. Yamashita, Y. Kurihara et al., "Mitophagy is primarily due to alternative autophagy and requires the MAPK1 and MAPK14 signaling pathways," *Autophagy*, vol. 11, no. 2, pp. 332–343, 2015.

[92] Z. Anton, A. Landajuela, J. H. Hervas et al., "Human Atg8-cardiolipin interactions in mitophagy: specific properties of LC3B, GABARAPL2 and GABARAP," *Autophagy*, vol. 12, no. 12, pp. 2386–2403, 2016.

[93] V. Gelmetti, P. De Rosa, L. Torosantucci et al., "PINK1 and BECN1 relocalize at mitochondria-associated membranes during mitophagy and promote ER-mitochondria tethering and autophagosome formation," *Autophagy*, vol. 13, no. 4, pp. 654–669, 2017.

[94] N. T. Ktistakis and S. A. Tooze, "Digesting the expanding mechanisms of autophagy," *Trends in Cell Biology*, vol. 26, no. 8, pp. 624–635, 2016.

[95] B. C. Hammerling, R. H. Najor, M. Q. Cortez et al., "A Rab5 endosomal pathway mediates Parkin-dependent mitochondrial clearance," *Nature Communications*, vol. 8, no. 1, p. 14050, 2017.

[96] E. Villa, S. Marchetti, and J. E. Ricci, "No Parkin zone: mitophagy without Parkin," *Trends in Cell Biology*, vol. 28, no. 11, pp. 882–895, 2018.

[97] N. Matsuda and K. Tanaka, "Cell biology: tagged tags engage disposal," *Nature*, vol. 524, no. 7565, pp. 294-295, 2015.

[98] D. A. Stevens, Y. Lee, H. C. Kang et al., "Parkin loss leads to PARIS-dependent declines in mitochondrial mass and respiration," *Proceedings of the National Academy of Sciences*, vol. 112, no. 37, pp. 11696–11701, 2015.

[99] J. F. Halling, S. Ringholm, J. Olesen, C. Prats, and H. Pilegaard, "Exercise training protects against aging-induced mitochondrial fragmentation in mouse skeletal muscle in a PGC-1α dependent manner," *Experimental Gerontology*, vol. 96, pp. 1–6, 2017.

[100] C. M. Gustafsson, M. Falkenberg, and N. G. Larsson, "Maintenance and expression of mammalian mitochondrial DNA," *Annual Review of Biochemistry*, vol. 85, no. 1, pp. 133–160, 2016.

[101] K. Peng, L. Yang, J. Wang et al., "The interaction of mitochondrial biogenesis and fission/fusion mediated by PGC-1α regulates rotenone-induced dopaminergic neurotoxicity," *Molecular Neurobiology*, vol. 54, no. 5, pp. 3783–3797, 2017.

[102] A. Stotland and R. A. Gottlieb, "α-MHC MitoTimer mouse: In vivo mitochondrial turnover model reveals remarkable mitochondrial heterogeneity in the heart," *Journal of Molecular and Cellular Cardiology*, vol. 90, pp. 53–58, 2016.

[103] J. Zhou, S. Y. Chong, A. Lim et al., "Changes in macroautophagy, chaperone-mediated autophagy, and mitochondrial metabolism in murine skeletal and cardiac muscle during aging," *Aging*, vol. 9, no. 2, pp. 583–599, 2017.

[104] M. A. Lampert, A. M. Orogo, R. H. Najor et al., "BNIP3L/NIX and FUNDC1-mediated mitophagy is required for mitochondrial network remodeling during cardiac progenitor cell differentiation," *Autophagy*, vol. 15, no. 7, pp. 1182–1198, 2019.

[105] D. Ryu, L. Mouchiroud, P. A. Andreux et al., "Urolithin A induces mitophagy and prolongs lifespan in C. elegans and increases muscle function in rodents," *Nature Medicine*, vol. 22, no. 8, pp. 879–888, 2016.

[106] S. Rizza, S. Cardaci, C. Montagna et al., "S-Nitrosylation drives cell senescence and aging in mammals by controlling mitochondrial dynamics and mitophagy," *Proceedings of the National Academy of Sciences*, vol. 115, no. 15, pp. E3388–e3397, 2018.

[107] S. Rizza and G. Filomeni, "Denitrosylate and live longer: how ADH5/GSNOR links mitophagy to aging," *Autophagy*, vol. 14, no. 7, pp. 1285–1287, 2018.

[108] N. Manzella, Y. Santin, D. Maggiorani et al., "Monoamine oxidase-A is a novel driver of stress-induced premature senescence through inhibition of parkin-mediated mitophagy," *Aging Cell*, vol. 17, no. 5, article e12811, 2018.

[109] Y. Kuroda, T. Mitsui, M. Kunishige et al., "Parkin enhances mitochondrial biogenesis in proliferating cells," *Human Molecular Genetics*, vol. 15, no. 6, pp. 883–895, 2006.

[110] C. Kukat, K. M. Davies, C. A. Wurm et al., "Cross-strand binding of TFAM to a single mtDNA molecule forms the mitochondrial nucleoid," *Proceedings of the National Academy of Sciences*, vol. 112, no. 36, pp. 11288–11293, 2015.

[111] G. Chimienti, A. Picca, F. Fracasso et al., "Differences in liver TFAM binding to mtDNA and mtDNA damage between aged and extremely aged rats," *International Journal of Molecular Sciences*, vol. 20, no. 10, p. 2601, 2019.

[112] L. Knuppertz, V. Warnsmann, A. Hamann, C. Grimm, and H. D. Osiewacz, "Stress-dependent opposing roles for mitophagy in aging of the ascomycete Podospora anserina," *Autophagy*, vol. 13, no. 6, pp. 1037–1052, 2017.

[113] H. Zhou, J. Wang, P. Zhu et al., "NR4A1 aggravates the cardiac microvascular ischemia reperfusion injury through suppressing FUNDC1-mediated mitophagy and promoting Mff-

[114] required mitochondrial fission by CK2α," *Basic Research in Cardiology*, vol. 113, no. 4, p. 23, 2018.

[114] H. Zhou, P. Zhu, J. Guo et al., "Ripk3 induces mitochondrial apoptosis via inhibition of FUNDC1 mitophagy in cardiac IR injury," *Redox Biology*, vol. 13, pp. 498–507, 2017.

[115] Y. Zhang, Y. Wang, J. Xu et al., "Melatonin attenuates myocardial ischemia-reperfusion injury via improving mitochondrial fusion/mitophagy and activating the AMPK-OPA1 signaling pathways," *Journal of Pineal Research*, vol. 66, no. 2, article e12542, 2019.

[116] W. Yu, M. Xu, T. Zhang, Q. Zhang, and C. Zou, "Mst1 promotes cardiac ischemia-reperfusion injury by inhibiting the ERK-CREB pathway and repressing FUNDC1-mediated mitophagy," *The Journal of Physiological Sciences*, vol. 69, no. 1, pp. 113–127, 2019.

[117] M. Tong, T. Saito, P. Zhai et al., "Mitophagy is essential for maintaining cardiac function during high fat diet-induced diabetic cardiomyopathy," *Circulation Research*, vol. 124, no. 9, pp. 1360–1371, 2019.

[118] S. Wang, Z. Zhao, Y. Fan et al., "Mst1 inhibits Sirt3 expression and contributes to diabetic cardiomyopathy through inhibiting Parkin-dependent mitophagy," *Biochimica et Biophysica Acta (BBA) - Molecular Basis of Disease*, vol. 1865, no. 7, pp. 1905–1914, 2019.

[119] C. C. Hsieh, C. Y. Li, C. H. Hsu et al., "Mitochondrial protection by simvastatin against angiotensin II-mediated heart failure," *British Journal of Pharmacology*, vol. 176, no. 19, pp. 3791–3804, 2019.

[120] X. Liu, S. Zhang, L. An et al., "Loss of Rubicon ameliorates doxorubicin-induced cardiotoxicity through enhancement of mitochondrial quality," *International journal of cardiology*, vol. 296, pp. 129–135, 2019.

[121] Y. Feng, N. B. Madungwe, C. V. da Cruz Junho, and J. C. Bopassa, "Activation of G protein-coupled oestrogen receptor 1 at the onset of reperfusion protects the myocardium against ischemia/reperfusion injury by reducing mitochondrial dysfunction and mitophagy," *British Journal of Pharmacology*, vol. 174, no. 23, pp. 4329–4344, 2017.

[122] Z. Zha, J. Wang, X. Wang, M. Lu, and Y. Guo, "Involvement of PINK1/Parkin-mediated mitophagy in AGE-induced cardiomyocyte aging," *International Journal of Cardiology*, vol. 227, pp. 201–208, 2017.

[123] B. Zhou, J. Kreuzer, C. Kumsta et al., "Mitochondrial permeability uncouples elevated autophagy and lifespan extension," *Cell*, vol. 177, no. 2, pp. 299–314.e16, 2019.

[124] B. Wang, J. Nie, L. Wu et al., "AMPKα2 protects against the development of heart failure by enhancing mitophagy via PINK1 phosphorylation," *Circulation Research*, vol. 122, no. 5, pp. 712–729, 2018.

[125] W. Zhang, S. Siraj, R. Zhang, and Q. Chen, "Mitophagy receptor FUNDC1 regulates mitochondrial homeostasis and protects the heart from I/R injury," *Autophagy*, vol. 13, no. 6, pp. 1080-1081, 2017.

[126] J. C. Campos, B. B. Queliconi, L. H. M. Bozi et al., "Exercise reestablishes autophagic flux and mitochondrial quality control in heart failure," *Autophagy*, vol. 13, no. 8, pp. 1304–1317, 2017.

[127] R. M. Whitaker, D. Corum, C. C. Beeson, and R. G. Schnellmann, "Mitochondrial biogenesis as a pharmacological target: a new approach to acute and chronic diseases,"

Annual Review of Pharmacology and Toxicology, vol. 56, no. 1, pp. 229–249, 2016.

[128] A. Vainshtein, E. M. Desjardins, A. Armani, M. Sandri, and D. A. Hood, "PGC-1α modulates denervation-induced mitophagy in skeletal muscle," *Skeletal Muscle*, vol. 5, no. 1, p. 9, 2015.

[129] D. Yeo, C. Kang, M. C. Gomez-Cabrera, J. Vina, and L. L. Ji, "Intensified mitophagy in skeletal muscle with aging is down-regulated by PGC-1alpha overexpression in vivo," *Free Radical Biology and Medicine*, vol. 130, pp. 361–368, 2019.

[130] M. Zhang, Y. Chu, J. Mowery et al., "Pgc-1αrepression and high-fat diet induce age-related macular degeneration-like phenotypes in mice," *Disease Models & Mechanisms*, vol. 11, no. 9, article dmm032698, 2018.

[131] J. F. Gill, G. Santos, S. Schnyder, and C. Handschin, "PGC-1α affects aging-related changes in muscle and motor function by modulating specific exercise-mediated changes in old mice," *Aging Cell*, vol. 17, no. 1, article e12697, 2018.

[132] M. Markaki, K. Palikaras, and N. Tavernarakis, "Novel insights into the anti-aging role of mitophagy," *International Review of Cell and Molecular Biology*, vol. 340, pp. 169–208, 2018.

[133] H. J. Weir, P. Yao, F. K. Huynh et al., "Dietary restriction and AMPK increase lifespan via mitochondrial network and peroxisome remodeling," *Cell Metabolism*, vol. 26, no. 6, pp. 884–896.e5, 2017.

[134] N. Quan, W. Sun, L. Wang et al., "Sestrin2 prevents age-related intolerance to ischemia and reperfusion injury by modulating substrate metabolism," *The FASEB Journal*, vol. 31, no. 9, pp. 4153–4167, 2017.

[135] M. Morita, J. Prudent, K. Basu et al., "mTOR controls mitochondrial dynamics and cell survival via MTFP1," *Molecular Cell*, vol. 67, no. 6, pp. 922–935.e5, 2017.

[136] A. Lang, R. Anand, S. Altinoluk-Hambuchen et al., "SIRT4 interacts with OPA1 and regulates mitochondrial quality control and mitophagy," *Aging*, vol. 9, no. 10, pp. 2163–2189, 2017.

[137] Y. Zheng, B. Shi, M. Ma, X. Wu, and X. Lin, "The novel relationship between Sirt3 and autophagy in myocardial ischemia–reperfusion," *Journal of Cellular Physiology*, vol. 234, no. 5, pp. 5488–5495, 2019.

[138] W. K. Chen, Y. L. Tsai, M. A. Shibu et al., "Exercise training augments Sirt1-signaling and attenuates cardiac inflammation in D-galactose induced-aging rats," *Aging*, vol. 10, no. 12, pp. 4166–4174, 2018.

[139] P. Dakik, Y. Medkour, K. Mohammad, and V. I. Titorenko, "Mechanisms through which some mitochondria-generated metabolites act as second messengers that are essential contributors to the aging process in eukaryotes across phyla," *Frontiers in Physiology*, vol. 10, p. 461, 2019.

[140] E. Katsyuba, A. Mottis, M. Zietak et al., "De novo NAD$^+$ synthesis enhances mitochondrial function and improves health," *Nature*, vol. 563, no. 7731, pp. 354–359, 2018.

[141] M. Yoshida, A. Satoh, J. B. Lin et al., "Extracellular vesicle-contained eNAMPT delays aging and extends lifespan in mice," *Cell Metabolism*, vol. 30, no. 2, pp. 329–342.e5, 2019.

[142] K. Palikaras, E. Lionaki, and N. Tavernarakis, "Coordination of mitophagy and mitochondrial biogenesis during ageing in *C. elegans*," *Nature*, vol. 521, no. 7553, pp. 525–528, 2015.

[143] I. Scott, B. R. Webster, C. K. Chan, J. U. Okonkwo, K. Han, and M. N. Sack, "GCN5-like protein 1 (GCN5L1) controls mitochondrial content through coordinated regulation of mitochondrial biogenesis and mitophagy," *Journal of Biological Chemistry*, vol. 289, no. 5, pp. 2864–2872, 2014.

[144] J. Nah, S. Miyamoto, and J. Sadoshima, "Mitophagy as a protective mechanism against myocardial stress," *Comprehensive Physiology*, vol. 7, no. 4, pp. 1407–1424, 2017.

[145] M. M. Senchuk, D. J. Dues, C. E. Schaar et al., "Activation of DAF-16/FOXO by reactive oxygen species contributes to longevity in long-lived mitochondrial mutants in Caenorhabditis elegans," *PLOS Genetics*, vol. 14, no. 3, article e1007268, 2018.

[146] Y. Li, Y. Xue, X. Xu et al., "A mitochondrial FUNDC1/HSC70 interaction organizes the proteostatic stress response at the risk of cell morbidity," *The EMBO Journal*, vol. 38, no. 3, 2019.

[147] S. Peleg, C. Feller, I. Forne et al., "Life span extension by targeting a link between metabolism and histone acetylation in Drosophila," *EMBO Reports*, vol. 17, no. 3, pp. 455–469, 2016.

[148] D. J. Baker and S. Peleg, "Biphasic modeling of mitochondrial metabolism dysregulation during aging," *Trends in Biochemical Sciences*, vol. 42, no. 9, pp. 702–711, 2017.

[149] V. I. Korolchuk, S. Miwa, B. Carroll, and T. von Zglinicki, "Mitochondria in cell senescence: is mitophagy the weakest link?," *EBioMedicine*, vol. 21, pp. 7–13, 2017.

[150] I. Parikh, J. Guo, K.-H. Chuang et al., "Caloric restriction preserves memory and reduces anxiety of aging mice with early enhancement of neurovascular functions," *Aging*, vol. 8, no. 11, pp. 2814–2826, 2016.

[151] R. Jumpertz, R. L. Hanson, M. L. Sievers, P. H. Bennett, R. G. Nelson, and J. Krakoff, "Higher energy expenditure in humans predicts natural mortality," *The Journal of Clinical Endocrinology & Metabolism*, vol. 96, no. 6, pp. E972–E976, 2011.

[152] P. D. Bhola and A. Letai, "Mitochondria–Judges and Executioners of Cell Death Sentences," *Molecular Cell*, vol. 61, no. 5, pp. 695–704, 2016.

[153] S. Marquez-Jurado, J. Diaz-Colunga, R. P. das Neves et al., "Mitochondrial levels determine variability in cell death by modulating apoptotic gene expression," *Nature Communications*, vol. 9, no. 1, p. 389, 2018.

[154] R. Shi, M. Guberman, and L. A. Kirshenbaum, "Mitochondrial quality control: the role of mitophagy in aging," *Trends in Cardiovascular Medicine*, vol. 28, no. 4, pp. 246–260, 2018.

[155] Y. Liu and B. Levine, "Autosis and autophagic cell death: the dark side of autophagy," *Cell Death & Differentiation*, vol. 22, no. 3, pp. 367–376, 2015.

[156] N. Sen, Y. K. Satija, and S. Das, "PGC-1α, a Key Modulator of p53, Promotes Cell Survival upon Metabolic Stress," *Molecular Cell*, vol. 44, no. 4, pp. 621–634, 2011.

[157] G. W. Dorn 2nd and R. N. Kitsis, "The mitochondrial dynamism-mitophagy-cell death interactome: multiple roles performed by members of a mitochondrial molecular ensemble," *Circulation Research*, vol. 116, no. 1, pp. 167–182, 2015.

[158] L. Partridge, J. Deelen, and P. E. Slagboom, "Facing up to the global challenges of ageing," *Nature*, vol. 561, no. 7721, pp. 45–56, 2018.

[159] K. H. Chen, X. Guo, D. Ma et al., "Dysregulation of HSG triggers vascular proliferative disorders," *Nature Cell Biology*, vol. 6, no. 9, pp. 872–883, 2004.

[160] Y. Chen, Y. Liu, and G. W. Dorn II, "Mitochondrial fusion is essential for organelle function and cardiac homeostasis," *Circulation Research*, vol. 109, no. 12, pp. 1327–1331, 2011.

[161] L. Fang, X. L. Moore, X. M. Gao, A. M. Dart, Y. L. Lim, and X. J. Du, "Down-regulation of mitofusin-2 expression in cardiac hypertrophy in vitro and in vivo," *Life Sciences*, vol. 80, no. 23, pp. 2154–2160, 2007.

[162] J. M. Son, E. H. Sarsour, A. Kakkerla Balaraju et al., "Mitofusin 1 and optic atrophy 1 shift metabolism to mitochondrial respiration during aging," *Aging Cell*, vol. 16, no. 5, pp. 1136–1145, 2017.

[163] L. Chen, Q. Gong, J. P. Stice, and A. A. Knowlton, "Mitochondrial OPA1, apoptosis, and heart failure," *Cardiovascular Research*, vol. 84, no. 1, pp. 91–99, 2009.

[164] L. Chen, T. Liu, A. Tran et al., "OPA1 mutation and late-onset cardiomyopathy: mitochondrial dysfunction and mtDNA instability," *Journal of the American Heart Association*, vol. 1, no. 5, article e003012, 2012.

[165] T. Varanita, M. E. Soriano, V. Romanello et al., "The OPA1-dependent mitochondrial cristae remodeling pathway controls atrophic, apoptotic, and ischemic tissue damage," *Cell Metabolism*, vol. 21, no. 6, pp. 834–844, 2015.

[166] Y. Ikeda, A. Shirakabe, Y. Maejima et al., "Endogenous Drp1 mediates mitochondrial autophagy and protects the heart against energy stress," *Circulation Research*, vol. 116, no. 2, pp. 264–278, 2015.

[167] M. Song, K. Mihara, Y. Chen, L. Scorrano, and G. W. Dorn 2nd, "Mitochondrial fission and fusion factors reciprocally orchestrate mitophagic culling in mouse hearts and cultured fibroblasts," *Cell Metabolism*, vol. 21, no. 2, pp. 273–286, 2015.

[168] M. Ding, J. Ning, N. Feng et al., "Dynamin-related protein 1-mediated mitochondrial fission contributes to post-traumatic cardiac dysfunction in rats and the protective effect of melatonin," *Journal of Pineal Research*, vol. 64, no. 1, article e12447, 2018.

[169] M. H. Disatnik, J. C. Ferreira, J. C. Campos et al., "Acute inhibition of excessive mitochondrial fission after myocardial infarction prevents long-term cardiac dysfunction," *Journal of the American Heart Association*, vol. 2, no. 5, article e000461, 2013.

[170] S. B. Ong, S. Subrayan, S. Y. Lim, D. M. Yellon, S. M. Davidson, and D. J. Hausenloy, "Inhibiting mitochondrial fission protects the heart against ischemia/reperfusion injury," *Circulation*, vol. 121, no. 18, pp. 2012–2022, 2010.

[171] A. Rana, M. Rera, and D. W. Walker, "Parkin overexpression during aging reduces proteotoxicity, alters mitochondrial dynamics, and extends lifespan," *Proceedings of the National Academy of Sciences*, vol. 110, no. 21, pp. 8638–8643, 2013.

[172] A. Hoshino, Y. Mita, Y. Okawa et al., "Cytosolic p53 inhibits Parkin-mediated mitophagy and promotes mitochondrial dysfunction in the mouse heart," *Nature Communications*, vol. 4, no. 1, p. 2308, 2013.

[173] J. Piquereau, R. Godin, S. Deschenes et al., "Protective role of PARK2/Parkin in sepsis-induced cardiac contractile and mitochondrial dysfunction," *Autophagy*, vol. 9, no. 11, pp. 1837–1851, 2013.

[174] A. H. Chaanine, D. Jeong, L. Liang et al., "JNK modulates FOXO3a for the expression of the mitochondrial death and mitophagy marker BNIP3 in pathological hypertrophy and in heart failure," *Cell Death & Disease*, vol. 3, no. 2, article e265, 2012.

[175] A. F. Fernandez, S. Sebti, Y. Wei et al., "Disruption of the beclin 1-BCL2 autophagy regulatory complex promotes longevity in mice," *Nature*, vol. 558, no. 7708, pp. 136–140, 2018.